

INTRODUCTION OF MEDIA AND REAGENTS FOR THE  
DETERMINATION OF ENVIRONMENTAL AND  
BIOLOGICAL SUBSTANCES BY HIGH  
PERFORMANCE CAPILLARY  
ELECTROPHORESIS

By

YEHIA SALEM MECHREF

Bachelor of Science

American University of Beirut

Beirut, Lebanon

1991

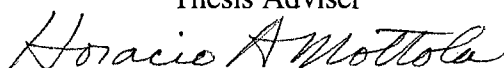
Submitted to the Faculty of the  
Graduate College of the  
Oklahoma State University  
in partial fulfillment of  
the requirements for  
the Degree of  
DOCTOR OF PHILOSOPHY  
July, 1996

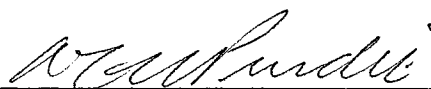
INTRODUCTION OF MEDIA AND REAGENTS FOR THE  
DETERMINATION OF ENVIRONMENTAL AND  
BIOLOGICAL SUBSTANCES BY HIGH  
PERFORMANCE CAPILLARY  
ELECTROPHORESIS

Thesis Approved:



Thesis Adviser









Dean of the Graduate College

## ACKNOWLEDGMENTS

First, my profound and sincere appreciation goes to my research advisor, Dr. Ziad El Rassi, whose advise, guidance, sincerity and devotion to his work and students have made this work possible. Being his student was an unforgettable experience that taught me hard work pays off. Although my time under his tutelage came to an end, I will be always indebted to him and very grateful that I had the opportunity to be his student.

I would also like to express cordial thanks to my committee members, Dr. Neil Purdie, Dr. Horacio A. Mottola and Dr. E. C. Nelson for their support and invaluable suggestions. It has been a great privilege to attend courses presided over by Dr. El Rassi, Dr. Purdie and Dr. Mottola. Also, I should thank Dr. K. Darrell Berlin for his valuable suggestions. I would like to thank Phillips Petroleum for supporting me with a fellowship.

Thanks are also in order for the people in our research group, Ying Zhang, Arron Karcher, Kevin Farmer and Changming Yang. Special thanks go to Jennifer Postelwait and Kim Wasserkrug for their friendships.

I acknowledge the encouragement and supports from many friends whom I knew on-campus and off-campus including Wassim Nashabeh without whom I would not have come to OSU, Tim and Gina Smith who are a true friends and I value and appreciate their friendship, Imad Abou-Zahar, Shawn Childress, Samir Tyagi as well as many others. It has been a great privilege to make the acquaintance of Ibrahim, Dania, Sarah and Ahmad Khalil and Mohammad and Nahiel Agha.

My thanks also go to my sisters and brothers, Mohammad, Mahmoud, Mysoon, Rania, Rami and Rasha who always believed in me. I should thank my mother-in-law,

Bahija, for tolerating the fact that her only child is far away from her and my father-in-law, Zafer, who may rest in peace.

My utterly thanks and love go to my wife, Reda, who have always been there for me. I will never forget her understanding of the long hours I have spent in the lab and hope to make up for the lost time. Her unconditional love and support were dearly needed and were provided constantly without request and they eased the stressful graduate life. Although this work bear my name, to me her name is printed next to mine. Thank you Reda, and I will always love you. Although my little angel, Farah Fayzah, is too young to comprehend what her father is doing, her innocent smiles relieve any stress.

This dissertation is dedicate to my parents, Salem and Fayzah, who never doubted my ability to achieve the goals I sat to myself. Their love and support have always motivated me to go through the hardships. I am honored and proud to be your son. This dissertation is for you and you are in my heart.

## TABLE OF CONTENTS

Chapter	Page
I.	INTRODUCTION AND SOME BASIC ASPECTS OF HIGH PERFORMANCE CAPILLARY ELECTROPHORESIS
Introduction .....	1
Historical Background and Development .....	3
Basic Principles .....	7
Electrophoretic Migration .....	7
Electroosmotic Flow .....	9
Analytical Parameters .....	13
Migration Time and Apparent Mobility .....	13
Separation Efficiency .....	14
Resolution and Selectivity .....	15
Factors Affecting the Efficiency of Separation in CZE .....	16
Modes of Operation .....	16
General Instrumentation and Capillary .....	21
Sample Injection .....	23
Detection in CE .....	25
Conclusions .....	26
References .....	27
II.	Capillary Zone Electrophoresis of Biomolecules
Introduction .....	30
Detection of Carbohydrates in CZE .....	31
Precolumn Derivatization of Carbohydrates .....	33
Derivatization Schemes .....	35
CE Analysis of Gangliosides .....	41
Solute-Wall Interaction in CZE of Proteins .....	44
Buffer Systems .....	45
Dynamically Coated Capillaries .....	46
Permanently Coated Capillaries .....	48
Covalently Bonded Phases .....	48
Physically Adhered Phases .....	52
Summary of Objectives and Rationales of Part I of the Dissertation .....	53
References .....	55
III.	Capillary Zone Electrophoresis of Derivatized Acidic Monosaccharides
Introduction .....	59
Materials and Methods .....	61
Reagents and Materials .....	61

Chapter	Page
Instruments and Capillaries .....	61
Mass Spectrometry Measurements .....	62
Derivatization of Acidic Carbohydrates .....	63
Results and Discussion .....	63
Precolumn Derivatization .....	63
CZE of Derivatized Monosaccharides .....	70
CZE at Low pH .....	70
CZE at high pH .....	73
On-Column Detection of the Derivatized Monosaccharides .....	77
Conclusions .....	80
References .....	82
 IV	
<b>CAPILLARY ELECTROPHORESIS OF CARBOXYLATED CARBOHYDRATES. 1. SELECTIVE PRECOLUMN DERIVATIZATION OF GANGLIOSIDES WITH UV ABSORBING AND FLUORESCENT TAGS</b>	
Introduction .....	84
Materials and Methods .....	86
Instruments and Capillaries .....	86
Reagents and Materials .....	86
Extraction of Gangliosides .....	87
Derivatization of Gangliosides .....	88
Neuraminidase Treatment .....	88
Results and Discussion .....	88
Precolumn Derivatization of Gangliosides .....	89
Capillary Electrophoresis of Gangliosides .....	94
Conclusions .....	107
References .....	110
 V.	
<b>CAPILLARY ELECTROPHORESIS OF CARBOXYLATED CARBOHYDRATES. 2. SELECTIVE PRECOLUMN DERIVATIZATION OF SIALO-OLIGOSACCHARIDES DERIVED FROM GANGLIOSIDES WITH 7- AMINONAPHTHALENE-1,3-DISULFONIC ACID FLUORESCING TAG</b>	
Introduction .....	112
Materials and Methods .....	113
Reagents and Materials .....	113
Instruments and Capillaries .....	113
Cleavage of Sialooligosaccharides from Gangliosides .....	114
Derivatization of Sialooligosaccharides .....	114
Results and Discussion .....	116
CZE with Sodium Phosphate Electrolyte System .....	116
CZE with Borate Electrolyte System .....	119
Conclusions .....	124
References .....	126

Chapter		Page
VI.	FUSED-SILICA CAPILLARIES WITH SURFACE-BOUND DEXTRAN LAYER CROSSLINKED WITH DIEPOXY POLYETHYLENE GLYCOL FOR CAPILLARY ELECTROPHORESIS OF BIOLOGICAL SUBSTANCES AT REDUCED ELECTROSMOTIC FLOW	
	Introduction .....	128
	Materials and Methods .....	130
	Instruments and Capillaries .....	130
	Reagents and Materials .....	130
	Capillary Coating .....	131
	Stability Studies .....	131
	Reproducibility Studies .....	131
	Derivatization of Acidic Mono- and Oligosaccharides .....	132
	Results and Discussion .....	132
	Coatings of capillaries .....	132
	Evaluation of the Coated Capillaries .....	132
	Electroosmotic Flow .....	132
	CZE of Basic Proteins .....	135
	Reproducibility and Stability of the Coatings .....	138
	CZE of Negatively Charged Species .....	142
	Acidic Proteins .....	142
	ANDSA Derivatives of Acidic Monosaccharides.....	142
	ANDSA Derivatives of Sialooligosaccharides Derived from Gangliosides .....	144
	Conclusions .....	147
	References .....	149
VII.	COUPLED CAPILLARY ELECTROPHORESIS AND CAPILLARY ENZYME MICROREACTORS HAVING SURFACE-IMMOBILIZED RNA-MODIFYING ENZYMES	
	Introduction .....	150
	Materials and Methods .....	151
	Reagents and Materials .....	151
	Instrument .....	152
	Capillary Column .....	152
	Enzyme Reactor Preparation .....	152
	Other Procedures .....	153
	Results and Discussion .....	155
	Adjustment of the Direction of EOF in the Separation Capillary .....	155
	RNase U <sub>2</sub> Capillary Enzyme Reactor .....	157
	RNase U <sub>2</sub> and T <sub>1</sub> Mixed Enzyme Reactor .....	163
	Digestion of tRNA <sup>Phe</sup> .....	168
	Conclusions .....	174
	References .....	175

Chapter		Page
VIII.	SOME BASIC ASPECTS OF MICELLAR ELECTROKINETIC CAPILLARY CHROMATOGRAPHY AND CHIRAL CAPILLARY ELECTROPHORESIS	
	Introduction .....	178
	Micellar Electrokinetic Capillary Chromatography .....	179
	Separation Principles .....	179
	Migration Behavior .....	180
	Neutral Analytes .....	180
	Charged Analytes .....	182
	Resolution in MECC .....	183
	Optimization of Separation in MECC .....	183
	Some Aspects of MECC with In Situ Charged Micelles .....	186
	Chiral Separations in CE .....	189
	Some General Aspects .....	189
	A Model for Chiral Separation .....	190
	Ligand Exchange .....	191
	Chiral Micelles .....	192
	Inclusion Complexation .....	193
	Affinity Interactions .....	196
	Proteins as Chiral Selectors .....	196
	Polysaccharides as Chiral Selectors .....	197
	Summary of Objectives and Rationales of Part II of the Dissertation .....	199
IX.	MICELLAR ELECTROKINETIC CAPILLARY CHROMATOGRAPHY WITH IN SITU CHARGED MICELLES. EXPANDING THE UTILITY OF ALKYLGLYCOSIDE-BORATE MICELLES TO ACIDIC AND NEUTRAL pH FOR CAPILLARY ELECTROPHORESIS OF DANSYL AMINO ACIDS AND HERBICIDES	
	Introduction .....	206
	Materials and Methods .....	207
	Instrument .....	207
	Reagents and Materials .....	207
	Results and Discussion .....	208
	Dependence of the Magnitude of the Migration Time Window on Borate Concentration .....	208
	Dependence of the Magnitude of the Migration Time Window on pH .....	212
	Correlation Between Capacity Factor and Carbon Number, $n_c$ , of Homologous Series .....	217
	Dependence of Capacity Factor on pH .....	218
	Illustrative Applications .....	220
	Phenoxy Acid Herbicides and their Esters .....	220
	Urea Herbicides .....	220
	Dansyl Amino Acids .....	225
	Conclusions .....	225
	References .....	228



X.	MICELLAR ELECTROKINETIC CAPILLARY CHROMATOGRAPHY WITH IN SITU CHARGED MICELLES. EVALUATION OF NOVEL CHIRAL MICELLES CONSISTING OF STEROIDAL-GLYCOSIDE SURFACTANT-BORATE COMPLEXES	
	Introduction .....	229
	Materials and Methods .....	233
	Capillary Electrophoresis Instrument .....	233
	Reagents and Materials .....	233
	Results and Discussion .....	235
	Variables Affecting the Chiral Recognition and the Electrokinetic Behavior of the Steroidal Glycoside- Borate Micellar Phases .....	235
	Electrolyte pH .....	235
	Borate Concentration .....	237
	Concentration of the Surfactant .....	246
	Organic Modifier .....	246
	Capillary Temperature .....	248
	Illustrative Enantiomeric Separations .....	253
	Troger's Base .....	253
	Dansyl Amino Acids .....	253
	Silvex Herbicide .....	256
	Conclusions .....	256
	References .....	259
XI.	PRECOLUMN DERIVATIZATION OF CHIRAL AND ACHIRAL PHENOXY ACID HERBICIDES WITH A FLUORESCENT TAG FOR ELECTROPHORETIC SEPARATION IN THE PRESENCE OF CYCLODEXTRINS AND MICELLAR PHASES	
	Introduction .....	261
	Materials and Methods .....	263
	Capillary Electrophoresis Instrument for Fluorescence Detection .....	263
	Capillary Electrophoresis Instruments for UV and Laser-Induced Fluorescence Detection .....	263
	Reagents and Materials .....	264
	Precolumn Derivatization .....	266
	Results and Discussion .....	267
	Extent of Derivatization and Limit of Detection .....	267
	Chiral Separation by CD-CE .....	271
	CE of ANDSA-Phenoxy Acid Herbicides by Mixed CDs .....	279
	CD-MECC .....	282
	Conclusions .....	284
	References .....	285

Chapter		Page
XII.	EVALUATION OF ALKYLGLUCOSIDE CHIRAL SURFACTANTS IN THE ENANTIOMERIC SEPARATION OF PHENOXY ACID HERBICIDES AND OTHER SPECIES	
	Introduction .....	287
	Materials and Methods .....	289
	Capillary Electrophoresis Instrument .....	289
	Reagents and Materials .....	289
	Results and Discussion .....	290
	Effect of Surfactant Concentration and Description of the Separation Principles .....	290
	Effect of pH and Ionic Strength .....	305
	Effect of Methanol .....	310
	Effect of Temperature .....	312
	Chiral Separation under Optimized Conditions .....	312
	Enantiomeric Separation of Other Solutes .....	317
	Dansyl Amino Acids .....	317
	1,1'-Binaphthyl-2,2'-diylhydrogen Phosphate .....	321
	Warfarin .....	321
	Bupivacaine .....	323
	Conclusions .....	323
	References .....	327
XIII	EVALUATION OF OCTYLMALTOPYRANOSIDE CHIRAL SURFACTANT IN THE ENANTIOMERIC SEPARATION OF FLUORESCENTLY LABELED PHENOXY ACID HERBICIDES AND THEIR LIF DETECTION	
	Introduction .....	329
	Materials and Methods .....	330
	Capillary Electrophoresis Instrument .....	330
	Reagents and Materials .....	331
	Precolumn Derivatization .....	331
	Fluorescence Measurements .....	331
	Field-Amplified Sample-Stacking .....	332
	Results and Discussion .....	334
	Effect of Tagging with ANDSA on the Enantiomeric Resolution .....	334
	Limit of Detection .....	337
	Field-Amplified Sample-Stacking of Ultra Diluted Samples .....	337
	Effect of Surfactant Concentration .....	339
	Effect of pH and Ionic Strength .....	342
	Effect of Methanol .....	346
	Conclusions .....	348
	References .....	349

## LIST OF TABLES

Table		Page
Chapter I		
I.	Sources of Zone Broadening in CE .....	17
II.	Modes of HPCE and their Basis of Separation .....	18
III.	Methods of Detection in HPCE .....	26
Chapter III		
I.	Mass-to-Charge Ratios (m/z) of Observed Ions for the Derivatized Monosaccharides .....	68
Chapter V		
I.	Structures, Abbreviations and Charge-to-Mass Ratios of Underivatized and ANDSA Derivatives of the Sialooligosaccharides Derived from Gangliosides .....	115
Chapter VI		
I.	EOF of the Different Capillaries Under the Separation Conditions .....	135
II.	Percentage Relative Standard Deviation (%RSD) of the Migration Times of Four Basic Proteins Separated on Different Coated Capillaries .....	138
Chapter VII		
I.	Possible Fragmentation of tRNA <sup>Phe</sup> by the Ribonucleases Under Investigation .....	171
Chapter VIII		
I.	Aggregation Numbers and CMC Values for Various Surfactants .....	185
II.	Proteins as Chiral Selectors and their Application .....	198
III.	Polysaccharides as Chiral Selectors in CE .....	199

Table	Page
Chapter IX	
I. Values of Slope, Intercept and R for the Correlation Between Capacity Factor, $k'$ , and Carbon Number in the Alkyl Chain of Alkyl Phenyl Ketones at Various pH Values .....	217
II. Values of Slope, Intercept and R for the Correlation Between Capacity Factor, $k'$ , and Carbon Number in the Alkyl Chain of Alkyl Phenyl Ketones at Various Borate Concentration .....	218
Chapter XI	
I. Percent Yield of the Precolumn Derivatization of Phenoxy Acid Herbicides with ANDSA .....	269
II. Resolution of Derivatized and Underivatized Phenoxy Acid Herbicide Enantiomers by CD-CE Using Various Cyclodextrins .....	276

## LIST OF FIGURES

Figure	Page
Chapter I	
1. Schematic Illustration of (a) the Electric Double-Layer at the Surface of the Fused-Silica Capillary, (b) the Electrical Double-Layer Potential Gradient and (c) the Flat Flow Profile of the Electroosmotic Flow (EOF) .....	10
2. Schematic Illustration of Ideal CZE Separation .....	12
3. Mode of Operation of CE .....	19
4. Instrumental Set-up of an In-House Assembled Capillary Electrophoresis Instrument and Full and Cross-Sectional View of the Capillary .....	22
5. Modes of Sample Injection in CE .....	24
Chapter II	
1. Schematic Illustration of Reductive Amination .....	37
2. Schematic Illustration of Condensation Reaction with PMP .....	38
3. Schematic Illustration of Derivatization with CBQCA .....	38
4. Schematic Illustrations of Derivatization with TRSE .....	39
5. Schematic Illustration of Condensation Reaction with Dansylhydrazine .....	40
6. Structures of the Gangliosides .....	42
Chapter III	
1. Derivatization Scheme .....	65
2. Structures of the Acidic Monosaccharides .....	66
3. CF-LSIMS Spectra of ANDSA- and SA-Glyceric Acid .....	67
4. Time Course for the Derivatization Reactions of Glyceric Acid with ANDSA and SA .....	69

Figure	Page
5. Electropherograms of SA Derivatives of Acidic Monosaccharides .....	71
6. Electropherograms of ANDSA Derivatives of Acidic Monosaccharides ...	72
7. Electropherograms of ANDSA Derivatives of Acidic Monosaccharides ...	74
8. Electropherogram of ANDSA Derivatives of Acidic Monosaccharides ....	76
9. Plots of Migration Times of ANDSA Derivatives of Acidic Monosaccharides Versus Borate Concentration .....	78
10. Plots of Migration Times of SA Derivatives of Acidic Monosaccharides Versus Borate Concentration .....	79

#### Chapter IV

1. Typical Electropherograms of SA (a) and ANDSA (b) Derivatives of the Ganglioside Mixture Type III from Sigma and ANDSA Derivative of Standard G <sub>D1a</sub> (c) .....	91
2. Monitoring of the Neuraminidase Action on the SA Derivative of G <sub>T1b</sub> by Capillary Electrophoresis .....	93
3. Time Course for the Derivatization Reactions of G <sub>T1b</sub> with ANDSA and SA .....	95
4. Electropherograms of Standard Gangliosides Derivatized with ANDSA .....	96
5. Electropherograms of Underivatized Gangliosides (mixture type III) .....	98
6. Electropherograms of Standard Underivatized Gangliosides .....	99
7. Electropherograms of Underivatized Gangliosides (mixture type III) .....	101
8. Plot of Average Plate Counts per Meter at Various $\alpha$ -CD Concentration in the Running Electrolyte .....	102
9. Typical Plots of Migration Time Versus Borate Concentration in the Running Electrolyte Obtained with ANDSA Derivatives of Standard Gangliosides .....	104
10. Typical Fluorescence Electropherogram of Mono-, Di- and Trisialogangliosides Derivatized with ANDSA .....	105
11. Electropherograms of Standard Underivatized Gangliosides .....	106
12. Electropherograms of Standard ANDSA Derivatives of Disialogangliosides .....	108
13. Electropherogram of Standard ANDSA-Disialogangliosides .....	109

Figure	Page
Chapter V	
1. Electropherograms of Underivatized (a) and ANDSA Derivatives (b) of Sialooligosaccharides Cleaved from Gangliosides .....	117
2. Electropherogram of ANDSA Derivatives of Sialooligosaccharides .....	120
3. Plots of Migration Times (a) and Electrophoretic Mobilities (b) of ANDSA Derivatives of Sialooligosaccharides <i>versus</i> Borate Concentration .....	122
4. Electropherograms of ANDSA Derivatives of Sialooligosaccharides .....	123
Chapter VI	
1. Plot of Electroosmotic Flow Versus pH of the Running Electrolyte .....	134
2. Typical Electropherograms of Four Standard Basic Proteins .....	136
3. Typical Electropherograms of Four Basic Proteins .....	139
4. Plots of Migration Times of Basic Proteins Versus Number of Washes with 0.010 M HCl .....	140
5. Plots of Migration Times of Basic Proteins Versus Number of Washes with 0.010 M NaOH .....	141
6. Typical Electropherogram of Acidic Proteins Obtained on a Dextran 150 kDa Coated Capillary .....	143
7. Structure of <i>N</i> -Acetylneuraminic Acid-ANDSA Derivative .....	145
8. Electropherograms of ANDSA Derivatives of Acidic Monosaccharides Obtained on a Dextran 150 kDa Coated Capillary .....	146
9. Electropherograms of ANDSA Derivatives of Sialooligosaccharides Derived from Gangliosides .....	148
Chapter VII	
1. Schematic of CE Instrument Showing the Coupling of the Capillary Enzyme Reactor to the Separation Capillary and the Arrangement Used for Jacketing the Microreactor with a Tygon Tube for Thermostating its Surrounding via a Circulating Water Bath .....	154
2. Plots of EOF (1) and Current (2) as a Function of Polybrene Percentage in the Running Electrolyte System .....	156
3. Plot of EOF Versus the pH of the Running Electrolyte .....	158
4. pH Dependence of the Activity of RNase U <sub>2</sub> .....	160

Figure	Page
5. Typical Electropherograms of Digested ApC Dinucleotide at Different pH Values .....	161
6. Temperature Dependence of the Activity of RNase U <sub>2</sub> .....	162
7. Electropherograms of Dinucleotides (a) and the Digest of Dinucleotides (b) Using RNase U <sub>2</sub> Enzyme Reactor .....	164
8. pH Dependence of the Activity of RNase T <sub>1</sub> .....	166
9. Electropherograms of Dinucleotides (a) and their Digest (b) by Mixed RNase U <sub>2</sub> and T <sub>1</sub> Capillary Reactor .....	167
10. Electropherograms of Dinucleotides (a) and their Digest (b) by Mixed RNase U <sub>2</sub> and T <sub>1</sub> Capillary Reactor .....	169
11. Electropherograms of tRNA <sup>Phe</sup> Digested by Passing Through RNase U <sub>2</sub> Capillary Reactor .....	170
12. Electropherograms of tRNA <sup>Phe</sup> Digested by Passing Through RNase T <sub>1</sub> and U <sub>2</sub> Mixed Capillary Reactor .....	173
 Chapter VIII 	
1. Schematic Illustrations of the Principles of MECC Separations with Anionic Surfactant .....	181
2. Structure of $\alpha$ -CD (a). Basic Features of native CDs (b) .....	194
3. Structure of 18-Crown-6-Ether Tetracarboxylic Acid .....	195
 Chapter IX 	
1. Effect of Borate Concentration on the Magnitude of the Migration Time Window .....	210
2. Typical Electropherograms of Alkyl Phenyl Ketones Obtained at Different Sodium Borate Concentrations .....	213
3. Effect of pH on the Magnitude of the Migration Time Window .....	214
4. Typical Electropherograms of Alkyl Phenyl Ketones at Various pH .....	216
5. Plots of Capacity Factor k' vs. pH of the Running Electrolyte .....	219
6. Structures of Two Phenoxy Acid Herbicides and Three Phenoxy Acid Herbicide Esters .....	221
7. Electropherogram of Phenoxy Acid Herbicides and their Esters .....	222



Figure	Page
8. Structures of Nine Urea Herbicides .....	223
9. Electropherograms of Urea Herbicides .....	224
10. Electropherogram of Dansyl Amino Acids .....	226
Chapter X	
1. Structures of Big CHAP (X= OH) and Deoxy Big CHAP (X = H) Surfactants .....	231
2. Structures of Model Chiral Solutes Used in this Study .....	234
3. Effect of pH on the Magnitude of the Migration Time Window .....	236
4. Electropherograms of BNOH Obtained with Deoxy Big CHAP at Various pH .....	238
5. Electropherograms of Standard BNPO <sub>4</sub> Enantiomers Obtained with Deoxy Big CHAP at Various pH .....	239
6. Electropherogram of BNPO <sub>4</sub> Obtained with Big CHAP at pH 9.0 in (a) and Electropherograms of BNOH Obtained with Big CHAP at pH 10.0 in (b) .....	240
7. Effect of Borate Concentration on the Magnitude of the Migration Time Window .....	242
8. Electropherograms of BNDA Enantiomers Obtained with Deoxy Big CHAP at Various Concentrations of Borate in the Running Electrolytes .....	243
9. Electropherograms of BNPO <sub>4</sub> Enantiomers Obtained with Deoxy Big CHAP at Various Concentrations of Borate in the Running Electrolytes .....	244
10. Electropherograms of BNOH Enantiomers Obtained with Big CHAP at Various Concentrations of Borate in the Running Electrolytes .....	245
11. Electropherograms of BNOH Obtained at Various Concentrations of Deoxy Big CHAP in the Running Electrolytes .....	247
12. Electropherograms of BNDA Enantiomers Obtained with Deoxy Big CHAP at Various Percentage of Methanol in the Running Electrolytes .....	249
13. Electropherograms of (a and b) BNOH and (c and d) BNPO <sub>4</sub> Enantiomers Obtained with Big CHAP at various Percentage of Methanol .....	250

Figure	Page
14. Electropherograms of BNDA Enantiomers Obtained with Deoxy Big CHAP at Various Capillary Temperatures .....	251
15. Electropherograms of BNOH Enantiomers Obtained with Big CHAP at Capillary Temperature of 15 °C (a) and 35 °C (b) .....	252
16. Electropherograms of Troger's Base Obtained with Deoxy Big CHAP .....	254
17. Electropherograms of Dansyl Amino Acids Obtained with Deoxy Big CHAP in (a) and (b) and Big CHAP in (c) .....	255
18. Electropherogram of Silvex a Phenoxy Acid Herbicide .....	257

#### Chapter XI

1. Structures of Phenoxy Acid Herbicides Studied .....	265
2. (a) Electropherograms of Six ANDSA-Phenoxy Acid Herbicides Obtained by CE-UV .....	268
3. Electropherogram of Nine ANDSA-Phenoxy Acid Herbicides Obtained by CE-LIF .....	270
4. Electropherograms of ANDSA-Phenoxy Acid Herbicides Obtained by CD-CE Using Lamp Operated Fluorescence Detector .....	272
5. Electropherograms of ANDSA-Phenoxy Acid Herbicides Obtained by CD-CE Using Lamp Operated Fluorescence Detector .....	273
6. Electropherograms of Underivatized Phenoxy Acid Herbicides Obtained by CD-CE .....	277
7. Resolution of the ANDSA-Phenoxy Acid Enantiomers as a Function of Chiral Selector Concentration .....	278
8. Electropherograms of ANDSA-Phenoxy Acid Herbicides Obtained by CD-CE and Mixed CD-CE Using Lamp Operated Fluorescence Detector .....	280
9. Electropherograms of ANDSA-Phenoxy Acid Herbicides Obtained by CD-CE and Mixed CD-CE Using Lamp Operated Fluorescence Detector .....	281
10. Electropherograms Comparing the Enantiomeric Separation of ANDSA-Phenoxy acid Herbicides Obtained with (a) CD-CE and (b) CD-MECC Using Lamp Operated Fluorescence Detector .....	283

#### Chapter XII

1. Structures of Dansyl Amino Acids, Bupivacaine and Warfarin .....	291
---	-----

Figure	Page
2. Electropherograms of Phenoxy Acid Herbicides Depicting the Effect of OG Concentration on Enantiomeric Resolution .....	293
3. A Scheme Illustrating the Separation Principles of Charged Species in the Presence of Neutral Micelles .....	294
4. Plots of the Average Effective Electrophoretic Mobility of Phenoxy Acid Herbicides Versus the Concentration of OG (a), NG (b) and OM (c) .....	296
5. Bar Graphs of the Enantiomeric Resolution of Phenoxy Acid Herbicides at Different OG Concentration .....	297
6. Bar Graphs of the Enantiomeric Resolution of Phenoxy Acid Herbicides at different NG Concentration .....	300
7. Electropherograms of Phenoxy Acid Herbicides Depicting the Effect of NG Concentration on the Enantiomeric Resolution .....	301
8. Bar Graphs of the Enantiomeric Resolution of Phenoxy Acid Herbicides at Different OM Concentration .....	303
9. Electropherograms of Phenoxy Acid Herbicides at Various OM Concentrations .....	304
10. Bar Graphs of the Enantiomeric Resolution of Phenoxy Acid Herbicides at Different pH Values of the Running Electrolyte .....	307
11. Electropherograms of Phenoxy Acid Herbicides at Different pH Values of the Running Electrolyte .....	308
12. Bar Graphs of the Enantiomeric Resolution of Phenoxy Acid Herbicides at Different Ionic Strength of the Running Electrolyte .....	309
13. Bar Graphs of the Enantiomeric Resolution of Phenoxy Acid Herbicides at Different Percentages of Methanol Added to the Running Electrolyte .....	311
14. Bar Graphs of the Enantiomeric Resolution of Phenoxy Acid Herbicides at Different Temperatures .....	313
15. Plots of the Average Electrophoretic Mobility of Phenoxy Acid Herbicides Enantiomers Versus Separation Temperature .....	314
16. Electropherograms of Phenoxy Acid Herbicides Depicting Optimum Enantiomeric Resolution Using NG (a) or OG (b) .....	315
17. Optimum Enantiomeric Resolutions of Phenoxy Acid Herbicides Using OM .....	316
18. Electropherograms of Dansyl Amino Acids .....	318

Figure	Page
19. Bar Graphs of the Enantiomeric Resolution of Dansyl Amino Acids at Different OM Concentration .....	319
20. Electropherograms of Dansyl Amino Acids .....	320
21. Electropherograms of 1,1'-Binaphthyl-2,2'-diylhydrogen Phosphate .....	322
22. Electropherograms of Warfarin .....	324
23. Electropherograms of Bupivacaine .....	325

### Chapter XIII

1. Fluorescence Spectra of ANDSA and ANDSA-2,2-CPPA .....	333
2. Electropherograms of Derivatized (a) and Underivatized (b) Phenoxy Acid Herbicides .....	235
3. Electropherograms of ANDSA-Phenoxy Acid Herbicides Obtained With (a) and Without (b and c) Field-Amplified Sample Stacking .....	338
4. Plots of the Average Effective Electrophoretic Mobilities of ANDSA-Phenoxy Acid Herbicides Versus OM Concentrations .....	340
5. Bar Graphs of the Enantiomeric Resolution of ANDSA-Phenoxy Acid Herbicides at Various OM Concentrations .....	341
6. Electropherograms of ANDSA-Phenoxy Acid Herbicides at Various OM Concentrations .....	343
7. Bar Graphs of the Enantiomeric Resolution of ANDSA-Phenoxy Acid Herbicides at Various Ionic Strengths of the Separation Electrolyte .....	345
8. Bar Graphs of the Enantiomeric Resolution of ANDSA-Phenoxy Acid Herbicides at Various Percentage of Methanol in the Separation Electrolyte .....	347

## LIST OF SYMBOLS AND ABBREVIATIONS

2-AP	2-aminopyridine
2-PPA	2-phenoxypropionic acid
6-AQ	6-aminoquinoline
2,2-CPPA	2-(2-chlorophenoxy)propionic acid
2,3-CPPA	2-(3-chlorophenoxy)propionic acid
2,4-CPPA	2-(4-chlorophenoxy)propionic acid
2,4-D	(2,4-dichlorophenoxy)acetic acid
2,4,5-T	(2,4,5-trichlorophenoxy)acetic acid
A	adenosine
$\alpha$	selectivity
$\alpha$ -CD	$\alpha$ -cyclodextrin
A>p	adenosine-2':3'-cyclic monophosphate
ACN	acetonitrile
AGP	$\alpha_1$ -acid glycoprotein
AHNS	4-amino-5-hydroxynaphthalene-2,7-disulfonic acid
ANDSA	7-aminonaphthalene-1,3-disulfonic acid
ANTS	8-aminonaphthalene-1,3,6-trisulfonic acid
ApC	adenylyl-(3'→5')-cytidine
ApG	adenylyl-(3'→5')-guanosine
APK	alkyl phenyl ketones
APTS	9-aminopyrene-1,4,6-trisulfonic acid
ApU	adenylyl-(3'→5')-uridine

$\beta$ -CD	$\beta$ -cyclodextrin
BF <sub>3</sub>	boron trifluoride etherate
Big CHAP	<i>N,N</i> -bis-(3-D-gluconamidopropyl)-cholamide
BNDA	1,1'-binaphthyl-2,2'-diamine
BNOH	1,1'-bi-2-naphthol
BNPO <sub>4</sub>	1,1'-binaphthyl-2,2'-diylhydrogen phosphate
BSA	bovine serum albumin
C	cytidine
CBHI	cellobiohydrolase I
CBQCA	3-(4-carboxybenzoyl)-2-quinolinecarboxyaldehyde
CD	cyclodextrin
CE	capillary electrophoresis
CF-LSIMS	continuous flow-liquid secondary ion mass spectrometry
CGE	capillary gel electrophoresis
CIEF	capillary isoelectric focusing
CITP	capillary isotachopheresis
CMC	critical micelle concentration
CTAB	cetyltrimethylammonium bromide
CZE	capillary zone electrophoresis
D	diffusion coefficient
$\delta$	thickness of the double layer
DAD	diode array detector
Deoxy Big CHAP	<i>N,N</i> -bis-(3-D-gluconamidopropyl)-deoxycholamide
$\Delta h$	difference in height between reservoirs
DHZ	5-dimethylaminonaphthalene-1-sulfonyl hydrazine
diepoxy PEG	polyethylene glycol diglycidyl ether

DM- $\beta$ -CD	heptakis-2,6-di-O-methyl- $\beta$ -cyclodextrin
DMF	N,N-dimethylformamide
DMSO	dimethylsulfoxide
DTAB	Dodecyltrimethylammonium bromide
$E$	electric field
$\epsilon$	dielectric constant
ED	electrochemical detection
EDAC	1-ethyl-3-(3-dimethylaminopropyl) carbodiimide
EOF	electroosmotic flow
$F_d$	drag force
$F_e$	electrical force
G	guanosine
$\gamma$ -CD	$\gamma$ -cyclodextrin
G>p	guanosine-2':3'-cyclic monophosphate
GC	gas chromatography
G <sub>D1a</sub>	disialoganglioside
G <sub>M1</sub>	monosialoganglioside
GpA	guanylyl-(3'→5')-adenosine
GpG	guanylyl-(3'→5')-guanosine
GpU	guanylyl-(3'→5')-uridine
G <sub>T1b</sub>	trisialoganglioside
$\eta$	viscosity
HP- $\beta$ -CD	hydroxypropyl- $\beta$ -cyclodextrin
HPC	hydroxypropyl cellulose
HPCE	high performance capillary electrophoresis
HSA	human serum albumin
$I$	current or ionic strength

I.D.	internal diameter
$\phi$	phase ratio
$K$	distribution coefficient
$\kappa$	Debye-Hückel constant
$k'$	capacity factor
KPFO	Potassium perfluorooctanoate
$L$	total length of capillary
$l$	effective length of the capillary column
LIF	laser-induced fluorescence
$\log \alpha$	methylene group selectivity
$\log \beta$	specific interaction between micellar and aqueous phases
LSIMS	liquid secondary ion mass spectrometry
$\mu_{\text{app}}$	apparent mobility
MECC	micellar electrokinetic capillary chromatography
MEGA 8	Octanoyl- <i>N</i> -methylglucamide
MEGA 9	nonanoyl- <i>N</i> -methylglucamide
MEGA 10	decanoyl- <i>N</i> -methylglucamide
$\mu_{\text{eo}}$	electroosmotic mobility
$\mu_{\text{ep}}$	electrophoretic mobility
$\mu_{\text{ep,eff}}$	effective electrophoretic mobility
$\mu_{\text{ep,mc}}$	electrophoretic mobility of micelle
MES	2-( <i>N</i> -morpholino)ethanesulfonic acid
MS	mass spectrometry
$N$	separation efficiency
$n$	peak capacity
NANA	<i>N</i> -acetylneuraminic acid
NaPFN	Sodium perfluorononanoate



$v_{app}$	apparent velocity
$n_c$	number of carbon atoms
$v_{eff}$	effective velocity
$v_{eo}$	electroosmotic velocity
$v_{ep}$	electrophoretic velocity
NG	nonyl- $\beta$ -D-glucopyranoside
$v_{mc}$	micelle velocity
$v_s$	solute velocity
O.D.	outer diameter
OG	octyl- $\beta$ -D-glucopyranoside
OM	octyl- $\beta$ -D-maltopyranoside
OVM	ovomucoid
PAA	phenylalkyl alcohols
PEG	polyethylene glycol
PEI	polyethyleneimine
pI	isoelectric point
PMP	1-phenyl-3-methyl-5-pyrazolone
PMPMP	1-(p-methoxy)phenyl-3-methyl-5-pyrazolone
PVA	polyvinyl alcohol
$q$	net charge
$R$	resistance
$r$	radius
$\rho$	surface charge density
$\rho_{mc}$	surface charge density of the micelle
RNA	ribonucleic acid
RNase T <sub>1</sub>	ribonuclease T <sub>1</sub>
RNase U <sub>2</sub>	ribonuclease U <sub>2</sub>

$R_s$	resolution
RSD	relative standard deviation
SA	sulfanilic acid
SC	Sodium cholate
SDC	Sodium deoxycholate
SDS	sodium dodecyl sulfate
$\sigma_L$	standard deviation of of a peak in length
STC	Sodium taurocholate
STDC	Sodium taurodeoxycholate
$t_M$	migration time
TM- $\beta$ -CD	heptakis-2,3,6-tri-O-methyl- $\beta$ -cyclodextrin
$t_{mc}$	migration time of micelle
$t_o$	migration time of bulk flow
$t_r$	retention time of solute in MECC
tRNA <sup>Phe</sup>	transfer ribonucleic acid specific for phenylalanine
TRSE	5-carboxytetramethylrhodamine succinimidyl ester
U	uridine
$\bar{v}$	partial specific volume of micelle
$V_{aq}$	volume of aqueous phase
$V_{mc}$	volume of micellar phase
$w_b$	width of peak at base
$w_h$	width of peak at half height
$w_i$	width of peak at inflection point
$\zeta$	zeta potential
$f$	translational friction coefficient

CHAPTER I  
INTRODUCTION AND SOME BASIC ASPECTS  
OF HIGH PERFORMANCE CAPILLARY  
ELECTROPHORESIS

Introduction

The practical importance of separation sciences stems from the fact that at least one separation process is almost inevitable in analytical or preparative studies of chemical or biological molecules. Among the various separation techniques that are available for the analyst, those based on differential migration processes (e.g., chromatography and electrophoresis) are the most widely used. In electrophoresis, separation is based on the differential migration of electrically charged particles or ions by attraction or repulsion in an electric field.

Capillary electrophoresis (CE), also known as high-performance capillary electrophoresis (HPCE), is a recent development of electrophoresis, combining the high resolving power of electrophoresis and the instrumentation and automation concepts of modern chromatography. The overall purpose of this combination is to miniaturize the instrumental set-up of traditional electrophoresis and extend the scope of applications of electrophoresis.

Regardless of the separation technique employed, there are two major transport processes that are occurring during any separation. First, the free-energy differences experienced by molecules in their physiochemical environment cause separative transport. The separation mechanism may be based on phase equilibria such as adsorption, extraction, and ion exchange, or on kinetic processes such as electrophoresis and dialysis. However,

for a separation to occur each individual solute must have unique transport properties regardless of the separation mechanism. The second process is the dispersive transport, or band broadening, and is the sum of various processes causing the dispersion of the zones about their center of gravity. Diffusion, convection, and restricted mass transfer are examples of dispersion processes. Therefore, unless dispersive transport is properly controlled, peaks can merge together even under conditions of excellent separative transport. In this regard, CE may be the finest example of optimizing both transport mechanisms to yield highly efficient separations. This may have partially contributed to the recent emerging of CE as a powerful analytical tool and complementary to other established techniques such as HPLC. Moreover, the prospects of high separation efficiencies, speed of analysis and high sensitivity have been the driving force for practical and fundamental research on CE by many analytical research laboratories.

This dissertation is concerned with furthering the development of CE by introducing and evaluating (i) novel separation media (e.g. novel micellar phases, chiral selectors), (ii) new capillary coating, (iii) selective precolumn derivatization schemes, and (iv) capillary enzyme microreactors for the separation and detection of a wide variety of biological, pharmaceutical and environmental solutes. These various interrelated topics are treated in two major parts. The first part is mainly concerned with concepts related to the analysis of biological molecules, and comprises six chapters (Chapters II-VII). The first chapter of this part (Chapter II) is an overview of CE of biomolecules. While Chapters III, IV and V introduce a novel and selective precolumn derivatization scheme for the CE separation and sensitive detection of acidic carbohydrates, Chapters VI and VII deal with the development of capillary column coating and immobilized enzyme microreactors for efficient CE analysis of oligosaccharides, proteins and ribonucleic acids. The second part of this dissertation (Chapters VIII-XIII) introduces novel separation media and reagents for the CE separation and detection of chiral and achiral environmental and pharmaceutical species. Chapter VIII provides an overview of the basic principles and practical aspects of

micellar electrokinetic capillary chromatography (MECC) and chiral capillary electrophoresis (CCE). The utility of MECC with *in-situ* charged micelles in acidic and neutral media is discussed in Chapter IX, while Chapter X introduces a novel chiral micellar system for enantiomeric separation by CCE. Chapters XI-XIII of this part focuses on the enantiomeric resolution of various optical isomers, including racemic mixtures of phenoxy acid herbicides, in the presence of cyclodextrins or chiral surfactants.

For clarity of presentations, besides providing general background information in chapter II of the first part and in chapter VIII of the second part of this dissertation, specific background information can be found in the introductory part of each chapter of this dissertation

The objective of this chapter is to (i) provide a historical background of CE, (ii) highlight its development, and (iii) review the fundamental concepts of CE separations, instrumentation, and modes of operation.

### Historical Background and Development

Capillary electrophoresis has a published history that can be traced back to as early as 1953 when Edstrom [1] used fine silk fibers of 15  $\mu\text{m}$  diameter and 1 to 2 cm in length for the determination of 100 pg of RNA contained within a single cell. The motivations of early scientists are similar to those of the current workers in the field. First, excellent heat transfer properties are attainable by the high surface-to-volume ratio of the capillary, thus allowing the use of high electric fields for fast and efficient separations. Second, CE provides high mass sensitivity which was recognized as valuable, particularly for the analysis of the components of single cells [2]. Nevertheless, CE has not been recognized as a powerful analytical technique until major advances in detection occurred during the 1980s, a period after which the technique had undergone an unprecedented exponential advancement. The reason behind such an advancement originates from a century of development in electrophoresis and instrumentation which provided the foundation for CE.

Before reaching its current advanced technological status, the CE techniques has evolved continuously during the last two decades. A direct predecessor of modern CE was first developed by Hjertén in 1967 [3]. The 3 mm i.d. columns used in this study were rotated to reduce the detrimental effects of convection caused by Joule heating. Although rotation did not affect heat dissipation, the rotation action caused a mixing to occur within the capillary, thus smoothing out the convective gradients. However, the advantages of using columns with smaller internal diameters were not realized until 1974 when Virtanen [4] used small diameter Pyrex glass columns (i.d. 200-500  $\mu\text{m}$ ). In this work, a potentiometric detection method for zone electrophoretic analysis of alkali cations was described. A few years later, Mikkers *et al.* [5] used a small diameter PTEF column (i.d. 200  $\mu\text{m}$ ) for the determination of inorganic and organic anions. The separation was attained in a short time (less than 10 min), and detection was performed using both ultraviolet (UV) and conductometric detection. Generally, these small diameter columns, or more commonly called capillaries, allowed a better heat dissipation and a more uniform thermal cross-section of the sample within the tube. Although all these early works showed improvement over what was achievable in traditional electrophoresis, they were hampered by low separation efficiency due to sample overloading originating from the poor detector sensitivity and large injection volumes.

These complicating issues were solved in 1981 when Jorgenson and Lukacs used 75  $\mu\text{m}$  capillaries and on-column fluorescence detection for the analysis of mixtures of dansyl and fluorescamine derivatives of amino acids, dipeptides and simple amines [6]. This work was a major advancement in CE in terms of separation efficiency and sensitivity, and undoubtedly marked the commencement of the HPCE era.

The 1980s and early 1990s witnessed important advancements in CE including the introduction of several separation modes. Isoelectric focusing [7] and gel electrophoresis [8] were successfully adapted to the capillary format. However, Cohen and Karger [9] were the first to demonstrate a highly efficient separations by capillary gel electrophoresis.

In 1984, a major breakthrough in CE was realized by the introduction of a new operation mode by Terabe *et al.* [10], the so-called micellar electrokinetic capillary chromatography (MECC). The MECC technique, which is based on the differential partitioning of the solutes into a charged micelle acting as a "pseudo-stationary" phase, permits the separation of small molecules, whether charged or neutral. As a result of the introduction of this technique as well as other electrokinetic capillary techniques, such as ligand exchange [11], ion exchange [12] and use of cyclodextrins [13], a wide variety of molecules, previously intractable by electrophoresis, could be analyzed by CE.

The issue of detection technology has remained fundamental to CE. Although CE instrumentation is simple, the development of rugged, simple and high-sensitivity detection technology remains a significant and important issue in CE. Walbroehl and Jorgenson [14] developed a fixed-wavelength on-column UV detector which alleviated the serious limitation of the short pathlength originated from the narrow i.d. capillaries. The detector developed had a "slit" width of only 100  $\mu\text{m}$ , thus providing a very good spatial resolution. The detector was linear over four orders of magnitude with detection limits as low as 15 pg for isoquinoline. Moreover, detectability was improved to the attomole level by utilizing laser-induced fluorescence (LIF) [15]. In 1988, Smith *et al.* [16] utilized electrospray to interface CE to mass spectrometry, while Wallingford and Ewing [2] developed a sensitive electrochemical detector, permitting the measurement of catecholamines in a single snail neuron. Other advancement in the area of detection was the utilization of indirect detection to measure solutes that neither absorb nor fluoresce [17]. Recently, special capillary designs are used to extend the optical pathway without increasing overall capillary area, thus improving detection without increasing the generated current and subsequent heating within the capillary. One of these designs is the bubble cell which offers a unique method to extend the pathway with nearly no degradation of separation efficiency (Chapter III). It is made by forming an expanded region, a bubble, directly within the capillary. This capillary is commercially available from Hewlett-Packard with a three times expansion. Up

to 15 times radial expansion has been demonstrated by glass-blowing [18]. However, due to several limitations including nonuniform flow and local Joule heating, the commercial version only offers a three fold improvement in detection sensitivity. Another design for increasing the path length in CE uses a Z-shaped capillary cell [19], with measurement along the long axis of the capillary. However, unlike the bubbled capillary, band broadening in the "Z" capillary is a significant problem, since the absorbance is integrated along the long axis of capillary. If a second band enters the long axis before the first band leaves, the peaks will overlap, thus degrading the separation efficiency.

Another major limitation of CE resided in the protein adherence to the capillary wall, a phenomenon that usually leads to poor separation efficiency and reproducibility, and most often irreversible adsorption of the solute. However, this problem was overcome by several developments including treated capillary walls [20-22] and conducting analysis at a pH values above the *pI* of the protein [23]. Although these methods diminished solute-wall interaction and allowed highly efficient separation of proteins by CE, the availability of hydrolytically stable and inert coating is still persisting. This dissertation addresses this problem by introducing a novel and stable capillary coating which is the subject of chapter VI.

Despite some shortcomings, the various original works on alleviating the detection and separation problems in CE have paved the way for the technique to emerge as a capable microseparation (or nanoseparation) technique for the analysis of neutral and ionic species of varying sizes. The analytical merits of CE have become evident by the national and international meetings dedicated to CE as well as by the availability of various commercial instruments since 1988.



## Basic Principles

### Electrophoretic Migration

When a current passes through an ionic solution, anions migrate toward the anode (positive electrode) and cations migrate toward the cathode (negative electrode) in equal quantity and electroneutrality of the solution is always maintained as a result of ionization of water. The conductivity of a solution is governed by the concentration and mobility of the ionic species in an electric field, while the mobility of ions is influenced by their charge-to-size ratio. The size of a molecule is determined by its molecular weight, its three dimensional structure and its hydration sphere. Therefore, the current generated by a running electrolyte is proportional to the ionic mobility of its cations and anions, and as a result, counterions must be appropriately chosen when preparing the running electrolyte to minimize the generated current.

In an electrical field, a charged species experiences an electrical force  $F_e$  which is equal to the product of its net charge  $q$  and the applied electric field strength  $E$ :

$$F_e = q \times E \quad (1)$$

and  $E$  is given by:

$$E = \frac{V}{L} \quad (2)$$

where  $L$  is the total length of the capillary and  $V$  is the applied voltage. The  $F_e$  force, which is positive for cations and negative for anions, drives the former toward the cathode and the latter toward the anode. Although the electrical force acting on a charged species is supposed to accelerate it, the species are not only affected by this force alone. A drag force opposite to the electrical force is experienced by the species as a result of their movement through the background buffer. This drag force  $F_d$  is directly proportional to the species electrophoretic velocity  $v$ , and is given by:

$$F_d = -f \times v \quad (3)$$

where  $f$  is the translational frictional coefficient and for small spherical ions can be expressed by Stokes' Law:

$$f = 6\pi\eta r \quad (4)$$

where  $\eta$  is the viscosity of the buffer through which the species are migrating and  $r$  is the radius of the species. The frictional drag is directly proportional to viscosity, size and electrophoretic velocity. Therefore, a charged species in an electric field will migrate at a limiting velocity dependent on the inherent charge and radius of the species as well as on the strength of the applied field and the viscosity of the buffer solution. This limiting velocity, also known as drift velocity, steady-state velocity or electrophoretic velocity ( $v_{ep}$ ), is attained when the electrical and drag forces balance each other. Thus, by equating equations (1) and (3) the mathematical expression of  $v_{ep}$  is given by:

$$v_{ep} = \frac{qE}{f} \quad (5)$$

Since the electrophoretic mobility,  $\mu_{ep}$ , is defined as the electrophoretic velocity of the solute per unit field strength, a combination of equation (4) and (5) will give the following mathematical expression for electrophoretic mobility:

$$\mu_{ep} = \frac{v_{ep}}{E} = \frac{q}{6\pi\eta r} \quad (6)$$

From this equation it is evident that small, highly charged species have high mobilities whereas large, minimally charged species have low mobilities. The magnitude of  $\mu_{ep}$  depends on the net charge  $q$  of a molecule and its frictional properties (size and shape, i.e.,  $r$ ). Note that the electrophoretic mobility usually listed in standard tables is a physical constant determined at the point of full solute ionization and extrapolated to infinite dilution. This is usually different from the experimentally determined value which is called effective

electrophoretic mobility and is highly dependent on pH and the composition of the running electrolyte.

### Electroosmotic Flow

In aqueous separation media, fused-silica surfaces, which are the materials of CE capillaries, possess an excess of negative charges mainly due to the ionization of the silanol group (SiOH) to the anionic form (SiO<sup>-</sup>). As a result of this, anionic species in the running electrolyte are repelled from the surface whereas counterions are attracted to the capillary wall. This attraction and repulsion will result in a spatial distribution of the ions, thus forming an electrical double-layer at the silica-solution interface and creating a potential gradient. The resulting ionic distribution is shown in Fig. 1a. Ions closest to the wall are tightly bound and immobile, forming what is known as the compact layer. Further from the wall is a diffuse and mobile region, while at a great distance from the wall the bulk solution is neutral. As a result of this spatial distribution of ions within the electrical double-layer, an electric potential gradient originates according to Stern-Gouy-Chapman theory [24] and is illustrated in Fig. 1b. The zeta potential  $\zeta$ , which is illustrated in Fig. 1b, is generally described as the potential at the plane of shear occurring when the liquid is forced to move by an external force (electrical field in the case of CE).

When a voltage is applied across the capillary length, the cations forming the diffuse double-layer are attracted toward the cathode. Since they are, solvated their movement drags the bulk solution in the capillary toward the cathode. This is a fundamental constituent of HPCE operation and is known as electroosmotic flow (EOF). Although the double-layer is perhaps 100 Å thick, EOF is transmitted throughout the diameter of the capillary, supposedly through hydrogen bonding of water molecules or other interaction forces between buffer constituents. The magnitude of EOF can be expressed in terms of velocity or mobility by [25]:

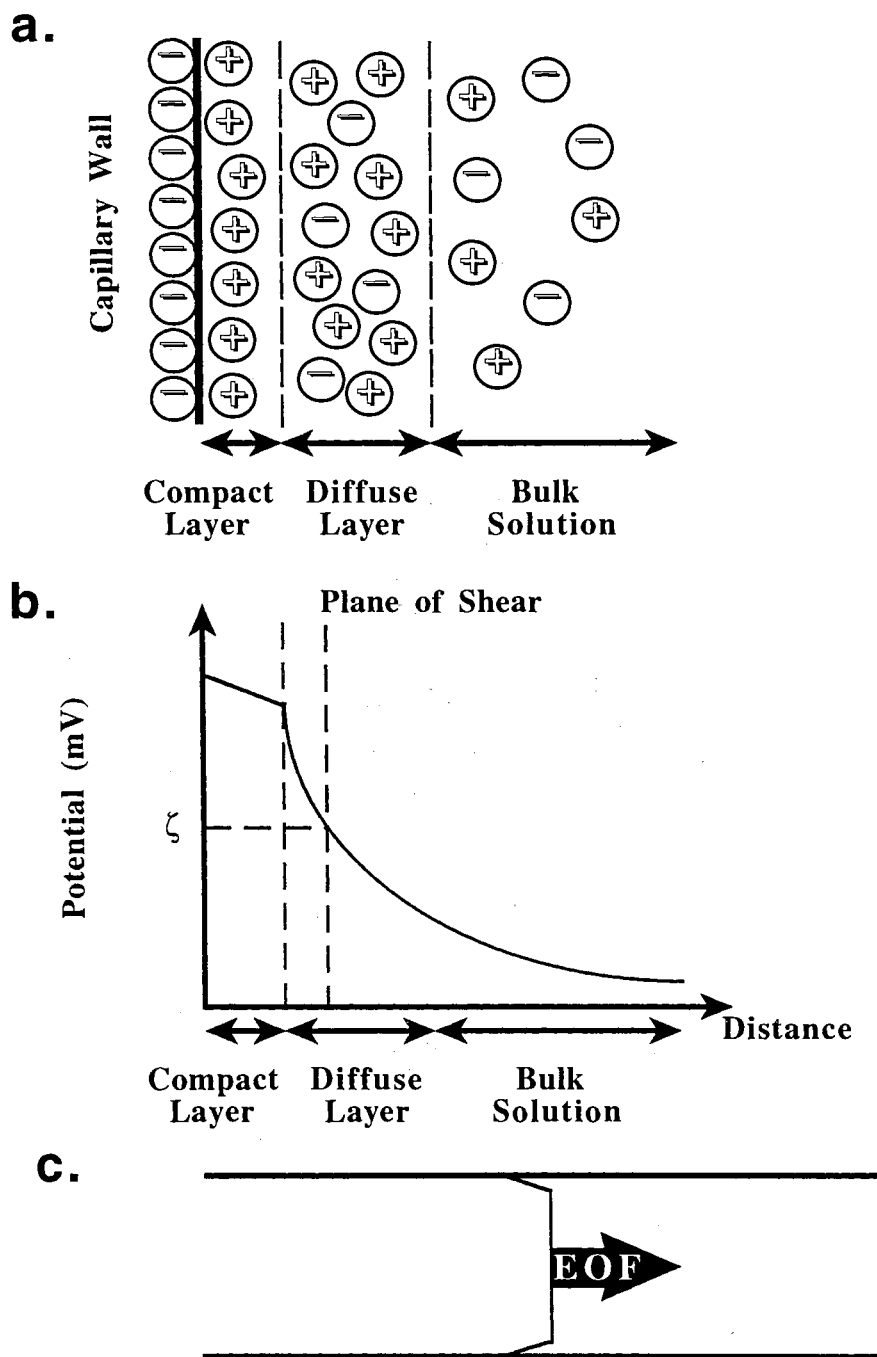


**Figure 1.** Schematic illustrations of (a) the electric double-layer at the surface of the fused-silica capillary, (b) the electrical double-layer potential gradient and (c) the flat flow profile of the electroosmotic flow (EOF).

$$v_{eo} = \mu_{eo}E = \frac{\epsilon\zeta}{4\pi\eta}E \quad (7)$$

where  $\mu_{eo}$  is the electroosmotic mobility. The zeta potential  $\zeta$  is governed by the surface charge on the capillary wall. Because this charge is strongly pH dependent, the magnitude of EOF varies with pH. At high pH, where the silanol groups are ionized, EOF is significantly greater than at low pH where silanol groups are less ionized. The zeta potential is also inversely proportional to the square root of the ionic strength of the electrolyte as described by the double-layer theory. Increasing the ionic strength compresses the double layer, decreases the zeta potential and reduces the EOF.

A unique feature of EOF is its flat flow profile (see Fig. 1c). This flat flow profile enhances separation efficiencies, since it does not directly contribute to the dispersion of the solute zones. This is in contrast to the flow generated by an external pump which yields a laminar or parabolic flow due to the shear force at the wall. Another benefit of EOF is that it causes movement of nearly all species, regardless of charge, in the same direction. Under normal operating conditions (i.e., cathodal flow), anions will be swept toward the cathode since the magnitude of the flow can be more than one order of magnitude greater than their electrophoretic mobilities. Therefore, cations, neutral species and anions can be electrophoresed in a single run. In this regard, cations migrate fastest since both their effective electrophoretic mobilities and EOF are in the same direction (Fig. 2a and b). Neutral species will co-migrate with the EOF, whereas anions will migrate last since their effective electrophoretic mobilities and EOF are in opposite direction. While EOF is usually beneficial, it often needs to be controlled. For example, at high pH the EOF may be too rapid, resulting in co-migration of solutes without separation. In addition, electrophoretic separation modes such as isoelectric focusing, isotachopheresis and capillary gel electrophoresis often require reduction or elimination of the EOF. The elimination or control of EOF will be further discussed in Chapter II.

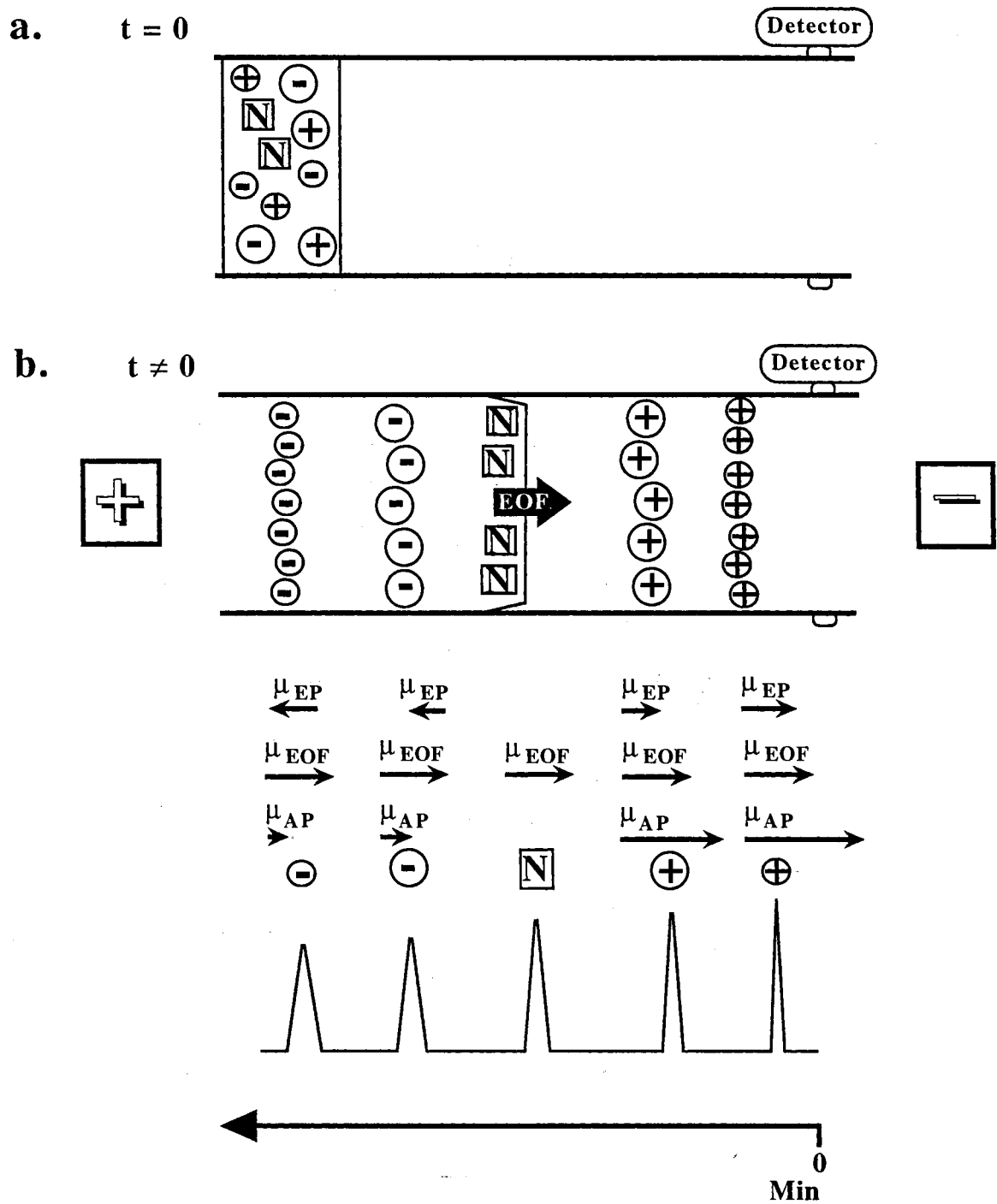


**Figure 2.** Schematic illustrations of ideal CZE separation before (a) and after (b) applying an electric field, and a hypothetical electropherogram.

## Analytical Parameters

Migration Time and Apparent Mobility

For separation in CE to occur, each solute must have a unique apparent mobility ( $\mu_{app}$ ) which is given by:

$$\mu_{app} = \mu_{ep} + \mu_{eo} \quad (8)$$

where  $\mu_{eo}$  is the electroosmotic mobility. Similarly the apparent velocity ( $v_{app}$ ) is given by:

$$v_{app} = v_{ep} + v_{eo} = (\mu_{ep} + \mu_{eo})E = (\mu_{ep} + \mu_{eo})\frac{V}{L} \quad (9)$$

where  $V$  is the applied voltage,  $E$  is the applied electric field and  $L$  is the total length of the capillary. The migration time,  $t_M$ , is the time required for a solute to migrate to the detection point, and is given by :

$$t_M = \frac{l}{v_{app}} = \frac{lL}{(\mu_{ep} + \mu_{eo})V} \quad (10)$$

where  $l$  is the length from the inlet of the capillary to the detection point. These two different lengths of the capillary are illustrated schematically in Fig. 4. The electroosmotic mobility,  $\mu_{eo}$ , which affects all solutes to the same extent can be calculated directly from the electropherogram by:

$$\mu_{eo} = \frac{v_{eo}}{E} = \frac{lL}{t_o V} \quad (11)$$

where  $t_o$  is the migration time of a neutral species such as dimethyl sulfoxide, acetone or mesityl oxide. The electrophoretic mobility,  $\mu_{ep}$ , is given by:

$$\mu_{ep} = \mu_{app} - \mu_{eo} = \frac{v_{ep}}{E} = \frac{lL}{(t_M - t_o)V} \quad (12)$$

where  $\mu_{app}$  is calculated using the observed migration time of the solute:

$$\mu_{\text{app}} = \frac{IL}{t_M V} \quad (13)$$

The  $\mu_{\text{ep}}$  can be either positive or negative depending on the charge of the solute and the polarity of the applied electric field.

### Separation Efficiency

Separation in CE results from the migration of the analytes in discrete zones, the length of which is strongly dependent on the dispersive processes that act on it. The efficiency, expressed in number of theoretical plates,  $N$ , is given by:

$$N = \left( \frac{l}{\sigma_L} \right)^2 \quad (14)$$

where  $\sigma_L$  is the standard deviation of the peak in unit of length. Under ideal separation conditions (that is small injection plug length, no solute-wall interaction, etc.) longitudinal diffusion (along the capillary) can be considered to be the only contributor to solute-zone broadening. Therefore, the efficiency can be related to the molecular diffusion term, which is given according to Einstein's law by:

$$\sigma_L^2 = 2Dt_M = \frac{2DlL}{\mu_{\text{ep}}V} \quad (15)$$

where  $D$  is the diffusion coefficient of the solute. By substituting equation (15) in equation (14), efficiency  $N$  is then given by:

$$N = \frac{\mu_{\text{ep}}^2 V l}{2DL} = \frac{\mu_{\text{ep}}^2 E l}{2D} \quad (16)$$

$N$  can be calculated directly from the electropherogram by using the same mathematical equation used in liquid chromatography [26]:

$$N = 4 \left( \frac{t_M}{w_i} \right)^2 = 5.54 \left( \frac{t_M}{w_h} \right)^2 = 16 \left( \frac{t_M}{w_b} \right)^2 \quad (17)$$



where  $w_i$ ,  $w_h$  and  $w_b$  are the peak widths for a Gaussian peak at the inflection point, half-height and base, respectively.

### Resolution and Selectivity

The selectivity factor,  $\alpha$ , and resolution,  $R_s$ , for two adjacent zones are given by [6, 27]:

$$\alpha = \frac{\Delta\mu_{ep}}{\bar{\mu}} = \frac{\Delta\mu_{ep}}{\bar{\mu}_{ep} + \mu_{eo}} \quad (18)$$

and

$$R_s = \frac{1}{4} \sqrt{N} \frac{\Delta\mu_{ep}}{\bar{\mu}} = \frac{1}{4\sqrt{2}} \Delta\mu_{ep} \sqrt{\frac{Vl}{DL(\bar{\mu}_{ep} - \mu_{eo})}} \quad (19)$$

respectively. When  $l = L$  equation (19) can be simplified to:

$$R_s = \frac{1}{4\sqrt{2}} \Delta\mu_{ep} \sqrt{\frac{V}{D(\bar{\mu}_{ep} - \mu_{eo})}} \quad (20)$$

In equations (18-20),  $\Delta\mu_{ep}$  is the difference in the electrophoretic mobilities of two adjacent zones,  $\bar{\mu}_{ep}$  is the average electrophoretic mobilities of two adjacent zones and  $\bar{\mu}$  is the average apparent mobilities of two adjacent zones. While separation efficiency increases linearly with voltage (see eq. 16), resolution increases with the square root of voltage. However, increasing both efficiency and resolution by increasing the voltage is limited by the Joule heat generated at high voltage. Resolution approaches infinity when the average electrophoretic mobility becomes equal, but opposite in sign, to the electroosmotic mobility (i.e.,  $\bar{\mu}_{ep} = \mu_{eo}$ ). However, analysis time will also approach infinity under these conditions.

### Factors Affecting the Efficiency of Separation in CZE

The separation efficiency described by equation 16 does not take into account other factors affecting band broadening. Therefore, the calculated separation efficiency using equation 17, which reflects all band broadening processes (through  $w$  of peak) that can occur simultaneously during solute migration, is usually less than the theoretical value estimated by the simplified equation 16. This is due to the fact that in addition to longitudinal diffusion, other contributors to zone broadening are usually present including temperature gradient induced by Joule heating, injection plug length and others so that the total variance,  $\sigma_T^2$ , of the observed peak is given by the sum of the contributing variances:

$$\sigma_T^2 = \sigma_D^2 + \sigma_{\Delta T}^2 + \sigma_i^2 + \sigma_{\Delta ke}^2 + \sigma_w^2 \quad (21)$$

molecular diffusion	+	Joule heating	+	injection volume	+	conductivity differences	+	solute-wall interaction
------------------------	---	------------------	---	---------------------	---	-----------------------------	---	----------------------------

A list of the important contributors to solute-zone broadening is depicted in Table I. Efficient separation in CE is achieved by controlling all of these dispersion processes. Among all the aforementioned sources of zone broadening sample adsorption, or solute-wall interaction, is the most significant for CZE of macromolecules (e.g., proteins).

### Modes of Operation

Capillary electrophoresis is a versatile technique partially because of its numerous modes of operation. The separation mechanisms of each mode are different, thus offering orthogonal and complementary information. The basic methods embraced by CE are (i) capillary zone electrophoresis (CZE), (ii) micellar electrokinetic capillary chromatography (MECC), (iii) capillary gel electrophoresis (CGE), (iv) capillary isoelectric focusing (CIEF), and (v) capillary isotachopheresis (CITP). The separation mechanisms of each mode are illustrated in Fig. 3 and the bases of separation are outlined in Table I. The same basic instrumental set-up is used for performing any of these modes.

TABLE I. Sources of Zone Broadening in CE.

Source of zone broadening	Comments
Longitudinal diffusion	<ul style="list-style-type: none"> <li>• Defines the fundamental limit of efficiency</li> <li>• Solutes with lower diffusion coefficients form narrower zones</li> </ul>
Joule heating	<ul style="list-style-type: none"> <li>• Leads to temperature gradient and laminar flow</li> </ul>
Injection plug length	<ul style="list-style-type: none"> <li>• Injection length should be less than the diffusion controlled zone lengths</li> <li>• Dilute samples often necessitate longer than ideal injection length</li> </ul>
Sample adsorption	<ul style="list-style-type: none"> <li>• Interaction of solutes with capillary walls cause severe peak tailing</li> </ul>
Mismatched conductivities of sample and buffer (electrodispersion)	<ul style="list-style-type: none"> <li>• Solutes with higher conductivities than the running buffer result in fronted peaks</li> <li>• Solutes with lower conductivities than the running buffer result in tailed peaks</li> </ul>
Unleveled buffer reservoirs	<ul style="list-style-type: none"> <li>• Generates laminar flow</li> </ul>
Detector cell size	<ul style="list-style-type: none"> <li>• Should be small relative to peak width</li> </ul>

CZE is the most widely used mode of CE because of its simplicity and versatility. This simplicity is because the capillary is only filled with buffer for performing the separation. As shown in Figs 2 and 3a, separation occurs as a result of solutes migration in distinct zones and at different velocities. Separation of both anionic and cationic species is possible because of the EOF (Fig. 2). Neutral solutes do not migrate on their own, but co-migrate with the EOF. CZE is not the only mode of CE in which "zonal"

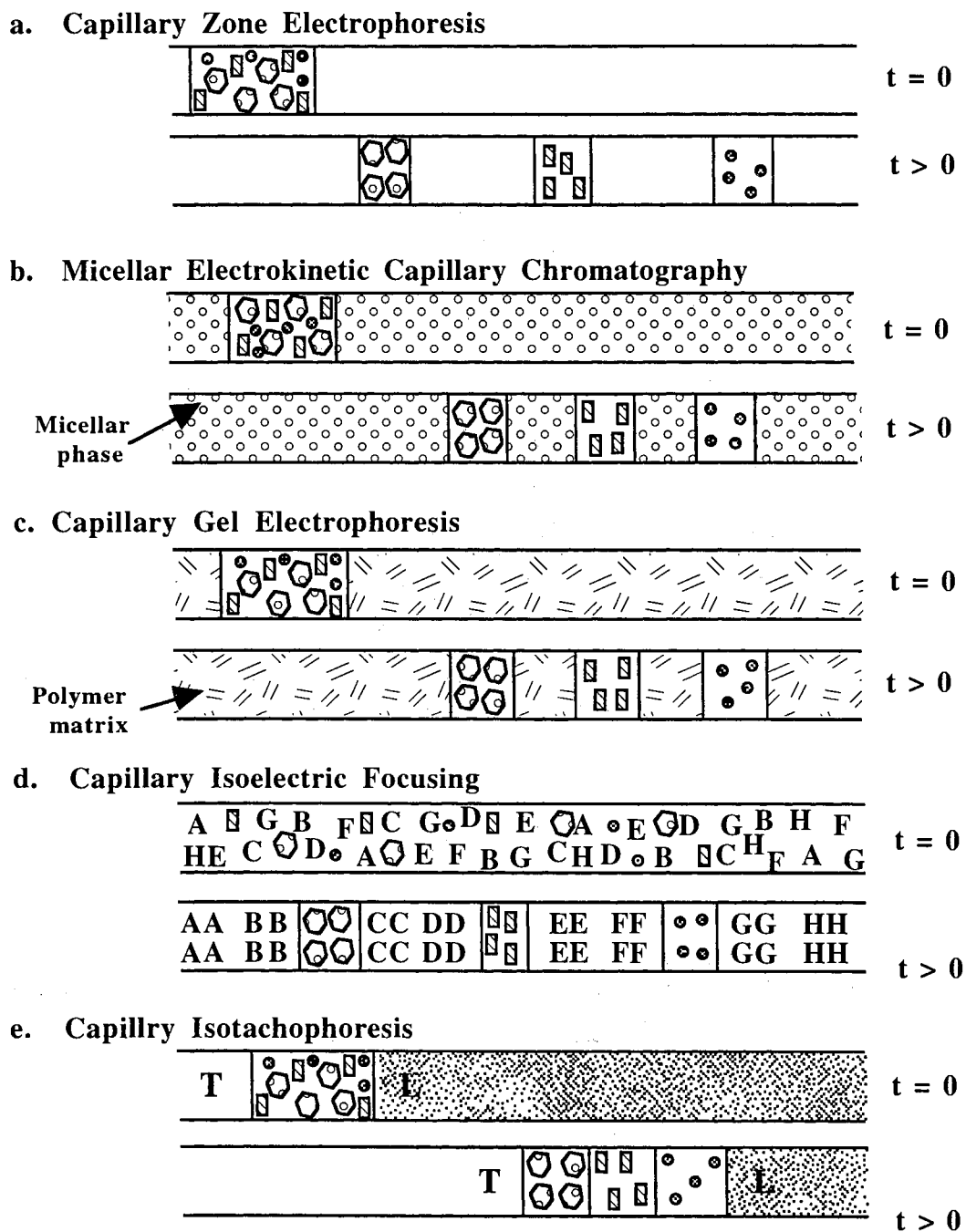
electrophoresis occurs. Other modes such as MECC and CGE are also zonal techniques; therefore, it is more appropriate to name CZE open-tube or free-solution electrophoresis.

TABLE II. Modes of HPCE and their Basis of Separation.

<b>Mode</b>	<b>Basis of separation</b>
Capillary zone electrophoresis (CZE)	Free solution mobility
Micellar electrokinetic capillary chromatography (MECC)	Hydrophobic/ionic interactions with micelles
Capillary gel electrophoresis (CGE)	Size and charge
Capillary isoelectric focusing (CIEF)	Isoelectric point
Capillary isotachopheresis (CITP)	Moving boundaries

As mentioned above, MECC, which was introduced by Terabe in 1984, is a hybrid of electrophoresis and chromatography. This mode will be discussed more extensively in Chapter VIII. The running electrolyte in MECC contains a surfactant at concentration above its critical micelle concentration, thus forming micelles. The separation in this mode is based on the differential partitioning of the analytes in the micellar "pseudo-stationary" phase, where hydrophobic analytes interact more strongly with the micelle than less hydrophobic ones (Fig. 3b). The surfactants and thus the micelles are usually charged and have an electrophoretic mobility. As a result, neutral solutes interacting with the micelles will acquire an effective electrophoretic mobility that is a function of their affinity for the micellar phase.

CGE has been most commonly employed for the size-based separation of macromolecules such as proteins and nucleic acids. The size separation is obtained by electrophoresis of the solutes through the capillary filled with cross-linked polyacrylamide gel or with a soluble polymer. The main separation mechanism in CGE is based on the differences in solute size as charged solutes migrate through the pores of the polymer



**Figure 3.** Mode of operation of CE. A, B, C, D, E, F, G and H, designate the ampholytes; T, terminating electrolyte; L, leading electrolyte.

network (Fig. 3c). The usefulness of the gels originates from the fact that they permit separation based on "molecular sieve". Furthermore, they are anti-convective media that (i) minimize solute diffusion and consequently band broadening, (ii) prevent solute adsorption to the capillary walls and (iii) eliminate EOF. Therefore, CGE separations with up to 30 million theoretical plates per meter have been reported [9]. However, for the gel to be a suitable electrophoretic media, it must have certain properties such as temperature stability and appropriate range of pore size. One drawback of this technique is that neutral solutes would not migrate through the gel, since EOF is suppressed in this mode of operation.

In CIEF, a pH gradient is formed within the capillary using ampholytes which are molecules that contain both acidic and basic moieties with pI values that cover the desired pH range of the CIEF experiment. The capillary is filled with a mixture of solutes and ampholytes, with a basic solution at the cathode and an acidic solution at the anode and upon application of the electric field a pH gradient is generated. The charged ampholytes and solutes migrate through the medium until they reach a pH region where their net charge equals zero (at their pI); this process is known as focusing. The overall separation process is depicted in Fig. 3d. Once the focusing process is completed, a steady-state is reached and the current drops to zero. Next the solutes and ampholytes are mobilized and the zones are passed in front of the detector. Mobilization can be achieved by application of pressure to the inlet of the capillary or by addition of salt to one of the reservoirs.

Another mode of operation is CITP, a moving boundary electrophoretic technique, where a combination of two buffer systems is used to create a state in which the separated zones all move at the same velocity. The zones remain sandwiched between the so-called leading (contains ions with higher mobility than the solutes) and terminating (contains ions with lower mobility than the solutes) electrolytes (Fig. 3e). In a single CITP experiment, either cations or anions can be separated.

## General Instrumentation and Capillary

A unique feature of CE is its remarkably simple instrumentation set-up. The basic instrumentation set-up of an in-house assembled HPCE instrument is illustrated in Fig. 4, and it consists of five major parts. A capillary is required for the separation, a high voltage power supply is needed to drive the separation, a detector (typically UV or fluorescence) is usually installed on-column to detect the migrating solute zones, and a plexiglass safety box equipped with a safety interlock enclosure is used to protect the operator from the high voltage. A microsyringe whose needle is connected to the capillary by a Teflon tube of an inner diameter that matches the outer diameter of the capillary is used for rinsing and refilling the capillary. Other additional features that are commonly found in commercial instruments include a temperature control system, an automated capillary flushing system to enhance system reproducibility, an automated injection system, an autosampler, and a computerized data acquisition system. Although the separation efficiency is not improved by actively cooling the capillary [28, 29], constant temperature is very important to achieve a reproducible migration time of the analyte and to adjust the selectivity.

While both glass and Teflon capillaries were used earlier [5, 6], today fused-silica capillary is almost exclusively used in CE. The capillary usually has a protective thin outer coating of polyimide which provides great strength and flexibility. A full and cross-sectional view of a fused-silica capillary is illustrated in Fig. 4. The capillary is prepared from the same high-purity silicon dioxide that is used for optical fibers. Capillary as thin as 2  $\mu\text{m}$  i.d. is commercially available; however, most workers use a 10-100  $\mu\text{m}$  i.d. A small section of the polyimide coating is removed from the capillary to provide an optical window for absorbance or fluorescence measurements. The coating can be removed with a gentle flame from a butane lighter, yet this often makes the capillary walls quite brittle. Electric heating removes the coating without damaging the capillary wall. However, heating will damage any coating on the interior wall of the capillary. Therefore, the outer coating of the capillary in this case is removed by using a concentrated sulfuric acid bath at 100 °C.

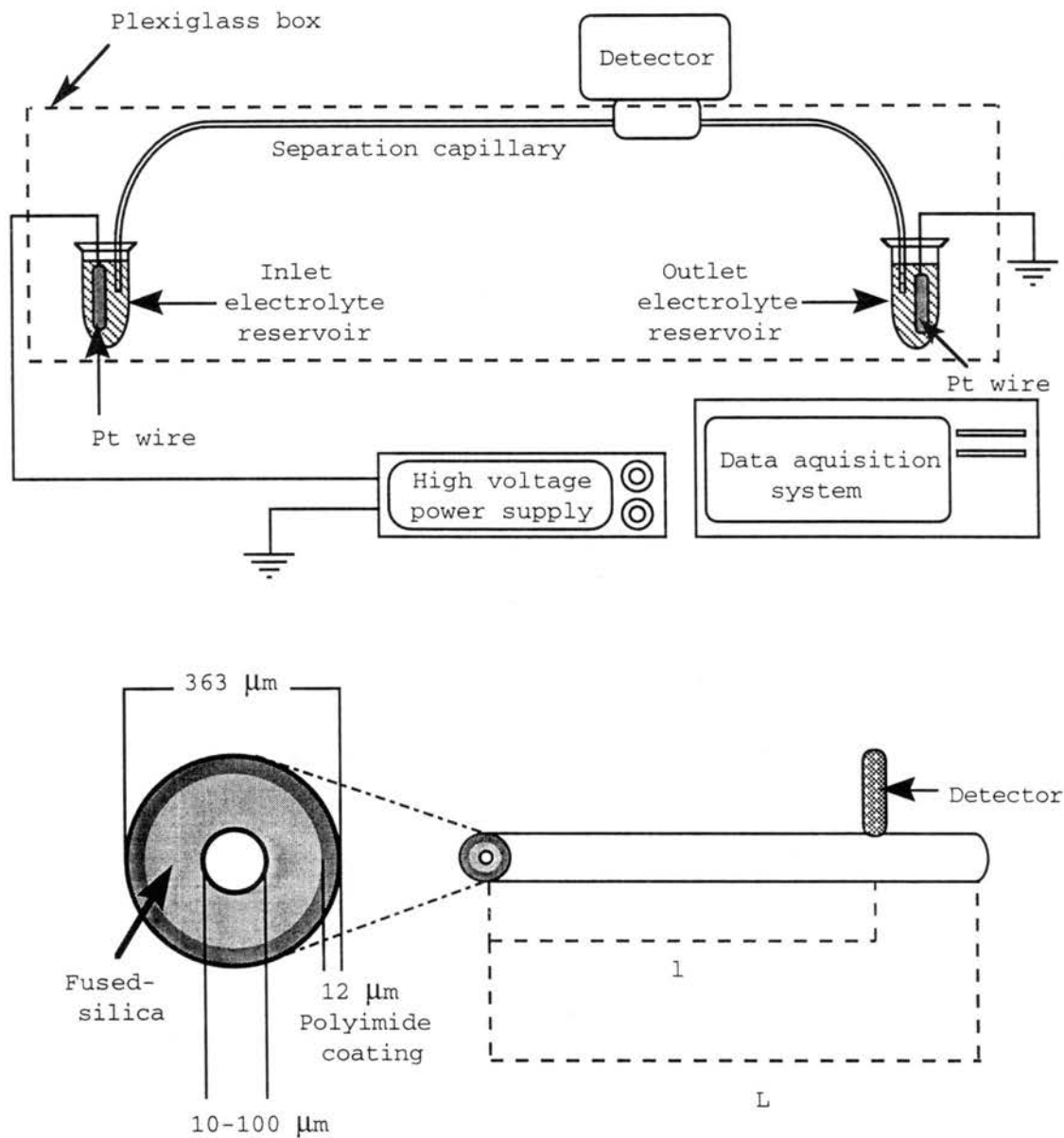


**Figure 4.** Instrumental set-up of an in-house assembled capillary electrophoresis instrument and full and cross-sectional view of the capillary.  $L$  is the total length of the capillary and  $l$  is the length of the capillary to the detection point.



## Sample Injection

Capillary electrophoresis is inherently a microseparation technique, and the capillaries typically used have a total volume ranging from a few nanoliters to few microliters depending on the length and the i.d. of the capillary. For example, the volume of a 50 cm long, 50  $\mu\text{m}$  i.d. capillary is about 1  $\mu\text{l}$ . Since only a small fraction of the capillary can contain sample to avoid excessive band broadening, only a minute amount of sample can be loaded onto the capillary. Quantitative sample injection in CE can be accomplished most commonly by hydrodynamic or electrokinetic methods (Fig. 5). Hydrodynamic sample injection is the most widely used approach. It can be achieved by application of (i) a pressure at the injection end of the capillary (Fig. 5a), (ii) a vacuum at the outlet end of the capillary (Fig. 5b), or by (iii) siphoning action (or gravity) attained by elevating the inlet reservoir relative to the outlet (Fig. 5c). While commercial instruments utilize either of the first two methods, the in-house assembled instruments employ the last method for sample injection. With hydrodynamic injection, the quantity of sample loaded is a function of the capillary dimensions, viscosity of the buffer in the capillary, the pressure difference across the capillary and the injection time. Electrokinetic (or electromigration injection) is achieved by replacing the electrolyte reservoir at the injection-end with the sample vial and applying a certain voltage (Fig. 5d). Usually, a field strength 3 to 5 times lower than that used for the electrophoretic separation is applied. In this way, analytes enter the capillary as a result of the action of both their migration and the pumping action of EOF. Quantity loaded is dependent on the electrophoretic mobility of the individual analytes. Therefore, more mobile ions are loaded to a greater extent than those less mobile. In addition, the quantity injected is dependent on the ionic strength of the sample matrix. Variation in conductivity, originating from the presence of large quantity of undetected ions such as sodium or chloride, results in differences in voltage drop and quantity loaded. As a result of these phenomena, electrokinetic injection is less reproducible than its hydrodynamic counterpart. Despite the aforementioned quantitative

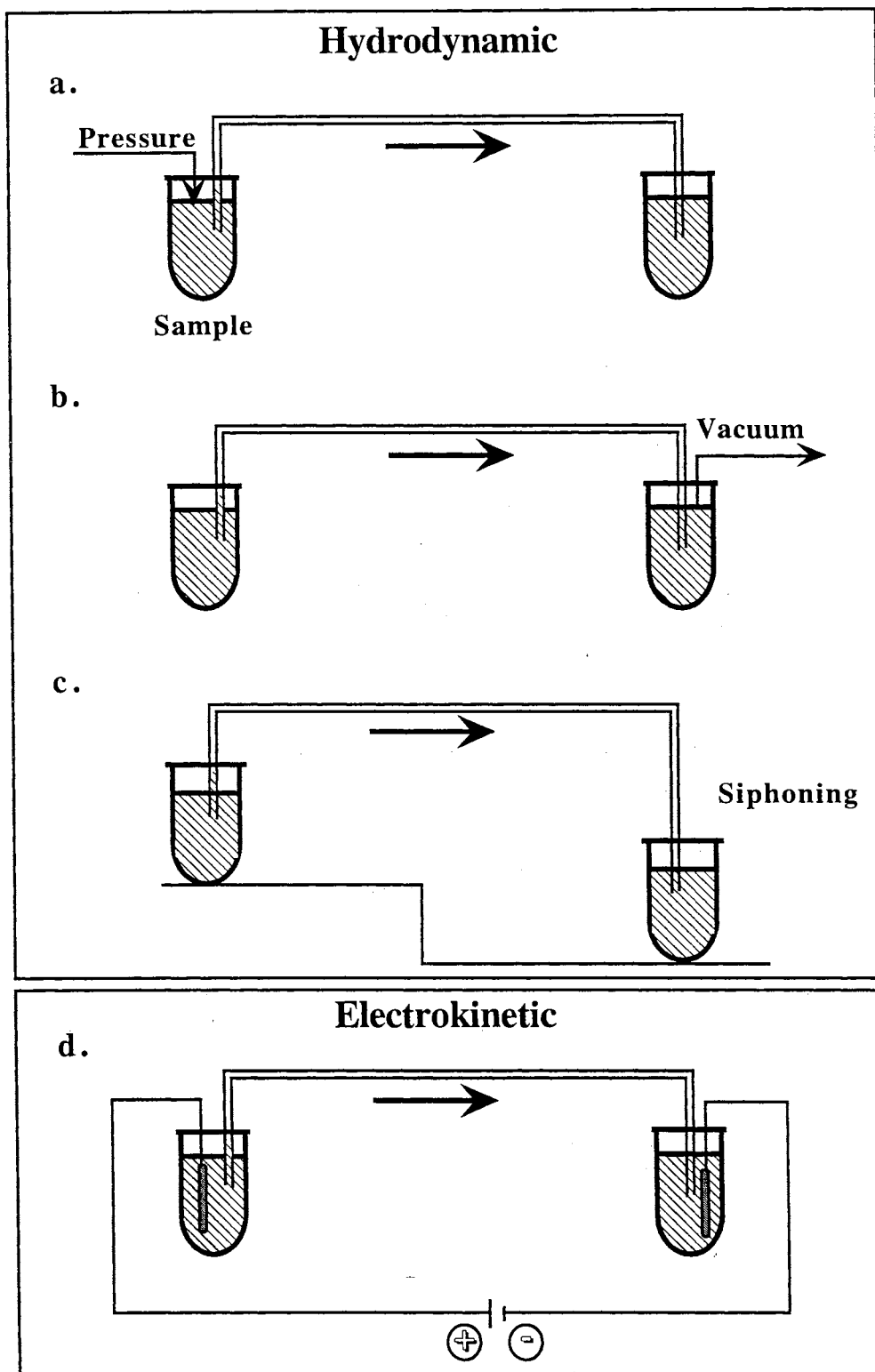


Figure 5. Modes of sample injection in CE.

limitations, electrokinetic injection is advantageous when viscous media or gels are employed in the capillary and when hydrodynamic injection is ineffective. In addition, electrokinetic injection can be used for concentrating the sample on column during or very shortly after sample injection. This is based on the conductivity differences between the sample and the running buffer, and is called "stacking". Under these conditions, a proportionally greater field will develop across the sample zone causing the ions to migrate faster upon application of the voltage. This remains true until they reach the running electrolyte boundary where they slow down and "stack" into a narrow zone. It should be noted that quantification with "sample stacking" can be difficult if the sample composition is not accurately known. In addition, under typical stacking conditions most of the voltage drop occurs in the stacking zone. The corresponding power generated can raise the temperature in the sample zone to almost 100°C. This can be of particular concern for thermally labile samples.

#### Detection in CE

Detection in HPCE has always been a significant challenge due to the small dimensions of the capillary. Although CE is performed on a nanoliter volumes of samples, it is not a trace analysis technique since concentrated analyte solutions or preconcentration methods are often necessary. A number of detection methods have been used in CE to surmount this challenge, many of which are similar to those employed in liquid column chromatography. However, UV detection is by far the most common. Table II lists many of the detection methods investigated, along with advantages/disadvantages. The research that will be described in this dissertation has utilized the first three methods of detection listed in table II.

TABLE III. Methods of Detection in HPCE [30].

Method	Advantages/disadvantages
UV-Vis absorption	<ul style="list-style-type: none"> <li>• Universal</li> </ul>
Fluorescence	<ul style="list-style-type: none"> <li>• Diode array offers spectral information</li> </ul>
Laser-induced fluorescence	<ul style="list-style-type: none"> <li>• Sensitive</li> </ul>
Amperometry	<ul style="list-style-type: none"> <li>• Usually requires sample derivatization</li> </ul>
Conductivity	<ul style="list-style-type: none"> <li>• Extremely sensitive</li> </ul>
Mass spectrometry	<ul style="list-style-type: none"> <li>• Usually requires sample derivatization</li> </ul>
Indirect UV, Fluorescence, amperometry	<ul style="list-style-type: none"> <li>• Expensive</li> </ul>
UV-Vis absorption	<ul style="list-style-type: none"> <li>• Sensitive</li> </ul>
Fluorescence	<ul style="list-style-type: none"> <li>• Selective but useful only for electroactive analytes</li> </ul>
Laser-induced fluorescence	<ul style="list-style-type: none"> <li>• Requires special electronics and capillary modification</li> </ul>
Amperometry	<ul style="list-style-type: none"> <li>• Universal</li> </ul>
Conductivity	<ul style="list-style-type: none"> <li>• Requires special electronics and capillary modification</li> </ul>
Mass spectrometry	<ul style="list-style-type: none"> <li>• Sensitive and offer structural information</li> </ul>
Indirect UV, Fluorescence, amperometry	<ul style="list-style-type: none"> <li>• Interface between MS and CE is complicated</li> </ul>
UV-Vis absorption	<ul style="list-style-type: none"> <li>• Universal</li> </ul>
Fluorescence	<ul style="list-style-type: none"> <li>• lower sensitivity than direct methods</li> </ul>

### Conclusions

In summary, this chapter provided an overview of the historical background and development of CE. It also discussed the basic principles, analytical parameters and the different modes of operation of CE. This chapter also described the instrumentation set-up, modes of injection and detection systems used in CE.

## References

1. Edstrom, J.E., *Nature*, 172 (1953) 908.
2. Wallingford, R.A. and Ewing, A.G., *Anal. Chem.*, 60 (1988) 258.
3. Hjertén, S., *Chromatogr. Rev.*, 9 (1967) 122.
4. Virtinen, R., *Acta. Polytech. Scand.*, 123 (1974) 1.
5. Mikkers, F.E.P., Everaerts, F.M. and Verheggen, T.P.E.M., *J. Chromatogr.*, 270 (1979) 11.
6. Jorgenson, J. and Lukacs, K.D., *Anal. Chem.*, 53 (1981) 1298.
7. Hjertén, S. and Zhu, M.-D., *J. Chromatogr.*, 346 (1985) 265.
8. Hjertén, S., *J. Chromatogr.*, 270 (1983) 1.
9. Cohen, A.S. and Karger, B.L., *J. Chromatogr.*, 397 (1987) 409.
10. Terabe, S., Otsuka, K., Ichikama, K., Tsuchiya, A. and Ando, T., *Anal. Chem.*, 56 (1984) 111.
11. Gozel, P., Gossman, E., Michelsen, H. and Zare, R.N., *Anal. Chem.*, 59 (1987) 44.
12. Terabe, S. and Isemura, T., *Anal. Chem.*, 62 (1990) 650.
13. Terabe, S., Ozaki, H., Otsuka, K. and Ando, T., *J. Chromatogr.*, 332 (1985) 211.
14. Walbroehl, Y. and Jorgenson, J.W., *J. Chromatogr.*, 315 (1984) 135.
15. Gassman, E., Kuo, J.E. and Zare, R.N., *Science*, 230 (1985) 813.
16. Smith, R.D., Olivares, J.A. and Nguyen, N.T., *Anal. Chem.*, 60 (1988) 436.
17. Kuhr, W.G. and Yeung, E.S., *Anal. Chem.*, 60 (1988) 1832.
18. Xue, Y. and Yeung, E.S., *Anal. Chem.*, 66 (1994) 144.
19. Bruin, G.J.M., Stegeman, G., Van Asten, A.C., Xu, X., Kraak, J.C. and Poppe, H., *J. Chromatogr.*, 559 (1991) 163.
20. Hjertén, S., *J. Chromatogr.*, 347 (1985) 191.
21. Nashabeh, W. and El Rassi, Z., *J. Chromatogr.*, 559 (1991) 367.
22. Smith, J.T. and El Rassi, Z., *High Resol. Chromatogr.*, 15 (1992) 573.

23. Lauer, H. and McManigill, D., *Anal. Chem.*, 58 (1986) 166.
24. Hunter, R.J., *Zeta Potential in Colloid Science*, London, Academic Press, 1981, Chapter 3.
25. Rice, C.L. and Whitehead, R., *J. Phys. Chem.*, 69 (1965) 4017.
26. Karger, B.L., Snyder, L.R. and Horváth, C., *An Introduction to Separation Science*, New York, John Wiley & Sons Inc., 1973.
27. Jorgenson, J. and Lukacs, K.D., *Science*, 222 (1983) 266.
28. Gobie, W.A. and Ivory, C.F., *J. Chromatogr.*, 516 (1990) 191.
29. Knox, J.H., *Chromatographia*, 26 (1989) 329.
30. Ewing, A.G., Wallingford, R.A. and Olefirowicz, T.M., *Anal. Chem.*, 61 (1989) 292.

PART I

## CHAPTER II

### CAPILLARY ZONE ELECTROPHORESIS OF BIOMOLECULES

#### Introduction

Capillary zone electrophoresis (CZE) is the most widely used mode of CE due to its simplicity and wide range of applications. As explained in Chapter I, separation by CZE occurs due to the differential migration of solutes in discrete zones, and the EOF facilitates the separation of both anionic and cationic solutes in a single run. In addition, separations by CZE are performed in a homogeneous carrier electrolyte. Many of the applications of CZE have been in the bioscience areas for the separation of peptides, proteins and more recently carbohydrates and glycoconjugates.

For attaining good separations by CZE the following criteria must be met: (i) the mobility of the solute of interest must differ from the mobility of other solutes in the sample, (ii) the background electrolyte must be homogenous with a uniform field strength distribution throughout the length of the capillary, (iii) the solutes or sample matrix elements must not interact or bind to the capillary wall and (iv) the buffer conductivity must significantly exceed the total conductivity of the sample components. While CZE separation of many biomolecules can be achieved in a bare fused-silica capillary, the separation of proteins can not be performed in such capillaries due to the presence of solute-wall interaction. Therefore, analysis of proteins by CZE can be only performed either in coated capillaries or highly alkaline running electrolytes where the proteins have the same net charge as that of the capillary wall, a condition that reduce protein adsorption.



Although carbohydrates do not exhibit solute-wall interaction, the difficulty associated with their CE analysis, generally, originates from the absence of an inherent charge and/or a detection center in their structures, both are necessary for detection and CE separation. While the absence of a detection center hinders the sensitive detection of carbohydrates by modern analytical separation techniques (including CE), the absence of a charge does not allow their direct differential migration and ultimately separation by CE. However, these obstacles were surmounted through various approaches which have exploited many of the inherent properties of carbohydrates. The polyhydroxy nature of carbohydrates allowed their charging either (i) by *in situ* conversion into charged species *via* complex formation with ions such as borate and metal cations or (ii) by the ionization of the hydroxyl groups at alkaline pH. While the presence of several functional groups in the carbohydrate structures (such as carbonyl and amino groups) permits their labeling with UV absorbing or fluorescent tags for their sensitive detection, other detection systems have also been utilized for the sensitive determination of carbohydrates including indirect UV and fluorescence detection as well as electrochemical detection.

This chapter will provide a survey of the methods developed for the CE analysis of carbohydrates, glycolipids (gangliosides) and proteins. First, an overview of the various approaches developed for the labeling of carbohydrate and of the CE analysis of gangliosides are provided. Second, a discussion of the various capillary column coating approaches that have been developed to improve the selectivity and efficiency of biomolecules separation is included. Finally, the objectives and rationales of our studies in part I are listed.

### Detection of Carbohydrates in CE

As stated above, most carbohydrates lack chromophores in their structures, a condition that hinders their detection at low concentrations. Therefore, several detection strategies have been developed to surmount this difficulty, including indirect UV and

fluorescence detection [1-6], electrochemical detection [7-13], dynamic labeling *via* complexation with absorbing or fluorescing ions or transition metals [14-17], and precolumn derivatization with a suitable chromophore and/or fluorophore.

Although the principle of indirect UV (or fluorescence) detection appears relatively simple and is significantly more sensitive than direct low wavelength UV of underivatized carbohydrates [18], it suffers from several limitations. First, the instability of the detection system which results in drift or disturbances of the baseline. Second, an indirect detection system requires working at a low concentration of background electrolyte in order to have efficient transfer ratios, a condition that results in lower separation efficiencies at higher sample concentration and the possibility of solute-wall interactions. A third disadvantage imposed by indirect detection in CE is the limitation in the selection of the composition and pH of the background electrolyte. In other words, there is not much room to manipulate selectivity and optimize separations. In fact, "neutral" carbohydrates are only partially ionized at the optimum pH normally used in indirect detection, i.e., pH~12, a condition that does not favor high resolution separation. Finally, another disadvantage is the limited linear dynamic range which is typically under two orders of magnitude. Therefore, the application of this mode of detection has been limited to fairly concentrated samples or whenever the analytes are not easily derivatized or cannot be detected otherwise.

Electrochemical techniques have been proven to be useful for the detection of underivatized carbohydrates. Moreover, electrochemical detection (ED) is an ideal mode of detection for microcolumn-based separation systems. This is because ED is based on an electrochemical reaction at the surface of the working electrode and is independent of cell volumes or path length. This is contrary to optical detectors whose response is dependent on path length. However, ED suffers from (i) the limitations imposed by the alkaline conditions needed for sensitive detection and differential electromigration which restricts the useful pH to a very narrow range, i.e., pH >12, and (ii) the non discriminative nature of amperometric detection which is known to yield a response not only for carbohydrates

but also for other analytes including amino acids, peptides, organic acids simple alcohols and aliphatic amines [19], a condition that may render peak assignment difficult and may lead to less accurate quantitative measurements.

As mentioned above, dynamic labeling of carbohydrates entails the formation of a complex between the carbohydrate molecules and the chromophore or fluorophore ions or a transition metal; such complexes allow the detection of carbohydrates at high wavelengths or by fluorescence. However, not all carbohydrates can complex with a fluorophore or chromophore; consequently, this strategy is only limited to few carbohydrate molecules that have the ability to form such complexes (e.g., cyclodextrin [14, 15], glycosaminoglycans with carboxylic groups [17], amylopectin and amylose [16]).

Based on the above discussion, it is apparent that the various mode of detection used for underivatized carbohydrates suffer from some limitations. Consequently, precolumn derivatization with a suitable chromophore or fluorophore constitutes an elegant approach to selective, sensitive and reproducible determination of carbohydrates. These detection strategies used in CE of carbohydrates have been extensively discussed recently by El Rassi and Mechref [20]. Nevertheless, only precolumn derivatization will be discussed in details in this chapter, since it pertains to the scope of this dissertation and constitutes the main focus of Chapters III-V.

### Precolumn Derivatization of Carbohydrates

Carbohydrates are generally tagged with a suitable chromophore or fluorophore to allow their detection at low levels. Since the tagging process brings about dramatic changes in the structure of the carbohydrate analytes, the selection of a suitable tag is crucial to the subsequent CE determination of the analytes. This is due to the fact that derivatization does not only allow the sensitive detection but also impart the derivatized solutes with different structural properties. In this regard, it is preferred that the tag also supplies the charge necessary for electrophoresis over a relatively wide range of pH or that

the tag imparts a hydrophobic character to the derivatives which allows the MECC separation of derivatized carbohydrates. Other essential criteria for a successful precolumn derivatization include (i) high yields, (ii) the formation of a single product for each species, (iii) the absence of detectable side products, (iv) a minimum sample work-out and clean-up and (v) no cleavage of an essential sugar residue, e.g., sialic acid residue.

In precolumn derivatization reactions, it is generally preferred that the tagging occurs at only one reactive functional group of the analyte and is complete so that a single derivative is obtained in high yields. The polyhydroxy nature of sugars is attractive as far as the attachment of a tag to the molecule is concerned. This route to derivatization has been used extensively in gas-liquid chromatography [21] in order to increase the volatility of carbohydrates and consequently facilitate their separation. However, derivatizing the hydroxyl groups would lead to multiple tagging of an analyte, and because the hydroxyl groups may vary in their relative reactivities, a distribution of derivatives would be obtained rather than a single product. In order to prevent multiple derivatization, other functional groups on the sugar molecule must be considered. The most popular sites for tagging include: (i) the carbonyl group in reducing sugars and (ii) the amino group in amino sugars. An additional tagging site is the carboxylic moiety in acidic sugars which has not been previously explored. To produce a single product in a given precolumn derivatization, the tag must possess only one reactive site for attachment to the analyte. For UV detection, the tagging agent should exhibit a high molar absorptivity at a given wavelength with minimal interferences from the running electrolyte to ensure highly sensitive detection of the derivatized carbohydrates. Likewise, in fluorescence a tagging agent should exhibit a high quantum efficiencies at a given excitation wavelength. These requirements become more crucial when dealing with extremely small sample volumes encountered in nano-scale separation techniques such as CE.

## Derivatization Schemes

Thus far, five different precolumn derivatization schemes have been introduced for the tagging of carbohydrates. These are illustrated in Figs 1-5.

First, the reductive amination is the most widely used tagging process [22, 23] and is illustrated in Fig. 1. So far, this precolumn derivatization has been the method of choice for the labeling of reducing saccharides. This has been facilitated by the availability of a large number of chromophores with amino functional groups [20]. Briefly, reductive amination of sugars involves the ring opening of the pyranose or furanose sugar to form the aldehyde or ketone, followed by a nucleophilic addition of the amino group of the labeling reagent to form a Schiff base (imine). Finally, reduction of this Schiff base by sodium cyanoborohydride results in the formation of a stable adduct as illustrated in Fig. 1. The yield of derivatization of carbohydrates by reductive amination as performed in solutions containing acetic acid was shown to depend on the acetic acid concentration [22, 24, 25]. This has prompted the investigation of the effect of the acid concentration as well as the  $pK_a$  of the acid used in the reductive amination of carbohydrates [26]. The organic acids were acetic, succinic, glycolic, L-malic, citric, malonic and maleic acid, with  $pK_a$ 's in the range of 1.91 to 4.75. Generally, the efficiency of the acid catalyst increased with increasing acid strength. Consequently, derivatization of carbohydrates in the presence of organic acids of higher strength than acetic acid caused a higher yield, an effect that is more pronounced for *N*-acetylamino sugars. This might be caused by the steric hindrance caused by the *N*-acetylamino group thus affecting the ring opening or the Schiff base formation. Optimum yield was attained using citric acid as the catalyst and conversion of a few nanomoles of neutral saccharides to the 9-aminopyrene-1,4,6-trisulfonic acid derivatives is achieved at 75°C in less than 60 min. Despite all these features, reductive amination suffers from two drawbacks. First, sialic acid residues at the non-reducing ends of the oligosaccharides derived from glycoproteins are labile in a strong acid at high concentration, conditions needed to perform reductive amination. Second, the need for

heating the reaction mixture is also not favorable when labeling sialic acid containing carbohydrates and will result in the cleavage of the sialic acid residue.

The following discussion overviews some of the most important tags used in the labeling of carbohydrates by reductive amination and provides a brief description of the detectability of the sugar derivatives obtained by this labeling procedure. Typically, reductively aminated sugar derivatives of 2-aminopyridine (2-AP) are usually detected in the UV at 240 nm at the 10 pmol level [22]. Also, these derivatives can be detected by fluorescence. 6-Aminoquinoline (6-AQ) is a useful tag for the detection and separation of carbohydrates by CE [27]. The 6-AQ derivatives showed a maximum absorbance at 270 nm, and the signal obtained was 8 times higher compared to that obtained with 2-AP derivatives under otherwise identical conditions [27]. The removal of excess 2-AP and 6-AQ is not required in CE since the derivatized carbohydrates migrate behind the excess tag, while in the case of acidic sugars, the derivatives and the derivatizing agent move in opposite directions [28]. Linhardt and co-workers [29] described the derivatization of *N*-acetylchitooligosaccharides with a negatively charged tag, 7-aminonaphthalene-1,3-disulfonic acid (ANDSA) *via* reductive amination. The ANDSA-derivatives were excited at 250 nm using an arc-lamp and the fluorescence was collected at 420 nm with detection limits in the femtomole range. UV detection was also described for sugar derivatives of ANDSA [29]. ANDSA has a fairly strong absorbance at 247 nm ( $\epsilon=3100 \text{ M}^{-1} \text{ cm}^{-1}$ ), but more importantly it supplies the charge necessary for rapid electrophoretic analysis of sugars in CE. Chiesa and Horváth [30] utilized a similar tag, 8-aminonaphthalene-1,3,6-trisulfonic acid (ANTS), for the derivatization and separation of maltooligosaccharides by CE which was first demonstrated in the derivatization of sugars separated in polyacrylamide slab gel electrophoresis [31]. ANTS not only supplies a strong chromophore, but also provides multiple negative charges even at low pH, which allows the rapid electrophoretic analysis. Using ANTS-derivatized glucose, as little as 15 femtomoles could be detected at 214 nm [30]. Using CE-LIF with a He-Cd laser at 325

nm, the limits of detection lies in the low attomole range, three orders of magnitude lower than in UV detection. Other aminonaphthalene sulfonic acid-based tags were introduced for the derivatization of carbohydrates by reductive amination [32] including the fluorescent tags 5-aminonaphthalene-2-sulfonic acid and 4-amino-5-hydroxynaphthalene-2,7-disulfonic acid. A very recent and interesting development in fluorescent labeling of carbohydrates has been the introduction of 9-aminopyrene-1,4,6-trisulfonic acid (APTS). [26, 33-35] for the HPCE-LIF of mono- and oligosaccharides. APTS derivatization of mono- and oligosaccharides did not only provide a detection center for the sugars with a substantially higher quantum efficiency than most of the commonly used fluorophore sugar derivatives, but also introduced three negatively charged groups which seem to ensure the separation of closely related structures [33, 35].

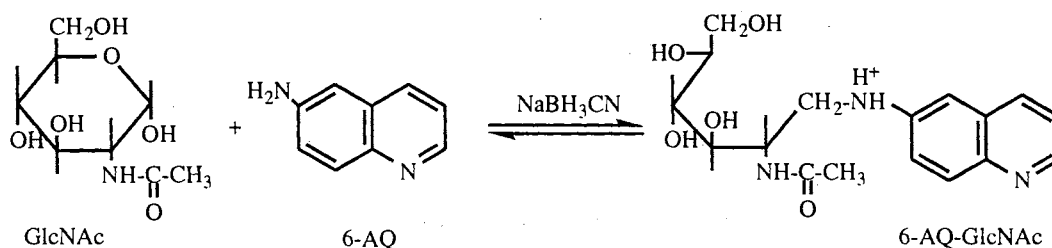


**Figure 1.** Schematic illustration of reductive amination where the reducing sugar is N-acetylglucosamine (GlcNAc) and the tag is 6-aminoquinoline (6-AQ) [27].

The second derivatization scheme is the base-catalyzed condensation between the carbonyl group of reducing carbohydrates and the active hydrogens of 1-phenyl-3-methyl-5-pyrazolone (PMP) or 1-(p-methoxy)phenyl-3-methyl-5-pyrazolone (PMPMP), forming bis-PMP and bis-PMPMP derivatives, respectively [36-39]. This derivatization procedure is illustrated in Fig. 2. PMP and PMPMP yield neutral sugar derivatives in acidic media, which become negatively charged in aqueous basic solutions due to the partial dissociation of the enolic hydroxyl group of the tags. Therefore, the weakly ionized derivatives do not separate well, and borate-based electrolytes [36, 38, 39] and/or micellar phases such as

sodium dodecyl sulfate (SDS) [40] are required to bring about differential electromigration and ultimately separation.

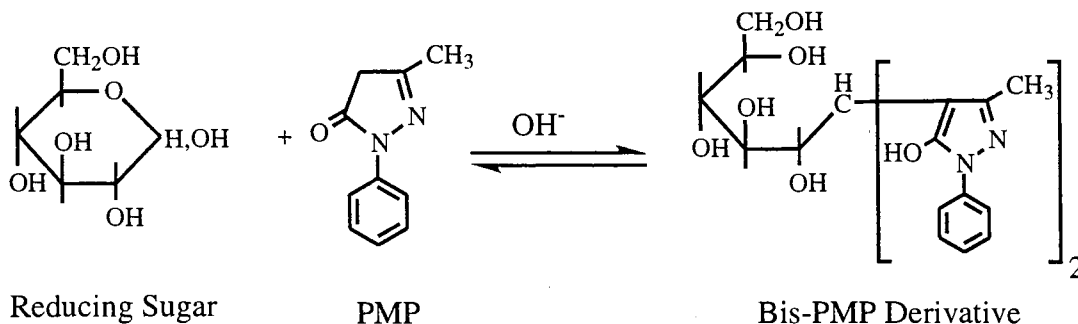


**Figure 2.** Schematic illustration of condensation reaction with PMP [39].

The third derivatization scheme involves the reductive amination of reducing carbohydrates with amines to yield 1-amino-1-deoxyalditols followed by reaction with 3-(4-carboxybenzoyl)-2-quinolinecarboxyaldehyde (CBQCA) in the presence of potassium cyanide (Fig. 3) [41, 42]. This labeling procedure, which was first introduced by Novotny and co-workers [41, 43-45], allows the detection of submicromolar concentration of CBQCA-sugar derivatives by LIF. CBQCA-sugar derivatives have an excitation maximum at 456 nm, which conveniently matches the 442 nm line of a He-Cd laser, and an emission maximum near 552 nm. Using CBQCA, attomole levels of amino sugars have been analyzed by LIF-CE [46]. One of the virtue of CBQCA derivatization is that the excess derivatizing agent does not have to be removed since the fluorogenic CBQCA does not interfere with the analysis. However, CBQCA is not available commercially.

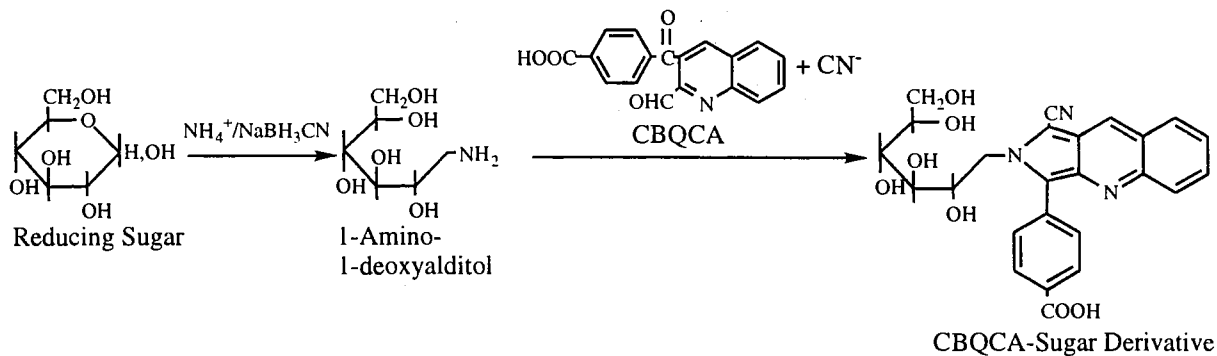


**Figure 3.** Schematic illustration of derivatization with CBQCA [42].



A fourth precolumn derivatization scheme also involves initially the reductive amination of reducing carbohydrates with amines to yield 1-amino-1-deoxyalditols followed by reaction with 5-carboxytetramethylrhodamine succinimidyl ester (TRSE) [47], (Fig. IV). This derivatization scheme was utilized recently in the derivatization of the six most abundant hexoses (i.e., glucose, galactose, mannose, fucose, glucosamine, galactosamine) found in mammalian with TRSE [47]. The detection limit of these derivatives was 100 molecules utilizing a post-column LIF detection in a sheath flow cuvette [47]. Although TRSE is a useful fluorescent label for aminated sugar monomers, the labeling reaction requires high sugar concentration to overcome the competition between the labeling reaction and the hydrolysis of the dye, thus rendering the analysis of some real sugar samples not feasible. In fact, the dye yielded two hydrolysis products as was reported by the authors [47].

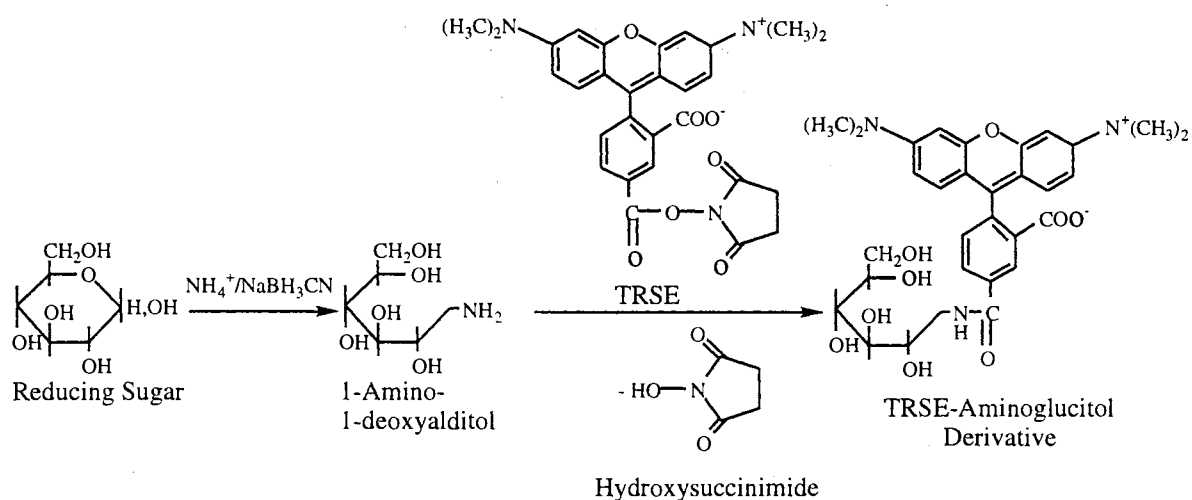


**Figure 4.** Schematic illustrations of derivatization with TRSE [47].

Lastly, condensation between the amine functional group in 5-dimethylaminonaphthalene-1-sulfonyl hydrazine (dansylhydrazine) with the aldehyde or ketone form of the sugar to form a stable imine or hydrazone product is illustrated in Fig. 5. Although this derivatization procedure was utilized recently (1996) to derivatize mono- and disaccharides directly with the fluorescent dansylhydrazine (DHZ) which reacts

specifically with aldehydes and ketones, it was originally performed by Avigad [48] in 1977 for use in thin layer chromatography. Similar procedures were also utilized in the analysis of carbohydrates [49, 50] and glycoproteins [51] by HPLC. The reaction was reported to be completed in only 15 min and allowed derivatization of sugars in the picomole range when performed in an organic medium or in a medium at high ratio in an organic solvent. The sugar-DHZ derivatives fluoresced at 530 nm when excited with a He-Cd laser at 325 nm. Under these conditions, the limit of detection of the derivatized mono- and disaccharides was 100 attomoles. This method was utilized for the determination of glucose in small volumes of biological samples such as tear fluid. However, this derivatization procedure produces several byproducts, which may interfere with the identification of the analyte peak.

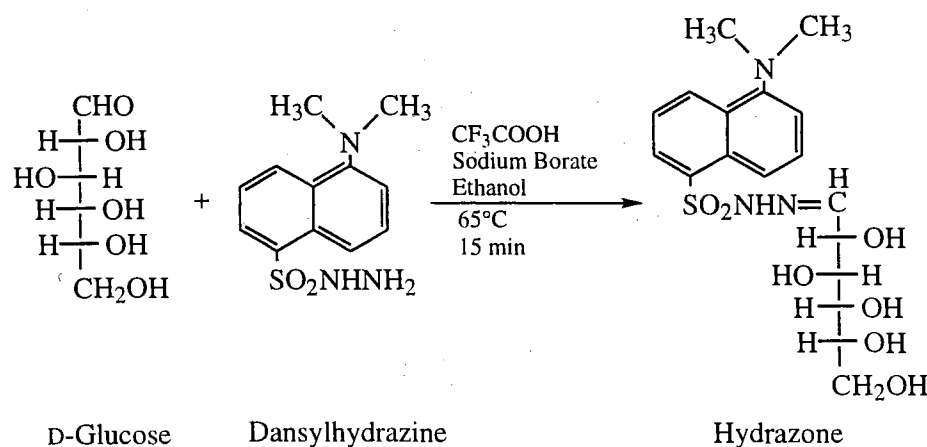


**Figure 5.** Schematic illustration of condensation reaction with dansylhydrazine [52].

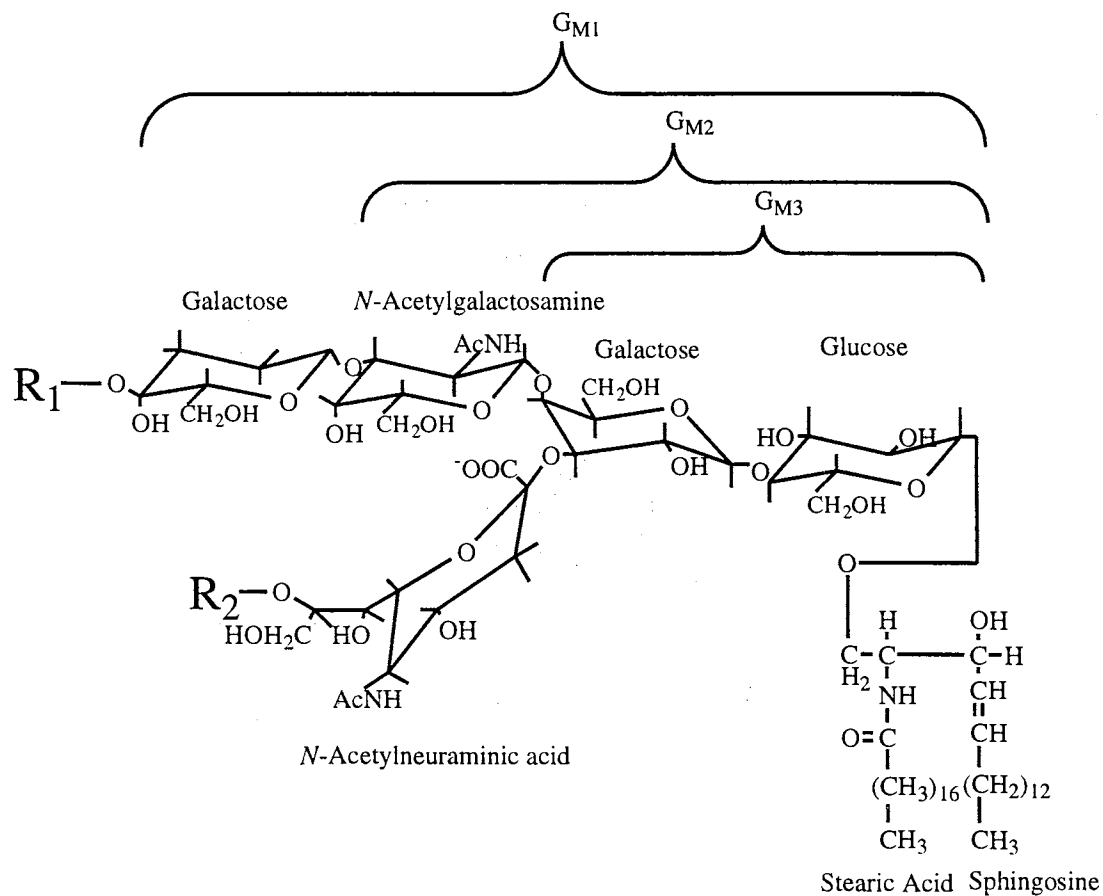
As can be seen from the above overview of the different labeling procedures developed so far, the utility of the carboxylic groups of acidic carbohydrate as a labeling site has not been yet exploited. Therefore, part of this dissertation research has focused on the development of a selective derivatization scheme utilizing the carboxylic group of acidic carbohydrates. This derivatization is developed to be performed at room temperatures and in slightly acidic media (pH 5.0), thus preventing the cleavage of sialic acid residues from carbohydrates. Chapters III-V discuss and evaluate this procedure, and its applications to

various carboxylated carbohydrates, e.g., acidic monosaccharides, sialooligosaccharides and gangliosides (sialoglycolipids)

### CE Analysis of Gangliosides

Since Chapter IV of this dissertation is concerned with the CE analysis of gangliosides, a brief survey of the previous work on CE of gangliosides is in order here.

A ganglioside molecule (for structure see Fig. 6) has a hydrophilic sialooligosaccharide chain and a hydrophobic moiety, i.e., ceramide, that consists of a sphingosine and fatty acid. Due to this inherent structural feature, the gangliosides are amphiphilic solutes forming stable micelles in aqueous solutions with very low critical micellar concentration values ( $10^{-8}$ - $10^{-10}$  M) [53]. Furthermore, gangliosides most often exist at low concentrations and their structures lack strong chromophores. Thus, two major obstacles must be overcome when developing a CE method for the analysis of gangliosides: the ability (i) to separate them as monomers and (ii) to detect them at low levels. Thus far, CE separation of gangliosides as monomers has been addressed recently by Yoo *et al.* [54]. On the other hand, Liu and Chan [45] applied CE to the study of the behavior of gangliosides in aqueous solutions. These researchers demonstrated that CZE can separate some ganglioside micelles, and consequently permitted the studies of the micellar properties of these amphiphilic species using untreated fused-silica capillaries and on-column direct UV detection at 195 nm. The ganglioside micelles were successfully analyzed within 10 min with mass sensitivity in the order of  $10^{-11}$  mol. Baseline resolution of a mixture of three ganglioside micelles, namely,  $G_{M1}$ ,  $G_{D1b}$  and  $G_{T1b}$ , was achieved using 2.5 mM potassium phosphate, pH 7.40, as the running electrolyte. The separation was mainly facilitated by the varying content of the sialic acid residues in the ganglioside micelles, which imparted them with different electrophoretic mobilities. The observed



- $G_{M1}$ ,  $R_1 = R_2 = H$   
 $G_{M2}$ ,  $R_2 = H$   
 $G_{M3}$ ,  $R_2 = H$   
 $G_{D1a}$ ,  $R_1 = N\text{-Acetylneuraminic acid (NeuNAc)}$ ,  $R_2 = H$   
 $G_{D1b}$ ,  $R_1 = H$ ,  $R_2 = \text{NeuNAc}$   
 $G_{D3} = G_{M3}$ ,  $R_2 = \text{NeuNAc}$   
 $G_{T1b}$ ,  $R_1 = R_2 = \text{NeuNAc}$

**Figure 6.** Structures of the gangliosides.

migration velocities of the ganglioside micelles seem to be largely unaffected in the pH range 7.0-11.0, and decreased monotonically when the pH was varied from 6.0 to 4.0. This is because of the diminishing dissociation of the carboxyl group of the sialic acid residues as the pH was decreased [45]. Increasing the ionic strength of the running electrolyte decreased the migration and broadened the peaks of the gangliosides. This may be due to the fact that increasing the ionic strength would decrease the electrostatic repulsion between the ganglioside monomers, thus increasing the number of monomers in the aggregates, and consequently the size of the ganglioside micelles. This increase in the size of the micelles would result in decreasing their migration velocity. The authors also studied the time course of mixed micelle formation of gangliosides. Both  $G_{D1b}$  and  $G_{T1b}$  were first separated into two distinct peaks after initial mixing. However, upon incubation at 37 °C, complete fusion between both micellar peaks could be observed in less than 2.5 hrs. The fusion process was temperature-dependent. In fact, at 50 °C the formation of mixed micelles between  $G_{D1b}$  and  $G_{T1b}$  was complete within 30 min. In contrast, no fusion of the ganglioside peaks was observed at 0 °C even after 75 hrs. The mixed micelle formation seems to be dependent on the sialic acid content of the individual gangliosides. Whereas mixed micelle formation between  $G_{D1b}$  and  $G_{D1a}$  and that between  $G_{D1b}$  and  $G_{T1b}$  required 1.5 and 3.0 hrs, respectively, the aggregation of  $G_{M1}$  with polysialogangliosides (i.e.,  $G_{D1b}$  and  $G_{T1b}$ ) was 6- to 36- fold slower, under otherwise identical incubation conditions. In addition, no fusion was observed between  $G_{M1}$  and  $G_{M2}$  after 2 days of incubation. Based on these observations it was suggested that polysialogangliosides (e.g.,  $G_{D1a}$  and  $G_{T1b}$ ) may have higher propensities than monosialoganglioside. Thus, the high resolution, high speed and quantitative aspects of CZE were clearly demonstrated in monitoring processes that may have important implications in the distribution and function of gangliosides in biological membranes.

One of the many elegant features of CE is the ease with which the electrophoretic behavior of the analytes can be altered through simple addition of specific reagents to the

running electrolyte. Among the many buffer additives described so far [55], cyclodextrins (CDs) are the most effective in promoting the separation of gangliosides. This is due to the fact that CDs can alter the electrophoretic behavior of a wide variety of compounds via inclusion complexes the extent of which is determined by the solute hydrophobicity and size [55]. Based on this, Yoo *et al.* [54] demonstrated the utility of CDs in the separation of native gangliosides at 185 nm. Among the various CDs,  $\alpha$ -CD was the best buffer additive as far as the separation is concerned. This may be due to the size of the cavity of  $\alpha$ -CD that best fit the lipid moiety of the gangliosides.

As can be noticed from the above discussion, the utility of HPCE in the separation of gangliosides (the sialic acid-containing glycosphingolipids) has not been yet fully exploited.

#### Solute-wall Interaction in CE of Proteins

From equation 16 in Chapter I, it can be predicted that macromolecules which have low diffusion coefficient ( $D \leq 5.0 \times 10^{-7} \text{ cm}^2 \text{ s}^{-1}$ ) such as proteins could be separated with separation efficiencies greater than one million plates. However, due primarily to solute-wall interaction, the separation efficiency can be extremely low when proteins are separated with uncoated capillaries. In fact, peak tailing and even complete adsorption of the solute can occur, depending on the kinetics of the adsorption-desorption processes. While slow adsorption-desorption kinetics causes peak broadening and tailing, irreversible adsorption leads to modification of the capillary wall and consequently irreproducible separations and no elution of solutes. In CE, the primary causes of solute adsorption to the capillary walls are the ionic interaction between cationic solutes and the negatively charged wall on one hand, and the hydrophobic interaction on the other hand. Although the large surface area-to-volume ratios of the capillary is beneficial for heat dissipation, it increases the probability of solute adsorption to the capillary wall. Several approaches have been utilized to reduce

solute-wall interaction including the use of (i) buffer systems, (ii) dynamically coated capillaries and (v) permanently coated capillaries.

### Buffer Systems

Solute-wall interaction was found to decrease as the concentration of the buffer increase [56, 57]. This is due to the decrease in the effective surface charge. However, this approach is limited by the increased current and subsequent Joule heating. This approach also prolongs analysis time as a result of the decrease in EOF. Despite these limitations, moderate buffer concentrations have been used to improve the efficiency of separation of coated capillaries. An alternative to the high electrolyte concentration is the use of the zwitterionic buffer systems [58]. Generally, zwitterions do not contribute to conductivity and as a result they can be used at very high concentrations, i.e., 2.0 M. Nevertheless, the use of zwitterions is limited by the  $pK_a$ 's of their ionizable group, and 2.0 M concentration introduces large background noise in UV detection.

Another approach to decrease solute-wall interaction is to perform the analysis at extreme pH. Biopolymers are anionic in buffers with pH 1-2 units above the pI of a given protein, thus repelling from the anionic capillary wall [56]. However, this approach suffers from two major limitations. First, the hydrophobic interaction between solute and wall is not eliminated. Second, proteins with high pI values ( $pI > 7$ ) are anionic at pH > 13, thus requiring buffers with high  $OH^-$  concentration which are too conductive and not useful due to Joule heating. In addition, at extreme pHs, conformational changes of some proteins occur with possible dissociation of multimeric proteins, loss of biological activity, and appearance of multiple peaks. On the other hand, at low pH (< 2-3) silanol groups of the fused-silica are protonated and uncharged. While EOF is nearly zero, under these conditions, most proteins are positively charged at such low pH and consequently migrate toward the cathode. Again, this approach suffers from several limitations including (i)

poor selectivity (ii) higher hydrophobic interaction between solute and wall and (iii) low solubility of proteins at low pHs.

### Dynamically Coated Capillaries

In dynamic coating an additive is included in the running electrolyte. These additives can interact with the wall and alter charge and hydrophobicity of the capillary wall. A number of substances adsorb to the silica wall *via* electrostatic interactions or hydrogen bonding. These substances are used as buffer additives to reduce solute-wall interaction as well as the EOF or even to reverse the latter's direction. The charge of the capillary surface can be reversed (from negative to positive) by the inclusion of cationic additives in the background electrolyte, thus reducing proteins adsorption. This reduction in protein adsorption is accomplished by using cationic surfactants, cationic polymers, or polyamines which will interact electrostatically with the capillary wall and, due to the presence of multiple positive charges, inverse the net charge on the capillary wall and consequently reverse the direction of the EOF.

Cetyltrimethylammonium bromide (CTAB), which is a cationic surfactant, has been utilized as a buffer additive for reducing the solute-wall interaction [59]. This approach involves a bilayer formation of hydrophobic chain at the wall, thus allowing high efficiency separation of basic proteins at neutral pH in low ionic strength buffer.

One of the amine derivatives which was shown to be an effective background electrolyte additive for reducing solute-wall interaction was the diamine derivative 1,4-diaminobutane [56]. However, diamines at low concentrations were not effective in the case of strongly basic proteins, such as lysozyme and cytochrome c. These proteins required high concentrations of spermine [60], 1,3-diaminopropane [61], 1,5-diaminopentane [62], or ethylenediamine [63]. Other amine derivatives that have been proven useful in reducing solute-wall interaction include triethylenetetramine, pentamethylpiperidine and *N,N,N',N'*-tetramethyl-1,3-butanediamine [64].



In addition, a cationic natural polymer (chitosan) has recently been used as a buffer additive [65]. The chitosan polymer, which is (1→4)-2-amino-2-deoxy-β-D-glucan resulting from the deacetylation of chitin, interacts with the capillary wall, thus reversing the direction of the EOF and reducing solute-wall interaction of proteins. However, as the buffer pH approaches the pK<sub>a</sub> value of chitosan the electrostatic repulsion between the proteins and the chitosan is possibly replaced by hydrogen bonding between the two, thus reducing the peak efficiency and ultimately limiting the use of this additive at high pH. The UV absorption of chitosan is also a drawback of this method since it reduces the detection sensitivity. The significant reduction in EOF or even the reversal of its direction in many cases is the only limitation of these buffer systems.

Non-ionic surfactants were also shown to be useful in preventing hydrophobic interaction between hydrophobic solutes and hydrophobically derivatized capillaries. Tween and Brij are two examples of such surfactants which dynamically coat derivatized C<sub>18</sub> capillaries, thus rendering these capillaries useful in the separation of proteins. Tween and Brij possess bulky polar head groups which render the C<sub>18</sub> capillary surface hydrophilic and suitable for protein separation [66, 67].

In addition, non-ionic polymeric molecules (e.g., hydroxypropylmethylcellulose and polyvinyl alcohol) have been used as additives in the background electrolytes to suppress the EOF *via* their adsorption to the capillary walls, thus drastically reducing EOF and preventing undesirable solute-wall interaction [68-70]. However, these additives increase the viscosity of the background electrolyte and consequently prolong the analysis time.

Although all these aforementioned dynamic coatings of the capillaries have been proven useful for particular applications, they all suffer from several drawbacks. First, biological conditions are sacrificed when performing the separation in the presence of these additives. The poor reproducibility of this approach is another major drawback. This poor reproducibility is due mainly to the fact that the coating is only adsorbed to the surface and

is continuously changing. Finally, the use of this approach eliminate the possibility for any post column analyses such as mass spectrometry which is sensitive to additives.

### Permanently Coated Capillaries

Another approach for controlling EOF and eliminating solute-wall interaction involves the development of coatings covalently bonded or physically adhered to the capillary wall. Although several coating approaches have been developed which involved different chemistry, an ideal surface modification procedure should, in principle, satisfy certain criteria. First, the bonded phases should completely cover the original silica, and the functions introduced should not interact with biopolymer solutes over a wide range of conditions. Second, the coating should exhibit a well defined or reproducible composition. Finally, the bonded phase should have high chemical stability and resistibility, in particular, to alkaline and acidic hydrolysis resulting from aqueous solvents routinely used in CE.

Covalently Bonded Phases. One of the first attempts at surface modification involved the sialylation of the capillary to reduce the EOF and improve the resolution of dansyl amino acids [71]. But this technique did not reduce the solute-wall interaction for proteins. In 1985 Hjertén [68] developed a technique where methylacryl groups were attached to the capillary walls and subsequently cross-linked with polyacrylamide to produce a fairly inert surface. This coating scheme totally eliminated the EOF and allowed the separation of human serum samples and nucleotides, yet the life-time of such capillaries was short. Along the same lines, Cobb *et al.* [72] reported the use of polyacrylamide-coated capillary similar to that described previously by Hjertén, yet the coating was bonded to the silica wall through a Si-C bond which is hydrolytically more stable than the Si-O-Si bond. Although the coating was proved to be useful and stable over a wide pH range, the coating scheme was long and complicated and involved three separate stages. In addition, this scheme is very difficult to reproduce and drastically reduces the EOF, thus prolonging the analysis time especially at physiological pH. Polyacrylamide has also been used in

conjunction with other linkers to modify the surface of the capillary [73]. In this method, a polymeric film containing vinyl double bonds was produced by using synthetic polyvinylmethylsiloxanediol combined with a cross-linker. Crosslinking and binding to the silica surface takes place in one step at room temperature, yet the structure of the cross-linker was not revealed in the paper. To the polymeric film, a crosslinked layer was covalently attached in two steps. First, linear polyacrylamide was grafted to the polysiloxane layer. Second, polyacrylamide chains were converted into polymethylol acrylamide by reacting with formaldehyde at pH 10 [73]. This method produced capillaries with EOF 150 times less than that of the bare capillary. In addition, under mild operation conditions (i.e., pH 4.4-8) the separation efficiency did not decrease during 600 consecutive analyses. However, like any other polyacrylamide columns, an increase in EOF is observed when used at a pH higher than 8.5, resulting from the partial hydrolysis of polyacrylamide. Recently, polyacryloylaminoethoxyethanol, which is more resistant to hydrolysis than polyacrylamide, was used for coating fused-silica capillaries [74]. In this method, the polymer was covalently attached to a silica surface previously modified with  $\alpha$ -methacryloxypropyl functionality which was achieved by catalytic hydrosilylation of allyl methacrylate on an SiH-modified fused-silica capillary. This coating produces capillaries, the lifetime of which is twice that of the conventional polyacrylamide when used at pH 8.5.

Bruin *et al.* [75] used  $\gamma$ -glycidoxypropyltrimethylsilane to attach polyethyleneglycol 600 (PEG 600) to the walls of the capillary. These capillaries were stable for several months when they were operated in 3-5 pH range, but their stability rapidly decreased at pH greater than 5. A diol coating, which was prepared by reacting the capillary wall with  $\gamma$ -glycidoxypropyltriethoxysilane followed by acid hydrolysis, was also reported by the same authors [76]. This coating exhibited lower separation efficiencies than the PEG 600 coating and also suffered instability at pH greater than 5. In the same report [76], maltose coating was prepared by reacting the capillary wall with  $\gamma$ -aminopropyltriethoxysilane and

then with maltose in the presence of cyanoborohydride. However, this coating exhibited lower separation efficiencies than the PEG 600 and diol coatings, and was susceptible to bacterial degradation due to the presence of the carbohydrate moiety.

In a different approach, our laboratory utilized PEG in two surface modification schemes to yield coated capillaries with moderate EOF [77]. In the first scheme,  $\gamma$ -glycidoxypropyltrimethoxysilane was covalently attached to the silanol groups on the capillary walls. Since the reaction was conducted in water, a glyceropropylpolysiloxane sub-layer was formed which was then reacted with an equimolar mixture of polyethylene glycol diglycidyl ether (Mr 600) and PEG 2000 or PEG 600 in dioxane to form the polyether chains of different lengths with one end or both ends covalently attached to the sub-layer. These coated capillaries were labeled as *fuzzy*. In the second scheme, the capillary wall was reacted with PEG 200 having triethoxysilane at both ends in dimethylformamide solution at 100°C. This coating resulted in the formation of polyether polysiloxane chains of which the monomeric units at both ends are covalently attached to the surface with possible interconnection. Capillaries prepared according to this method are called *interlocked* coated capillaries.

Hydrophobic C<sub>18</sub> capillary columns for the separation of acidic and basic proteins in the presence of nonionic surfactants were introduced by Towns and Regnier [78] to reduce solute-wall interaction. The capillary wall was first reacted with octadecyltrichlorosilane in methylene chloride as the solvent to produce a C<sub>18</sub> surface that is similar to that used in reversed phase chromatography. Next, non-ionic surfactants were hydrophobically adsorbed onto the C<sub>18</sub> phase forming a thick hydrophilic layer.

Solute-wall interaction can be eliminated by coating the capillary with polymers having the same net charge as the proteins, thus inducing coulombic repulsive forces between the analyte and the surface of the capillary. Towns and Regnier [66] developed capillaries having positively charged polyethyleneimine (PEI) layers by cross-linking PEI with ethylene glycol diglycidyl ether in the presence of triethylamine. This coating was only

useful for the analysis of basic proteins, since acidic proteins exhibited solute-coating interaction.

An interesting surface modification was recently introduced by our laboratory and yielded capillaries with switchable EOF (anodal/cathodal) [79]. The resulting capillary surface is a composite of material consisting of unreacted silanol groups, a layer of positively charged quaternary ammonium functions, and a hydrophilic layer of long polyether chains. This method involved reacting the capillary with bis(2-hydroxyethyl)-aminopropyltriethoxysilane followed by reacting it with diepoxy PEG 600 and finally with PEG 200. As a result of the presence of positively and negatively charged groups on the capillary wall, the magnitude and the direction of EOF could be manipulated by adjusting the pH of the running electrolyte. In addition, the polyether chains reduced the solute-wall interaction with either the unreacted silanol groups or the introduced quaternary ammonium groups.

Also, zero and constant or variable anodal EOF capillaries were recently developed by our laboratory [28]. In case of the zero EOF capillaries, large molecular weight hydroxypropyl cellulose was deposited on the capillary wall and produced a "zero" EOF. The coating procedure involved the reaction of the silanol functional groups of the capillary walls first with  $\gamma$ -glycidoxypropyltrimethoxysilane and then with hydroxypropyl cellulose. These "zero" flow capillaries were further functionalized with a charged polyethyleneimine layer to which polyether layer was covalently attached, thus producing a positively charged surface and creating a variable anodal EOF. However, this anodal EOF was relatively weak because of the high viscosity of the coated wall imparted by the hydroxypropyl cellulose layer. A stronger and constant anodal EOF (i.e., EOF is not a function of the electrolyte pH) was attained when the capillary walls were first coated with methylated polyethyleneimine hydroxyethylated which contains a high density of quaternary ammonium group.

Physically Adhered Phases. Another approach for coating fused-silica capillaries involves the adsorption of polymers to the capillary wall, thus forming a thin-film coating. Schomburg and coworkers [80] thermally immobilized polyvinyl alcohol (PVA) on the walls of the capillaries. In their procedure, capillaries were flushed with aqueous PVA solution which was then discharged with nitrogen gas. Finally, the immobilization of PVA coating is achieved by heating the capillary at 140°C for several hours. This coating provides high separation efficiencies for basic and acidic proteins over nearly the whole pH range in which proteins are stable, but this coating procedure yielded prolonged analysis time due to the completely suppressed EOF in the pH range between 3 and 10. In addition, this thermal immobilization provides higher separation efficiency than dynamic coating with PVA. Another procedure based on polymer adsorption was recently reported by Busch *et al.* [81] where the capillaries were coated with a thin-film of cellulose acetate. The coating procedure is very simple and only involves the filling of the capillary with cellulose acetate solution, followed by flushing with helium. The coating allowed the separation of basic proteins with column efficiency up to  $1 \times 10^6$  plates per meter. This coating procedure is simple, stable and easy to produce. In addition, other cellulose derivatives can be used, too. However, the coating is not stable above pH 7.5.

Recently, Erim *et al.* [82] reported a simple method for the preparation of PEI coating based on the physical adherence of high-molecular-mass PEI. The PEI layer is coated on the silica surface by flushing the capillary with a solution of high-molecular-mass PEI. The physically adsorbed layer of PEI was shown to be very stable in a pH range of 3-11. In addition, chitosan, a cationic natural polymer, was also used to coat the inner walls of fused-silica capillaries [65]. This involved the flushing of the capillaries with 0.1% solution of chitosan between runs. However, unlike the PVA coating, the separation efficiency obtained using this flushing method was lower than that obtained using chitosan as a buffer additive.

The aforementioned coating schemes are the most important approaches that have been developed to reduce or eliminate solute-wall interaction. Note that most of these coatings suffer from limitations including either the short-term stability or the reproducibility of the coating procedure. Although great improvements in CE separation of proteins have been achieved by the aforementioned methods, a universal method for the efficient separation of basic and acidic proteins has not been developed, and therefore, more work is still needed in this direction. This dissertation addresses this need by developing a novel capillary coating which is the subject of Chapter VI.

#### Summary of Objectives and Rationales of Part I of the Dissertation

In part I of this dissertation, we have three major objectives: (i) to develop a novel and selective precolumn derivatization scheme for the labeling of acidic carbohydrates and glycolipids, (ii) to further develop the concept of capillary enzymophoresis which involves the coupling of capillary enzyme microreactors to capillary electrophoresis for selectively modifying minute amounts of biochemicals prior to CE separation, and (iii) to introduce a new capillary coating that is highly stable in basic and acidic media for the reproducible and efficient CE separation of biological substances.

The derivatization scheme developed involves the formation of an amide bond between the carboxylic acid functional group of acidic carbohydrates and glycoconjugates, and the amino group of a suitable tagging agent, thus providing a highly selective labeling scheme. Acidic monosaccharides, sialooligosaccharides, and gangliosides (sialoglycolipids) were derivatized according to this labeling method and the extent of derivatization has been evaluated. Also, electrolyte systems which permit the CE analysis of gangliosides have been developed. These aspects are presented in Chapters III-V.

As a continuation of recent work from our laboratory on capillary enzymophoresis, Chapter VII further evaluate this concept by developing capillary enzyme reactors having surface-immobilized RNA-modifying enzymes for selectively fragmenting and altering

nucleic acid fragments in order to facilitate their identification and to allow the simultaneous on-line digestion and mapping of minute amounts of transfer ribonucleic acids.

Finally, to further contribute to the development of CE in the area of large biomolecules, a highly stable hydrophilic capillary coating with reduced EOF was designed. The stable coating which is discussed in Chapter VI was achieved through the covalent attachment of branched, high molecular weight dextrans and subsequent cross-linking of polyether chains on the inner surface of fused-silica capillaries.

For detailed rationales and objectives of the various interrelated research projects of this doctoral dissertation, the reader is advised to refer to the introductory sections of each chapter that follows.



## References

1. Garner, T.W. and Yeung, E.S., *J. Chromatogr.*, 515 (1990) 639.
2. Kuhr, W.G. and Yeung, E.S., *Anal. Chem.*, 60 (1988) 1832.
3. Richmond, M.D. and Yeung, E.S., *Anal. Biochem.*, 210 (1993) 245.
4. Vorndran, A.E., Oefner, P.J., Scherz, H. and Bonn, G.K., *Chromatographia*, 33 (1992) 163.
5. Xu, X., Kok, W.T. and Poppe, H., *J. Chromatogr. A*, 716 (1995) 231.
6. Lu, B. and Westerlund, D., *Electrophoresis*, 17 (1996) 325.
7. Colón, L.A., Dadoo, R. and Zare, R.N., *Anal. Chem.*, 65 (1993) 476.
8. Zhou, W. and Baldwin, R.P., *Electrophoresis*, 17 (1996) 319.
9. Ye, J. and Baldwin, R.P., *J. Chromatogr. A*, 687 (1994) 141.
10. O'Shea, T.J., Lunte, S.M. and LaCourse, W.R., *Anal. Chem.*, 65 (1993) 948.
11. Weber, P.L. and Lunte, S.M., *Electrophoresis*, 17 (1996) 302.
12. Lu, W. and Cassidy, R.M., *Anal. Chem.*, 65 (1993) 2878.
13. LaCourse, W.R. and Owens, G.S., *Electrophoresis*, 17 (1996) 310.
14. Penn, S.G., Chiu, R.W. and Monnig, C.A., *J. Chromatogr. A*, 680 (1994) 233.
15. Lee, Y. and Lin, T., *Electrophoresis*, 17 (1996) 333.
16. Brewster, J.D. and Fishman, M.L., *J. Chromatogr. A*, 693 (1995) 382.
17. Toida, T. and Linhardt, R.J., *Electrophoresis*, 17 (1996) 341.
18. Yeung, E.S. and Kuhr, W.G., *Anal. Chem.*, 63 (1991) 275.
19. Johnson, D.C. and LaCourse, W.R., in El Rassi, Z., Ed., *Carbohydrate Analysis: High Performance Liquid Chromatography and Capillary Electrophoresis*, Amsterdam, Elsevier, 1995, p. 391.
20. El Rassi, Z. and Mechref, Y., *Electrophoresis*, 17 (1996) 275.
21. El Rassi, Z. and J.T., Smith., in El Rassi, Z., Ed., *Carbohydrate Analysis: High Performance Liquid Chromatography and Capillary Electrophoresis*, Amsterdam, Elsevier, 1995, p. 607.

22. Honda, S., Iwase, S., Makino, A. and Fujiwara, S., *Anal. Biochem.*, 176 (1989) 72.
23. Hase, S., in El Rassi, Z., Ed., *Carbohydrate Analysis: High Performance Liquid Chromatography and Capillary Electrophoresis*, Amsterdam, Elsevier, 1995, p. 555.
24. Klockow, A., Widmer, H.M., Amadó, R. and Paulus, A., *Fresenius J. Anal. Chem.*, 350 (1994) 415.
25. Schwaiger, H., Oefner, P., Huber, C., Grill, E. and Bonn, G.K., *Electrophoresis*, 15 (1994) 941.
26. Evangelista, R.A., Gutman, A. and Chen, F.-T.A., *Electrophoresis*, 17 (1996) 347.
27. Nashabeh, W. and El Rassi, Z., *J. Chromatogr.*, 600 (1992) 279.
28. Smith, J.T. and El Rassi, Z., *Electrophoresis*, 14 (1993) 396.
29. Lee, K., Kim, Y. and Linhardt, R., *Electrophoresis*, 12 (1991) 636.
30. Chiesa, C. and Horváth, C., *J. Chromatogr.*, 645 (1993) 337.
31. Jackson, P., *Anal. Biochem.*, 196 (1991) 238.
32. Stefansson, M. and Novotny, M., *J. Am. Chem. Soc.*, 115 (1993) 11573.
33. Evangelista, R.A., Liu, M. and Chen, F., *Anal. Chem.*, 67 (1995) 2239.
34. Guttman, A. and Pritchett, T., *Electrophoresis*, 16 (1995) 1906.
35. Chen, F. and Evangelista, R.A., *Anal. Biochem.*, 230 (1995) 273.
36. Honda, S., Yamamoto, K., Suzuki, S., M., U. and Kakehi, K., *J. Chromatogr.*, 588 (1991) 327.
37. Honda, S., Akao, E., Suzuki, S., Okuda, M., Kakehi, K. and Nakamura, J., *Anal. Biochem.*, 180 (1989) 351.
38. Honda, S., Ueno, T. and Kakehi, K., *J. Chromatogr.*, 608 (1992) 289.
39. Honda, S., Suzuki, S., Nose, A., Yamamoto, K. and Kakehi, K., *Carbohydr. Res.*, 215 (1991) 193.
40. Chiesa, C., Oefner, P.J., Zieske, L.R. and O'Neill, R.A., *J. Cap. Elec.*, 2 (1995) 175.

41. Liu, J., Shirota, O., Wiesler, D. and Novotny, M., *Proc. Natl. Acad. Sci. USA*, 88 (1991) 2302.
42. Novotny, M.V. and Sudor, J., *Electrophoresis*, 14 (1993) 373.
43. Sudor, J. and Novotny, M., *Proc. Natl. Acad. Sci. USA*, 90 (1993) 9451.
44. Liu, J., Shirota, O. and Novotny, M., *Anal. Chem.*, 64 (1992) 973.
45. Liu, Y. and Chan, K.-F.J., *Electrophoresis*, 12 (1991) 402.
46. Liu, J., Shirota, O. and Novotny, M., *Anal. Chem.*, 63 (1991) 413.
47. Zhao, J.Y., Diedrich, P., Zhang, Y., Hindsgaul, O. and Dovichi, N.J., *J. Chromatogr. B*, 657 (1994) 307.
48. Avigad, G., *J. Chromatogr.*, 139 (1977) 343.
49. Alpenfels, W.F., *Anal. Biochem.*, 114 (1981) 153.
50. Mopper, K. and Johnson, L., *J. Chromatogr.*, 256 (1983) 27.
51. Eggert, F.M. and Jones, M., *J. Chromatogr.*, 333 (1985) 123.
52. Perez, S.A. and Colón, L.A., *Electrophoresis*, 17 (1996) 352.
53. Ulrich-Bott, B. and Wiegandt, H., *J. Lip. Res.*, 25 (1984) 1233.
54. Yoo, Y.S., Kim, Y.S., Jhon, G.-J. and Park, J., *J. Chromatogr. A*, 652 (1993) 431.
55. Issaq, J.I., Janini, G.M., Chan, K.C. and El Rassi, Z., *Adv. Chromatogr.*, 35 (1995) 101.
56. Lauer, H. and McManigill, D., *Anal. Chem.*, 58 (1986) 166.
57. Green, J.S. and Jorgenson, J.W., *J. Chromatogr.*, 478 (1989) 63.
58. Bushey, M.M. and Jorgenson, J.W., *J. Chromatogr.*, 480 (1989) 301.
59. Tsuda, T., *HRC, J. High. Resolut. Chromatogr.*, 10 (1987) 622.
60. Dolnik, V., Liu, J., Banks, J.F. and Novotny, M.V., *J. Chromatogr.*, 480 (1989) 321.
61. Bullock, J.A. and Yuan, L.C., *J. Microcol. Sep.*, 3 (1991) 241.
62. Rohlicek, V. and Deyl, Z., *J. Chromatogr.*, 494 (1989) 87.

63. Song, L., Ou, Q. and Yu, W., *J. Chromatogr.*, 657 (1993) 175.
64. Corradini, D. and Cannarsa, G., *LC-GC*, 14 (1996)
65. Yao, Y.J. and Li, S.F.Y., *J. Chromatogr. A*, 663 (1994) 97.
66. Towns, J. and Regnier, F., *J. Chromatogr.*, 516 (1990) 69.
67. Dougherty, A.M., Woolley, C.L., Williams, D.L., Swaile, D.F., Cole, R.O. and Sepaniak, M.J., *J. Liq. Chromatogr.*, 14 (1991) 907.
68. Hjertén, S., *J. Chromatogr.*, 347 (1985) 191.
69. Gilges, M., Husmann, H., Kleemib, M.-H., Motsch, S.R. and Schomburg, G., *J. High Resolut. Chromatogr.*, 15 (1992) 452.
70. Gordon, M.J., Lee, K.-J. and Zare, R.N., *Anal. Chem.*, 63 (1991) 69.
71. Jorgenson, J. and Lukacs, K.D., *Anal. Chem.*, 53 (1981) 1298.
72. Cobb, K., Dolnik, V. and Novotny, M., *Anal. Chem.*, 62 (1990) 2478.
73. Schmalzing, D., Pigeo, C.A., Foret, F., Carrilho, E. and Karger, B.L., *J. Chromatogr. A*, 652 (1993) 149.
74. Chiari, M., Nesi, M., Sandoval, J.E. and Pesek, J.J., *J. Chromatogr. A*, 717 (1995) 1.
75. Bruin, G.J.M., Chang, J.P., Kuhlman, R.H., Zegers, K., Kraak, J.C. and Poppe, H., *J. Chromatogr.*, 471 (1989) 429.
76. Bruin, G.J.M., Huisden, R., Kraak, J.C. and Poppe, H., *J. Chromatogr.*, 480 (1989) 339.
77. Nashabeh, W. and El Rassi, Z., *J. Chromatogr.*, 559 (1991) 367.
78. Towns, J. and Regnier, F., *Anal. Chem.*, 63 (1991) 1126.
79. Smith, J.T. and El Rassi, Z., *HRC, J. High Resol. Chromatogr.*, 15 (1992) 573.
80. Gilges, M., Kleemiss, M.H. and Schomburg, G., *Anal. Chem.*, 66 (1994) 2038.
81. Bush, M.H.A., Kraak, J.C. and Poppe, H., *J. Chromatogr. A*, 695 (1995) 287.
82. Erim, F.B., Cifuentes, A., Poppe, H. and Kraak, J.C., *J. Chromatogr. A*, 708 (1995) 356.

CHAPTER III  
CAPILLARY ZONE ELECTROPHORESIS OF DERIVATIZED  
ACIDIC MONOSACCHARIDES

Introduction

Most carbohydrate species do not possess strong chromophores in their structures, a condition that precludes their direct detection in the UV at low levels. To overcome this difficulty, carbohydrates are generally tagged with a suitable chromophore or fluorophore prior to separation, a process referred to as precolumn derivatization. In capillary electrophoresis, it is preferable that the tagging agent be charged over a relatively wide pH range, and that the derivatization reaction leads to a single derivative in high yield. The hydroxyl groups of carbohydrates are attractive sites for tagging, but the possible formation of more than one derivative precludes their use as tagging sites. Therefore, other functional groups of the carbohydrate molecules must be considered for the attachment of chromophores or fluorophores. The carbonyl group in reducing carbohydrates is by far the most widely used site for derivatization. The amino and carboxylic groups of amino and acidic sugars, respectively, are also potential anchoring sites for chromophores.

Exploiting the reactivity of the reducing end of saccharides, precolumn derivatizations *via* reductive amination for various mono- and oligo-saccharides have been reported [1-6]. Using reductive amination, our laboratory has demonstrated the utility of 6-aminoquinoline [2], a strong UV absorbing and fluorescing tag. Carbonyl groups of carbohydrates can be also coupled with amines to form imines or glycosylamines [7,8]. However, this derivatization reaction yields relatively instable derivatives, and leads to the formation of syn/anti isomers and anomeric mixtures.

Hara *et al.* [9,10] made use of a derivatization reaction, which was initially proposed for gas chromatographic studies [11], for the prelabeling of sialic acids (e.g., *N*-acetylneuraminic acid and its acetyl derivatives and *N*-glycolylneuraminic acid) with 1,2-diamino-4,5-methylenedioxybenzene, a fluorogenic reagent for  $\alpha$ -keto acids, and the derivatives were separated by reversed-phase HPLC. This method of derivatization can only be employed for free  $\alpha$ -keto acids that exist in the linear form, and it can not be used for the derivatization of  $\alpha$ -keto acids that exist in the lactone form (i.e., cyclic ester form). Therefore, this method of derivatization can not be employed for the derivatization of glycoconjugates containing sialic acid moieties such as glycolipids or glycoproteins.

The present study is concerned with the introduction of a selective precolumn derivatization for carboxylated saccharides in the free or conjugated forms by the formation of an amide bond between the carboxylic group of the analyte and the amino group of the derivatizing agent using a well established chemical reaction [12,13]. Two different derivatizing agents were evaluated, sulfanilic acid (a UV absorbing tag) and 7-aminonaphthalene-1,3-disulfonic acid (a UV absorbing and fluorescent tag). Both derivatizing agents possess strong acidic groups, namely sulfonic groups, which are fully ionized over a wide range of pH. Besides providing the chromophore or fluorophore for the sensitive detection of carbohydrates, the new derivatization reaction described here replaces the weak acidic group (i.e., carboxylic acid group) of the analyte by a stronger acidic group (i.e., sulfonic acid group) which ensure permanent negative charges on the derivatives. This has allowed the achievement of separation of closely related acidic monosaccharides at low and high pH with detection sensitivities down to low femtomoles. In addition, this novel derivatization method eliminated the need for sample clean up. The application of the present precolumn derivatization to the labeling of sialic acid containing glycoconjugates is the subject of Chapter IV and V.

## Materials and Methods

### Reagents and Materials

The following acidic monosaccharides: L-glyceric acid, D-gluconic acid, D-galacturonic acid, and *N*-acetylneuraminic acid (NANA), as well as 1-ethyl-3-(3-dimethylaminopropyl) carbodiimide hydrochloride (EDAC) were purchased from Sigma Chemical Co. (St. Louis, MO, U.S.A.). The derivatizing agents 7-amino-1,3-naphthalene disulfonic acid (ANDSA) and sulfanilic acid (SA) were purchased from TCI America, Inc. (Portland, OR, U.S.A.). Reagent grade sodium phosphate dibasic, hydrochloric acid, sodium hydroxide and boric acid granular were purchased from Fisher Scientific (Pittsburgh, PA, U.S.A.). Deionized water was used to prepare the running electrolyte and the sample solutions. The running electrolytes were filtered with 0.2  $\mu\text{m}$  Whatman syringless filters obtained from Baxter Diagnostics Inc. (McGaw Park, IL, U.S.A.) to avoid column plugging and minimize baseline noise.

### Instruments and Capillaries

The instrument for capillary electrophoresis was assembled in-house from commercially available components [2]. It is comprised of two high-voltage power supplies of positive and negative polarity, Models MJ30P400 and MJ30N0400, respectively, from Glassman High Voltage (Whitehouse Station, NJ, U.S.A.) and a UV-Vis variable wavelength detector, Model 200, equipped with a cell for on-column capillary detection from Linear Instrument (Reno, NV, U.S.A.). The detection wavelength was set at 247 nm for the UV detection. For fluorescence detection of the derivatized monosaccharides, a spectrofluorescence detector Model FL-750 BX from McPherson Instrument (Acton, MA, U.S.A.) with variable excitation wavelength was used. The excitation wavelength was set at 315 nm, and 400 nm sharp cut-off long wavelength absorption filter was used as the emission filter. The electropherograms were recorded

with a Shimadzu computing integrator Model CR5A (Columbia, MD, U.S.A.). Some portions of the work were performed on an HP <sup>3D</sup>capillary electrophoresis instrument from Hewlett Packard (Waldbronn, Germany) equipped with a real time UV-visible diode array detector (DAD) in the 190-600 nm range, and a data analysis software similar to HPLC <sup>3D</sup>Chemstation.

Fused-silica capillary columns of 50  $\mu\text{m}$  I.D. and 365  $\mu\text{m}$  O.D. were obtained from Polymicro Technology (Phoenix, AZ, U.S.A.). Extended light path capillaries from Hewlett Packard were also used in some portions of the studies. All capillaries used in this study were uncoated since the analytes are negatively charged and would repulse from the like-charged capillary surface. The running electrolyte was renewed after every run.

The derivatized acidic monosaccharides were introduced into the capillary as thin plugs by means of hydrodynamic injection for approximately 5 seconds at 15 cm differential height between inlet and outlet ends of the capillary. This translates to an injected sample volume of 1.4 nL.

### Mass Spectrometry Measurements

All mass spectra were obtained with a VG ZAB2-SE instrument (VG Analytical Ltd., Manchester, UK). The instrument is equipped with a VG II-150 data acquisition system. Liquid secondary ion mass spectrometry (LSIMS) was performed with a cesium ion gun operated at 32 kV. The negative secondary ions were accelerated at 6 kV. The mass range scanned was 100 to 950 m/z at a rate of 10 seconds/decade. An instrument resolution of approximately 1000 was used in acquiring the spectra. Calibration was made using cesium iodide on the probe tip.

For continuous flow-liquid secondary ion mass spectrometry (CF-LSIMS), the spectra were obtained by a single scan, and no signal averaging was applied. The mobile phase was a 1:1 mixture of water and methanol containing 2%(w/v) triethanolamine (TEA) adjusted to pH 10.5 with ammonium hydroxide. A flow-rate of 4.5  $\mu\text{L}/\text{min}$  was supplied



to the source by a  $\mu$ LC-500 syringe pump (ISCO, Inc., Lincoln, U.S.A.). The mobile phase was delivered by a 50  $\mu$ m fused-silica capillary, that was approximately 80.0 cm in length from the micro injector to the source. A 1.0  $\mu$ L loop was used in the microinjector (Valco, Houston, TX, U.S.A.).

#### Derivatization of Acidic Carbohydrates

Acidic monosaccharides were tagged with ANDSA or SA as follows. Typically, an aliquot of 60  $\mu$ L of 100 mM aqueous solution of EDAC (pH 5.0) was first added to 1.0 mg of acidic monosaccharides in solid form (approx. 5.50  $\mu$ mole of carboxyl groups). Occasionally, the reaction was carried out with as little as 0.1 mg of acidic monosaccharides. Generally, the amount of sample that can be derivatized could be scaled down even further provided that the final sample volume does not drop below a certain size from which an injection can be made and the sample concentration stays in the range of the detection limit. This was followed by adding an aliquot of 100  $\mu$ L of 100 mM aqueous solution of the derivatizing agent. The reaction mixture was stirred for at least 2 hrs at room temperature. Following, the reaction mixture containing the derivatized acidic monosaccharides was analyzed by capillary electrophoresis without any sample clean up from excess derivatizing agent and other components of the reaction mixture.

### Results and Discussion

#### Precolumn Derivatizations

As described above, the derivatization of acidic monosaccharides was performed with SA and ANDSA through a condensation reaction between the amino group of the derivatizing agent and the carboxyl group of the monosaccharide molecules, to form a peptide link by acid catalyzed removal of water in the presence of EDAC. The presence of a carbodiimide, e.g., EDAC, is required to promote the formation of the peptide bond. Carbodiimides are a class of compounds used in many condensation reactions [12,13].

EDAC was selected because of its high solubility in aqueous solutions where hydrophilic carbohydrates are well dissolved. The derivatization reaction proceeds according to the schemes shown in Fig. 1 where R<sup>n</sup>NH<sub>2</sub> is either SA or ANDSA, and R<sub>1</sub>COOH can be any of the acidic carbohydrates illustrated in Fig. 2.

In these derivatization reactions, the amount of added carbodiimide must be carefully controlled to avoid the formation of side products. In other words, the number of moles of added EDAC should not exceed the number of moles of reacting carboxyl groups. This is because the SA and ANDSA possess sulfonic acid groups which are known to react exothermally with carbodiimide to give side products [12,13]. In fact, side products were observed in a control reaction where the derivatizing agent and carbodiimide were mixed together without the analytes. However, the side products were not detected when the acidic monosaccharides were present in the mixture and the amount of EDAC was equivalent or slightly exceeding that of the analytes.

To characterize the derivatized sugars, real-time spectral analysis of pure SA and ANDSA as well as of their sugar derivatives was performed on-line by the diode array detector (DAD) of the commercial instrument used in this study. The spectra of SA and ANDSA showed maximum absorbance (i.e.,  $\lambda_{\max}$ ) at 251 nm with molar absorptivities of  $6.0 \times 10^4$  and  $9.7 \times 10^4 \text{ cm}^{-1}\text{M}^{-1}$ , respectively. The  $\lambda_{\max}$  for the SA and ANDSA derivatives of acidic monosaccharides shifted slightly toward lower wavelengths and was about 247 nm.

To assess the identity of the different derivatized monosaccharides, CF-LSIMS was performed on aliquots of SA and ANDSA sugar derivatives as described above. The mass-to-charge ratios of the observed ions for the derivatized sugars are summarized in Table I, while typical CF-LSIMS spectra are shown in Fig. 3. The absence of traces of underivatized sugars in the various spectra may indicate that the derivatization proceed to completion. Since the ANDSA used was a monopotassium salt, CF-LSIMS spectra

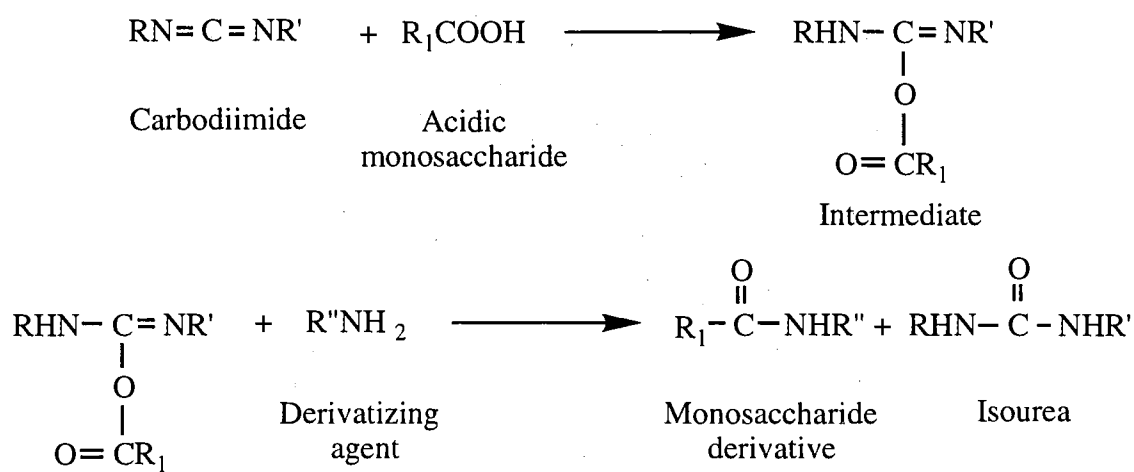


**Figure 1.** Derivatization scheme

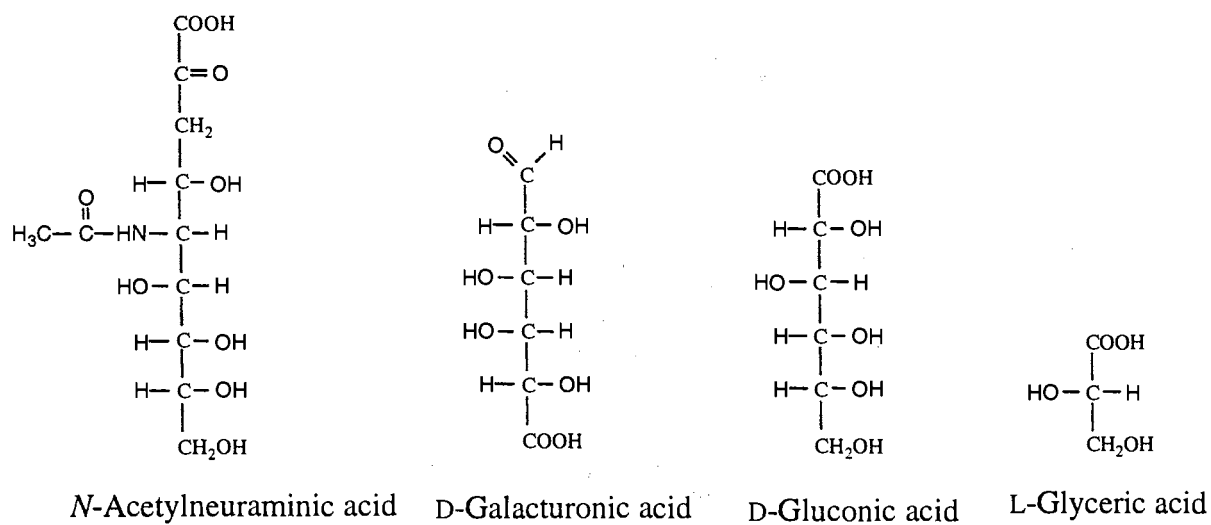


**Figure 2.** Structures of the acidic monosaccharides labeled according to the derivatization scheme illustrated in Fig. 1.

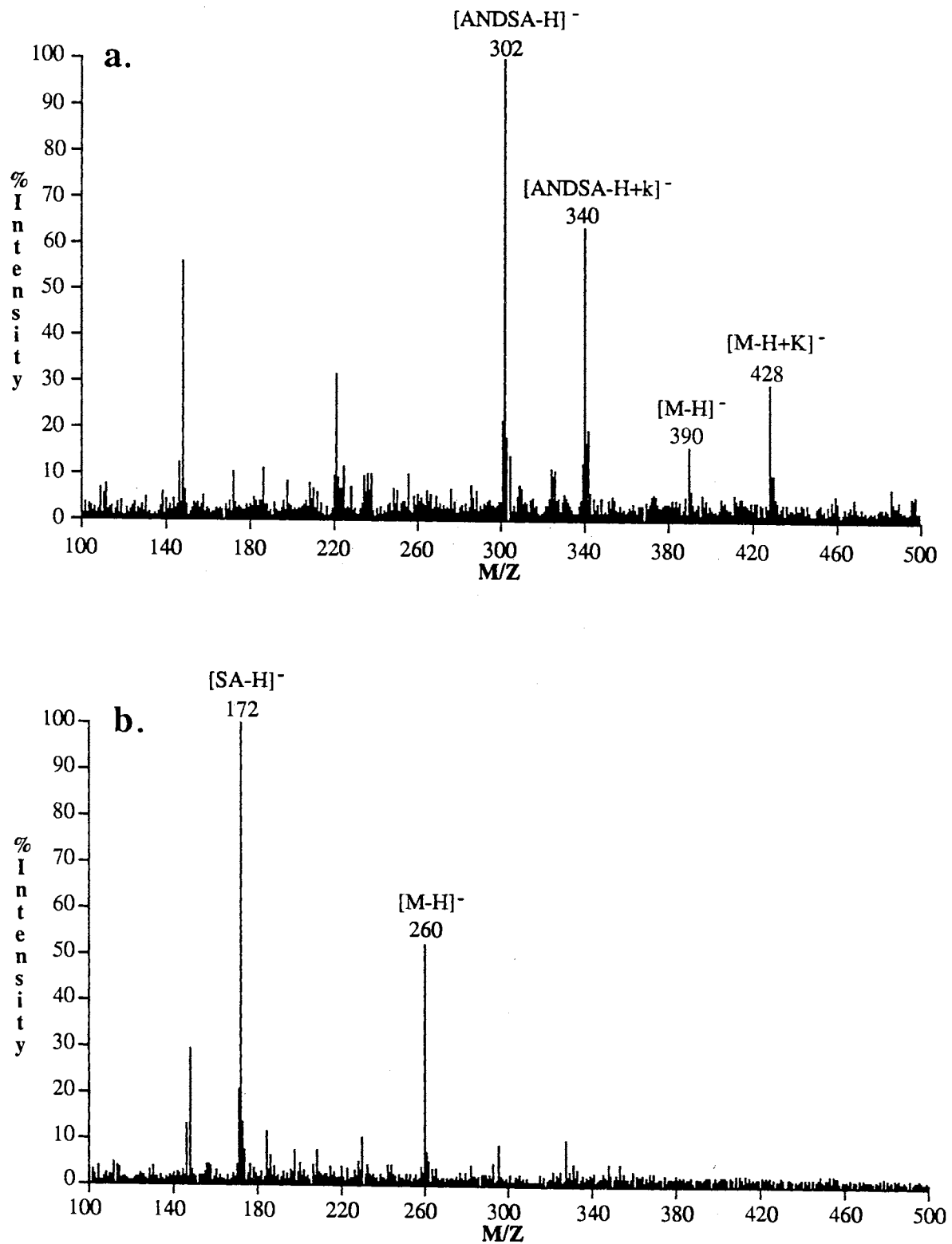


**Figure 3.** CF-LSIMS spectra of ANDSA- and SA-glyceric acid in (a) and (b), respectively.

obtained with ANDSA derivatives showed two peaks for each derivative, one peak corresponds to the adduct between the ANDSA sugar derivative and potassium ion while the other peak corresponds to the free ANDSA sugar derivative (i.e., without the potassium ion).

TABLE I. Mass-to-Charge Ratios (m/z) of Observed Ions for the Derivatized Monosaccharides.

Derivatized monosaccharides	m/z of observed ion	
	[M-H] <sup>-</sup>	[M-H+K] <sup>-</sup>
ANDSA	302	340
SA	172	—
ANDSA-gluconic acid	480	518
SA-gluconic acid	350	—
ANDSA-Galacturonic acid	478	516
SA-galacturonic acid	348	—
ANDSA-glyceric acid	390	428
SA-glyceric acid	260	—
ANDSA-NANA	593	631
SA-NANA	463	—

The progress of the derivatization reactions with SA and ANDSA was monitored by capillary electrophoresis using glyceric acid as the model solute. The reaction mixtures were analyzed by capillary electrophoresis at various time intervals. The time course of the derivatization reactions with SA and ANDSA are shown in Fig. 4 in terms of plots of peak height versus time. As shown in Fig. 4, the derivatization of the acidic monosaccharide

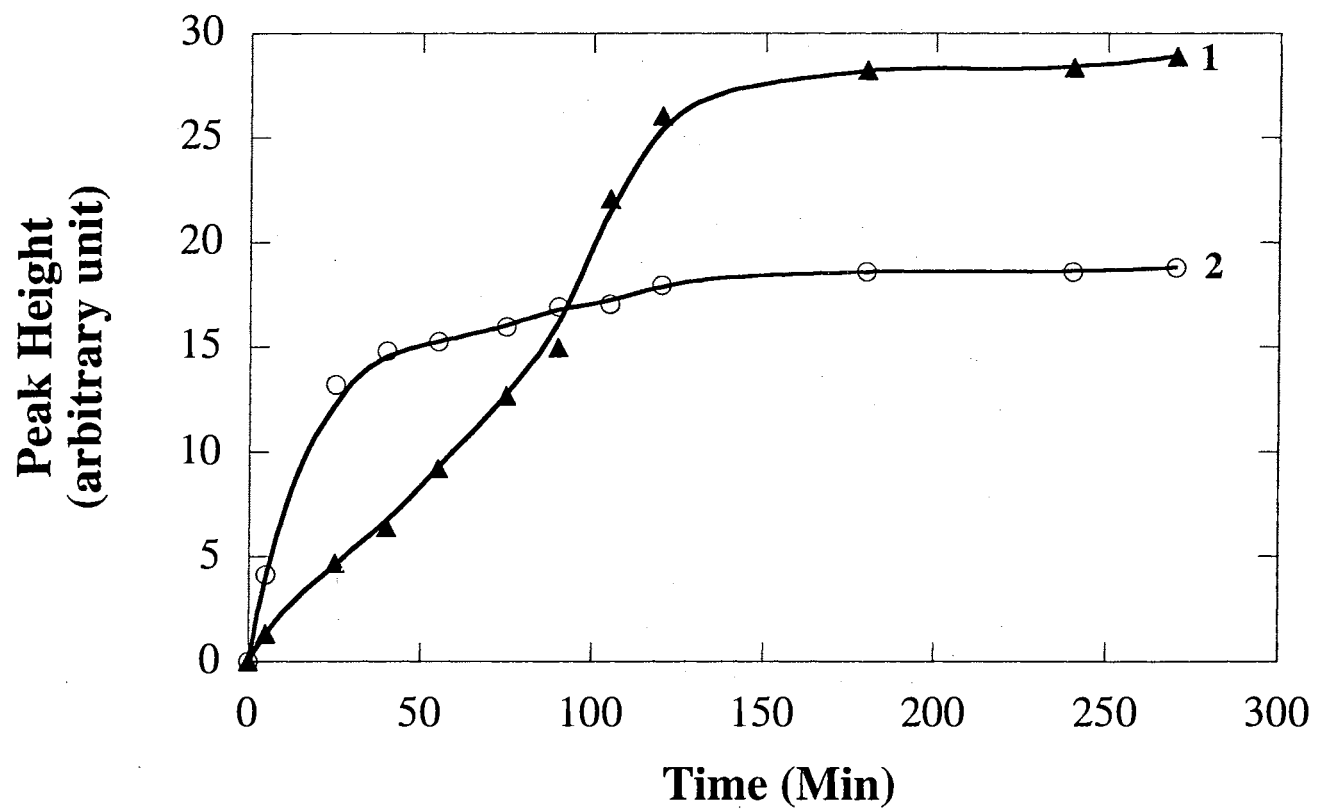


**Figure 4.** Time course for the derivatization reactions of glyceric acid with ANDSA (curve 1) and SA (curve 2).

proceeded at a faster rate with SA than with ANDSA. The derivatization with SA reached a steady state in almost one hour, while that with ANDSA required almost two and a half hours to reach the steady state. This may be due to differences in collision rates arising from differences in the molecular weights of the two derivatizing agents.

#### CZE of Derivatized Monosaccharides

Four different types of acidic monosaccharides were selected as model solutes in order to evaluate the effectiveness of the derivatization reaction under investigation. These were glyceric acid (the simplest acidic monosaccharide), gluconic acid (an aldonic acid), galacturonic acid (a uronic acid), and *N*-acetylneuraminic acid. The aldonic acids are the initial oxidation products of aldoses. Mild oxidation of an aldose results in the conversion of its aldehyde group to a carboxylic function thereby yielding an aldonic acid [14]. On the other hand, the specific oxidation of the primary alcohol group of aldoses yields uronic acids [14]. Unlike aldonic acids, uronic acids can assume the pyranose, furanose, and linear forms. Therefore uronic acids are still considered to be reducing sugars [15].

CZE at Low pH. The precolumn derivatization described in this study replaces the carboxylic group of the sugars with a strong acidic group, i.e., sulfonic group, which is fully ionized in the entire pH range. Thus, the derivatives can be electrophoresed at low pH as well as at high pH. In the pH range 2.0-3.5, and using an untreated fused-silica capillary with electrolytes of moderate ionic strength (e.g.,  $\geq 50$  mM), the electroosmotic flow (EOF) is almost not existent or very negligible. Under these conditions, and using a high voltage power source of negative polarity, negatively charged molecules will migrate toward the anode and will not be retarded by the EOF. Figures 5 and 6 illustrates the electropherograms of SA and ANDSA sugar derivatives, respectively, performed at pH 2.0, 2.5 and 3.0. As expected, the solutes eluted in the order of decreasing charge-to-mass ratio. In the case of SA derivatives, at pH 2.0 and 2.5 the derivatizing agent migrates away



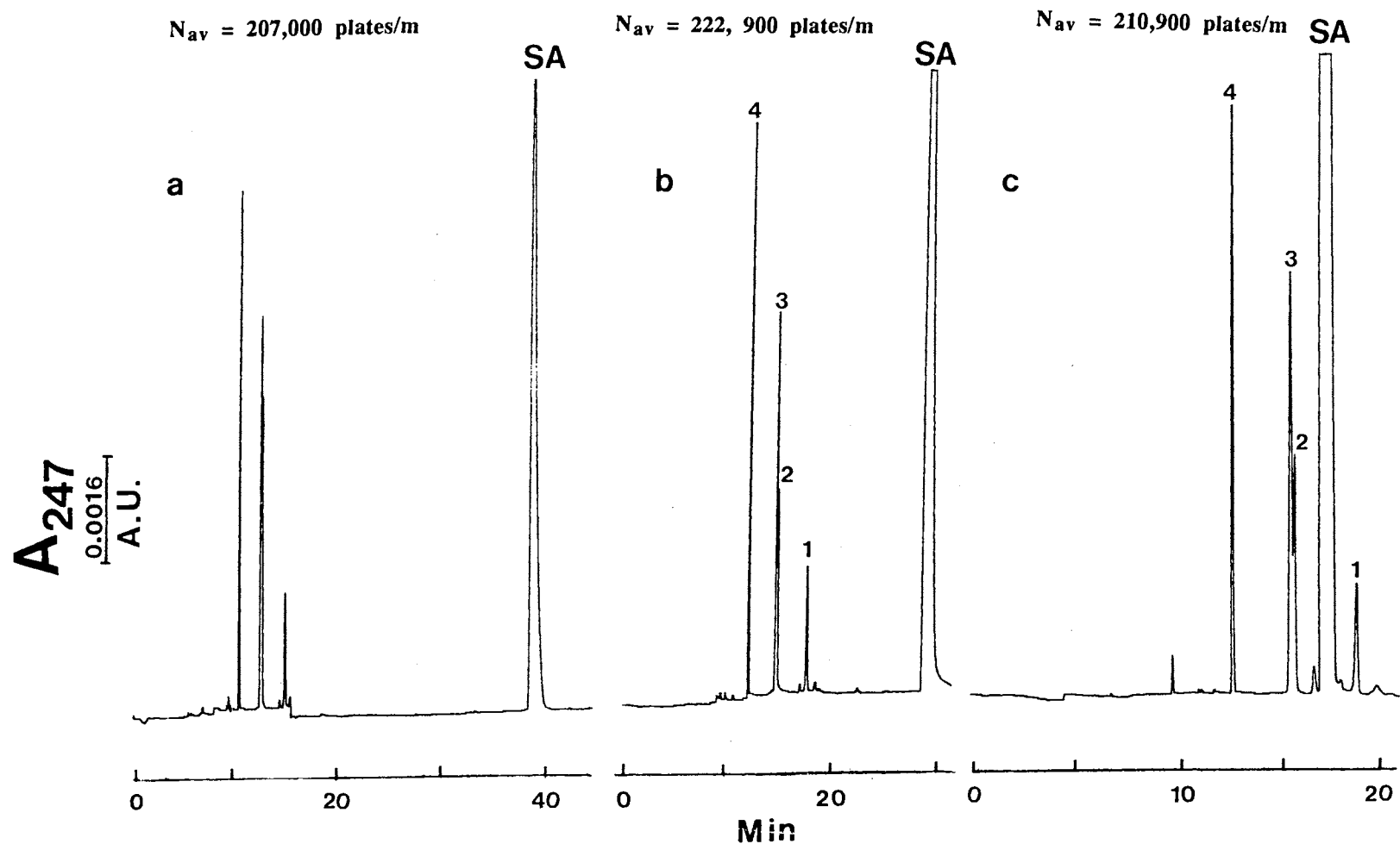


**Figure 5.** Electropherograms of SA derivatives of acidic monosaccharides. Separation capillary, untreated fused-silica, 50 cm (to detection point), 80 cm (total length) x 50  $\mu$ m I.D.; electrolytes, 100 mM phosphate at pH 2.0, 2.5 and 3.0 in (a), (b) and (c), respectively; running voltage, -20 kV; UV detection at 247 nm. Solutes: 1, NANA; 2, gluconic acid; 3, galacturonic acid; 4, glyceric acid; SA, sulfanilic acid.

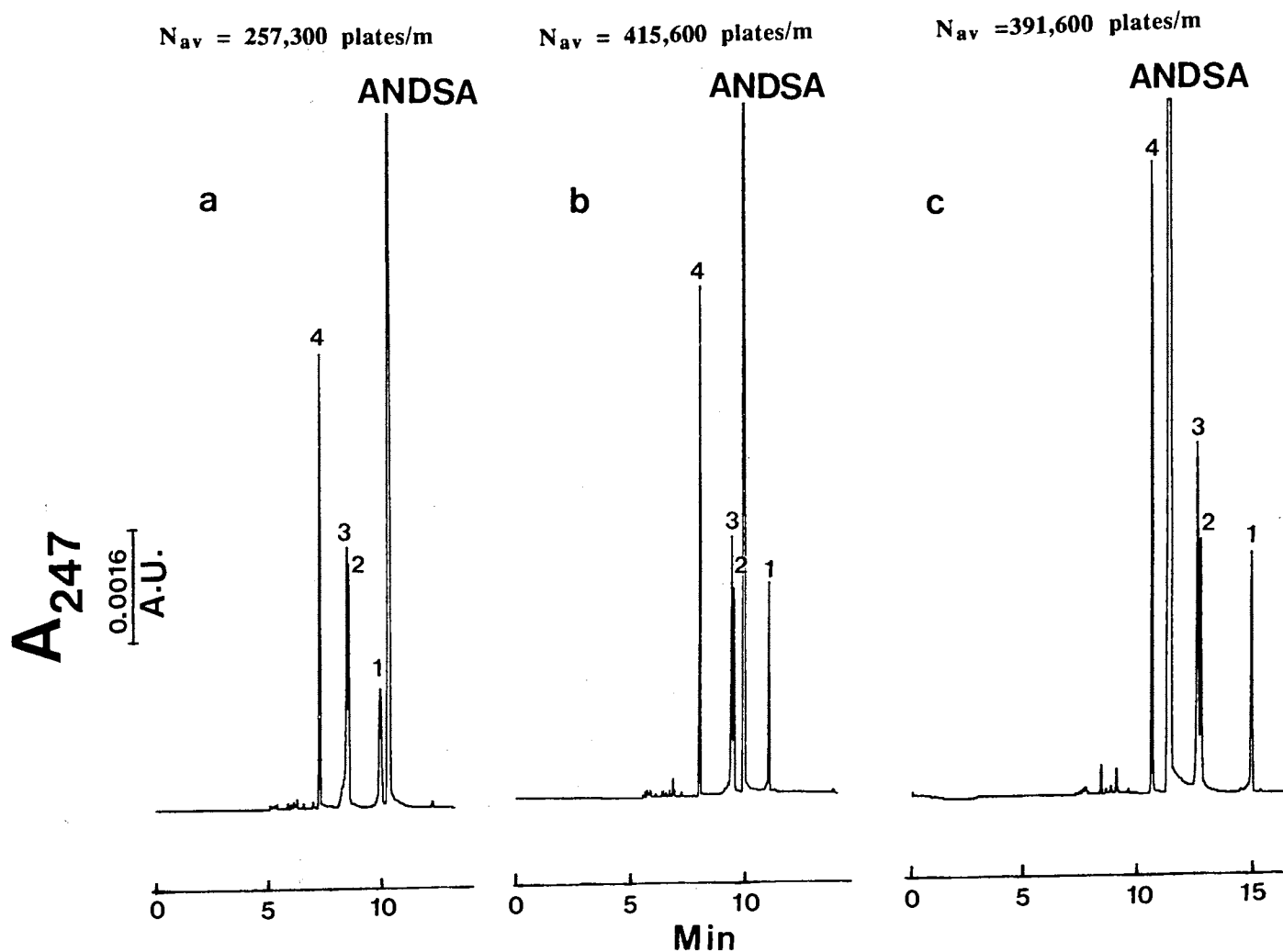


**Figure 6.** Electropherograms of ANDSA derivatives of acidic monosaccharides. Electrolytes, 100 mM phosphate at pH 2.0, 2.5 and 3.0 in (a), (b) and (c), respectively. Other conditions are as in Fig. 3. Solutes: 1, NANA; 2, gluconic acid; 3, galacturonic acid; 4, glyceric acid; ANDSA, 7-amino-1,3-naphthalene disulfonic acid.

from the derivatized molecules. SA has a sulfonic group as well as an amino group. Therefore, lowering the pH will ionize the amino group ( $pK_a = 3.23$ ) making it positively charged while the sulfonic group is negatively charged. The overall result of lowering the pH is a decrease in the net negative charge of the SA molecule which slow its migration toward the anode (see Fig. 5a, b, and c). The same effect is also observed with ANDSA (Fig. 6), but ANDSA has two sulfonic groups so that in the pH range 2.0-3.0, its net negative charge is higher than that of SA and consequently ANDSA migrated faster than SA in this system. In all cases, increasing the electrolyte pH from 2.0 to 3.0 increased slightly the migration times of the derivatized sugars, see Figs. 5 and 6. This may be attributed to a slight increase in the EOF (although the flow is extremely low) which is in the opposite direction to the electrophoretic mobilities of the analytes.

Another advantage of using electrolytes of low pH is the high separation efficiencies (the values of  $N$  is indicated on the electropherograms) when compared to those obtained with electrolyte systems of high pH described below.

CZE at High pH. At high pH, two different electrolyte systems were utilized, namely sodium borate and sodium phosphate. Figure 7 illustrates typical electropherograms obtained with ANDSA derivatives of the acidic monosaccharides using 50 mM sodium phosphate, pH 10.0, as the running electrolyte and a high voltage power source of positive polarity. Because the capillary is untreated, a strong electroosmotic flow ( $6.06 \times 10^{-4} \text{ cm}^2\text{V}^{-1}\text{sec}^{-1}$ ) in the direction of the cathode (which is at ground potential) was obtained. Apparently, this flow was capable of sweeping the negatively charged saccharides toward the cathode past the detection point. Since this EOF is in the opposite direction to the electrophoretic migration of the negatively charged analytes, the sulfonated sugar derivatives eluted in the order of increasing charge-to-mass ratios, i.e., NANA, which has the lowest charge-to-mass ratio, eluted first and was followed by gluconic acid, galacturonic acid, and glyceric acid. Although, galacturonic acid differed from gluconic

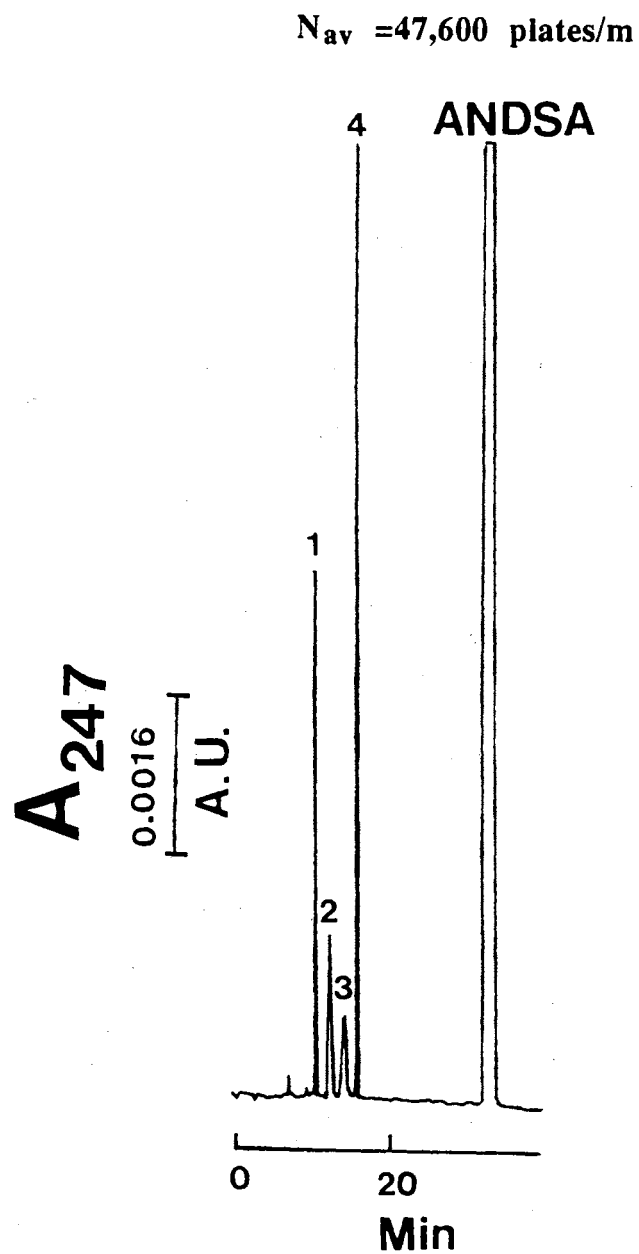


**Figure 7.** Electropherograms of ANDSA derivatives of acidic monosaccharides. Electrolyte, 50 mM phosphate, pH 10.0; running voltage +20 kV. Other conditions are as in Fig. 3. Solutes: 1, NANA; 2, gluconic acid; 3, galacturonic acid; 4, glyceric acid; ANDSA, 7-amino-1,3-naphthalene disulfonic acid.

acid by only  $0.16 \times 10^{-4}$  and  $0.17 \times 10^{-4}$  unit of charge-to-mass ratio in the case of SA and ANDSA derivatives, respectively, the two saccharides were baseline separated. This complete separation from gluconic acid may be attributed to the fact that galacturonic acid in aqueous solution can exist in linear as well as cyclic configurations, i.e., it differs from gluconic acid in molecular shape. The SA derivatives eluted in the same order, and also yielded approximately the same plate counts (results not shown) as that of ANDSA sugar derivatives but the analysis time was shorter by a factor of 2.35. This is because the former derivatives are singly negatively charged while the latter are doubly negatively charged.

It is well established that at alkaline pH, borate ions form *in situ* anionic complexes with carbohydrates [16,17], thus facilitating their separation by electrophoresis [18]. In general, vicinal hydroxyl groups (i.e., diols) with *cis* configuration form more stable complexes than *trans* diols [16,17]. Figure 8 portrays a typical electropherogram obtained with the ANDSA derivatives of the monosaccharides using 100 mM borate (pH 10.0), a positive polarity high voltage power source and an on column fluorescence detector. As with the phosphate electrolyte system, the electroosmotic flow is very strong ( $6.22 \times 10^{-4} \text{ cm}^2 \text{ V}^{-1} \text{ sec}^{-1}$ ) and its direction is toward the cathode, which is at ground potential. This strong EOF was capable of sweeping the negatively charged analytes past the detector. When compared to the preceding electrolyte system based on sodium phosphate, borate complexation is a better approach for carbohydrate separation providing an enhanced selectivity, compare Fig. 7 to Fig. 8. Glyceric acid is the most retarded solute thus indicating stronger complexation with borate than the other derivatized sugars. This finding corroborate earlier observation [16] in that  $\alpha$ -hydroxy acids such as glyceric acid form strong complexes with borate a trend that was "explained by assuming that the carboxyl group is hydrated to  $\text{C}(\text{OH})_3$ , as a result of which a very favorable situation prevails in these acids for the formation of a boric acid complex" [16]. It should be noted

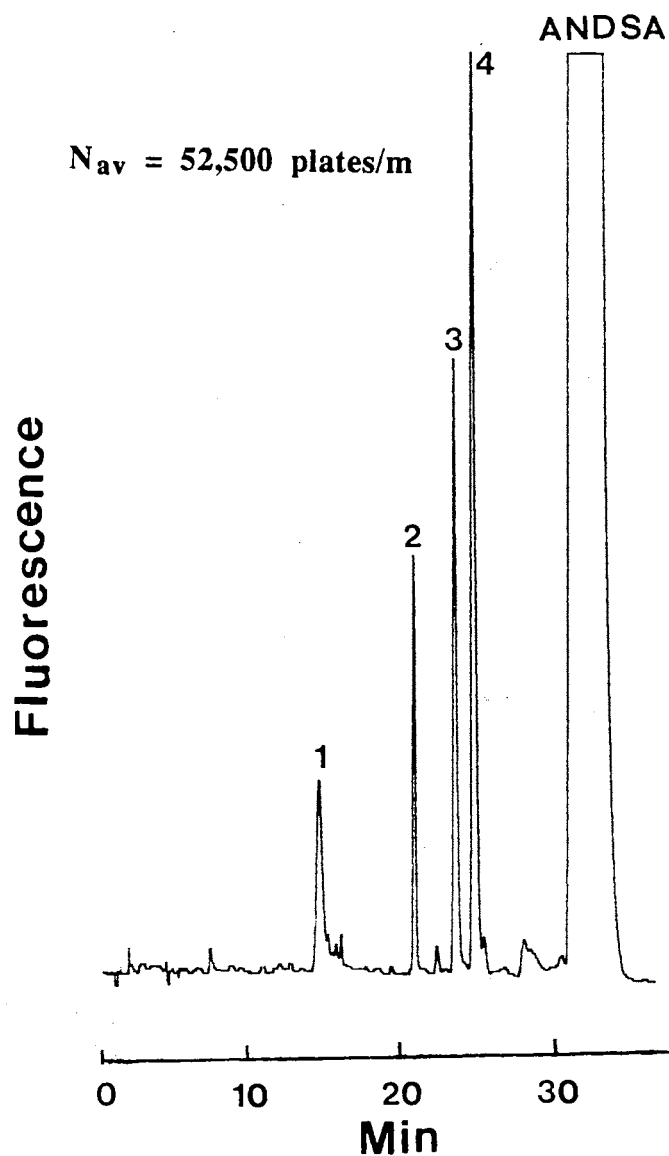


**Figure 8** Electropherogram of ANDSA derivatives of acidic monosaccharides. Electrolyte, 100 mM borate, pH 10.0; running voltage, +20 kV. Fluorescence detection, excitation wavelength = 315 nm, sharp cut-off long absorption filter of 400 nm was used as an emission filter. Other conditions are as in Fig. 3. Solutes: 1, NANA; 2, gluconic acid; 3, galacturonic acid; 4, glyceric acid; ANDSA, 7-amino-1,3-naphthalene disulfonic acid.

also that glyceric acid is the smallest acidic monosaccharide. Galacturonic acid, which has two pairs of vicinal hydroxyl groups in the *cis* configuration at C3/C4 and C1/C2, formed strong complex with borate and eluted before glyceric acid. The cyclic NANA has only three vicinal hydroxyl groups in the glycerol moiety of the molecule. This property coupled with the fact that NANA has the biggest size among the monosaccharides studied may explain its short migration time. Since gluconic acid is a linear monosaccharide, the hydroxyl groups will occupy a favorable position with reference to one another to undergo complexation with borate [19]. Figure 9 illustrates the behavior of the ANDSA derivatives at various borate concentration. As expected, the migration time increases with borate concentration because the amount of sugar-borate complex increases according to the law of mass action. As can be seen in Fig. 9, the best compromise in terms of analysis time and resolution is reached when the running electrolyte was 100 mM borate. In total, at pH 10 and borate concentration  $\geq 100$  mM, the elution order of the sugars parallels that obtained with phosphate. Also, the plate count is about the same as in the case of phosphate, pH 10. The major difference is an enhanced resolution among the analytes in the presence of borate in the running electrolyte. As shown in Fig. 10, the SA derivatives showed similar elution pattern to that of the ANDSA derivatives. The major difference between both derivatives is that the SA-sugars were better resolved at pH 10.5 (i.e., 0.5 pH unit higher than with ANDSA) and required adding one and a half times more borate in the running electrolyte (i.e.,  $\geq 150$  mM) than the ANDSA derivatives. This is expected since the magnitude of the net negative charge of the SA derivatives is increased as the extent of borate complexation with carbohydrates is increased by rising the pH and borate concentration.

#### On Column Detection of the Derivatized Monosaccharides

The tagging of the acidic monosaccharides with SA and ANDSA allowed their detection in the UV and fluorescence at low levels. ANDSA is a fluorescent tagging agent

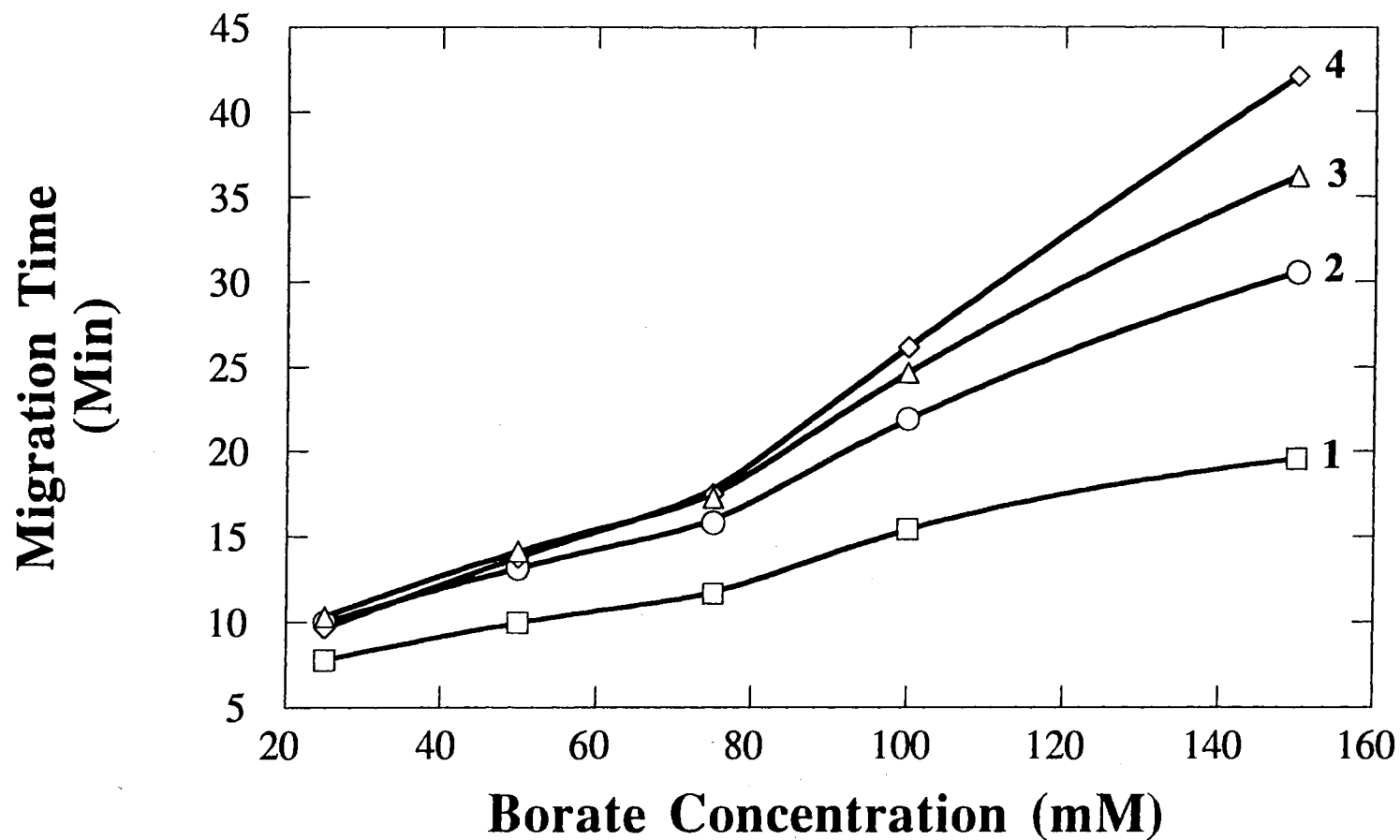


**Figure 9.** Plots of migration times of ANDSA derivatives of acidic monosaccharides versus borate concentration. Electrolytes, sodium borate at various concentration, pH 10.0; running voltage, +20 kV, pH 10.0. Other conditions are as in Fig. 3. Symbols: 1, NANA; 2, gluconic acid; 3, galacturonic acid; 4, glyceric acid.



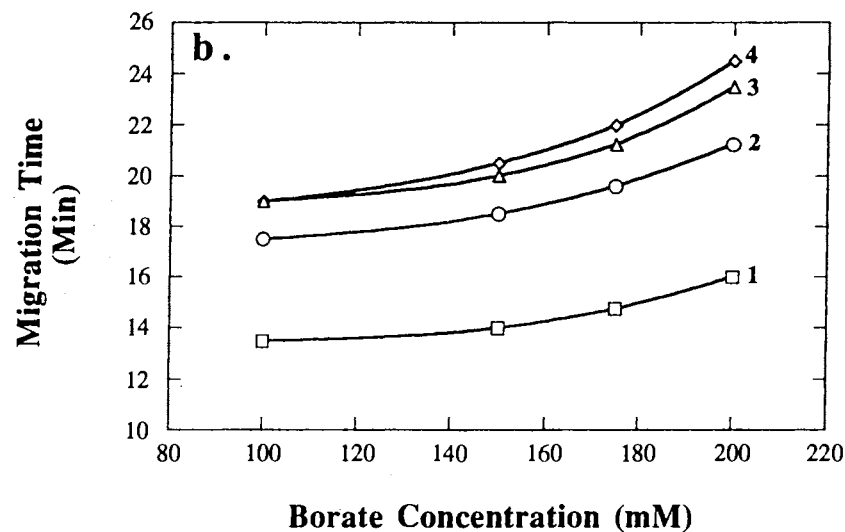
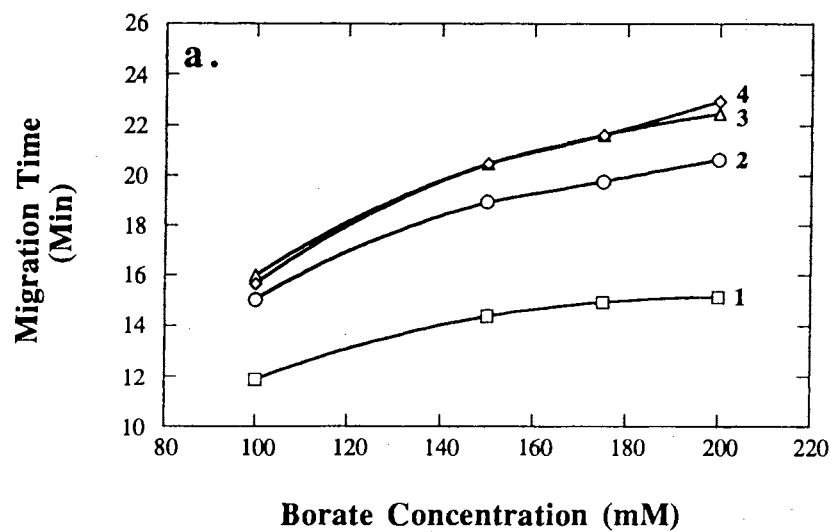


**Figure 10.** Plots of migration times of SA derivatives of acidic monosaccharides versus borate concentration. Electrolytes, sodium borate at various concentration, pH 10.0 and 10.5 in (a) and (b), respectively; running voltage, +20 kV. Other conditions are as in Fig. 3. Lines: 1, NANA; 2, gluconic acid; 3, galacturonic acid; 4, glyceric acid.

with a maximum excitation signal at 315 nm and a maximum emission signal at 420 nm [20]. A typical electropherogram with on column fluorescence detection using a 200 W xenon-mercury lamp as the radiation source is portrayed in Fig. 8. The minimum detectable quantity of SA derivatives with a UV detector is ca. 30 femtomoles, while that of ANDSA derivatives is ca. 15 femtomoles using regular fused-silica capillaries with a light path equal to the capillary inner diameter. These results corroborate well with the fact that the molar absorptivity of ANDSA is almost twice that of SA, see above. The fluorescence detection of ANDSA derivatives exhibited higher sensitivity than the UV detection, with a minimum detectable quantity of approximately 0.6 femtomole; a decrease by a factor of 25 with respect to the UV detection. These figures were improved when extended light path capillaries obtained from HP were utilized. These capillaries contain a three-times expanded diameter section (bubble) at the point of detection. This design is expected to improve sensitivity up to a factor of three over the standard capillaries without sacrificing resolution. Experimentally, in our case, the sensitivity is improved by a factor of 2.85. This lower the minimum detectable amount of ANDSA derivatives to ca. 5.3 femtomoles, and that of SA derivatives to 10.5 femtomoles. The HP extended path capillaries could not be mounted on the in-house fluorescence instrument to evaluate the performance of the capillary design in this mode of detection. However, and on the basis of the UV detection, one can predict that the minimum detectable amount could be lowered by a similar factor to that in the UV, which should allow the detection of ANDSA derivatives down to 0.2 femtomole, i.e., ca. 200 attomoles.

### Conclusions

In summary, we have developed and evaluated a precolumn derivatization reaction for acidic carbohydrates to allow their sensitive detection by on column UV and/or fluorescence monitoring. The reaction exploited the reactivity of the carboxyl group of sugars which can be readily condensed with an amino group of a given tagging agent in the

presence of a water soluble carbodiimide. The derivatization reaction has several advantages including (i) specific attachment of the tag, (ii) relatively rapid reaction with high yields, (iii) little or no sample clean up and (iv) replacement of the weak carboxylic acid by a strong sulfonic acid, thus imparting permanent negative charge to the sugar molecule over a wide pH range. These features allowed the high resolution separation of acidic carbohydrates with sensitivities down to very low femtomole levels by UV and fluorescence detection.

## References

1. Honda, S., Iwase, S., Makino, A. and Fujiwara, S., *Anal. Biochem.*, 176 (1989) 72.
2. Nashabeh, W. and El Rassi, Z., *J. Chromatogr.*, 600 (1992) 279.
3. Nashabeh, W. and El Rassi, Z., *J. Chromatogr.*, 514 (1990) 57.
4. Lee, K.-B., Al-Hakim, A., Loganathan, D. and Linhardt, R., *Carbohydr. Res.*, 214 (1991) 155.
5. Liu, J., Shiota, O. and Novotny, M., *Proc. Natl. Acad. Sci. USA*, 88 (1991) 2302.
6. Honda, S., Ueno, T. and Kakehi, K., *J. Chromatogr.*, 608 (1992) 289.
7. Pigman, W., in Pigman, W., Ed., *The Carbohydrates*, Academic Press, New York 1957, p. 406.
8. Gottschalk, A., in Gottschalk, A., Ed., *Glycoproteins*, Vol. 5, part A, Elsevier, Amsterdam 1972, p. 141.
9. Hara, S., Takemori, Y., Yamaguchi, M., Nakamura, M. and Okura, Y., *Anal. Biochem.*, 164 (1987) 138.
10. Hara, S., Yamaguchi, M., Takemori, Y., Furuhata, K., Ogura, H. and Nakamura, M., *Anal. Biochem.*, 179 (1989) 162.
11. Langenbeck, U., Mohring, H. and Dieckmann, K., *J. Chromatogr.*, 115 (1975) 65.
12. Khorana, H.G., *Chem. Revs*, 53 (1953) 145.
13. Khorana, H. G., *J. Chem. Soc.*, (1952) 2081.
14. Theander, O., in : Pigman, W. and Horton, D., Eds., *The Carbohydrates, Chemistry and Biochemistry*, 2nd edit., Vol. IB, Academic Press, New York, 1980, p.1014.
15. Voet, D. and Voet, J., *Biochemistry*, John Wiley, New York 1990, 1018.
16. Boeseken, J., *Adv. Carbohydr. Chem.*, 4 (1949) 189.
17. Foster, A.B., *Adv. Carbohydr. Chem.*, 12 (1957) 81.
18. El Rassi, Z., *Adv. Chromatogr.*, 34 (1994) 177.
19. Davis, H.B. and Mott, C.J.B., *J. Chem. Soc. Faraday I*, 76 (1980) 1991.

20. Lee, K.-B., Kim, Y.-S., and Linhardt, R., *Electrophoresis*, 12 (1991) 636.

## CHAPTER IV

### CAPILLARY ELECTROPHORESIS OF CARBOXYLATED CARBOHYDRATES. 1. SELECTIVE PRECOLUMN DERIVATIZATION OF GANGLIOSIDES WITH UV ABSORBING AND FLUORESCENT TAGS

#### Introduction

Gangliosides are sialic acid-containing glycosphingolipids found in nearly all vertebrate tissues [1, 2]. They reside in the plasma membrane and can act as receptor binding sites on the cell surface. A ganglioside molecule has a hydrophilic sialooligosaccharide chain and a hydrophobic moiety, i.e. ceramide, that consists of a sphingosine and fatty acid [3], see Fig. 6 of Chapter II. The sialic acid residues, which determines the negative charge of the ganglioside molecule, seems to be involved in regulating the physiological capabilities of gangliosides such as reactivity with toxins, viruses, antibodies and growth factors [4-6].

Growing interest in the numerous and important biological functions of gangliosides has engendered the need for capable separation techniques for their isolation and determination. Chromatography in its various forms has been a widely used technique in the isolation of gangliosides [3, 7-10]. As with most of other carbohydrate species, one of the major difficulties encountered in the analysis of gangliosides is the lack of chromophores in their molecules. This inherent property hinders their determination at low levels since their detection in the UV below 200 nm is met with relatively low sensitivity. The low detectability of underivatized gangliosides is also problematic because most gangliosides are often only available in minute amounts. Thus, besides the need for sensitive detection methodologies there is also a strong demand for microcolumn separation

methods of high resolving power and small sample requirements. In this regard, high performance capillary electrophoresis (HPCE) is the alternative technique for the analytical separation and determination of gangliosides. In fact, HPCE has already been briefly explored in the separation of underivatized gangliosides using low wavelength UV detection [11, 12].

To overcome the detectability problem, several precolumn derivatization reactions have been already reported for the tagging of gangliosides, and in particular prior to separation by high performance liquid chromatography (HPLC). UV-absorbing perbenzoyl [13,14] and *p*-nitrobenzyloxyamine derivatives [15] are typical examples. Although, the sensitivity of these procedures was sufficiently high, the reactions were not specific for gangliosides and moreover, prewashing to remove reagents and by-products was necessary prior to separation. Nakalayashi and co-workers [10] introduced a specific precolumn derivatization of gangliosides based on the formation of an ester bond between *p*-bromophenacyl bromide reagent and the carboxylic group of the sialic acid moieties, and demonstrated its suitability for the analysis of the derivatives by HPLC. Although convenient to regenerate the original molecule, the susceptibility of the ester bond to hydrolysis makes this specific derivatization [10] rather unsuitable for the production of stable derivatives.

Similar to HPLC, with HPCE it is preferable that precolumn derivatization be selective. In addition, the tag should be charged or if it is neutral, its attachment to the carbohydrate molecule should not eliminate the already existing charge of the solute molecule so that separation in an electric field would be possible. Very recently, we have shown that these two requirements are readily met by exploiting the reactivity of the carboxylic group of acidic monosaccharides [16], see Chapter III. Since gangliosides are sialic acid containing glycolipids, the carboxylic groups of the sialic acid residues can also be readily tagged as in the case of carboxylated monosaccharides. The tagging procedure [16] involves the formation of a stable amide bond between the carboxylic group of the

sugar analyte and the amino group of the derivatizing agent, e.g. 7-aminonaphthalene-1,3-disulfonic acid or sulfanilic acid, in the presence of water-soluble carbodiimide. Besides providing the chromophore or fluorophore, the derivatization reaction utilized here replaces the weak carboxylic acid group of the gangliosides by the strong sulfonic acid group, thus ensuring permanent negative charges on the derivatives over the entire pH range.

This study is a logical continuation to our recent contribution to the area of separation of minute amounts of acidic carbohydrates by HPCE. Herein we report (i) the evaluation of the new derivatization procedure in the selective tagging of carboxylated glycoconjugates, e.g. gangliosides, and (ii) the introduction of novel electrolyte systems for the separation of gangliosides in capillary electrophoresis.

## Materials and Methods

### Instruments and Capillaries

The instrument for capillary electrophoresis was assembled in-house from commercially available components [16-18] and a description of the instruments used is included in Chapter III.

### Reagents and Materials

Gangliosides  $G_{M1}$ ,  $G_{D1a}$ , and  $G_{D3}$  were extracted from bovine brain as described below and elsewhere [19]. Ganglioside type III mixture (containing approx. 20% N-acetylneuraminic acid) and standard monosialoganglioside ( $G_{M1}$ ) from bovine brain were purchased from Sigma Chemical Co. (St. Louis, MO, USA). Standard disialogangliosides ( $G_{D1a}$ ,  $G_{D1b}$ , and  $G_{D3}$ ) and trisialoganglioside ( $G_{T1b}$ ) were obtained from Sigma and from Matreya Inc. (Pleasant Gap, PA, USA). Neuraminidase from *Clostridium perfringens* and MEGA 10 (decanoyl-*N*-methylglucamide) surfactant were purchased from Calbiochem Corp. (LaJolla, CA, USA).  $\alpha$ -Cyclodextrin ( $\alpha$ -CD) was donated by the American Maize-Products Co. (Hammond, IN, USA). Reagent grade sodium phosphate monobasic,



hydrochloric acid, sodium hydroxide, boric acid granular, and HPLC-grade acetonitrile (ACN) were obtained from Fisher Scientific (Pittsburgh, PA, USA). Poly(vinyl alcohol) (PVA), 87-89% hydrolyzed (M.W. 124 000-186 000) and hydroxypropyl cellulose (HPC) of average M.W. 100 000 were purchased from Aldrich (Milwaukee, WI, USA). A reversed-phase HPLC column, C<sub>18</sub>-silica Microsorb-MW, with 5 µm mean particle diameter and 100 Å mean pore diameter was purchased from Rainin Instrument Co. (Woburn, MA, U.S.A.). This column was used in purifying the side products of the derivatization reactions. The sources of the other materials used in this chapter are the same as those listed in Chapter III.

### Extraction of Gangliosides

Approximately 500 grams of bovine brain tissues were extracted. Tissues were homogenized and extracted twice with 1 500 mL of chloroform/methanol (2:1, v/v) and once with isopropanol/hexanes/water (55:25:20, v/v/v). Following Folch's partition [20] the upper layer glycolipids were subjected to DEAE-Sephadex column chromatography to separate neutral and acidic glycolipids (sulfatide and gangliosides) [21]. The acidic glycolipids were eluted in three fractions with increasing salt concentration. The monosialogangliosides were eluted with 0.05 M NH<sub>4</sub>OAC in MeOH, sulfatide and the disialogangliosides with 0.15 M NH<sub>4</sub>OAC in MeOH and polysialogangliosides with 0.45 M NH<sub>4</sub>OAC in MeOH. The lower phase glycolipids were acetylated and subjected to column chromatography with Florisil [22]. Further purification of the gangliosides was performed by HPLC with a Varian model 9012 HPLC system using a column (1 x 100 cm) of Latrobeads (6RS-8010, Latron, Tokyo, Japan) and eluted at 2.0 mL/min with a 200 min gradient of isopropanol/hexanes/water [19, 23] from 55 : 44 : 1 (v/v/v) to 55 : 20 : 25 (v/v/v). Further purification of individual glycolipids was accomplished by preparative high performance thin layer chromatography (HPTLC) with the use of chloroform/methanol/water (55:40:10, v/v/v containing 0.02% CaCl<sub>2</sub>). Separated

glycolipids were visualized with ultraviolet light after being sprayed with 0.1% primuline in 80% aqueous acetone. Once visualized, individual glycolipids were recovered from HPTLC plates by scraping followed by sonication in isopropanol/hexanes/water (55:25:20, v/v/v).

#### Derivatization of gangliosides

Gangliosides were tagged with ANDSA or SA as previously described in ref. [16] (Chpter III). Briefly, an aliquot of 50  $\mu\text{L}$  of 100 mM aqueous solution of EDAC, pH 5.0, was initially added to sub-microgram amounts of solid gangliosides and the mixture was stirred for 1 hr. Then, 50.0  $\mu\text{L}$  of 100 mM aqueous solution of the derivatizing agent were added and the mixture was stirred for an additional 1.5 hrs. Subsequently, the entire reaction mixture containing the derivatized gangliosides, excess derivatizing agent and other components of the reaction mixture was analyzed by capillary zone electrophoresis (CZE).

#### Neuraminidase Treatment

An aliquot of 20.0  $\mu\text{L}$  of the SA derivative of  $\text{G}_{\text{T1b}}$  aqueous solution was added to 7.0  $\mu\text{L}$  of neuraminidase (i.e., 0.028 units), dissolved in 50.0  $\mu\text{M}$  sodium acetate buffer, pH 5.0, and the mixture incubated at 37  $^{\circ}\text{C}$  for 72 hrs [24-26]. Aliquots of the reaction mixture were taken at various time intervals and analyzed by CZE.

### Results and Discussion

Throughout the various studies concerning the electrophoretic behavior of derivatized gangliosides, the results were compared to those obtained with their underivatized counterparts in order to assess the various changes that might have been caused by the precolumn labeling of the different gangliosides.

In evaluating the suitability of the various electrophoretic systems under consideration, gangliosides type III mixture, which was purchased from Sigma, as well as

individual gangliosides were utilized. The type III mixture may contain essentially  $G_{M1}$ ,  $G_{D1a}$ ,  $G_{D1b}$  and  $G_{T1b}$  since it is known that mammalian brains generally contain these four major gangliosides [3,27] in the concentration ratios of 2:3.5:1:1.5, respectively [27].

#### Precolumn Derivatization of Gangliosides

The use of low wavelengths (e.g., 195 nm or 185 nm) for the detection of underivatized gangliosides impairs the utility of many buffer systems because at these wavelengths the components of the electrolyte systems starts to absorb substantially in the UV, thus leading to high background signals. The lack of suitable chromophores in ganglioside molecules makes their detection impossible at high wavelengths where many useful running electrolytes are UV transparent. To overcome this difficulty, and permit the sensitive detection at higher wavelengths, the gangliosides were derivatized with SA and ANDSA according to established procedures for carboxylated carbohydrates which were recently introduced by our laboratory [16]. The precolumn derivatization reaction involves a condensation reaction between the free amino group of the derivatizing agent and the free carboxyl group of the ganglioside to form a peptide link by acid-catalyzed removal of water in the presence of EDAC. The carbodiimide EDAC, which is required to promote the formation of the peptide bond [28,29], was selected because of its high solubility in aqueous solutions. The derivatization proceeds according to the scheme illustrated in Fig. 1 of Chapter III.

Individual gangliosides as well as Sigma type III ganglioside mixture were derivatized according to the above scheme. Typical electropherograms of both SA and ANDSA derivatives of type III mixture are displayed in Fig. 1. The excess of derivatizing agent eluted at 23 min for SA (Fig. 1a) while it did not elute in reasonable time in the case of ANDSA (Fig. 1b) when 15 kV were used as the running voltage. The detection wavelength was set at 247 nm since the UV spectra of both derivatizing agents, i.e., SA and ANDSA, as well as the gangliosides derivatives showed maximum absorbance at 247

nm. Returning to Fig. 1, the signal of disialogangliosides ( $G_{DS}$ ) is much greater than that of  $G_{M1}$  and  $G_{T1b}$ . As stated above, there are more  $G_{DS}$  in the mixture than mono- and trisialogangliosides. Since  $G_{T1b}$  and  $G_{DS}$  have three and two derivatization sites, respectively, under exhaustive precolumn derivatization conditions two and three chromophores could be attached to  $G_{T1b}$  and  $G_{DS}$ , respectively. This would explain the difference between peak height ratios of derivatized and underivatized gangliosides (compare Fig. 1 and Fig. 5c).

As can be seen in Fig. 1a and b, in addition to the derivatized gangliosides, by-products are also produced in the precolumn derivatization reaction. The by-products were detected by UV at 247 nm (in the case of SA and ANDSA) and by fluorescence in the case of ANDSA. This suggests that both by-products possess the derivatizing agents as part of the molecule. This was further confirmed by the electrophoretic behaviors of the by-products when varying the pH of the running electrolyte. The SA by-product seems to be neutral at  $\text{pH} \geq 5$  and positively charged at  $\text{pH} < 5$  as inferred from its migration with or ahead of the marker of the electroosmotic flow (EOF), respectively. The by-product of ANDSA has a net negative charge at  $\text{pH} \geq 5$  and neutral at  $\text{pH} < 5$  as indicated by the migration time of its peak with respect to that of the EOF marker. The  $\text{pK}_a$  values of the amino groups of SA and ANDSA are in the range of 3-4 [30]. Together, these observations imply that the by-product of SA has involved reaction with the sulfonic acid group of the SA molecule while leaving its amino group unsubstituted. The same conclusion could be drawn regarding the ANDSA by-product whereby one sulfonic acid group of the molecule has been involved in the reaction while the other sulfonic acid group and the amino group were left unsubstituted. In fact, studies made by  $^1\text{H}$  NMR and  $^{13}\text{C}$  NMR on an HPLC purified fraction of the by-product of ANDSA agreed with these observations. Both modes of NMR suggested the presence of alkylated moieties attached to the derivatizing agent which may indicate that the by-product is the result of the reaction between the derivatizing agent and the carbodiimide.

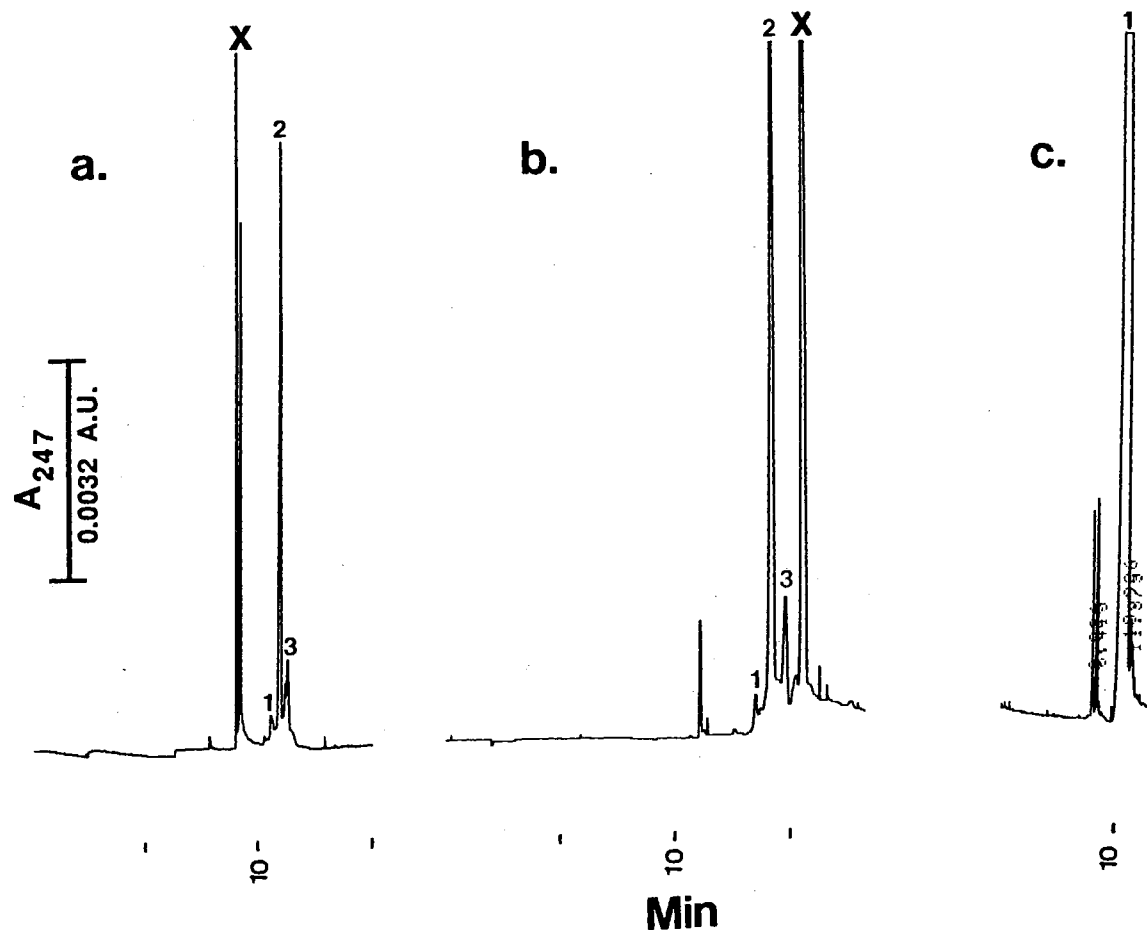


**Figure 1.** Typical electropherograms of SA (a) and ANDSA (b) derivatives of the ganglioside mixture type III from Sigma and ANDSA derivative of standard  $G_{D1a}$  (c). Capillary, 80.0 cm (total length), 50.0 cm (to detection)  $\times$  50  $\mu$ m i.d.; running voltage, 15.0 kV in (a) and (b) and 20.0 kV in (c). Running electrolytes: (a) and (b): 150 mM borate containing 15.0 mM  $\alpha$ -CD, pH 10.0; (c) 10 mM sodium phosphate, pH 7.0, containing 15.0 mM  $\alpha$ -CD. Peak assignments in (a) and (b): 1 =  $G_{M1}$ , 2 =  $G_{D1a}$  and  $G_{D1b}$ , 3 =  $G_{T1b}$ , x = by-product; in (c): 1 =  $G_{D1a}$ .

The by-products were seen when the amount of ganglioside added to the reaction mixture was not well controlled. With almost all ganglioside samples we did not have sufficient quantities that would allow the accurate weighing of a known and desirable amount. In other words, the side product was observed only when the amount of carbodiimide far exceeded the amount of analyte in the reaction mixture. In fact, when the reaction was made such that for each mole of carboxylic group, one mole of EDAC and two moles of SA or ANDSA were added, the derivatization reaction did not lead to the formation of detectable amount of side product as was the case of  $G_{D1a}$  (Fig. 1c). The absence of by-products was also observed with acidic monosaccharides reported earlier [16] whenever the ratio of 1:1:2 of sugar : carbodiimide : derivatizing agent was utilized.

To confirm the occurrence of the derivatization at the sialic acid site, the derivatized trisialoganglioside SA- $G_{T1b}$  was treated with neuraminidase (for structure, see Fig. 6 in Chapter II). Neuraminidase is an exoglycosidase which catalyzes the hydrolysis of the linkage joining a terminal sialic acid residue to a D-galactose or a D-galactosamine residue [31]. Since  $G_{M1}$  is resistant to neuraminidase, and  $G_{T1b}$  is hydrolyzed more rapidly than  $G_{Ds}$  [32], the cleavage of  $G_{T1b}$  with neuraminidase should result in the production of  $G_{M1}$  and  $G_{D1b}$  [25,26]. This is shown in Fig. 2 where SA derivatized  $G_{T1b}$  gave one peak before treatment with neuraminidase and three peaks after exhaustive treatment with neuraminidase. Two additional peaks have also appeared which were assumed to correspond to the cleaved mono- and disialic acid residues. The relatively intense peak that appeared at 19.2 min may be the SA derivative of sialic acid cleaved from  $G_{T1b}$  to yield  $G_{D1b}$  (i.e., the  $R_1$  residue, see Fig. 6 in Chapter II) while the less intense peak that eluted at 13.1 min may correspond to the SA derivative of disialic acid cleaved from  $G_{T1b}$  to yield  $G_{M1}$  (i.e., the  $R_2$ -sialic acid residues, see Fig. 6 in Chapter II). The assumption that the less intense peak is that of the disialic acid and the more intense peak is that of the sialic acid monomer, corroborates well with the fact that the amount of  $G_{M1}$  produced is much less than that of the  $G_{D1b}$ . The excess SA was observed at 23.1 min.

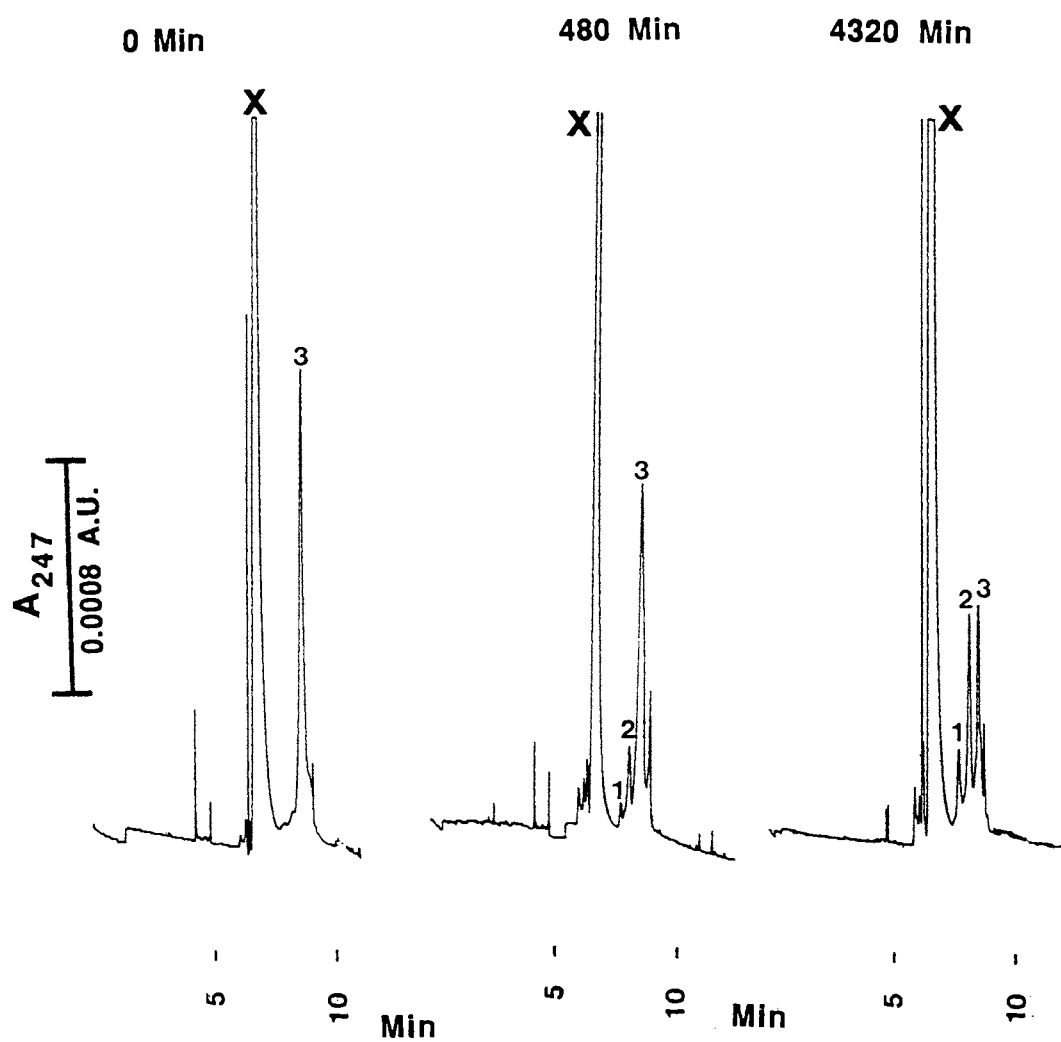


**Figure 2.** Monitoring of the neuraminidase action on the SA derivative of GT1b by capillary electrophoresis. Conditions as in Fig. 1a and b. Peak assignments: 1 = GM<sub>1</sub>, 2 = GD<sub>1b</sub>, 3 = GT<sub>1b</sub>, x = by-product.

The progress of the derivatization reaction with SA and ANDSA was monitored by CZE using the type III ganglioside mixture. Typical time course plots for SA-G<sub>T1b</sub> and ANDSA-G<sub>T1b</sub> are shown in Fig. 3 in terms of integrated peak heights versus time. In all cases, the precolumn derivatization reaction proceeded at a faster rate with SA than with ANDSA. The derivatization with SA reached a steady state in almost 1 hr, while that with ANDSA required almost 2.5 hrs to reach the steady state. These results corroborate earlier findings with carboxylic monosaccharides [16] (Chapter III), and may be attributed to differences in collision rates arising from differences in the molecular weights of the two derivatizing agents.

#### Capillary Electrophoresis of Gangliosides

It is well established that gangliosides exist as stable micelles in aqueous solutions with critical micellar concentration (CMC) in the range of  $10^{-10}$  -  $10^{-8}$  M [10, 33]. This phenomenon hinders the efficient separation of gangliosides as monomeric species in neat aqueous media. Consequently, an organic solvent or an additive capable of breaking the micelles is needed. In this study, acetonitrile and other additives were added individually to the running electrolytes used in separating the gangliosides. One virtue of the precolumn derivatization is that SA and ANDSA derivatives have maximum absorptivity at 247 nm far removed from low UV wavelengths (e.g., 195 nm) where only few solvents and light buffers can be used. In addition, ANDSA derivatives are readily detected by fluorescence.

HPLC grade acetonitrile (ACN) was used as the organic modifier for the separation of gangliosides because its UV cut-off is 185 nm. Figure 4 shows the separation of standard derivatized gangliosides at basic and neutral pH. At both pHs, and in the absence of acetonitrile in the running electrolyte the ANDSA-gangliosides eluted as a single broad peak with no separation, see Fig. 4a and c. The inclusion of 50% ACN in the running electrolyte has apparently brought about the break up of aggregation and in turn the separation of the gangliosides. The same trend was also observed with the underivatized



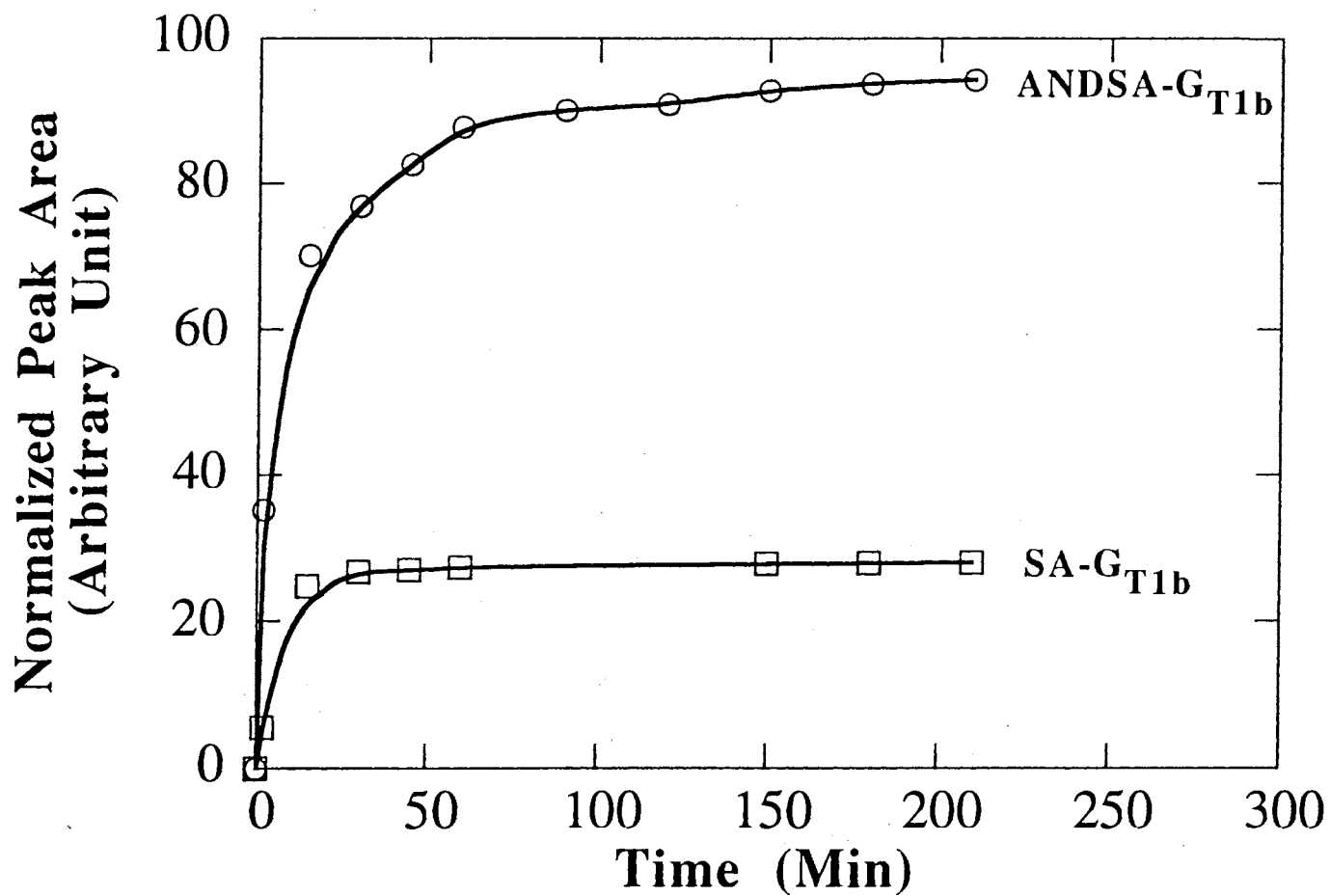


**Figure 3.** Time course for the derivatization reactions of G<sub>T1b</sub> with ANDSA and SA. The reaction mixture was subjected to CZE at different time interval using conditions of Fig. 1a and b.

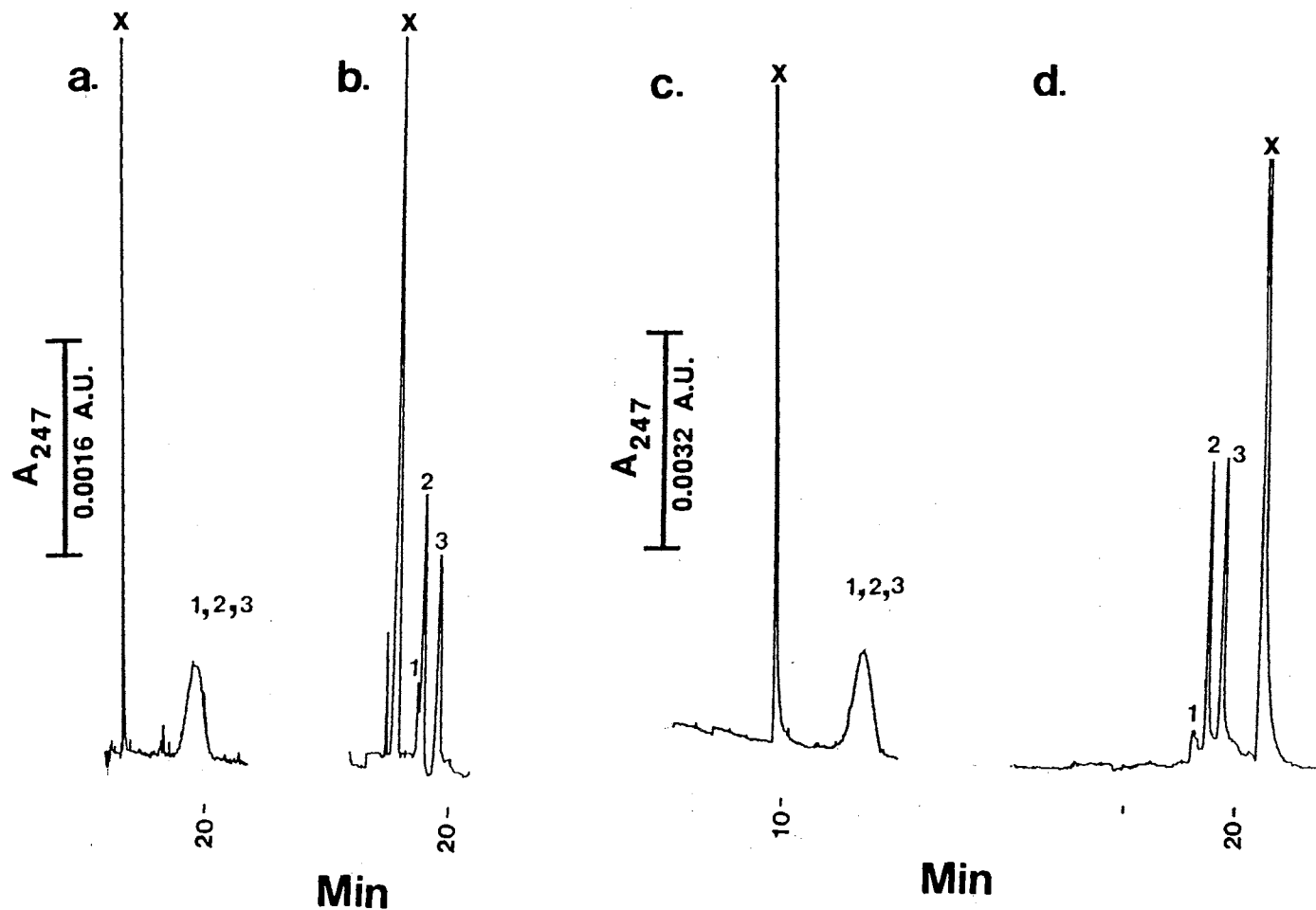


**Figure 4.** Electropherograms of standard gangliosides derivatized with ANDSA at neutral (a and b) and high pH (c and d) in the presence (b and d) and absence (a and c) of acetonitrile in the running electrolyte. In (a) and (b): running electrolyte, 25 mM sodium phosphate, pH 7.0, at 0% (a) and 50% v/v (b) acetonitrile; running voltage, 25.0 kV. In (c) and (d): running electrolyte, 10 mM sodium phosphate, pH 10.0 at 0% (c) and 50% v/v (d) acetonitrile; running voltage, 20 kV. Samples: 1 = GM1, 2 = GD<sub>1a</sub>, 3 = GT<sub>1b</sub>. Other conditions as in Fig. 1.

gangliosides (type III mixture) shown in Fig. 5, where 50% v/v ACN concentration seems to be the optimum amount which yielded the best separation in terms of resolution and sharpness of the migrating zones. The derivatization of the carbohydrate moiety of the gangliosides seems not to introduce undesirable effects as far as the aggregation of these species is concerned. In fact, both derivatized and underivatized gangliosides behaved similarly when electrophoresed with acetonitrile-rich electrolytes. In all cases, at ACN concentration below 30% (v/v), the gangliosides co-migrated indicating that the different analytes traveled through the capillary as a mixed micelle. As the ACN concentration increased above 30%, the different gangliosides migrated as monomers or oligomers and their migration mobility was greatly affected by their charge-to-mass ratio (Fig. 5). As can be seen in Fig. 5, only three different peaks were detected, which were identified by spiking the mixture with standard samples of the different gangliosides. The disialoganglioside isomers,  $G_{D1a}$  and  $G_{D1b}$ , co-migrated since both molecules have the same charge-to-mass ratio. Optimum separation conditions were achieved at 50% (v/v) ACN since at 60% ACN the gain in resolution was on the expense of broader peaks and at 70% ACN the efficiency dropped by a factor of almost two.

To further optimize the hydro-organic electrolyte system just described, the effects of phosphate concentration and pH of the running electrolyte were examined. As expected, increasing the ionic strength of the running electrolyte decreased the electroosmotic flow which resulted in increasing the migration time of the gangliosides through the capillary (Fig. 6). More importantly, for amphiphilic gangliosides increasing the ionic strength of the running electrolyte reduces the CMC value. In fact, it has been shown that the CMC of  $G_{M1}$  decreased by a factor of three when going from pure water to 50 mM sodium acetate buffer [34]. As can be seen in Fig. 6, the effect of increasing buffer ionic strength seems to be more pronounced for the monosialoganglioside  $G_{M1}$  since electrostatic repulsion between the polar head groups of singly charged amphiphilic species can be shielded at much lower salt concentration, a phenomenon that favors aggregation and reduction of

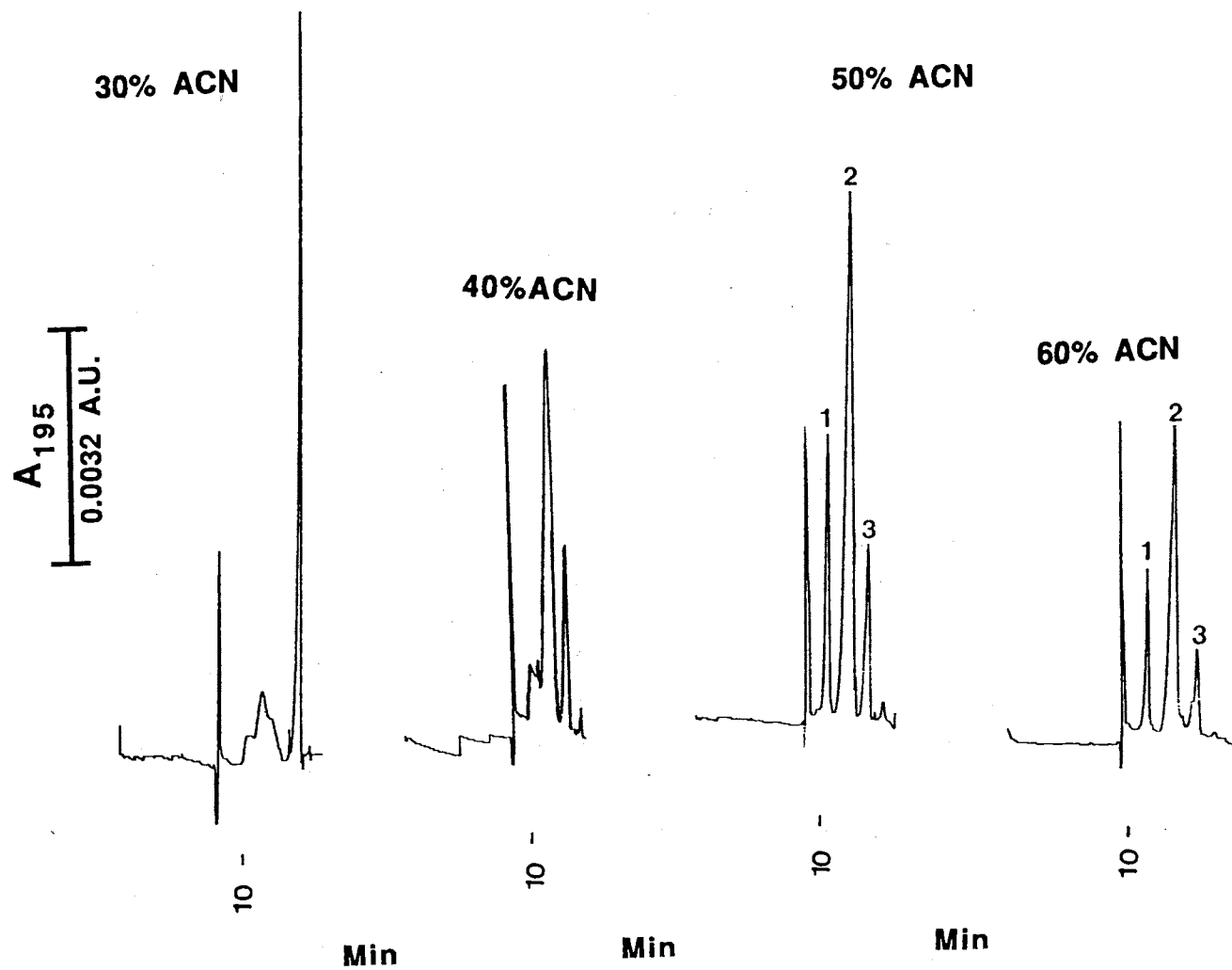


**Figure 5.** Electropherograms of underivatized gangliosides (mixture type III). Running electrolytes: 5.0 mM sodium phosphate, pH 7.50, at various % (v/v) acetonitrile; running voltage, 15.0 kV. Peak assignments: 1 = GM<sub>1</sub>, 2 = GD<sub>1a</sub> and GD<sub>1b</sub>, 3 = GT<sub>1b</sub>. Other conditions as in Fig. 1.

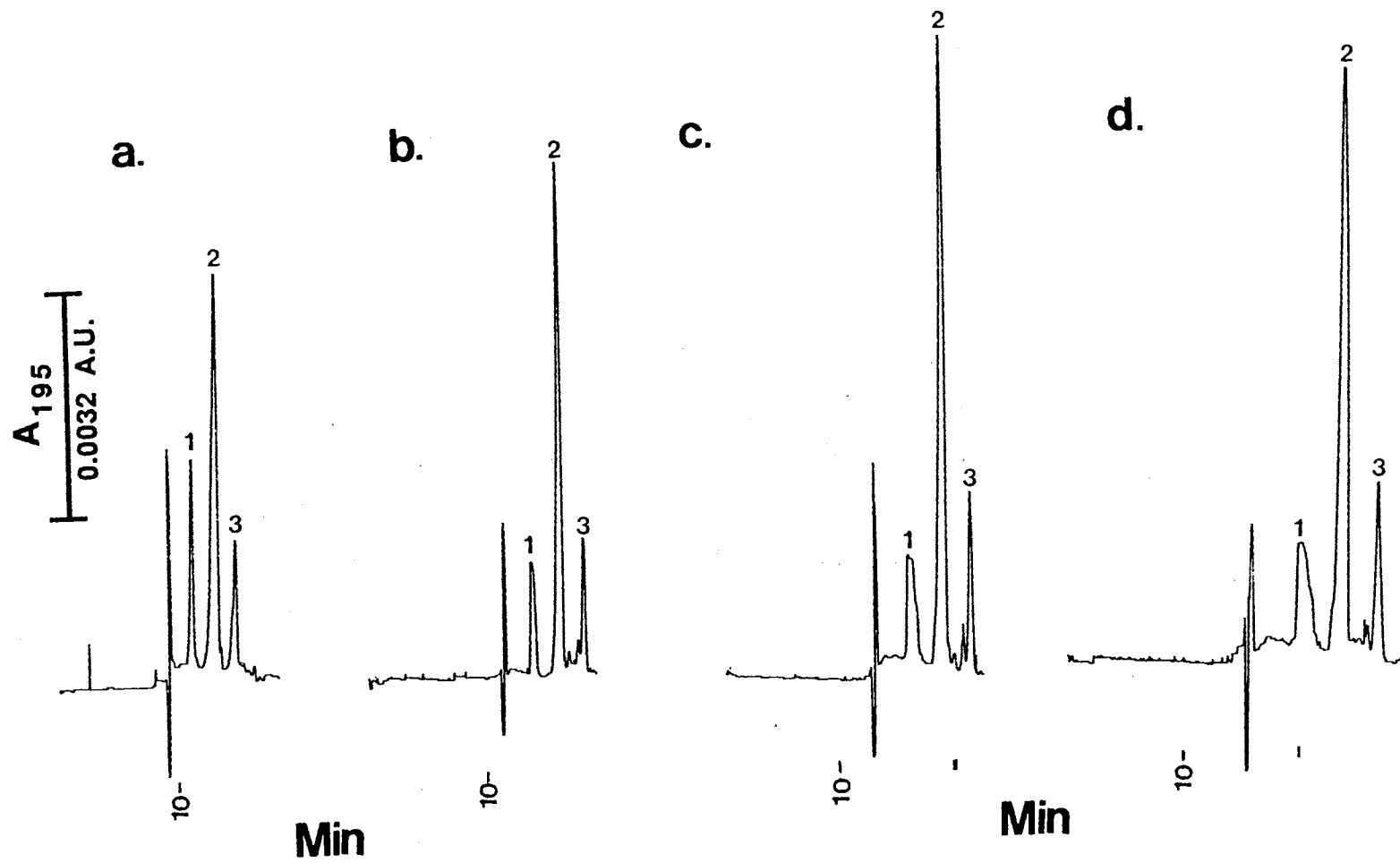


**Figure 6.** Electropherograms of standard underivatized gangliosides. Running electrolytes: sodium phosphate buffers, pH 7.50, containing 50% (v/v) acetonitrile at 5.0, 15.0, 25.0 and 35.0 mM sodium phosphate in a, b, c and d, respectively. Average number of theoretical plates per meter: 25 200, 14 400, 13 200 and 16 700 in a, b, c and d, respectively. Peak assignments: 1 = GM<sub>1</sub>, 2 = GD<sub>1a</sub> and GD<sub>1b</sub>, 3 = GT<sub>1b</sub>. Other conditions as in Fig. 1.

CMC in aqueous solution. This may explain the decrease in the sharpness of the  $G_{M1}$  peak as the concentration of phosphate buffer increased. Optimum separation efficiencies in terms of number of theoretical plates were achieved at 5.0 mM phosphate buffer concentration.

Increasing the pH of the running electrolyte from 5.0 to 8.0 did not greatly affect the electroosmotic flow (fluctuated between  $8.5$  and  $9.0 \times 10^{-4} \text{ cm}^2 \text{ V}^{-1} \text{ sec}^{-1}$ ), nor the electrophoretic mobility of the different gangliosides (results not shown). For instance, the electrophoretic mobility of  $G_{M1}$  only increased from  $2.0$  to  $2.5 \times 10^{-4} \text{ cm}^2 \text{ V}^{-1} \text{ sec}^{-1}$ . This might be due to the presence of the acetonitrile in the running electrolyte.

One of the shortcomings of the hydro-organic buffer systems evaluated above is that  $G_{D1a}$  and  $G_{D1b}$  were not separated. To provide other buffer systems that are useful for the separation of gangliosides in their monomeric forms,  $\alpha$ -CD was used as a buffer additive. It has been shown that  $\alpha$ -CD has the ability to break up the micellar form of the different gangliosides mixtures in a borate electrolyte [12]. In fact, and as can be seen in Fig. 7a, the ganglioside mixture type III could be separated into its mono-, di- and trisialogangliosides in the presence of  $\alpha$ -CD. Although, 7 mM  $\alpha$ -CD was sufficient for keeping the different gangliosides as monomers, a 15 mM  $\alpha$ -CD concentration was used because this amount yielded the highest plate count as shown in Fig. 8.

The effect of borate complexation with the oligosaccharide moiety of gangliosides was studied at three different borate concentrations to determine the best conditions for the separation of the two disialoganglioside isomers,  $G_{D1a}$  and  $G_{D1b}$ . As can be seen in Fig. 7, 100 mM borate provided partial separation between the two isomers and a further increase in borate concentration did not improve the resolution (Fig. 7c). This may indicate that the changes in the charge density between the isomers due to borate complexation may not be sufficiently high to allow their complete separation. As expected, increasing the borate concentration increased the migration time due to increasing the extent of complexation of the carbohydrate moieties of the gangliosides with borate and to decreasing

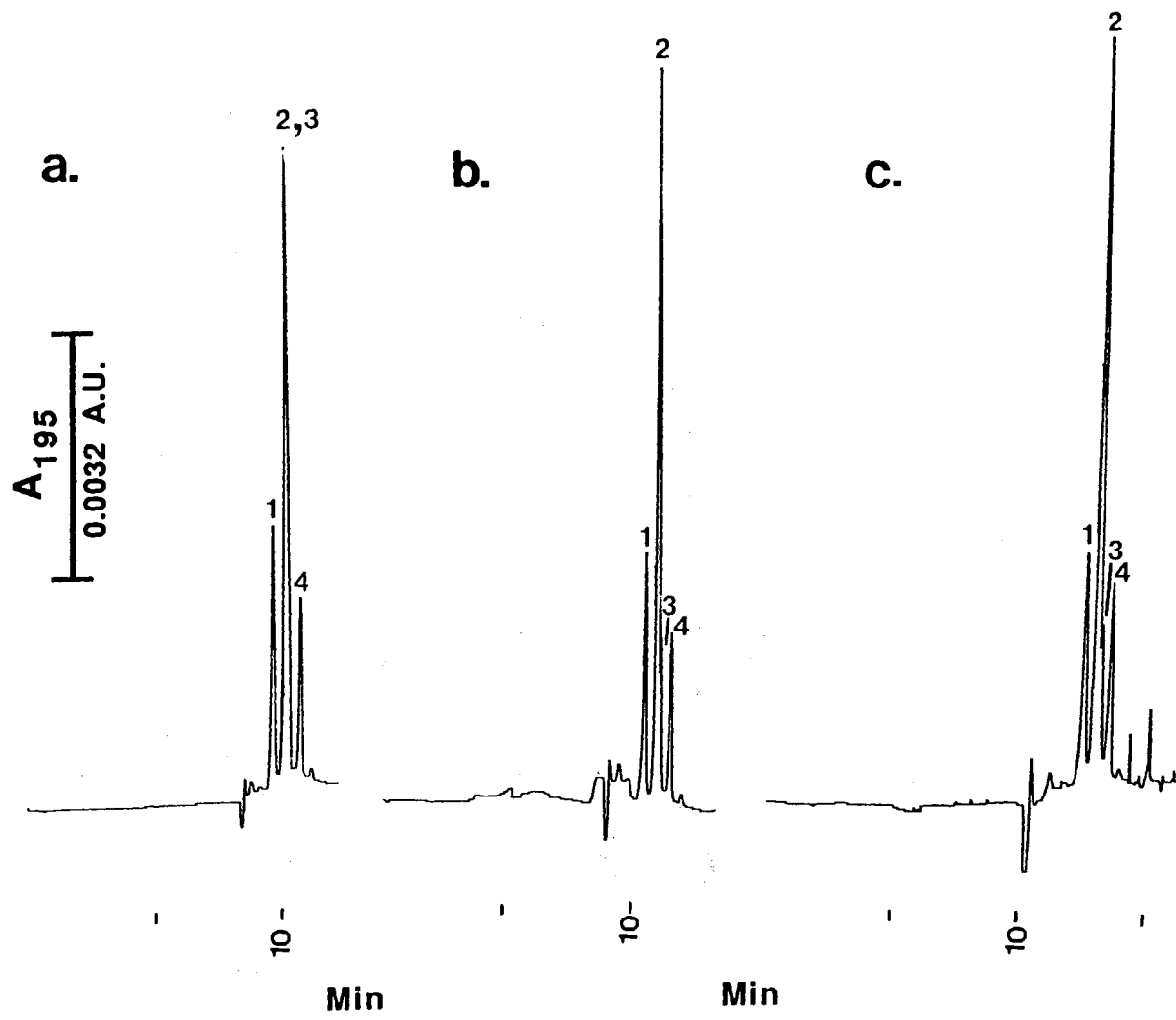


**Figure 7.** Electropherograms of underivatized gangliosides (mixture type III). Running electrolytes, borate buffers containing 15.0 mM  $\alpha$ -CD, pH 10.0, at 50, 100 and 150 mM borate in (a), (b) and (c), respectively. Peak assignments: 1 = G<sub>M1</sub>, 2 = G<sub>D1a</sub>, 3 = G<sub>D1b</sub>, 4 = G<sub>T1b</sub>. Other conditions as in Fig. 1.

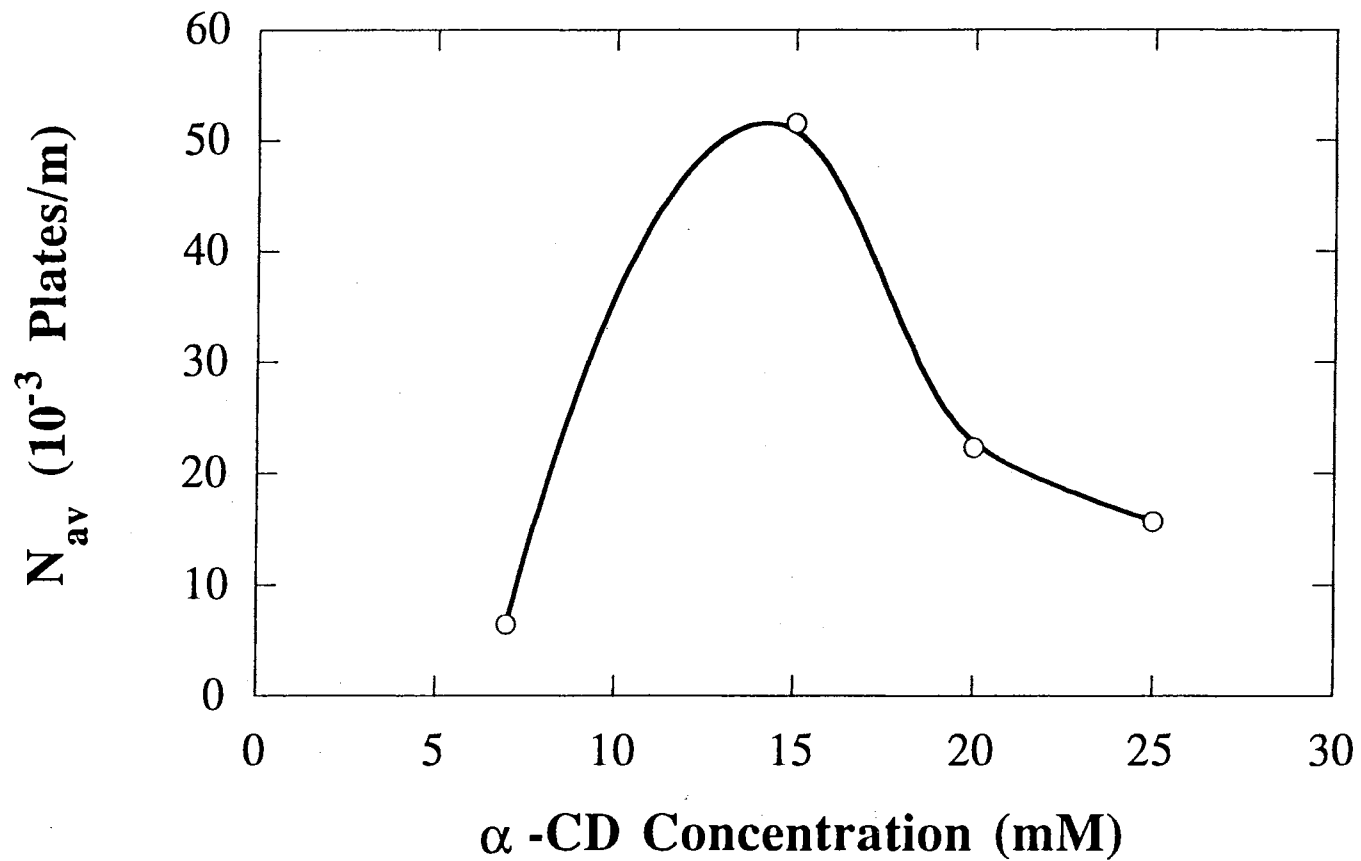


**Figure 8.** Plot of average plate counts per meter at various  $\alpha$ -CD concentration in the running electrolyte. Running electrolytes, 150 mM borate, pH 10.0, at various concentration of  $\alpha$ -CD. Other conditions as in Fig. 1.



the EOF. It should be noted that the electrophoretic velocity of the solutes is in the opposite direction to the EOF. The same trend was also observed with ANDSA-gangliosides when the borate concentration was varied in the presence of  $\alpha$ -CD (Fig. 9). As with the underivatized gangliosides, increasing the borate concentration resulted in a partial separation between the isomers but at the expense of longer analysis time. As can be seen in Fig. 9, the complexation between borate and the individual gangliosides occurs to the same extent as indicated by the parallel increase of the migration time with the increase in borate concentration. This may indicate that the sialic acid does not contribute significantly to borate complexation since the only difference in the carbohydrate moieties of the various gangliosides is the number of sialic acids.

ANDSA is a fluorescent tagging agent. It has a maximum excitation signal at 315 nm and a maximum emission signal at 420 nm [35]. This allowed the fluorescence detection of the ANDSA derivatives of gangliosides as shown in Fig. 10.

As shown above, the hydro-organic electrolyte system containing ACN and the  $\alpha$ -CD buffer system did not provide adequate resolution for the disialoganglioside isomers, i.e.,  $G_{D1a}$  and  $G_{D1b}$ , despite the fact that they were very efficient in breaking up micelle formation. Therefore, there is a need to add hydrophobic or hydrophilic selectors to the electrolyte to provide sufficient selectivity. To evaluate some potential additives, three model disialogangliosides were used including  $G_{D1a}$ ,  $G_{D1b}$  and  $G_{D3}$ .  $G_{D3}$  has a smaller molecular weight than the two isomers  $G_{D1a}$  and  $G_{D1b}$  since its carbohydrate moiety is a tetrasaccharide with two sialic acid residues (see Fig. 6 of Chapter II). The charge-to-mass ratios of  $G_{D1a}$ ,  $G_{D1b}$  and  $G_{D3}$  are  $1.09 \times 10^{-3}$ ,  $1.09 \times 10^{-3}$ , and  $1.35 \times 10^{-3}$ , respectively.

In addition to the fact that the  $\alpha$ -CD and ACN electrolyte systems provided marginal or no resolution between  $G_{D1a}$  and  $G_{D1b}$ , they did not allow the complete resolution of  $G_{D1a}$  and  $G_{D1b}$  from  $G_{D3}$  as shown in Fig. 11a and b. As can be seen in these figures, phosphate electrolyte containing 50% ACN yielded a better separation between  $G_{D3}$  and the other two disialoganglioside isomers. Similar results were obtained

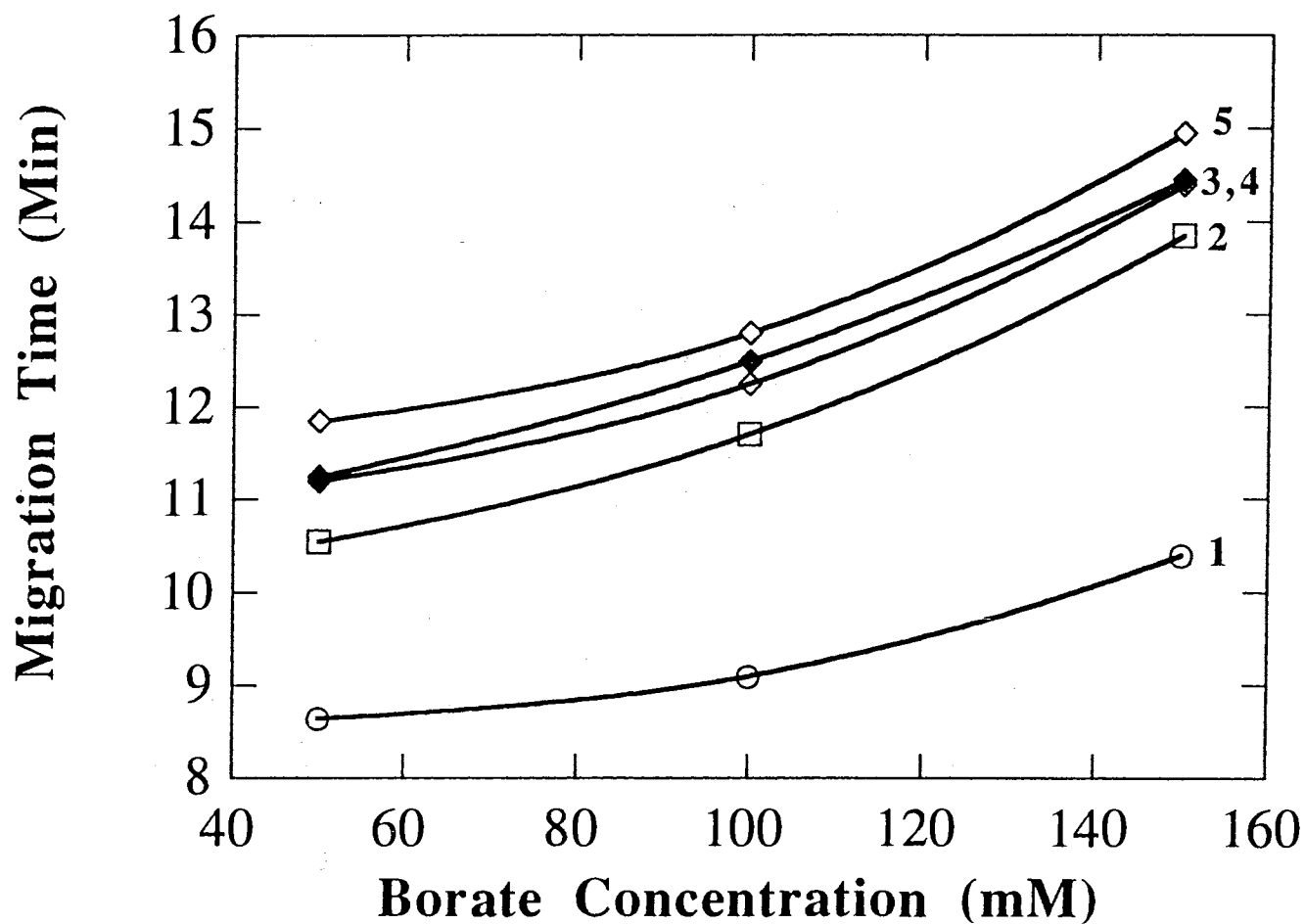


**Figure 9.** Typical plots of migration time versus borate concentration in the running electrolyte obtained with ANDSA derivatives of standard gangliosides. Symbols: 1 = DMSO, 2 =  $G_{M1}$ , 3 =  $G_{D1a}$ , 4 =  $G_{D1b}$ , 5 =  $G_{T1b}$ . Other conditions as in Fig. 7.

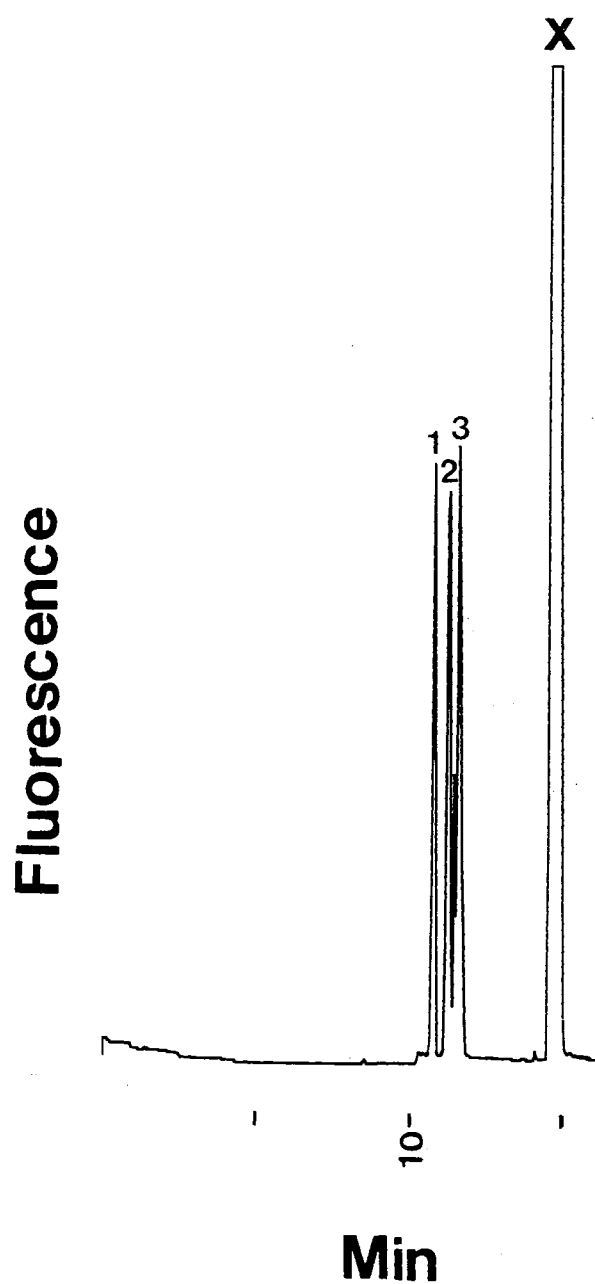


**Figure 10.** Typical fluorescence electropherogram of mono-, di- and trisialogangliosides derivatized with ANDSA. Running electrolyte, 10 mM sodium phosphate, pH 12.0, containing 15.0 mM  $\alpha$ -CD; running voltage, 18.0 kV. Peak assignments: 1 = GM1, 2 = GD1a, 3 = GT1b, x = by product. Other conditions as in Fig. 1.

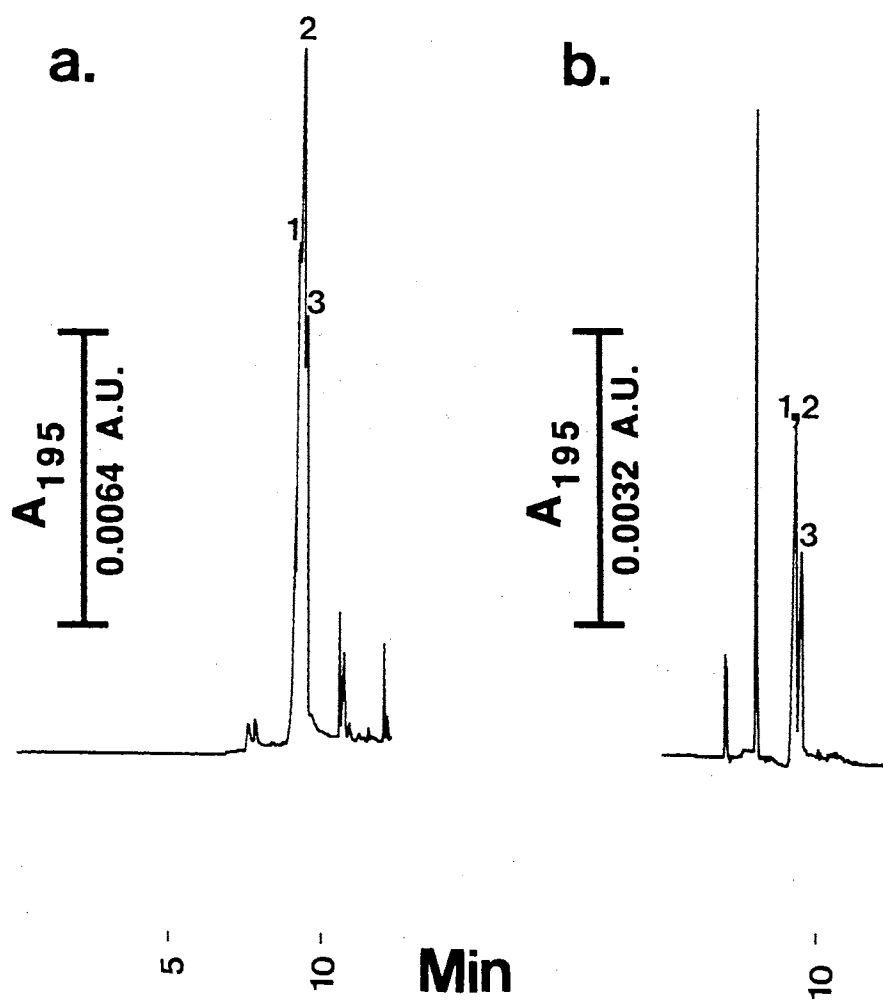


**Figure 11.** Electropherograms of standard underivatized gangliosides. (a) Running electrolyte, 50 mM borate containing 15 mM  $\alpha$ -CD, pH 10.0; running voltage 20.0 kV. (b) Running electrolyte, 10 mM sodium phosphate, pH 7.0 containing 50% (v/v) acetonitrile; running voltage, 25.0 kV. Samples: 1 = GD<sub>1a</sub>, 2 = GD<sub>1b</sub>, 3 = GD<sub>3</sub>. Other conditions as in Fig. 1.

with the derivatized  $G_{D1a}$ ,  $G_{D1b}$  and  $G_{D3}$ .

To enhance the selectivity of the electrophoretic system and to achieve separation of the  $G_{Ds}$ , hydrophilic interaction was superimposed on the electrophoretic process by including HPC or PVA in the running electrolytes in addition to  $\alpha$ -CD. The amount of these additives were varied, and best results were attained at 0.5 % (v/v), see Fig. 12a and b.

In another set of experiments, hydrophobic interaction was exploited to achieve the separation of the  $G_{Ds}$ . In this regard, the possibility of using micellar electrokinetic capillary chromatography (MECC) was considered by investigating the usefulness of *in situ* charged micelles recently introduced by our laboratory [36,37]. *In situ* micellar systems are based on the complexation of alkylglycoside surfactants and borate, a phenomenon that provides micelles with adjustable surface charge density. As seen in Fig. 13, a micellar electrolyte system consisting of 50 mM borate, 5 mM MEGA 10 and 15 mM  $\alpha$ -CD gave a baseline separation and a high plate count for the  $G_{Ds}$ . The pH of the electrolyte was adjusted to 6 to ensure a different migration time between the analytes and the by-product.

### Conclusions

The selective precolumn derivatization of gangliosides involving the carboxylic acid groups of the sialic acid residues has proved suitable for the analysis of small amounts of these sialoglycolipids by HPCE. This attractive feature in conjunction with the unique selectivities offered by the various electrolyte systems developed in the present studies are expected to facilitate the determination of gangliosides in small tumors.

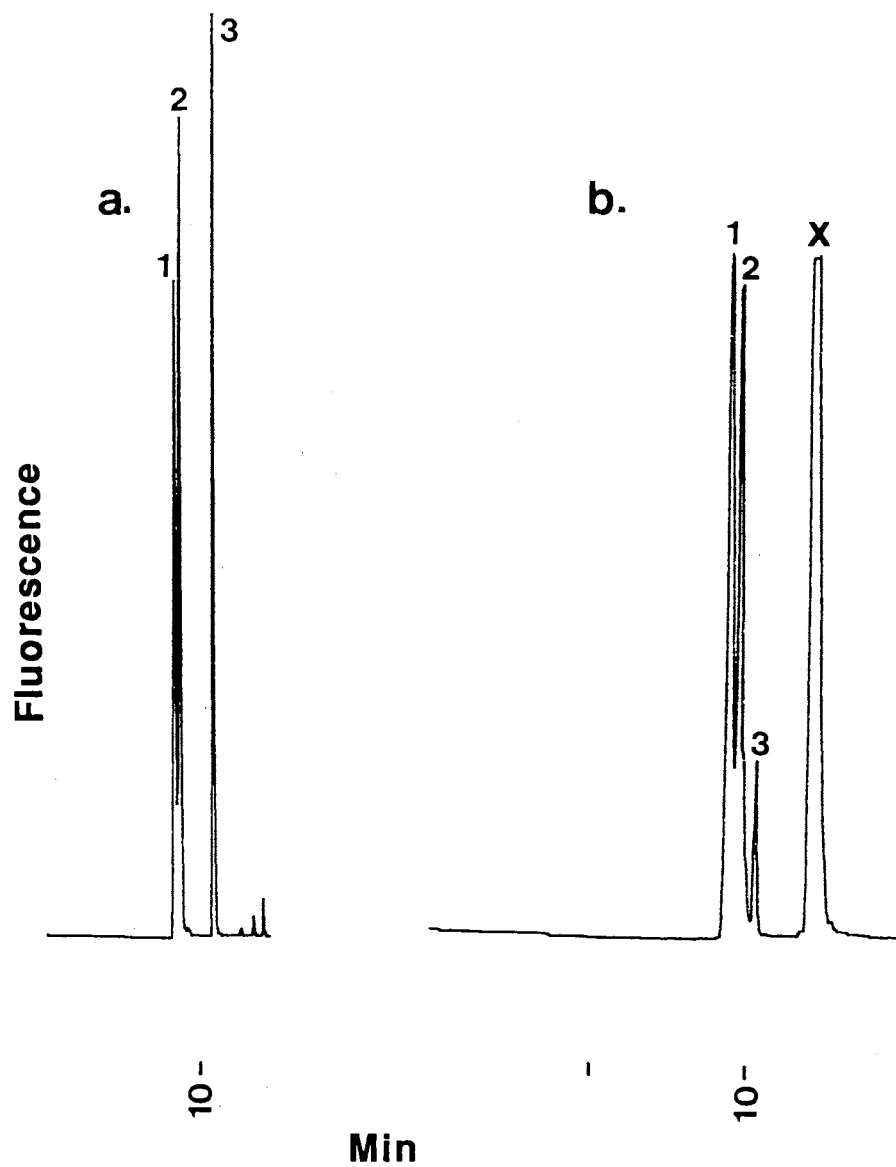


**Figure 12.** Electropherograms of standard ANDSA derivatives of disialogangliosides. Running electrolytes, 10 mM sodium phosphate, pH 12.0, containing 15 mM  $\alpha$ -CD and 0.5% HPC in (a) or 0.5% PVA in (b); running voltage, 18.0 kV. Peak Assignments: 1 =  $G_{D1a}$ , 2 =  $G_{D1b}$ , 3 =  $G_{D3}$ , x = by-product. Other conditions as in Fig. 1.

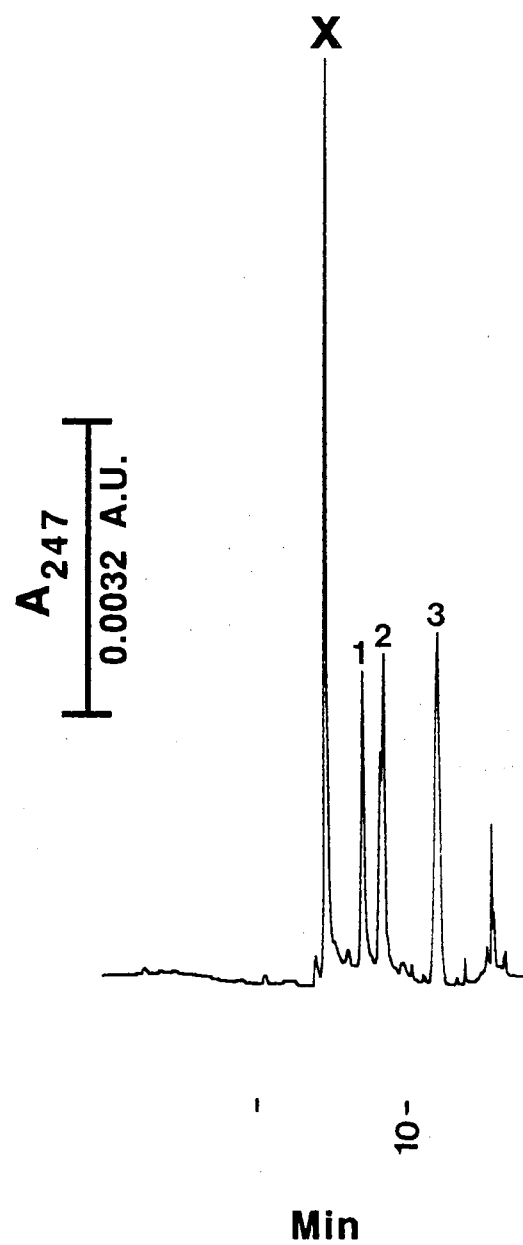


**Figure 13.** Electropherogram of standard ANDSA-disialogangliosides. Running electrolyte, 50 mM borate, pH 6.0 containing 5.0 mM MEGA surfactant and 15.0 mM  $\alpha$ -CD. Peak assignments and other conditions as in Fig. 12.

## References

1. Svennerholm, L., *J. Neurochem.*, 10 (1963) 613.
2. Wiegandt, H., in Weigandt, H., Ed., *Glycolipids*, Elsevier, Amsterdam, 1985, p. 199.
3. Leeden, R. and Yu, R., *Methods Enzymol.*, 83 (1982) 139.
4. Van Heyningen, W., *J. Gen. Microbiol.*, 20 (1959) 291.
5. Hakomori, S., *Proc. Natl. Acad. Sci. U.S.A.*, 67(1970) 1791.
6. Spiegel, S. and Fishman, P., *Proc. Natl. Acad. Sci. U.S.A.*, 84 (1987) 141.
7. Smith, D.F. and Torres, B.V., *Methods Enzymol.*, 179 (1989) 30.
8. Ladisch, S. and Gillard, B., *Methods Enzymol.*, 138 (1987) 300.
9. Kannagi, R., Watanabe, K. and Hakomori, S.-I., *Methods Enzymol.*, 138 (1987) 3.
10. Nakalayashi, H., Iwamori, M. and Naga, Y., *J. Biochem.*, 96 (1984) 977.
11. Liu, Y. and Chan, K.-F.J., *Electrophoresis*, 12 (1991) 402.
12. Yoo, Y., Kim, Y., John, G.-J., and Park, J., *J. Chromatogr. A*, 652 (1993) 431.
13. Bremer, E., Gross, S. and McClure, R., *J. Lipid Res.*, 20 (1979) 1028.
14. Lee, W., Westrick, M. and Macher, B., *Biochim. Biophys. Acta*, 712 (1982) 489.
15. Traylar, T., Koontz, D. and Hogan, E., *J. Chromatogr.*, 272 (1983) 9.
16. Mechref, Y. and El Rassi, Z., *Electrophoresis*, 15 (1994) 627.
17. Nashabeh, W. and El Rassi, Z., *J. Chromatogr.*, 514 (1990) 57.
18. Nashabeh, W. and El Rassi, Z., *J. Chromatogr.*, 600 (1992) 279.
19. Ostrander, G.K., Levery, S.B., Hakomori, S. and Holmes, E.H., *J. Biol. Chem.*, 263 (1988) 3103.
20. Folch, J., Arson, S. and Meath, J.A., *J. Biol. Chem.*, 191 (1951) 819.
21. Yu, R.K. and Ledeen, R.W., *J. Lipid Res.*, 13 (1972) 680.
22. Saito, T. and Hakomori, S., *J. Lipid Res.*, 12 (1971) 257.
23. Watanabe, K. and Arao, Y., *J. Lipid Res.*, 22 (1981) 1020.
24. Kilar, F. and Hjerten, S., *J. Chromatogr.*, 480 (1989) 35.



25. Montreuil, J., Bouquelet, S., Debray, H., Fournet, B., Spik, G. and Strecker, G., in Chaplin, M. and Kennedy, J., Eds., *Carbohydrate Analysis A Practical Approach*, IRL Press Limited, Oxford, 1986, p. 143.
26. Schauer, R., *Adv. Carbohydr. Chem. Biochem.*, 40 (1982) 132.
27. Ando, S., Chang, N.-C. and Yu, R., *Anal. Biochem.*, 89 (1978) 437.
28. Khorana, H., *Chem. Rev.*, 53 (9153) 145.
29. Khorana, H., *J. Chem. Soc.*, (1952) 2081.
30. Dean, J.A., *Lange's Handbook of Chemistry*, McGraw Hill, Inc., New York, 1985.
31. Voet, D. and Voet, J., *Biochemistry*, John Wiley, New York, (1990), p. 1018.
32. Kuhn, R. and Wiegandt, H., *Z. Naturforsch. B*, 18 (1963) 541.
33. Ulrich-Bott, B. and Wiegandt, H., *J. Lip. Res.*, 25 (1984) 1233.
34. Rauvala, H., *Eur. J. Biochem.*, 97 (1979) 555.
35. Lee, K.-B., Kim, Y.-S. and Linhardt, R., *Electrophoresis*, 12 (1991) 636.
36. Cai, J. and El Rassi, Z., *J. Chromatogr.*, 608 (1992) 31.
37. Smith, J.T., Nashabeh, W. and El Rassi, Z., *Anal. Chem.*, 66 (1994) 1119.

## CHAPTER V

### CAPILLARY ELECTROPHORESIS OF CARBOXYLATED CARBOHYDRATES. 2. SELECTIVE PRECOLUMN DERIVATIZATION OF SIALO-OLIGOSACCHARIDES DERIVED FROM GANGLIOSIDES WITH 7-AMINONAPHTHALENE-1,3- DISULFONIC ACID FLUORESCING TAG

#### Introduction

In recent years, there has been an increasing awareness of the many important biological roles of the oligosaccharide chains (i.e., glycans) of glycoproteins and glycolipids [1-3], and as a consequence, the analytical methodologies used for their determination are continuously evolving. Along these lines, the analysis of carbohydrates has recently emerged as one of the new fascinating applications of capillary electrophoresis [4-7]. This is not surprising, since when carbohydrates are appropriately tagged with ionizable fluorophores or chromophores that provide the center for sensitive detection and the charge for electrophoresis, capillary electrophoresis (CE) becomes the analytical technique of choice yielding an unprecedented resolution and permitting the determination of complex carbohydrates at low levels. A unique virtue of CE is its capability to analyze very small sample volumes, a feature that is very important for the analysis of most complex carbohydrates which often exist in minute amounts.

This report, which is a continuation to our recent studies involving precolumn labeling of acidic carbohydrates [8,9], see Chapters III and IV, is focused on demonstrating the potential of CE in the separation of fluorescently labeled sialooligosaccharides derived from gangliosides. Gangliosides are sialic acid-containing glycosphingolipids found in nearly all vertebrate tissues [10,11]. The sialooligosaccharide

moieties used in these studies were cleaved from gangliosides by digesting with an endoglycosidase that hydrolyzes the linkage between the oligosaccharide chain and ceramide of glycosphingolipid [12], yielding a mixture of deconjugated oligosaccharides and ceramides. The released sialooligosaccharides were then isolated and subsequently tagged with ANDSA (a fluorescing and UV absorbing label) to overcome detectability problems associated with carbohydrates. This was achieved by a precolumn derivatization procedure which has been recently introduced by our laboratory for the tagging of acidic monosaccharides [8] (Chapter III) and gangliosides [9] (Chapter IV). The tagging procedure exploits the chemical reactivity of the carboxylic acid groups of acidic carbohydrates, and involves the formation of a stable amide bond between the carboxylic acid group of the carbohydrate analyte and the amino group of the derivatizing agent, e.g., 7-aminonaphthalene-1,3-disulfonic acid (ANDSA), in the presence of water-soluble carbodiimide [8].

The ANDSA derivatives of sialooligosaccharides cleaved from gangliosides were analyzed under various electrolyte conditions in order to optimize the separation of the various derivatives by capillary electrophoresis.

## Materials and Methods

### Reagents and Materials

Gangliosides  $G_{M1}$ ,  $G_{M2}$ ,  $G_{M3}$  and  $G_{D3}$  were extracted from bovine brain as described elsewhere [9, 13]. Other materials are the same as those listed in Chapters III and IV.

### Instruments and Capillaries

The instrument for capillary electrophoresis was assembled in-house from commercially available components [8, 14] and was described in Chapter IV.

Fused-silica capillary columns of 50  $\mu\text{m}$  I.D. and 365  $\mu\text{m}$  O.D. were obtained from Polymicro Technology (Phoenix, AZ, U.S.A.). All capillaries used in this study were uncoated since the analytes are negatively charged and would repulse from the like-charged capillary surface. The running electrolyte was renewed after every run. Under this condition, the reproducibility of migration time in % RSD was about 0.9 and 2.0 with borate and phosphate electrolyte systems, respectively. The derivatized sialooligosaccharides were introduced into the capillary as thin plugs by means of hydrodynamic injection for approximately 5 s at 15 cm differential height between inlet and outlet ends of the capillary.

#### Cleavage of Sialooligosaccharides from Gangliosides

Reaction mixtures containing 100  $\mu\text{g}$  of the sialoganglioside, 150  $\mu\text{g}$  sodium cholate, and 0.5 units of ceramide-glycanase (1 unit will hydrolyze 1 nmol of sialoganglioside per minute at pH 5.0, 37 °C) in 200  $\mu\text{l}$  of 50 mM sodium acetate buffer, pH 5.0, were incubated at 37 °C and monitored at one hour intervals by thin layer chromatography. Reactions were terminated after 4 hours by addition of 1.0 mL of chloroform:methanol (2:1 v/v) prior to centrifugation at 7,000xg. Following centrifugation, the aqueous layer was removed and the procedure repeated twice. The oligosaccharide containing aqueous layers were combined and dried under nitrogen purge. The structures of the different sialooligosaccharides derived from gangliosides used in this study are shown in Table I. Two of the sialooligosaccharides, namely sialooligo-G<sub>D1a</sub> and G<sub>D1b</sub>, are structural isomers that only differ in the position of one of the sialic acid groups.

#### Derivatization of Sialooligosaccharides

Seven different sialooligosaccharides (see Table I) were tagged with ANDSA as previously described in Chapter III [8, 9]. Briefly, an aliquot of 5  $\mu\text{L}$  of 100 mM aqueous solution of EDAC, pH 5.0, was initially added to sub-microgram amounts of

sialooligosaccharides dissolved in distilled water. Then, 10.0  $\mu$ L of 100 mM aqueous solution of the derivatizing agent were added, and the mixture was stirred for 2.0 hrs at room temperature. Subsequently, the entire reaction mixture containing the derivatized sialooligosaccharides, excess derivatizing agent, and other components of the reaction mixture was analyzed by capillary zone electrophoresis (CZE).

TABLE I. Structures, Abbreviations and Charge-to-Mass Ratios of Underivatized and ANDSA Derivatives of the Sialooligosaccharides Derived from Gangliosides.

Structure	Abbreviation	Charge-to-mass ratio $\times 10^3$	
		Underivatized	ANDSA-derivatives
$\text{Gal}\beta 1 \rightarrow 3\text{GalNAc}\beta 1 \rightarrow 4\text{Gal}\beta 1 \rightarrow 4\text{Glc}$ $\begin{array}{c} 3 \\ \uparrow \\ 2\alpha\text{NeuAc} \end{array}$	Sialooligo-G <sub>M1</sub>	1.00	1.56
$\text{GalNAc}\beta 1 \rightarrow 4\text{Gal}\beta 1 \rightarrow 4\text{Glc}$ $\begin{array}{c} 3 \\ \uparrow \\ 2\alpha\text{NeuAc} \end{array}$	Sialooligo-G <sub>M2</sub>	1.20	1.79
$\text{Gal}\beta 1 \rightarrow 3\text{GalNAc}\beta 1 \rightarrow 4\text{Gal}\beta 1 \rightarrow 4\text{Glc}$ $\begin{array}{cc} 3 & 3 \\ \uparrow & \uparrow \\ 2\alpha\text{NeuAc} & 2\alpha\text{NeuAc} \end{array}$	Sialooligo-G <sub>D1a</sub>	1.55	2.16
$\text{Gal}\beta 1 \rightarrow 3\text{GalNAc}\beta 1 \rightarrow 4\text{Gal}\beta 1 \rightarrow 4\text{Glc}$ $\begin{array}{c} 3 \\ \uparrow \\ 2\alpha\text{NeuAc} \end{array}$ $\begin{array}{c} 3 \\ \uparrow \\ 2\alpha\text{NeuAc} \end{array}$	Sialooligo-G <sub>D1b</sub>	1.55	2.16
$\text{Gal}\beta 1 \rightarrow 3\text{GalNAc}\beta 1 \rightarrow 4\text{Gal}\beta 1 \rightarrow 4\text{Glc}$ $\begin{array}{c} 3 \\ \uparrow \\ 2\alpha\text{NeuAc} \end{array}$ $\begin{array}{c} 3 \\ \uparrow \\ 2\alpha\text{NeuAc} \end{array}$	Sialooligo-G <sub>T1b</sub>	1.90	2.47
$\text{Gal}\beta 1 \rightarrow 4\text{Glc}$ $\begin{array}{c} 3 \\ \uparrow \\ 2\alpha\text{NeuAc} \end{array}$	Sialooligo-G <sub>M3</sub>	1.58	2.18
$\text{Gal}\beta 1 \rightarrow 4\text{Glc}$ $\begin{array}{c} 3 \\ \uparrow \\ 2\alpha\text{NeuAc} \end{array}$	Sialooligo-G <sub>D3</sub>	2.17	2.68

## Results and Discussion

### CZE with Sodium Phosphate Electrolyte System

Figure 1a shows the CZE of underivatized sialooligosaccharides using 100 mM sodium phosphate, pH 6.0, as the running electrolyte and UV detection at 195 nm. Like most carbohydrate species, the sialooligosaccharides, which do not possess strong chromophores in their structures, cannot be directly detected in the UV at low levels. In fact, the concentration of the sample used for generating the electropherogram in Fig. 1a was relatively high (i.e., in the order of  $10^{-3}$  M). Despite the high sample concentration used, the detector has to be set at low attenuation (high sensitivity), a condition that explains the noisy baseline obtained. In addition, two pairs of sialooligosaccharides were not resolved namely  $G_{D1a}$  and  $G_{D1b}$  as well as  $G_{T1b}$  and  $G_{D3}$ . It should be noted that the use of 195 nm as the detection wavelength excludes the use of many useful electrolyte systems as the separation media because at this low wavelength the components of the running electrolyte may absorb UV light.

To improve the detectability of the analytes, the sialooligosaccharides were precolumn labeled with ANDSA, a fluorescing and also UV absorbing tag. Figure 1b shows a typical electropherogram of the derivatives obtained under the same running conditions as in Fig. 1a with on column fluorescence detection. The minimum detectable quantity of the ANDSA derivatives of sialooligosaccharides was approximately 0.6 femtomole, which is the same as that of carboxylated monosaccharides we reported earlier [8]. In addition to significantly improving the detectability of the sialooligosaccharides, the precolumn derivatization, described in this report, has another important virtue. For each sialic acid residue, the precolumn derivatization with ANDSA replaces the weak carboxylic acid group of the analyte by two stronger sulfonic acid groups. As can be seen in Fig. 1b, the presence of permanent charges on the molecule, which were imparted by the strong sulfonic acid groups, resulted in an overall improved separation of the derivatives. The

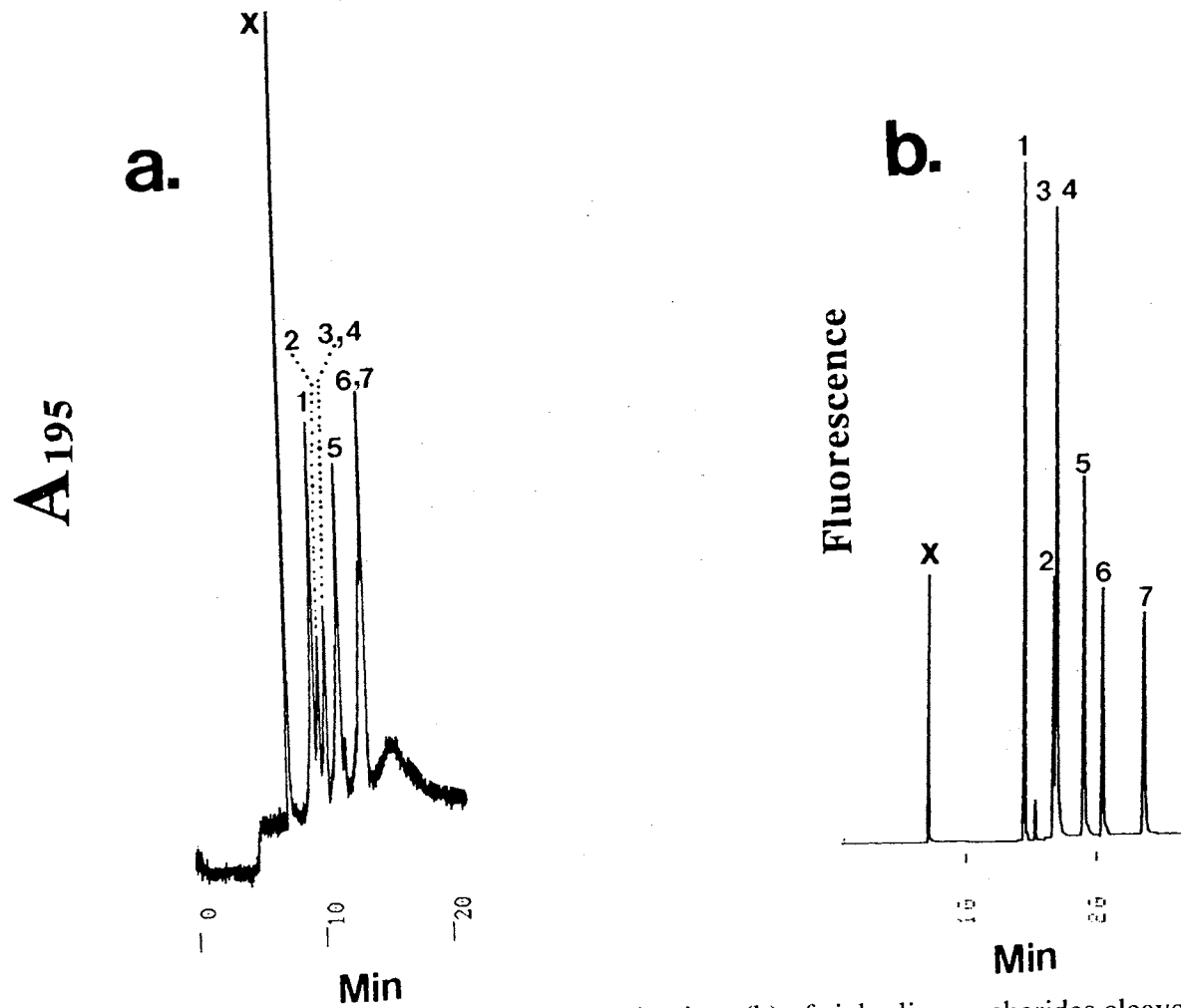


**Figure 1.** Electropherograms of underivatized (a) and ANDSA derivatives (b) of sialooligosaccharides cleaved from gangliosides. Capillary, 50/80 cm x 50  $\mu$ m i.d.; running voltage 20 kV. Running electrolyte: 100 mM phosphate, pH 6.0. Peak assignments: x = by-product, 1 = Sialooligo-G<sub>M1</sub>, 2 = Sialooligo-G<sub>M2</sub>, 3 = Sialooligo-G<sub>D1a</sub>, 4 = Sialooligo-G<sub>D1b</sub>, 5 = Sialooligo-G<sub>T1b</sub>, 6 = Sialooligo-G<sub>M3</sub>, 7 = Sialooligo-G<sub>D3</sub>.

average plate counts per meter increased by a factor of greater than seven upon labeling, i.e., from 22 000 to 161 000 plates/m when going from underivatized to derivatized sialooligosaccharides under otherwise identical electrophoretic conditions. It should be noted that the high separation efficiency observed in the case of ANDSA-sialooligosaccharides is due in part to the much smaller amount injected. The separation shown in Fig. 1b agrees well with what should be expected. In fact, with the exception of the two isomers  $G_{D1a}$  and  $G_{D1b}$ , the sialooligosaccharides have different charge-to-mass ratios as shown in Table I. Although the two isomers are different in molecular shape, this difference may not be significant to afford the separation of the two isomers under the conditions of the present experiment.

Using 100 mM sodium phosphate, pH 6.0, as the running electrolyte, and an electric field of positive polarity, the negatively charged ANDSA derivatives of the sialooligosaccharides, migrated against the EOF. Under this condition, the different analytes migrated in the order of increasing charge-to-mass ratios. By inspecting Fig. 1b, it can be seen that this held true for all the derivatized sialooligosaccharides except  $G_{T1b}$ . The migration of a given analyte through the separation channel is affected not only by its charge-to-mass ratio but also by its structure, which influences the magnitude of the frictional force exerted on the analyte as it moves through the separation media. This may be the reason for the faster migration of sialooligo- $G_{T1b}$  than sialooligo- $G_{M3}$ , toward the detection end of the capillary. Also, this may explain the elution of sialooligo- $G_{M2}$  in close proximity to sialooligo- $G_{D1a}$  and sialooligo- $G_{D1b}$ . Returning to Fig. 1b, the first peak is assumed to be that of the by-product of the precolumn derivatization reaction, which was tentatively identified by NMR and fluorescence characteristic as an adduct between ANDSA and EDAC [9].

Since the present precolumn derivatization imparts the oligosaccharides with permanent charges through the strong sulfonic acidic groups of the ANDSA tag, the derivatives can be electrophoresed at both low and high pH. With electrolyte systems of



moderate ionic strength (*e.g.*,  $\geq 50$  mM sodium phosphate) and at  $\text{pH} \leq 3.5$ , untreated fused-silica capillaries usually exhibit a negligible EOF. Under these conditions, and using a high voltage power source of negative polarity, negatively charged ANDSA-oligosaccharides will migrate toward the anode by their own electrophoretic mobility. Figure 2a and b illustrates the electropherograms of ANDSA derivatives of the sialooligosaccharides using two sodium phosphate electrolytes of different ionic strengths, namely 50 mM and 100 mM at pH 3.5. The average plate counts per meter were ca. 187 000 and 113 000 when using 50 and 100 mM sodium phosphate solutions as the running electrolytes, respectively. As expected, the species eluted in the reverse order with respect to that observed at pH 6.0 using an electric field of positive polarity (compare to Fig. 1b). With the exception of  $\text{G}_{\text{T}1\text{b}}$ , the elution pattern is in the order of decreasing charge-to-mass ratio. The slow migration velocity of sialooligo- $\text{G}_{\text{T}1\text{b}}$  with respect to sialooligo- $\text{G}_{\text{M}3}$  can be attributed to a structure effect as mentioned above. Increasing the ionic strength of the electrolytes resulted in resolving sialooligo- $\text{G}_{\text{M}2}$  from sialooligo- $\text{G}_{\text{D}1\text{a}}$  and  $\text{G}_{\text{D}1\text{b}}$ .

The excess tagging agent ANDSA eluted first (see Fig. 2) simply because the ANDSA molecule has two negative charges and smaller molecular weight than all the oligosaccharide analytes. This will allow ANDSA to migrate faster in an electric field of negative polarity.

#### CZE with Borate Electrolyte System

As shown above, sodium phosphate electrolyte systems did not offer enough selectivity to separate the ANDSA derivatives of sialooligo- $\text{G}_{\text{D}1\text{a}}$  and sialooligo- $\text{G}_{\text{D}1\text{b}}$  isomers. This initiated the investigation of the potentials of alkaline borate electrolyte systems at different borate concentrations in order to evaluate the extent to which borate would complex with the ANDSA derivatives of the sialooligosaccharides, and in turn optimize their separation. It is well established that at an alkaline pH, borate ions form *in situ* anionic complexes with carbohydrates [15, 16], thus facilitating their separation by

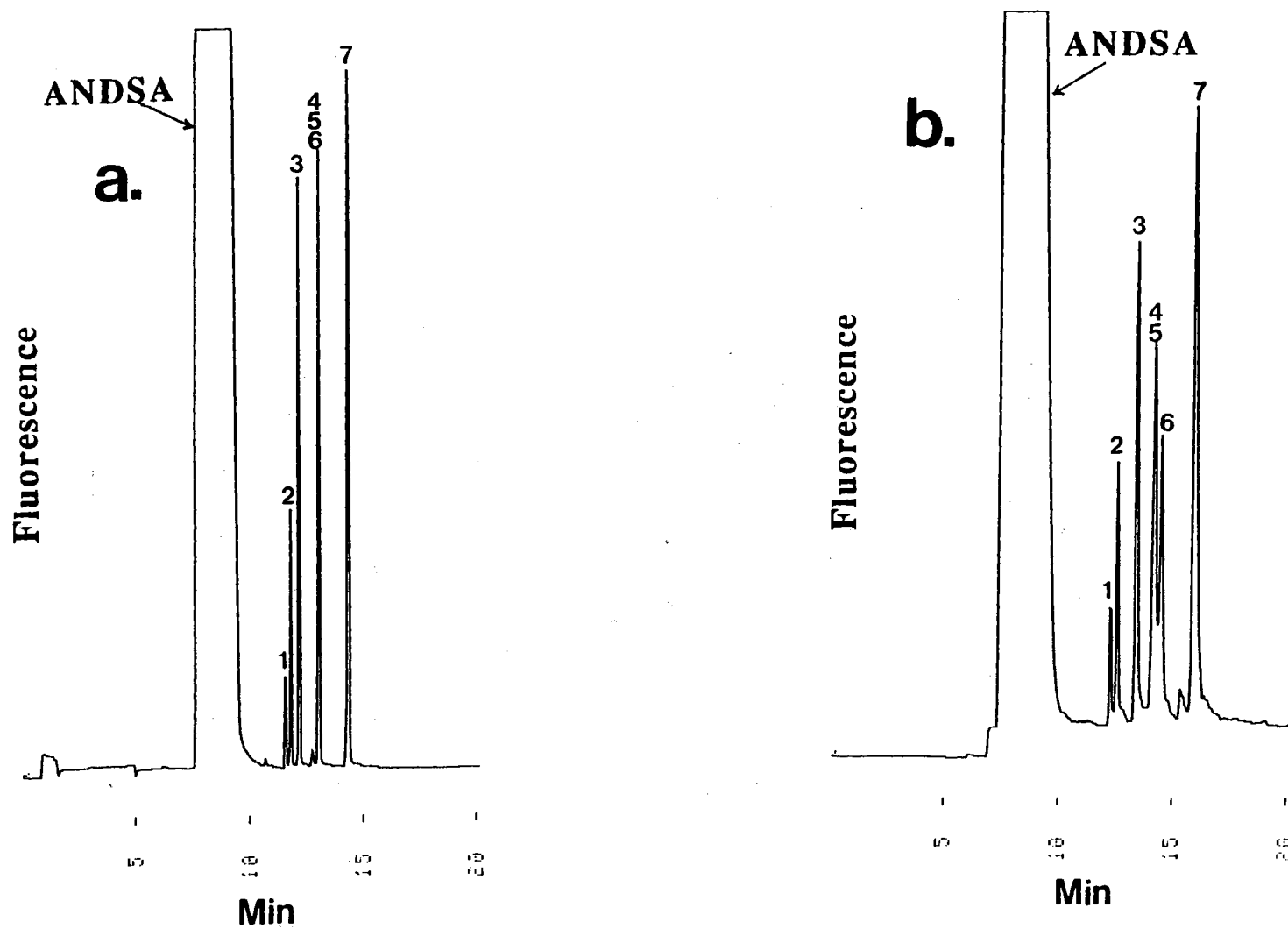


**Figure 2.** Electropherogram of ANDSA derivatives of sialooligosaccharides. Electrolytes, 50 mM and 100 mM phosphate, pH 3.5 in (a) and (b), respectively. Running voltage -20 kV. Peak assignments and other conditions as in Fig. 1.

capillary electrophoresis [4, 5]. As can be seen in Fig 3a, the migration times of the derivatives as well as that of the EOF marker increased as the borate concentration increased. Increasing borate concentration will increase the ionic strength of the running electrolyte and in turn decrease the EOF (i.e., increase the migration time of the neutral marker). Increasing the ionic strength results in (i) decreasing the zeta potential of the capillary wall as well as the thickness of the electric layer at the capillary-electrolyte interface and (ii) increasing the viscosity of medium. These two effects will lead to significant decrease in the EOF.

To better understand the effect of borate concentration on the overall separation, the electrophoretic mobilities of the derivatives are plotted in Fig. 3b. As expected, the electrophoretic mobilities of the ANDSA-oligosaccharide derivatives decreased with increasing the ionic strength of the running electrolyte (i.e., increasing borate concentration). As the borate concentration in the running electrolyte is increased, the extent of solute-borate association is also increased. But, this complexation increments the charge of the sulfonated derivatives by a narrow margin that is overshadowed by (i) the increase in the electrolyte viscosity and (ii) the decrease in the zeta potential of the analytes. These two phenomenon explain the decrease in the electrophoretic mobilities of the derivatives. Thus the increase in the observed migration times of the solute is mainly a reflection of the decrease in the EOF.

The elution pattern of the ANDSA-oligosaccharide derivatives at various borate concentration is displayed in Fig. 4. As can be seen in this figure, there is an optimum concentration of borate at which a complete separation of the different analytes including the structural isomers was achieved. The average plate counts per meter were 192 000, 318 000 and 400 000 with 50, 75 and 125 mM borate electrolytes, respectively. The optimum concentration is 75 mM borate (Fig. 4 b), and presumably corresponds to the situation where the amount of borate added has (i) yielded some difference in the charge-to-mass ratios between the two isomers and (ii) magnified the differences in the charge-to-

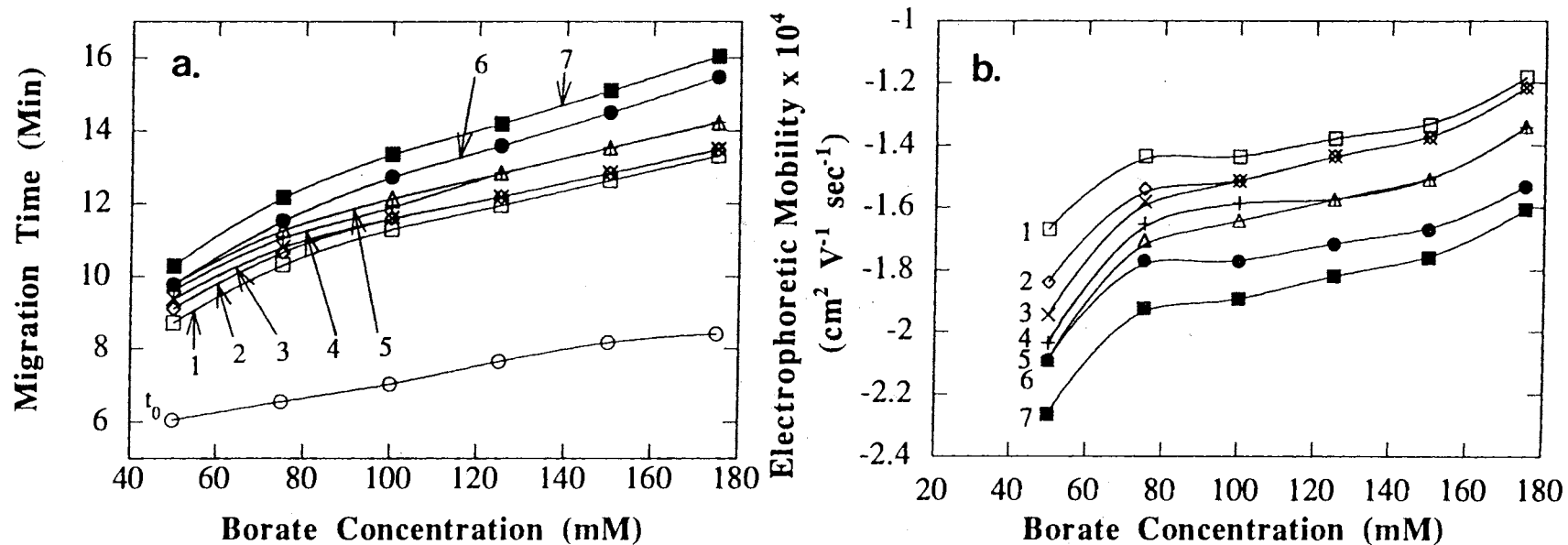


**Figure 3.** (a) Plot of migration times of ANDSA derivatives of sialooligosaccharides *versus* borate concentration. (b) Plot of electrophoretic mobilities of the same derivatives *versus* borate concentration. Electrolytes, sodium borate at various concentrations, pH 10; running voltage 20 kV. Samples:  $t_0$  = DMSO, 1 = Sialooligo- $G_{M1}$ , 2 = Sialooligo- $G_{M2}$ , 3 = Sialooligo- $G_{D1a}$ , 4 = Sialooligo- $G_{D1b}$ , 5 = Sialooligo- $G_{T1b}$ , 6 = Sialooligo- $G_{M3}$ , 7 = Sialooligo- $G_{D3}$ . Other conditions as in Fig. 1.

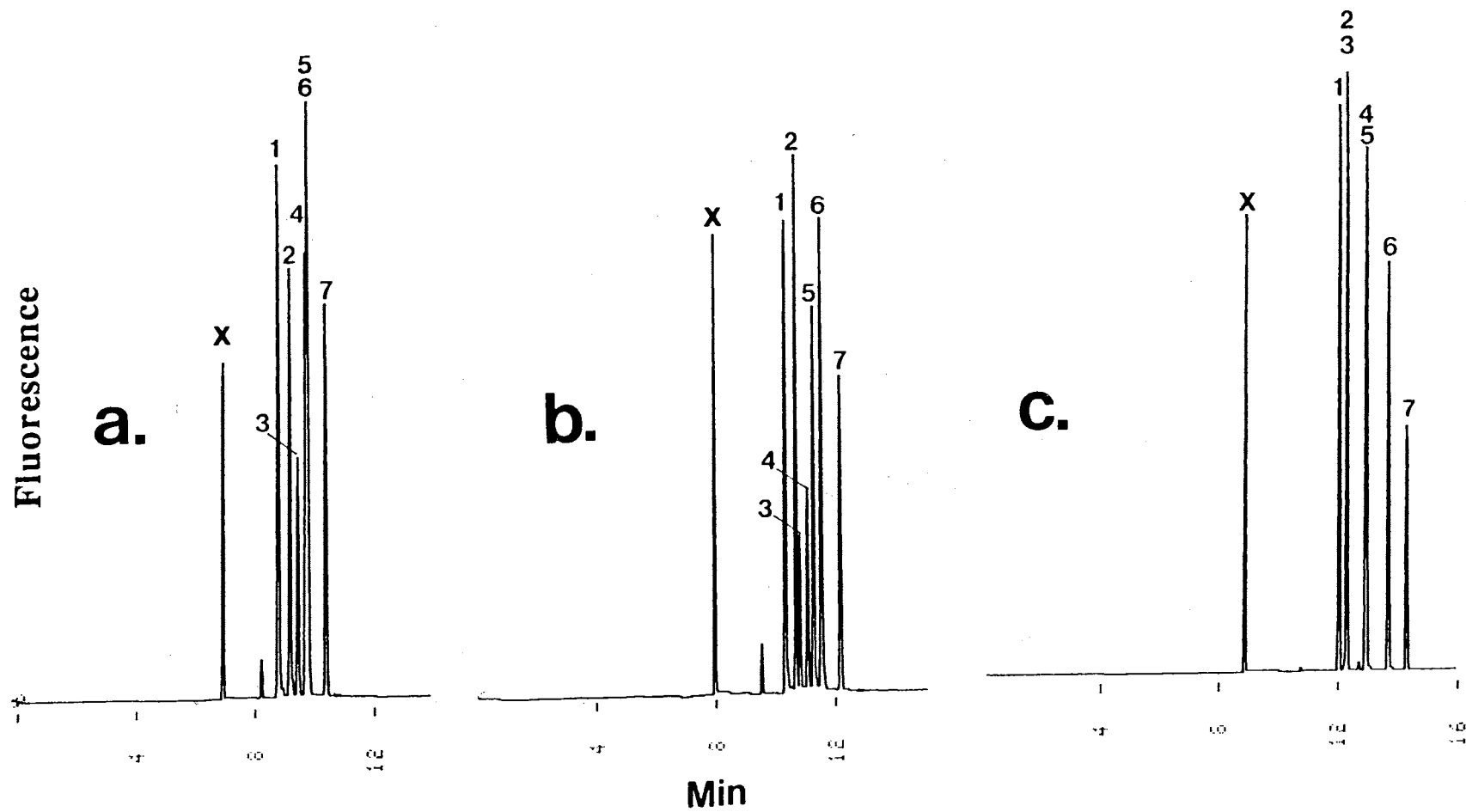


**Figure 4.** Electropherograms of ANDSA derivatives of sialooligosaccharides. Electrolytes, sodium borate buffers pH 10, at 50, 75 and 125 mM borate in (a), (b) and (c), respectively. Other conditions as well as peak assignments are as in Fig. 1.

mass ratios between the other analytes before the amount of added borate starts to obliterate differences in charge-to-mass ratios, a condition that caused  $G_{M2}$  and  $G_{D1a}$  as well as  $G_{D1b}$  and  $G_{T1b}$  to co-elute. Overall, the quality of separation diminished as the borate concentration was increased in the range 100-175 mM.

To summarize, the effect of added borate on separation may be explained as follows. Borate complexation with oligosaccharides occurs mainly at the outermost sugar residue toward the non reducing end of the molecule [17], and the extent of this complexation is usually decreased by the presence of a charged moiety [4, 5, 18], which is made up by the ANDSA tag of the derivatized sialooligosaccharides. This may explain why the two isomers sialooligo- $G_{D1a}$  and sialooligo- $G_{D1b}$  can be resolved from each other upon borate complexation. The outermost galactose residue in sialooligo- $G_{D1b}$  has enabled the complexation with borate at the *cis*-oriented hydroxyl groups at C-3 and C-4 of this residue, thus imparting another negative charge on this oligosaccharide. On the other hand, the outermost sugar residue of sialooligo- $G_{D1a}$  is a tagged sialic acid that usually complex less with borate [8] and in the same time decreases the extent of borate complexation with the neighboring galactose residue (see structures in Table I). The additional charge imparted by borate complexation on sialooligo- $G_{D1b}$  might also explain why it can not be resolved from sialooligo- $G_{T1b}$  at higher borate concentration. Similar considerations may apply for explaining the behavior of sialooligo- $G_{M2}$  and sialooligo- $G_{D1a}$ .

### Conclusions

We have demonstrated the suitability of precolumn derivatization of sialooligosaccharides, derived from gangliosides, with ANDSA fluorescing tag at the carboxylic acid group of the sialic acid residue of these oligosaccharides. This tagging process, which was primarily aimed at increasing the detectability of the oligosaccharides cleaved from gangliosides, resulted also in improving the resolution of these carbohydrates by capillary electrophoresis over a wide range of pH. The separation of the ANDSA

derivatives of sialooligosaccharides under investigation was best achieved when a running electrolyte of 75 mM borate, pH 10.0, was used. We believe the utility of this procedure will be multitudinous. For example, the methodology developed here may prove useful in examining alterations in carbohydrates moieties of gangliosides of tumors associated with chemical hepatocarcinogenesis. The conditions described in this report are also expected to be readily applicable to the precolumn derivatization and separation of other sialooligosaccharides such as those derived from glycoproteins.

## References

1. Paulson, J.C., *Trends Biochem. Sci.*, 14 (1989) 271.
2. Stults, C.L.M., Sweeley, C.C. and Macher, B.A., *Methods Enzymol.*, 179 (1989) 167.
3. Hakomori, S. and Igarashi, Y., *Adv. Lipid Res.*, 25 (1993) 147.
4. El Rassi, Z., *Adv. Chromatogr.*, 34 (1993) 177.
5. El Rassi, Z. and Nashabeh, W., in: El Rassi, Z., Ed., *Carbohydrate Analysis: High Performance Liquid Chromatography and Capillary Electrophoresis*, Elsevier, Amsterdam 1995, p. 447.
6. Novotny, M.V. and Sudor, J., *Electrophoresis*, 14 (1993) 373.
7. El Rassi, Z. and Smith, J.T., in: El Rassi, Z., Ed., *Carbohydrate Analysis: High Performance Liquid Chromatography and Capillary Electrophoresis*, Elsevier, Amsterdam 1995, p. 607.
8. Mechref, Y. and El Rassi, Z., *Electrophoresis*, 15 (1994) 627.
9. Mechref, Y., Ostrander, G.K. and El Rassi, Z., *J. Chromatogr.A*, 695 (1995) 83.
10. Svennerholm, L., *J. Neurochem.*, 10 (1963) 613.
11. Wiegandt, H., in Weigandt, H., Ed., *Glycolipids*, Elsevier, Amsterdam 1985, p. 199.
12. Li, Y.-T. and Li, S.-C., *Methods Enzymol.*, 179 (1989) 479.
13. Ostrander, G. K., Levery, S. B., Hakomori, S. and Holmes, E. H., *J. Biol. Chem.*, 263 (1988) 3103.
14. Nashabeh, W. and El Rassi, Z., *J. Chromatogr.*, 514 (1990) 57.
15. Boeseken, J., *Adv. Carbohydr. Chem.*, 4 (1949) 189.
16. Foster, A. B., *Adv. Carbohydr. Chem.*, 12 (1957) 81.
17. Honda, S., Makino, A., Suzuki, S. and Kaheki, K., *Anal. Biochem.*, 191 (1990) 228.



18. Van Duin, M. , Peters, J.A., Kiebomm, A.P.G. and Van Bekkum, H., *Tetrahedron*, 41 (1985) 3411.

CHAPTER VI

FUSED-SILICA CAPILLARIES WITH SURFACE-BOUND DEXTRAN LAYER  
CROSSLINKED WITH DIEPOXY POLYETHYLENE GLYCOL FOR  
CAPILLARY ELECTROPHORESIS OF BIOLOGICAL  
SUBSTANCES AT REDUCED ELECTRO-  
OSMOTIC FLOW

Introduction

Due to its high resolving power and simple operational aspects, open tubular capillary zone electrophoresis (CZE) is currently the most popular branch of capillary electrophoresis. Although CZE with fused silica capillaries is being increasingly used in the area of biopolymers, its application to the separation of proteins is hampered by the Coulombic attraction between the negatively charged fused silica surface and the polyionic protein solutes. This solute-wall interaction is most often manifested by a substantial band broadening and in some cases is accompanied by irreversible adsorption of the solute to the capillary walls.

Several approaches have been described to alleviate solute-silica interaction including the derivatization of the silanol groups on the surface of fused-silica capillaries with hydrophilic coatings (for more details see Refs 1 and 2, and Chapter II). Although approaches such as the use of electrolytes of low [3] or high pH [4], high ionic strength buffers [5], buffers with zwitterionic components [6], etc. were shown useful, the covalent attachment of bonded phases [7,8] to the silica surface proved to be the most effective solution to the problems associated with solute adsorption on the inner walls of fused silica capillaries.

A wide variety of permanent coatings have been proposed by different investigators, including neutral and charged coatings [1,2]. Our laboratory has described different types of coatings, including surface-bonded hydroxylated polyether capillaries with reduced EOF [9], hydrophilic coatings with switchable EOF [10] and multilayered coatings having zero or constant (pH independent) anodal EOF [11]. It has to be noted that there is no one single coating that will suit all types of applications. For instance, while in some applications a moderate EOF of defined direction (anodal or cathodal) is needed to allow the analysis of both negatively and positively charged solute in a single electrophoretic run, in other cases the EOF must be eliminated or reduced in order to allow an enhanced resolution for closely related species.

This chapter introduces a hydrophilic coating based on high molecular weight dextran polysaccharides. The coating procedure is simple and highly reproducible involving three major steps. The silica surface is first coated with an oligomeric epoxy silane layer. In a second step, dextran is covalently attached to the epoxy layer in the presence of boron trifluoride ( $\text{BF}_3$ ), a Lewis acid catalyst. In a third step, the dextran is crosslinked with diepoxy polyethylene glycol in the presence of  $\text{BF}_3$ . It should be mentioned that dextran was recently coated onto fused silica capillary by Hjertén and Kubo [12] using a rather lengthy procedure involving the conversion of dextran to allyl dextran before bonding of the polysaccharide to the capillary inner wall. The method described in the present report is much simpler, utilizes commercially available compounds and involves the stabilization of the bonded dextran layer by crosslinking with PEG. As will be demonstrated, in addition to being highly stable and reproducible, the coating resulted in reducing the EOF and solute-wall interaction. This allowed the separation of basic proteins with high separation efficiencies and permitted the separation of very closely related sialooligosaccharides derived from gangliosides.

## Materials and Methods

### Instruments and Capillaries

A Beckman P/ACE instrument (Beckman Instrument, Fullerton, CA, USA), Model 5510 equipped with a diode array detector was used in this study. Detection was performed at 214 nm for proteins and 250 nm for ANDSA derivatives of carbohydrates, and the data were analyzed by System Gold software from Beckman Instrument using an IBM personal computer. In all experiments, the temperature of the capillary was maintained at 25°C by the instrument thermostating system. The samples were introduced as thin plugs into the capillary via high pressure injection mode where one second of injection introduces 1.2 nL of sample. Capillaries were obtained from the same source stated in Chapter III.

### Reagents and Materials

Lysozyme from turkey egg white, cytochrome C from horse heart, ribonuclease A and  $\alpha$ -chymotrypsinogen A both from bovine pancreas, ovalbumin, trypsin inhibitor type (I-S) from soybean,  $\beta$ -lactoglobulin A and B from bovine milk,  $\alpha$ -lactalbumin from human milk, L-glyceric acid, D-gluconic acid, D-galacturonic acid, D-glucuronic acid, D-galacturonic acid, N-acetylneuraminic acid (NeuNAc) and dextrans with average  $M_r$ s of 45 000, 71 000 and 150 000 Da produced by *Leuconostoc mesenteroides* were purchased from Sigma Chemical Co. (St. Louis, MO, USA).  $\gamma$ -Glycidoxypropyltrimethoxysilane, polyethylene glycol (PEG) of  $M_r$  200, boron trifluoride etherate ( $\text{BF}_3$ ), dimethylsulfoxide (used as an inert EOF tracer) and 1,4-dioxane were purchased from Aldrich (Milwaukee, WI, USA). Polyethylene glycol diglycidyl ether of  $M_r$  200 (diepoxy PEG) was obtained from Polysciences (Warrington, PA, USA). Other materials were obtained from the same sources stated in chapters III-V

### Capillary Coating

Fused-silica capillaries of different lengths were coated with dextrans of different molecular weights according to the following procedure. Capillaries were first etched with 1.0 M NaOH for 15 min followed by washing with deionized water for 15 min. Then, the capillary was filled with an aqueous solution containing 10% (v/v)  $\gamma$ -glycidoxypropyltrimethoxysilane and allowed to react at 96°C for 20 min in a laboratory oven. This step was repeated three times. Next, the capillary was flushed with dried 1,4-dioxane for 15 min and then with 2.5 mL dried dioxane saturated with dextran and containing 1% (v/v)  $\text{BF}_3$  at a flow rate of 0.5 mL/hr. Finally, the capillary was perfused with 10% (v/v) of both polyethylene glycol diglycidyl ether ( $M_r$  200) and polyethylene glycol (PEG) of  $M_r$  200 in dried dioxane containing 1% (v/v)  $\text{BF}_3$  for two hours. The modified capillaries were stored in HPLC-grade methanol. Throughout the surface treatment of fused silica capillaries, a single-syringe infusion pump (Cole-Parmer Instruments, Niles, IL, USA) was used for washing and flushing the capillaries with the different solutions.

### Stability Studies

The stability of the different coated capillaries was tested by flushing the capillaries with corrosive aqueous solutions such as 0.010 M HCl or 0.010 M NaOH for 10 min between runs and then equilibrating the column with the running electrolyte for 5 min before each run. These washes were repeated separately 10 times for each solution.

### Reproducibility Studies

The reproducibility of the coatings was evaluated by comparing protein migration times from run-to-run, day-to-day and column-to-column. The calculations of percentage relative standard deviation (%RSD) for run-to-run were based on five successive measurements separated by 5 min washing with HPLC-grade methanol and 5 min equilibration with the

running electrolyte. For day-to-day, %RSD calculations were based on a total of 15 measurements made on five different days (5 sets of 3 measurements each). For column-to-column, %RSD was calculated using data collected from three columns prepared on three different days.

### Derivatization of Acidic Mono- and Oligosaccharides

Acidic monosaccharides as well as sialooligosaccharides derived from gangliosides were tagged with ANDSA as previously described [13-15] (Chapters III-V).

## Results and Discussion

### Coatings of capillaries

The dextran polysaccharides from *Leuconostoc mesenteroides* used in this study have a backbone of D-glucose linked predominantly by  $\alpha$ -D(1 $\rightarrow$ 6) which is mainly branched at  $\alpha$ -D(1 $\rightarrow$ 3). The branched nature and hydrophilic character of the dextran polysaccharides make them very attractive candidates for the coating of fused silica capillaries. A branched coating sticking out of the surface will certainly hinder biopolymers (such as proteins) from getting in close proximity of the charged silica surface thus diminishing their electrostatic interactions with the surface silanols. As described in the experimental section, besides the covalent attachment of a layer of dextran to the capillary surface via an epoxy activated primary layer, the branched dextran was further stabilized by crosslinking with diepoxy PEG. In this crosslinking step, the addition of regular PEG to the reaction mixture is to provide long hydrophilic chain for the efficient crosslinking of the high molecular weight polysaccharides.

### Evaluation of the Coated Capillaries

Electroosmotic Flow. The electroosmotic flow (EOF) whose magnitude reflects the surface charge characteristics as well as the surface coverage with a given coating, was

measured for the different dextran coated capillaries, and the results were compared to those obtained on bare fused-silica capillaries (see Fig. 1). The EOF measurements were performed with 25 mM phosphate electrolyte at different pH values (5-10 at an interval of one pH unit) and an electric field strength of 25 kV. Generally, the EOF of the coated capillaries was reduced to varying degrees for the different dextrans over the whole pH range studied when compared to the EOF obtained with uncoated fused silica capillaries. As expected, dextran 150 kDa capillary showed the most pronounced decrease and an almost constant EOF in the pH range 5-8 (see Fig. 1). For instance, at pH 7.0, the EOF of the dextran 150 kDa capillary was reduced 9 times, while at pH 10.0 the EOF was about 7.5 times less than that on the uncoated capillary. The dextran 71 kDa and 45 kDa coated capillaries showed also a reduced EOF, but to a lesser extent than that for 150 kDa.

As shown above, the reduction in the magnitude of EOF was more pronounced as the molecular weight of dextran used in the coating increased. This observation suggests that (i) the masking of the silanol groups of the capillary walls is more effective as the molecular weight of the dextran is increased and (ii) the viscosity of the coated wall is much greater with dextran of higher molecular weight.

To cut down on the time of analysis, the EOF measurements were made under conditions of low ionic strength (25.0 mM sodium phosphate) and high voltage (25 kV) whereby the magnitude of the EOF is relatively high, and consequently the migration time of the EOF marker is relatively short. This was undertaken to qualitatively ascertain the extent of shielding of the silanols provided by the coating when compared to bare fused silica capillaries. On the other hand, when the coated capillaries were evaluated under the separation conditions for proteins which normally involve the use of electrolytes of higher ionic strength or containing a zwitterionic agent (e.g., MES) the values of EOF of the different capillaries were much lower than the values reported in Fig. 1. The EOF values obtained under the separation conditions are depicted in Table I. Again, and as can be seen in this table, with the separation buffer consisting of citrate/MES whose ionic strength is

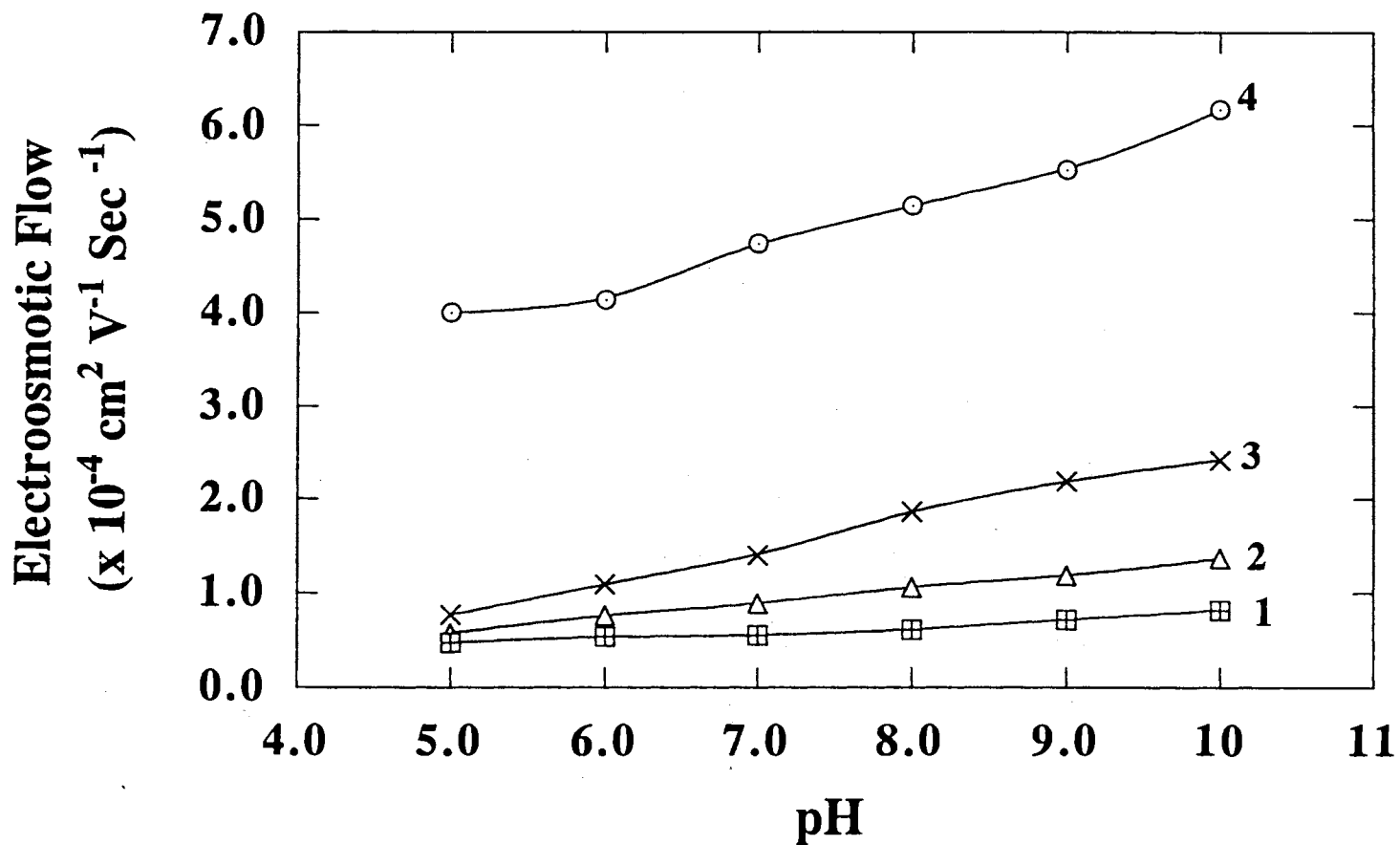


**Figure 1.** Plot of electroosmotic flow versus pH of the running electrolyte. Capillary, 47 cm total length (40 cm effective length) x 50  $\mu\text{m}$  I.D.. Running electrolyte, 0.025 M phosphate buffer at different pH; applied voltage, 25 kV; detection, UV at 214 nm; inert tracer, DMSO. Curves 1, dextran 150 kDa; 2, dextran 71 kDa; 3, dextran 45 kDa; 4, bare fused-silica capillary.



TABLE I. EOF of the Different Capillaries Under the Separation Conditions.

Separation conditions	EOF	EOF	EOF
	(cm <sup>2</sup> V <sup>-1</sup> sec <sup>-1</sup> ) Dextran 45 kDa	(cm <sup>2</sup> V <sup>-1</sup> sec <sup>-1</sup> ) Dextran 71 kDa	(cm <sup>2</sup> V <sup>-1</sup> sec <sup>-1</sup> ) Dextran 150 kDa
20 mM citrate/MES			
pH 6.0	5.30x10 <sup>-5</sup>	4.85x10 <sup>-5</sup>	4.26x10 <sup>-5</sup>
23.5 kV			
100 mM phosphate			
pH 5.0	3.30x10 <sup>-5</sup>	2.64x10 <sup>-5</sup>	2.28x10 <sup>-5</sup>
15 kV			

relatively low and the running voltage is quite high, the EOF is almost twice as higher as that obtained at lower applied voltage with the higher ionic strength sodium phosphate buffer system.

CZE of Basic Proteins. Four standard basic proteins (lysozyme, pI = 11.0; cytochrome C, pI = 10.7; ribonuclease A, pI = 9.4; and  $\alpha$ -chymotrypsinogen A, pI = 9.5) were used as model test solutes to evaluate the different coated capillaries using two different electrolyte systems. Figure 2 illustrates typical electropherograms of the four standard proteins using 0.10 M phosphate buffer, pH 5.0, as the running electrolyte. Under these conditions, the EOF is significantly reduced (see Table I).

The average plate counts per meter,  $N_{av}$ , were 195 000, 252 000 and 570 000 plates/m, for dextran 45 kDa, 71 kDa and 150 kDa coated capillaries, respectively. The high  $N_{av}$  values observed suggest an effective shielding of the silanol groups of the capillary walls by the branched dextran and in turn minimized solute-wall interaction. The separation efficiency of the four basic proteins increased as the molecular weight of dextran used for capillary coatings increased, a behavior that parallels that of the EOF.

To further characterize the capillaries under investigation, the four basic standard proteins were analyzed using 20 mM citrate/MES, pH 6.0, as the running electrolyte.

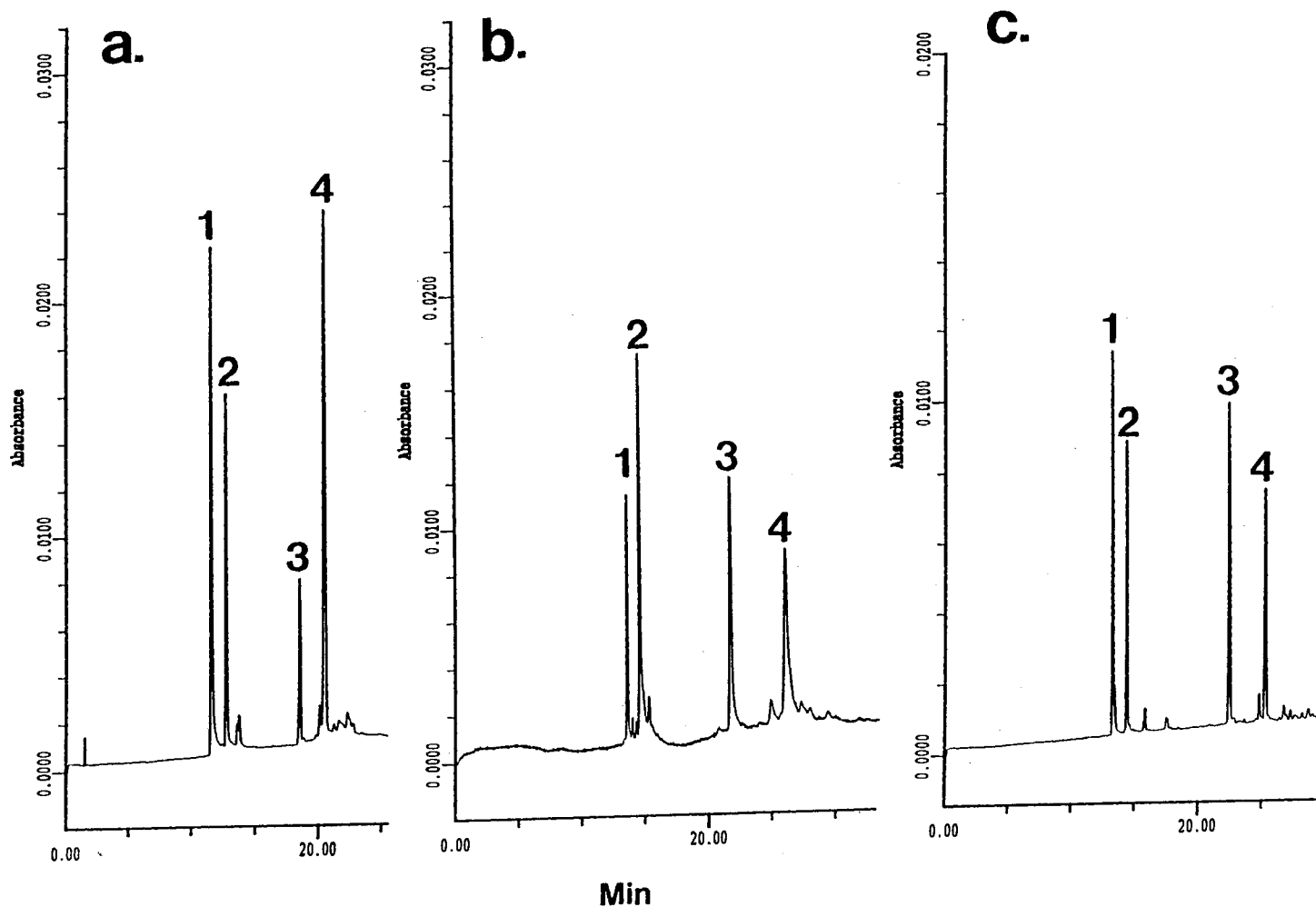


**Figure 2.** Typical electropherograms of four standard basic proteins obtained with dextran 45 kDa (a), dextran 71 kDa (b) and dextran 150 kDa (c). Running electrolyte, 0.10 M phosphate, pH 5.0; pressure injection, 1 sec; applied voltage, 15 kV. Samples: 1, lysozyme; 2, cytochrome C; 3, ribonuclease A; 4,  $\alpha$ -chymotrypsinogen A. Other conditions as in Fig. 1.

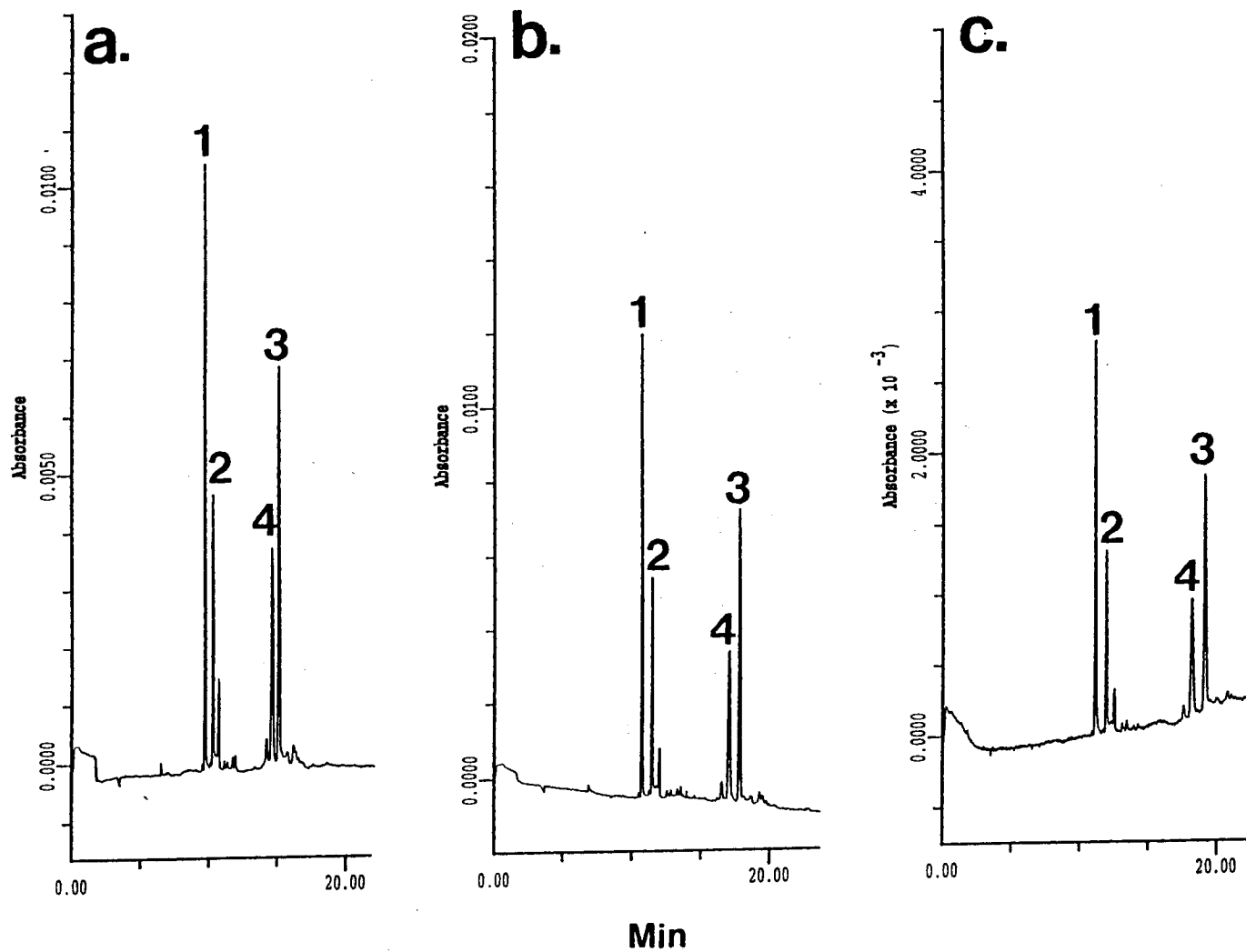
Figure 3 depicts typical electropherograms obtained under these running conditions. The observed  $N_{av}$  values followed the same trend as that obtained in the case of sodium phosphate electrolyte systems. The  $N_{av}$  values were 260 000, 375 000 and 395 000 plates/m for dextran 45 kDa, 71 kDa and 150 kDa capillaries, respectively. It should be noted that, in all cases, the citrate/MES electrolyte systems yielded different selectivity as far as the reversal in the elution order of ribonuclease A and  $\alpha$ -chymotrypsinogen A is concerned, compare Figs 2 and 3.

Reproducibility and Stability of the Coatings. Table II summarizes the run-to-run, day-to-day and column-to-column migration time reproducibility expressed in terms of percent relative standard deviation (% RSD) with four standard basic proteins (i.e., lysozyme, cytochrome C, ribonuclease A and  $\alpha$ -chymotrypsinogen A) at pH 6.0. As can be seen in Table 2, the values of the %RSD are relatively low indicating that the three different dextran coatings are highly reproducible. Dextran 45 kDa showed more reproducibility from run-to-run than the other two, while dextran 150 kDa showed more reproducibility from day-to-day and column-to-column.

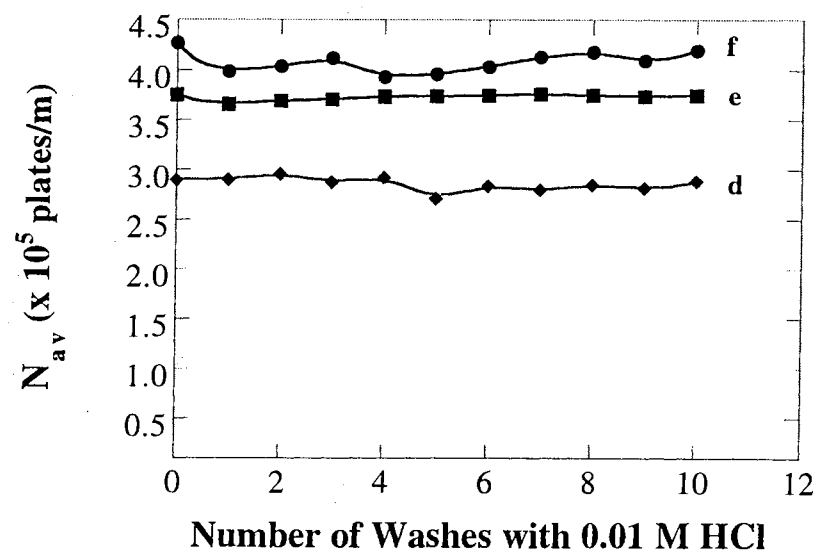
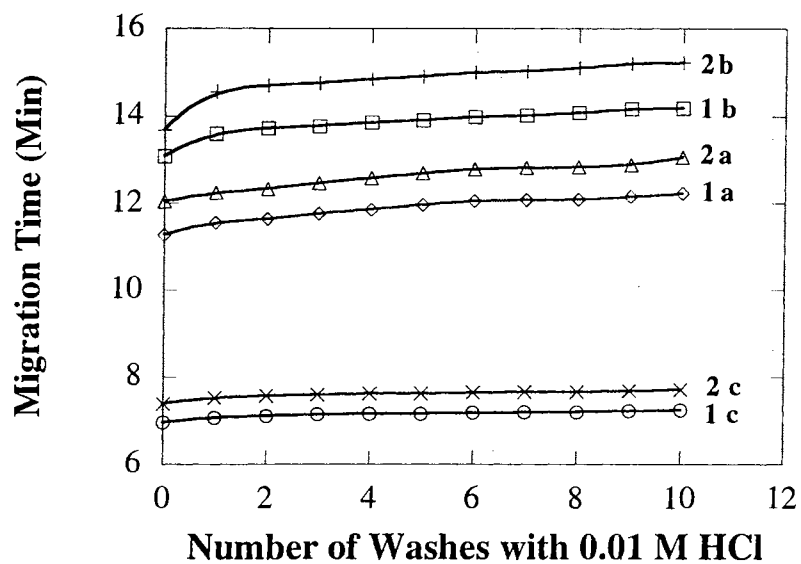
The stability of the dextran-PEG coated capillaries was tested under harsh conditions which involved washing the various capillaries with a strong base solution or strong acid solution before performing the separations of the standard basic proteins, namely lysozyme, cytochrome C, ribonuclease A and  $\alpha$ -chymotrypsinogen A. The different washings were carried out as explained in the experimental section. The results are shown in Figs 4 and 5 in terms of changes in migration time and  $N_{av}$  values of the standard basic proteins as a function of the number of wash. As can be seen in Fig. 4, which illustrates data pertaining to washing the capillaries with 0.010 M HCl, the coatings are quite unaffected by the exposure to solutions of low pH as manifested by the minimal variations in migration times observed on both dextran 150 kDa and 71 kDa capillaries, with the former showing less variation than the later. However, the migration times of basic proteins obtained with dextran 45 kDa capillary varied substantially subsequent to

TABLE II. Percentage Relative Standard Deviation (%RSD) of the Migration Times of Four Basic Proteins Separated on Different Coated Capillaries. Capillary, 47 cm total length (40 cm effective length) x 50  $\mu$ m I.D.; electrolyte, 0.020 M citrate/MES, pH 6.0; pressure injection, 1 sec; applied voltage, 23.5 kV (see experimental for other details).

Proteins	%RSD								
	Dextran 45 kDa			Dextran 71 kDa			Dextran 150 kD		
	run-to- run	day-to- day	column- to-column	run-to- run	day-to- day	column- to-column	run-to- run	day-to- day	column- to-column
Lysozyme	0.34	0.54	1.50	0.11	0.41	1.42	0.35	0.41	1.53
Cytochrome C	0.48	1.70	2.00	0.15	0.64	1.65	0.42	0.56	1.64
Ribonuclease A	0.58	2.00	2.30	0.14	0.93	1.84	0.54	0.61	1.79
$\alpha$ -Chymotrypsinogen A	0.67	2.15	2.45	0.30	0.95	1.96	0.54	0.64	1.89



**Figure 3.** Typical electropherograms of four basic proteins obtained with dextran 45 kDa (a), dextran 71 kDa (b) and dextran 150 kDa (c). Running electrolyte, 0.020 M citrate/MES, pH 6.0; pressure injection, 1 sec; applied voltage, 23.5 kV. Samples as in Fig. 2. Other conditions as in Fig. 1.



**Figure 4.** Plots of migration times of basic proteins versus number of washes with 0.010 M HCl obtained with dextran 45 kDa (a), dextran 71 kDa (b) and dextran 150 kDa (c). Also, plots of  $N_{av}$  versus number of washes with 0.010 M HCl obtained with dextran 45 kDa (d), dextran 71 kDa (e) and dextran 150 kDa (f). Capillary, 47 cm total length (40 cm effective length)  $\times$  50  $\mu$ m I.D. for dextran 45 kDa and 71 kDa, and 37 cm total length (30 cm effective length)  $\times$  50  $\mu$ m I.D. for dextran 150 kDa. Running electrolyte, 0.020 M citrate/MES pH 6.0; pressure injection, 1 sec; applied voltage, 23.5 kV. curves: 1, lysozyme; 2, cytochrome C.

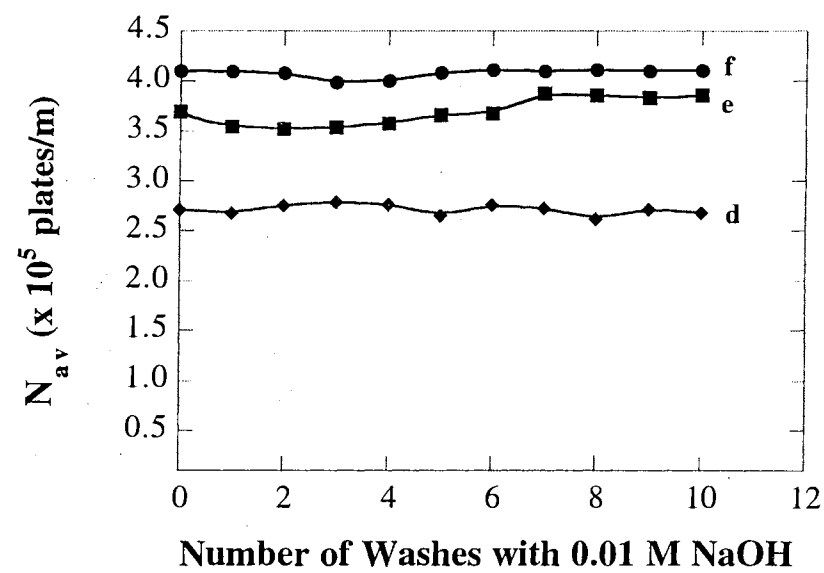
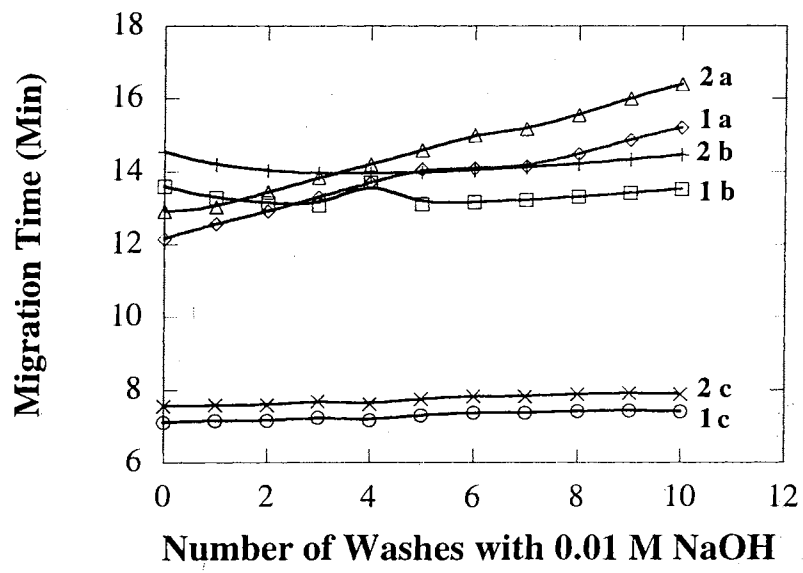


**Figure 5.** Plots of migration times of basic proteins versus number of washes with 0.010 M NaOH obtained with dextran 45 kDa (a), dextran 71 kDa (b) and dextran 150 kDa (c). Also, plots of  $N_{av}$  versus number of washes with 0.010 M NaOH obtained with dextran 45 kDa (d), dextran 71 kDa (e) and dextran 150 kDa (f). Symbols and other conditions as in Fig. 4.

these washes. This finding may suggest that the extent of crosslinking and attachment of dextran to the surface is not sufficiently high for the low molecular weight dextran.

In another set of experiments, the capillaries were tested for stability by washing them with 0.010 M NaOH. The results obtained here resemble those observed with the acidic washes with the exception that the dextran 45 kDa capillary suffered substantial changes in migration time from successive washes with 0.01 M NaOH as shown in Fig. 5. Dextran 71 kDa and 150 kDa capillaries showed excellent stability at high pH which make them very useful for the analysis of negatively charged species at high pH in the negative polarity mode (see below).

### CZE of Negatively Charged Species

Acidic Proteins. In addition to demonstrating the usefulness of the capillaries in CZE of basic proteins, we have also evaluated their utility in the analysis of acidic proteins at reduced EOF using an electric field in the negative polarity as shown in Fig. 6. Since the dextran 150 kDa capillary showed the highest separation efficiency with basic proteins, we have selected this capillary to carry out the separation of some standard acidic proteins. As can be seen in Fig. 6, five acidic proteins namely ovalbumin, trypsin inhibitor,  $\beta$ -lactoglobulin A,  $\beta$ -lactoglobulin B and  $\alpha$ -lactalbumin could be separated in 30 min with an  $N_{av}$  value of 111,000 plates/m using 0.10 M sodium phosphate, pH 7.0, as the running electrolyte. This plate number is much less than that observed with the basic proteins. Very recently, we have reported similar observations with capillary having hydroxypropyl cellulose coating [11]. One possible explanation for the relatively low efficiency is probably the presence of some hydrophobic interaction between the acidic proteins under investigation and the coating. It should be mentioned that these acidic proteins are of higher molecular weight than the basic ones utilized in the above study.

ANDSA Derivatives of Acidic Monosaccharides. The utility of the dextran-PEG coated capillaries in separation of biological species other than proteins was evaluated by



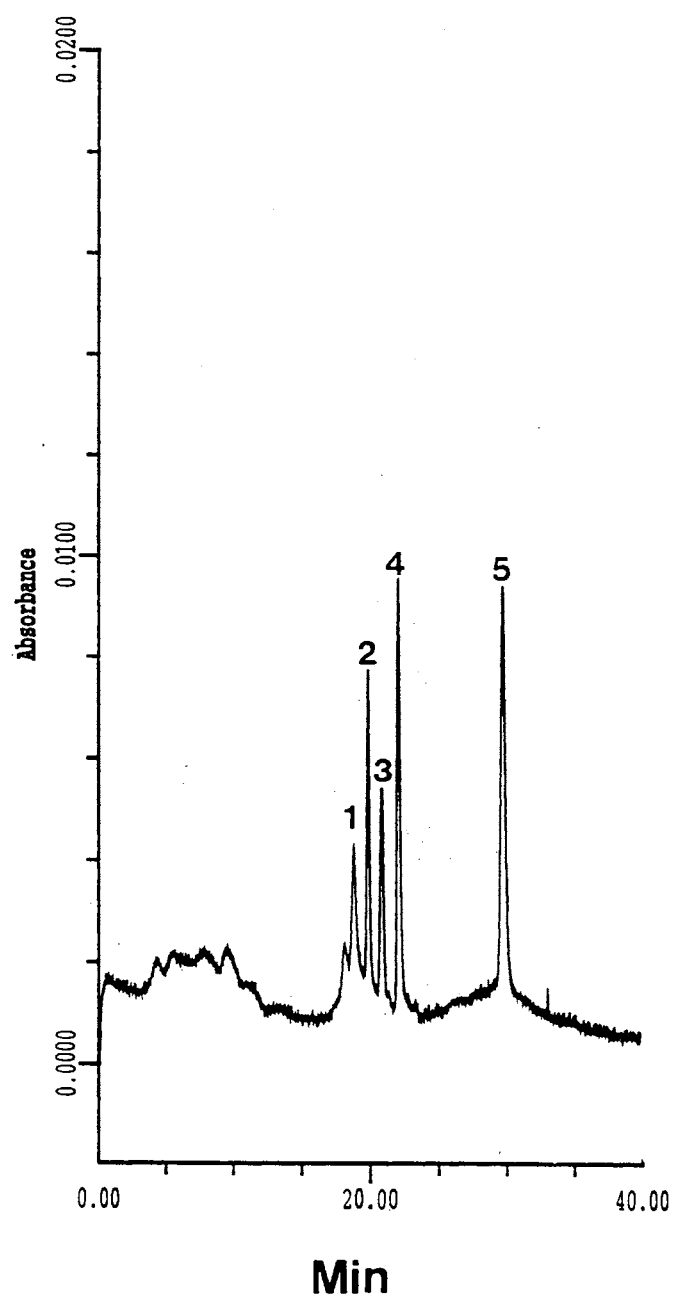


**Figure 6.** Typical electropherogram of acidic proteins obtained on a dextran 150 kDa coated capillary. Running electrolyte, 0.10 M phosphate pH 7.0; pressure injection, 1 sec; applied voltage, -15 kV. Samples: 1, ovalbumin; 2, trypsin inhibitor; 3,  $\beta$ -lactoglobulin A; 4,  $\beta$ -lactoglobulin B; 5,  $\alpha$ -lactalbumin. Other conditions as in Fig. 1.

analyzing ANDSA derivatives of acidic monosaccharides using an electric field of negative polarity. Under this condition, a very low EOF in the direction opposite to that of the electrophoretic mobility of the separated analytes is present which would in principle benefit the separations by enhancing resolution. In addition, the charge on the solutes and the capillary surface are of the same sign, which will preclude sorptive interactions. A typical example of the ANDSA-monosaccharide derivatives is shown in Fig. 7 for *N*-acetylneuraminic acid.

In this selective precolumn derivatization, which has been introduced by our laboratory [13-15] and described in Chapters III-V, the labeling of acidic carbohydrates is based on the reactivity of the carboxyl acid group, which in the presence of carbodiimide can react with the amine group of an appropriate tag to form an amide bond as shown in Fig. 7 for the case of *N*-acetylneuraminic acid and 7-aminonaphthalene-1,3-disulfonic acid (ANDSA). As can be seen, the ANDSA derivatives are negatively charged and the derivatization introduces an extra negative charge on the analyte, i.e., each carboxylic acid group on the analyte is replaced by two sulfonic acid groups. Figure 8 shows the separation of six ANDSA derivatives of acidic monosaccharides on dextran 150 kDa capillary using an electric field of negative polarity. The separation was completed in almost 10 min with 100 mM borate buffer, pH 10, as the running electrolyte. Using these conditions, a significantly longer analysis time (25 min) was required to achieve the separation on an uncoated capillary (results not shown) when an electric field of positive polarity was used. It should be noted that the elution order was reversed in the case of uncoated capillary. In both cases, the resolution of the different analytes is due to the extent of borate complexation with each analyte in the mixture [13].

ANDSA Derivatives of Sialooligosaccharides Derived from Gangliosides. Again, dextran 150 kDa capillary was also examined in the CZE of ANDSA derivatives of sialooligosaccharides derived from gangliosides. As in the case of acidic monosaccharides, the precolumn derivatization takes place on the carboxylic acid group of the sialic acid

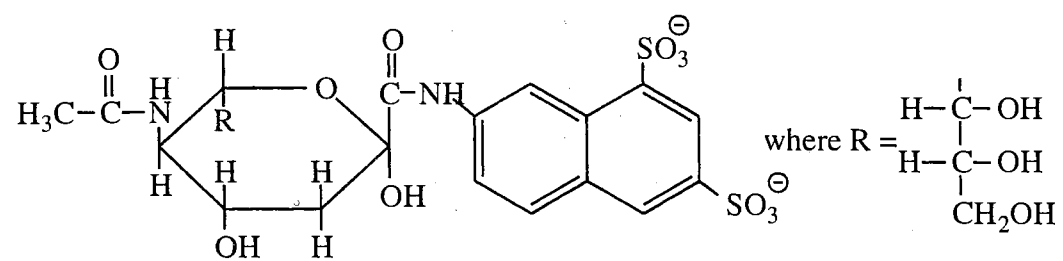


**Figure 7.** Structure of *N*-Acetylneuraminic acid-ANDSA derivative.

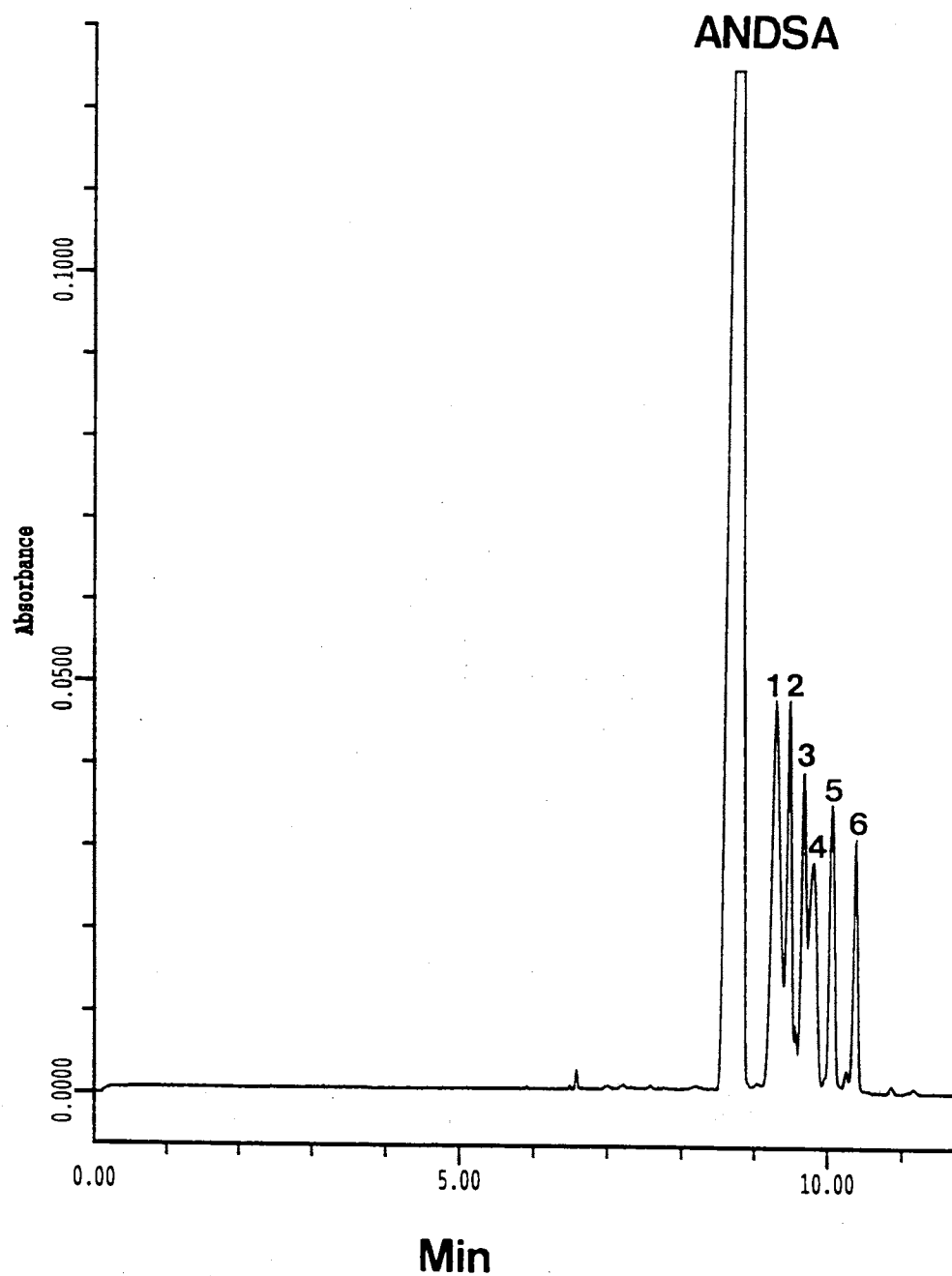


**Figure 8.** Electropherograms of ANDSA derivatives of acidic monosaccharides obtained on a dextran 150 kDa coated capillary. Running electrolyte, 0.10 M borate, pH 10.0; pressure injection, 1 sec; applied voltage, -15 kV; detection, UV at 250 nm. Sample: 1, D-glucuronic acid; 2, D-glyceric acid; 3, D-galactonic acid; 4, D-galacturonic acid; 5, D-gluconic acid; 6, *N*-acetylneuraminic acid. Other conditions as in Fig. 1.

residue, i.e., NeuNAc residue; for structures see Table I of Chapter V. Figure 9 illustrates a typical electropherogram of seven ANDSA derivatives of sialooligosaccharides performed with an electric field in the negative polarity.

As can be seen from the structures of the sialooligosaccharides illustrated in Table I of Chapter V, two of the analytes are structural isomers, yet they were completely separated when the separation was conducted in 0.10 M sodium phosphate buffer, pH 7.0 ( Fig. 9). The two structural isomers were not resolved when the separation was conducted on uncoated capillary in the positive polarity electric field [15], see Fig. 1b in Chapter V. The separation on the coated capillary had an  $N_{av}$  value of 419 000 plates/m.

### Conclusions

Due to its branched structure and hydrophilic character, dextran crosslinked with PEG behaves as a suitable coating for fused silica capillaries by minimizing solute-wall interaction. The dextran coating crosslinked with PEG created a surface layer of high viscosity which in combination with its shielding effect of the surface silanols have substantially reduced the EOF. The reduced solute-wall interaction, the hydrophilic nature of the dextran-PEG coating and the minimized EOF have facilitated the separation of basic and acidic proteins as well as the separation of closely related mono- and oligosaccharides with relatively high separation efficiency.

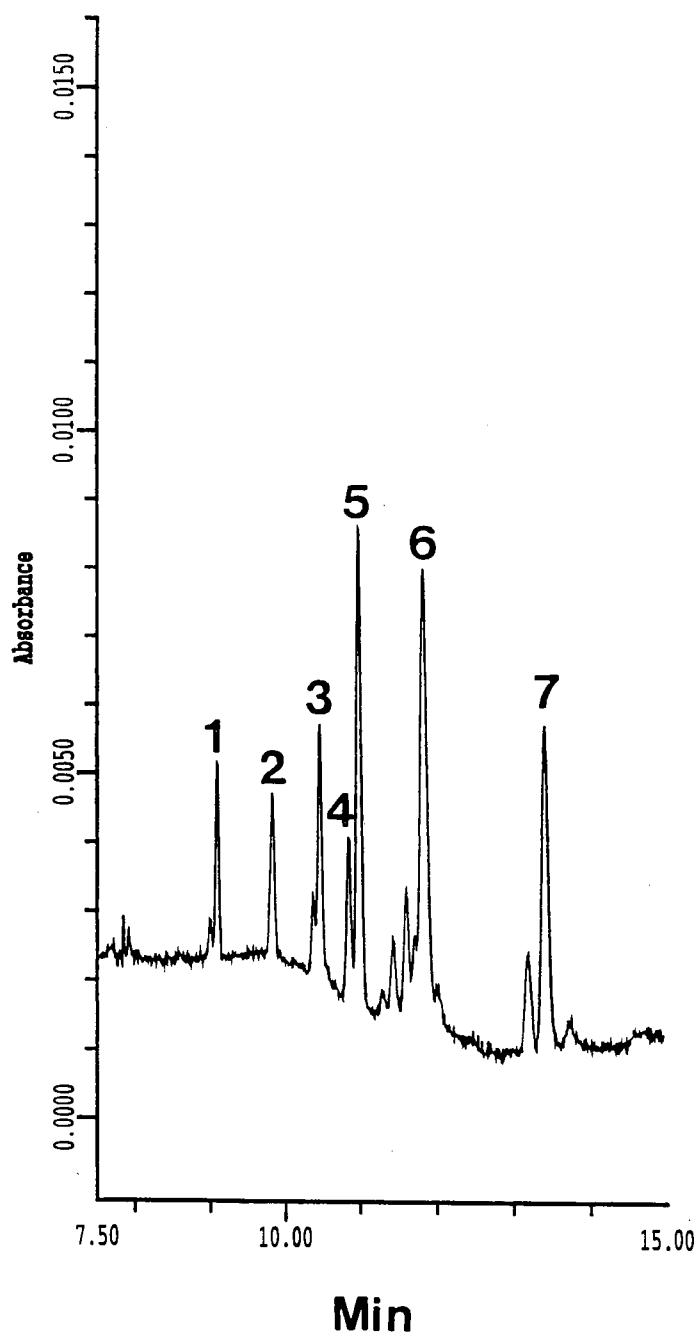


**Figure 9.** Electropherograms of ANDSA derivatives of sialooligosaccharides derived from gangliosides obtained on a dextran 150 kDa coated capillary. Running electrolyte, 0.10 M phosphate pH 7.0; pressure injection, 1 sec; applied voltage, -15 kV; detection, UV at 250 nm. Sample: 1, Sialooligo-G<sub>D3</sub>; 2, Sialooligo-G<sub>M3</sub>; 3, Sialooligo-G<sub>T1b</sub>; 4, Sialooligo-G<sub>D1b</sub>; 5, Sialooligo-G<sub>D1a</sub>; 6, Sialooligo-G<sub>M2</sub>; 7, Sialooligo-G<sub>M1</sub>. Other conditions as in Fig. 1.

## References

1. El Rassi, Z. and Nashabeh, W., in El Rassi, Z., Ed., *Carbohydrate Analysis: High Performance Liquid Chromatography and Capillary Electrophoresis*, Elsevier, Amsterdam 1994, p. 267.
2. Issaq, H.J., Janini, G.M., Chan, K.C. and El Rassi, Z., *Adv. Chromatogr.*, 35 (1995) 101.
3. McCormick, R., *Anal. Chem.*, 60 (1988) 2322.
4. Lauer, H.H. and McManigill, D., *Anal. Chem.*, 58 (1986) 166.
5. Green, S. and Jorgenson, J.W., *J. Chromatogr.*, 478 (1989) 63.
6. Bushey, M.M. and Jorgenson, J.W., *J. Chromatogr.*, 1989, 480, 301-310.
7. Hjertén, S., *J. Chromatogr.*, 347 (1985) 191.
8. Cobb, K., Dolnik, V. and Novotny, M., *Anal. Chem.*, 62 (1990) 2478.
9. Nashabeh, W. and El Rassi, Z., *J. Chromatogr.*, 559 (1991) 367.
10. Smith, J. T. and El Rassi, Z., *HRC, J. High Resolut. Chromatogr.*, 15 (1992) 573.
11. Smith, J. T. and El Rassi, Z., *Electrophoresis*, 14 (1993) 396.
12. Hjertén, S. and Kubo, K., *Electrophoresis*, 14 (1993) 390.
13. Mechref, Y. and El Rassi, Z., *Electrophoresis*, 15 (1994) 627.
14. Mechref, Y., Ostrander, G.K. and El Rassi, Z., *J. Chromatogr. A*, 695 (1995) 83.
15. Mechref, Y., Ostrander, G.K. and El Rassi, Z., *Electrophoresis*, 16 (1995) 1499.

CHAPTER VII

CAPILLARY ENZYMOPHORESIS OF NUCLEIC ACID FRAGMENTS USING  
COUPLED CAPILLARY ELECTROPHORESIS AND CAPILLARY  
ENZYME MICROREACTORS HAVING SURFACE-  
IMMOBILIZED RNA-MODIFYING  
ENZYMES

Introduction

The need for selectively modifying minute amounts of biochemicals prior to analysis while not introducing any significant dilution in the sample being analyzed, has always led to the search for specific reagents as well as to the development of new and suitable microdevices for microanalysis. The microscale capabilities of capillary electrophoresis (CE) and the high specificity of enzymes were soon realized in biochemical analysis by combining CE and enzyme microreactors in an off- or on-line types of arrangement [1-4]. Along these lines, free solution enzyme-catalyzed reactions in capillary to assay enzyme activity [5-7] or to digest a protein for peptide mapping [8] were also developed.

Recently, our laboratory introduced open-tubular capillary enzyme reactors with various immobilized RNA-modifying enzymes, e.g. ribonuclease T<sub>1</sub>, hexokinase and adenosine deaminase [2,3], for the modification of nucleic acid fragments prior to analysis by CE. For this combination of CE and capillary enzyme microreactors, we coined the term capillary enzymophoresis [3]. In our initial work [3], we have shown that capillary enzymophoresis is a suitable approach for (i) locating peaks (i.e., identifying sample components) on the electropherogram, (ii) improving the selectivity of the electrophoretic



system, (iii) facilitating the quantitative determination of analytes with good accuracy, (iv) on line digestion and mapping of minute amounts of transfer ribonucleic acids (tRNAs) and (v) the simultaneous synthesis and separation of nanogram quantities of oligonucleotides.

As a continuation of our recent work in the area of capillary enzymophoresis [2,3], this report is concerned with further developing the concept of coupling capillary enzyme reactor to capillary electrophoresis. In this regard, capillary enzyme reactors with immobilized RNase U<sub>2</sub> or RNase T<sub>1</sub> as well as with mixed RNase T<sub>1</sub> and U<sub>2</sub> were developed and evaluated under different conditions, including pH and temperature. These reactors proved useful in modifying RNA fragments prior to CE separation and in mapping minute amounts of tRNAs by CE.

## Materials and Methods

### Reagents and Materials

Ribonuclease U<sub>2</sub> (RNase U<sub>2</sub>) from *Ustilago sphaerogena* [EC 3.1.27.4], ribonuclease T<sub>1</sub> (RNase T<sub>1</sub>) from *Aspergillus oryzae* [EC 3.1.27.3] were obtained from Pharmacia Biotech Inc. (Piscataway, NJ, U.S.A.). Transfer ribonucleic acid specific for phenylalanine (tRNA<sup>Phe</sup>) from brewers yeast, guanylyl-(3'→5')-adenosine (GpA), guanylyl-(3'→5')-uridine (GpU), guanylyl-(3'→5')-guanosine (GpG), adenylyl-(3'→5')-cytidine (ApC), adenylyl-(3'→5')-guanosine (ApG), adenylyl-(3'→5')-uridine (ApU), adenosine-2':3'-cyclic monophosphate (A>p), guanosine-2':3'-cyclic monophosphate (G>p), adenine (A), guanine (G), uracil (U), and cytosine (C) were purchased from Sigma Chemical Co. (St. Louis, MO, U.S.A.).  $\gamma$ -Aminopropyltriethoxysilane was obtained from Hüls of America (Bristol, PA, U.S.A.). Hexadimethrine bromide (polybrene) and glutaric dialdehyde were obtained from Aldrich (Milwaukee, WI, U.S.A.). Ammonium bifluoride and citric monobasic sodium salt were obtained from Fisher Scientific (Pittsburgh, PA, U.S.A.). Other chemical were obtained from the same sources listed in Chapters III and IV.

## Instrument

The instrument for capillary electrophoresis was assembled in-house from commercially available components, resembled previously reported systems [9] and is described in Chapter III.

## Capillary Columns

Fused-silica capillary columns of 50  $\mu\text{m}$  I.D and 365  $\mu\text{m}$  O.D. were purchased from Polymicro Technology (Phoenix, AZ, U.S.A.). All capillaries used in this study were coated in-house with fuzzy polyether chain according to previously described procedures [10].

## Enzyme Reactor Preparation

Fused-silica capillaries of 50  $\mu\text{m}$  I.D. and various lengths were coated with RNase T<sub>1</sub> or RNase U<sub>2</sub> or with a mixture of both enzymes. The immobilization of the enzymes was carried out according to a procedure described earlier [3]. Briefly, the capillaries were first etched with ammonium bifluoride according to the procedure described by Onuska *et al.* [11]. Then, the etched capillaries were filled with 10% (v/v) aqueous solution of  $\gamma$ -aminopropyltriethoxysilane and allowed to react at 95°C for 30 min. This step was repeated five times. Next, the capillary was perfused with a 1.0% (v/v) solution of glutaric dialdehyde in 50 mM phosphate, pH 7.0, for 2 hrs at a flow rate of 0.5 ml/hr. Following, the enzyme of interest dissolved in phosphate solution was recycled through the capillary reactor for 3 hrs at the same flow rate and left to stand overnight. Finally, unreacted aldehyde functional groups were scavenged with 50 mM Tris-HCl, pH 7.5. All the enzyme capillary reactors were stored in water at 5 °C when they were not in use.

### Other Procedures

The enzyme capillary reactor was connected to the separation capillary using PTFE tube which has an inner diameter that matches the outer diameter of the capillary columns used. A thin plug of the substrates were introduced by electrokinetic injection for 5 sec at -15 kV. Then, the substrate was forced to traverse the length of the capillary enzyme reactor by raising the electrolyte inlet vial 15 cm higher than the outlet vial. Next, the two capillaries were disconnected and the CZE separation was carried out as soon as the substrate plug entered into the separation capillary. The time required for the substrate to traverse the length of the reactor was estimated from the electropherogram obtained with the substrate which was allowed to traverse both the enzyme reactor and separation capillaries lengths passing the detection point. This time was also calculated by applying the mathematical relationship reported earlier [3]. The calculated and experimental values were in good agreement.

The reactivity of the enzyme reactors was studied at different temperatures using the configuration shown in Fig. 1. In this configuration, the capillary enzyme reactor was inserted in a tygon tube which served as a water jacket and the temperature was controlled by a water circulating bath.

In experiments involving the digestion of tRNA<sup>Phe</sup>, the tRNA<sup>Phe</sup> solutions were prepared by dissolving this substrate in 150 mM citrate at a certain pH (that is the pH of the subsequent digestion) and 5 M urea and heated at 55 °C for 10 min before it was introduced into the capillary enzyme reactors. This procedure is carried out to ensure the existence of tRNA<sup>Phe</sup> in its primary structure in the solutions. The dinucleotide samples were prepared by first dissolving the standard dinucleotides in distilled water, and then an aliquot was mixed with the electrolyte solution to be used in the subsequent digestion in a 1:1 ratio before the dinucleotide sample was introduced into the capillary enzyme reactor.

The separation capillary was successively flushed with water, methanol, water, and fresh buffer between runs to ensure reproducible separations. The capillary enzyme reactor

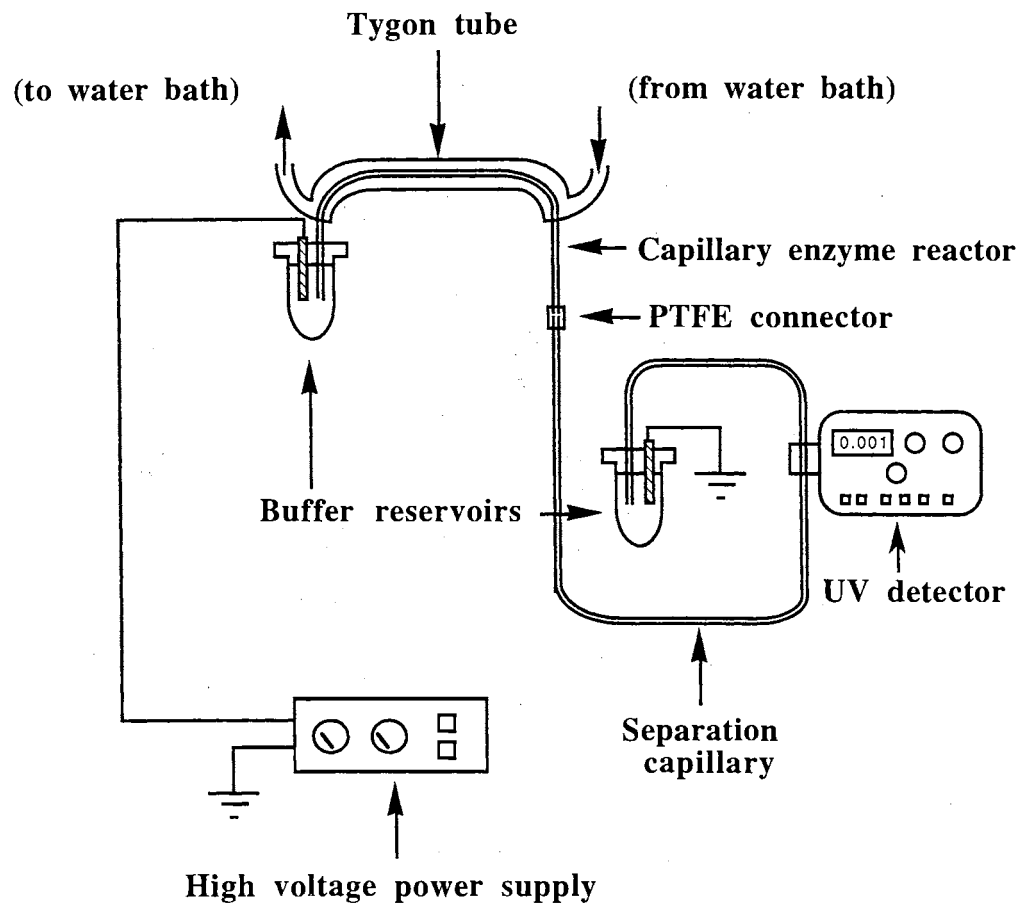


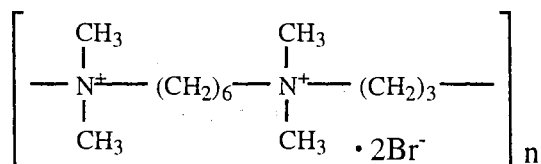
**Figure 1.** Schematic of CE instrument showing the coupling of the capillary enzyme reactor to the separation capillary and the arrangement used for jacketing the microreactor with a tygon tube for thermostating its surrounding via a circulating water bath.

was always flushed and stored in water between runs.

## Results and discussion

### Adjustment of the Direction of EOF in the Separation Capillary

Nucleic acids are negatively charged species, and therefore their rapid separation by electrophoresis requires the use of an electric field of negative polarity. Separations in the negative polarity are better performed when the usual cathodal EOF (i.e., in the direction of the cathode) is extremely low or when the EOF is anodal (i.e., in the direction of the anode). Since the capillaries used in our studies exhibited a moderate cathodal EOF, a mean for inverting the direction of the flow was needed in order to achieve the separation of the various nucleic acids and their bases in a single electrophoretic run. In this regard, we selected hexadimethrine bromide (polybrene) which is a polymer of *N,N,N',N'*-tetramethylhexamethylenediamine and trimethylene bromide having a molecular formula of  $(C_{13}H_{30}Br_2N_2)_n$  and the following molecular structure:



Similar to other reported cationic buffer additives [4,12,13], this multi-positively charged polymer interacts with the unreacted negatively charged silanol groups on the surface of the fuzzy polyether capillary, thus converting the net charge of the inner capillary surface to positive, and as a result the EOF is inverted from cathodal to anodal [14]. Figure 2 depicts the observed EOF of the fuzzy polyether coated capillary obtained with running electrolytes containing various percentage of polybrene. Also shown in Fig. 2 is the current generated as a function of polybrene percentage in the running electrolyte. Since polybrene is a polycationic species, the ionic strength of the running electrolyte increases sharply as more

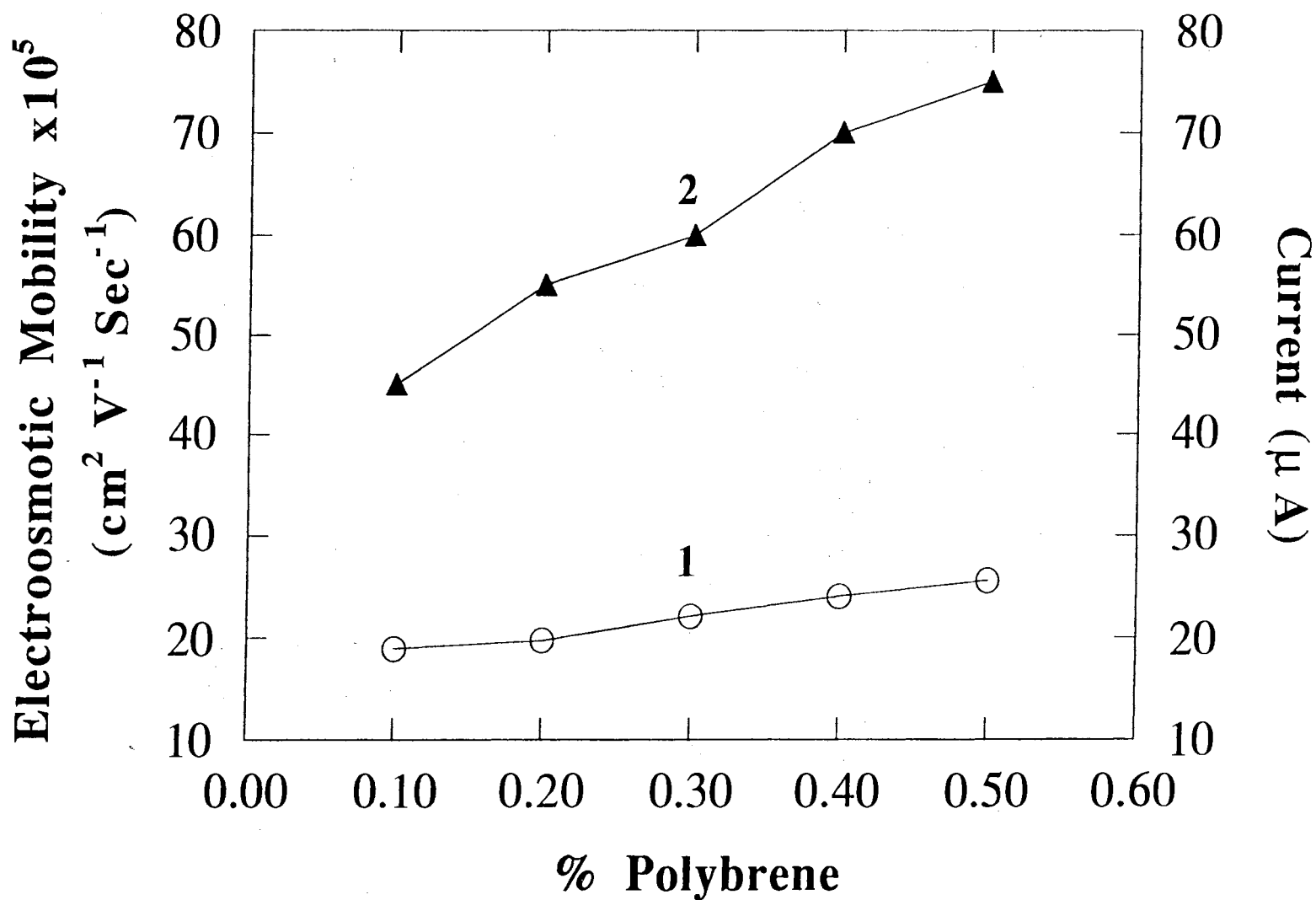


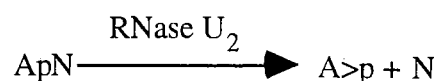
**Figure 2.** Plots of EOF (1) and current (2) as a function of polybrene percentage in the running electrolyte system. Capillary, 40/70 cm x 50 μm I.D., fuzzy polyether coated capillary; running electrolyte, 15 mM citrate, pH 3.5, containing different % (w/w) of polybrene; voltage, -28 kV. DMSO was used as the EOF neutral marker.

polybrene is included in the running electrolyte. This results in increasing the current generated and in turn the joule heating. Increasing the amount of polybrene in the running electrolyte from 0.10 to 0.50% (w/w) increased the EOF by a factor of 1.35; however, the current was almost doubled. Therefore, 0.10 % polybrene (w/w) was used throughout the study in order to keep the current generated in an acceptable range for an in-house built electrophoresis instrument that is without a temperature control system.

As can be seen in Fig. 3 the anodal EOF decreased as the pH values of the running electrolyte increased. This is because of the increasing ionization of the unreacted surface silanol groups with pH. Thus, for the same amount of polybrene used in the electrolyte, the positive charge density of the capillary decreases as the pH is raised, a condition that leads to decreasing EOF.

#### RNase U<sub>2</sub> Capillary Enzyme Reactor

Ribonuclease U<sub>2</sub> is an endoribonuclease specific for adenylic acid [15,16]. RNase U<sub>2</sub> cleaves phosphodiester bonds between 3'-adenylic acid residues and the 5'-hydroxyl groups of adjacent nucleotidyl residues (ApN). This leads to the formation of an adenosine-2':3'- cyclic monophosphate (A>p) and a nucleoside (N) according to the following reaction scheme:



The catalytic activity of immobilized RNase U<sub>2</sub> capillary reactor towards different dinucleotides was evaluated by CZE under different conditions. The substrate was first introduced as a thin plug into the capillary enzyme reactor, which was connected to the separation capillary as described in materials and methods. Using gravity flow, the thin plug was then allowed to traverse the length of the reactor and to enter the separation capillary. As the plug has entered the tip of the separation capillary the microreactor was disconnected and the digest was analyzed by CZE at -28 kV. In this experiment, 25 min

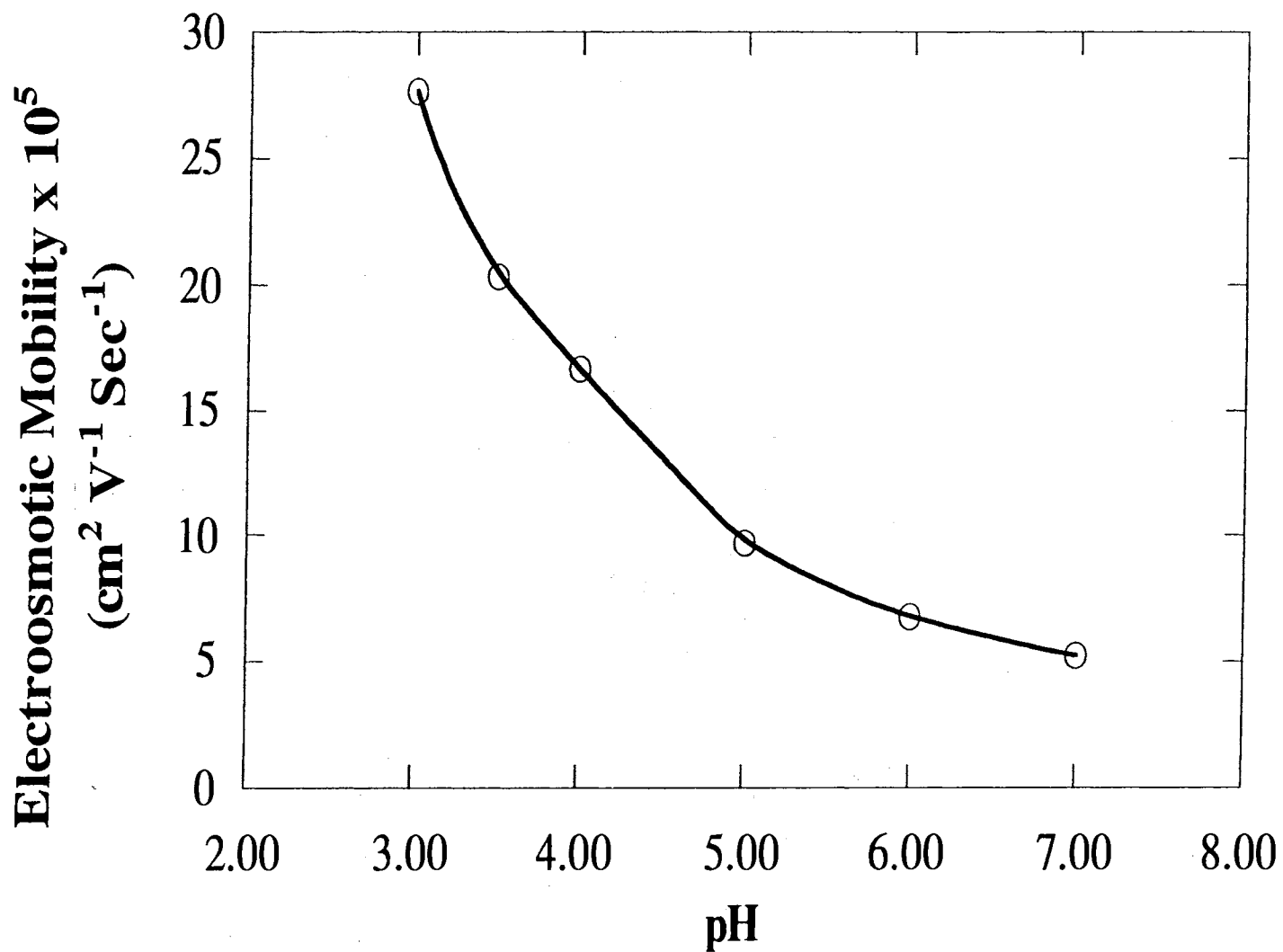


**Figure 3.** Plot of EOF versus the pH of the running electrolyte. Running electrolyte, 15 mM citrate containing 0.10% (w/w) polybrene at various pH values. Other conditions as in Fig. 2.



were required for the substrate to traverse the 15 cm RNase U<sub>2</sub> reactor. This experimental set up was employed to evaluate the reactivity of the RNase U<sub>2</sub> towards the digestion of ApC, ApG, and ApU dinucleotides at different pH values and temperatures. The dinucleotide ApA was not used since it has been reported that this substrate undergoes little or no digestion by RNase U<sub>2</sub> [17]. As can be seen in Fig. 4, RNase U<sub>2</sub> digests ApC more readily than the other two dinucleotides under otherwise identical conditions. In all cases, the enzyme exhibited a maximum activity at pH 3.5. ApC dinucleotide was completely digested by RNase U<sub>2</sub>, while only 40% and 35% of ApG and ApU, respectively, were digested by RNase U<sub>2</sub> at ambient temperature and pH 3.5. This optimum pH value is more acidic than the value reported in the literature for free solution enzymatic digestion [18,19]. The reported pH dependence of the activity of RNase U<sub>2</sub> in free solution has a maximum activity at pH 4.5 which decreases as the pH value was varied around this optimal value, and the enzyme showed little or no activity at pH value less than 2.5 and greater than 5.5 [19]. This difference in enzyme activity between the immobilized and free enzyme could be explained by the change in the microenvironment pH in the vicinity of the immobilized enzyme since the capillary walls are partially charged. On the other hand, the order of reactivity of RNase U<sub>2</sub> towards the different dinucleotides is in agreement with that observed in free solution [19]. These results imply that the immobilization of the enzyme did not affect its specificity but rather shifted its activity toward acidic conditions. Figure 5 depicts electropherograms of ApC digest at different pH values.

The reactivity of the immobilized enzyme was also investigated at various temperatures. In principle, the activity of an enzyme increases with temperature up to a certain value above which the enzyme denatures and loses its activity. Figure 6 displays temperature dependence of the activity of RNase U<sub>2</sub> towards the digestion of the three dinucleotides. Increasing the temperature of the enzyme reactor from 20 to 30 °C increased slightly the activity of the immobilized enzyme. As the temperature was increased above this range, the activity of the immobilized enzyme decreased sharply. As can be seen in

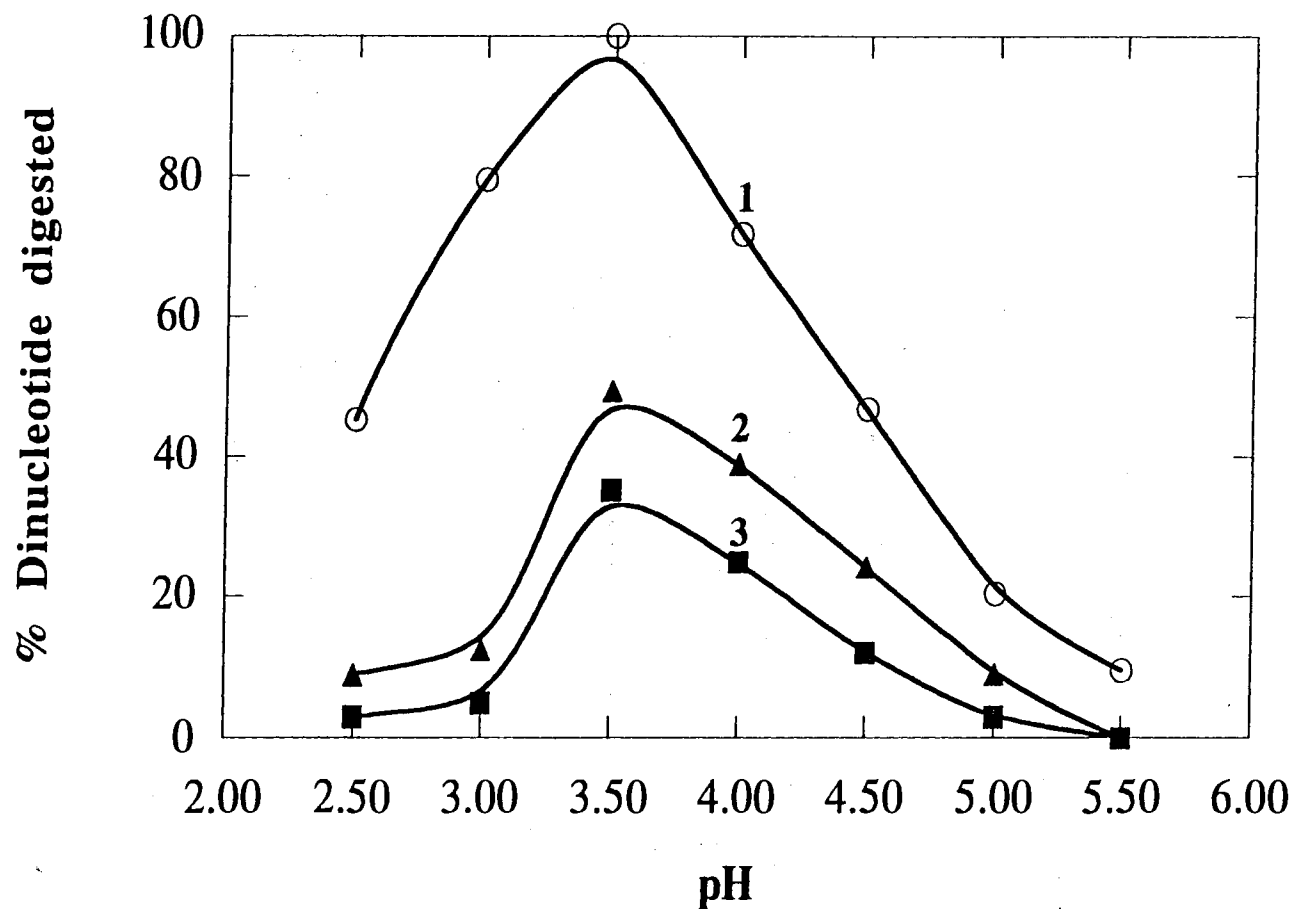


**Figure 4.** pH dependence of the activity of RNase U<sub>2</sub>. The % dinucleotide digested was calculated from peak areas using sulfanilic acid as internal standard. Digestion conditions: the dinucleotide samples were passed through the capillary enzyme reactor (15 cm x 50 μm I.D.), as explained in materials and methods, which was filled with the running electrolyte used in the separation step. Running electrolytes, 15 mM sodium citrate containing 0.1% (w/w) polybrene at various pH values; voltage, -28 kV. Other conditions as in Fig. 2. Curves: 1, ApC; 2, ApG; 3, ApU.

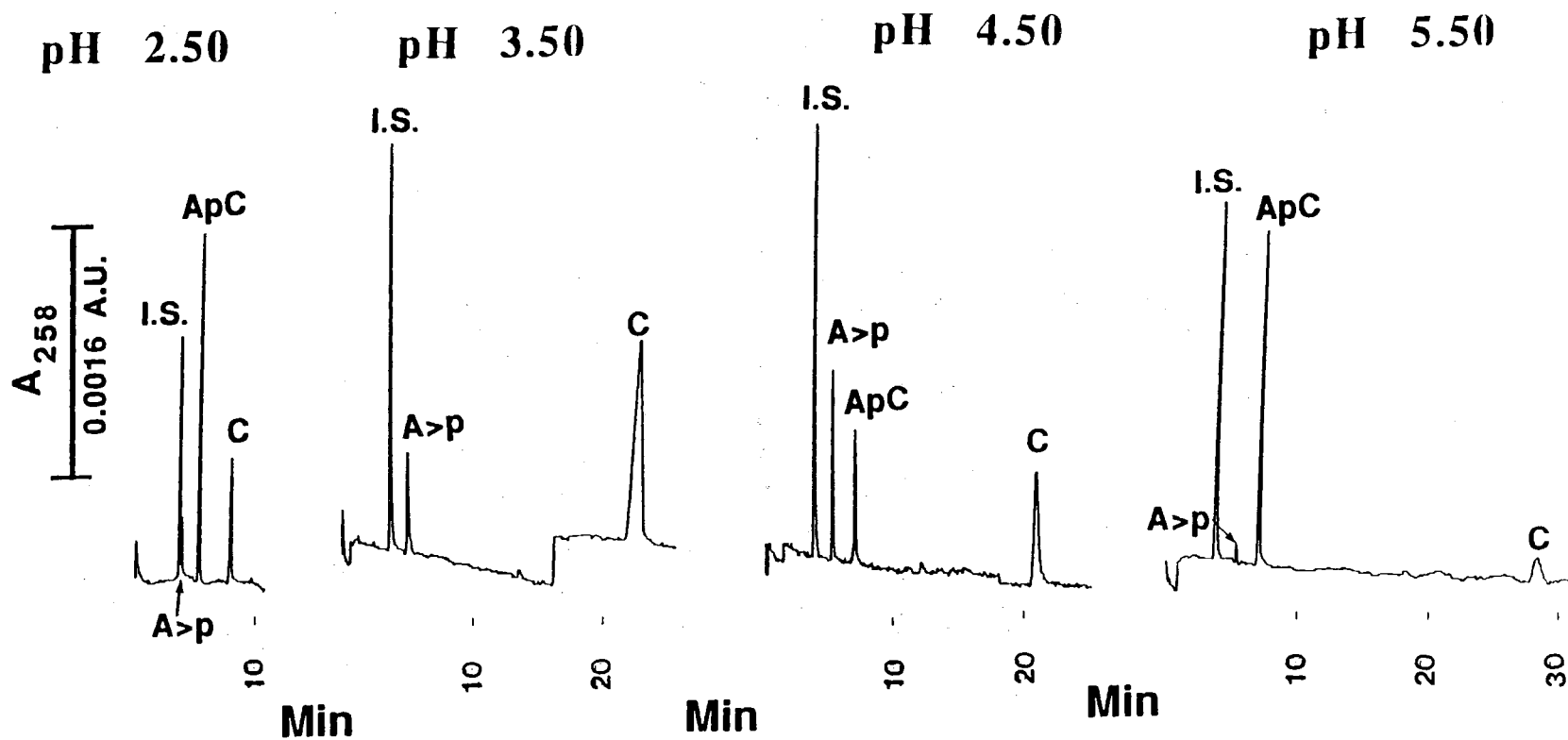


**Figure 5.** Typical electropherograms of digested ApC dinucleotide at different pH values after passing through RNase U<sub>2</sub> capillary reactor (15 cm x 50 μm I.D.). Running electrolytes, 15 mM citrate containing 0.10% (w/w) polybrene at pH 2.50, 3.50, 4.5 and 5.5; voltage, -28 kV. Other conditions as in Figs 2 and 4.

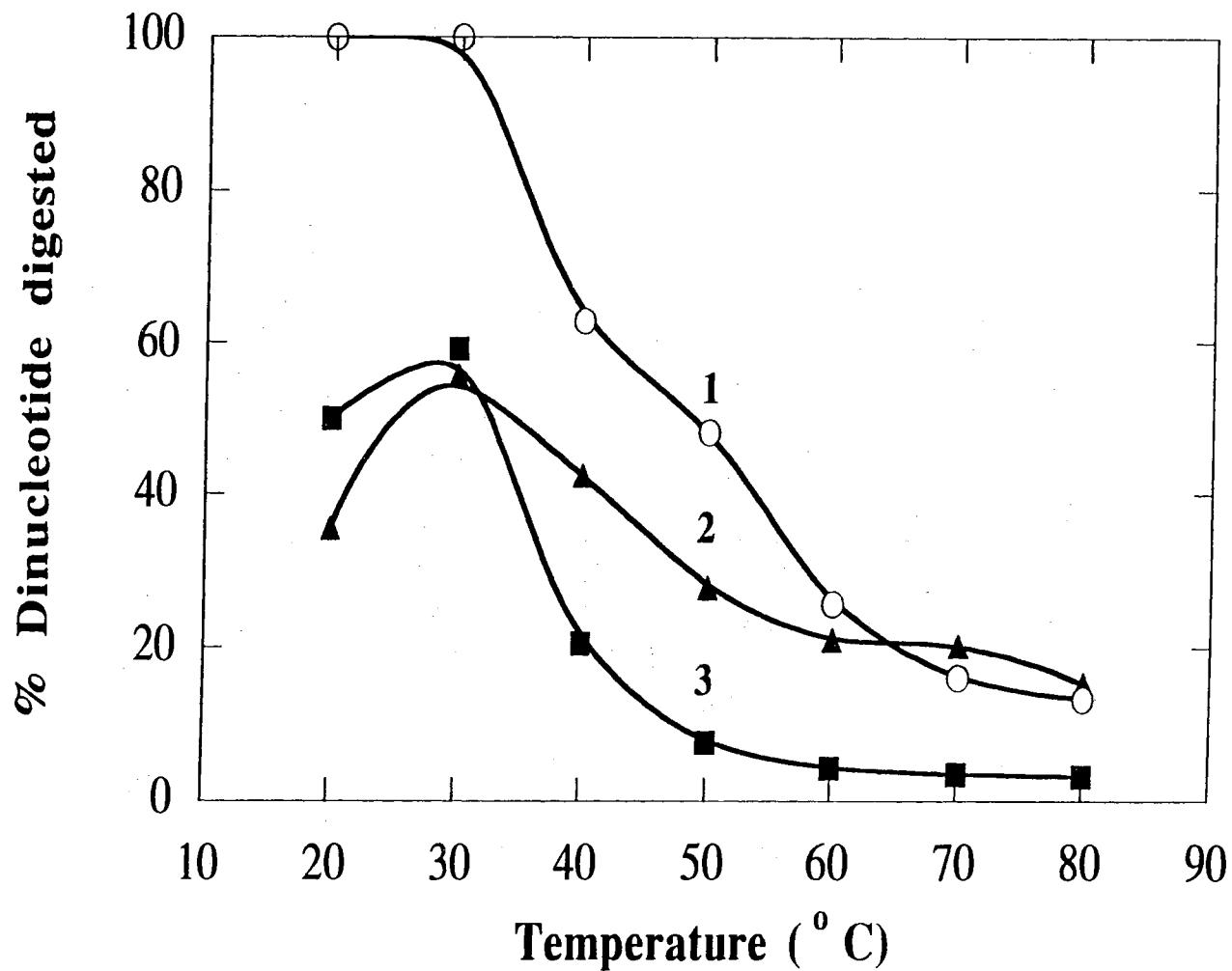


**Figure 6.** Temperature dependence of the activity of RNase U<sub>2</sub>. The % dinucleotide digested was calculated from peak areas using sulfanilic acid as internal standard. The reactor temperature was varied through the arrangement shown in Fig. 1. Running electrolyte, 15 mM sodium citrate, pH 3.5, containing 0.1% (w/w) polybrene. Curves: 1, ApC; 2, ApU; 3, ApG. Other conditions as in Figs 2 and 4.

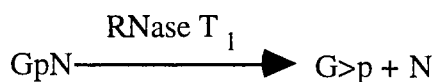
Fig. 6, it is interesting to note that while the activity of the enzyme towards the digestion of ApC and ApG decreased significantly at temperature above 30°C, the enzymic activity towards the digestion of ApU was much less affected. In the temperature range 50 to 60 °C, the activity of the enzyme towards ApC and ApG decreased more rapidly than towards ApU. This temperature dependence might be explained by the change in the enzyme conformation as the temperature was varied. Thus, the enzyme might have acquired a conformation that changed the accessibility or configuration of its specific site which in turn would have resulted in varying the activity of the enzyme.

Figure 7 depicts an electropherogram of the digest of three dinucleotides performed on RNase U<sub>2</sub> capillary enzyme reactor at optimum temperature and pH, i.e., 30°C and pH 3.5. All ApC has been converted to A>p and C while ApG and ApU have been digested partially to A>p and U and G, respectively.

In summary, enzymophoresis with capillaries having immobilized enzymes is a useful tool for (i) the rapid and accurate evaluation of immobilized enzymes over a wide range of conditions consuming insignificant amounts of enzymes and other reagents and (ii) the identification of small amounts of biological species via the appearance and disappearance (or decrease) of peaks for products and substrates, respectively. For instance, when the electropherogram digested sample is compared to that of undigested sample, each dinucleotide can be identified by the appearance of two new peaks on the electropherogram after the sample has passed through the enzyme reactor.

#### RNase U<sub>2</sub> and T<sub>1</sub> Mixed Enzyme Reactor

RNase T<sub>1</sub> cleaves specifically the phosphodiester bonds between 3'-guanylic acid residues and the 5'-hydroxyl groups of adjacent nucleotidyl residues as follows [15,20]:



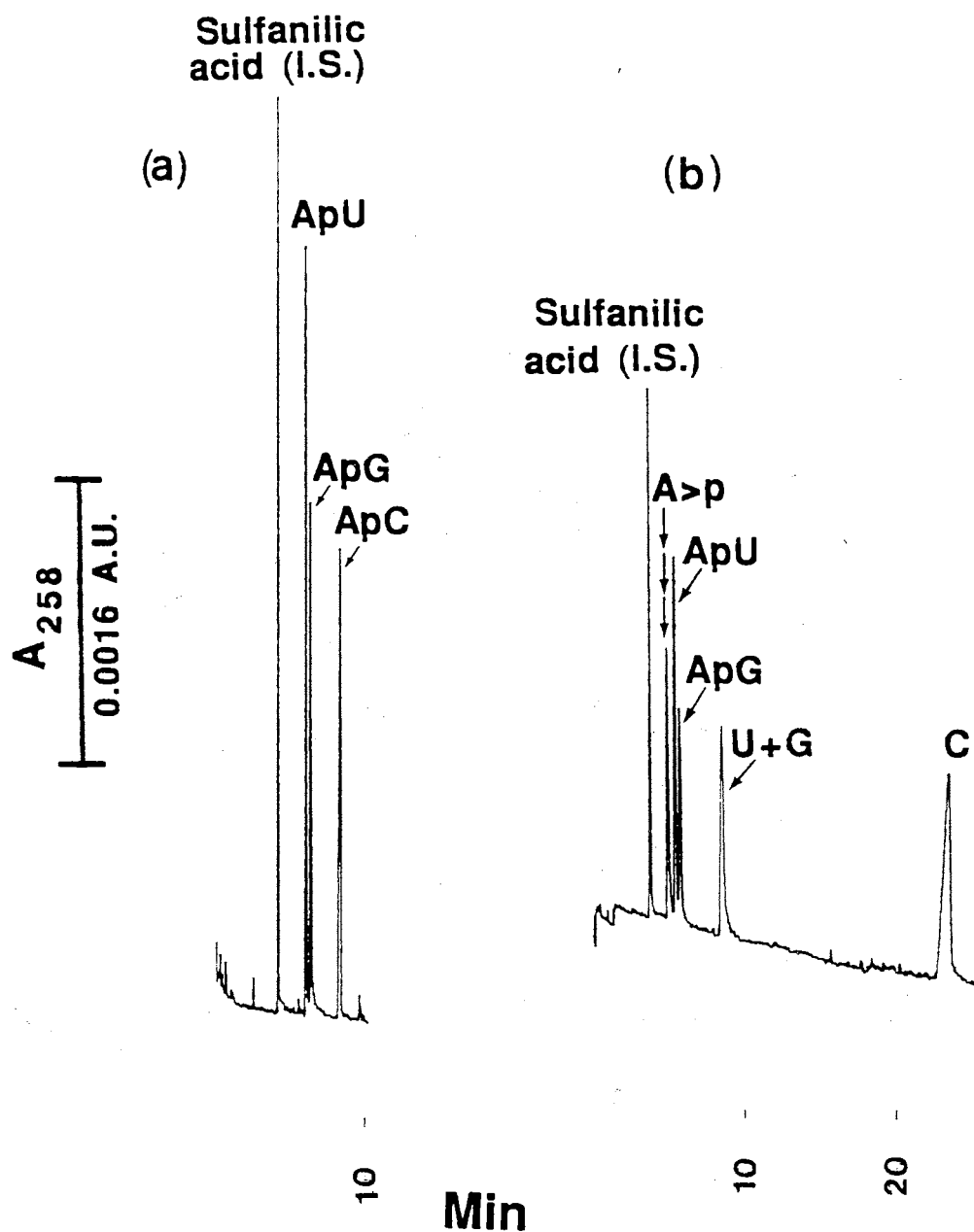


**Figure 7.** Electropherograms of dinucleotides (a) and the digest of dinucleotides (b) using RNase U<sub>2</sub> enzyme reactor. Temperature of the reactor, 30°C. Running electrolyte, 15 mM sodium citrate, pH 3.5, containing 0.10% (w/w) polybrene. Other conditions as in Figs 2 and 4.

were N is any nucleotidyl residue. The specific activity of the most purified RNase U<sub>2</sub> is one tenth that of the RNase T<sub>1</sub> [19]. Egami et al. [21] reported that RNase T<sub>1</sub> in free solution is most active at about pH 7.5 and that 50% of the maximal activity remains at pH 5.5 and 8. These findings disagree with those of our studies with the immobilized enzyme. As shown in Fig. 8, there is a broad range of optimum pH ( $4.5 < \text{pH} < 8.5$ ) for the immobilized RNase T<sub>1</sub> as evaluated by CZE. The enzyme conserved 75% of its maximal activity at pH 2.0 and 9.0. This may indicate that the immobilization of RNase T<sub>1</sub> has enhanced the stability of the enzyme and limited its pH dependence. When compared to free solution enzyme, the difference observed in pH-dependency of the activity of the immobilized enzyme may be contributed to the microenvironmental effect arising from the immobilization process as explained above.

The fact that immobilized RNase U<sub>2</sub> and T<sub>1</sub> possess different optimum pH values prompted us to construct a mixed enzyme reactor. A mixed enzyme reactor of RNase U<sub>2</sub> and T<sub>1</sub> could be used under those conditions where one of the enzyme is catalytically active while the other is totally or partially inactive. This mixed enzyme reactor could be employed in the simultaneous identification of adenine and guanine containing RNA fragments.

The mixed capillary enzyme reactor was evaluated using GpN and ApC dinucleotides. Since the reactor was 20 cm long, 35 min were required for the substrate to traverse the reactor at 15 cm height difference between inlet and outlet reservoirs. Typical electropherograms obtained in the absence or presence of the enzyme reactor are displayed in Figs 9 and 10. As can be seen in Fig 9, at pH 3.5 RNase U<sub>2</sub> possesses its highest activity as manifested by the total conversion of ApC into A>p and C while RNase T<sub>1</sub> is still active to a certain degree as noticed from the partial cleavage of the different GpN to G>p and N. Conversely, when the same mixture was allowed to pass through the reactor at pH 5.5 where RNase U<sub>2</sub> is almost inactive while RNase T<sub>1</sub> is highly active, GpN dinucleotides were completely cleaved while ApC was not (see Fig. 10). The unreactivity

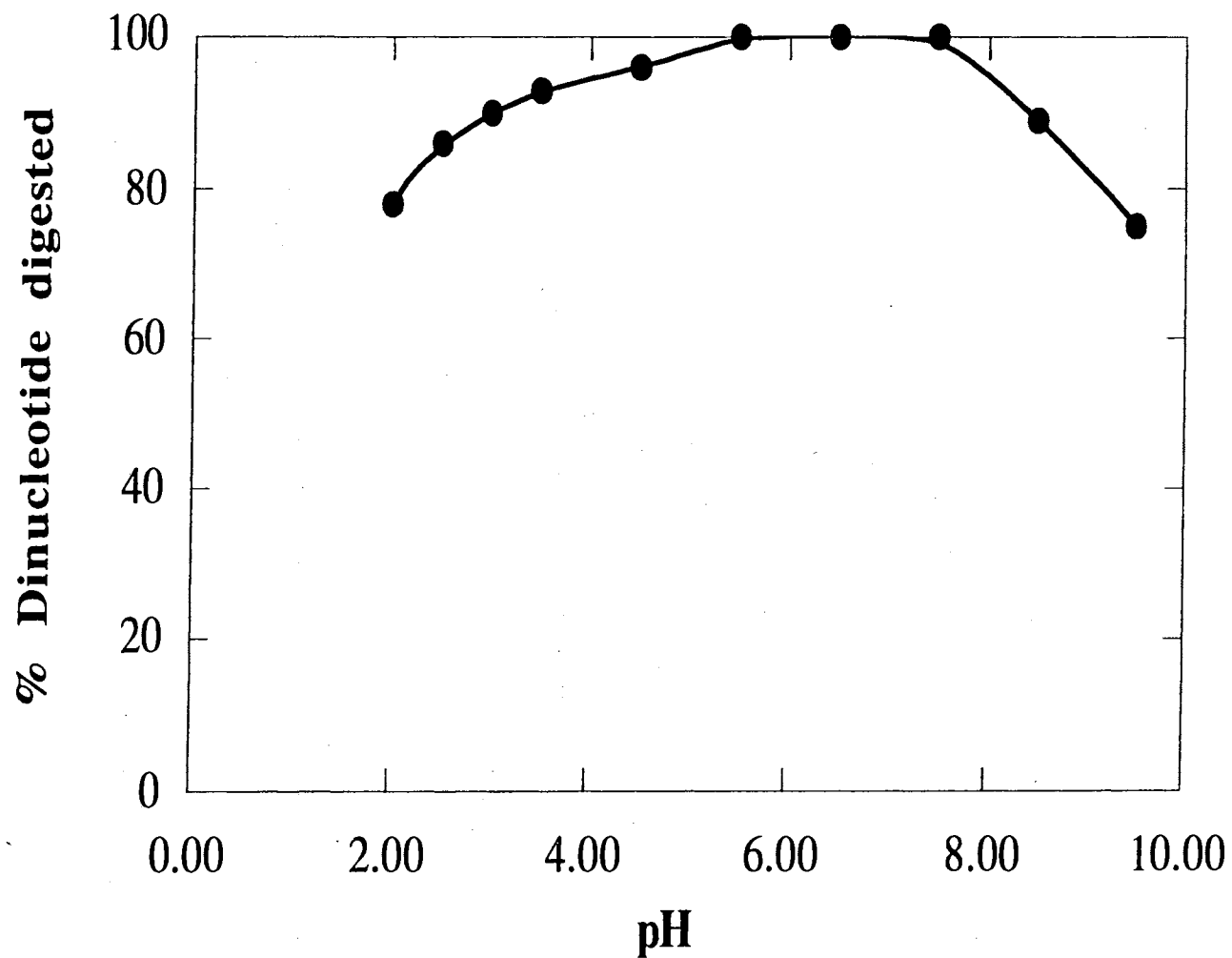


**Figure 8.** pH dependence of the activity of RNase T<sub>1</sub>. The % GpA digested was calculated from peak areas using sulfanilic acid as internal standard. Running electrolyte, 15 mM sodium citrate at various pH containing 0.10 % (v/v) polybrene. Other conditions as in Figs 2 and 4.



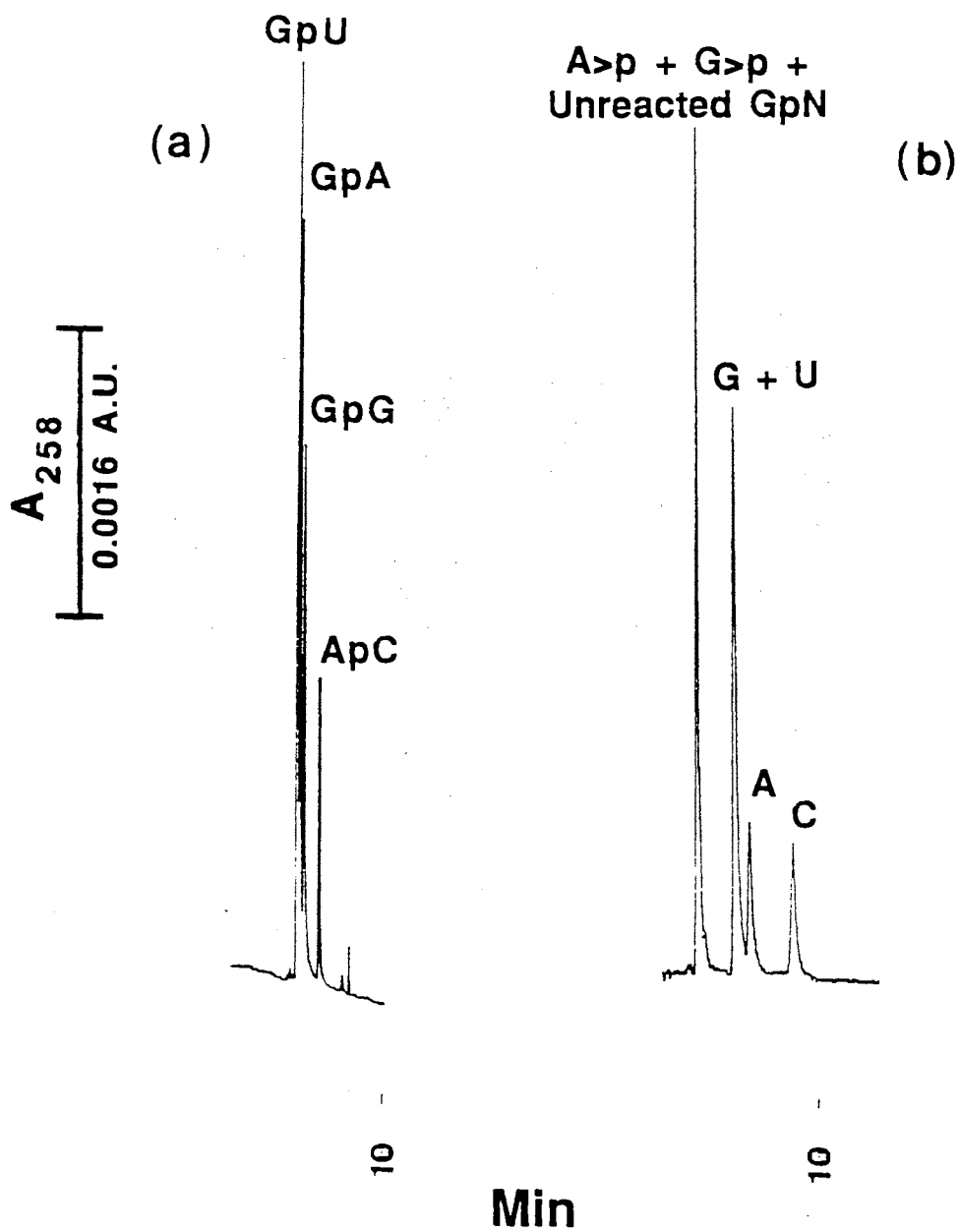


**Figure 9.** Electropherograms of dinucleotides (a) and their digest (b) by mixed RNase  $U_2$  and  $T_1$  capillary reactor (20 cm x 50  $\mu$ m I.D.). Running electrolyte. 15 mM sodium citrate, pH 3.50, containing 0.10 (w/w) polybrene. Other conditions as in Figs 2 and 4.

of RNase U<sub>2</sub> towards ApC is also confirmed by the absence of a peak for C which should have appeared at 20 min. The comparison of Fig. 9b and Fig. 10b, shows the effect of pH on the resolution of the nucleosides which are the products of the digestion of dinucleotides. At pH 3.5, while G and U coeluted, A and C were resolved from each other and from the peak of G + U. At pH 5.5, the three nucleosides U, G and A coeluted while C migrated slower and appeared at ca. 20 min. This is because at pH 5.5 U, G and A nucleosides are neutral, while C is partially positively charged. In fact, the  $pK_a$  values of A, G and C are 3.5, 2.1 and 4.2, respectively [22]. Since the first  $pK_a$  value of U is 9.2, this nucleoside is neutral at  $pH < 8.2$ , and starts to become negatively charged at  $pH > 8.2$  [22]. Thus, with the exception of C, the nucleosides are neutral at pH 5.5 and as a result they co-migrate in CZE.

#### Digestion of tRNA<sup>Phe</sup>

tRNA<sup>Phe</sup> comprises 76 nucleotide residues. Exhaustive digestion of tRNA<sup>Phe</sup> with RNase U<sub>2</sub> leads to the formation of 15 different oligonucleotides, see Table I. Two of these fragments (a trimer and a pentamer) contain the sequence ApA at their ends, and therefore may hydrolyze further to produce two adenosine monophosphate. However, this seems to be unlikely since ApA residue is somewhat resistant to the action of RNase U<sub>2</sub>. Typical electropherograms of tRNA<sup>Phe</sup> passed through the RNase U<sub>2</sub> capillary reactor are displayed in Fig. 11 a and b. They were obtained by carrying the CZE separation at pH 3.5 and 5.5. In both cases, the digestion was performed at pH 3.5. The electrophoresis of the digest at pH 3.5 seems to yield better resolution among the various fragments. This may be explained by the greater differences in the charges of the fragments at this low pH where, with the exception of U, the base constituents will protonate differently. However, in both cases, the number of peaks observed closely matches the number of fragments expected to be produced as a result of the digestion.

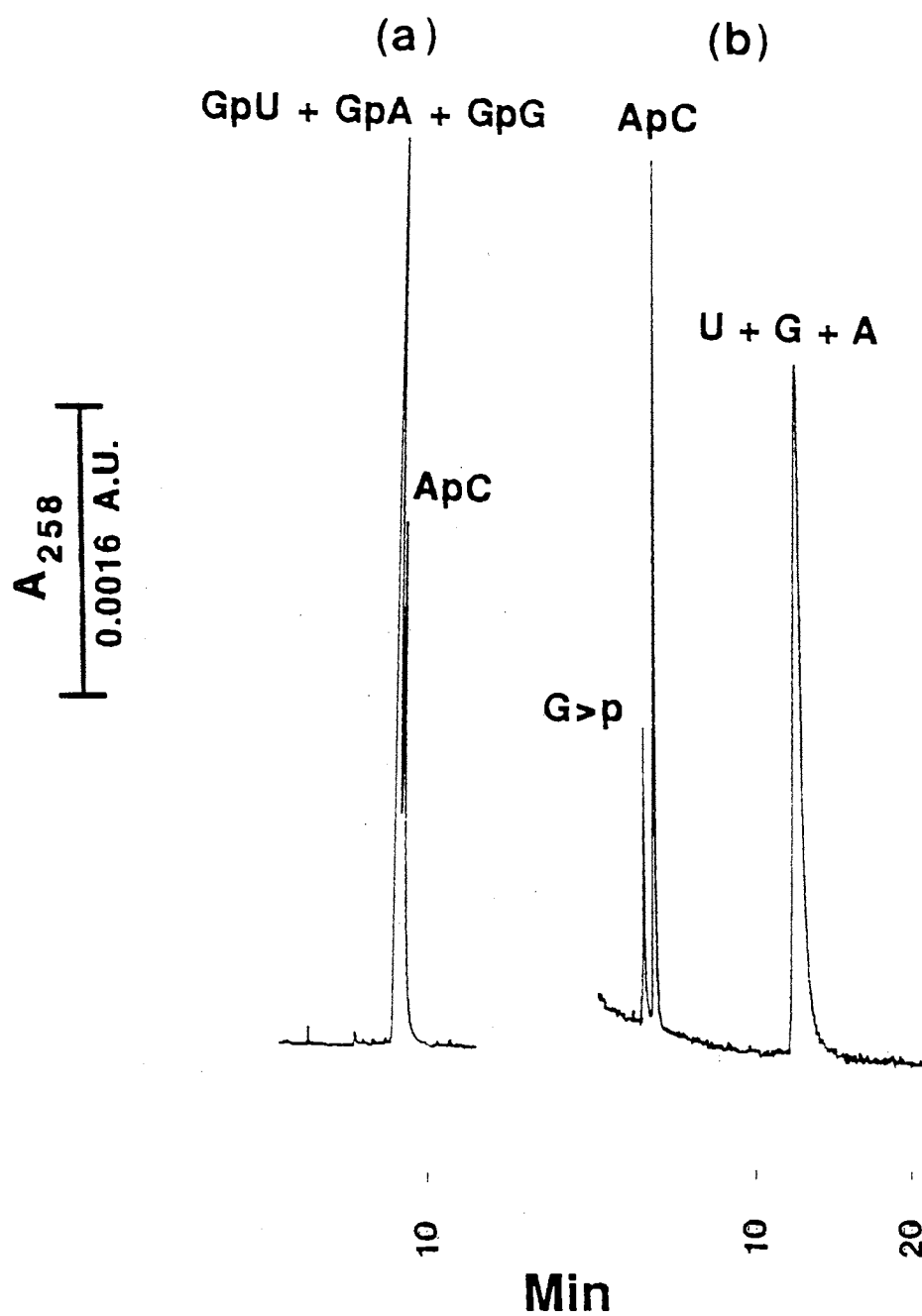


**Figure 10.** Electropherograms of dinucleotides (a) and their digest (b) by mixed RNase U<sub>2</sub> and T<sub>1</sub> capillary reactor (20 cm x 50 μm I.D.). Running electrolyte, 15 mM citrate, pH 5.5, containing 0.10% (w/w) polybrene. Other conditions as in Figs 2 and 4.

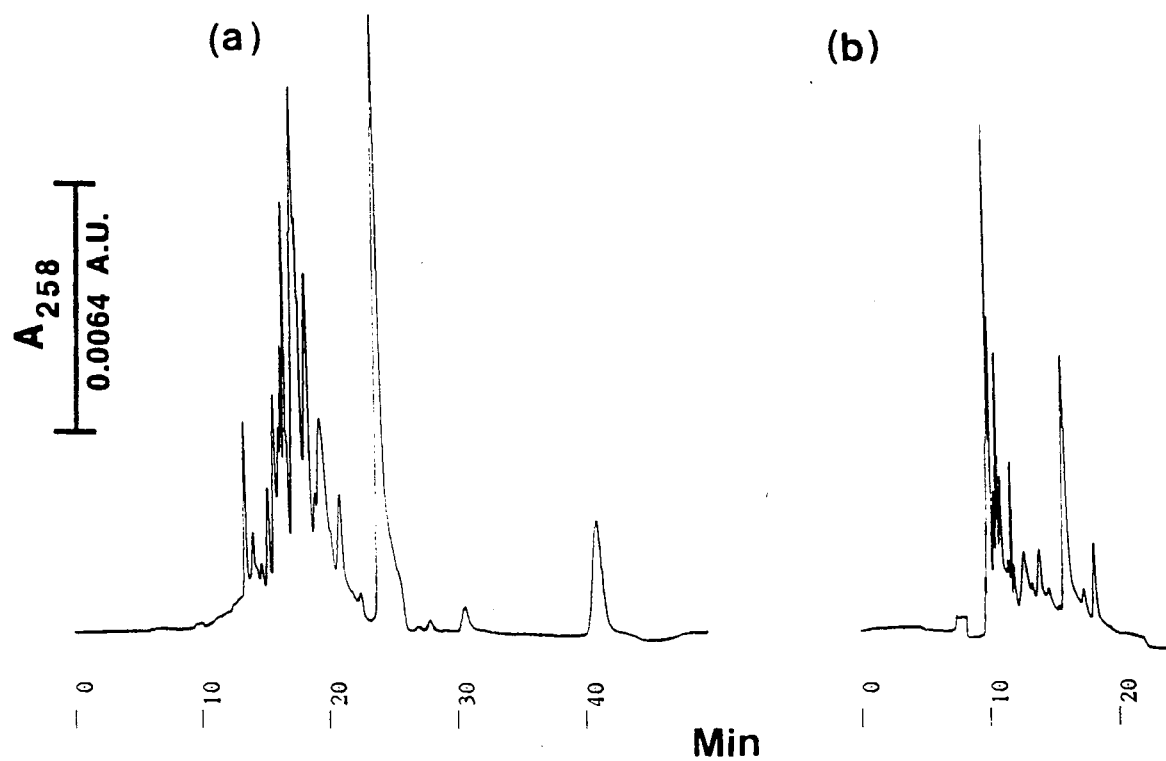


**Figure 11.** Electropherograms of tRNA<sup>Phe</sup> digested by passing through RNase U<sub>2</sub> capillary reactor (15 cm x 50 μm I.D.). The tRNA<sup>Phe</sup> sample was prepared as explained in materials and methods at pH 3.5. During the digestion, the capillary enzyme reactor was filled with 50 mM sodium citrate, pH 3.5, containing 0.10 % (w/w) polybrene. The separation was carried out with 50 mM sodium citrate at pH 3.50 (a) and 5.5 (b) containing 0.10 % (w/w) polybrene; voltage, -15 kV. Other conditions as in Fig. 2.

TABLE I. Possible Fragmentation of tRNA<sup>Phe</sup> by the Ribonucleases Under Investigation.

RNase U <sub>2</sub> fragments	RNase T <sub>1</sub> fragments	RNase U <sub>2</sub> /T <sub>1</sub> fragments
	4 Gp pGp	10 Gp 6 Ap m <sup>2</sup> Gp pGp
2 GA CA YA	3 AG CG UG Cm <sup>2</sup> <sub>2</sub> G	2 CA AA YA CG Cm <sup>2</sup> <sub>2</sub> G UG
GAA CCA-OH	DDG	CCA DDG CCA-OH
UCCA UUUA	TψCG CCAG	UCCA UUUA CUCA UUCG ψm <sup>5</sup> CUG TψCG
mCUmGAA pGCGGA m <sup>2</sup> GCUCA	CUCAG CACCA-OH	mCUmGAA
Gcm <sup>2</sup> <sub>2</sub> GCCA ψm <sup>5</sup> CUGGA UUCGCA GDDGGGA	m <sup>7</sup> GUCm <sup>5</sup> CUG AAUUCG AUUUAm <sup>2</sup> G	m <sup>7</sup> GUCm <sup>5</sup> CUG
	AUCCACAG	
	AmCUmGAAYAψm <sup>5</sup> CUG	
		Gm <sup>7</sup> GUCm <sup>5</sup> CUGUGTψCGA

A, Adenosine; C, cytidine; m<sup>5</sup>C, 5-methylcytidine; mC, 2-O-methylcytidine; D, 5,6-dihydrouridine; G, guanosine; mG, 2-O-methylguanosine; m<sup>7</sup>G, N<sup>7</sup>-methylguanosine; m<sup>2</sup>G, N<sup>2</sup>-methylguanosine; m<sup>2</sup><sub>2</sub>G, N<sup>2</sup>,N<sup>2</sup>-dimethylguanosine; Y, invariant pyrimidine; ψ, pseudouridine; T, ribothymidine.

On the other hand, the exhaustive digestion of tRNA<sup>Phe</sup> with RNase T<sub>1</sub> leads to the formation of 14 different oligonucleotides, and two different mononucleotides, see Table I. RNase U<sub>2</sub> and T<sub>1</sub> mixed capillary enzyme reactor is expected to produce more fragments

than each of the individual enzyme under conditions where both enzymes are fully or partially active. A total of 21 fragments could be obtained, four of which are mononucleotides, see Table I. It should be mentioned that the fragments obtained with a mixed enzyme reactor will be shorter than the fragments generated with a single enzyme reactor. As can be seen in Table I, the exhaustive digestion by the mixed enzymes leads to 6 dimers, 3 trimers, 6 tetramers, only one pentamer and one hexamer.

The mixed reactor was employed for the digestion of tRNA<sup>Phe</sup> under two different pH values. As expected (see Fig. 12a), the mixed reactor produced a different electropherogram of the digested tRNA<sup>Phe</sup> than that obtained with RNase U<sub>2</sub> reactor under otherwise the same conditions. This electropherogram corresponds to the digested tRNA<sup>Phe</sup> at pH 3.5 where RNase U<sub>2</sub> is fully active while RNase T<sub>1</sub> is partially active. Figure 12b illustrates the electropherogram of tRNA<sup>Phe</sup> digested at pH 7.0 where RNase U<sub>2</sub> is inactive while RNase T<sub>1</sub> is fully active. The digestion under the two different conditions gave different number of peaks since the activity of the two enzymes varied by varying the pH values at which the digestion took place.

A simple comparison of Fig. 11a to Fig. 12a reveals that the fragments in the latter case eluted faster than in the former case. As shown in Table I, this is consistent with the fact that the fragments produced by the mixed enzyme reactor (Fig. 12a) are smaller in size than the ones produced by RNase U<sub>2</sub> enzyme reactor (Fig. 11a).

In all cases, the digestion may not be exhaustive under the conditions used in the capillary enzyme reactor whereby only a single pass of the sample was performed and the contact time is relatively short. Under these circumstances, the random cleavage may lead to the formation of random cuts and in turn longer pieces than those displayed in Table I may be produced.

In summary, the schemes provided here may prove useful in providing rapid fingerprinting of minute amounts of tRNAs, especially altered t-RNAs which have been used for the investigation of proteins biosynthesis as well as for the study of protein-

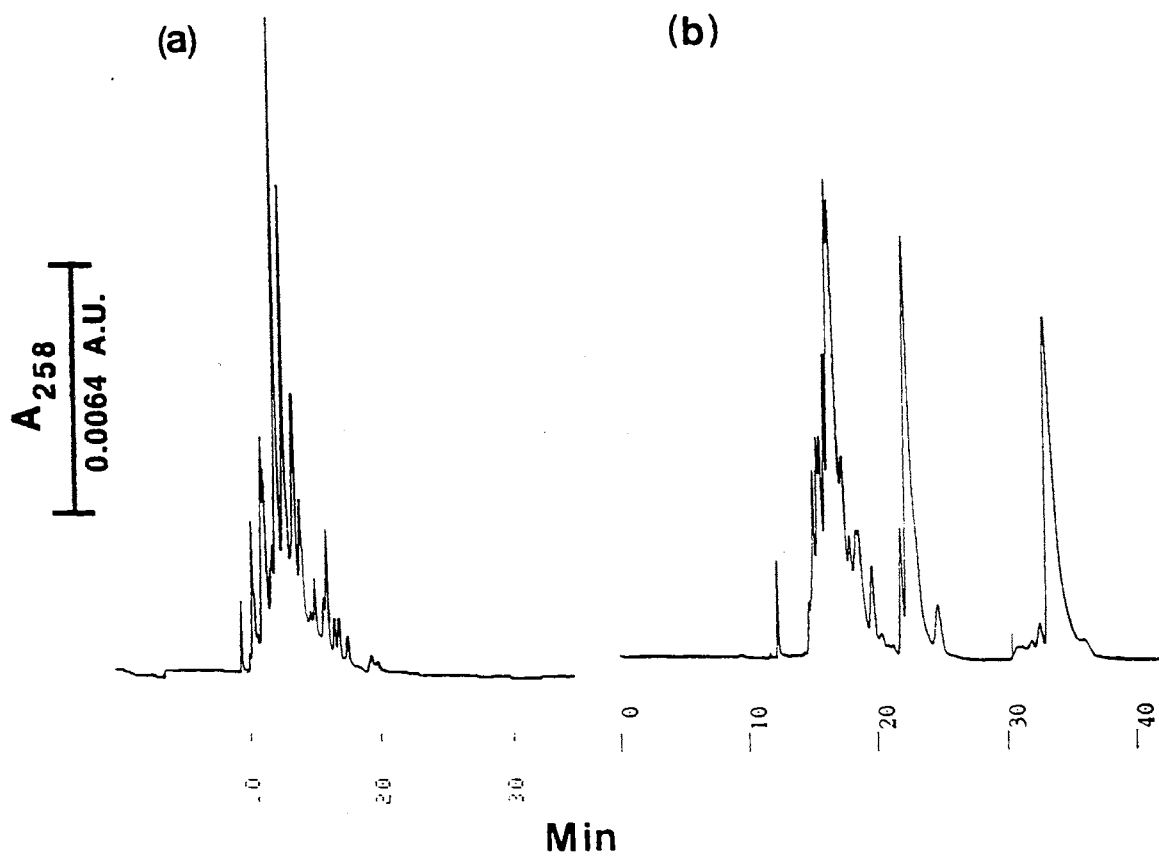


**Figure 12.** Electropherograms of tRNA<sup>Phe</sup> digested by passing through RNase T<sub>1</sub> and U<sub>2</sub> mixed capillary reactor (20 cm x 50 μm I.D.). The tRNA<sup>Phe</sup> samples were prepared as explained in materials and methods at pH 3.5 (a) and pH 7.0 (b). Running electrolytes, 50 mM sodium citrate, pH 3.5 (a) or pH 7.0 (b) containing 0.1% (w/w) polybrene ; voltage, -15 kV. Other conditions as in Fig. 2.

nucleic acid interactions [23]. For such molecules, it is important that the relevant modification occurs only once or few times in each tRNA molecule. Therefore, the availability of methods as those described above should prove useful for the rapid monitoring of the extent of such modification reactions on the microscale.

### Conclusions

RNA modifying enzymes, e.g., RNase T<sub>1</sub> and RNase U<sub>2</sub> can be effectively immobilized on the walls of fused silica capillaries either individually or as mixed enzymes. In all cases, the immobilized RNase T<sub>1</sub> and RNase U<sub>2</sub> conserved their enzymic activity and exhibited acceptable chemical and thermal stability. The preparation of the various microreactors was relatively simple involving standard immobilization chemistry. Furthermore, the capillary enzyme reactors having mixed enzymes or individual enzymes were useful in selectively modifying small amounts of RNA fragments, e.g., dinucleotides and tRNAs, before capillary electrophoresis separation. Capillaries with mixed enzymes immobilized on their walls could be used under pH conditions where either both enzymes are active or one is active while the other is inactive. This configuration permitted the realization of a unique modification of a given RNA fragment by a single pass through the capillary enzyme reactor. The immobilization process allowed not only the multiple reuse of the same batch of enzyme for modifying several RNA samples but also maintained the enzymic activity over a broader pH range with respect to the soluble enzyme.



## References

1. Cobb, K. A., Novotny, M., *Anal. Chem.*, 61 (1989) 2226.
2. Nashabeh, W., El Rassi, Z. *15<sup>th</sup> International Symposium on Column Liquid Chromatography*, Lecture #L53, Basel, Switzerland, June 3-7, 1991.
3. Nashabeh, W., El Rassi, Z., *J. Chromatogr.*, 596 (1992) 251.
4. Amankwa, L. A. Kuhr, W. G., *Anal. Chem.*, 64 (1992) 1610.
5. Bao, J. M., Regnier, F. E., *J. Chromatogr.*, 608 (1992) 217.
6. Avila, L. Z., Whitesides, G. M., *J. Org. Chem.*, 58 (1993) 5508.
7. Xue, Q., Yeung, E. S., *Anal. Chem.*, 66 (1994) 1175.
8. Chang, H. T., Yeung, E. S., *Anal. Chem.*, 65 (1993) 2947.
9. Mechref, Y., El Rassi, Z., *Electrophoresis*, 15 (1994) 319.
10. Nashabeh, W., El Rassi, Z., *J. Chromatogr.*, 559 (1991) 367.
11. Onuska, F. I., Comba, M. E., Bistricki, T., Wilkinson, R. J., *J. Chromatogr.*, 142 (1977) 117.
12. Emmer, A., Jansson, M., Roeraade, J., *J. Chromatogr.*, 547 (1991) 544.
13. Wiktorowicz, J. E., Colburn, J. C., *Electrophoresis*, 11 (1990) 769.
14. Oefner, P. J., *Electrophoresis*, 16 (1995) 46.
15. D'Alessio, J. M., in Rickwood, D. and Hames, B.D., Eds, *Gel Electrophoresis of Nucleic Acids. A practical Approach*; IRL Press, Oxford, 1982, p. 173.
16. Uchida, T., Egami, F., in P. D. Boyer, Ed., *The Enzymes*; Academic Press, New York, 1971, Vol. IV, p. 205.
17. Brownlee, G. G., *Determination of Sequences in RNA*, North-Holland, Amsterdam, 1972, p 199-200.
18. Donis-Keller, H., Maxam, A. M., Gilbert, W., *Nucl. Acid Res.*, 4 (1977) 2527.
19. Arima, T., Uchida, T., Egami, F., *Biochem. J.*, 106 (1968) 601.
20. Uchida, T., Egami, F., *Methods Enzymol.*, 12 (1967) 228.

21. Egami, F., Takashi, K., Uchida, T., *Progress Nucleic Acid Res. Molec. Biol.*, 3 (1964) 59.
22. Bloomfield, V. A., Crothers, D. M., Tinoco, I., *Physical Chemistry of Nucleic Acids*, Harper and Row, New York, 1974, p. 75.
23. Mathias, M. Strenbach, H., *Methods Enzymol.*, 59 (1979) 182.

PART II

## CHAPTER VIII

### SOME BASIC ASPECTS OF MICELLAR ELECTROKINETIC CAPILLARY CHROMATOGRAPHY AND CHIRAL CAPILLARY ELECTROPHORESIS

#### Introduction

One major breakthrough in CE has been the interception of micellar electrokinetic capillary chromatography (MECC) in 1984 by Terabe and coworkers [1]. Micellar electrokinetic capillary chromatography has enlarged the scope of CE applications to include the separation of neutral solutes and to solving separation problems that were, otherwise, intractable by CE. Separation in MECC is based on the differential solubilization of solutes into a charged micellar phase which usually consists of an electrolyte solution containing charged surfactant at a concentration above its critical micelle concentration (CMC).

Another major progress in CE is the introduction of the concept of chiral capillary electrophoresis (CCE) for the separation of optical isomers. Since the first report on CCE by Gassmann *et al.* in 1985 [2], which exploited the ligand exchange mechanism for enantiomeric separation, several important approaches for CCE have been reported and have been discussed in two recent reviews [3, 4]. The suitability of CE for enantiomeric separation is primarily due to the unique selectivity and high separation efficiencies of CE which are well suited for the determination of solutes having low separation factors as is often the case with enantiomers. Another major advantage of CE is that separation is performed in homogenous solution which can be easily altered to optimize enantiomeric resolution. In addition, the low consumption of expensive chiral selectors and reagents has

made CE a highly cost-effective separation technique relative to other methods such as high-performance liquid chromatography, gas-liquid chromatography and supercritical fluid chromatography.

Since the separation achieved by either CCE or MECC is based on electrokinetic phenomena, they belong to the same class of separation methods, the so-called electrokinetic capillary chromatography (EKC). Generally, separations in EKC are based on the chromatographic principle of partitioning of the solute between the surrounding medium and a pseudo-stationary phase included in the running electrolyte. This partitioning is based on the solubilization of the solute in the micellar phase for MECC, whereas it is based on the interactions (e.g., hydrophobic, polar interactions) between the solute and the chiral selector included in the running electrolyte for CCE. The pseudo-stationary phase is the micellar phase in MECC, while it is the chiral selector in CCE. In many instances, enantiomeric separations of solutes are attained by MECC using chiral surfactants or mixed achiral surfactants/chiral additives. Due to the similarity and close ties between MECC and CCE, they are jointly discussed in this chapter.

The aim of this chapter is to provide an overview of some basic concepts of MECC and CCE and to outline the objectives and rationales of part II of the dissertation.

## Micellar Electrokinetic Capillary Chromatography

### Separation Principles

The separation principles of neutral solutes by MECC are schematically illustrated in Fig. 1. Ionic micelles are used as a pseudo-stationary phase, which dynamically interact with the analytes. Above CMC, the surfactant molecules included in the running electrolyte aggregate to form a micelle which is in a dynamic equilibrium with the surfactant monomers.

Although, in the presence of an electric field, an anionic micelle migrates toward the anode by its electrophoretic mobility which is a function of the micelle's size and charge as

given by equation (6) in Chapter I, it will be swept toward the cathode by the EOF which is stronger than the electrophoretic mobilities of most anionic micelles when used under neutral or alkaline separation conditions. Thus, there are two phases inside the capillary in MECC: an aqueous phase moving at the velocity of the EOF and a micellar phase whose apparent mobility is in the same direction as the EOF but moving at a much slower velocity than the EOF. This creates the so-called "migration time window" (see Fig. 1d) which extends from the time of an unretained solute,  $t_0$  to  $t_{mc}$ , the migration time of a solute that partitions totally in the micelle.

Separations of neutral solutes in MECC are based on their differential partitioning into the micelle. Very polar solutes which do not interact with the micelle migrate with the EOF, whereas very hydrophobic solutes that are completely solubilized in the micelle migrate with the micelle. Solutes with an intermediate hydrophobicity will migrate between those two zones (A and S in Fig. 1c and d) and their separation will depend on the distribution coefficient of each solute.

### Migration Behavior

Neutral Analytes. The equation describing the relationship between the migration time of an analyte,  $t_M$ , and the capacity factor,  $k'$ , is given by [1]:

$$t_M = \frac{1 + k'}{1 + (t_0 / t_{mc})k'} t_0 \quad (1)$$

$k'$  is given by:

$$k' = \frac{n_{mc}}{n_{aq}} \quad (2)$$

where  $n_{mc}$  and  $n_{aq}$  are the total moles of the analyte incorporated into the micelle and that in the aqueous phase, respectively. Equation 1 can be rearranged to give:

$$k' = \frac{t_M - t_0}{(1 - t_M / t_{mc})t_0} \quad (3)$$

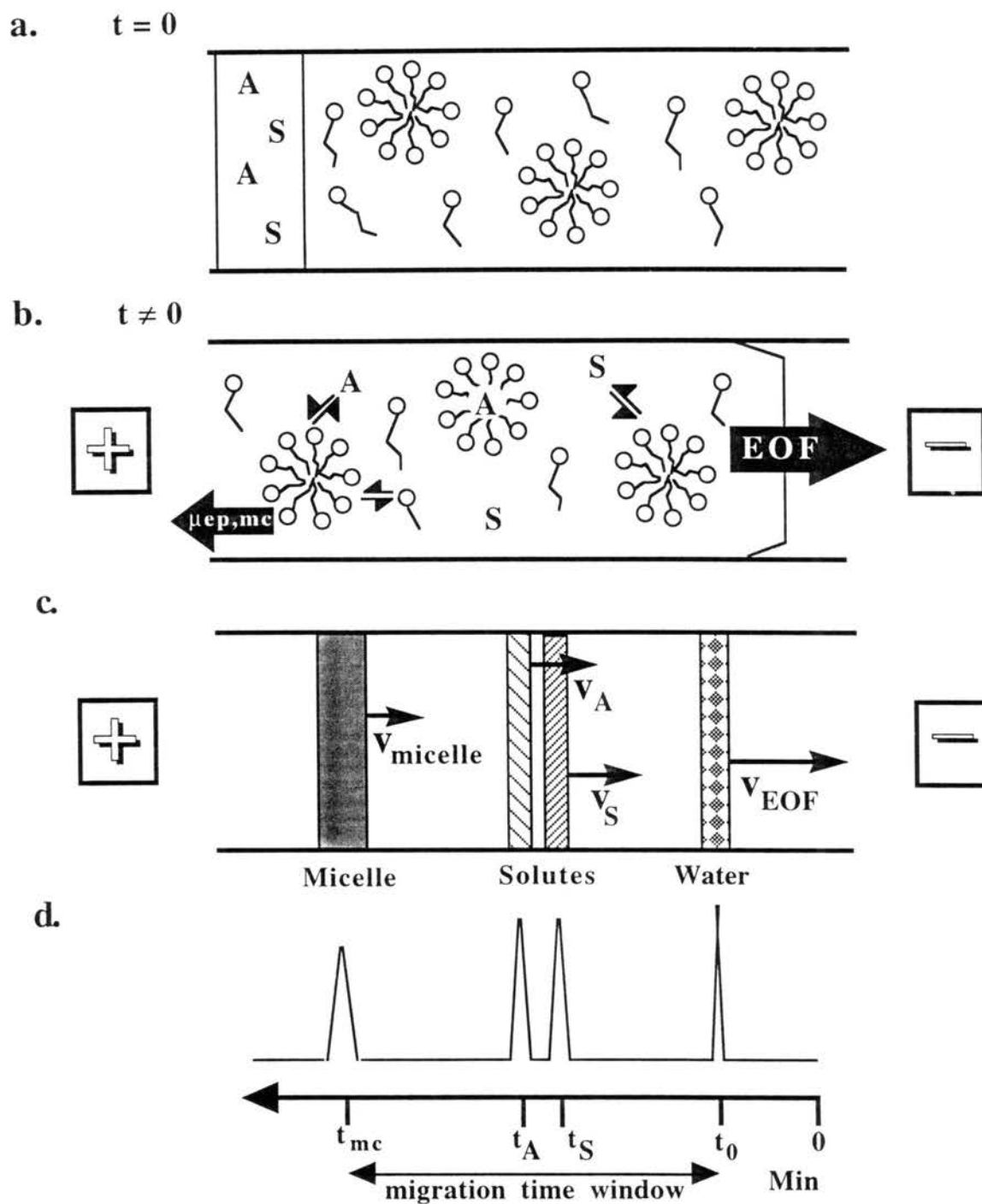


**Figure 1.** Schematic illustrations of the principles of MECC separations with an anionic surfactant. (a) Sample introduction, (b) application of electric field, (c) various migration zones and (d) ideal electropherogram. A and S, analytes;  $\mu_{ep,mc}$ , electrophoretic mobility of the micelle; EOF, electroosmotic flow.

where  $t_0$  and  $t_{mc}$  are the migration times of an unretained solute and that of the micelle, respectively. Equation (3) is a modification of the normal chromatographic description of capacity factor,  $k'$ , to account for the movement of the pseudo-stationary phase. In fact, when  $t_{mc} = \infty$  (as in chromatography),  $k'$  expression will be exactly that of chromatography. Equation (3) is used to calculate the capacity factor from the migration time obtained from the electropherogram.

The effective electrophoretic mobility of a neutral analyte,  $\mu_{ep}^*$  can be related to the capacity factor by [5]:

$$\mu_{ep}^* = \frac{k'}{1+k'} \mu_{ep,mc} \quad (4)$$

where  $\mu_{ep,mc}$  is the effective electrophoretic mobility of the micelle. From equation (4), a given charged analyte acquires an effective electrophoretic mobility as a result of its incorporation in the micelle, and the magnitude of such mobility is proportional to the fraction of the analyte incorporated in the micelle. In the same way, the apparent electrophoretic mobility of a neutral analyte,  $\mu_s^*$ , is given by:

$$\mu_s^* = \mu_{ep}^* + \mu_{eo} \quad (5)$$

where  $\mu_{eo}$  is the electroosmotic mobility.

Charged Analytes. Unlike neutral analytes, charged analytes have their own effective electrophoretic mobility which depends on the fraction of the ionized form and the hydrodynamic volume of the analyte, as well as the pH of the running electrolyte. Both ionized and unionized forms of the analyte may interact with the micelle. Therefore, a quantitative description of the migration of a negatively charged analyte should take into consideration  $\mu_{eo}$ ,  $\mu_{ep,mc}$ , the effective electrophoretic mobility of the ionized analyte,  $\mu_{A^-}$ , the binding constants of the unionized,  $K_{HA}$ , and ionized,  $K_{A^-}$ , forms of the analyte



with the micelle, and the dissociation constant,  $K_a$ , of the analyte. The capacity factor, taking into consideration the aforementioned parameters, is given by [6, 7]:

$$k' = \frac{v_{ep,s,mc} - v_{ep,s,0}}{v_{ep,mc} - v_{ep,s,mc}} \quad (6)$$

where  $v_{ep,s,mc}$  and  $v_{ep,s,0}$  are the electrophoretic velocity of the analyte in the presence and absence of the micelle, respectively. The migration behavior of cationic analytes in the presence of an anionic micelle is more complex, due to the formation of an ion-pair between the analyte and the monomeric anionic surfactant.

### Resolution in MECC.

Resolution,  $R_s$ , of two species in MECC can be described by:

$$R_s = \underbrace{\left( \frac{\sqrt{N}}{4} \right)}_{\text{Efficiency}} \underbrace{\left( \frac{k_2'}{k_2' + 1} \right)}_{\text{Retention}} \underbrace{\left( \frac{1 - t_0/t_{mc}}{1 + (t_0/t_{mc})k_1'} \right)}_{\text{Selectivity}} \underbrace{\left( \frac{\alpha - 1}{\alpha} \right)}_{\text{Selectivity}} \quad (7)$$

where  $\alpha$  is the selectivity factor and is given by  $k_2'/k_1'$  and the ratio  $t_0/t_{mc}$  is defined as the elution range parameter which is a reflection of the migration time window.

### Optimization of Separation in MECC

From equation (7), resolution can be improved by optimizing efficiency, selectivity, and/or the capacity factor. Among these parameters, capacity factor is the most easily adjusted. This is accomplished, usually, by changing the surfactant concentration [8], adding an organic modifier [9], or by selecting a micellar phase with different hydrophobic character [10].

Generally, the capacity factor increases linearly with increasing surfactant concentration according to the following equation:

$$k' = K\bar{v}([S] - \text{CMC}) \quad (8)$$

where  $\bar{v}$  is the partial specific volume of the micelle,  $[S]$  is the surfactant concentration and CMC is the critical micelle concentration. However, increasing the surfactant concentration is limited by Joule heating associated with increasing the concentration of ionic surfactants (i.e., increase in the generated current). Therefore, the use of a high electric field is often avoided at high surfactant concentration, and as a result the analysis time is prolonged.

Organic modifiers can be added to manipulate micellar structure and properties or solute-micelle interaction. Accordingly, organic modifiers have been classified into two classes based on their action. While organic modifiers that manipulate micellar structure and properties, such as 1-heptanol, causes an increase of  $k'$  by increasing the partition coefficient [11], modifiers that manipulate solute-micelle interaction (e.g., organic solvents, urea, glucose and ion pairing agents) cause a decrease in  $k'$  [12].

Selectivity in MECC can be easily manipulated by varying the physical nature (e.g., size, charge, geometry) of the micelle by using different surfactants. A suitable MECC surfactant should meet the following criteria: (i) the surfactant must have a moderate CMC value; (ii) micellar solution must be homogenous and UV transparent; (iii) the micellar phase must have low viscosity. Table I lists some common surfactants with the corresponding values of their CMC and aggregation number.

While most surfactants are not specific, others have very specific selectivity. For example, bile salts, such as sodium cholate, which are naturally occurring steroidal surfactants that form helical micelle, were shown to have unique selectivity for steroidal-like solutes [14].

In addition to changing the surfactant type, the addition of co-surfactant also alters the properties of a micellar phase, thus modifying the selectivity of the micellar system. Several groups have recently explored various mixed micelle systems [15-17]. While our laboratory have recently investigated the effect of the mixing of cationic surfactants of various alkyl chain lengths on selectivity [18], other groups have added nonionic surfactants to ionic micellar phases to alter the selectivity of the system [16]. In addition,

our laboratory have recently used butylboronate to alter the selectivity of in situ charged micelles by decreasing the critical micelle concentration (i.e., increasing the hydrophobic character of the micelle) [19].

TABLE I. Aggregation Numbers and CMC Values for Various Surfactants

Surfactant (type, name)	Acronym or Trade name	Aggregation number <sup>a</sup>	CMC (mM) <sup>b</sup>
<b>Anionic</b>			
Sodium dodecyl sulfate	SDS	62	8.1
Sodium perfluorononanoate	NaPFN	NA	9.1
Potassium perfluorooctanoate	KPFO	NA	30
<b>Cationic</b>			
Cetyltrimethylammonium bromide	CTAB	78	1.3
Dodecyltrimethylammonium bromide	DTAB	55	15
<b>Nonionic</b>			
Heptyl- $\beta$ -D-glucoside	HG	NA	79
Octyl- $\beta$ -D-glucoside	OG	84	20-25
Octanoyl sucrose	OS	NA	24.4
Octanoyl- <i>N</i> -methylglucamide	MEGA 8	NA	58
Nonaoyl- <i>N</i> -methylglucamide	MEGA 9	NA	19-25
Decanoyl- <i>N</i> -methylglucamide	MEGA 10	NA	6-7
<b>Bile salts</b>			
Sodium cholate	SC	2	9-15
Sodium deoxycholate	SDC	3-12	2-6
Sodium taurocholate	STC	4	3-11
Sodium taurodeoxycholate	STDC	6	1-4

<sup>a</sup>&<sup>b</sup> obtained from Ref.[13]

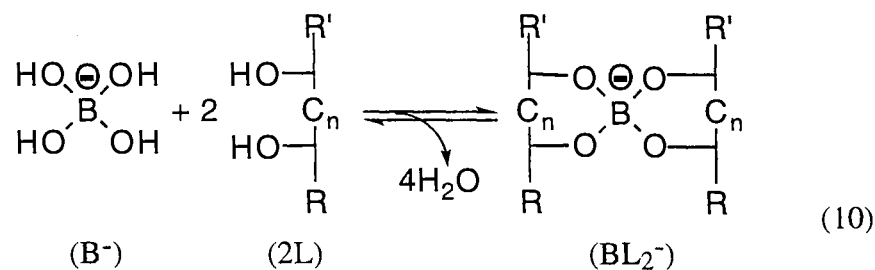
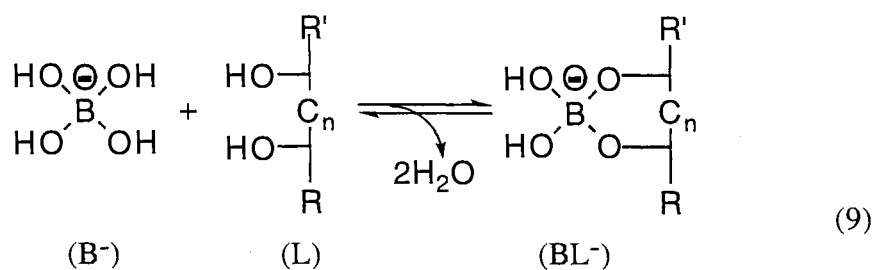
NA not available

Also, resolution is improved by extending the migration time window. As mentioned above, neutral solutes migrate between  $t_{mc}$  and  $t_0$  (i.e., the migration time window). The migration time window can be varied by controlling the EOF or using anionic surfactants with high mobility. Many organic modifiers (e.g., methanol, 2-propanol and acetonitrile) interact with the capillary wall, thus reducing EOF and in turn

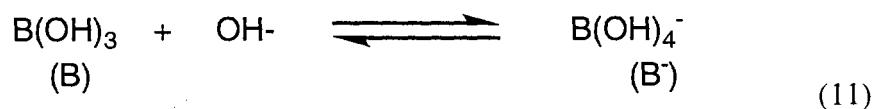
increasing the migration time window. However, the amount of organic modifier added is limited by the effect of the modifier on the CMC, aggregation number and micellar dissociation, and by the significant decrease in efficiency associated with the addition of organic modifiers to the running electrolyte. Metal salts and ion-pairing agents have been added to anionic surfactants to reduce the migration time window. These counter ions are electrostatically attached to the charged surface of the micelle, thus reducing  $\mu_{ep,mc}$ .

A novel concept for adjusting the migration time window was introduced recently by our laboratory, and involved the use of in situ charged micelles [19-24]. This approach uses neutral glycosidic surfactants which are readily converted to anionic micelles via complexation of the glycosidic moiety of the surfactant with borate ions. Therefore, the charge density of the micelle can be adjusted by varying the concentration of borate ions in the background electrolyte or varying the pH of the background electrolyte, and as a result the migration time window can be varied to optimize resolution.

Some Aspects of MECC with In Situ Charged Micelles. In general, the polyol moiety of glycosidic surfactants can complex with borate according to the following equilibria [25, 26]:



where  $BL^-$  and  $BL_2^-$  are the mono- and di-esters, respectively, L is the glycosidic surfactant and  $n = 0$  or 1. Equilibrium (9) is very much driven to the right, whereas equilibrium (10) is dependent upon the position of the hydroxyl groups in the polyol. Tetrahydroxyborate ions,  $B(OH)_4^-$ , are the predominant species in aqueous boric acid solution at an alkaline pH, according to the following equilibrium:



Therefore, borate complexation is more effective under these conditions. For an additional treatment of borate complexation with polyolic compounds, see Chapter IX.

Mono- and dicomplex borate esters coexist in aqueous solutions [26, 27], and their molar ratio is affected by (i) the relative concentration of borate ions and polyol molecules, (ii) the position of the hydroxyl groups in the polyol and (iii) the presence of substituents. The dicomplex is favored at high polyol:borate ratio [26], and its quantity is directly dependent on the position of the two hydroxyl groups of the polyol. The less favorable the position of the hydroxyl groups the smaller is the quantity of the dicomplex, and at large excess of borate, the quantity of dicomplexes becomes negligible.

Since mono- and di- complex formation is an equilibrium process, all glycosidic surfactants in borate media will readily possess negative charge the magnitude of which is influenced by the position of the equilibria and therefore by the stability of the complex. At constant surfactant concentration, according to equilibria (9-11), the complex concentration increases with increasing borate concentration or pH, according to the law of mass action. Therefore, for in situ charged micelles, the adjustment of the surface charge density of the micelle, and consequently the migration time window is based on varying the extent of complexation between the glycosidic surfactant and borate ions. The overall surface charge density of the micelle can be given by [20]:

$$\rho_{mc} = \frac{[S \cdot B]}{[S \cdot B] + [S]} \rho_{mc-c} \quad (12)$$

or by:

$$\rho_{mc} = \frac{\rho_{mc-c}}{1 + \frac{[S]}{[S \cdot B]}} \quad (13)$$

where  $\rho_{mc-c}$  is the limiting charge density of the glycosidic surfactant-borate micelle,  $[S \cdot B]$  is the total concentration of the complexed surfactant (i.e., mono- and dicomplex), and  $[S]$  is the concentration of uncomplexed surfactant. The higher the charge density the more negative the micelle. While any increase in the borate concentration or pH, at constant surfactant concentration, will result in a decrease in the ratio  $[S]/[S \cdot B]$ , and therefore a larger  $\rho_{mc}$ , an increase in the surfactant concentration, at constant pH and borate concentration, will yield an increase in the ratio  $[S]/[S \cdot B]$ , and as a result,  $\rho_{mc}$  will decrease, see equation 12 or 13. Therefore, these readily tuned features of the micelle would allow the tailoring of the elution range for a given separation problem. It should be noted that changing the charge of the micelle through borate complexation may produce small changes in the size of the micelle [20]. In a recent study involving an octylglucoside surfactant [28], it was shown that increasing the ionic strength up to 0.20, the CMC of the surfactant was largely unaffected.

Unlike the traditionally used micelles which are characterized by a fixed surface charge density, the resolution in MECC with in situ charged micelles can be optimized through adjusting both  $k'$  and  $t_{mc}$ . Therefore, MECC with in situ charged micelles can be utilized in the separation of neutral or charged solutes that could not be resolved in traditional MECC because of their similar selectivities.

## Chiral Separations in CE

### Some General Aspects

The importance of chirality in biological phenomena, chemical synthesis and design of pharmaceutical agents have been the driving force for the development of various separation methods by high-performance liquid chromatography, gas chromatography, thin layer chromatography and recently CE. Although the various separation methods proved useful in the separation of chiral compounds, those based on CE offer additional advantages including higher separation efficiencies and resolution and lower consumption of samples and buffers.

The enantiomeric separation of chiral compounds is a difficult task since both optical isomers possess similar physico-chemical properties. In CE, both optical isomers have the same electrophoretic mobility in an achiral background electrolyte. Therefore, it is necessary to create a difference in the effective mobilities of the optical isomers in order to achieve enantiomeric resolution in CE. This can be achieved directly by placing the racemic mixture in a chiral environment which forms with the enantiomers labile diastereoisomeric complexes differing in stability, and consequently in effective mobility, or indirectly (through precolumn derivatization) by forming stable diastereoisomers of different mobilities.

The indirect separation method is based on the reaction of a racemic mixture with a pure chiral reagent (R or S), thus producing two diastereoisomers that will be resolved using an achiral electrophoretic system. The major advantage of this method originates from the fact that the enantiomeric separation is achieved in a simple buffer system without any chiral additive. However, this method suffers from several drawbacks. The method is time consuming, requires a highly pure chiral reagent and is only applicable to enantiomers that have reactive functional groups and identical reaction kinetics. As a result of these

drawbacks, the direct separation methods are more popular for enantiomeric resolution by CE.

In the direct separation methods, the chiral selector is either added to the background electrolyte, bound to the capillary wall, or included in a gel matrix. The enantiomeric separation is achieved by the formation of labile diastereoisomeric complexes as a result of the interaction between the optical isomers and the chiral selector. The separation of the two enantiomers is attained only if the two diastereoisomers formed possess different stability constants, thus causing the two enantiomers to migrate with different velocities. The selection of a suitable chiral selector is the only drawback of the direct chiral separation methods. Several types of chiral selectors and different separation mechanisms have been employed in CE for the enantiomeric resolution of a wide range of analytes. These mechanisms include (i) ligand exchange, (ii) chiral micelles, (iii) inclusion complexation and (iv) affinity interaction.

#### A Model for Chiral Separation

A useful model for chiral separation of two optical isomers R and S which interact with a single chiral selector (C) was described by Wern and Row [29, 30]. In the absence of C, R and S have the same effective mobility,  $\mu_1$ . The actual mobilities of the complexes formed between R, S and C (i.e., RC and SC) are also the same and are designated as  $\mu_2$ . The interaction between the optical isomers and the chiral selector is given by the following two equilibria:



If the exchange of R or S between the free and complexed species is rapid, the apparent mobility of X ( $\bar{\mu}_X$ ) which is either R or S is given by:



$$\bar{\mu}_X = \left( \frac{[X]}{[X] + [XC]} \right) \mu_1 + \left( \frac{[XC]}{[X] + [XC]} \right) \mu_2 \quad (16)$$

By substituting  $K_{XC}$  into equation (16),  $\bar{\mu}_X$  is given by:

$$\bar{\mu}_X = \frac{\mu_1 + \mu_2 K_{XC}[C]}{1 + K_{XC}[C]} \quad (17)$$

Using equation (17) in terms of R and S, the difference in the effective electrophoretic mobility of the optical isomers,  $\Delta\bar{\mu}$ , is given by:

$$\Delta\bar{\mu} = \bar{\mu}_R - \bar{\mu}_S = \frac{(\mu_1 - \mu_2)(K_{SC} - K_{RC})[C]}{1 + (K_{RC} + K_{SC})[C] + K_{RC}K_{SC}[S]^2} \quad (18)$$

Therefore, chiral resolution is possible only if  $\Delta\bar{\mu}$  is not equal zero (i.e., effective electrophoretic mobilities of the optical isomers are different). This is true if the two enantiomers have different affinities for the chiral selector, i.e.,  $K_{RC}$  and  $K_{SC}$  are different and not zero, and the electrophoretic mobilities of the free and complexed enantiomers are different, i.e.,  $\mu_1 \neq \mu_2$ . The effect of the chiral selector concentration on enantiomeric resolution is apparent in equation (18), since  $\Delta\bar{\mu} = 0$  if  $[C] = 0$  or  $[C]$  is very large. Therefore, a maximum enantiomeric resolution is attained at a certain concentration of the chiral selector above or below which enantiomeric resolution decreases.

### Ligand Exchange

The ligand exchange mechanism, first introduced by Danakov in chromatography [31], was applied for the enantiomeric separation of dansyl amino acids [32, 33] and  $\alpha$ -hydroxy acids [34] by CE. The separation is based on the interaction between a metal complex with a chiral ligand added to the background electrolyte and the two enantiomers to be resolved. The detection sensitivity of the method is limited by the UV absorption of the metal complex. However, this problem can be solved by using different detectors such as those based on laser-induced fluorescence [32].

### Chiral Micelles

Micellar electrokinetic capillary chromatography has been successfully employed for the enantiomeric separation of various chiral analytes. Chiral recognition can be achieved in MECC by using a chiral micelle or by incorporating a chiral selector into the micellar phase. As explained above, separation in MECC is based on the differential partitioning of the analyte between the aqueous phase and the micellar phase; therefore, using a chiral micelle which interact differently with optically active analytes will not only induce electrophoretic separation but also enantiomeric separation. Typical chiral micelles include sodium N-dodecanoyl-L-valinate and sodium N-dodecanoyl-L-alaninate which were applied to the separation of several amino acid derivatives namely 3,5-dinitrobenzoyl-amino acids, 4-nitrobenzoyl-amino acids, benzoyl-O-isopropyl ester-amino acids and phenylthiohydantoin-amino acids [35-37]. Other important chiral micelles are the bile salts which proved useful for the enantiomeric separation of dansyl amino acids, binaphthyl derivatives and some pharmaceuticals [14, 38-42]. Poly(sodium-N-undecylenyl-L-valinate) is also another chiral micelle that has been used for the enantiomeric separation of 1,1'-bi-2,2'-naphthol and laudanosine [43].

Typical mixed achiral surfactant/chiral surfactant systems include the use of SDS (achiral surfactant) combined with digitonin [44] glycyrrhizic acid and  $\beta$ -escin [45] which are naturally occurring chiral surfactants.

### Inclusion Complexation

Cyclodextrins (CDs) or crown-ether derivatives have been used successfully to obtain enantiomeric resolution in CE through an inclusion complexation mechanism. In this separation mechanism, the optical isomers (guest compounds) fit the cavity of the chiral selector (host compound), thus forming host-guest or inclusion-complexes. For enantiomeric resolution to be achieved, the two diastereoisomeric complexes formed during the electrophoretic analysis, must have different stability constants.

Native CDs are cyclic oligosaccharides consisting of six, seven, or eight glucopyranose units, and are known as  $\alpha$ -,  $\beta$ -, or  $\gamma$ -CD, respectively (Fig. 2a). The shape of CDs is similar to that of a truncated cone with a hydrophobic cavity of different size depending on the number of glucose units and the substituent groups of the CD (Fig. 2b). Their cavity is relatively hydrophobic, while the outside is relatively hydrophilic due to the presence of hydroxyl groups.

Many CD derivatives, other than the native  $\alpha$ -,  $\beta$ - and  $\gamma$ -CD, have been developed to increase water solubility, modify cavity shape, or introduce a special function. These derivatives include glycosylated- $\alpha$ -CD [46], heptakis-2,6-di-O-methyl- $\beta$ -CD (DM- $\beta$ -CD) [47-51], heptakis-2,3,6-tri-O-methyl- $\beta$ -CD (TM- $\beta$ -CD) [47, 51-54], hydroxyethyl- $\beta$ -CD (HE- $\beta$ -CD) [54] and hydroxypropyl- $\beta$ -CD (HP- $\beta$ -CD) [46, 54-57].

In addition, charged CDs were also introduced and evaluated for the separation of uncharged optical isomers. These charged CD derivatives are 6A-methylamino- $\beta$ -CD [58], 6A,6D-dimethylamino- $\beta$ -CD [58], 4-Sulfoethyl-ether- $\beta$ -CD [59], mono-(6- $\beta$ -aminoethylamino-6-deoxy)- $\beta$ -CD [60] and carboxymethyl- $\beta$ -CD [61, 62, 59]. Also, carboxymethyl- $\beta$ -CD polymer, a polyelectrolyte charged CD, was evaluated as chiral selector [63].

Cyclodextrins and CD derivatives were used in the various mode of CE including CZE [49, 50, 58, 64, 65], ITP [66-68], CGE [69, 70] and MECC [19, 22, 71]. Each of these mode of operation has its advantages and disadvantages. Several experimental parameters influence the inclusion complexation, and consequently the stereoselectivity, including the type and concentration of CD, applied voltage, capillary temperature and length, buffer ionic strength and electroosmotic flow.

Crown ethers are the other chiral additives used to achieve enantiomeric resolution in CE by inclusion-complexation mechanism. The structure of a representative of crown ether derivatives (18-crown-6-ether tetracarboxylic acid) is illustrated in Fig. 3.

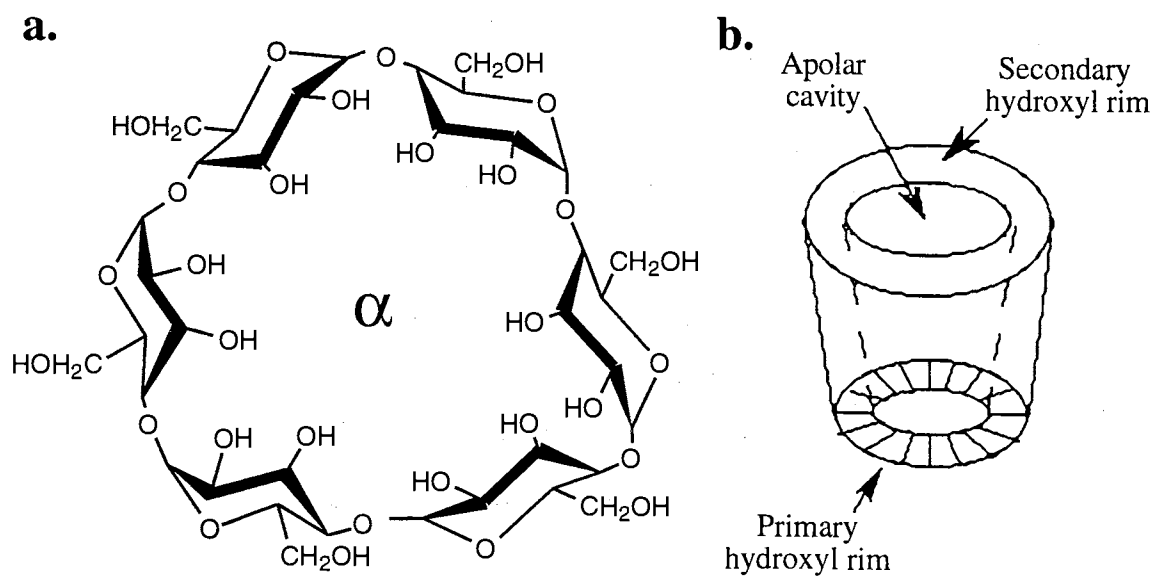


**Figure 2.** Structure of  $\alpha$ -CD (a). Basic features of the native CDs (b).

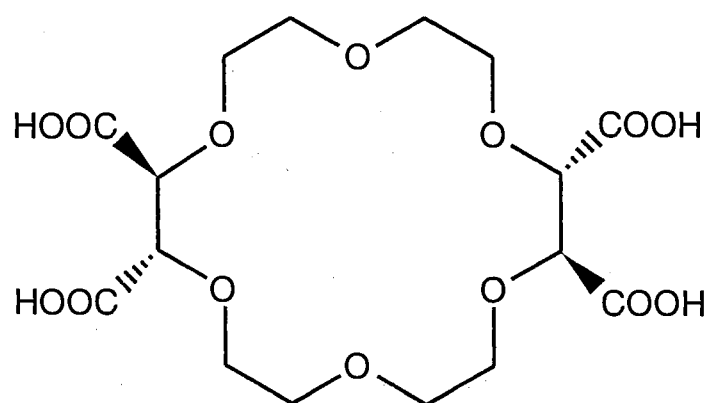


**Figure 2.** Structure of 18-Crown-6-ether tetracarboxylic acid

These cyclic molecules are capable of forming inclusion complexes with several inorganic and organic ions in which the analyte (guest compound) fits into the cavity, forming weak bonds (ion-dipole) with the etheroatoms (O and S) of the crown ether. Unlike CDs inclusion-complexation where the hydrophobic part of the analyte fits in the cavity, the inclusion-complexation of crown ethers include the hydrophilic part of the analyte. The inclusion of the amino group of the analyte is crucial for the enantiomeric resolution. Applications using 18-crown-6-ether tetra carboxylic acid as a chiral selector include a wide range of amino derivatives, such as amino acids [72], amines and peptides [73], and amino alcohols and sympathomimetic drugs [74]. The major drawback of crown ether is that  $K^+$ ,  $NH_4^+$  and  $Na^+$  salts should be avoided in preparing the electrolyte, because these cations compete with the analytes in the inclusion process.

#### Affinity Interactions

Proteins as Chiral Selectors. Proteins which are natural biopolymers with helical conformation are able to interact selectively with a wide number of small size compounds (e.g., pharmaceuticals), and are good chiral selectors for performing chiral separation by CE. This chiral separation is based on stereoselective interaction between the protein and the two optical isomers, thus forming two labile diastereoisomers complexes in dynamic equilibria during the electrophoretic run. For enantiomeric resolution to be realized, the stability constants of the two diastereoisomeric complexes must be different and consequently the electrophoretic mobility of the optical isomers will be different. Tanaka *et al.* [75] described a theoretical model for enantiomeric separation with proteins as chiral selectors, assuming a model similar to that reported by Wren and Rowe [29, 30] described above. According to this model, the difference in the apparent mobilities,  $\Delta\mu_{ap}$ , between the enantiomers is given by:

$$\Delta\mu_{ap} = \frac{(\mu_S - \mu_P)(K_2 - K_1)[P]}{1 + (K_2 + K_1)[P] + K_1K_2[P]^2} \quad (19)$$

where P is the protein used as the chiral selector,  $K_1$  and  $K_2$  are the binding constants of the enantiomeric pair, and  $\mu_S$  and  $\mu_P$  are the electrophoretic mobility of the free enantiomers and the protein, respectively. The mobility of the complexes is assumed to be that of the protein, i.e.,  $\mu_P$ .

Although proteins have been successfully employed as chiral selectors in CE, several drawbacks are encountered. Proteins may adsorb to the surface of the capillary, thus varying EOF and consequently reducing the system reproducibility. Moreover, the sensitivity in the low UV range is hindered by the protein high UV absorption. Protein may not be pure and may not be stable under the operating conditions. Employing any of the approaches described in Chapter II to eliminate solute-wall interaction such as coating the capillaries or including additives in the background electrolyte have been used to prevent the adsorption of proteins used as chiral selectors. Table II lists the various proteins which have been utilized, so far, for the separation of enantiomers in CE.

Polysaccharides as Chiral Selectors. In addition to proteins, various natural products can be used as chiral selectors in CE. Polysaccharides such as cellulose and amylose have been successfully used for enantioseparations by HPLC. Many cellulose derivatives are commercially available as HPLC columns and have been found effective in promoting chiral separations.

Thus far, the application of polysaccharides as chiral selectors in CE has been very limited and only few papers have reported their use as chiral selectors in CE. These saccharides used are listed in Table III.

TABLE II. Proteins as Chiral Selectors and their Application.

Protein	CE mode of operation	Solutes	Ref.
Bovine serum albumin (BSA)	CZE CGE	Benzoin, dansyl amino acids, ibuprofen, leucovorin, promethazine and warfarin	[76-78] [79, 80]
Ovomucoid (OVM)	CZE	Benzoin, chlorpheniramine, eperisone and tolperisone	[81]
$\alpha_1$ -acid glycoprotein (AGP)	CZE	Alprenolol, benzoin, cyclophosphamide, disopyramide, hexobarbital, metoprolol, oxprenolol, pentobarbital and promethazine	[77]
Human serum albumin (HSA)	CZE	2,3-Dibenzoyl tartaric acid, N-2,4-dinitrophenyl glutamic acid, 3-indolelactic acid and kynurenine	[82]
Fungal cellulase	CZE	Pindolol	[77]
Cellobiohydrolase I (CBHI)	CZE	Alprenolol, labetalol, metoprolol, pindolol and propranolol	[83]
Avidin	CZE	Flurbiprofen, ibuprofen, ketoprofen, leucovorin, vanilmandelic acid and warfarin	[84]
Casein	CZE	DNP-Amino acids	[85]



TABLE III. Polysaccharides as Chiral Selectors in CE.

Saccharides	Solutes	Ref.
Maltodextrin (linear $\alpha$ -(1-4)-linked glucose polymer)	Flurbiprofen, ibuprofen, carprofen, suprofen, indoprofen and coumarinic drugs	[86, 87]
Dextrin 10 (linear $\alpha$ -(1-4)-linked glucose polymer)	4-Amino-5-hydroxy- 2,7- naphthalenedisulfonic acid-monosaccharides	[88]
Dextran sulfate (linear $\alpha$ -(1-4)-linked glucose polymer having a sulfated group in the molecule)	Trimetoquinol and clentiazem	[89]
Heparin (di-, tetra-, or hexasaccharides composed of uronic acid and glucosamine)	Antimalarial drugs Antihistamine drugs	[90]

As shown above, enantiomeric separation of different classes of compounds can be easily and rapidly achieved by CE, with good reproducibility and at a very low cost. Therefore, chiral separation in CE is emerging as the ultimate analytical technique for the enantiomeric separation of racemic analytes of physiological, pharmaceutical and environmental importance.

#### Summary of Objectives and Rationales of Part II of the Dissertation

Micellar electrokinetic capillary chromatography and chiral capillary electrophoresis have substantially enhanced the utility of CE as an analytical technique in various scientific fields. Micellar electrokinetic capillary chromatography with in situ charged micelle is a very powerful separation system where the resolution is optimized by varying several parameters. However, the potentials of this system has not been evaluated yet under acidic or neutral conditions or for enantiomeric separations. Thus, it is the objective of this part of the dissertation to address these needs.

On the other hand, CCE has several advantages over other separation methods used for chiral separation. One of these advantages is the simplicity associated with changing the chiral selectors included in the background electrolyte, thus providing a cost-effective approach and permitting an easy way to determine the chiral selector needed for achieving the enantiomeric separation of a given racemic mixture. Chiral recognition is a specific process that can be best described by a key-and-lock model. In this regard, a chiral selector or system that would work for a given racemic mixture(s) may not provide an enantioselectivity to another racemic mixture. Therefore, there is an urgent need for novel chiral systems to be used in CCE. This dissertation addresses this need by introducing and evaluating novel chiral micellar systems and selectors for CCE.

Part II of the dissertation, dealing with MECC and CCE, is divided into two sections. The first section is focused on expanding the applicability of MECC with in situ charged micelle to include separations under acidic and neutral conditions, on one hand, and enantiomeric separations on the other hand. The latter objective is achieved through the introduction and evaluation of glycosidic-steroidal surfactants as borate complexes. The second section of Part II of this dissertation is aimed at the development of CD-CE systems for the enantiomeric resolution of fluorescently labeled phenoxy acid herbicides in a single run through the development of a mixed CD system, and the subsequent detection by CE/LIF at the 0.2 ppb. Also in the second section of Part II, novel neutral surfactants (three alkylglycoside surfactants) are introduced and characterized as chiral selectors over a wide range of operating conditions with various enantiomeric species. In the presence of these surfactants, a field amplified injection technique was implemented for the determination of phenoxy acid herbicides in ultra diluted samples at the concentration level of  $10^{-11}$ M or 2.2 ppt, a concentration much lower than that encountered in environmental matrices.

## References

1. Terabe, S., Otsuka, K., Ichikama, K., Tsuchiya, A. and Ando, T., *Anal. Chem.*, 56 (1984) 111.
2. Gassmann, E., Kuo, J.E. and Zare, R.N., *Science*, 230 (1985) 813.
3. Fanali, S., Cristalli, M., Vespalec, R. and Bocek, P., 7 (1994) 1.
4. Nishi, H. and Terabe, S., *J. Chromatogr. A*, 694 (1995) 245.
5. Ghowsi, K., Foley, J.P. and Gale, R.J., *Anal. Chem.*, 62 (1990) 2714.
6. Otsuka, K., Terabe, S. and Ando, T., *J. Chromatogr.*, 348 (1985) 39.
7. Khaledi, M.G., Smith, S.C. and Strasters, J.K., *Anal. Chem.*, 63 (1991) 1820.
8. Terabe, S., Ozaki, H., Otsuka, K. and Ando, T., *J. Chromatogr.*, 332 (1985) 211.
9. Balchunas, A.T. and Sepaniak, M.J., *Anal. Chem.*, 59 (1987) 1466.
10. Janini, G.M. and Issaq, H.J., *J. Liq. Chromatogr.*, 15 (1992) 927.
11. Aiken, J.H. and Huie, C.W., *J. Microcol. Sep.*, 5 (1993) 95.
12. Sepaniak, M.J., *HRC, J. High Resolut. Chromatogr.*, 13 (1990) 679.
13. Neugebauer, J., *A Guid to the Properties and Uses of Detergents in Biology and Biochemistry*, Calbiochem-Novabiochem Corp., San Diego (1994).
14. Terabe, S., Shibata, M. and Miyshita, Y., *J. Chromatogr.*, 480 (1989) 403.
15. Balchunas, A.T. and Sepaniak, M.J., *Anal. Chem.*, 60 (1988) 617.
16. Rasmussen, H.T., Goebel, L.K. and McNair, H.M., *J. high Resolut. Chromatogr.*, 14 (1991) 25.
17. Wallingford, R.A., Curry, P.D. and Ewing, A.G., *J. Microcol. Sep.*, 1 (1989) 23.
18. Crosby, D.L., Masters Thesis, Oklahoma State University, (1993)
19. Smith, J.T. and El Rassi, Z., *Electrophoresis*, 15 (1994) 1248.
20. Cai, J. and El Rassi, Z., *J. Chromatogr.*, 608 (1992) 31.
21. Smith, J.T. and El Rassi, Z., *J. Cap. Elec.*, 1 (1994) 136.
22. Smith, J.T., Nashabeh, W. and El Rassi, Z., *Anal. Chem.*, 66 (1994) 1119.
23. Smith, J.T. and El Rassi, Z., *J. Chromatogr. A*, 685 (1994) 131.

24. Smith, J.T. and El Rassi, Z., *J. Microcol. Sep.*, 6 (1994) 127.
25. Van Duin, M., Peters, J.A., Kieboom, A.P.G. and Van Bekkum, H., *Tetrahedron*, 41 (1985) 3411.
26. Makkee, M., Kieboom, A.P.G. and van Bekkum, H., *Recl. Trav. Chim. Pays-Bas*, 104 (1985) 230.
27. Kennedy, G.R. and How, M.J., *Carbohydr. Res.*, 28 (1973) 13.
28. Brito, R.M. and Vaz, W.L.C., *Anal. Biochem.*, 152 (1986) 250.
29. Wren, S.A.C. and Rowe, R.C., *J. Chromatogr.*, 609 (1992) 363.
30. Wren, S.A.C. and Rowe, R.C., *J. Chromatogr.*, 603 (1992) 235.
31. Danankov, V.A. and Rogozhin, S.V., *J. Chromatogr.*, 60 (1971) 280.
32. Gozel, P., Gossman, E., Michelsen, H. and Zare, R.N., *Anal. Chem.*, 59 (1987) 44.
33. Gassmann, E., Kuo, J.E. and Zare, R.N., *Science*, 230 (1985) 813.
34. Desiderio, C., Aturki, Z. and Fanali, S., *Electrophoresis*, 15 (1994) 864.
35. Otsuka, K. and Terabe, S., *J. Chromatogr.*, 515 (1990) 221.
36. Otsuka, K. and Terabe, S., *Electrophoresis*, 11 (1990) 982.
37. Dobashi, A., Ono, T., Hara, S. and Yamaguchi, J., *J. Chromatogr.*, 480 (1989) 413.
38. Nishi, H., Fukuyama, T., Matsuo, M. and Terabe, S., *J. Microcol. Sep.*, 1 (1989) 234.
39. Nishi, H., Fukuyama, T., Matsuo, M. and Terabe, S., *Anal. Chim. Acta.*, 236 (1990) 281.
40. Nishi, H., Fukuyama, T., Matsuo, M. and Terabe, S., *J. Chromatogr.*, 515 (1990) 233.
41. Cole, R.O., Sepaniak, M.J. and Hinze, W.L., *J. High Resol. Chromatogr.*, 13 (1990) 579.
42. Okafo, G.N., Bintz, C., Clarke, S.E. and Camilleri, P., *J. Chem. Soc. Chem. Commun.*, 1189 (1992)

43. Wang, J.A. and Warner, I.M., *Anal. Chem.*, 66 (1994) 3773.
44. Otsuka, K. and S., T., *J. Chromatogr.*, 515 (1990) 221.
45. Ishihama, Y. and Terabe, S., *J. Liq. Chromatogr.*, 16 (1993) 933.
46. Sepaniak, M.J., Cole, R.D. and Clark, B.K., *J. Liq. Chromatogr.*, 15 (1992) 1023.
47. Soini, H., Riekkola, M.L. and Novotny, M.V., *J. Chromatogr.*, 608 (1992) 265.
48. Nardi, A., Ossicini, L. and Fanali, S., *Chirality*, 4 (1992) 56.
49. Fanali, S., *J. Chromatogr.*, 474 (1989) 441.
50. Fanali, S., *J. Chromatogr.*, 545 (1991) 437.
51. Lin, J.M., Nakagama, T., Okazawa, T., Wu, X.Z. and Hobo, T., *Fresenius J. Anal. Chem.*, 354 (1996) 451.
52. Mayer, S. and Schurig, V., *HRC, J. High Resolut. Chromatogr.*, 15 (1992) 129.
53. Wren, S.A.C. and Rowe, R.C., *J. Chromatogr.*, 635 (1993) 113.
54. Peterson, T.E., *J. Chromatogr.*, 630 (1993) 353.
55. penn, S.G., Goodall, D.M. and Loran, J.S., *J. Chromatogr.*, 636 (1993) 149.
56. Aumatell, A., Wells, R.J. and Wong, D.K.Y., *J. Chromatogr.*, 686 (1994) 293.
57. Cladrowa-Runge, S., Hirz, R., Kenndler, E. and Rizzi, A., *J. Chromatogr. A*, 710 (1995) 339.
58. Nardi, A., Eliseev, A., Bocek, P. and Fanali, S., *J. Chromatogr.*, 638 (1993) 247.
59. Chankvetadze, B., Endresz, G., Bergenthal, D. and Blaschke, G., *J. Chromatogr. A*, 717 (1995) 245.
60. Terabe, S., *Trends Anal. Chem.*, 8 (1989) 129.
61. Schmitt, T. and Engelhardt, H., *Chromatographia*, 37 (1993) 475.
62. Schmitt, T. and Engelhardt, H., *HRC, J. High Resolut. Chromatogr.*, 16 (1993) 525.
63. Aturki, Z. and Fanali, S., *J. Chromatogr. A*, 680 (1994) 137.
64. Fanali, S. and Bocek, P., *Electrophoresis*, 11 (1990) 757.
65. Altria, K.D., Goodall, D.M. and Rogan, M.M., *Chromatographia*, 34 (1992) 19.

66. Snopek, J., Jelinek, I. and Smolkova-Keulemansova, E., *J. Chromatogr.*, 438 (1988) 211.
67. Snopek, J., Jelinek, I. and Smolkova-Keulemansova, E., *J. Chromatogr.*, 472 (1989) 308.
68. Snopek, J., Soini, H., Novotny, M., Smolkova-Keulemansova, E. and Jelinek, I., *J. Chromatogr.*, 559 (1991) 215.
69. Guttman, A., Paulus, A., Cohen, A.S., Grinberg, N. and Karger, B.L., *J. Chromatogr.*, 448 (1988) 41.
70. Cruzado, I.D. and Vigh, G., *J. Chromatogr.*, 608 (1992) 421.
71. Nishi, H., Fukuyama, T. and Terabe, S., *J. Chromatogr.*, 553 (1991) 503.
72. Kuhn, R., Stoecklin, F. and Erni, F., *Chromatographia*, 33 (1992) 32.
73. Kuhn, R., Erni, F., Bereuter, T. and Hausler, J., *Anal. Chem.*, 64 (1992) 2815.
74. Hohne, E., Kraus, G.J. and Gubitz, G., *HRC, J. High Resolul. Chromatogr.*, 15 (1992) 698.
75. Tanaka, Y., Matsubara, N. and Terabe, S., *Electrophoresis*, 15 (1994) 848.
76. Barker, G.E., Russo, P. and Hartwick, R.A., *Anal. Chem.*, 64 (1992) 3024.
77. Busch, S., Kraak, J.C. and Poppe, H., *J. Chromatogr.*, 635 (1993) 119.
78. Sun, P., Wu, N., Barker, G.E. and Hartwick, R.A., *J. Chromatogr.*, 648 (1993) 475.
79. Sun, P., Wu, N., Barker, R.A., Hartwick, N., Grinberg, N. and Kaliszan, R., *J. Chromatogr. A*, 652 (1993) 247.
80. Birnbaum, S. and Nilsson, S., *Anal. Chem.*, 64 (1992) 2872.
81. Ishihama, Y., Oda, Y., Asakawa, N., Yoshida, Y. and Sato, T., *J. Chromatogr. A*, 666 (1994) 193.
82. Vespalec, R., Sustacek, V. and Bocek, P., *J. Chromatogr. A*, 638 (1993) 255.
83. Valtcheva, L., Mohammad, J., Pettersson, G. and Hjertén, S., *J. Chromatogr.*, 638 (1993) 263.

84. Tanaka, Y., Matsubara, N. and Terabe, S., *Electrophoresis*, 16 (1995)
85. Wistuba, D., Diebold, H. and Schurig, V., *Microcol. Sep.*, 7 (1995) 17.
86. D'Hulst, A. and Verbeke, N., *J. Chromatogr.*, 608 (1992) 275.
87. D'Hulst, A. and Verbeke, N., *Electrophoresis*, 15 (1994) 854.
88. Stefansson, M. and Novotny, M., *J. Am. Chem. Soc.*, 115 (1993) 11573.
89. Nishi, H., Nakamura, K., Nakai, H., Sato, T. and Terabe, S., *Electrophoresis*, 16 (1995) 865.
90. Stalcup, A.M. and Agyei, N.M., *Anal. Chem.*, 66 (1994) 3054.

## CHAPTER IX

# MICELLAR ELECTROKINETIC CAPILLARY CHROMATOGRAPHY WITH IN SITU CHARGED MICELLES. EXPANDING THE UTILITY OF ALKYLGLYCOSIDE- BORATE MICELLES TO ACIDIC AND NEUTRAL pH FOR CAPILLARY ELECTROPHORESIS OF DANSYL AMINO ACIDS AND HERBICIDES

### Introduction

Several types of *in situ* charged micelles for use in micellar electrokinetic capillary chromatography (MECC) of neutral and charged species have been recently introduced and characterized by our laboratory [1-7]. These new micellar phases are essentially anionic complexes formed between alkyl- [2-7] or steroidal-glycoside [1] surfactants and borate or boronate anions. *In situ* charged micelles possess many unique and attractive features including: (i) an adjustable surface charge density (ii) a weaker hydrophobic character than the traditional alkyl surfactants, and (iii) chiral selectivity. In addition, and as a result of the variable surface charge density, *in situ* charged micelles allow the manipulation of the migration time window and in turn the optimization of analysis time, resolution and peak capacity *via* changing pH and borate or boronate concentration of the running electrolyte.

Thus far, the usefulness of *in situ* charged micelles in the alkaline pH range in MECC of chiral and achiral polyaromatics, pesticides, amino acids, barbiturates and medicarpins and precursors has been demonstrated [1-7]. In this chapter, the useful pH range of *in situ* charged micelles will be extended to the acidic as well as neutral pH.

In earlier reports on *in situ* charged micelles [2, 3], we have demonstrated by <sup>11</sup>B NMR studies that alkylglycoside surfactants with acyclic sugar head groups, such as



MEGA surfactants, have 3 to 5 fold higher affinity for borate ions than their counterparts with cyclic sugar head groups (e.g., octylglucoside, octylmaltoside). This observation, which corroborates well previous findings [8] in that linear sugars complex stronger with borate than cyclic ones, prompted us to select the MEGA surfactants for our present studies at lower pH range. The principles of *in situ* charged micelles have been discussed in previous contributions from our laboratory [2, 3, 7] (see Chapter VIII), and the complexation of borate with polyols have been briefly described recently by El Rassi [9], El Rassi and Nashabeh [10], and Hoffstetter-Kuhn et al. [11]. For simplicity, the term "borate ions" or "borate" is used in this chapter to refer to all kinds of borate species. But, whenever a specific borate species is involved the exact term is utilized instead.

## Materials and Methods

### Instrument

The instrument for capillary electrophoresis was assembled in-house from commercially available components [2, 12] and is described in Chapter III. The detection wavelength was set at 240 nm for the detection of phenoxy acid herbicides and phenoxy ester herbicides as well as urea herbicides, 254 nm for the detection of alkyl phenyl ketones and dansyl amino acids and 340 nm for the detection of Sudan III.

Fused-silica capillary columns of 50  $\mu\text{m}$  I.D. and 365  $\mu\text{m}$  O.D. were obtained from Polymicro Technology (Phoenix, AZ, USA). Throughout the present study, the total length of the capillary was 80 cm while the separation length was 50 cm.

### Reagents and Materials

Nonanoyl-*N*-methylglucamide (MEGA 9) and decanoyl-*N*-methylglucamide (MEGA 10) were purchased from Calbiochem Corp. (La Jolla, CA, USA). All herbicides were purchased from ChemService (West Chester, PA, USA). Sudan III, which was used as the tracer of the migration time of the micelle, and alkyl phenyl ketones were

obtained from Aldrich Chemical Co. (Milwaukee, WI, USA). Dansyl amino acids were purchased from Sigma Chemical Co. (St. Louis, MO, USA). Other reagents were obtained from the same sources listed in the previous chapters.

## Results and Discussion

### Dependence of the Magnitude of the Migration Time Window on Borate Concentration

As shown in Fig. 1a, the migration time window of the micellar phase under investigation increased with borate concentration, and to a larger extent at borate concentration higher than 500 mM. This increase is primarily due to the decrease in the electroosmotic flow, EOF, (see Fig. 1b) given the fact that the electrophoretic mobility of the MEGA 9-borate micelle decreased slightly in the range 100 to 600 mM borate or remained almost the same at borate concentrations above 600 mM as shown in Fig. 1b. Since by increasing the borate concentration in the running electrolyte, the values of both the electroosmotic velocity,  $v_{eo}$ , and electrophoretic velocity of the micelle,  $v_{ep(mc)}$ , are decreasing and approaching each other (see Fig. 1b), the difference between the two velocities will decrease with increasing borate concentration. Due to the fact that the electroosmotic velocity and electrophoretic velocity of the micelle are of opposite sign, and according to the following equation, which relates the migration time of the micelle,  $t_{mc}$ , to  $v_{eo}$ ,  $v_{ep(mc)}$  and the separation distance in the capillary,  $l$ ,

$$t_{mc} = \frac{l}{v_{eo} + v_{ep(mc)}} \quad (I)$$

$t_{mc}$  will increase, and consequently the breadth of the migration time window will enlarge with increasing borate concentration, see Fig. 1a.

Aqueous borate solutions contain tetrahydroxyborate anion, which is formed according to the following equilibrium,



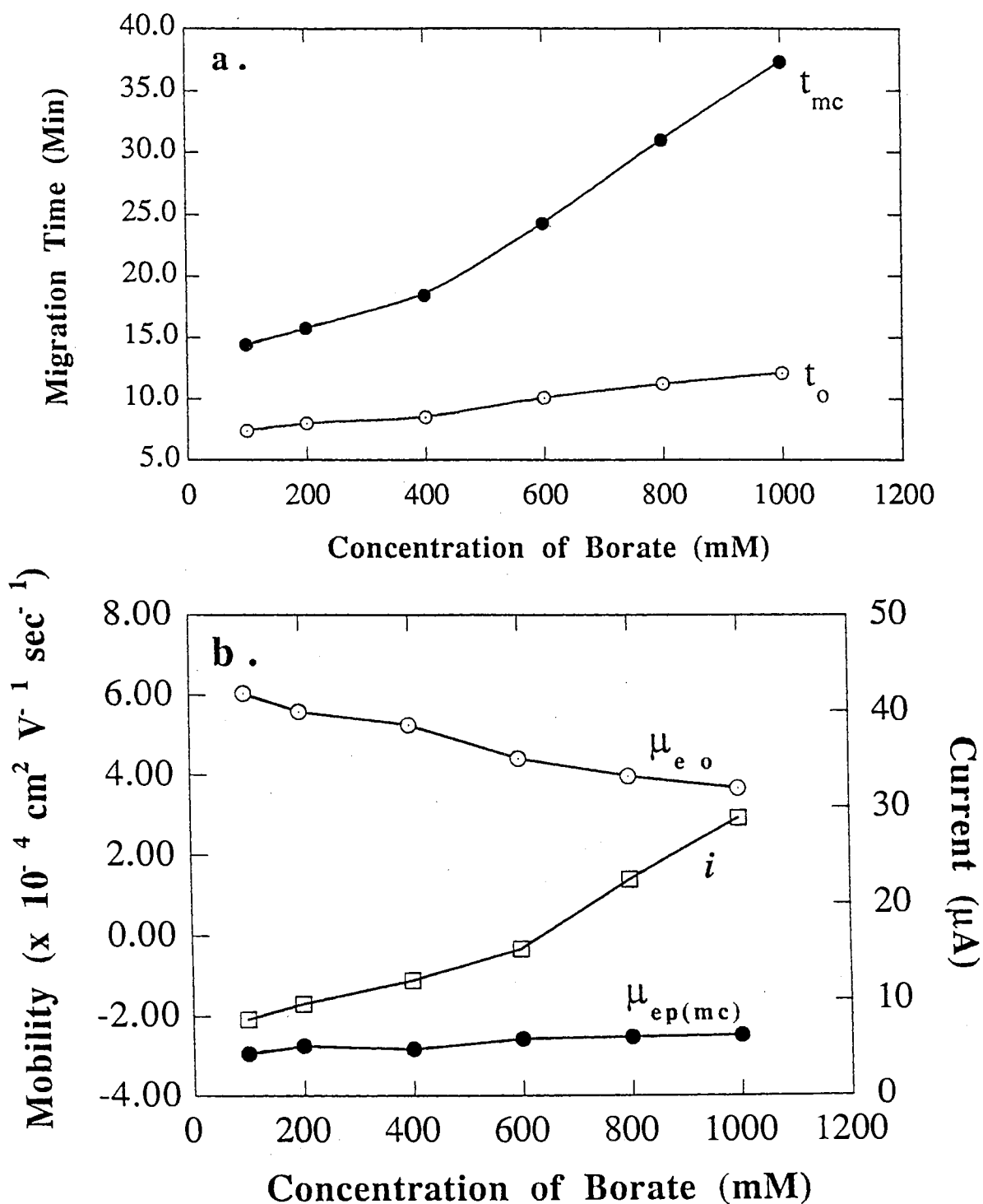
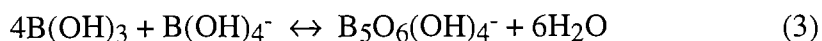
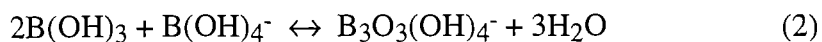
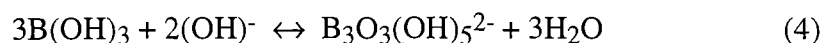


**Figure 1.** Effect of borate concentration on the magnitude of the migration time window in (a) and the electrophoretic mobility of the micelle as well as the electroosmotic mobility and current in (b). Separation capillary, bare fused-silica, 50.0 cm / 80.0 cm x 50  $\mu\text{m}$  i.d.; running electrolyte, 5.0 mM sodium phosphate containing 50.0 mM MEGA 9 and various borate concentration, pH 7.0; running voltage, 15.0 kV; t<sub>mc</sub> tracer, sudan III; t<sub>o</sub> marker, methanol.

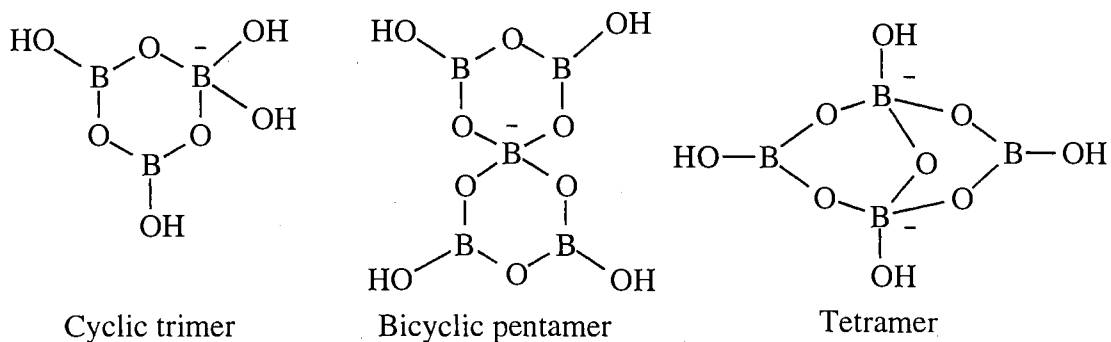
as well as polyborate anions [13-15] such as  $B_3O_3(OH)_4^-$ ,  $B_5O_6(OH)_4^-$ ,  $B_3O_3(OH)_5^{2-}$  and  $B_4O_5(OH)_4^{2-}$ . Singly charged trimer and pentamer borate anions are formed, respectively, by the following equilibria [16]:



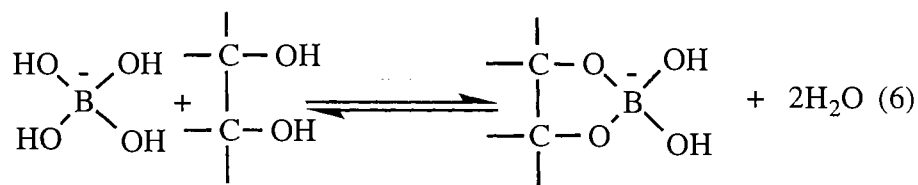
while doubly charged trimer and tetramer anions are produced, respectively, by the two following equilibria:



Whereas equilibria 1 and 2 are predominant at low borate concentration (e.g.,  $\leq 200$  mM), the other polyborate anions formed by equilibria 3, 4 and 5 become important species at high borate concentration [15]. For three of these polyborate anions the following structures were suggested [16, 17]:



The complexation of borate with compounds having vicinal hydroxyl groups, such as the MEGA surfactant used in this study, is thought to occur mainly *via* the reaction of the tetrahydroxyborate ion  $B(OH)_4^-$  and the polyolic compound according to the following equilibrium:



In fact, equilibrium 6 is favored when the O-O distances for the vicinal diol in the polyol compound and for the hydroxyls in the borate ion are on the order of 2.4 Å. This distance is that of the O-O in the tetrahedral boron [18]. On this basis, among polyborate anions, only the cyclic trimer will have the probability to complex with the polyol head group of the MEGA surfactant. However, it can be suggested that due to steric hindrance, the cyclic triborate will complex less than the tetrahydroxyborate anion with a given polyolic compound.

Returning to Fig. 1b, the decrease in the EOF and electrophoretic mobility of the micelle can be explained as follows. At 100 mM borate, pH 7.0, the electrophoretic mobility of the micelle ( $\mu_{ep(mc)}$ ) is quite high which is indicative of the formation of complexing borate ions, e.g., tetrahydroxyborate and cyclic trimer. As the amount of added boric acid was increased between 200 and 1000 mM,  $\mu_{ep(mc)}$  decreased. This may indicate that the concentration of polyborate species such as those shown in equilibria 3, 4 and 5 had increased, a phenomenon that would increase the ionic strength of the running electrolyte without further increasing the surface charge density of the micelle. In fact, and as shown in Fig. 1b, the current  $i$ , which is an indirect measure of the magnitude of the ionic strength, has increased with borate concentration over the concentration range studied. As discussed above, the polyborate species such as  $B_5O_6(OH)_4^-$ ,  $B_3O_3(OH)_5^{2-}$  and  $B_4O_5(OH)_4^{2-}$  are unlikely to complex with vicinal diols. Thus, since increasing the ionic strength of the running electrolyte is accompanied by little or no further increase in the surface charge density of the micelle, the net result is a decrease in the electrophoretic mobility of the MEGA-borate micelle. The decrease in EOF is due to increasing the ionic strength of the running electrolyte. Moreover, the decrease in both parameters (i.e., EOF and electrophoretic mobility of the micelle) may be in part attributed to increasing the viscosity of the running electrolyte at high borate concentration.

Figure 2 displays a typical electropherograms of alkyl phenyl ketones obtained at various borate concentrations. As can be seen in this figure, increasing the borate

concentration of the running electrolyte have resulted in longer analysis time, i.e., wider migration time window. The rationale of being able to change the migration time window is well illustrated in Fig. 2, whereby the solutes can be completely resolved in less than 15 min using a running electrolyte with borate concentration as low as 100 mM at pH 7.0.

#### Dependence of the Magnitude of the Migration Time Window on pH

The effect of the pH of the running electrolyte on the magnitude of the migration time window is shown in Fig. 3a. Increasing the pH of the running electrolyte between pH 3.5 and 6.5 is accompanied by an increase in EOF and electrophoretic mobility of the micelle (see Fig. 3b). The increase in the EOF with increasing pH is due to the ionization of the silanol groups on the inner capillary walls, while the increase in the electrophoretic mobility of the micelle is indicative of increasing the charge density of the micelle. At 400 mM borate in the running electrolyte, increasing the pH between 3.5 and 6.5 may have resulted in yielding higher amounts of complexing borate anions such as tetrahydroxyborate and cyclic trimer anions. This means that equilibria 1 and 2 shifted to the right as the pH was increased (high  $\text{OH}^-$  concentration).

On the other hand, at  $\text{pH} > 6.5$  and using 400 mM boric acid in the running electrolyte, the EOF decreased with increasing pH of the medium. This decrease in the EOF may be attributed to a higher ionic strength at elevated pH as more borate ions are produced. In fact, Fig. 3b shows the sharp increase in the current at  $\text{pH} > 6.5$ , which is reflective of an increase in the ionic strength of the running electrolyte. Moreover, the electrophoretic mobility of the micelle decreased slightly or stayed the same at pH values greater than 6.5. This may reflect that the magnitude of the increase in the ionic strength is greater than that of the surface charge density of the micelle. It is likely that at 400 mM borate concentration,  $\text{pH} > 6.5$ , non complexing polyborates start to be produced in a significant amount so that the increase in the ionic strength of the running electrolyte would outweigh the increase in the surface charge density of the micelle.

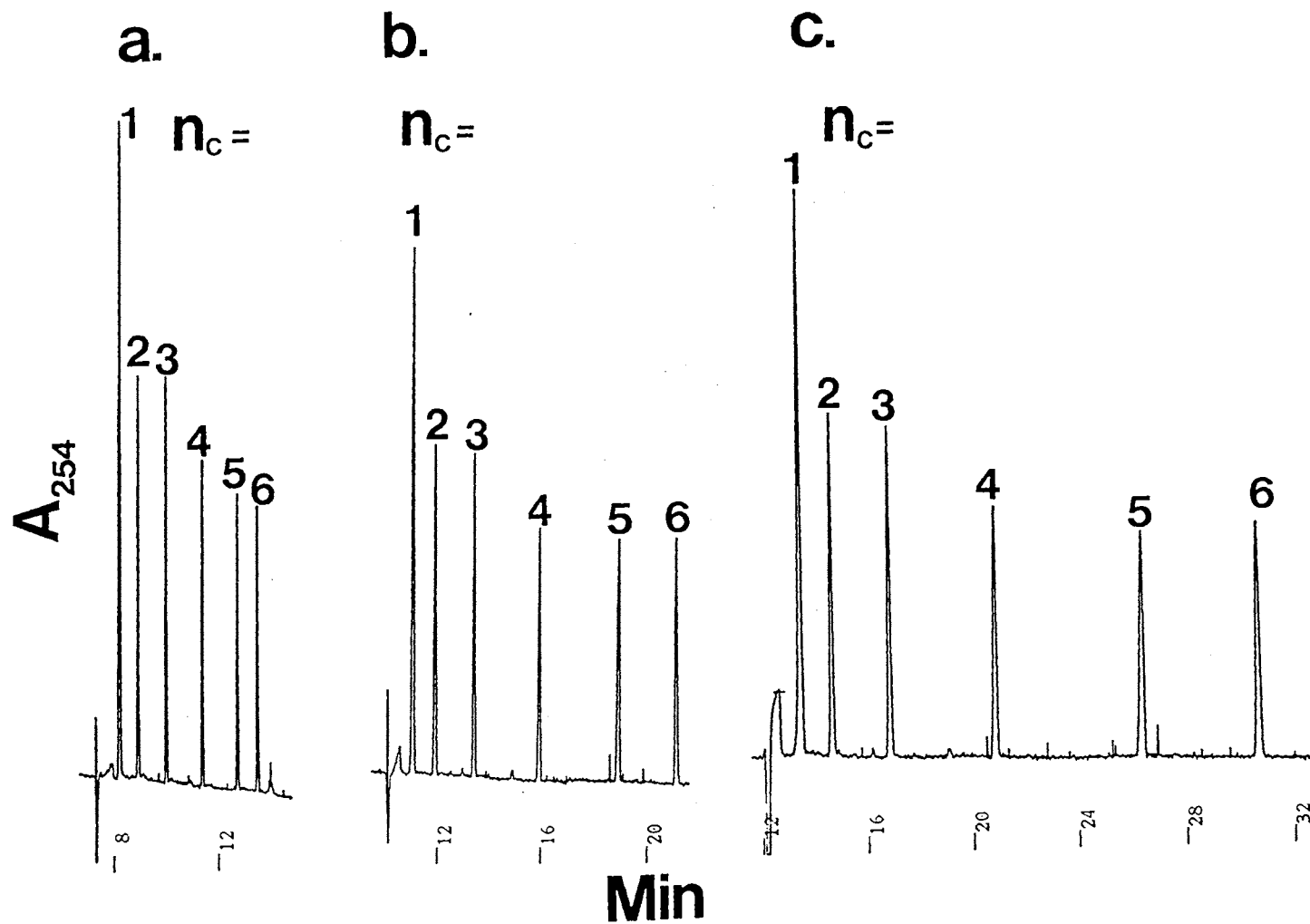


**Figure 2.** Typical electropherograms of alkyl phenyl ketones obtained at different sodium borate concentrations. Running electrolytes, 5.0 mM sodium phosphate containing 50.0 mM MEGA 9, pH 7.0, at various borate concentration: 100 mM (a), 600 mM (b) and 1000 mM (c). Solutes: 1, acetophenone; 2, propiophenone; 3, butyrophenone; 4, valerophenone; 5, hexanophenone; 6, heptanophenone. Other conditions as in Fig. 1.

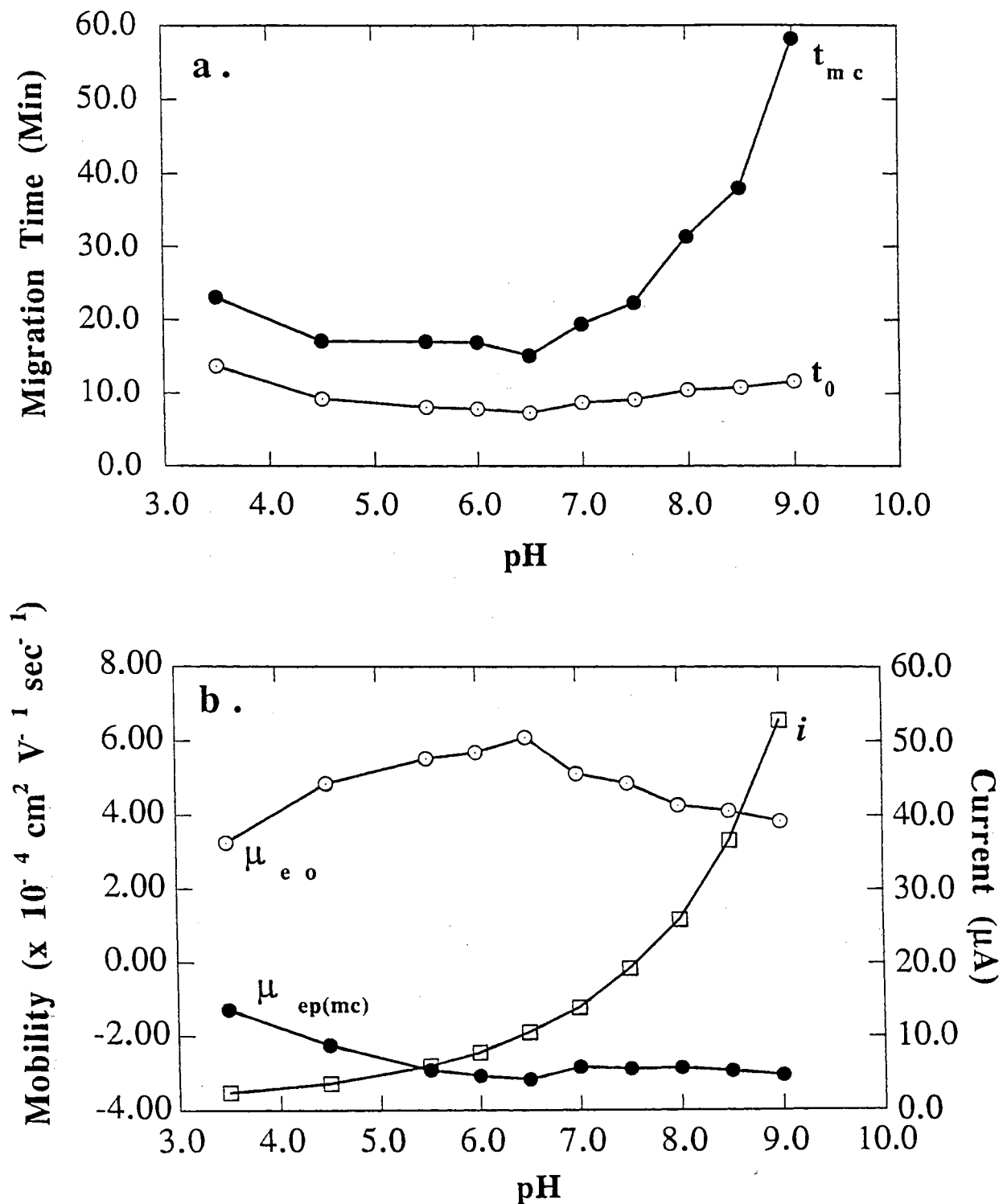


**Figure 3.** Effect of pH on the magnitude of the migration time window in (a) and the electrophoretic mobility of the micelle as well as the electroosmotic mobility and current in (b). Running electrolyte, 5.0 mM sodium phosphate containing 50.0 mM MEGA 9 and 400 mM borate at various pH values. Other conditions as in Fig. 1.



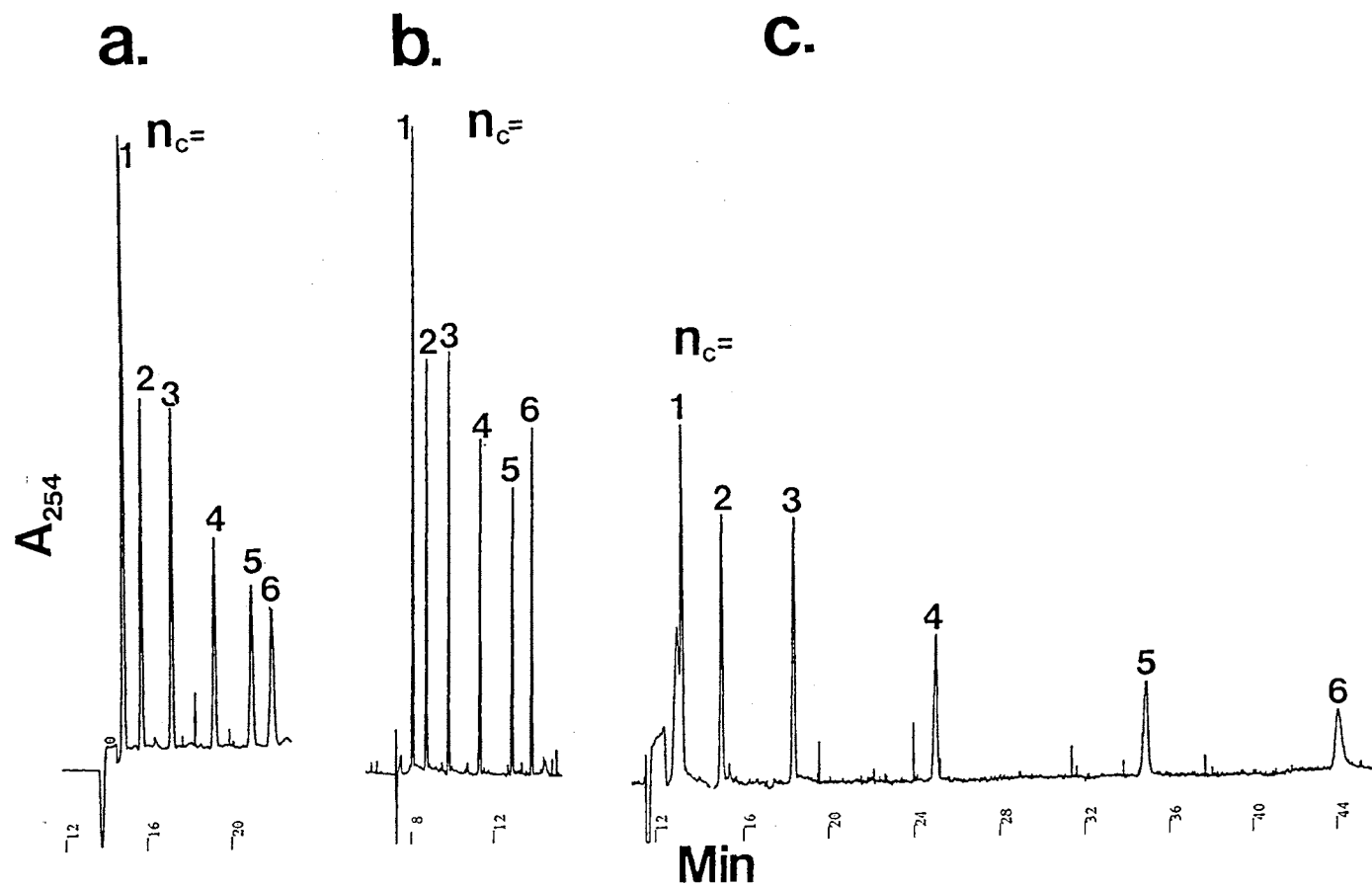
The increase in the breadth of the migration time window at pH values of 7.0 and above is the result of the decrease in the difference between the electroosmotic velocity and the electrophoretic velocity of the micelle (see eqn I). As can be seen in Fig. 3a, in the pH range 3.5-6.5 the migration time window exhibits almost constant breadth. This can be attributed to the fact that both the EOF and the electrophoretic mobility of the micelle increased by almost the same factor.

Figure 4 shows representative electropherograms of alkyl phenyl ketones at various pH values. Using 400 mM borate even at a pH as low as 3.5, a negative charge can be introduced into the micelle and the separation of the various solutes can be achieved. As in the case of various borate concentration (see Fig. 2), the results obtained at various pH (see Fig. 4) show the advantage of being able to manipulate the migration time window. Using 400 mM borate at pH 6.5 as the running electrolyte seems to provide the fastest analysis time with excellent resolution among the various homologous solutes.

In summary, using relatively high borate concentration (e.g., 400 mM) in the running electrolyte, the migration time window and the analysis time of the *in situ* charged micellar system can be varied conveniently with changing pH. This represents a definitive advantage over traditionally used micelles such as sodium dodecyl sulfate (SDS) which are characterized by a fixed surface charge density. In fact, with the MEGA-borate micelles, the EOF remains stronger in magnitude than the electrophoretic mobility of the *in situ* charged micelles, thus allowing the migration of the micelle toward the cathodic end over a wide pH range. This was not the case of the SDS micelle, where it was shown that the direction of the micelle was reversed as the pH was lowered to below pH 5.0 [19]. Under this condition, weakly or non partitioning solutes into the micellar system would be very retarded or would not elute.

#### Correlation Between Capacity Factor and Carbon Number, $n_c$ , of Homologous Series

The retention behavior of alkyl phenyl ketones, having alkyl chains with carbon



**Figure 4.** Typical electropherograms of alkyl phenyl ketones at various pH. Running electrolyte, 5.0 mM sodium phosphate containing 50.0 mM MEGA 9 and 400 mM borate, at pH 3.5 (a), 6.5 (b) and 9.0 (c). Solutes: 1, acetophenone; 2, propiophenone; 3, butyrophenone; 4, valerophenone; 5, hexanophenone; 6, heptanophenone. Other conditions as in Fig. 1.

number,  $n_c$ , from 1 to 6, was examined using a MEGA 9-borate micellar phase. Plots of the logarithmic capacity factors ( $\log k'$ ) of the alkyl phenyl ketone homologous solutes versus  $n_c$  of the homologous series at different pH values and borate concentration yielded straight lines, and the linear regression data are listed in Tables I and II.

TABLE I. Values of Slope, Intercept and R for the Correlation Between Capacity Factor,  $k'$ , and Carbon Number in the Alkyl Chain of Alkyl Phenyl Ketones [ $\log k' = (\log \alpha) n_c + \log \beta$ ] at Various pH Values<sup>a</sup>.

pH	$\log \beta$	$\log \alpha$	R
3.5	-1.04	0.360	0.999
4.5	-1.03	0.367	0.999
5.5	-0.97	0.340	0.999
6.5	-0.97	0.330	0.999
7.5	-1.03	0.340	0.999
8.5	-1.09	0.350	0.999

<sup>a</sup>[MEGA 9] = 50 mM; [Borate] = 400 mM; [Phosphate] = 5 mM; 15.0 kV.

These data are in accordance with those reported previously with MEGA 9-borate micelle phase at  $\text{pH} \geq 9$  [2], and follow the linear expression

$$\log k' = (\log \alpha) n_c + \log \beta$$

where the slope  $\log \alpha$  is a measure of methylene group ( $\text{CH}_2$ ) or hydrophobic selectivity which characterizes nonspecific interactions, while the intercept  $\log \beta$  reflects the specific interactions between the residue of the molecule and the aqueous and micellar phases. This equation implies a constant contribution to the free energy of transfer of the solute between the aqueous phase and the micellar phase with each  $\text{CH}_2$  increment in the chain length of the homologous series. The data obtained at acidic and neutral pH values were in good agreement with those reported previously at  $\text{pH} \geq 9$  [2] to the extent that the slope and the

intercept values are almost identical. This would suggest that the retention behavior of these micellar phases towards uncharged solutes at neutral and acidic pH conditions is similar to that obtained at alkaline conditions.

TABLE II. Values of Slope, Intercept and R for the Correlation Between Capacity Factor,  $k'$ , and Carbon Number in the Alkyl Chain of Alkyl Phenyl Ketones [ $\log k' = (\log \alpha) n_c + \log \beta$ ] at Various Borate Concentration<sup>a</sup>.

[Borate], mM	$\log \beta$	$\log \alpha$	$R$
100	-0.92	0.34	0.999
200	-1.10	0.37	0.999
400	-1.02	0.33	0.999
600	-1.12	0.34	0.999
800	-1.10	0.34	0.999
1000	-1.15	0.34	0.999

<sup>a</sup> [MEGA 9] = 50 mM; pH 10.0; [Phosphate] = 5 mM; 15.0 kV.

#### Dependence of Capacity Factor on pH

Figure 5 shows the dependence of the capacity factor on pH. As expected, the value of the capacity factor remained more or less constant over the pH domain studied. These results agree with those observed at higher pH domain [2]. The capacity factors of the first four solutes of the homologous series were practically unaffected by pH, while the  $k'$  of the other two solutes ( $n_c = 5$  and 6) showed slight decrease and some fluctuations as the pH was changed. The slight fluctuations are within the range of experimental errors while the decrease in retention may be attributed to increasing Joule heating as a result of increasing the current with pH.

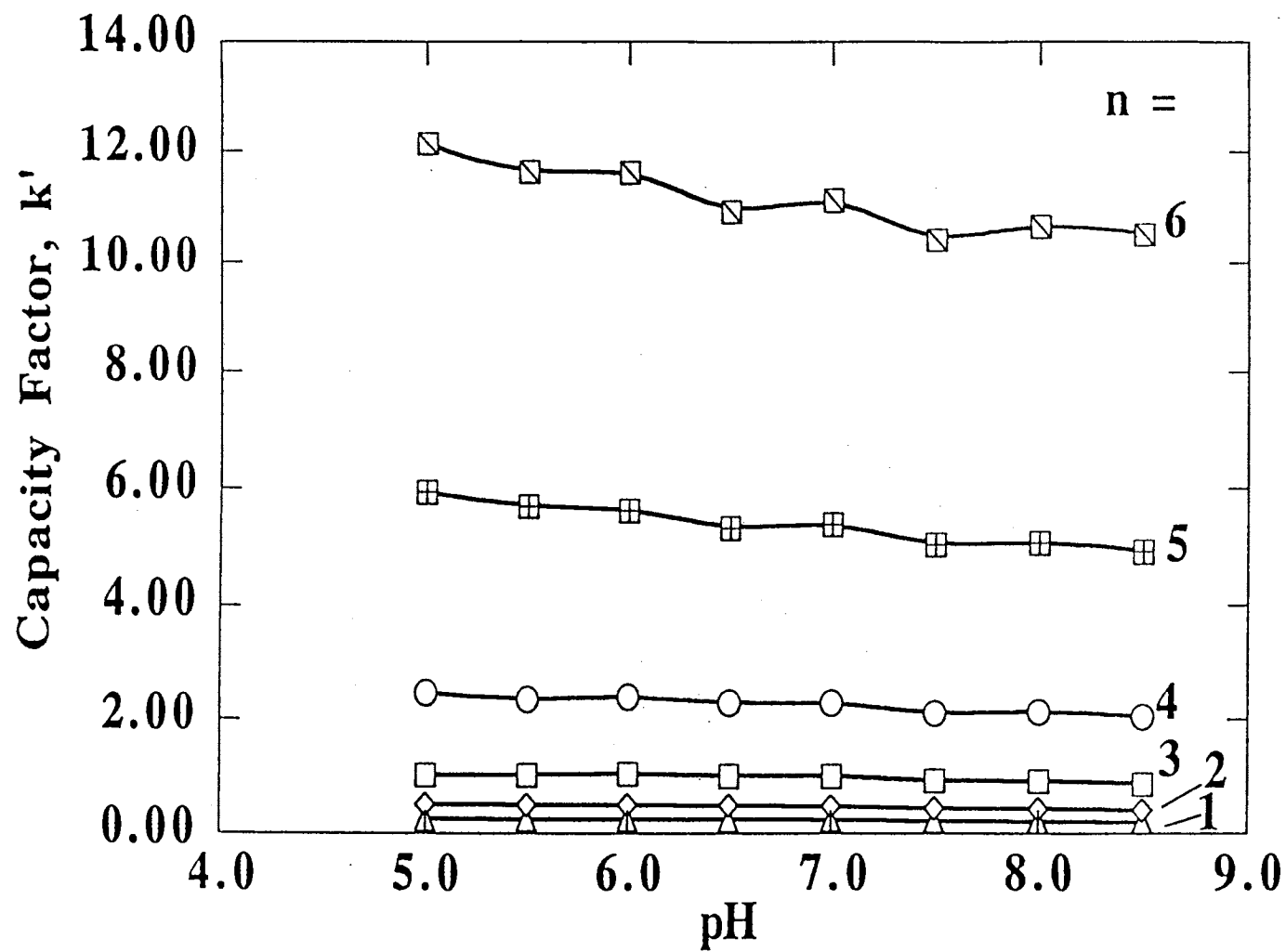


Figure 5. Plots of capacity factor  $k'$  vs. pH of the running electrolyte. Solutes as in Fig. 2. Other conditions as in Fig. 1.

### Illustrative Applications

Phenoxy Acid Herbicides and their Esters. An advantage of the MEGA-borate micellar phase at low pH resides in its ability to separate acidic herbicides and their esters. The separation of ester herbicides employing MEGA-borate micellar phases at alkaline pH values was not successful due to the fact that esters hydrolyze readily in alkaline media (results not shown). Figure 7 illustrates the separation of a mixture of five herbicides (see Fig. 6 for structures) consisting of two acidic herbicides (silvex and 2,4,5-T) and three ester herbicides namely 2,4-D isopropyl ester, 2,4-D butyl ester and 2,4,5-T isopropyl ester.

The separation was carried out using 200 mM sodium borate containing 50 mM MEGA 9 and 5.0 mM sodium phosphate, pH 7.0. Under these separation conditions, silvex and 2,4,5-T are negatively charged and as a result they associate very weakly with the negatively charged MEGA-borate micellar phase, thus migrating mostly by their own electrophoretic mobility faster than the other three analytes. The ester herbicides are neutral and therefore their elution order reflects their relative hydrophobicity. The separation is completed in less than 15 min with an average plate count of 325 000 plates/m.

Urea Herbicides. Fig. 9a and b illustrates the separation of nine urea herbicides (for structures, see Fig. 8) using MEGA 10-borate micellar phases at pH 5.0 and 7.0, respectively. With the exception of terbacil, the elution order of the components of the standard mixture is the same as that reported in an earlier study [2] using the same micellar phase but at pH 10.0. At pH 5.0 and 7.0, terbacil eluted first while at pH 10.0 it migrated slower than monuron and fluometuron [2]. This illustrates the advantages of being able to utilize a given *in situ* charged micellar phase over a wide range of pH, as far as changing the selectivity of the MECC system is concerned. The average plate counts per meter were 224 000 and 189 000 at pH 5.0 and 6.0, respectively.

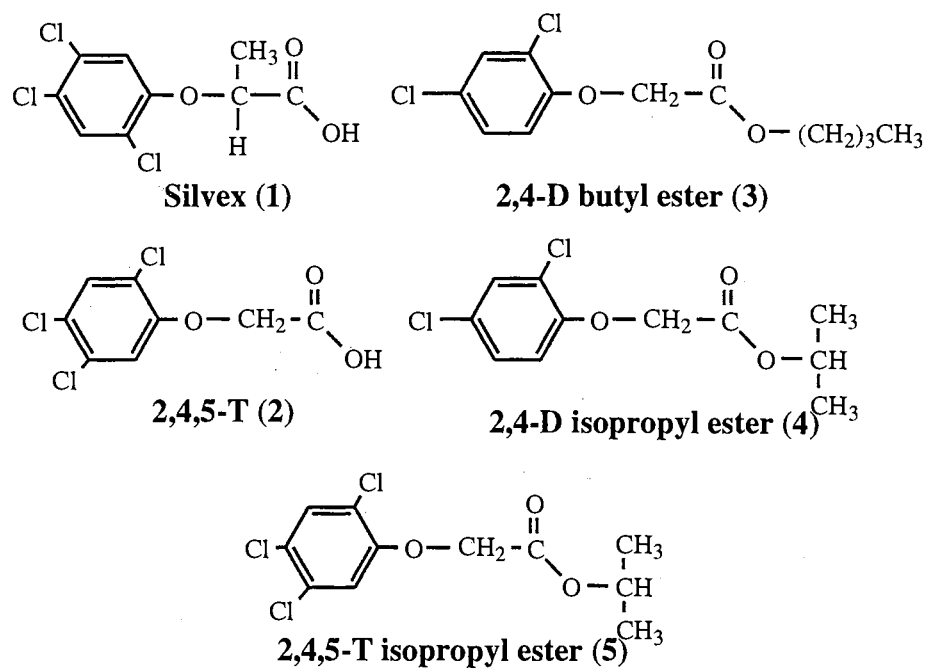


**Figure 6.** Structures of two phenoxy acid herbicides and three phenoxy acid herbicide esters. Numbers in brackets correlate with peak designation in Fig. 7.

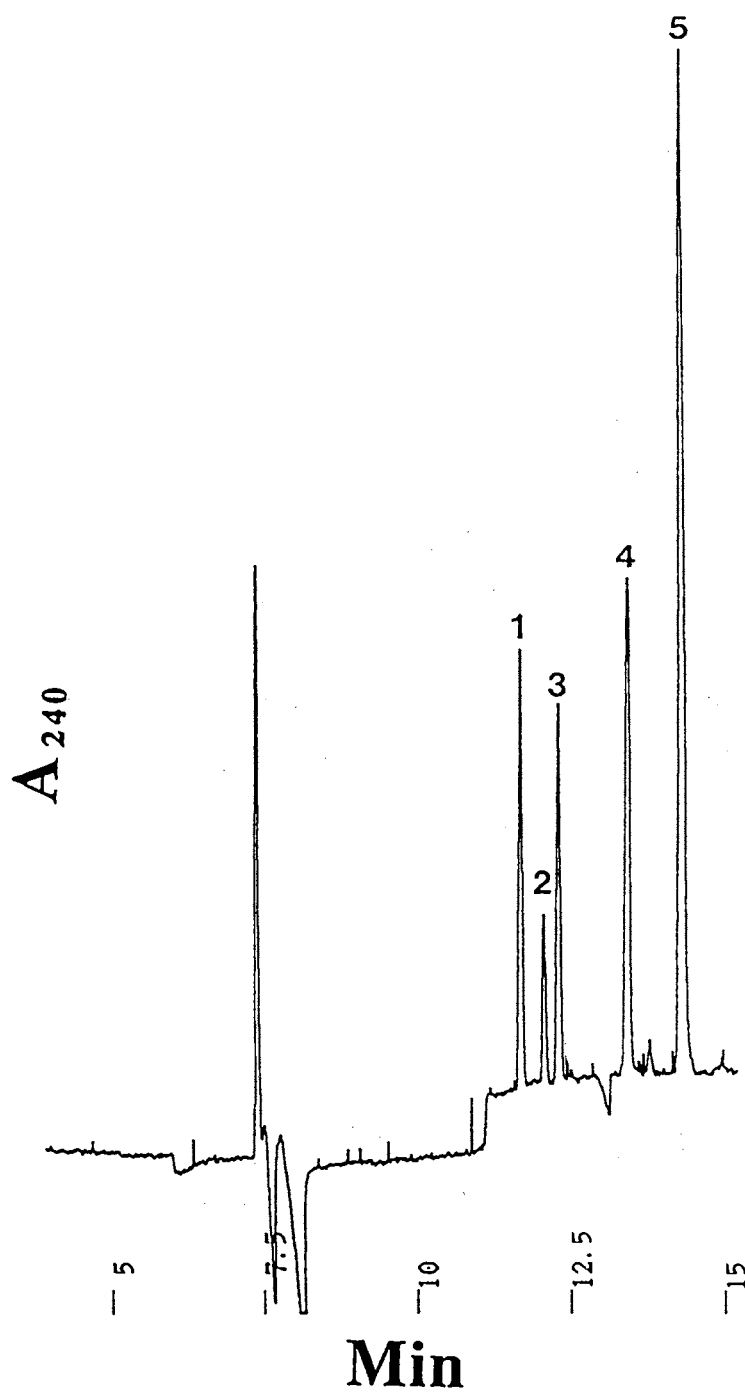


**Figure 7.** Electropherogram of phenoxy acid herbicides and their esters. Running electrolyte, 5.0 mM sodium phosphate containing 50.0 mM MEGA 9 and 400 mM borate, pH 7.0. Solutes: 1= silvex; 2= 2,4,5-T; 3= 2,4-D butyl ester; 4= 2,4-D isopropyl ester; 5= 2,4,5-T isopropyl ester. Other conditions as in Fig. 1.



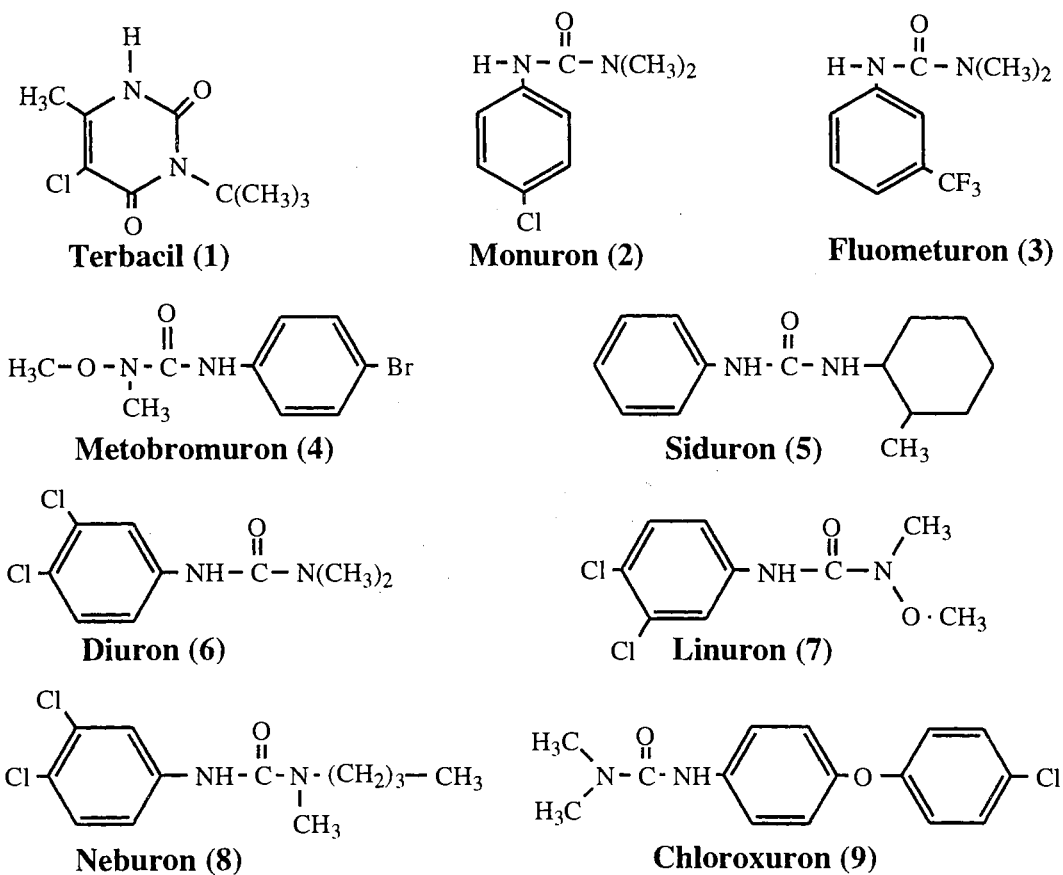


**Figure 8.** Structures of nine urea herbicides. Numbers in brackets correlate with peak designation in Fig. 9.

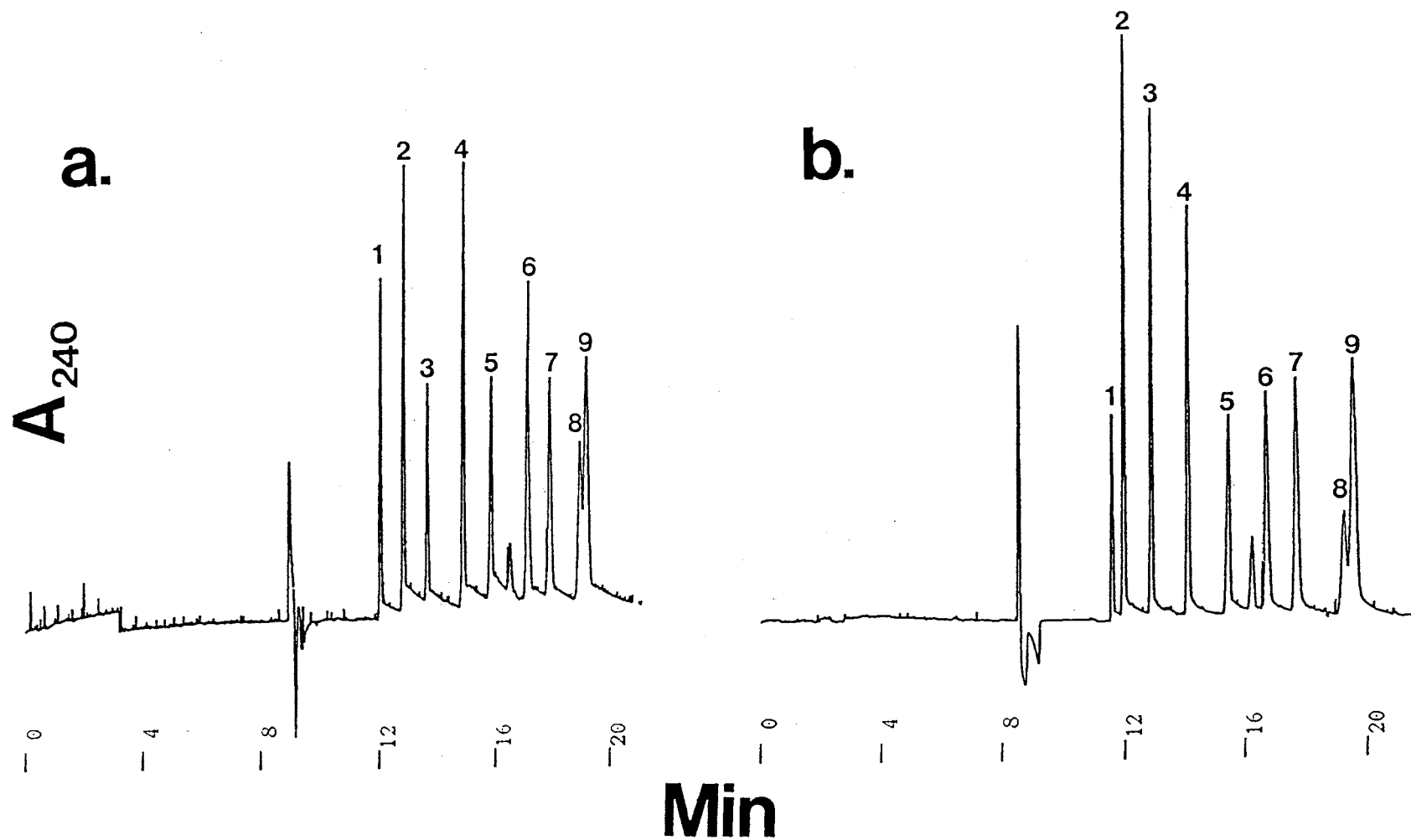


**Figure 9.** Electropherograms of urea herbicides. Running electrolytes, 5.0 mM sodium phosphate containing 50.0 mM MEGA 10 and 400 mM borate, pH 5.0, in (a) or 200 mM borate, pH 7.0 in (b). Solutes: 1, terbacil; 2, monuron; 3, fluometuron; 4, metobromuron; 5, siduron; 6, diuron; 7, linuron; 8, neburon; 9, chloroxuron. Other conditions as in Fig. 1.

Dansyl Amino Acids. Figure 10 illustrates the electropherogram of 15 dansyl amino acids using MEGA 10-borate micellar phase at pH 7.0. As can be seen in this figure, the system provided a baseline separation of 13 dansyl amino acids. The order of migration of the different analytes was the same as that observed in an earlier study using the same micellar phase but at pH 10.0 [2]. Although, dansylated glutamine, asparagine and threonine co-migrated at pH 7.0, the resolution among the other thirteen dansyl amino acids is much better than that obtained at pH 10.0 [2]. difference between the two separations may be attributed to differences in the degree of ionization of the solutes at pH 7.0 and 10.0. The separation was achieved in less than 24 minutes with an average plate count of 332 000 plates/meter.

### Conclusions

In conclusion, MECC using micelles based on alkylglycoside-borate complexes, i.e., *in situ* charged micelles, was demonstrated over a wide range of pH including acidic media. The surfactants used in this study were of the alkyl-*N*-methylglucamide (MEGA) types that possess a linear sugar moiety as the polar head group. These surfactants showed the ability to complex with borate even at acidic pH, thus expanding the pH range over which *in situ* charged micelles can be used in MECC. The electrokinetic behavior of the MEGA-borate micelle at acidic and neutral pH using relatively high borate concentration was different than that observed at alkaline pH using lower borate concentration. These studies which were performed at high borate concentration suggested the formation of polyborates which increased the ionic strength and viscosity of the running electrolyte without further increasing the surface charge density of the micelle. This led to decreasing the electrophoretic mobility of the micelle and the electroosmotic flow with increasing borate concentration. The net result was an increase in the migration time window at increasing borate concentration. Moreover, the magnitude of the migration time window could be adjusted by varying the pH of the running electrolyte over the pH range from 3.5

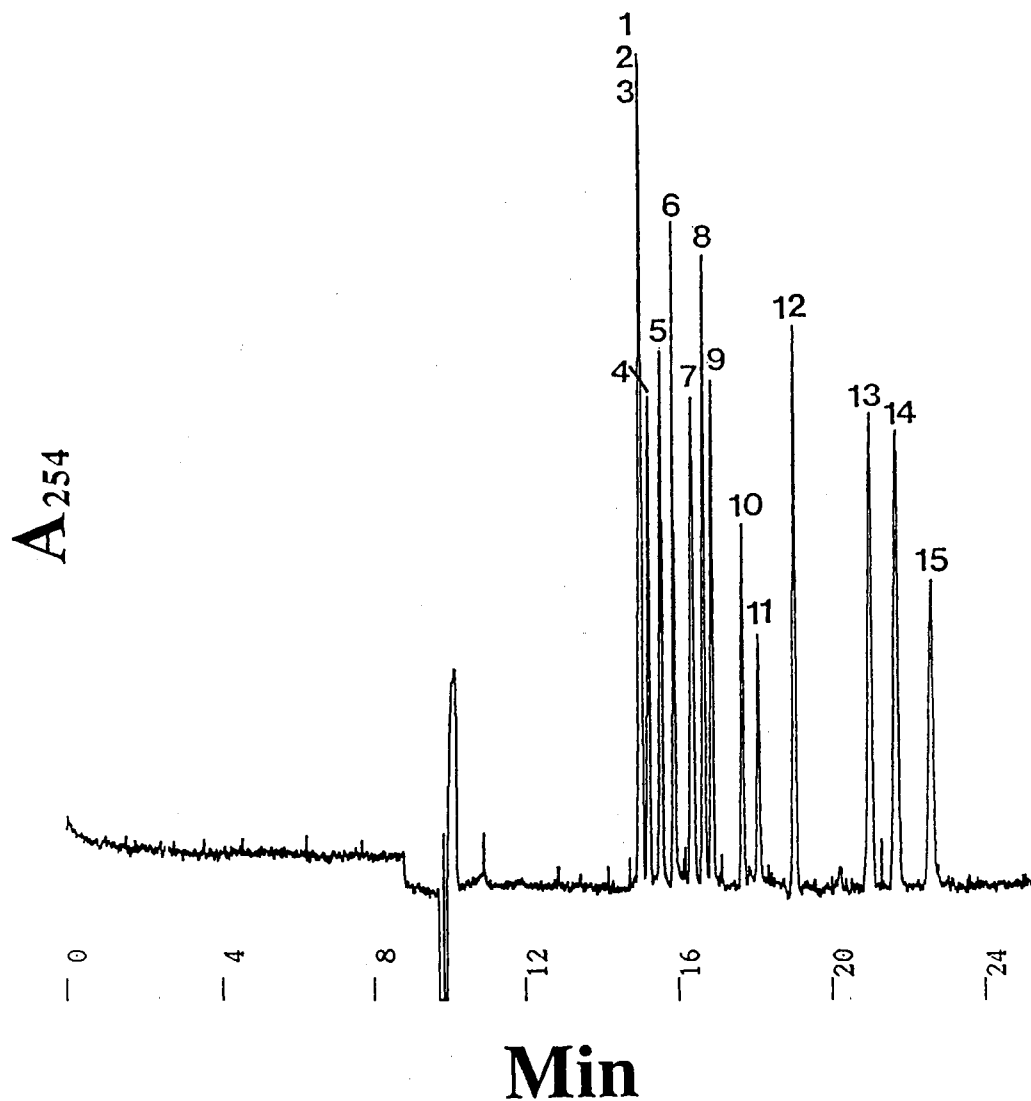


**Figure 10.** Electropherogram of dansyl amino acids. Running electrolyte, 400 mM borate containing 100 mM MEGA 10, pH 7.0. Solutes: 1, glutamine; 2, asparagine; 3, threonine; 4, serine; 5, valine; 6, methionine; 7, glycine; 8, isoleucine; 9, leucine; 10, arginine; 11, phenylalanine; 12, tryptophan; 13, glutamic acid; 14, aspartic acid; 15, cysteic acid. Other conditions as in Fig. 1.

to 9.0. The MEGA-borate systems proved useful for the separation of phenoxy acid herbicides and their esters, urea herbicides, dansyl amino acids and aromatics.

## References

1. Mechref, Y. and El Rassi, Z., *J. Chromatogr. A*, 724 (1995) 285.
2. Smith, J.T., Nashabeh, W. and El Rassi, Z., *Anal. Chem.*, 66 (1994) 1119.
3. Smith, J.T. and El Rassi, Z., *J. Microcol. Sep.*, 6 (1994) 127.
4. Smith, J.T. and El Rassi, Z., *Electrophoresis*, 15 (1994) 1248.
5. Smith, J. T. and El Rassi, Z., *J. Chromatogr. A*, 685 (1994) 131.
6. Smith, J.T. and El Rassi, Z., *J. Cap. Elec.*, 1 (1994) 136.
7. Cai, J. and El Rassi, Z., *J. Chromatogr.*, 608 (1992) 31.
8. Davis, H.B. and Mott, C.J.B., *J. Chem. Soc. Faraday I*, 76: 1991 (1980)
9. El Rassi, Z., *Adv. Chromatogr.*, 34 (1994) 177.
10. El Rassi, Z. and Nashabeh, W., in El Rassi, Z., Ed., *Carbohydrate Analysis: High Performance Liquid Chromatography and Capillary Electrophoresis*, Elsevier, Amsterdam, 1995, p. 267.
11. Hoffstetter-Kuh, S., Paulus, A., Gassmann, E. and Widmer, H.M., *Anal. Chem.*, 63 (1991) 1541.
12. Mechref, Y., Ostrander, G.K. and El Rassi, Z., *J. Chromatogr. A*, 695 (1995) 83.
13. Ingri, N., *Acta Chem. Scand.*, 16 (1962) 439.
14. Ingri, N., *Acta Chem. Scand.*, 17 (1963) 581.
15. Anderson, J.L., Eyring, E.M. and Whittaker, M.P., *J. Phys. Chem.*, 68 (1964) 1128.
16. Momii, R.K. and Nachtrieb, N.H., *Inorg. Chem.*, 6 (1967) 1189.
17. Ingri, N. *Sv. Kem. Tidskr.*, 75 (1963) 199.
18. Christ, C.C., Clark, J.R. and Evans, H.T., *Acta Cryst.*, 11 (1958) 761.
19. Otsuka, K. and Terabe, S., *J. Microcol. Sep.*, 1(1989) 150.

## CHAPTER X

# MICELLAR ELECTROKINETIC CAPILLARY CHROMATOGRAPHY WITH IN SITU CHARGED MICELLES. EVALUATION OF NOVEL CHIRAL MICELLES CONSISTING OF STEROIDAL-GLYCOSIDE SURFACTANT- BORATE COMPLEXES

### Introduction

Chirality is an important phenomenon in various fields including the pharmaceutical and agrochemical research and industries. Because of the increasing awareness of the different physiological effects of the enantiomeric components of racemic mixtures, recently there has been a strong need for various analytical methods for the recognition of molecular chirality and for the separation of enantiomeric compounds. In this regard, various stereoselective separation methods by gas, liquid and supercritical fluid chromatography as well as by capillary electrophoresis have been introduced. Very recently, the various aspects of enantiomeric separations by different chromatographic and electrophoretic techniques, as well as new developments in this branch of separation sciences, have been reviewed and reported in a special issue of the *Journal of Chromatography* [1].

The potentials of capillary electrophoresis in enantiomeric separations were first demonstrated as early as 1985 when the era of CE was just at its early stages [2]. In this first report on CE of enantiomers, several DL-amino acids bearing a dansyl group were resolved by a ligand exchange mechanism and detected by laser induced fluorescence [2]. This work has paved the way to other important approaches for enantiomeric separations by CE including chiral micelles [3] or chirally derivatized micelles [4], micellar phases with

chiral additives [5] or mixed chiral-achiral micelles [6], inclusion complexation (e.g., cyclodextrins and crown ethers) in open tubular format [7, 8] or in a gel filled capillary [9] and affinity interactions involving saccharides [10] or proteins [11, 12]. The details of these various approaches have been described in several recent reviews on CE of enantiomers [13-17]. Each of the different methods has provided a solution for a limited number of enantiomers, and there is no one single approach or chiral selector that has accommodated all enantiomeric separations. This fact has been the driving force for the search of new chiral selectors [17-22, 6] to allow the enantiomeric resolution of a wider range of racemates. Another important aspect of undergoing research in CE of enantiomers has been directed toward optimization of separation and better understanding of the underlying phenomena [23, 24].

This chapter is concerned with the investigation of the potentials of novel chiral in situ charged micelles in micellar electrokinetic capillary chromatography of enantiomers. The novel chiral micellar phases under investigation are essentially based on steroidal glycoside surfactants as borate complexes (see below). The concept of in situ charged micelles for use in MECC was recently introduced by our laboratory [25-30], and has proved useful in the separations of a wide range of species. However, this recent approach has not been yet exploited in MECC of enantiomers. Thus, the present report is a continuation of our previous work and is aimed at enlarging the scope of the applications of in situ charged micelles to include enantiomeric separations.

As shown in Fig. 1, Big CHAP and Deoxy Big CHAP are two nonionic surfactants containing a cholic or deoxycholic steroidal moiety, respectively, and a bisgluconamidopropyl polar group. These chiral, steroidal glycoside surfactants combine both the structural features of bile salts (chiral surfactants) and glycosidic surfactants (in situ charged, and also chiral surfactants [31]) through the steroidal portion and the polyolic polar groups, respectively. This would make such surfactants very attractive for chiral MECC using the concept of in situ charged micelles. In analogy with the reported



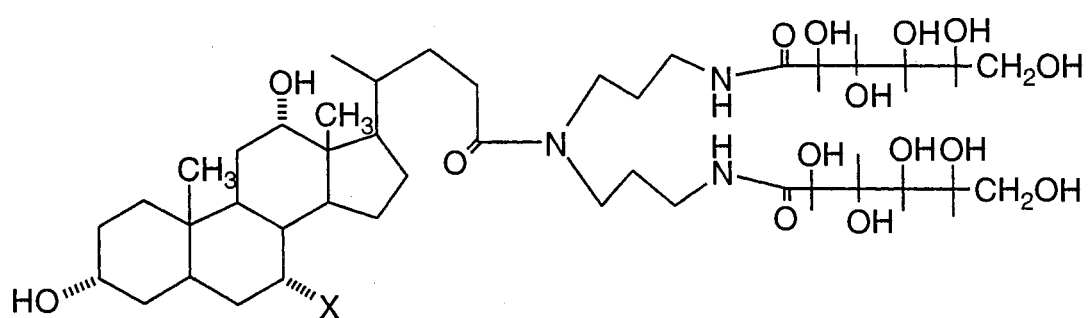


**Figure 1.** Structures of Big CHAP (X= OH) and Deoxy Big CHAP (X = H) surfactants.

behaviors of bile salt surfactants [32], it is believed that (i) the chiral steroidal moieties of Big CHAP and Deoxy Big CHAP render the micelle hydrophobic and hydrophilic simultaneously and (ii) the steroidal glycoside surfactants would form small micelles also called primary micelles via hydrophobic interaction between the non-polar faces of the steroidal monomers [33]. It has been reported that Big CHAP and deoxy Big CHAP have small aggregation numbers of 10 and 8-16, and CMC values of 3.4 and 1.1-1.4 mM, respectively [34]. Furthermore, since both surfactants possess two polar sugar groups, it is believed that their solubilization behavior is different from that of their bile salt counterparts as well as from that of the alkyl type surfactants including alkylglycoside surfactants. The relatively stronger hydrophilic character of Big CHAP and Deoxy Big CHAP should yield different enantioselectivity than that observed with bile salts and other more hydrophobic chiral surfactants. Also, because of the presence of two bulky sugar groups, one can envision that these surfactants would be more suitable for the separation of moderately hydrophobic chiral and achiral compounds, which usually associate strongly with alkyl based micellar phases and do not separate from each other [35].

Although Big CHAP and Deoxy Big CHAP surfactants are neutral, a charge can be introduced into their molecules via the complexation of the polyolic polar groups, i.e., the sugar moiety, with borate. This feature confers to the steroidal glycoside micelles an adjustable surface charge density similar to the previously described in situ charged micelles [25-30]. This renders the steroidal glycoside surfactants very attractive for difficult separations such as racemates. The possibility of in situ charging of Big CHAP and Deoxy Big CHAP through borate complexation offers the freedom of adjusting the migration time window of the micelles and consequently allowing the optimization of enantiomeric resolutions, analysis time and peak capacity. The migration time window of in situ charged micelles can be readily adjusted by varying the surface charge density of the micelles through changing the borate concentration and/or the pH of the running electrolyte [26-30].

Thus far, most chiral surfactants that have been described for MECC of enantiomers [22, 36] do not have a freely adjustable migration time window as the in situ charged micelles described here, and for some of them a mixed micellar system with SDS was employed either to increase the migration time window [37] or to render the chiral micelles amenable to the separation of neutral enantiomers [6].

## Materials and Methods

### Capillary Electrophoresis Instrument

The instrument for capillary electrophoresis used in this study was a Beckman P/ACE instrument (Beckman Instrument, Fullerton, CA, USA) and it is described in Chapter VI. Detection was performed at 240 nm using a diode array detector (DAD). The fused-silica capillaries were obtained from Polymicro Technology (Phoenix, AZ, U.S.A.) and had the dimensions of 50 cm / 57 cm with an I.D. of 50  $\mu\text{m}$  and an O.D. of 365  $\mu\text{m}$ . Unless otherwise stated, the temperature of the capillary was maintained at 15  $^{\circ}\text{C}$  by the instrument thermostating system. Samples were injected as methanol-water solutions by applying pressure of 0.5 psi for various lengths of time.

### Reagents and Materials

The following enantiomers: (S)-(-)-1,1'-binaphthyl-2,2'-diamine (BNDA), (R)-(+)-1,1'-binaphthyl-2,2'-diamine, ( $\pm$ )-1,1'-bi-2-naphthol (BNOH), (S)-(-)-1,1'-binaphthyl-2,2'-diylhydrogen phosphate (BNPO<sub>4</sub>), (R)-(+)-1,1'-binaphthyl-2,2'-diylhydrogen phosphate and troger's base were purchased from Aldrich (Milwaukee, WI, USA). Silvex (2-(2,4,5-trichlorophenoxy)propionic acid) was obtained from Chem Service (West Chester, PA, USA). All dansyl amino acids (Dns-AA), namely DL-leucine, DL-methionine, DL-phenylalanine, and DL-tryptophan cyclohexylammonium salts were purchased from Sigma Chemical Co. (St. Louis, MO, USA). The structures of the model solutes used in this study are given Fig. 2. N,N-bis-(3-D-Gluconamidopropyl)-cholamide

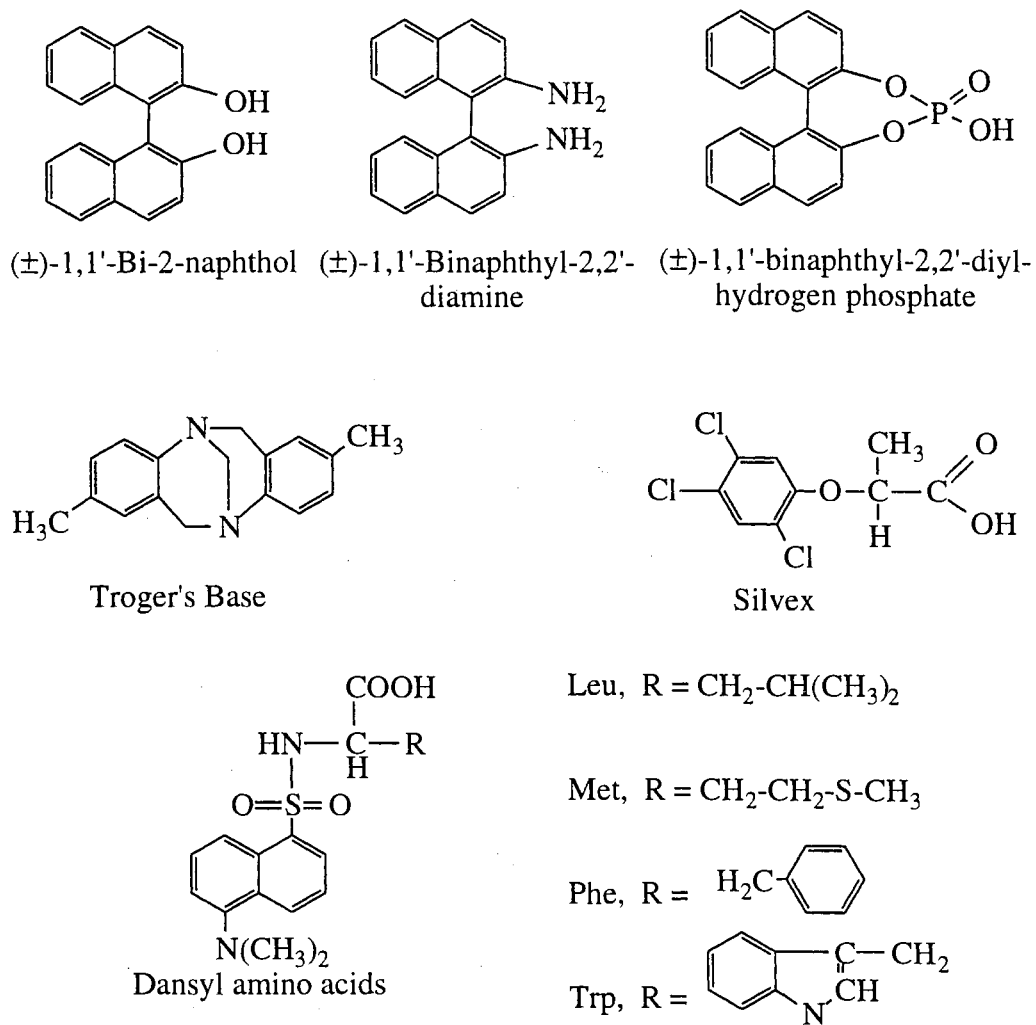


**Figure 2.** Structures of model chiral solutes used in this study.

(Big CHAP) and *N,N*-bis-(3-D-gluconamidopropyl)-deoxycholamide (Deoxy Big CHAP) were purchased from Calbiochem (La Jolla, CA, USA).

## Results and Discussion

### Variables Affecting the Chiral Recognition and the Electrokinetic Behavior of the Steroidal Glycoside-Borate Micellar Phases

The chiral recognition and selectivity of the steroidal glycoside surfactants in chiral MECC were evaluated using three different binaphthyl compounds as the model enantiomers under various conditions including the pH of the running electrolyte, borate and surfactant concentration, amount and nature of organic modifier, and capillary temperature.

Electrolyte pH. Figure 3 illustrates the relationship between the breadth of the migration time window and the pH of the running electrolyte. As can be seen in Fig. 3,  $t_{mc}$  increased sharply with pH due to increasing the surface charge density of the micelle, which resulted from increasing the concentration of the Big CHAP-borate complexes at higher pH values. Under this condition, the electrophoretic mobility of the micelle in the opposite direction to the electroosmotic flow (EOF) increased, thus yielding an increase in  $t_{mc}$ . In addition, the sharp increase in  $t_{mc}$  at pH 11.5 might be due in part to the ionization of the hydroxyl groups of the sugar moieties of the surfactant. On the other hand,  $t_0$  increased only slightly over the pH range studied due to the increase in the ionic strength of the running electrolyte at higher pH. This decreased the zeta potential of the capillary walls thus causing the EOF to decrease. The silanol groups of the fused-silica surface are fully ionized in the pH range 8-12, and consequently the charge density of the capillary inner surface is virtually constant. Overall, the net result of increasing the pH of the running electrolyte is a significant increase in the migration time window of the in situ charged chiral micellar phase.

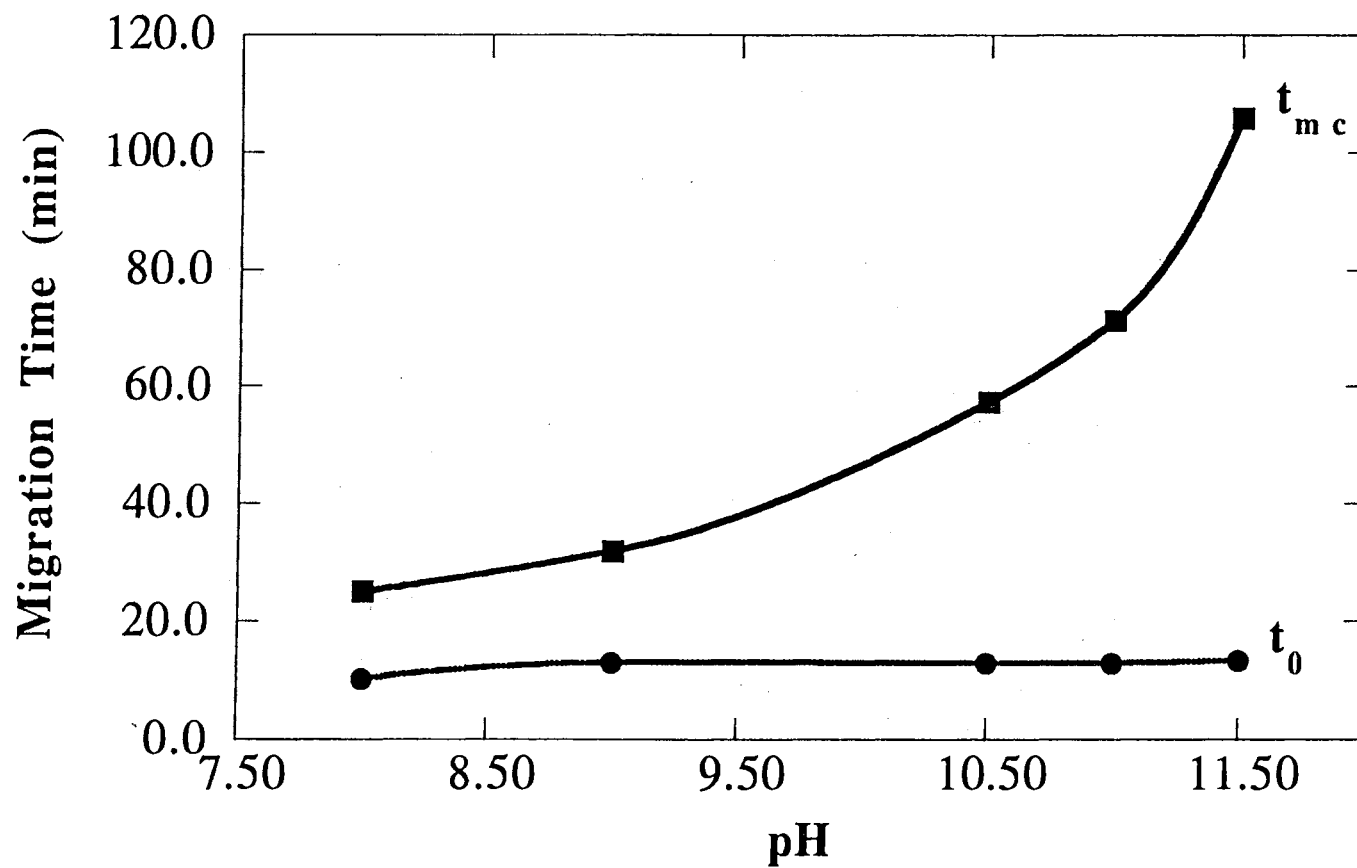


**Figure 3.** Effect of pH on the magnitude of the migration time window. Capillary, untreated fused-silica, 50/57 cm x 50  $\mu$ m I.D.; running electrolytes, 46 mM Big CHAP, 200 mM borate at various pH; running voltage, 15.0 kV; tracers, Sudan III (for  $t_{mc}$ ) and methanol (for  $t_0$ ).

Figure 4 illustrates the effect of pH of the running electrolyte on the enantiomeric resolution of BNOH using the Deoxy Big CHAP surfactant. As can be seen, the enantiomeric resolution of BNOH racemic mixture increased  $R_s = 0.90$  at pH 8.0 and 9.0 to  $R_s = 1.60$  at pH 10.0. BNPO<sub>4</sub> enantiomers showed a continuous increase in resolution as the pH of the running electrolyte increased (Fig. 5).  $R_s$  increased from 1.95 at pH 8.0 to 2.20 at pH 9, then to 2.80 at pH 10.0 and finally to 4.00 at pH 11.0. In addition, the order of migration of the BNPO<sub>4</sub> enantiomers was inverted at pH 11.0 (see Fig. 5). In general, the increase in resolution with increasing pH is the result of increasing the magnitude of the migration time window of the micellar system under investigation (see Fig. 3). Since increasing the pH results in increasing the electrophoretic velocity of the micelle in the opposite direction to the EOF, which in turn leads to increasing  $t_{mc}$ , the enantiomer which associates more with the micelle migrates slower than the one showing less affinity to the micelle, and consequently the migration order of the enantiomers is inverted. Note that at pH 11.0, and in the positive polarity mode, i.e., using positive potential at the injection end, the net mobility of the micelle is less than that of BNPO<sub>4</sub>.

Under the same operating conditions as in the preceding experiments, Big CHAP showed lower enantiomeric resolution than Deoxy Big CHAP. The enantiomeric resolution of BNPO<sub>4</sub> enantiomers increased slightly from  $R_s = 0.5$  to  $R_s = 0.6$  when going from pH 8.0 to pH 9.0 and then leveled off at the value of  $R_s = 0.6$  at pH 10.0 and 11.0 with no inversion in the elution order. A typical electropherogram obtained at pH 9.0 is shown in Fig. 6a. Thus, different chiral surfactants would yield different selectivity. Again, in the case of BNOH, the enantiomeric resolution with Big CHAP was much less than that observed with Deoxy Big CHAP, compare Fig. 6b (pH 10.0,  $R_s = 0.8$ ) to Fig. 4c (pH 10,  $R_s = 1.6$ ).

Borate Concentration. The effect of borate concentration on the breadth of the migration time window is illustrated in Fig. 7. As expected, the migration time window increased as the borate concentration increased. The sharp increase in  $t_{mc}$  is due to the

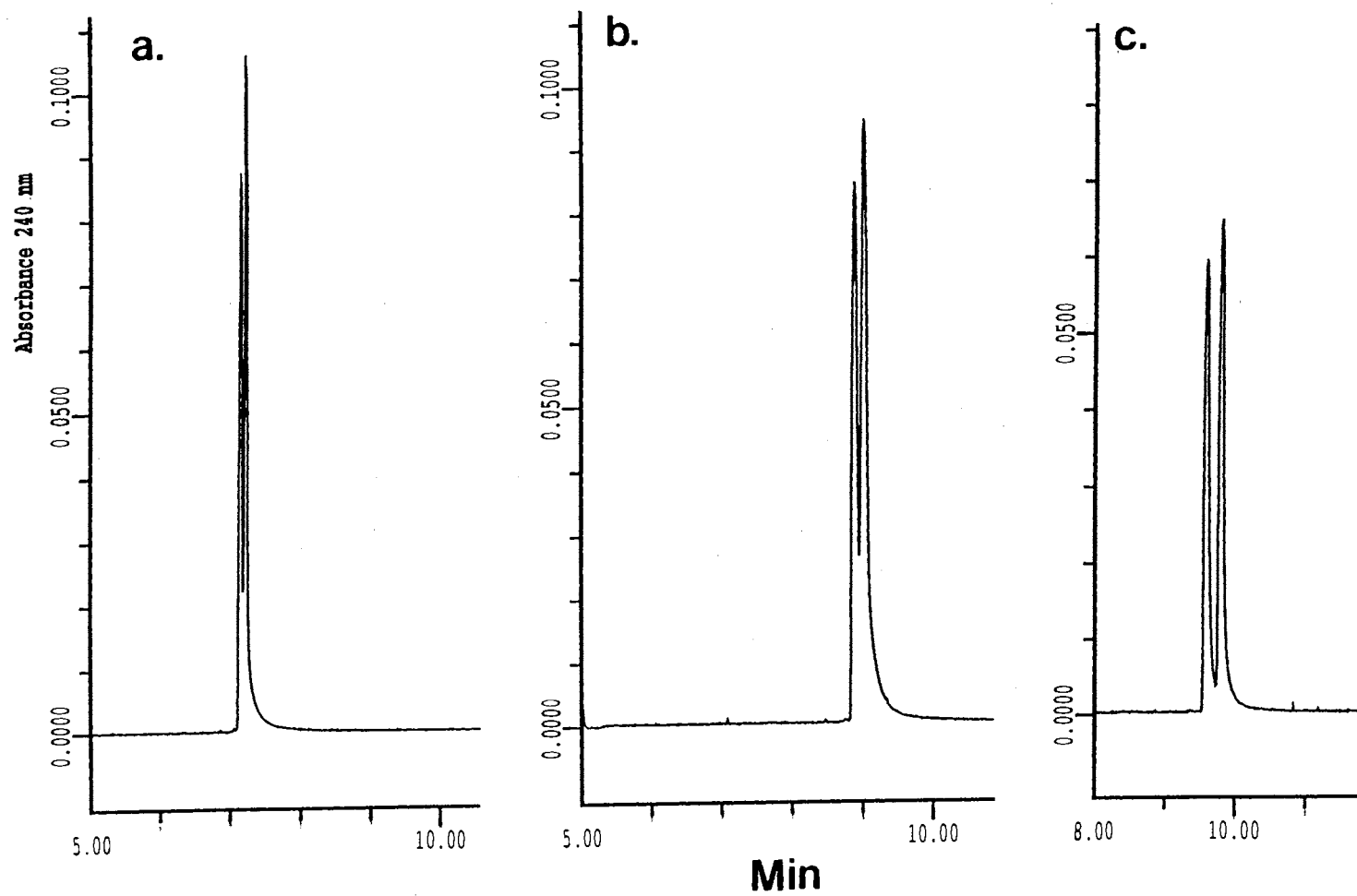


**Figure 4.** Electropherograms of BNOH obtained with Deoxy Big CHAP at various pH. Capillary, untreated fused-silica, 50/57 cm x 50  $\mu$ m I.D.; running electrolytes, 15 mM Deoxy Big CHAP, 50 mM borate at pH 8.0 (a), 9.0 (b) and 10.0 (c); capillary temperature, 15  $^{\circ}$ C; voltage, 20 kV.



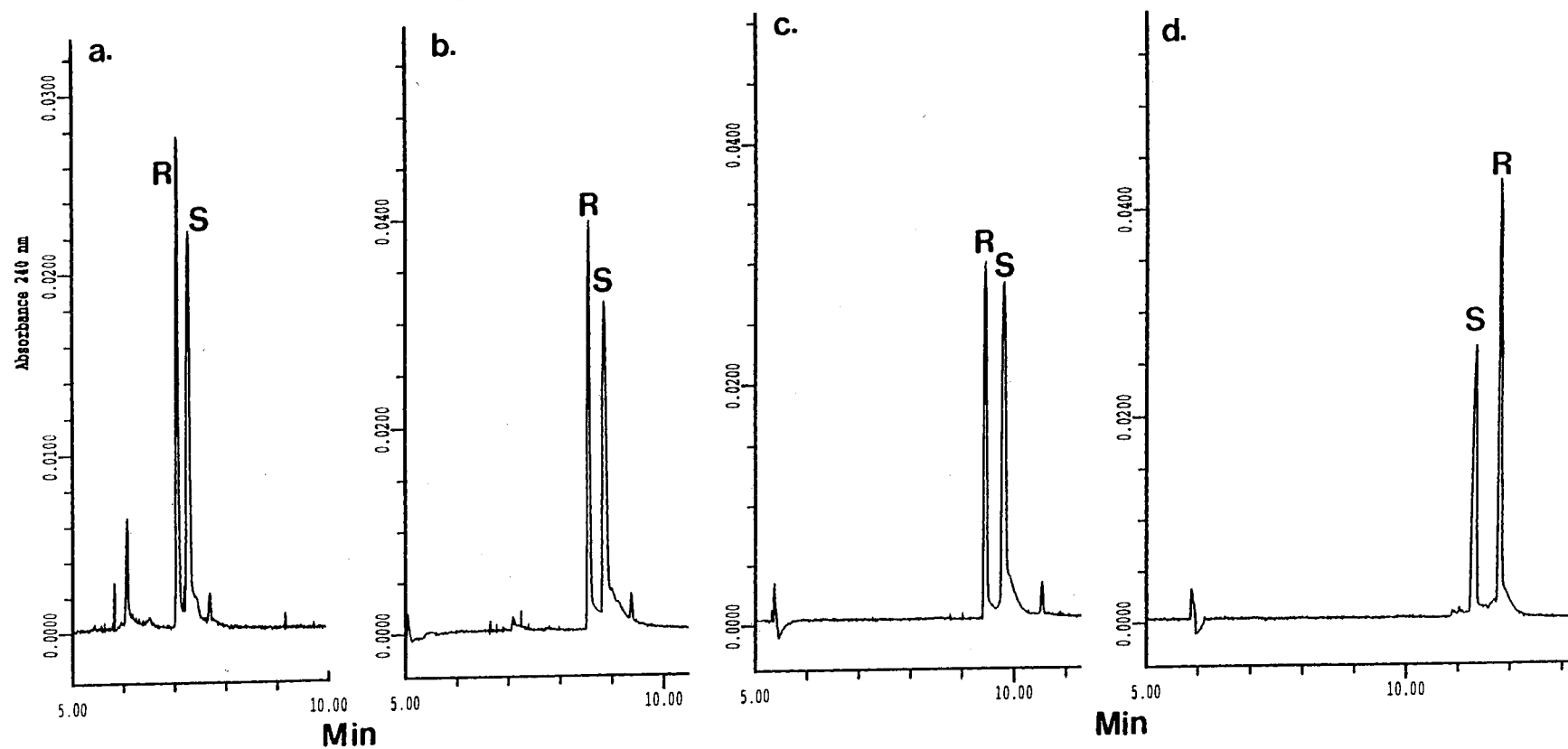


**Figure 5.** Electropherograms of standard  $\text{BNPO}_4$  enantiomers obtained with Deoxy Big CHAP at various pH: 8.0 (a), 9.0 (b), 10.0 (c) and 11.0 (d). Conditions as in Fig. 3.

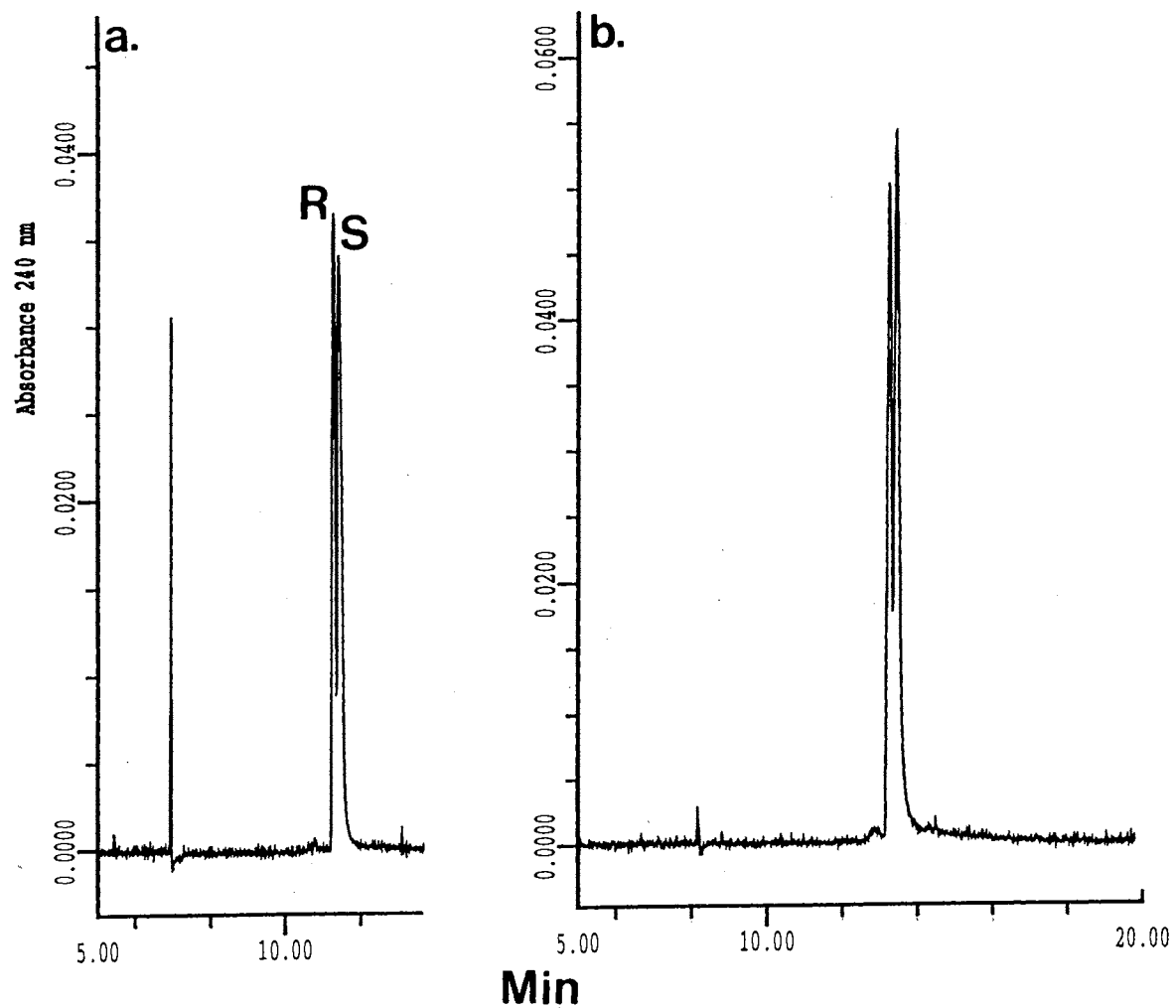


**Figure 6.** (a) Electropherogram of  $\text{BNPO}_4$  enantiomers obtained with Big CHAP at pH 9.0. (b) Electropherograms of BNOH obtained with Big CHAP at pH 10.0. Capillary, untreated fused-silica, 50/57 cm x 50  $\mu\text{m}$  I.D.; running electrolytes, 50 mM borate containing 20 mM Big CHAP, pH 9.0 (a) or pH 10.0 (b) and 10 % (v/v) methanol; capillary temperature, 15  $^\circ\text{C}$ ; voltage, 20 kV.

increase in the charge density of the micelle as a result of increasing the Big CHAP-borate complex concentration caused by the increase in borate concentration. On the other hand, the slight increase in  $t_0$  is due to the higher ionic strength and viscosity of the running electrolyte at high borate concentration.

As expected, the concentration of borate in the running electrolyte largely influenced enantiomeric resolution, see Fig. 8. As can be seen in Fig. 8, at 25 mM borate, BNDA enantiomers almost coeluted. By doubling the concentration of borate to 50 mM a significant increase in resolution was realized ( $R_s = 1.26$ ). Enantiomeric resolution kept increasing as the borate concentration increased and finally a resolution of 1.67 was obtained at 150 mM borate. The same trend was observed for BNOH enantiomers with the difference that even at 25 mM,  $R_s$  was nearing unity and then kept rising and reached a value of almost 2.0 at 150 mM borate (results not shown). In the case of BNPO<sub>4</sub>, even at 25 mM borate the enantiomeric resolution was quite high ( $R_s = 1.86$ ). This is because for a charged solute, such as BNPO<sub>4</sub>, that is strongly associating with the chiral surfactant, there is virtually no need to charge the micelle to obtain baseline resolution. As can be seen in Fig. 9, charging the micelle through the addition of borate has slowed the migration of the enantiomers. The net result is a sharp rise in  $R_s$  from 1.86 to 2.80 when going from 25 to 50 mM borate. At borate concentration higher than 50 mM the  $R_s$  decreased and then leveled off between 75 and 150 mM at a value of 1.5-1.6. The decline in  $R_s$  at high borate concentration is perhaps due to the slightly broader peaks. The peak broadening here may be caused by a longer residence time in the capillary column, i.e., more longitudinal diffusion.

For Big CHAP surfactant the effect of borate concentration in the running electrolyte on the enantiomeric resolution of BNOH is illustrated in Fig. 10. At 25 mM borate no enantiomeric resolution was obtained. By doubling the borate concentration to 50 mM a resolution of 0.7 is realized. By going to 100 and 150 mM borate this resolution stays almost the same. On the other hand, the BNPO<sub>4</sub> enantiomeric mixture showed

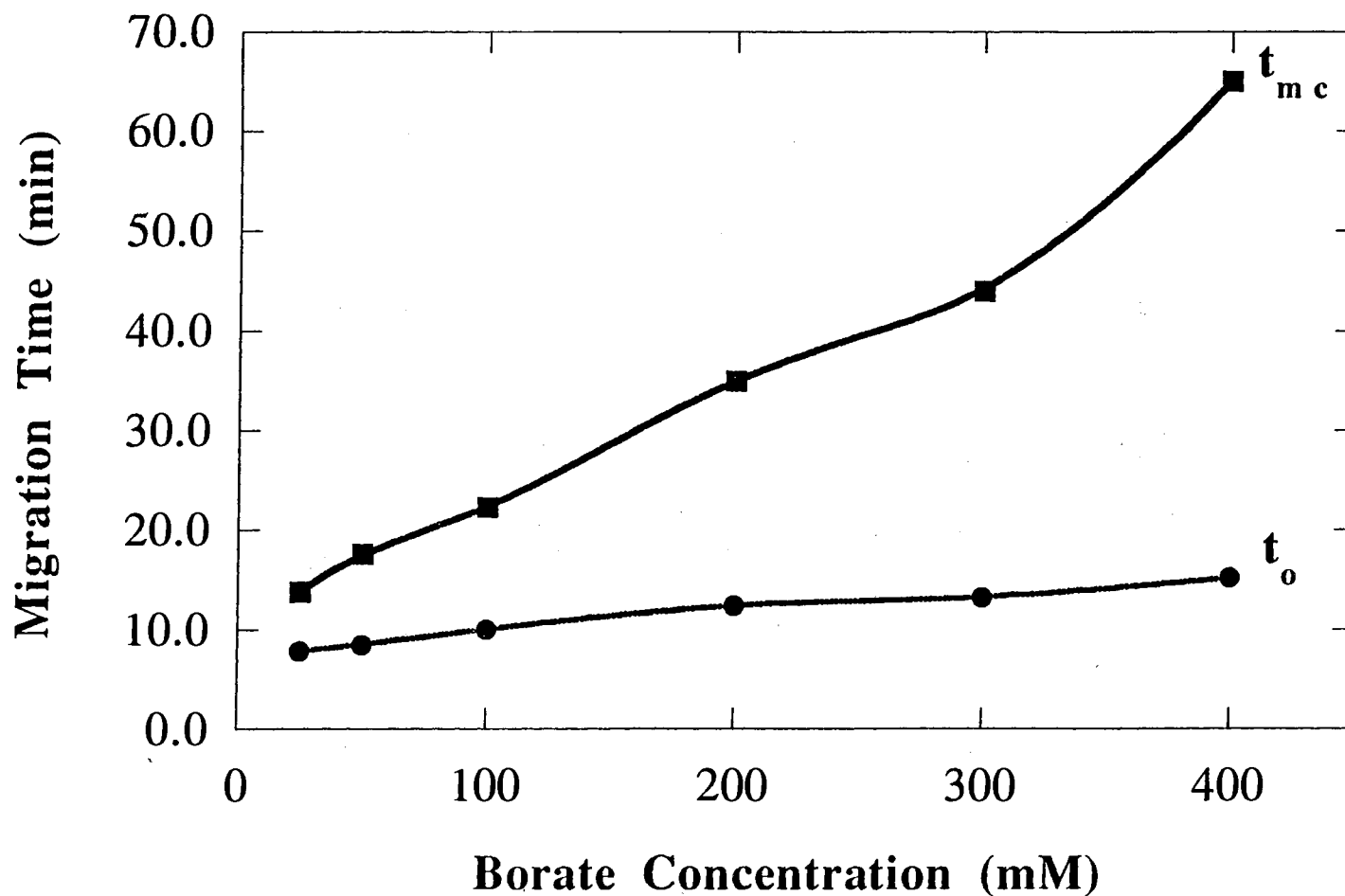


**Figure 7.** Effect of borate concentration on the magnitude of the migration time window. Running electrolytes, 9 mM Big CHAP at various concentrations of borate, pH 10. Other conditions as in Fig. 2.

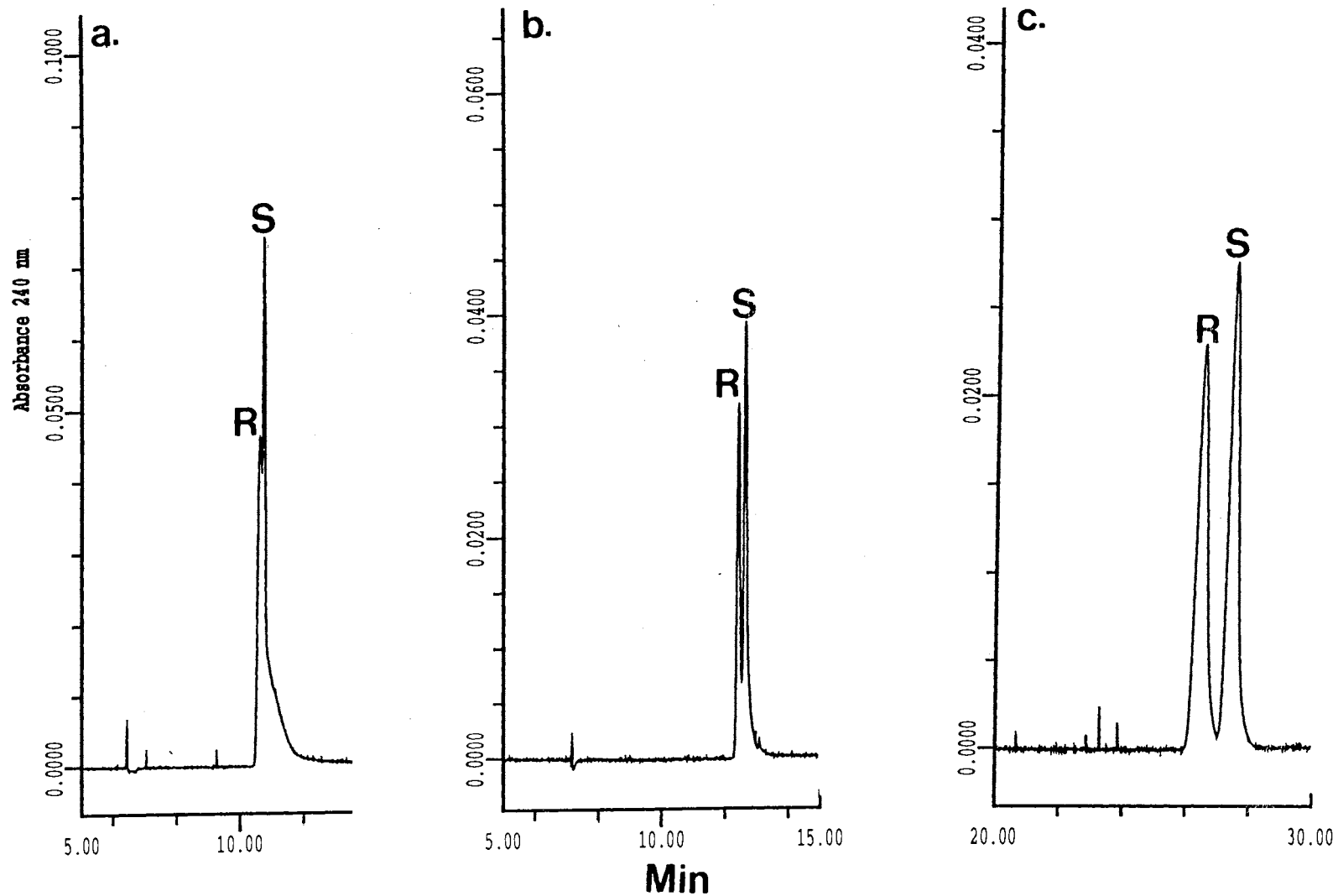


**Figure 8.** Electropherograms of BNDA enantiomers obtained with deoxy Big CHAP at various concentrations of borate in the running electrolytes. Capillary, untreated fused-silica, 50/57 cm x 50  $\mu$ m I.D.; running electrolytes, 25 mM (a), 50 mM (b), or 150 mM (e) sodium borate containing 15 mM Deoxy Big CHAP (pH 10.0) and 10 % (v/v) methanol; capillary temperature, 15  $^{\circ}$ C; voltage, 20 kV.

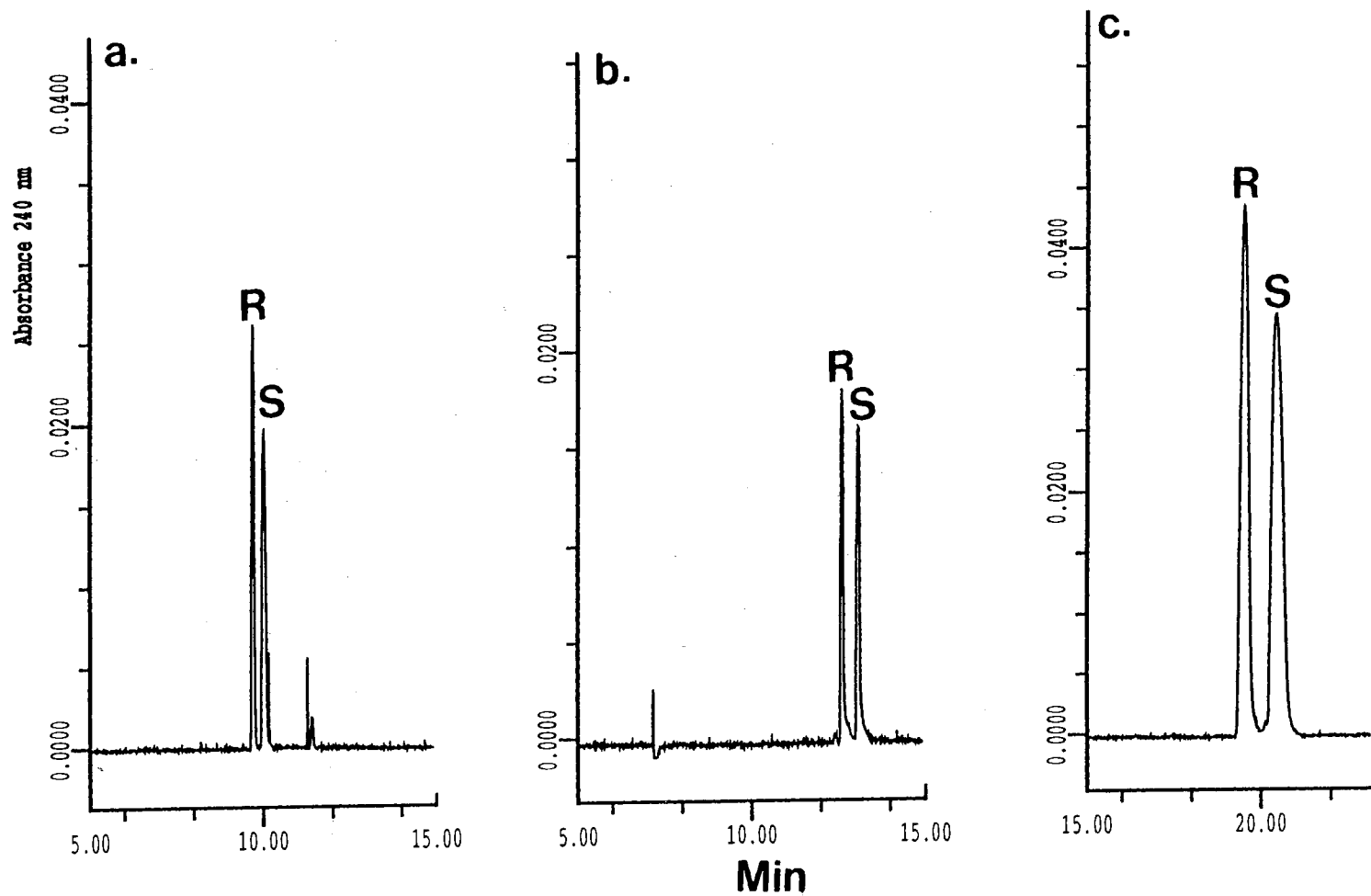


**Figure 9.** Electropherograms of BNPO<sub>4</sub> enantiomers obtained with Deoxy Big CHAP at various concentrations of borate in the running electrolytes: 25 mM (a), 50 mM (b) and 100 mM (c). Conditions as in Fig. 8.

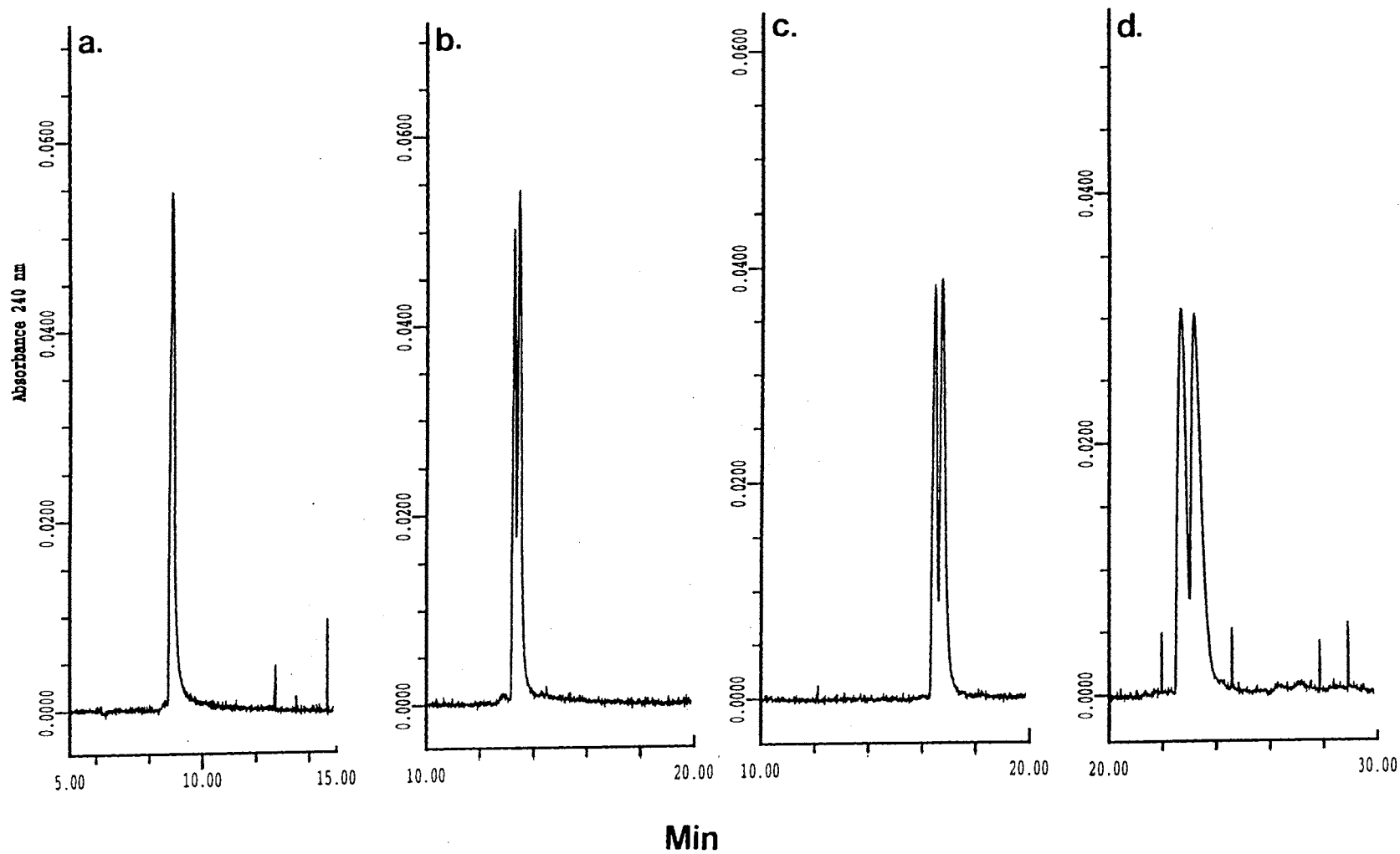


**Figure 10.** Electropherograms of BNOH enantiomers obtained with Big CHAP at various concentrations of borate in the running electrolytes: 25 mM (a), 50 mM (b), 100 mM (c) and 150 mM (d). Conditions as in Fig. 8.

maximum component resolution ( $R_s = 0.60$ ) when the 50 mM borate buffer was used (results not shown). The separation efficiency of this analyte decreased substantially as the concentration of borate increased to 100 mM and above.

Concentration of the Surfactant. Since the surfactant is also the chiral selector responsible for enantiomeric separations, the use of the appropriate concentration of the surfactant is crucial for optimum enantiomeric resolution. In fact, there is an optimum chiral selector concentration to achieve a maximum enantiomeric resolution [38]. Figure 11 illustrates the effect of the surfactant concentration on the enantiomeric resolution of BNOH. Maximum enantiomeric resolution was achieved when the concentration of Deoxy Big CHAP was 10 mM. It increased from an  $R_s = 1.0$  at 5 mM surfactant to an  $R_s = 1.7$  at 10 mM surfactant. Thereafter,  $R_s$  decreased to 1.2 at 15 mM despite the significant gain in separation efficiency at this surfactant concentration, see Fig. 11c. At 20 mM  $R_s$  decreased further to 1.1 and at 25 mM and above no enantiomeric resolution was observed.  $\text{BNPO}_4$  showed a maximum enantiomeric resolution ( $R_s \approx 2.5$ ) when 10 to 15 mM deoxy Big CHAP was used. This is a substantial increase from a value of 1.5 that was observed at 5 mM surfactant. The resolution decreased to 1.8 when going to 20 mM and reached a value of 1.3 at 30 mM surfactant. In terms of separation efficiency, the maximum value was obtained in the range 10 to 20 mM surfactant ( $N_{\text{av}}$  varied between 100,000 and 140,000 plates/m in this range).

Big CHAP also showed maximum enantiomeric resolution at 20 mM surfactant in the running electrolyte, but the chiral selectivity of this surfactant was substantially less than that of the Deoxy Big CHAP (results not shown).

Organic Modifier. Using deoxy Big CHAP as the chiral surfactant, the enantiomeric resolution of BNDA increased substantially with increasing % methanol in the running electrolyte. As can be seen in Fig. 12 very little enantiomeric resolution was achieved at 0% and 5% methanol in the running electrolyte, and an almost baseline



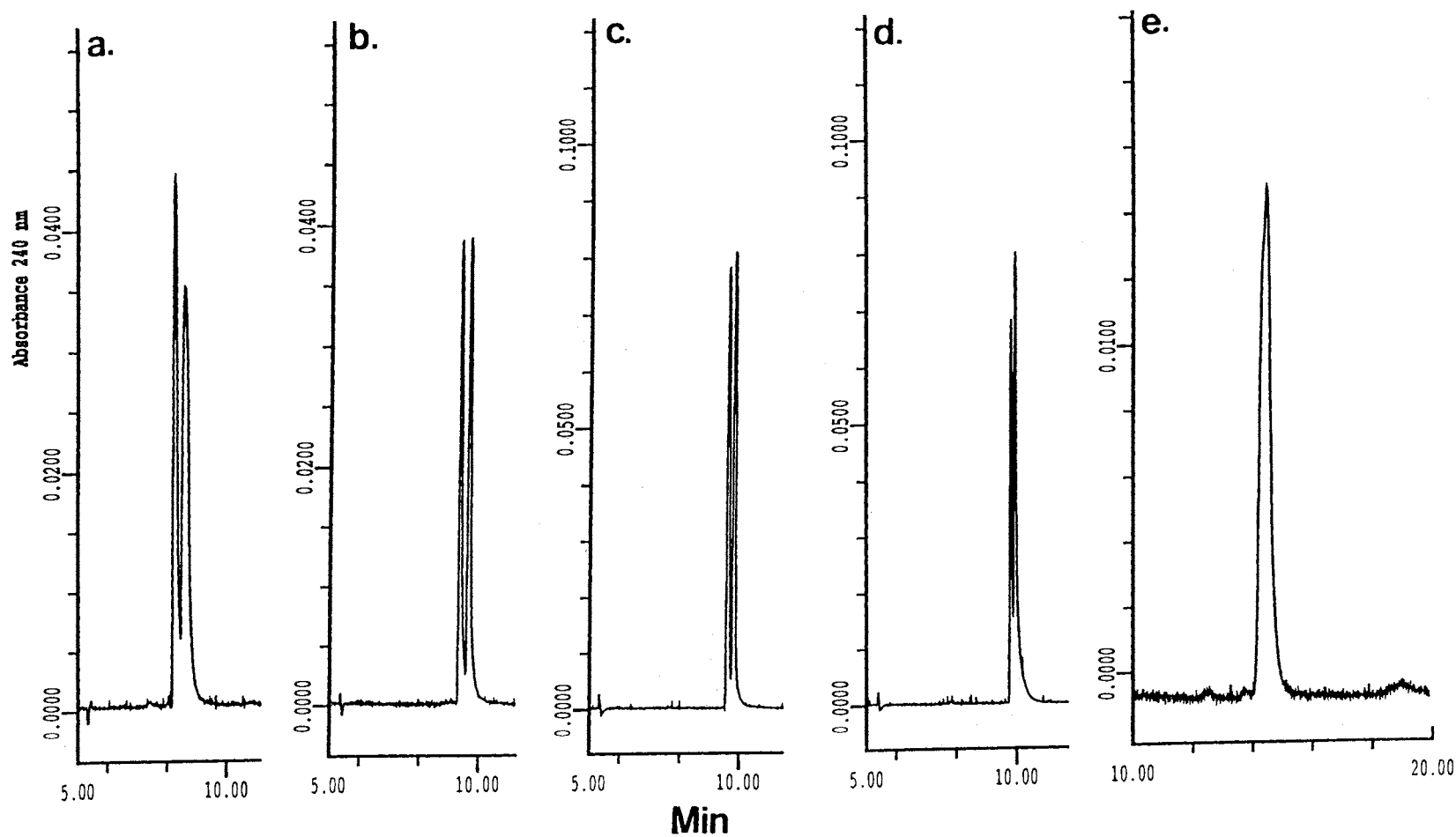


**Figure 11.** Electropherograms of BNOH obtained at various concentrations of Deoxy Big CHAP in the running electrolytes. Capillary, untreated fused-silica, 50/57 cm x 50  $\mu$ m I.D.; running electrolytes, 50 mM sodium borate containing 5 mM (a), 10 mM (b), 15 mM (c), 20 mM (d) or 25 mM (e) Deoxy Big CHAP, pH 10; capillary temperature, 15  $^{\circ}$ C; voltage, 20 kV.

resolution is obtained at 10% ( $R_s = 1.3$ ) and 15% methanol ( $R_s = 1.4$ ). For  $\text{BNPO}_4$  and  $\text{BNOH}$ , which showed relatively high resolution ( $R_s = 2.65$  and  $1.60$ , respectively) in the absence of methanol the addition of  $\text{MeOH}$  for up to 10 % had virtually no effect on resolution (results not shown).

In the case of Big CHAP, the addition of methanol to the running electrolyte increased the resolution of  $\text{BNOH}$  enantiomers but not that of  $\text{BNPO}_4$  enantiomers. As can be seen in Fig. 13 a and b,  $R_s$  between  $\text{BNOH}$  enantiomers has more than doubled from 0.30 to 0.70 when going from 0% to 10% methanol. On the other hand,  $R_s$  between  $\text{BNPO}_4$  enantiomers did not change and stayed equal to 0.6 when going from 0% to 10% methanol, see Fig. 13c and d. The addition of methanol adjusts the analyte-micelle interaction to give favorable enantiomeric separation conditions.

Capillary Temperature. The two glycoside-steroidal surfactants seem to exhibit greater enantioselectivity towards flat and rigid molecules such as the binaphthyls. This observation corroborates earlier findings with chiral bile salt surfactants [14], which have structure features similar to Big CHAP and Deoxy Big CHAP through the steroidal part of the surfactant molecule. Thus, temperature should play a major role in the enantiomeric resolution since temperature affects solute rigidity. As shown in Fig. 14, resolution between  $\text{BNDA}$  enantiomers decreased from 1.67 to 0.89 when going from 15°C to 35°C passing through  $R_s = 1.2$  at 25 °C. On the other hand, the enantiomeric resolution ( $R_s \approx 2.0$ ) of  $\text{BNOH}$  was almost unaffected by the temperature (results not shown).

As stated above and under all circumstances, Big CHAP exhibited less enantiomeric resolution than deoxy Big CHAP for the same analytes. In fact, the enantiomeric separation of  $\text{BNDA}$  was not achieved. In addition, the temperature effect was more pronounced and, as can be seen in Fig. 15, resolution of  $\text{BNOH}$  was almost completely lost as the temperature increased from 15 ° to 35 °C. Also,  $\text{BNPO}_4$  showed a substantial decrease in enantiomeric resolution from  $R_s = 0.57$  at 15 °C to  $R_s = 0.34$  at 35°C (results not shown). This decrease in resolution might be due to the loss of the structural rigidity of

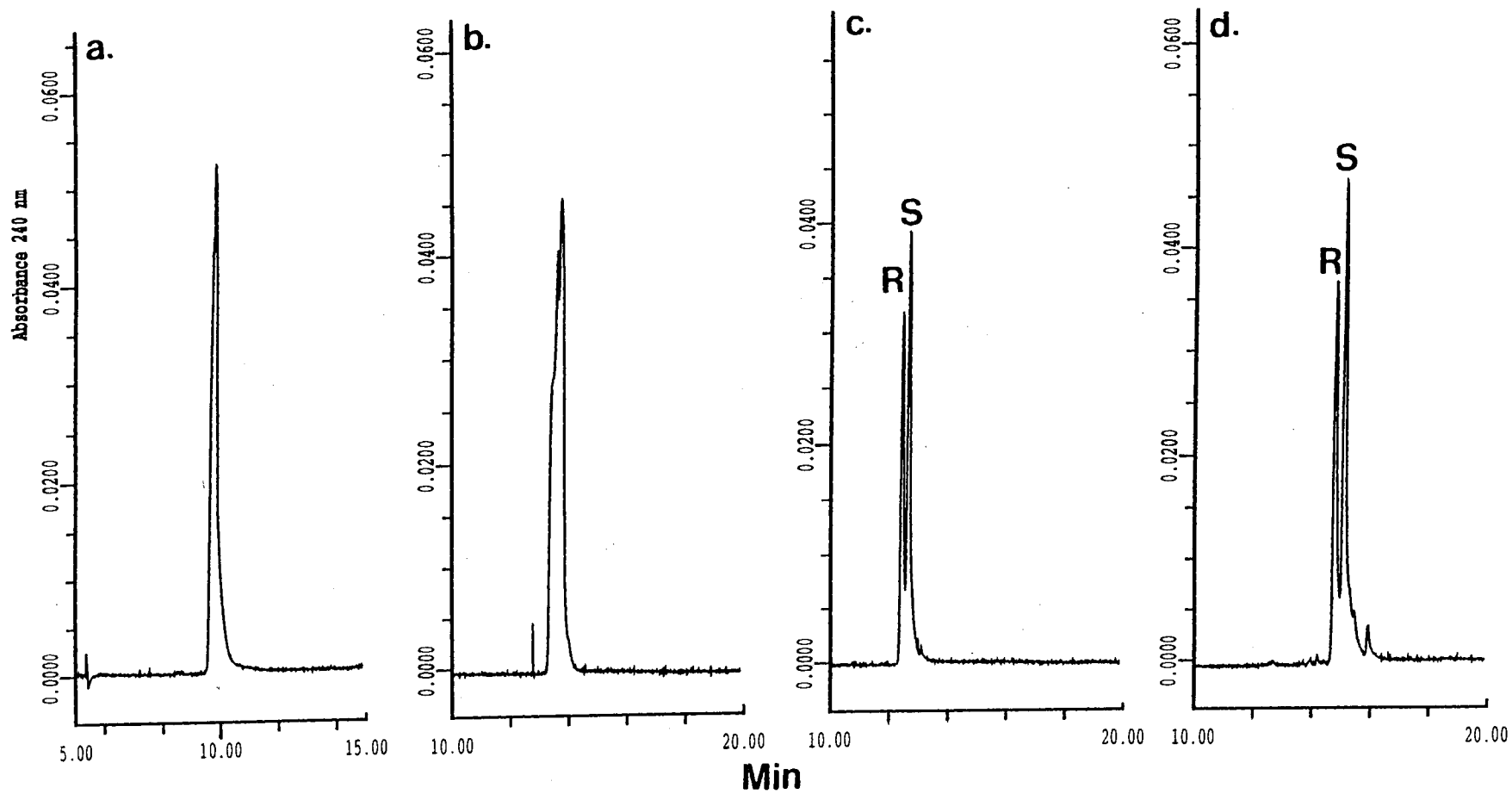


**Figure 12.** Electropherograms of BNDA enantiomers obtained with deoxy Big CHAP at various percentage of methanol in the running electrolytes. Capillary, untreated fused-silica, 50/57 cm x 50  $\mu$ m I.D.; running electrolyte, 50 mM borate containing 15 mM Deoxy Big CHAP (pH 10) and 0 % (a), 5 % (b), 10 % (c) or 15 % (d) methanol; voltage, 20 kV.

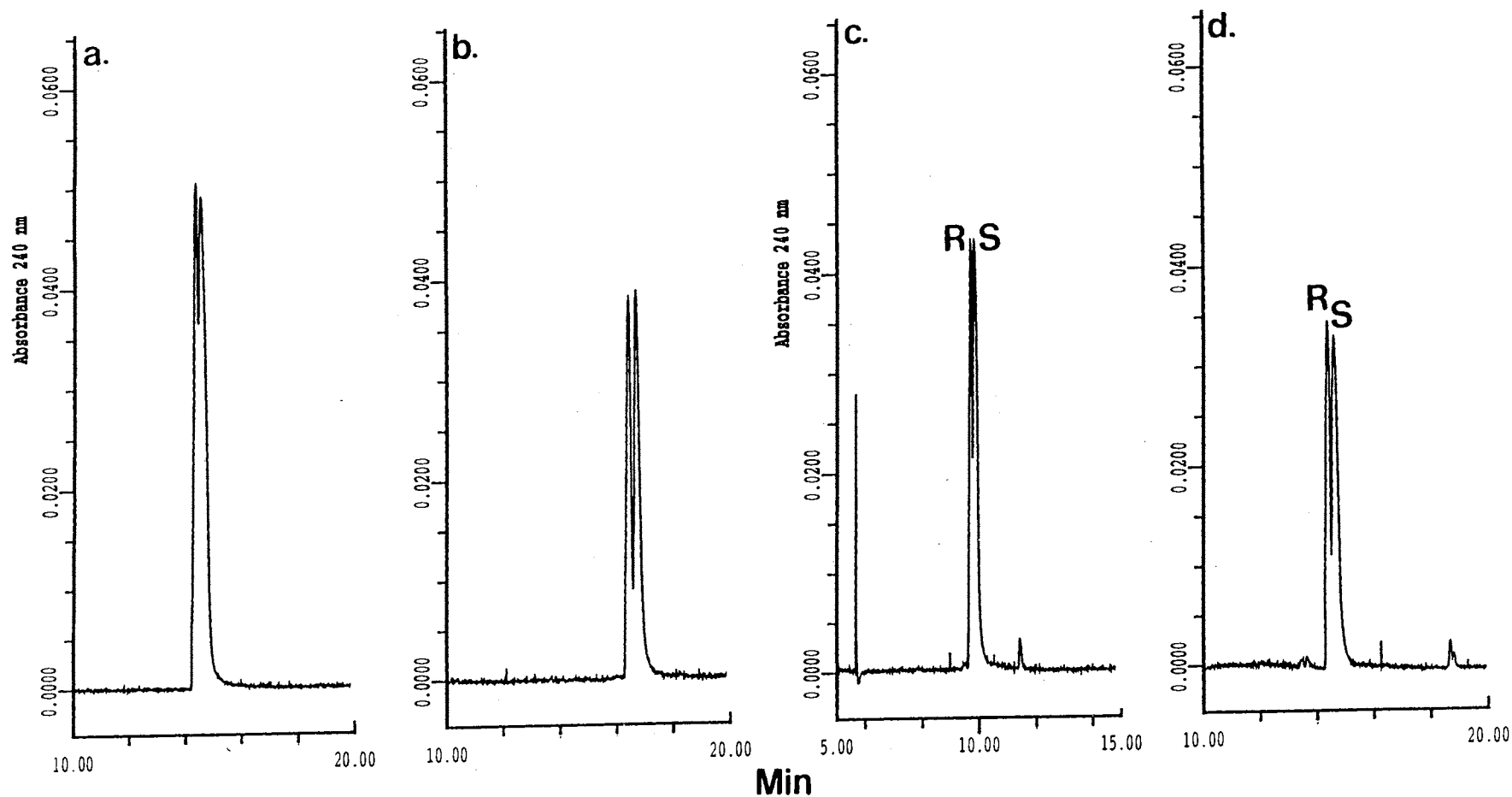


**Figure 13.** Electropherograms of (a and b) BNOH and (c and d) BNPO<sub>4</sub> enantiomers obtained with Big CHAP at various percentage of methanol in the running electrolytes. Capillary, untreated fused-silica, 50/57 cm x 50 μm I.D.; running electrolytes, 50 mM sodium borate containing 20 mM Big CHAP (pH 10.0) and 0% (a and c) or 10 % (b and d) methanol; capillary temperature, 15 °C; voltage, 20 kV.

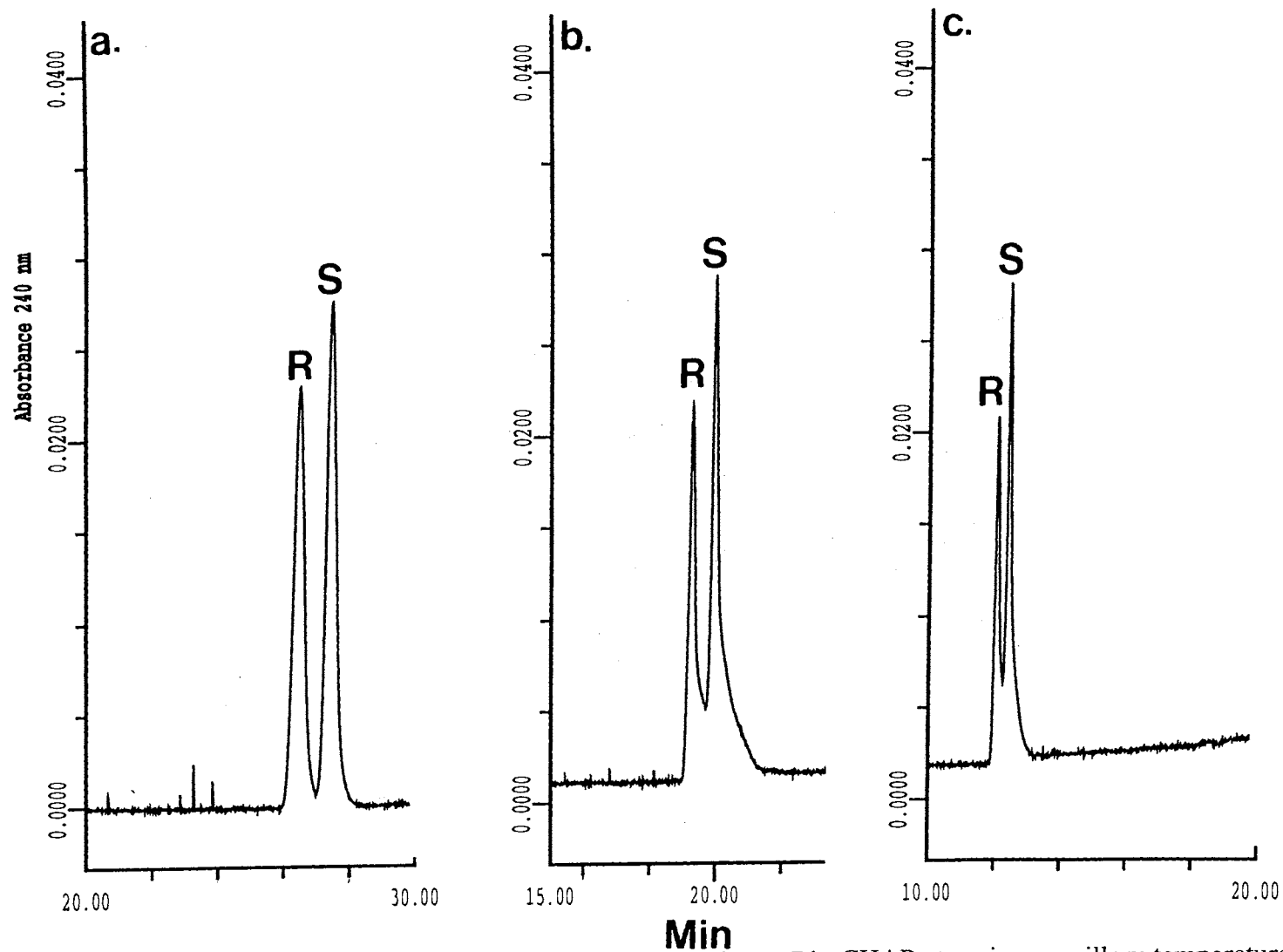


**Figure 14.** Electropherograms of BNDA enantiomers obtained with deoxy Big CHAP at various capillary temperatures. Capillary, untreated fused-silica, 50/57 cm x 50  $\mu$ m I.D.; running electrolytes, 150 mM sodium borate containing 15 mM deoxy Big CHAP, pH 10.0; capillary temperature, 15 (a), 25 (b) and 35  $^{\circ}$ C (c); voltage 20 kV.

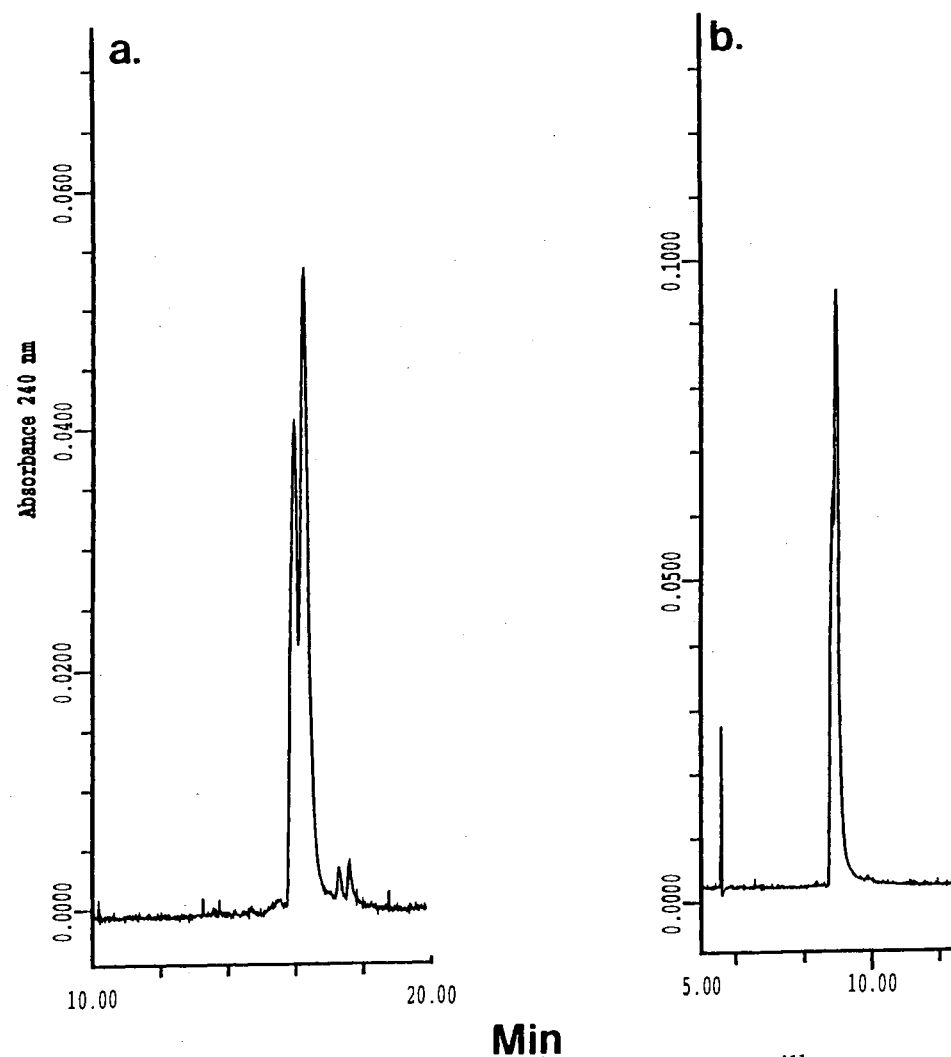


**Figure 15.** Electropherograms of BNOH enantiomers obtained with Big CHAP at capillary temperature of 15 °C (a) and 35 °C (b). Capillary, untreated fused-silica, 50/57 cm x 50  $\mu$ m I.D.; running electrolytes, 75 mM sodium borate containing 20 mM Big CHAP (pH 10.0) and 10% (v/v) methanol; voltage, 20 kV.

the solutes as expected with temperature increase.

### Illustrative Enantiomeric Separations

Troger's Base. The enantiomeric resolution of troger's base required different conditions than those optimal for the separations of the enantiomers of the binaphthyl derivatives. Higher surfactant and borate concentrations as well as organic solvents were needed to induce different enantiomeric association with the chiral micelle and in turn different enantiomeric mobilities. In addition, troger's base enantiomers were better resolved when acetonitrile was used as the organic modifier as compared to methanol (compare Fig. 16b and c).

Dansyl Amino Acids. Four pairs of DL-dansyl amino acids, namely leucine, methionine, phenylalanine and tryptophan, were electrochromatographed with the chiral micelles under investigation. As shown in Fig. 17, Deoxy Big CHAP showed better chiral selectivity than Big CHAP (compare Fig. 17b and c) for all the four dansyl amino acid enantiomers. Again, and because of the weaker chiral recognition of the surfactant toward dansyl amino acids, the surfactant concentration needed to achieve the chiral separation was higher than that required for binaphthyl derivatives. As can be seen in Fig 17, the separation of dansyl amino acid enantiomers could be achieved at pH 10.0. This chiral selectivity is significantly different than that encountered with bile salts, e.g., taurodeoxycholate, which were shown to exhibit chiral recognition toward amino acids at very acidic pH only [3].

As in the case of binaphthyls, here also the concentration of borate was found to be very crucial for the enantiomeric separations of dansyl amino acids. Figure 17 a and b shows the effect of borate concentration in the running electrolyte on the enantiomeric separation of dansyl amino acids. The enantiomeric separation increased significantly as the borate concentration was increased from 150 mM to 300 mM (compare Fig. 17a and b). Increasing the borate concentration above 300 mM did not improve the enantiomeric

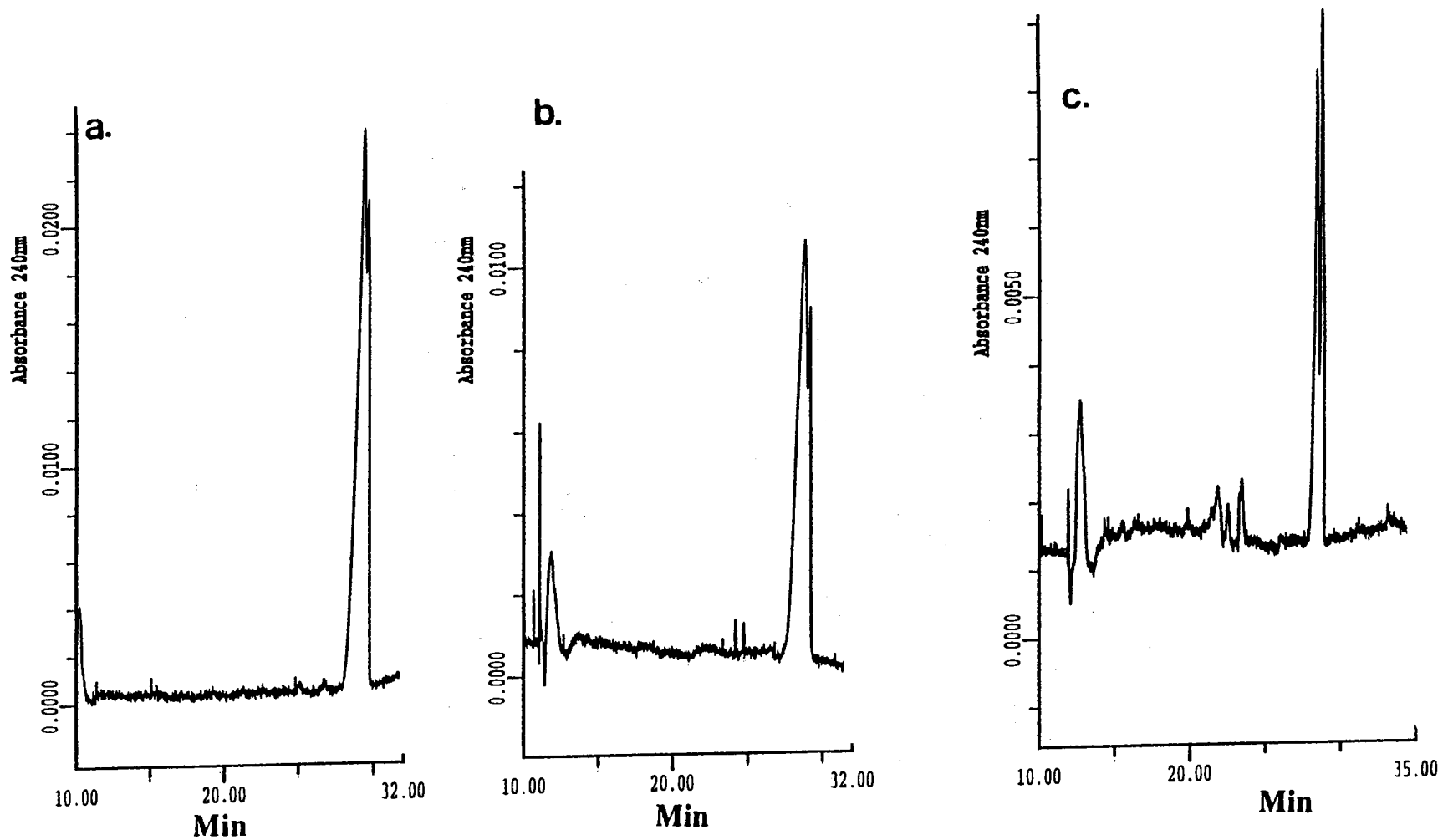


**Figure 16.** Electropherograms of troger's base obtained with Deoxy Big CHAP. Capillary, untreated fused-silica, 50/57 cm x 50  $\mu$ m I.D.; running electrolytes, 250 mM sodium borate containing 30 mM Deoxy Big CHAP (pH 10.0) and 0% organic solvent (a), 10% v/v methanol (b) or 10% v/v acetonitrile (c); voltage, 20 kV.



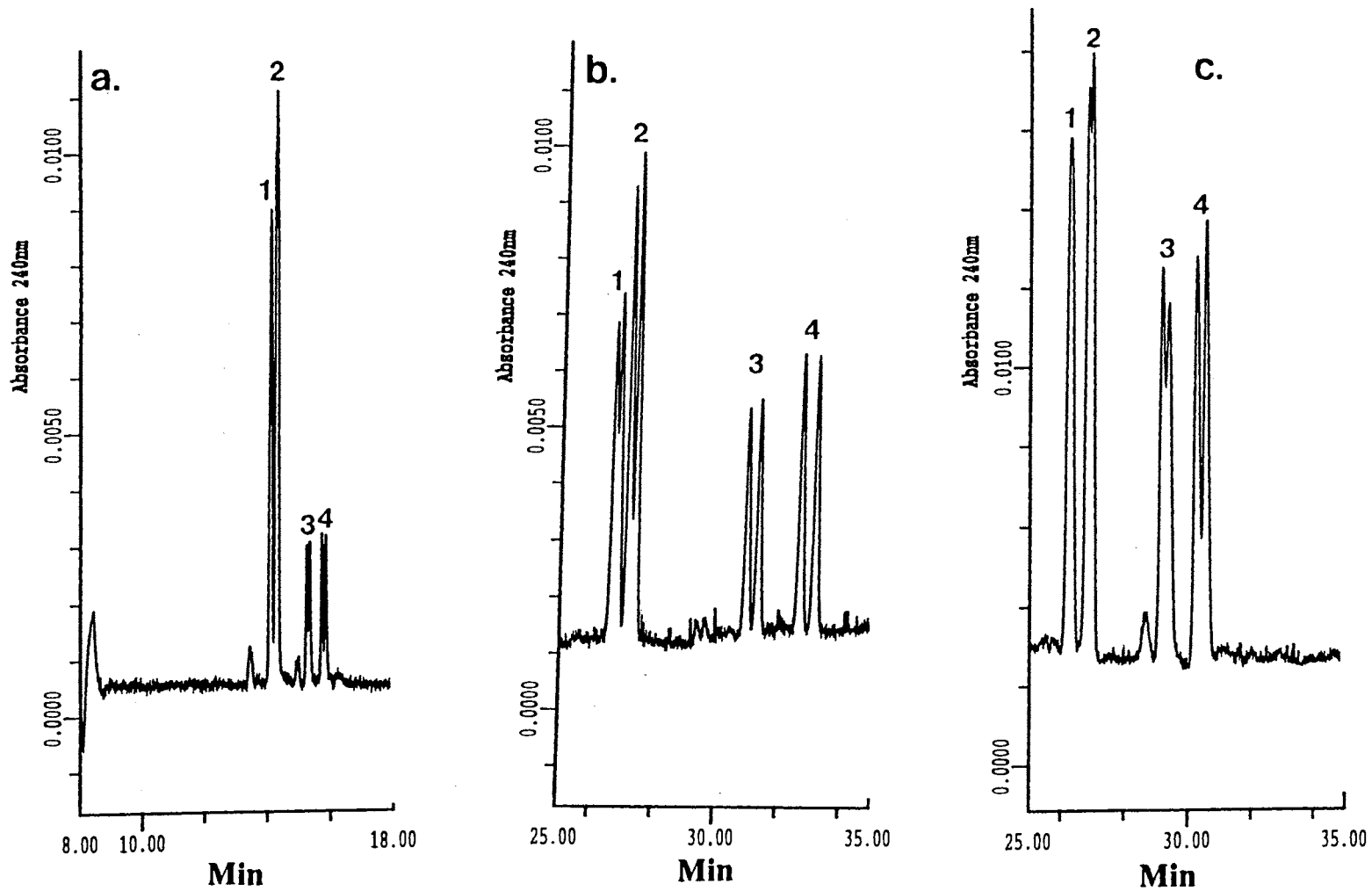


**Figure 17.** Electropherograms of dansyl amino acids obtained with deoxy Big CHAP in (a) and (b) and Big CHAP (c). Capillary, untreated fused-silica, 50/57 cm x 50  $\mu$ m I.D.; running electrolytes, 50 mM surfactant in 150 mM sodium borate (a) or in 300 mM sodium borate (b) and (c), pH 10; capillary temperature, 15  $^{\circ}$ C; voltage, 20 kV. Solutes: 1, D and L Dns-leucine; 2, D and L Dns-methionine; 3, D and L Dns-phenylalanine; 4, D and L tryptophan.

resolution, while the analysis time increased due to the decrease in the EOF and increase in  $t_{mc}$ .

Silvex Herbicide. Silvex is a phenoxy acid herbicide with a chiral center. Enantiomeric separation of this analyte was achieved using high borate concentration in the running electrolyte and relatively high surfactant concentration. Such chiral separation is illustrated in Fig. 18. Note that the addition of organic modifiers in the case of silvex did not improve the chiral separation, but rather decreased it. This behavior resembles that observed with the dansyl amino acids.

### Conclusions

Novel in situ charged micelles having chiral selectivity, namely *N,N*-bis (3-D-gluconamidopropyl)-cholamide and -deoxycholamide (denoted by Big CHAP and Deoxy Big CHAP, respectively), were evaluated in micellar electrokinetic capillary chromatography of enantiomers. The two neutral steroidal-glycoside surfactants (i.e., Big CHAP and Deoxy Big CHAP) could be charged readily via borate complexation, and consequently the surface charge density of their corresponding micelles could be conveniently adjusted through varying borate concentration and pH of the running electrolyte. This allowed the manipulation of the migration time window of the Big CHAP- and Deoxy Big CHAP-borate micellar systems over a certain range. As a result the enantiomeric resolution of a given racemic mixture could be optimized by varying the pH and borate concentration of the running electrolyte. In addition, the stereoselectivity of the chiral steroidal micelles could be further tuned by changing the concentration and nature of the organic modifier and surfactant as well as by adjusting the temperature of the capillary column. In general, resolution increased with (i) increasing pH and borate concentration of the running electrolyte and (ii) decreasing capillary temperature. On the other hand, there was an optimum organic modifier and surfactant concentration for which maximum resolution was obtained. Big CHAP-borate micelles were less stereoselective than Deoxy

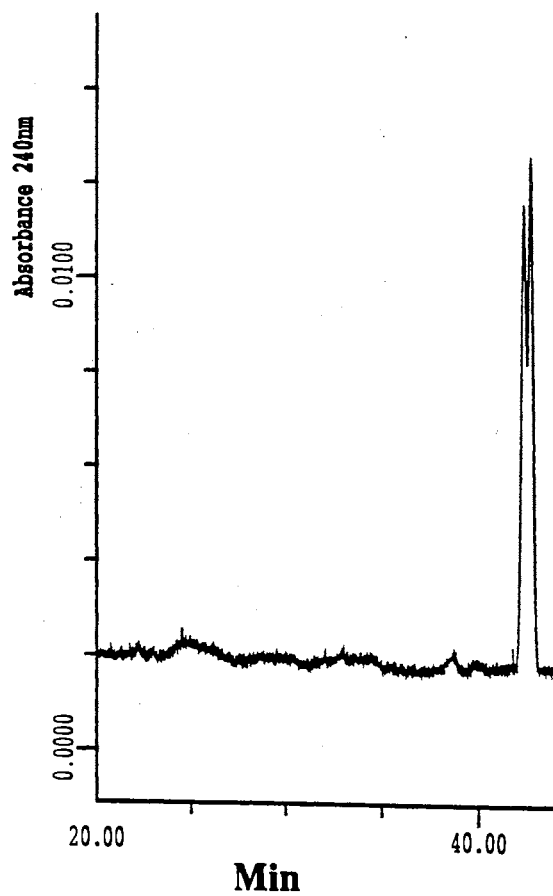


**Figure 18.** Electropherogram of silvex a phenoxy acid herbicide. Running electrolyte, 50 mM Deoxy Big CHAP, 400 mM borate, pH 10.0. Other conditions as in Fig. 17.

Big CHAP-borate micellar systems under otherwise identical conditions. The novel micellar phases were useful for the separation of binaphthyl enantiomers, troger's base, dansyl amino acid enantiomers and silvex herbicide optical isomers.

## References

1. Lindner, W. (Guest Editor), *Chiral Separations. Fundamental Aspects and Applications*, *J. Chromatogr. A*, 666 (1994).
2. Gassmann, E., Kuo, J. E. and Zare, R.N., *Science*, 230 (1985) 813.
3. Terabe, S., Shibata, M., and Miyashita, Y., *J. Chromatogr.*, 480 (1989) 403.
4. Dobashi, A., Ono, T., Hara, S. and Yamaguchi, J., *J. Chromatogr.*, 480 (1989) 413.
5. Terabe, S., Miyashita, Y., Ishihama, Y. and Shibata, O., *J Chromatogr.*, 636 (1993) 47.
6. Otsuka, K. and Terabe, S., *J. Chromatogr.*, 515 (1990) 221.
7. Khun, R., Erni, F., Bereuter, T. and Hausler, J., *Anal. Chem.*, 64 (1992) 2815.
8. Snopek, J., Jelinek, I. and Smolkova-Keulemansova, E., *J. Chromatogr.*, 438 (1988) 211.
9. Guttman, A., Paulus, A., Cohen, A.S., Grinberg, N. and Karger, B.L., *J. Chromatogr.*, 448 (1988) 41.
10. D'Hulst, A. and Verbeke, N., *J. Chromatogr.*, 608 (1992) 275.
11. Busch, S., Kraak, J. and Poppe, H., *J. Chromatogr.*, 635 (1993) 119.
12. Barker, G.E., Russo, P. and Hartwick, A., *Anal. Chem.*, 64 (1992) 3023.
13. Novotny, M., Soini, H. and Stefansson, M., *Anal. Chem.*, 66 (1994) 646.
14. Terabe, S., Otsuka, K. and Nishi, H., *J. Chromatogr. A*, 666 (1994) 295.
15. Terabe, S., Chen, N. and Otsuka, K., *Adv. Electrophoresis*, 7 (1994) 87.
16. Ward, J.W., *Anal. Chem.*, 66 (1994) 633.
17. Fanali, S., Cristalli, M., Vespalec, R. and Bocek, P., *Adv. Electrophoresis*, 7 (1994) 1.
18. Stalcup, A.M. and Agyel, N.M., *Anal. Chem.*, 66 (1994) 3054.
19. Soini, H., Stefansson, M., Riekkola, M.-L. and Novotny, M.V., *Anal. Chem.*, 66 (1994) 3477.

20. Wang, J. and Warner, I.M., *Anal. Chem.*, 66 (1994) 3773.
21. Talt, R.J., Thompson, D.O., Stella, V.J. and Stobaugh, J.F., *Anal. Chem.*, 66 (1994) 4013.
22. Otsuka, K., Karuhaka, K., Higashimori, M. and Terabe, S., *J. Chromatogr. A*, 680 (1994) 317.
23. Penn, S.G., Bergström, E.T., Goodall, D.M. and Loran, J.S., *Anal. Chem.*, 66 (1994) 2866.
24. Rawjee, Y.Y., Williams, R.L. and Vigh, G., *Anal. Chem.*, 66 (1994) 3777.
25. Smith, J.T. and El Rassi, Z., *J. Cap. Elec.*, 1 (1994) 136.
26. Smith, J.T. and El Rassi, Z., *J. Chromatogr. A*, 685 (1994) 131.
27. Smith, J.T. and El Rassi, Z., *Electrophoresis*, 15 (1994) 1248.
28. Smith, J.T., Nashabeh, W. and El Rassi, Z., *Anal. Chem.*, 66 (1994) 1119.
29. Smith, J.T. and El Rassi, Z., *J. Microcol. Sep.*, 6 (1994) 127.
30. Cai, J. and El Rassi, Z., *J. Chromatogr.*, 608 (1992) 31.
31. Mechref, Y. and El Rassi, Z., *J. Chromatogr. A*, submitted
32. Fisher, L. and Oakenfall, D., *Aust. J. Chem.*, 32 (1979) 31.
33. Attwood, D. and Florence, A. T., *Surfactant Systems, Their Chemistry Pharmacy and Biology*, Chapman and hall, London, 1983.
34. Hjelmeland, L.M., Klee, W.A. and Osborne, J., *Anal. Biochem.*, 130 (1983) 485.
35. Terabe, S., Otsuka, K. and Ando, T., *Anal. Chem.*, 57 (1985) 834.
36. Mazzeo, J.R., Grover, E.R., Swartz, M.E. and Peterson, J.S., *J. Chromatogr. A*, 680 (1994) 125.
37. Otsuka, K., Kawahara, J., Tatekawa, K. and Terabe, S., *J. Chromatogr.*, 559 (1991) 209.
38. Wren, S.A.C. and Rowe, R.C., *J. Chromatogr.*, 603 (1992) 235.

## CHAPTER XI

### PRECOLUMN DERIVATIZATION OF CHIRAL AND ACHIRAL PHENOXY ACID HERBICIDES WITH A FLUORESCENT TAG FOR ELECTROPHORETIC SEPARATION IN THE PRESENCE OF CYCLODEXTRINS AND MICELLAR PHASES

#### Introduction

Phenoxy acid herbicides are important agrochemicals, especially in the control of weeds in cereal crops [1]. Due to their relatively polar nature, ionic character and low volatility, phenoxy acid herbicides are perfectly suitable for determination by capillary electrophoresis. Thus far, only a few reports have appeared on CE of phenoxy acid herbicides as well as other herbicides [2-12]. Most of these recent contributions from our laboratory [2-5,12] and others [6,8,10,11] have focused on (i) understanding the electrophoretic behavior and (ii) developing electrolyte systems for the separation of phenoxy acid herbicides. Only two research papers have shown the determination of these pollutants at the low ppb levels [7,9]. One of these two reports [7], demonstrated that by combining a solid phase extraction step and a field amplified injection, the detection of phenoxy acid herbicides from dilute water samples can become feasible, while the second paper [9] showed that by derivatizing phenoxy acid herbicides with 5-(aminoacetamido)fluorescein, the determination of the herbicides at low levels by CE laser-induced fluorescence is then possible. Although 5-(aminoacetamido)fluorescein fluoresces intensely, the derivatization of phenoxy acid herbicides with this tagging agent yielded many side products [9]. In addition, the fluorescein derivatives were reported to deteriorate rather rapidly within 12 hr [9].

Besides the need for highly sensitive separation methods for the determination of herbicides in environmental samples, there is also a need for determining the enantiomeric components of phenoxy acid herbicides. Generally, herbicides are produced as racemic mixtures despite the fact that most often only one enantiomer is biologically active while the other can be viewed as an impurity [13]. As the individual isomers of chiral phenoxy acid herbicides have widely differing biological activities, it is important to be able to determine the amount of each enantiomers. Thus far, only two reports [6,10] have attempted the chiral separation of some phenoxy acid enantiomers.

Due to the possibilities of different separation principles in CE, e.g., ligand exchange, micellar electrokinetic capillary chromatography (MECC), inclusion complexation, affinity interactions, etc., chiral separations by CE have witnessed a steady growth, which has been outlined by several recent review articles [14-18]. Despite the major progress in chiral CE, there is still room for improvements as far as the optimization of enantiomeric separations is concerned so that the resolution of a wider range of racemates could be achieved.

The present chapter describes electrophoretic systems for the chiral and achiral high resolution separation of fluorescently labeled phenoxy acid herbicides, and their detection at low ppb levels by laser induced fluorescence detection. In this regard, a new precolumn derivatization scheme which is selective, free of side products and quantitative for the fluorescent tagging of phenoxy acid herbicides is demonstrated. The present research is a continuation to our previous contributions to the area of CE of herbicides [2-5,12,19-23], and also to enlarging the scope of applications of the selective precolumn derivatization of carboxylated species which we have introduced recently and demonstrated its utility in the CE of carboxylated monosaccharides [24], sialooligosaccharides [25] and sialogangliosides [26], see Chapters.III-V



## Materials and Methods

### Capillary Electrophoresis Instrument for Fluorescence Detection

The instrument for capillary electrophoresis/fluorescence detection was assembled in-house from commercially available components [24,25] and is described in Chapter III. Fused-silica capillary columns of 50  $\mu\text{m}$  I.D. and 365  $\mu\text{m}$  O.D. were obtained from Polymicro Technology (Phoenix, AZ, U.S.A.). All capillaries used in this study were uncoated since the analytes are negatively charged and would repulse from the like-charged capillary surface. The lengths of the capillaries used for the fluorescence study were 50 cm (to detector) / 80 cm (total length).

The derivatized herbicides were introduced into the capillary as thin plugs by means of hydrodynamic injection for approximately 5 s at 15 cm differential height between inlet and outlet ends of the capillary. Between runs, the capillary was flushed successively with 0.1M NaOH, distilled water and running electrolyte for 1 min each. Using this conditioning procedure, the migration time reproducibility in %RSD ( $n = 5$ ) was in the range 2.1–3.9.

### Capillary Electrophoresis Instruments for UV and Laser-Induced Fluorescence Detection

A Beckman P/ACE instrument (Fullerton, CA, U.S.A.), Model 5510 equipped with a diode array detector was used for the electrophoresis of underivatized phenoxy acid herbicides and the assessment of the extent of their derivatization and this instrument is described in Chapter VI. Detection was performed at 230 nm. For laser-induced fluorescence (LIF) detection, a P/ACE Model 5010 equipped with an Ominichrome (Chino, CA, U.S.A.) Model 3056-8M He-Cd laser multimode, 8 mW at 325 nm and a laser headcoupler to a standard SMA-906 fiber connector was used. The fluorescence emission band-pass filter of  $420 \pm 2$  nm was purchased from Corion (Holliston, MA, U.S.A.). The laser beam was rejected with a cut-on filter at 400 nm from Corion. Both instruments were equipped with a data handling system comprising an IBM personal computer and a System

Gold software. The resulting signal was fed to the computer for storage and real time display of the electropherograms. The fused-silica capillaries had the dimensions of 50 cm (to detector)/ 57 cm (total length) with an I.D. of 50  $\mu\text{m}$  and an O.D. of 365  $\mu\text{m}$ . The temperature of the capillary was maintained at 30°C by the instrument thermostating system. Samples were pressure injected at 0.034 bar (i.e., 3.5 kPa).

### Reagents and Materials

Phenoxy acid herbicides including (2,4-dichlorophenoxy)acetic acid (2,4-D), (2,4,5-trichlorophenoxy)acetic acid (2,4,5-T), 2-phenoxypropionic acid (2-PPA), 2-(4-chloro-2-methylphenoxy)propionic acid (mecoprop), 2-(2-chlorophenoxy)propionic acid (2,2-CPPA), 2-(3-chlorophenoxy)propionic acid (2,3-CPPA), 2-(4-chlorophenoxy)propionic acid (2,4-CPPA), 2-(2,4-dichlorophenoxy)propionic acid (dichlorprop) and silvex were purchased from Aldrich (Milwaukee, WI, U.S.A.) and from Chem Service (West Chester, PA, U.S.A.). The structures of the model solutes used in this study are given in Fig. 1. Two of the solutes are achiral, namely 2,4-D and 2,4,5-T while the remaining seven herbicides are chiral. Decanoyl-*N*-methylglucamide (MEGA 10) was purchased from Calbiochem Corp. (La Jolla, CA, U.S.A.). 1-Ethyl-3-(3-dimethylaminopropyl) carbodiimide hydrochloride (EDAC), and 2,6-di-O-methyl- $\beta$ -CD (DM- $\beta$ -CD) and 2,3,6-tri-O-methyl- $\beta$ -CD (TM- $\beta$ -CD) were purchased from Sigma Chemical Co. (St. Louis, MO, U.S.A.). The derivatizing agent 7-aminonaphthalene-1,3-disulfonic acid (ANDSA) and  $\alpha$ -cyclodextrin ( $\alpha$ -CD) and  $\gamma$ -cyclodextrins ( $\gamma$ -CD) were purchased from TCI America, Inc. (Portland, OR, U.S.A.).  $\beta$ -Cyclodextrin ( $\beta$ -CD) and hydroxylpropyl- $\beta$ -CD (HP- $\beta$ -CD) were donated by the American Maize-Products Co. (Hammond, IN, USA). The chemicals used in the preparation of electrolytes as well as the 0.2  $\mu\text{m}$  Uniprep Syringeless filters used in the filtration of the electrolyte were purchased

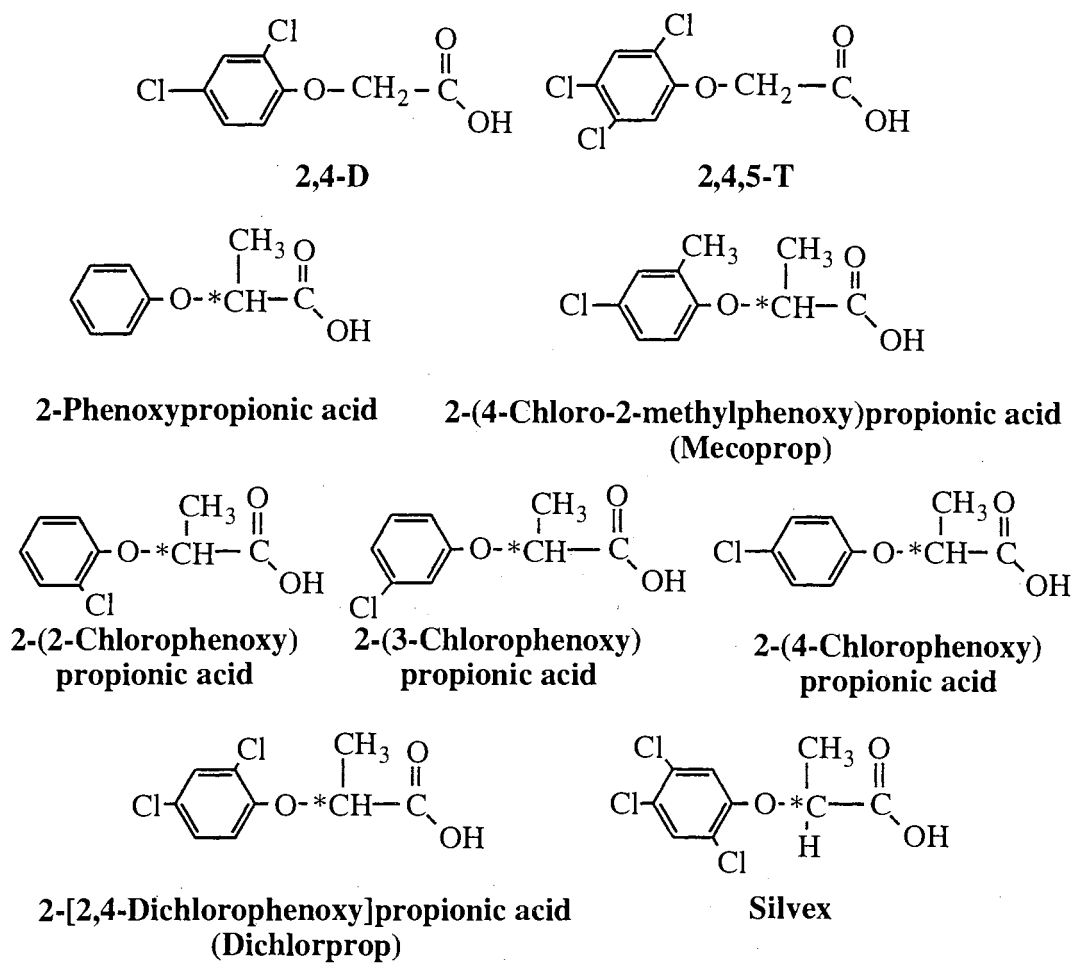
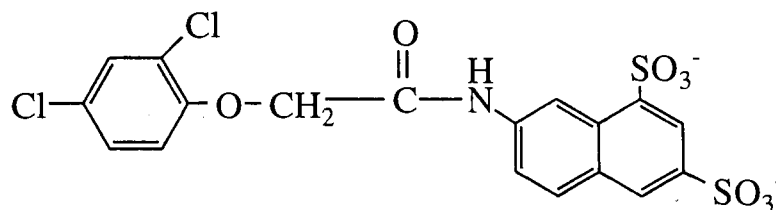


**Figure 1.** Structures of phenoxy acid herbicides studied.

from Fisher Scientific (Pittsburgh, PA, U.S.A.). All solutions were prepared with deionized water.

### Precolumn Derivatization

Nine different phenoxy acid herbicides (see above) were tagged with ANDSA according to the procedure we previously described for acidic carbohydrates [24-26] (Chapters III-V) with slight modification. Briefly, an aliquot of 5  $\mu\text{L}$  of  $5.0 \times 10^{-5}$  M acetonitrile solution of the analyte was initially mixed with 10  $\mu\text{L}$  of  $5.0 \times 10^{-5}$  M ANDSA dissolved in 50 mM phosphate buffer, pH 3.0. Next, an aliquot of 5  $\mu\text{L}$  of  $5.0 \times 10^{-5}$  M aqueous solution of EDAC, pH 5.0, was added, and the mixture was stirred for 2.0 hrs at room temperature. The  $5.0 \times 10^{-5}$  M concentration level was used to generate derivatized sample solutions for all the systematic studies that were carried out using the lamp operated fluorescence detector. For LIF studies, the concentrations of the stock solutions of the analytes as well as of the ANDSA and EDAC were in  $10^{-7}$  M range. This concentration range was used for the systematic studies with CE-LIF that involved the separation of the 9 derivatized phenoxy acid herbicides, see Fig. 3. In all cases, the entire reaction mixture containing the derivatized phenoxy acid herbicides, excess derivatizing agent, and other components of the reaction mixture was analyzed by CE. A typical example of ANDSA-phenoxo acid herbicides is shown herein



**ANDSA derivative of 2,4-D**

## Results and Discussion

### Extent of derivatization and limit of detection

The extent of ANDSA precolumn derivatization of the nine phenoxy acid herbicides under investigation was assessed by CE using UV detection at 230 nm. This wavelength corresponds to the maximum of the characteristic absorption band of the underivatized herbicides as determined from the spectral scans obtained with the diode array detector of the P/ACE instrument. The ANDSA-phenoxy acid herbicides showed an intense absorption band at 250 nm, and two other less intense absorption bands at 230 and 300 nm. The overlaid electropherograms of five of the phenoxy acid herbicides derivatized with ANDSA shown in Fig. 2a, clearly illustrate that the derivatization is free of side products and very quantitative, and in most cases the peak corresponding to the underivatized solute (marked with an asterisk) is hardly visible. In fact, the % yield of derivatization (see Table I) was 88% or greater for all analytes and as high as 99.7% for 2,2-CPPA. The percentage yield of the derivatization procedure was estimated by integrating the peak areas of the underivatized phenoxy acid herbicides resulting from the CE analysis of stock solutions of the underivatized analytes and their corresponding derivatized mixtures. In all cases, the concentrations of the stock solutions were high enough to stay in the range of the limits of detection of underivatized herbicides in the UV at 230 nm. As typical examples, in the derivatization of mecoprop and 2,4,5-T which showed 88% yield, the stock solutions of both analytes were at  $1.4 \times 10^{-3}$  M so that the % yield could be assessed with certainty.

Another important feature of the precolumn derivatization described here is the replacement of the weak carboxylic acid group of each phenoxy acid herbicide by two strong sulfonic acid groups in the ANDSA tag. This renders the analytes amenable to CE analysis over a wide range of pH due to the complete ionization of the sulfonic acid groups. In addition, the derivatives are very stable for a long period of time as manifested by the

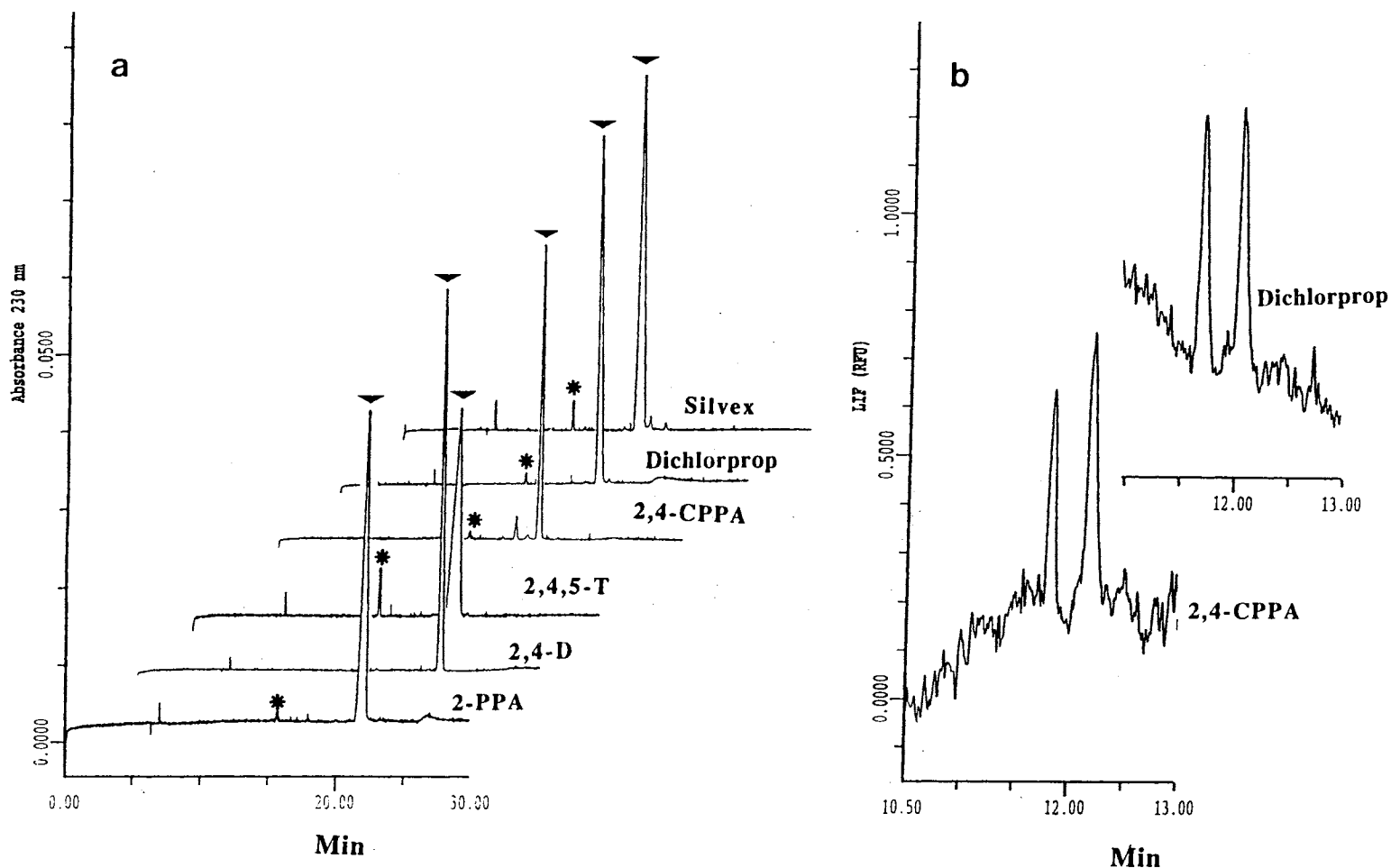


**Figure 2.** (a) Electropherograms of six ANDSA-phenoxy acid herbicides obtained by CE-UV. Running electrolytes, 100 mM phosphate, pH 6.5; capillary, 57 cm (50 cm to detection) x 50  $\mu$ m I.D.; voltage, 18 kV; current, 55  $\mu$ A; column temperature, 30°C; UV detection at 230 nm. ▶ ANDSA-derivatives; \* underivatized. (b) Electropherograms of 2 phenoxy acid herbicides obtained by CE-LIF. Running electrolyte: 25 mM phosphate, 600 mM borate, pH 5.0, containing 10 mM TM- $\beta$ -CD; voltage, 20 kV; current, 36  $\mu$ A; other conditions as in (a).

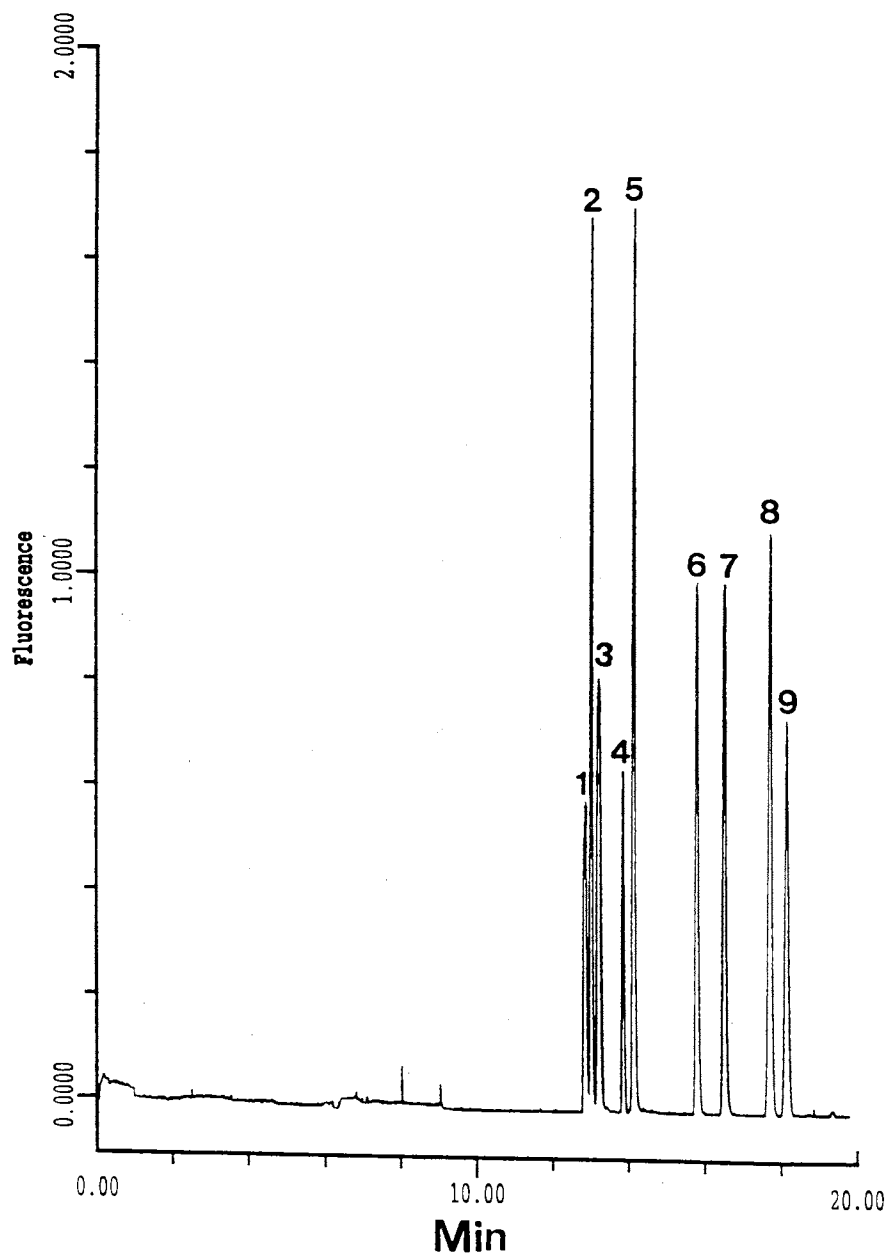
constancy of the fluorescence signal obtained from their aqueous solutions.

TABLE I. Percent Yield of the Precolumn Derivatization of Phenoxy Acid Herbicides with ANDSA.

Phenoxy acid herbicide	Peak areas (arbitrary unit)		% Derivatized
	Before derivatization	After derivatization	
Silvex	3.08	0.31	90.0
Mecoprop	3.47	0.43	88.0
Dichlorprop	3.50	0.22	94.0
2,2-CPPA	3.27	0.01	99.7
2,3-CPPA	3.45	0.01	99.6
2,4-CPPA	5.73	0.20	96.0
2-PPA	3.20	0.25	92.0
2,4,5-T	3.00	0.38	88.0
2,4-D	3.63	0.12	96.8

On the average, the UV limit of detection was enhanced by almost one order of magnitude from  $1.0 \times 10^{-4}$  M (10 picomole) to  $3.0 \times 10^{-5}$  M (0.36 picomole) as a result of derivatization. This limit of detection was decreased by two orders of magnitude (i.e.,  $2.5 \times 10^{-6}$  M, 2.26 femtomole) by fluorescence detection when compared to underivatized solutes. Further enhancement in detectability was attained by LIF detection whereby the limit of detection was pushed down to  $1 \times 10^{-9}$  M (or 3.6 attomoles), which is 5 orders of magnitude lower than in the UV. This limit of detection is about 0.2 ppb, a concentration at which environmental herbicide samples are expected to occur. This concentration was attained by successive dilution of the derivatized mixture at  $10^{-7}$  M (see experimental). As shown in Fig. 2b, the derivatization can be successfully performed on solutions containing initially  $1 \times 10^{-9}$  M phenoxy acid herbicides, and the resulting signal-to-noise ratio from CE-LIF analysis is better than 3.

Figure 3 shows a typical electropherogram of the nine ANDSA-phenoxy acid herbicides obtained by LIF detection at 18 kV using a running electrolyte of 200 mM borate, pH 10, containing 5 mM  $\alpha$ -CD. Besides the baseline resolution of the nine ANDSA-herbicides, Fig. 3 also features the absence of any noticeable side products as a



**Figure 3.** Electropherogram of nine ANDSA-phenoxy acid herbicides obtained by CE-LIF. Running electrolyte, 200 mM borate, pH 10.0, containing 5 mM  $\alpha$ -CD; current, 65  $\mu$ A. Peaks: (1) dichlorprop, (2) 2,4-D, (3) mecoprop, (4) 2,3-CPPA, (5) 2,4-CPPA, (6) silvex, (7) 2,4,5-T, (8) 2,2-CPPA, (9) 2-PPA. Other conditions as in Fig. 2.



result of the precolumn derivatization with ANDSA. In the absence of  $\alpha$ -CD, silvex migrated first (at  $\sim 17$  min) and 2-PPA last (at  $\sim 19.5$  min) while the following groups of solutes:(dichlorprop/mecoprop/2,4,5-T), (2,3-CPPA/2,4-CPPA) and (2,4-D/2,2-CPPA) co-migrated in that order in between silvex and 2-PPA. As will be shown below  $\alpha$ -CD caused the enantiomeric separation of only two chiral phenoxy acid herbicides at pH 5.0 and virtually no chiral recognition at pH 10.0.

#### Chiral Separation by CD-CE

The extent of the enantiomeric separation of the seven optically active herbicides attained upon the addition of 10 mM of  $\alpha$ -CD,  $\beta$ -CD,  $\gamma$ -CD, HP- $\beta$ -CD, DM- $\beta$ -CD, or TM- $\beta$ -CD to the phosphate/borate electrolyte system (25 mM phosphate, 600 mM borate, pH 5.0) is shown in Figs 4 and 5. The borate/phosphate electrolyte system was selected because one of the aims of the present investigation was the comparison of CD-CE to CD-MECC in the chiral separation of the herbicides. This electrolyte system was previously shown effective in converting in situ the MEGA surfactant to a negatively charged micelle even at pH 5.0 through borate complexation with the sugar head group of MEGA [12]. As demonstrated in that earlier work, the borate complexation imparted the surfactant with the necessary charge, and in turn a reasonable migration time window to achieve the MECC of various charged and neutral compounds. For an in-depth description of this in situ charged micellar system see Refs 4 and 12. When comparing the borate (600 mM)/phosphate (25 mM) electrolyte system at pH 5.0, which was used throughout the study, to a regular buffered electrolyte (e.g., 25 mM acetate, pH 5.0), there was virtually no major difference between both types of electrolytes as far as the migration time and the enantioselectivity are concerned (results not shown).

Returning to Figs 4 and 5, as expected, the various CDs did not only show different enantiomeric selectivity but also different migration patterns among the various analytes. While  $\alpha$ -CD caused the enantiomeric separation of 2,3-CPPA and slight splitting

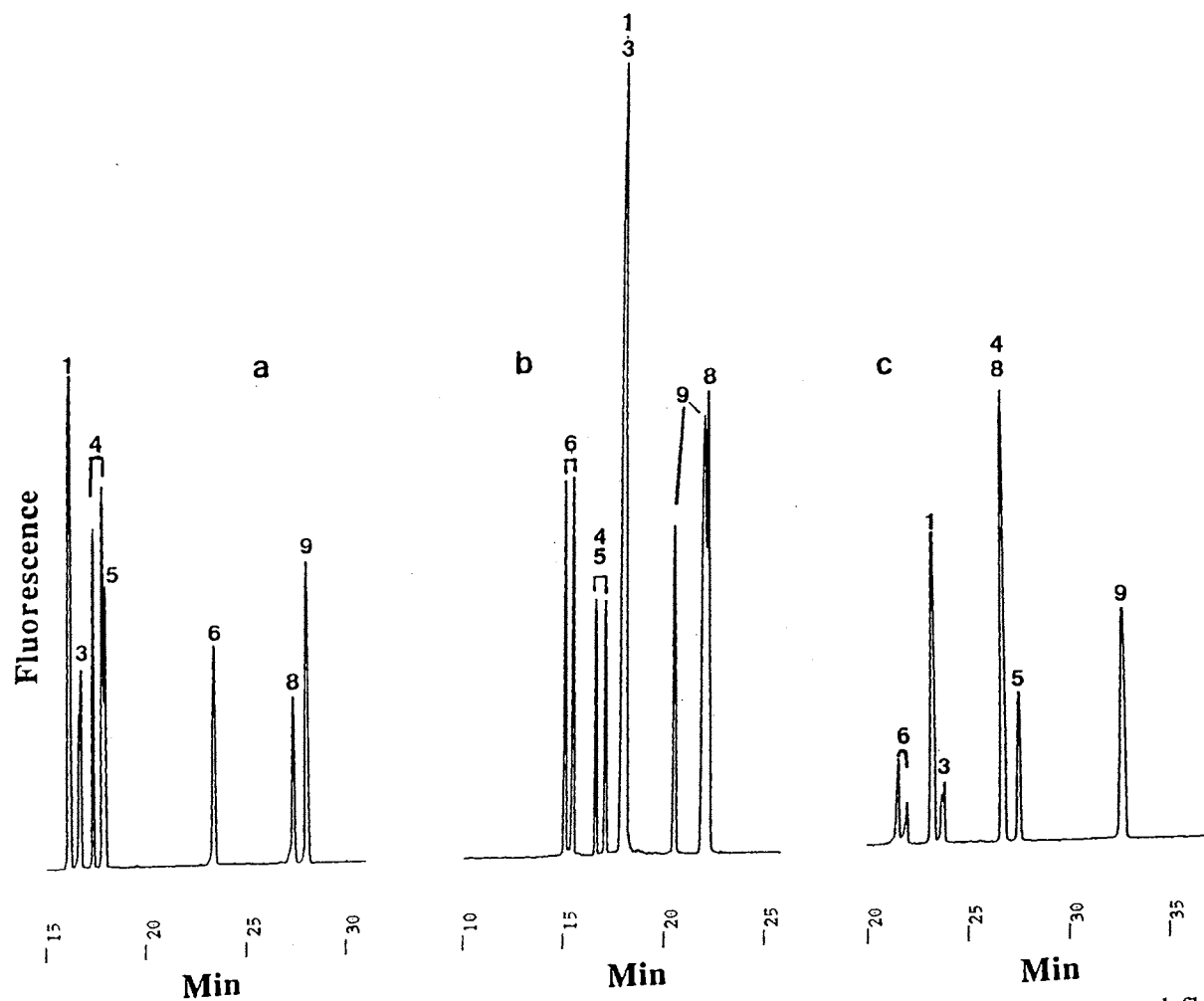


**Figure 4.** Electropherograms of ANDSA-phenoxy acid herbicides obtained by CD-CE using lamp operated fluorescence detector. Running electrolytes, 25 mM sodium phosphate, 600 mM borate, pH 5.0, containing 10 mM (a)  $\alpha$ -CD, (b)  $\beta$ -CD and (c)  $\gamma$ -CD; capillary, 80 cm (50 cm to detection) x 50  $\mu$ m I.D.; voltage, 20 kV; current, 10  $\mu$ A. Peaks: (1) dichlorprop, (3) mecoprop, (4) 2,3-CPPA, (5) 2,4-CPPA, (6) silvex, (8) 2,2-CPPA, (9) 2-PPA.

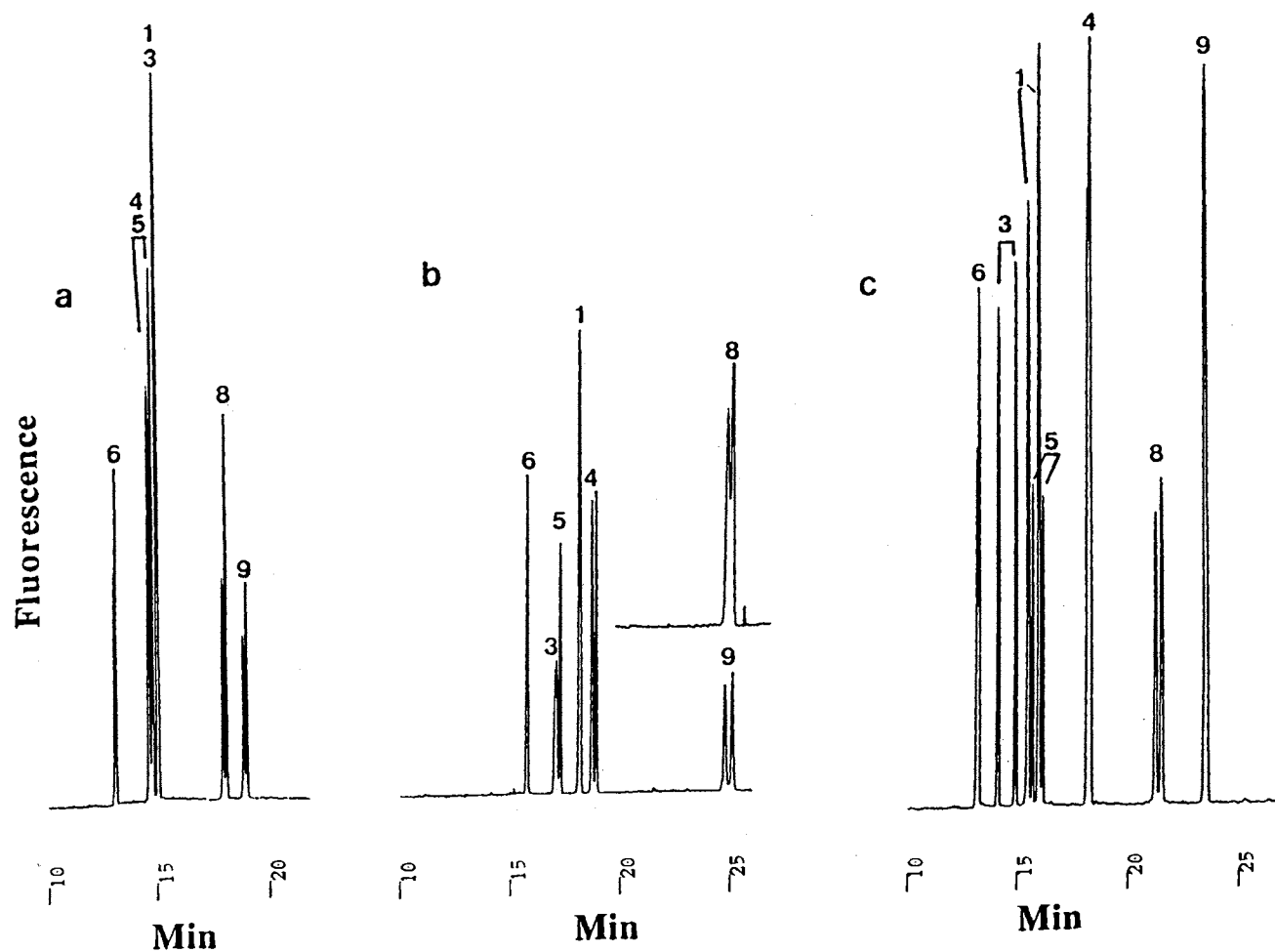


**Figure 5.** Electropherograms of ANDSA-phenoxy acid herbicides obtained by CD-CE using lamp operated fluorescence detector. Running electrolyte, 25 mM sodium phosphate, 600 mM borate, pH 5.0, containing 10 mM (a) HP- $\beta$ -CD, (b) DM- $\beta$ -CD and (c) TM- $\beta$ -CD. Peaks: (1) dichlorprop, (3) mecoprop, (4) 2,3-CPPA, (5) 2,4-CPPA, (6) silvex, (8) 2,2-CPPA, (9) 2-PPA. Other conditions as in Fig. 4.

of mecoprop (Fig. 4a),  $\gamma$ -CD allowed the enantiomeric separation of silvex and slight splitting of mecoprop, see Fig. 4c. Among the unmodified CDs,  $\beta$ -CD afforded the best enantiomeric separation with a baseline chiral resolution of silvex, 2,4-CPPA, 2,3-CPPA and 2-PPA. However, several analytes coeluted including the enantiomerically separated 2,3-CPPA and 2,4-CPPA. It is true that  $\alpha$ -CD did not yield a substantial enantiomeric separation, yet it produced the best CE separation of the analytes (Fig. 4a). The migration order of the different analytes varied as the nature of the CD was changed. Generally, the electrophoretic mobility of the CD-analyte complex is lower than that of the free (uncomplexed) analyte, and the stronger this complexation was the faster the analyte migrated toward the detection point, i.e., in the same direction as the electroosmotic flow. In the absence of CDs, the migration order of the phenoxy acid herbicides under investigation is silvex first, dichlorprop second, mecoprop third, 2,2-CPPA, 2,3-CPPA and 2,4-CPPA co-migrated forth, and 2-PPA last. This migration order was not observed with any of the CDs used, and the change in the migration order in the presence of CDs is the result of different complexation strength between the analytes and the CDs.

The enantioselectivity of the  $\beta$ -CD is enhanced when the chiral selector is trimethylated. As can be seen in Fig. 5c, TM- $\beta$ -CD allowed the enantiomeric baseline separation of mecoprop, dichlorprop, 2,4-CPPA and 2-PPA, and a partial enantiomeric separation of silvex and 2,3-CPPA. Moreover, the TM- $\beta$ -CD yielded a better achiral CE separation than other CDs. Hydroxylation and dimethylation of  $\beta$ -CD (i.e., HP- $\beta$ -CD and DM- $\beta$ -CD) are not as effective as trimethylation (i.e., TM- $\beta$ -CD) in bringing about enantiomeric separation (see Fig. 5a and b). With HP- $\beta$ -CD not only less chiral recognition was observed but also less resolution among the various analytes. In fact, 2,3-CPPA and 2,4-CPPA as well as mecoprop and dichlorprop co-migrated. With DM- $\beta$ -CD, only 2,3-CPPA and 2-PPA enantiomers were well resolved. Thus, by rendering the CD more hydrophilic by introducing a hydroxypropyl group as in HP- $\beta$ -CD, and by elongating the depth of the cavity by dimethylation as in DM- $\beta$ -CD, did not provide the guest-host

interaction needed for enhanced enantiomeric separation. An additional methyl group is needed (i.e., TM- $\beta$ -CD) to yield a deeper cavity [18] and in turn the complexation required for the enantiomeric separation of a larger number of analytes. However, the guest-host interaction with TM- $\beta$ -CD is still not enough to allow the enantiomeric separation of all the analytes studied in this report.

To assess the impact of precolumn derivatization on the chiral separation of the various enantiomeric herbicides, the enantiomeric resolution of the derivatized and underivatized herbicides obtained with the various CDs were estimated, and the results are summarized in Table II. In all cases, the derivatization enhanced the enantiomeric separation when compared to the underivatized herbicides under otherwise identical electrophoretic conditions. The cavities of  $\gamma$ -CD and  $\alpha$ -CD are too large or too small, respectively, to ensure the chiral recognition through the key and lock mechanism, thus providing only a limited enantiomeric separation of the analytes.

Typically, the effect of precolumn derivatization on chiral recognition can be assessed by comparing Fig. 6 to Fig. 5c. The tagging of the analytes with ANDSA enhanced the chiral resolution of the derivatized mecoprop, dichlorprop and 2,4-CPPA, and in addition brought about the enantiomeric separation of those that were not resolved when underivatized such as 2,2-CPPA and 2,3-CPPA (see Figs 6 and 5c, and Table II). The only exception is that upon derivatization the chiral resolution of silvex is hindered.

The effect of CD concentration on the chiral resolution of the various ANDSA-phenoxy acid herbicide enantiomers is shown in Fig. 7. As it can be seen in this figure, the resolution-concentration dependency is a complex function varying significantly from one CD to another and from a chiral solute to another. In general, and in the concentration domain studied, the enantiomeric resolution reached an optimum at a certain CD concentration which varied from solute to another. For instance, increasing the TM- $\beta$ -CD concentration from 5 to 20 mM decreased the enantiomeric separation of mecoprop, 2,4-

TABLE II. Resolution of Derivatized and Underivatized Phenoxy Acid Herbicide Enantiomers by CD-CE Using Various Cyclodextrins. Electrolytes: 25 mM sodium phosphate containing 600 mM borate and 10.0 mM CD, pH 5.0.

	$\alpha$ -CD		$\beta$ -CD		$\gamma$ -CD		DM- $\beta$ -CD		HP- $\beta$ -CD		TM- $\beta$ -CD	
	DER	UND	DER	UND	DER	UND	DER	UND	DER	UND	DER	UND
<b>Silvex</b>	0	0	2.54	0.39	2.43	0	0	0	0.2	0.10	0.85	3.03
<b>Mecoprop</b>	0.29	0.80	0	0.15	0.53	0	0.45	1.44	0	0.57	7.04	2.49
<b>Dichlorprop</b>	0.14	0.67	0	0	0	0	0	0	0	0.75	3.76	1.05
<b>2,4-CPPA</b>	0	0.430	3.43	1.0	0	0	0	0	0.97	0.35	5.63	1.08
<b>2,3-CPPA</b>	2.63	0.27	3.33	1.68	0	0	1.28	0	2.45	1.0	0.20	0
<b>2,2-CPPA</b>	0	0	0	0	0	0	0.79	0	1.29	0	1.76	0
<b>2-PPA</b>	0	0	5.68	1.24	0	0	1.89	0	1.39	0	0	0

DER = Derivatized phenoxy acid herbicides; UND = underivatized.

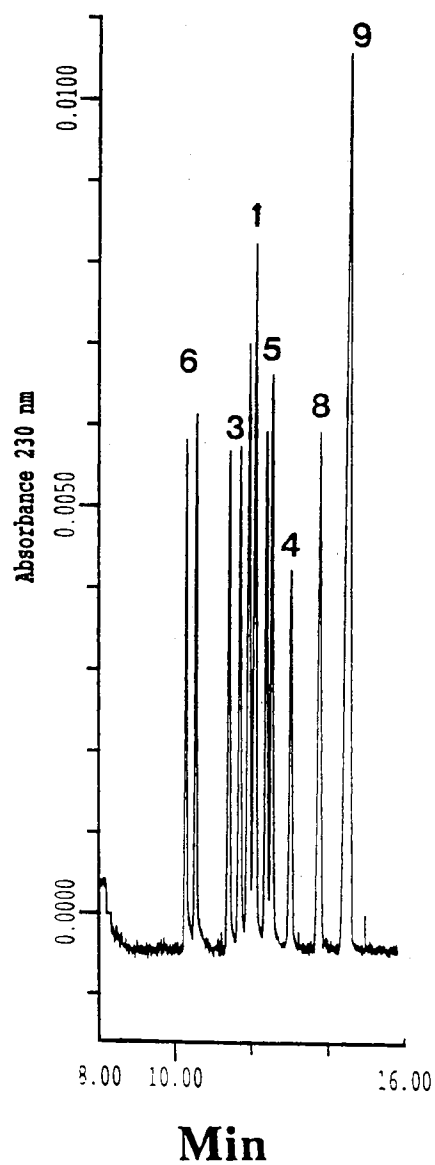


**Figure 6.** Electropherograms of underivatized phenoxy acid herbicides obtained by CD-CE. Running electrolyte, 25 mM sodium phosphate, 600 mM borate, pH 5.0, containing 10 mM TM- $\beta$ -CD; capillary, 57 cm (50 cm to detection)  $\times$  50  $\mu$ m I.D; voltage, 250 V/cm. (1) dichlorprop, (3) mecoprop, (4) 2,3-CPPA, (5) 2,4-CPPA, (6) silvex, (8) 2,2-CPPA, (9) 2-PPA.

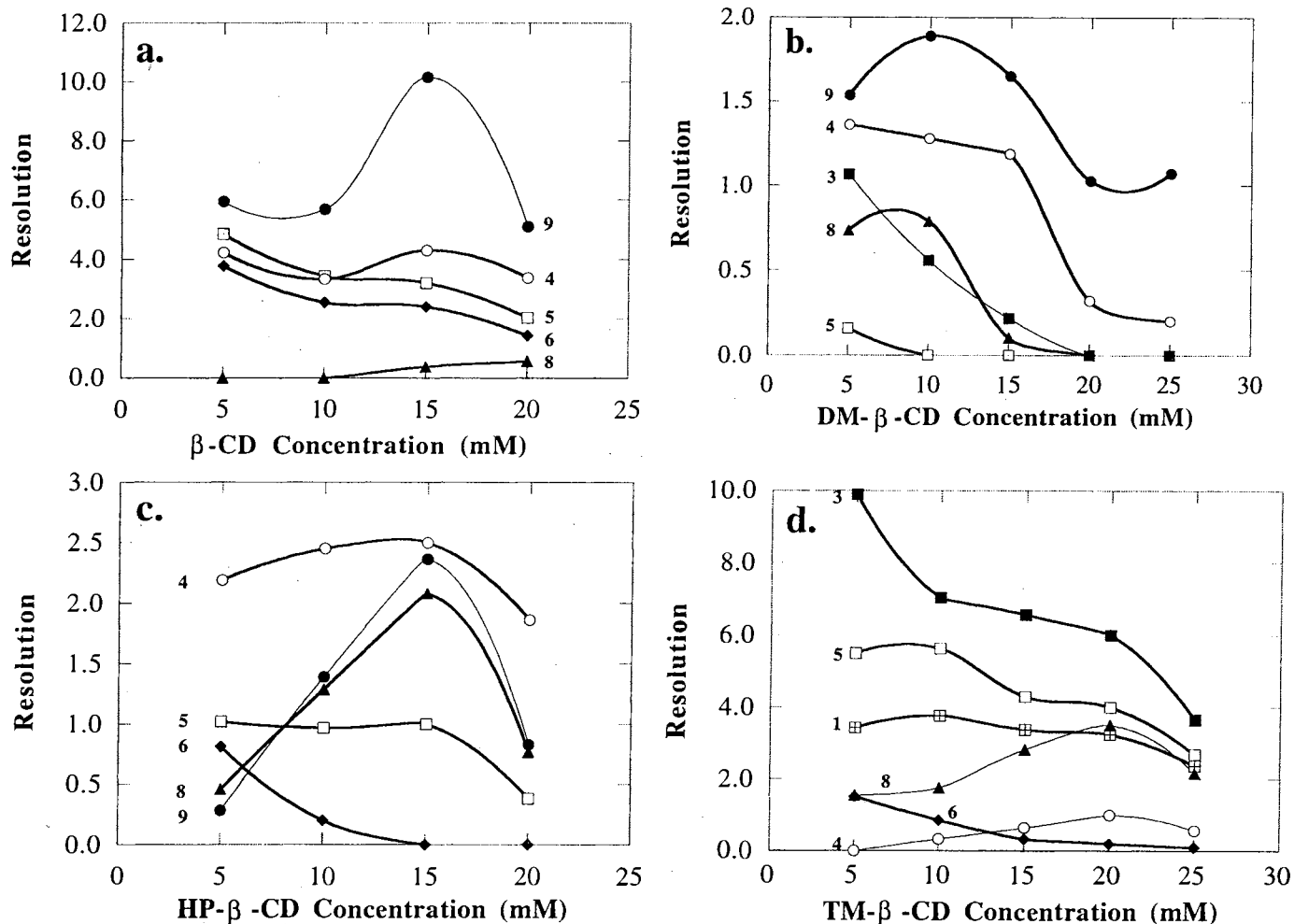


**Figure 7.** Resolution of the ANDSA-phenoxy acid enantiomers as a function of chiral selector concentration: (a)  $\beta$ -CD, (b) DM- $\beta$ -CD, (c) HP- $\beta$ -CD and (d) TM- $\beta$ -CD. Running electrolyte, 25 mM sodium phosphate, 600 mM borate, pH 5.0, containing various concentrations of (a)  $\beta$ -CD, (b) DM- $\beta$ -CD, (c) HP- $\beta$ -CD and (d) TM- $\beta$ -CD. Lines: (1) dichlorprop, (3) mecoprop, (4) 2,3-CPPA, (5) 2,4-CPPA, (6) silvex, (8) 2,2-CPPA, (9) 2-PPA. Other conditions as in Fig. 4.



CPPA and silvex and to a lesser extent that of dichlorprop, while it enhanced the enantiomeric resolution of 2,3-CPPA and 2,2-CPPA. However, the enantiomeric resolution of all the analytes decreased at TM- $\beta$ -CD concentration above 20 mM.

#### CE of ANDSA-Phenoxy Acid Herbicides by Mixed CDs

Since the various CDs exhibited different chiral selectivity toward the ANDSA-herbicides, it is obvious that electrolyte systems composed of mixed CDs should yield a unique chiral selectivity that can not be achieved by neither of the CDs alone. Figure 8 shows the effect of mixed TM- $\beta$ -CD and  $\gamma$ -CD on the enantiomeric resolution of the various chiral solutes. It is clear that the chiral selectivity achieved in this electropherogram is due to the combined effect of the chiral recognition of  $\gamma$ -CD, which allowed the separation of silvex enantiomers, and that of TM- $\beta$ -CD, which resolved the four other enantiomers.

In another set of experiments, the enantiomeric separation of the chiral analytes under investigation was examined with electrolyte systems containing mixed  $\beta$ -CD and TM- $\beta$ -CD. Silvex, 2,4-CPPA, 2,3-CPPA and 2-PPA were enantiomerically separated when a running electrolyte containing 5 mM  $\beta$ -CD was used as shown in Fig. 9a. On the other hand, silvex, mecoprop, dichlorprop, 2,4-CPPA and 2-PPA were enantiomerically separated when the running electrolyte contained 5 mM TM- $\beta$ -CD as shown in Fig. 9b. On the basis of these results one can assume that using a running electrolyte containing 5 mM each of  $\beta$ -CD and TM- $\beta$ -CD would result in the enantiomeric separation of all the analytes. With the exception of silvex all the other analytes were resolved into their enantiomers (Fig. 9c). The loss of enantiomeric resolution for silvex may have resulted from the fact that one of the mixed CD interacts more strongly with one of the isomers [say the (+) isomer] while the other mixed CD interacts strongly with the other isomer [say the (-) isomer]. Under this condition, where the enantiomeric selectivity of mixed CDs is opposite to one another, the enantiomeric resolution would be lost upon mixing. This

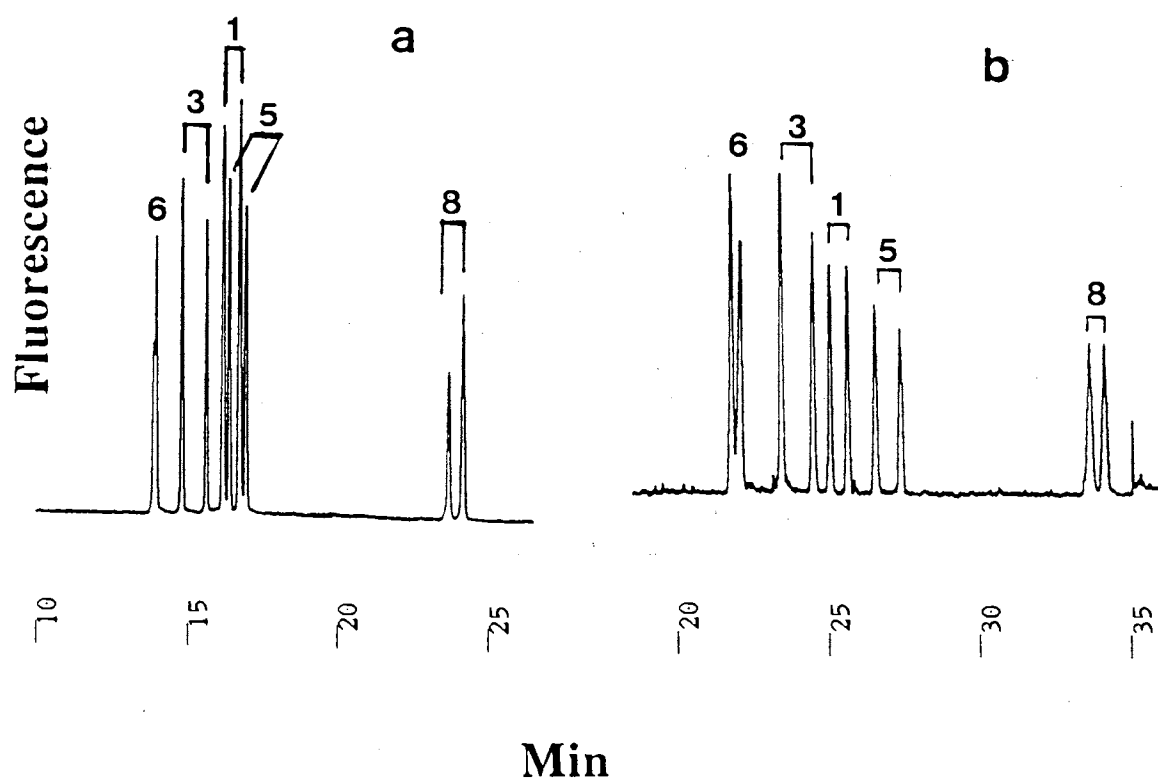


**Figure 8.** Electropherograms of ANDSA-phenoxy acid herbicides obtained by CD-CE and mixed CD-CE using lamp operated fluorescence detector. Running electrolytes, 25 mM sodium phosphate, 600 mM borate, pH 5.0, containing (a) 15 mM TM- $\beta$ -CD and (b) 15 mM TM- $\beta$ -CD and 25 mM  $\gamma$ -CD. Peaks: (1) dichlorprop, (3) mecoprop, (5) 2,4-CPPA, (6) silvex, (8) 2,2-CPPA. Other conditions as in Fig. 4.

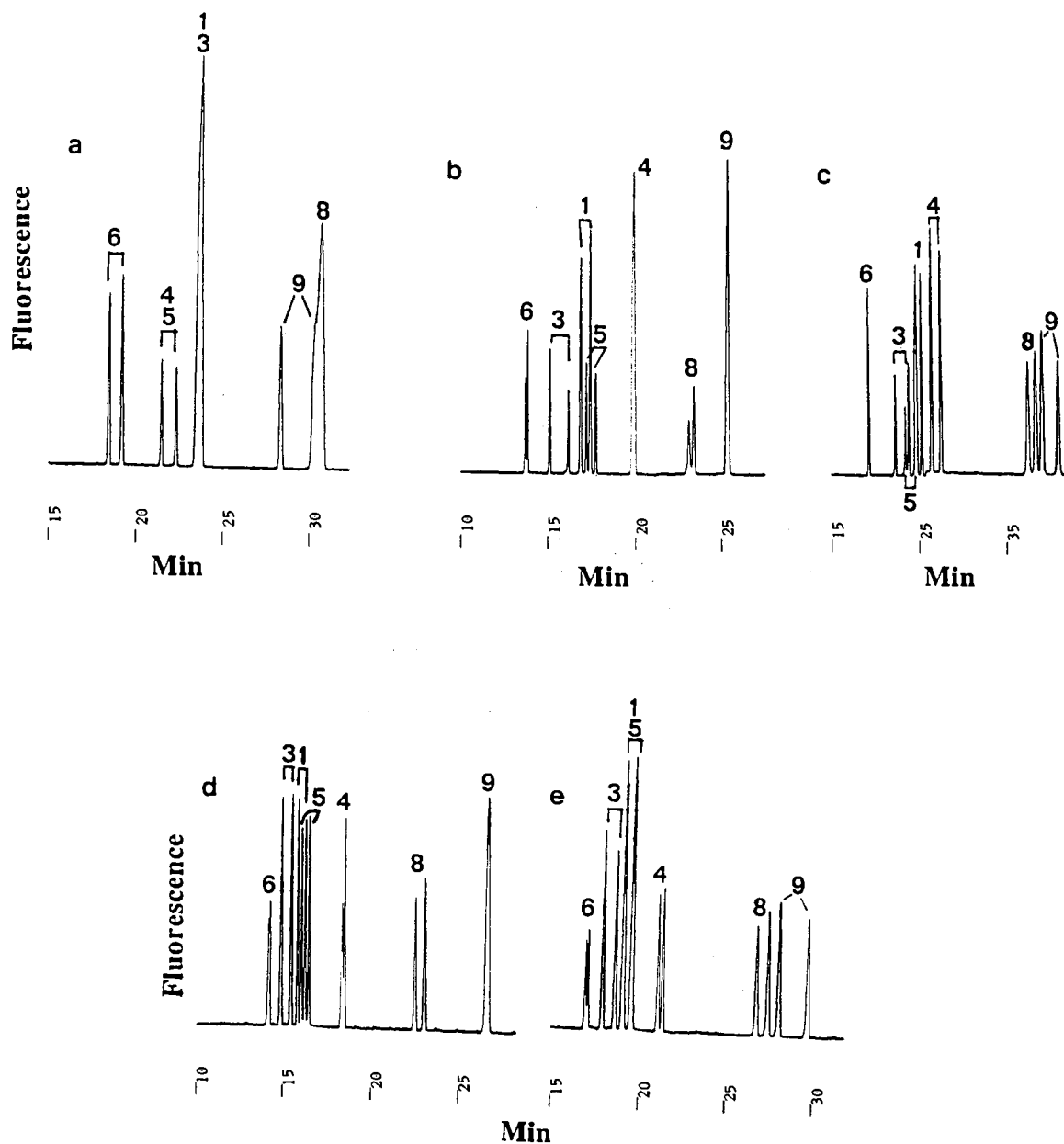


**Figure 9.** Electropherograms of ANDSA-phenoxy acid herbicides obtained by CD-CE and mixed CD-CE using lamp operated fluorescence detector. Running electrolytes, 25 mM sodium phosphate, 600 mM borate, pH 5.0, containing (a) 5 mM  $\beta$ -CD, (b) 5 mM TM- $\beta$ -CD and (c) 5 mM of each TM- $\beta$ -CD and  $\beta$ -CD, (e) 30 mM TM- $\beta$ -CD and (d) 5 mM  $\beta$ -CD and 30 mM TM- $\beta$ -CD. Peaks: (1) dichlorprop, (3) mecoprop, (4) 2,3-CPPA, (5) 2,4-CPPA, (6) silvex, (8) 2,2-CPPA, (9) 2-PPA. Other conditions as in Fig. 4.

explanation was further supported by the fact that the enantiomeric separation of silvex was restored when the two CDs were mixed at a certain concentration where silvex enantiomeric resolution in the presence of one of the chiral selectors was diminished. TM- $\beta$ -CD caused a very slight enantiomeric separation at 30 mM concentration (Fig. 9d). Therefore, mixing of 30.0 mM TM- $\beta$ -CD and 5.0 mM  $\beta$ -CD resulted in the enantiomeric separation of silvex and all the others. The only drawback is that dichlorprop and 2,4-CPPA enantiomers coeluted, Fig. 9e.

### CD-MECC

Using CD individually or mixed for the separation of closely related enantiomers may not provide enough selectivity among the various analytes, see Fig. 10a. In other words, two pairs of closely related enantiomers may exhibit very similar partitioning into the CD phase, and consequently do not separate from each other. This suggested the inclusion of a micellar phase into the electrolyte system to achieve the desired enantiomeric selectivity as well as resolution of the different analytes.

The concept of in situ charged micelles for use in MECC as well as its applicability to the separation of a wide variety of analytes was recently introduced by our laboratory [2-5,20]. The utility of these micellar systems was very recently expanded to include neutral and acidic pH electrolytes [12]. Since the chiral selectivity of CDs is optimum under acidic conditions [15], TM- $\beta$ -CD was added to MEGA 10-borate, pH 5.0. Figure 10b illustrates the effect of the presence of MEGA 10 on the achiral resolution between the individual analytes. The presence of the micellar system provided better resolution between the individual solutes, especially between 2,4-CPPA and dichlorprop. It should be noted that the high borate concentration was needed to charge the micelle at pH 5.0 where borate anions are not the major species [12].

While the addition of MEGA-10 to the chiral electrolyte has decreased the chiral resolution of TM- $\beta$ -CD (see Figure 10 b), the inclusion of MEGA 10 in the electrolyte

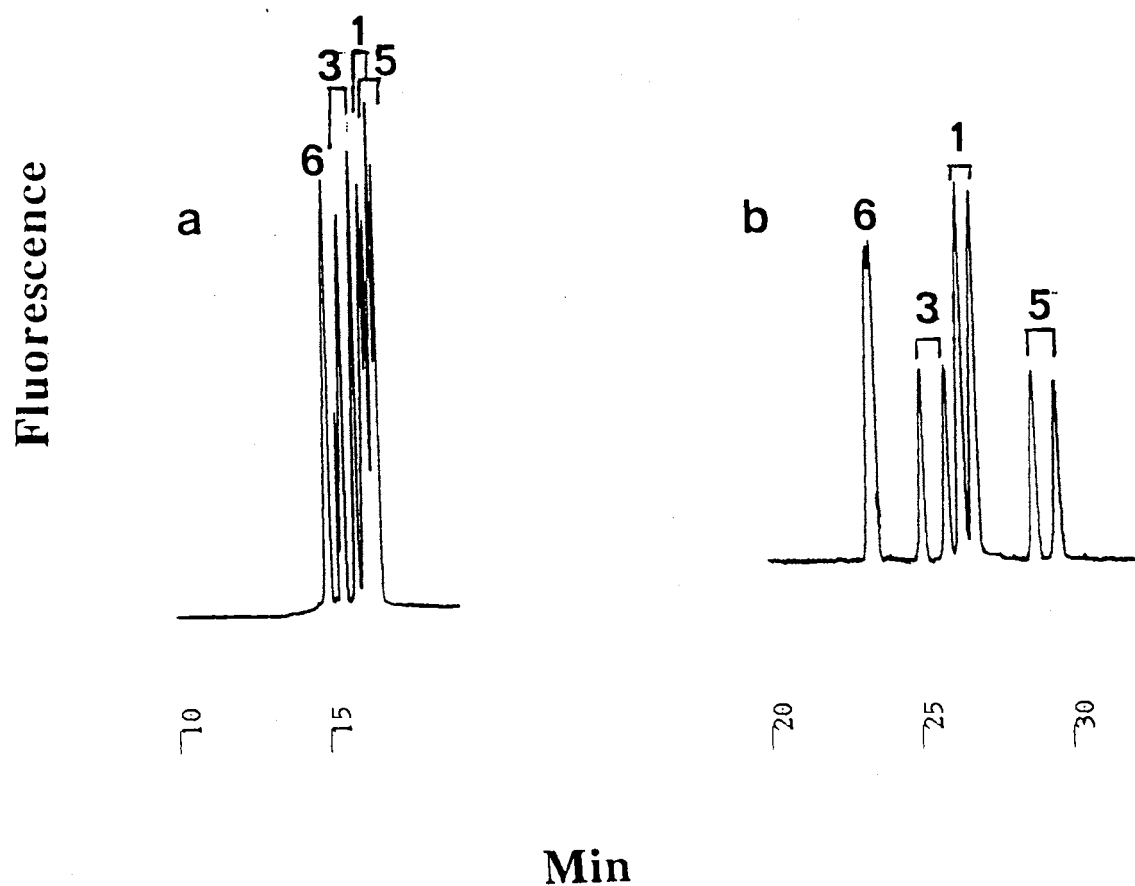


**Figure 10.** Electropherograms comparing the enantiomeric separation of ANDSA-phenoxy acid herbicides obtained with (a) CD-CE and (b) CD-MECC using lamp operated fluorescence detector. Running electrolytes, 600 mM borate, 10 mM sodium phosphate pH 5.0 containing (a) 25 mM TM- $\beta$ -CD and (b) 50 mM MEGA 10 and 25 mM TM- $\beta$ -CD; current,  $< 5 \mu\text{A}$ . (1) dichlorprop, (3) mecoprop, (4) 2,3-CPPA, (6) silvex. Other conditions as in Fig. 4.

containing DM- $\beta$ -CD, which caused only slight enantiomeric separation when used alone, resulted in the loss of chiral selectivity of DM- $\beta$ -CD, results not shown.

The effect of TM- $\beta$ -CD concentration on the resolution in the presence and absence of MEGA 10 for four phenoxy acid herbicides (dichlorprop, mecoprop, 2,4-CPPA, and silvex) was also studied. Even at high TM- $\beta$ -CD concentration, the enantiomeric separation achieved was lower in the presence than in the absence of the micellar system (results not shown). This might be due to the fact that the MEGA monomers are associating with CD molecules thus competing with the analyte for the binding sites involved in the chiral recognition.

### Conclusions

A novel, selective precolumn derivatization reaction was introduced and evaluated in the fluorescence labeling of phenoxy acid herbicides with ANDSA. The ANDSA-phenoxy acid derivatives were readily detected by capillary electrophoresis/laser-induced fluorescence (CE-LIF) at 0.2 ppb, a concentration at which environmental herbicide samples are expected to occur. The precolumn derivatization was very quantitative (99.7 % yield) and produced stable derivatives and no side products. Furthermore, the ANDSA-phenoxy acid herbicide enantiomers exhibited higher chiral resolution than their underivatized counterparts in the presence of CD in the running electrolyte. Several native and modified CDs were investigated in the enantiomeric separation of chiral phenoxy acid herbicides. The best enantioselectivity was achieved using TM- $\beta$ -CD as the chiral selector. To achieve the enantiomeric resolution of a large number of ANDSA-phenoxy acid enantiomers, electrolyte systems based on mixed CDs were utilized and evaluated. Mixed CDs based on  $\beta$ -CD and TM- $\beta$ -CD proved to be the most effective as far as the enantiomeric resolution of the chiral analytes is concerned. To provide different selectivity for the various ANDSA-phenoxy acid herbicides, novel micellar systems containing cyclodextrins were evaluated and were shown to improve CE separation.

## References

1. Tekel', J. and Kovacicova, J., *J. Chromatogr.*, 643 (1993) 291.
2. Smith, J.T. and El Rassi, Z., *J. Chromatogr. A*, 685 (1994) 131.
3. Smith, J.T. and El Rassi, Z., *Electrophoresis*, 15 (1994) 1248.
4. Smith, J.T., Nashabeh, W. and El Rassi, Z., *Anal. Chem.*, 66 (1994) 1119.
5. Smith, J.T. and El Rassi, Z., *J. Microcol. Sep.*, 6 (1994) 127.
6. Nielen, M.W.F., *J. Chromatogr.*, 637 (1993) 81.
7. Nielen, M.W.F., *Trends Anal. Chem.*, 2 (1993) 345.
8. Wu, Q., Claessens, H.A. and Cramers, C.A., *Chromatographia*, 34 (1992) 25.
9. Jung, M. and Brumley, W.C., *J. Chromatogr. A*, 717 (1995) 299.
10. Garrison, A.W., Schmitt, P. and Kettrup, A., *J. Chromatogr. A*, 688 (1994) 317.
11. Brumley, W.C. and Brownrigg, C.M., *J. Chromatogr.*, 646 (1993) 377.
12. Mechref, Y., Smith, J.T. and El Rassi, Z., *J. Liq. Chromatogr.*, 18 (1995) 3769.
13. Ariens, E.J., Wuis, E.W. and Veringa, E.J.J., *Biochem. Pharmacol.*, 37 (1988) 9.
14. Novotny, M., Soini, H. and Stefansson, M., *Anal. Chem.*, 66 (1994) 646.
15. Terabe, S., Otsuka, K. and Nishi, H., *J. Chromatogr. A*, 666 (1994) 295.
16. Terabe, S.; Chen, N. and Otsuka, K., *Adv. Electrophoresis*, 7 (1994) 87.
17. Ward, J.W., *Anal. Chem.*, 66 (1994) 633.
18. Fanali, S.; Cristalli, M.; Vespalec, R. and Bocek, P., *Adv. Electrophoresis*, 7 (1994) 1.
19. Mechref, Y. and El Rassi, Z., *J. Chromatogr. A*, 724 (1996) 285.
20. Cai, J. and El Rassi, Z., *J. Chromatogr.*, 608 (1992) 31.
21. Cai, J. and El Rassi, Z., *J. Liq. Chromatogr.*, 15 (1992) 1179.
22. Cai, J. and El Rassi, Z., *J. Liq. Chromatogr.*, 15 (1992) 1193.
23. Smith, J.T. and El Rassi, Z., *J. Cap. Elec.*, 1 (1994) 136.
24. Mechref, Y. and El Rassi, Z., *Electrophoresis*, 15 (1994) 627.
25. Mechref, Y., Ostrander, G.K. and El Rassi, Z., *Electrophoresis*, 16 (1995) 1499.

26. Mechref, Y., Ostrander, G.K. and El Rassi, Z., *J. Chromatogr. A*, 695 (1995) 83.



## Chapter XII

# EVALUATION OF ALKYLGLUCOSIDE CHIRAL SURFACTANTS IN THE ENANTIOMERIC SEPARATION OF PHENOXY ACID HERBICIDES AND OTHER SPECIES

### Introduction

As discussed earlier in Chapter VII, chiral capillary electrophoresis (CCE) is increasingly employed in the enantiomeric separation of various kinds of racemic mixtures. This is due to the fact that CCE is a simple, rapid and practical method yet providing high separation efficiency, and requiring small sample and reagent volumes. Various direct and indirect CCE approaches have been exploited in enantiomeric separation. One direct approach involves inclusion complexation in the presence of cyclodextrins (CDs) either in an open tubular format [1-10] or CDs immobilized in gel filled capillaries [11,12] or CDs bonded to the walls of fused silica capillaries [13,14]. Also, inclusion complexation was performed in the presence of crown ethers [15]. A second direct approach for CCE is based on solubilization by chiral micelles [16-18] or microemulsions [19]. Other direct approaches include (i) affinity interaction in the presence of proteins [20,21] or polysaccharides [22] and (ii) ligand-exchange complexation [23,24]. Finally, derivatization to diastereoisomers forms the basis for indirect methods for chiral separation by CE [25,26]. The details of these various methods have been described in several recent reviews on CE of enantiomers [27], and also in Chapter VIII.

Very recently, our laboratory has introduced novel chiral micellar systems based on steroidal-glycoside surfactant-borate complexes [28] for the separation of several optical isomers including binaphthyl, troger's base, dansyl amino acid and silvex herbicide

enantiomers (Chapter X). In a more recent report, we evaluated the use of mixed CDs in the separation of fluorescently labeled phenoxy acid herbicide enantiomers [29] (Chapter XI).

Thus far, all chiral separation involving micellar phases were performed with charged chiral micelles [30,31], in situ charged micelles [28] (see Chapter X), mixed achiral charged micelles/CDs [18,32] or mixed achiral charged micelles/chiral micelles [16,33]. This chapter, which is a continuation of our previous efforts in the area of CCE (see Chapters X and XI), reports for the first time the use of uncharged alkylglucoside chiral micelles in the separation of charged enantiomers such as phenoxy acid herbicides, organics and pharmaceutical compounds. There are two major rationales for using phenoxy acid herbicides as model chiral solutes for evaluating the alkylglucoside chiral surfactants under investigation: (i) they are important agrochemicals, especially in the control of weeds in cereal crops [34], and (ii) they have systematic structural differences, e.g., nature, location and number of substitution on the benzene ring, as well as a structural similarity (i.e., the chiral center) which make them attractive enantiomeric solutes for evaluating chiral selectors.

As will be shown in this chapter, the use of uncharged micelles in CCE offers a great deal of advantages in terms of tuning enantioselectivity which can be manipulated by various operational variables such as the surfactant concentration, the ionic strength and pH of the running electrolyte, and the capillary temperature. The neutral surfactants used in this chapter are namely *n*-octyl- $\beta$ -D-glucopyranoside (OG), *n*-nonyl- $\beta$ -D-glucopyranoside (NG) and *n*-octyl- $\beta$ -D-maltopyranoside (OM). All these surfactants resemble each other in terms of being neutral chiral surfactant possessing a saccharide polar head group. However, the OM surfactant possesses a maltoside chiral head group with different characteristic micellar solubilization toward a given set of solutes as was manifested by its electrokinetic behavior in MECC of a wide range of neutral and charged solutes [35,36].

The OG and NG differ from each other in the alkyl tail, where the former has one carbon atom less than the latter.

## Materials and Methods

### Capillary Electrophoresis Instrument

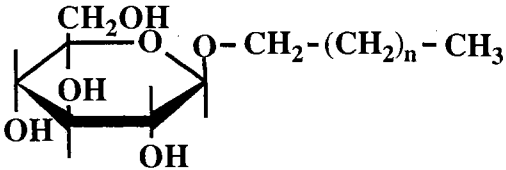
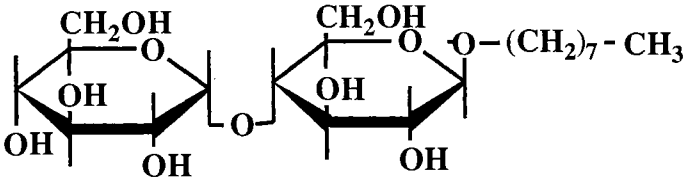
The capillary electrophoresis instrument used in this study was the as that described in Chapter VI. Detection was performed at 230 nm and the resulting signal was fed to the computer for archiving and real time display of the electropherograms. The fused-silica capillaries were obtained from Polymicro Technology (Phoenix, AZ, U.S.A.) and had the dimensions of 50 cm (to detection window) and 57 cm (total length) with an I.D. of 50  $\mu\text{m}$  and an O.D. of 365  $\mu\text{m}$ . Unless otherwise stated, the temperature of the capillary was maintained at 15°C by the instrument thermostating system. Samples were pressure injected as methanol-water solutions at 0.034 bar (i.e., 3.5 kPa) for various lengths of time.

### Reagents and Materials

n-Octyl- $\beta$ -D-glucopyranoside (OG), n-nonyl- $\beta$ -D-glucopyranoside (NG) and n-Octyl- $\beta$ -D-maltopyranoside (OM) surfactants were purchased from Anatrace (Mumee, OH, USA), Sigma Chemical Co. (St. Louis, MO, USA) and Calbiochem (La Jolla, CA, USA), respectively. The structures and the critical micellar concentration (CMC) of these surfactants are shown in Table I. Phenoxy acid herbicides including silvex, 2-(2,4-dichlorophenoxy)propionic acid (dichlorprop), 2-(4-chloro-2-methylphenoxy)propionic acid (mecoprop), 2-(4-chlorophenoxy)propionic acid (2,4-CPPA), 2-(3-chlorophenoxy)propionic acid (2,3-CPPA), 2-(2-chlorophenoxy)propionic acid (2,2-CPPA), and 2-phenoxypropionic acid (2-PPA) were purchased from Aldrich (Milwaukee, WI, USA) and from Chem Service (West Chester, PA, USA). The structures of the phenoxy acid herbicides used in this study are given in Fig. 1 of Chapter XI. (S)-(-)-1,1'-

Binaphthyl-2,2'-diylhydrogen phosphate (BNPO<sub>4</sub>), (R)-(+)-1,1'-binaphthyl-2,2'-diylhydrogen phosphate and (±) warfarin were purchased from Aldrich (Milwaukee, WI, USA). All dansyl amino acids (Dns-AA), namely DL-tryptophan, DL-phenylalanine DL-leucine, DL-methionine, and DL-valine cyclohexylammonium salts as well as bupivacaine (1-butyl-N-[2,6-dimethylphenyl]-2-piperidinecarboxamide) were purchased from Sigma Chemical Co. (St. Louis, MO, USA). The structure of BNPO<sub>4</sub> is illustrated in Fig. 2 in Chapter X. Structures of other solutes are shown in Fig. 1. All Other chemicals used in this study were obtained from the same sources listed in Chapter III.

TABLE I. Structures and CMCs of the Alkylglucopyranosides Used in this Study.

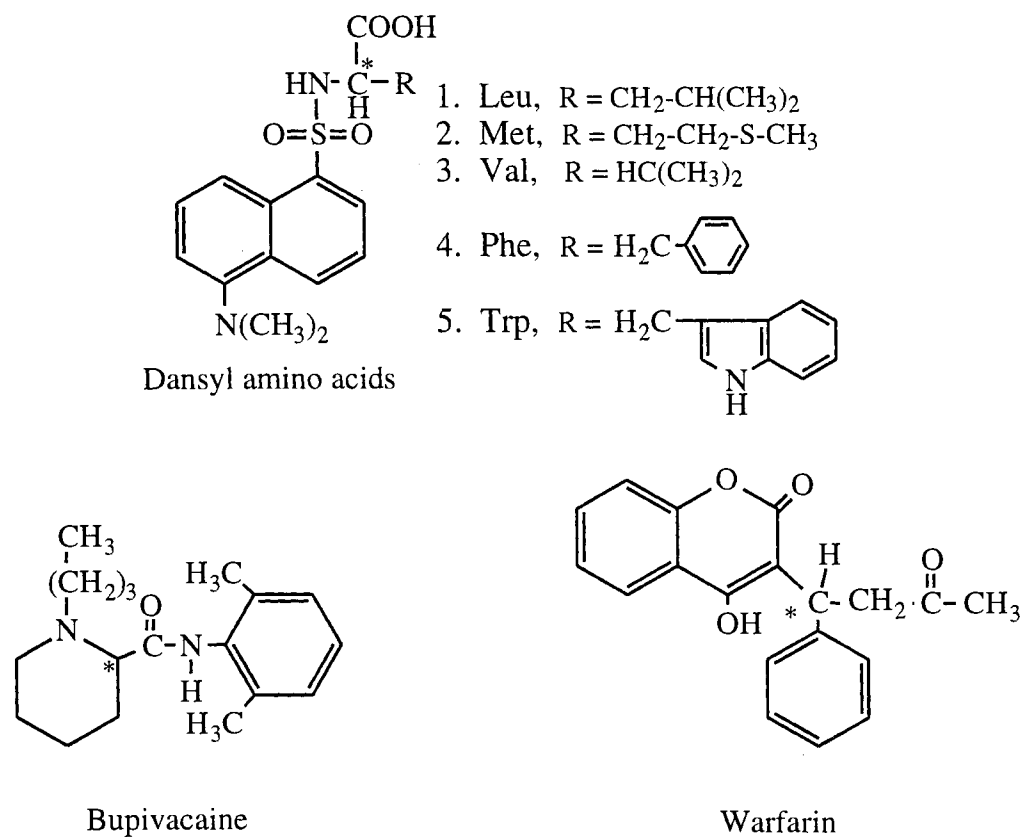
Structure and name of surfactant	Abbreviation	CMC (mM) <sup>a</sup>
		
n = 6: Octyl-β-D-glucopyranoside	OG	25
n = 7: Nonyl-β-D-glucopyranoside	NG	6.5
	OM	23.4

<sup>a</sup> obtained from Ref. [37]

## Results and Discussion

### Effect of Surfactant Concentration and Description of the Separation Principles

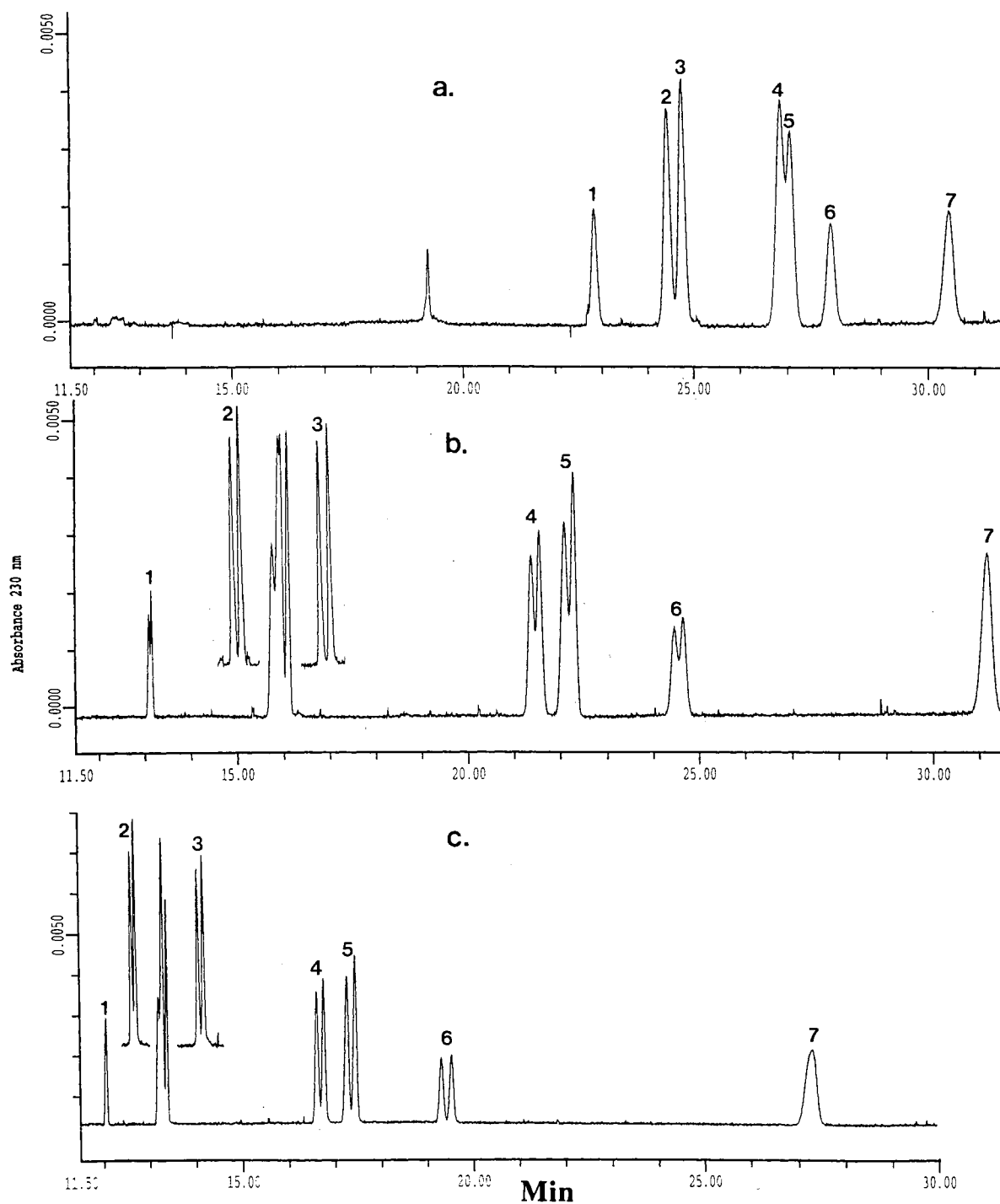
In aqueous media and above the CMC value, the monomers of the nonionic



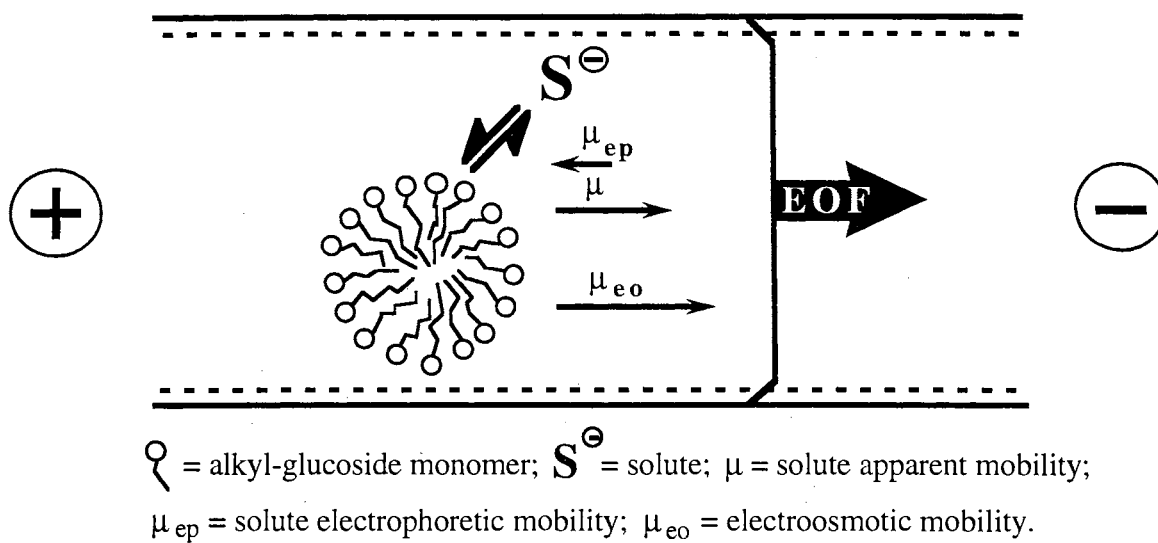
**Figure 1.** Structures of dansyl amino acids, bupivacaine and warfarin used in this study.

alkylglucoside surfactants undergo aggregation thus forming micelles with the hydrophilic sugar group protruding from the surface of the micelles. The chiral selectivity of such surfactants originates from the presence of the chiral sugar head groups. Figure 2 illustrates the electropherograms of phenoxy acid herbicides obtained at three different OG concentrations. As shown in this figure, chiral resolution is achieved only at surfactant concentration above CMC, indicating that the presence of the chiral surfactant in the micellar form is critical for chiral recognition. In other words, solute-micelle association *via* polar and hydrophobic interactions are important components for the enantiomeric separation. On this basis, the enantiomeric resolution is achieved when the two enantiomers exhibit different association constants with the chiral micelles (see Chapter VIII).

A schematic illustration of the separation principles of anionic solutes (e.g., phenoxy acid herbicides) in the presence of the alkylglucoside micellar phases is depicted in Fig. 3. While the neutral micelles of the alkylglucoside surfactants migrate at the velocity of the electroosmotic flow (EOF), the electrophoretic mobility of an anionic analyte is opposite in direction to the cathodal EOF. Thus, the effective electrophoretic mobility and in turn the migration time of an anionic solute (e.g., a phenoxy acid herbicide) will decrease as the magnitude of its association with the neutral micelle will increase. In other words, the stronger is the interaction between the analyte and the micelle the higher the apparent mobility of the anionic analyte, and consequently the faster its migration toward the cathode. This is seen in Fig. 2 where the migration time of silvex decreased from ca. 23 min to ca. 13 min when going from 10 mM OG to 60 mM OG while the migration time of the least interacting herbicide 2-PPA was slightly affected by the presence or the absence of the micelle, and decreased from ca. 31 min to ca. 27 min when increasing OG concentration from 10 to 150 mM. The slight increase in the migration time of 2-PPA when going from 10 to 60 mM OG can be attributed to the increase in the viscosity of the running electrolyte.



**Figure 2.** Electropherograms of phenoxy acid herbicides depicting the effect of OG concentration on enantiomeric resolution. Conditions: running electrolyte, 200 mM sodium phosphate, pH 6.5, containing 10 mM OG in (a), 60 mM OG in (b) and 150 mM OG in (c); capillary, 50 cm (to detection window) 57 cm (total length) x 50  $\mu\text{m}$  I.D.; voltage, 20 kV; temperature 15°C. Peaks, 1 = silvex, 2 = dichlorprop, 3 = mecoprop, 4 = 2,4-CPPA, 5 = 2,3-CPPA, 6 = 2,2-CPPA, 7 = 2-PPA.



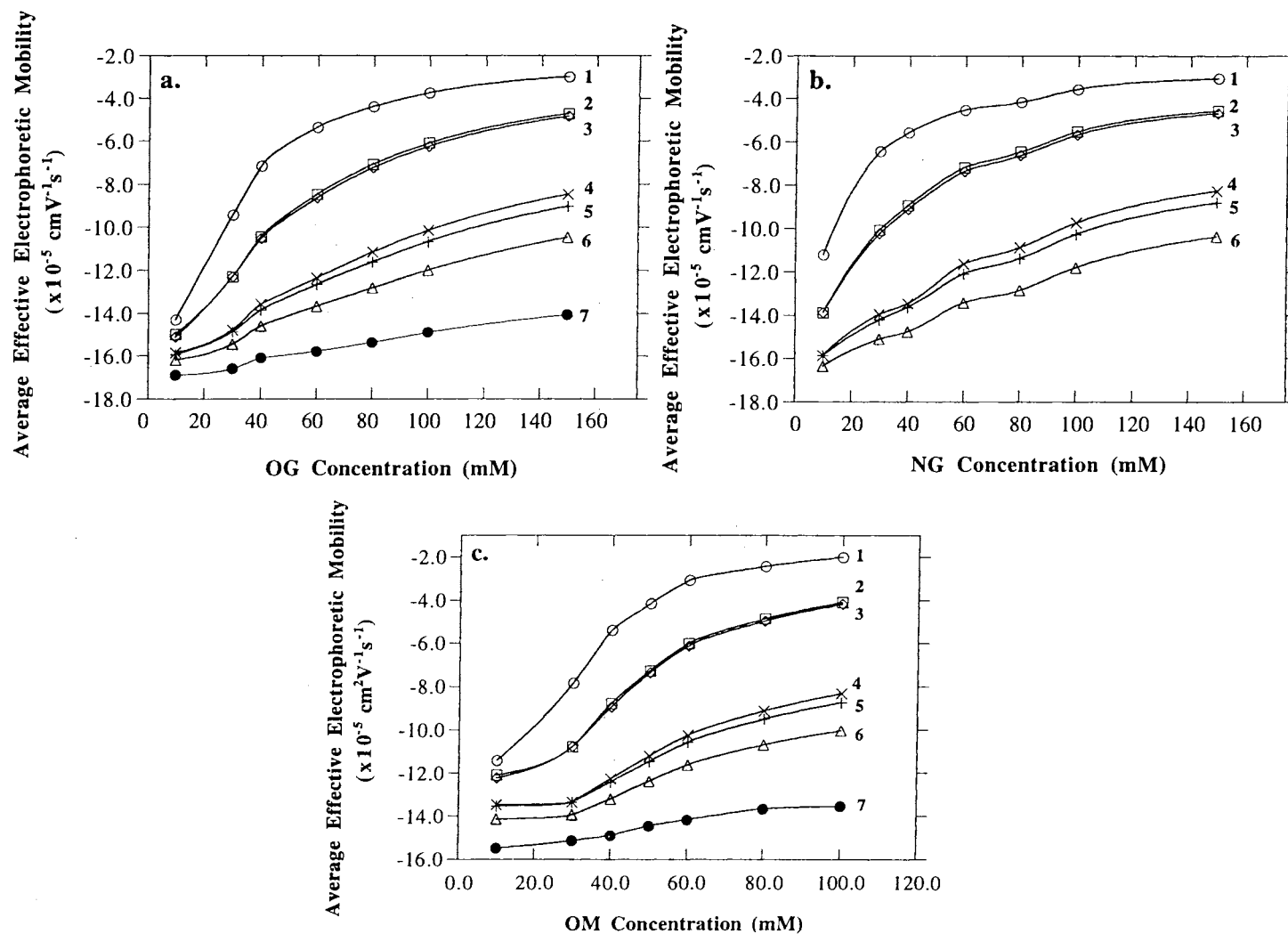
**Figure 3.** A scheme illustrating the separation principles of charged species in the presence of neutral micelles.



Figure 4 illustrates the variation in the average of the effective electrophoretic mobility of phenoxy acid herbicide enantiomers as a function of OG, NG and OM concentrations. In all cases, the effective electrophoretic mobility of the analytes decreased as the concentration of the surfactant increased. This is due to the fact that by increasing the surfactant concentration  $[S]$ , the micellized surfactant concentration ( $[S] - \text{CMC}$ ) is increased, and consequently the number of micelles interacting with a given solute at any instant increases. The net result is an increase in the time the solute spend in the micellar phase. As shown in Fig. 4, silvex, dichlorprop and mecoprop exhibited a sharp decrease in their effective electrophoretic mobilities up to 60 mM OG and OM and up to 30 mM NG, and this decrease became shallower at higher surfactant concentrations. The effective electrophoretic mobility of the other analytes, 2,4-CPPA, 2,3-CPPA, and 2,2-CPPA, decreased almost monotonically with increasing the surfactant concentrations in the range studied. It should be noted that the decrease in mobility at higher surfactant concentration is also partly due to the increase in the electrolyte viscosity.

Generally, and with uncharged surfactants, the magnitude of solute association with the micelle should increase with increasing solute hydrophobicity. Therefore, the order of the hydrophobicity of the different phenoxy acid herbicides seems to decrease in the following order, silvex >> dichlorprop > mecoprop >> 2,4-CPPA > 2,3-CPPA > 2,2-CPPA >> 2-PPA, which is the reversal of their migration order. This correlates with the number, nature and position of non-polar groups substituted on the phenyl group. The hydrophobicity of analytes increases as the number of nonpolar substituents on the phenyl group increases. In addition, a methyl group is less hydrophobic than a chlorine group, and a chlorine in a *para* substitution renders the analyte more hydrophobic than a chlorine in *meta* and *ortho* position, respectively (i.e., the closer is the chlorine atom to the oxygen atom the weaker the hydrophobicity of the phenoxy acid herbicides).

The effect of OG concentration on the enantiomeric resolution of the phenoxy acid herbicides under investigation is illustrated in Fig. 5. The optimum surfactant



**Figure 4.** Plots of the average effective electrophoretic mobility of phenoxy acid herbicides versus the concentration of OG (a), NG (b) and OM (c) in the running electrolyte. Conditions: running electrolyte, 200 mM sodium phosphate, pH 6.5, containing various concentration of OG in (a) and NG in (b), and 175 mM sodium phosphate, pH 6.5, containing various concentrations of OM in (c); capillary, 50 cm (to detection window) 57 cm (total length)  $\times$  50  $\mu\text{m}$  I.D.; voltage, 20 kV; temperature 15°C. Lines, 1 = silvex, 2 = dichlorprop, 3 = mecoprop, 4 = 2,4-CPPA, 5 = 2,3-CPPA, 6 = 2,2-CPPA, 7 = 2-PPA.

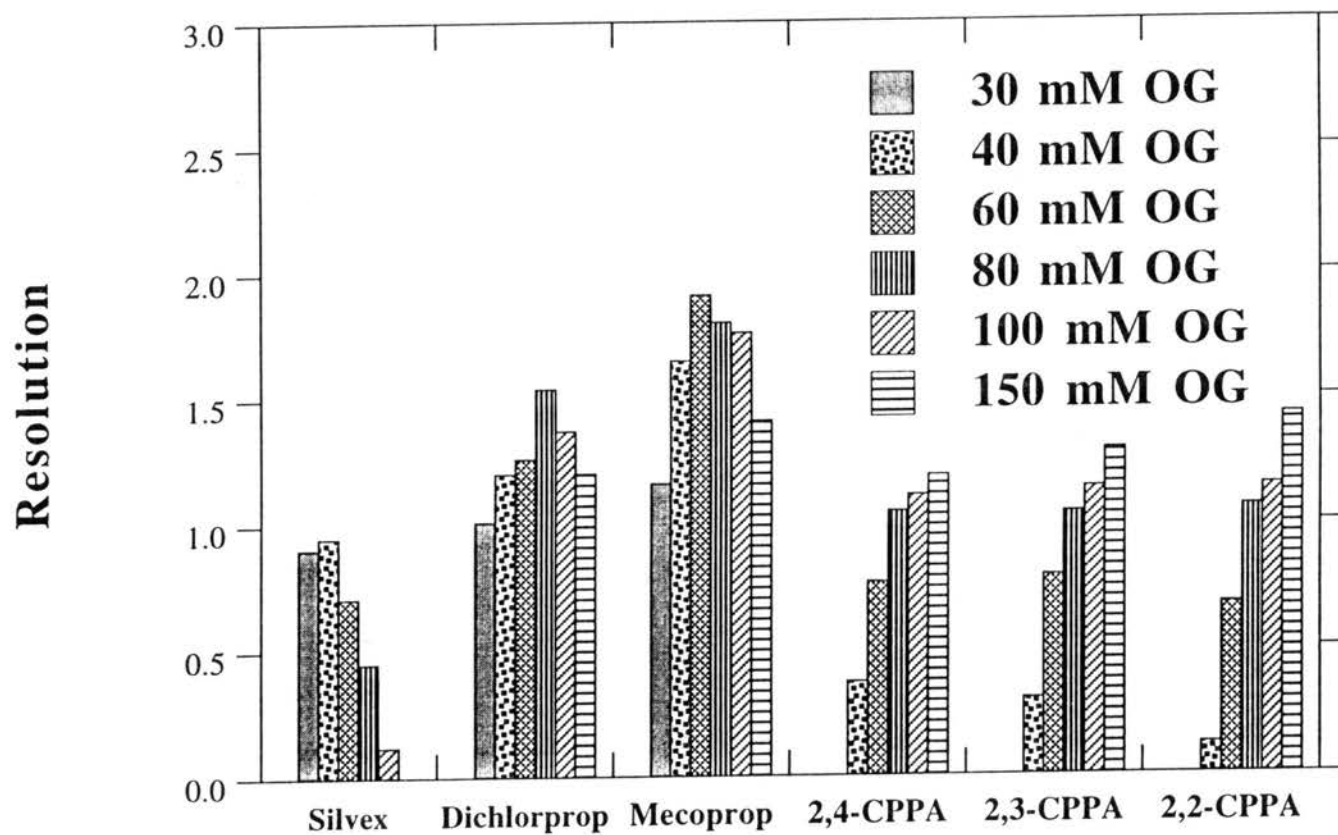


**Figure 5.** Bar graphs of the enantiomeric resolution of phenoxy acid herbicides at different OG concentration. Experimental conditions as in Fig. 2.

concentration for maximum enantiomeric resolution seems to decrease as the extent of the analyte solubilization in the OG micelle increases, which in the case of phenoxy acid herbicides seems to correlate with the hydrophobicity of the analyte. Generally, solute solubilization is believed to occur at a number of different sites in the micelle [38]: (i) on the surface of the micelle, i.e., at the micelle-solvent interface; (ii) between the hydrophilic head groups; (iii) in the so-called palaside layer of the micelle between the hydrophilic groups and the first few carbon atoms of the hydrophobic tails that comprise the outer core of the micellar interior; (iv) more deeply in the palaside layer; and (v) in the inner core of the micelle. Due to their ionic nature, the phenoxy acid herbicides are likely to be solubilized mainly in locus (ii) between the individual molecules of the surfactants in the palaside layer with the polar group of the solute, which is also the chiral center, oriented toward the polar, chiral group of the alkylglucoside surfactant and the nonpolar portion oriented toward the interior of the micelle. Depth of penetration in the palaside layer depends on the ratio of polar to nonpolar structures in the phenoxy acid herbicide molecules, with the less polar compounds penetrating more deeply than the more polar (i.e., less substituted) phenoxy acid herbicides. The depth of penetration will affect the enantioselectivity of the system. The deeper the solute will penetrate, the more its optical center will be pulled away from interacting with the chiral head group of the surfactant molecule, and consequently will cause a decrease in enantioselectivity. On the other extreme of the spectrum, the weaker the solubilization of the solute in the micelle, the less probable is the association between the micelle and the solute chiral centers, and the less is the enantiomeric resolution. Silvex, the most hydrophobic species among the analytes used in this study, attained maximum enantiomeric resolution at 40 mM OG, while the enantiomeric resolution of the weakly hydrophobic solutes namely 2,4-CPPA, 2,3-CPPA and 2,2-CPPA improved as OG concentration increased. Increasing the surfactant concentration results in increasing the concentration of the chiral centers in the overall micellar phase as well as increasing the nonpolar phase ratio in the electrolyte system.

Thus, for silvex, increasing OG concentration beyond 40 mM would have provided more chiral centers in the micellar phase than the optimum value for maximum resolution and/or increasing the OG concentration has resulted in the solute interacting more with the nonpolar portion than with the sugar chiral head groups in the palaside layer of the micelle. The enantiomeric resolution of the two solutes of intermediate hydrophobicity, namely mecoprop and dichlorprop, reached maximum values at 60 and 80 mM, respectively. The optimum surfactant concentration for maximum resolution is in the low range for hydrophobic solutes and in the high range for the less hydrophobic ones. The decrease in migration time for all the analytes as the concentration of OG increased is apparent by comparing Fig. 2a, b and c.

The alkyl chain of NG has one more carbon atom than the alkyl chain of OG, and the CMC value of NG is four times lower than that of OG (see Table I). As a result, the NG concentration needed to attain enantiomeric resolution is less than that needed for OG (compare Fig. 5 and 6). However, the dependence of enantiomeric resolution on NG concentration followed the same trend as that observed with OG. In other words, optimum enantiomeric resolution was attained for silvex at low NG concentration, for dichlorprop and mecoprop at intermediate NG concentration, and for 2,4-CPPA, 2,3-CPPA, 2,2-CPPA at high NG concentration. Again, no enantiomeric resolution of 2-PPA was observed even at 150 mM NG. The electropherograms of the phenoxy acid herbicides obtained at various NG concentrations are illustrated in Fig. 7 a, b and c. Note, silvex, dichlorprop and mecoprop were enantiomerically separated using 10 mM NG, since the CMC value of NG is 6.5 mM. Moreover, at this low surfactant concentration 2,4-CPPA and 2,3-CPPA as well as dichlorprop and mecoprop co-migrated. Again, as the concentration of the surfactant increased the migration time of the analytes decreased in a proportion that reflected the hydrophobicity of the analytes. The migration time of 2-PPA exceeded 45 min at 10 and 60 mM NG and decreased substantially to ca. 27 min at 150 mM NG.

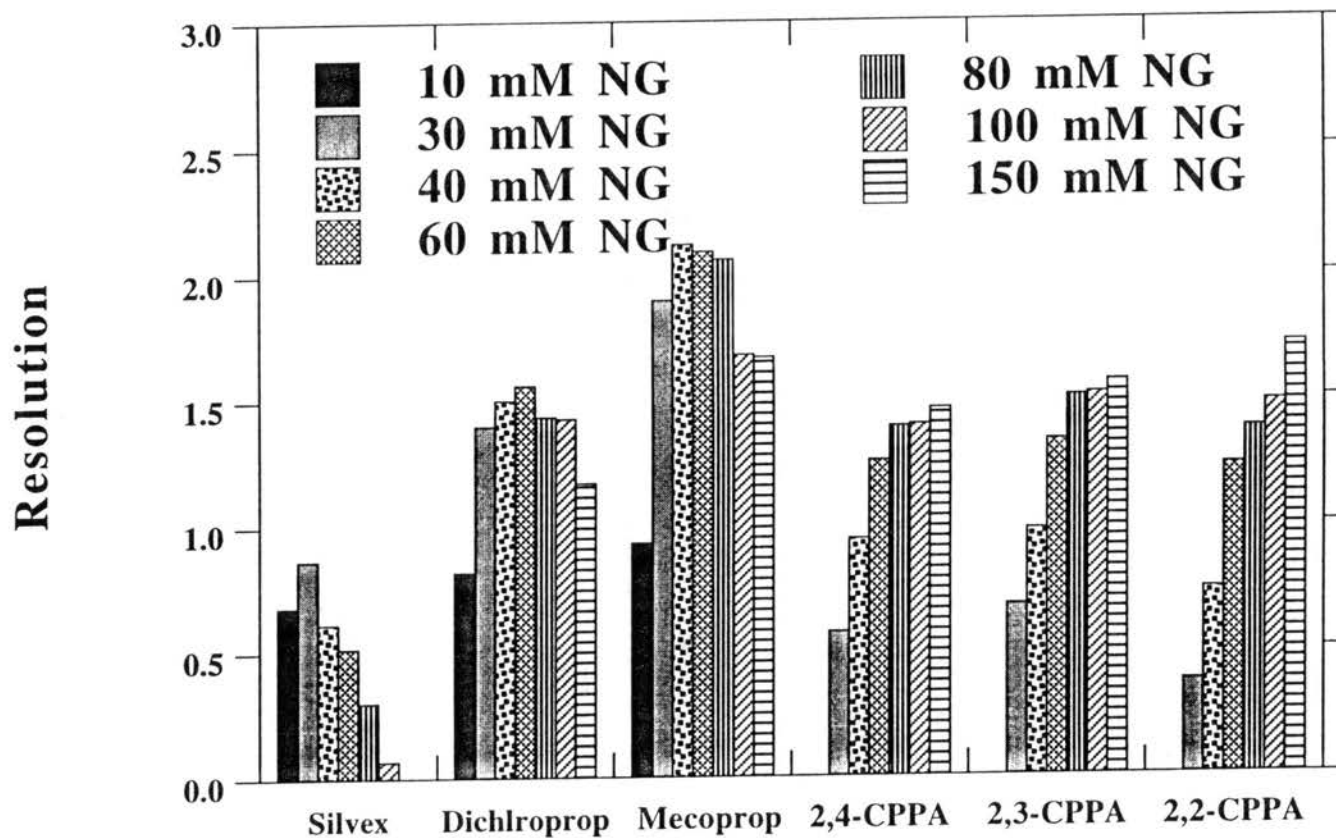


**Figure 6.** Bar graphs of the enantiomeric resolution of phenoxy acid herbicides at different NG concentrations. Conditions: running electrolyte, 200 mM sodium phosphate, pH 6.5, containing various NG concentrations. Other experimental conditions as in Fig. 4.

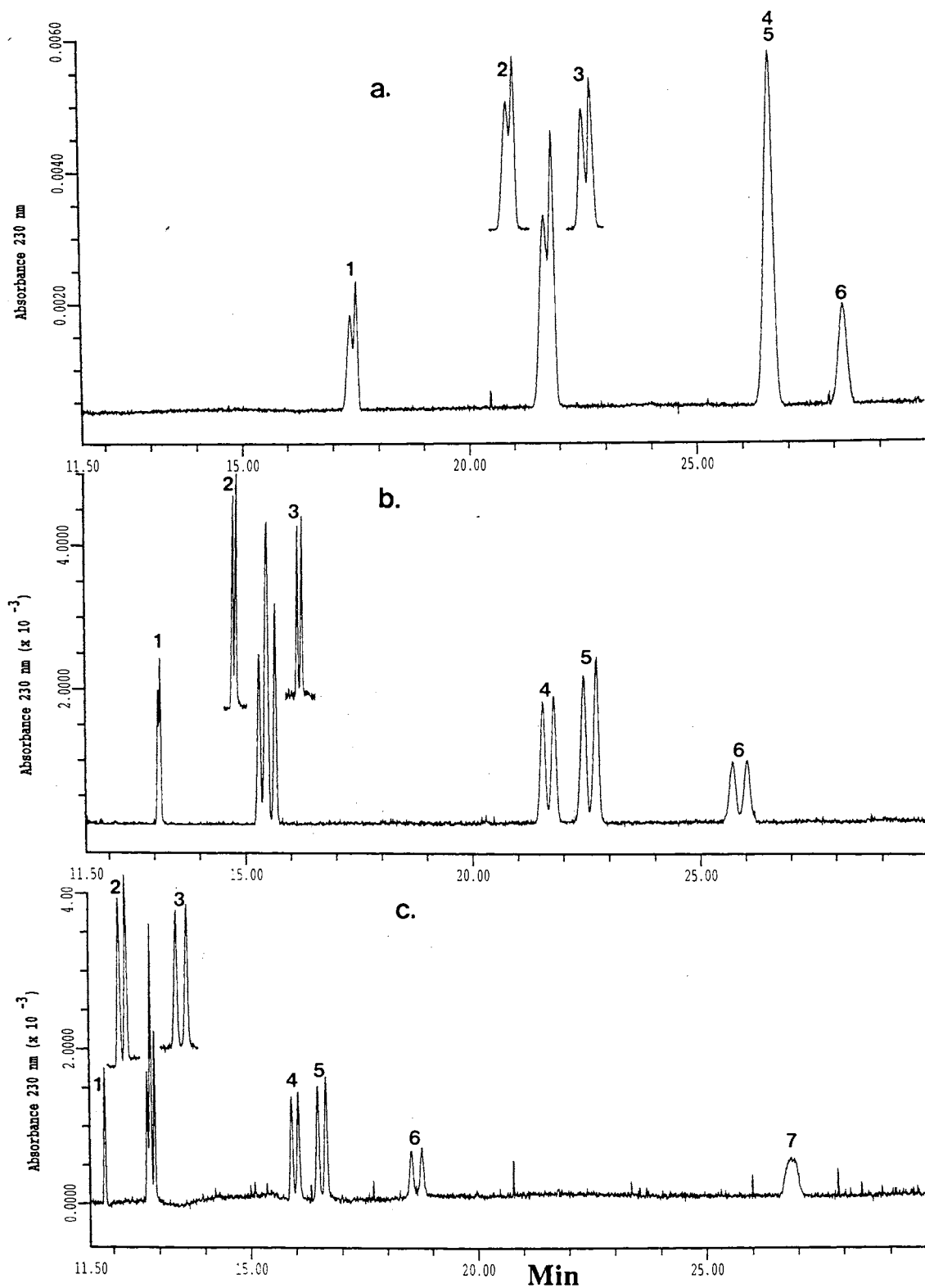


**Figure 7.** Electropherograms of phenoxy acid herbicides depicting the effect of NG concentration on enantiomeric resolution. Conditions: running electrolyte, 200 mM sodium phosphate, pH 6.5, containing 10 mM NG in (a), 60 mM NG in (b) and 150 mM NG in (c). Other conditions as in Fig. 4. Peaks, 1 = silvex, 2 = dichlorprop, 3 = mecoprop, 4 = 2,4-CPPA, 5 = 2,3-CPPA, 6 = 2,2-CPPA, 7 = 2-PPA.

The polar head of OM has one more glucopyranoside unit than the polar head of either OG or NG, thus increasing the chiral centers in the micelle as well as altering its characteristic micellar solubilization. As a result, the values of the enantiomeric resolution of the phenoxy acid herbicides obtained OM were higher than those attained using OG or NG (compare Fig. 8 to Fig. 5 and 6). However, the dependence of the enantiomeric resolution on OM concentration (see Fig. 8) followed the same trend observed with OG and NG. Optimum enantiomeric resolution for silvex, which is the most hydrophobic analyte, was attained at surfactant concentration of 30 mM (just above the CMC) while it decreased at higher OM concentrations. 2-PPA, the least hydrophobic analyte, was not enantiomerically separated even at a very high OM concentration, while the enantiomeric resolution of the weakly hydrophobic 2,4-, 2,3- and 2,2-CPPA increased as the OM concentration increased. The enantiomeric resolution of the solutes of intermediate hydrophobicity (e.g., dichlorprop and mecoprop) attained its maximum at an intermediate value, i.e., 60 mM OM. As can be seen in Fig. 9a, no enantiomeric resolution was observed for all analytes at surfactant concentration lower than CMC. Increasing the surfactant concentration results in increasing the phase ratios of both the chiral centers and the nonpolar phase of the micellar phase. Thus, for silvex, increasing OM concentration beyond 30 mM would have provided more chiral centers in the micellar phase than the optimum value for maximum resolution and/or increasing the OM concentration has resulted in the silvex solute undergoing more interaction with the nonpolar portion than the chiral maltoside head groups in the palaside layer of the micelle, thus causing enantiomeric resolution to decrease at elevated surfactant concentration. These same effects also explain the behavior of the other phenoxy acid herbicides such that the optimum surfactant concentration for maximum resolution is in the low range for hydrophobic solutes and in the high range for the less hydrophobic ones. Again, the decrease in migration time for all the analytes as the concentration of the surfactant increased is apparent for OM by comparing Fig. 9a, b and c.



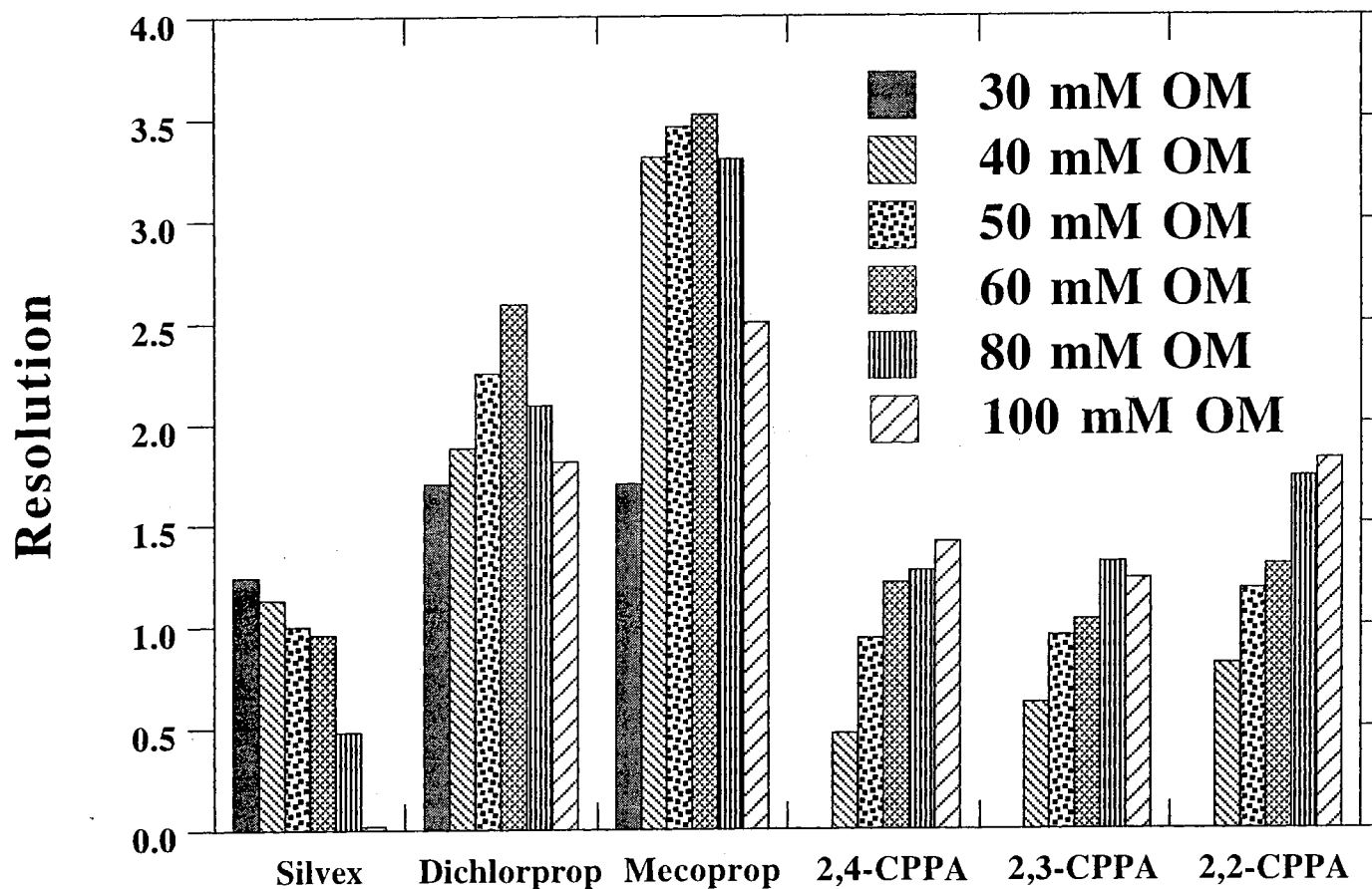


**Figure 8.** Bar graphs of the enantiomeric resolution of phenoxy acid herbicides at different OM concentrations. Conditions: running electrolyte, 175 mM sodium phosphate, pH 6.5, containing various concentrations of OM; voltage, 25 kV; capillary, bare fused-silica, 50 cm (to detection window) 57 cm (total length) x 50  $\mu$ m I.D.; separation temperature, 15°C.

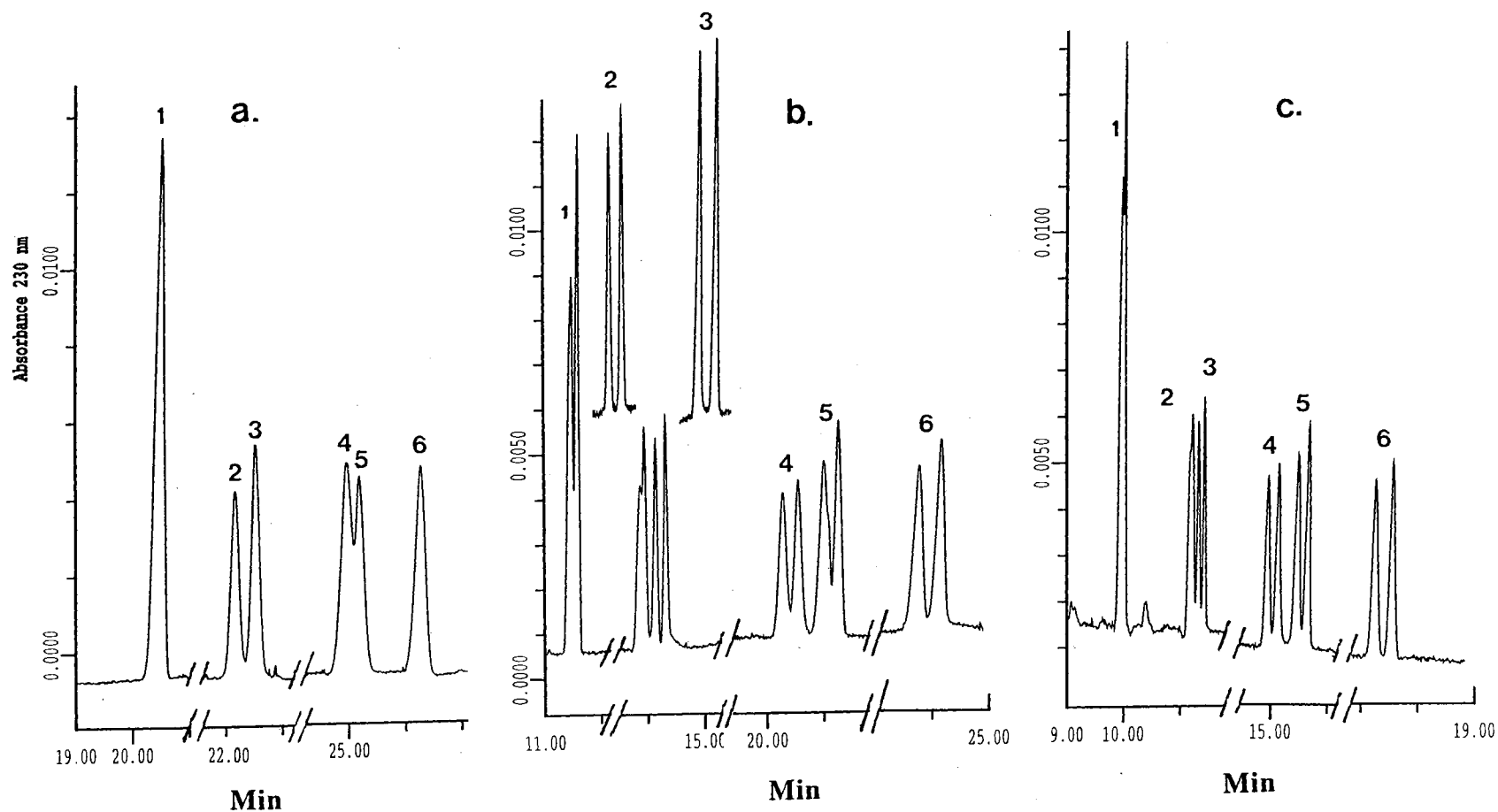


**Figure 9.** Electropherograms of phenoxy acid herbicides at various OM concentrations. Conditions: running electrolytes, 175 mM sodium phosphate, pH 6.5, containing 10 mM OM in (a), 60 mM OM in (b), and 100 mM OM in (c). Other conditions as in Fig. 8. Peaks, 1 = silvex, 2 = dichlorprop, 3 = mecoprop, 4 = 2,4-CPPA, 5 = 2,3-CPPA, 6 = 2,2-CPPA, 7 = 2-PPA.

In summary, the chiral selectivity of the alkylglucoside surfactants is based on the interaction between the analyte and the optically active sugar residue of the surfactant in the micellar phase. This was deduced from the fact that the enantiomeric selectivity toward the phenoxy acid herbicides was not achieved using the alkylglucoside surfactants at concentration below CMC. In the concentration range above CMC, increasing the concentration of the surfactant increases the micellized surfactant concentration, i.e.,  $[S]$ -CMC, thus ensuring an increasing number of chiral sites in the micellar form. However, optimum enantiomeric resolution is attained at a certain surfactant concentration, and this concentration is in turn dependent on the hydrophobicity of the analytes. As expected, and because of the lower CMC value, increasing the length of the alkyl tail of the surfactant leads to an optimum enantiomeric resolution at lower surfactant concentration. Also, increasing the number of glucose units in the polar head results in achieving higher enantiomeric resolution. Other factors were also found to influence the enantiomeric resolution including the pH and the ionic strength of the buffer, the use of methanol, as well as the separation temperature, see below.

#### Effect of pH and Ionic Strength

Because of the ionic nature of the phenoxy acid herbicides, the pH has a strong influence on their migration and interaction with the alkylglucoside micelle, and consequently on their enantiomeric resolution. First, with the exception of the solutes of intermediate hydrophobicity such as mecoprop and dichlorprop, which showed a maximum resolution at pH 6, increasing the pH of the running electrolyte decreased resolution in the pH range studied, see Fig. 10. This may be due to the decreasing solute-micelle interaction arising from increasing the ionization of the solutes with increasing pH. As far as the resolution of the majority of the enantiomers is concerned, higher enantiomeric resolutions were attained at pH 5.0 (Fig. 11a) than at pH 7.0 (Fig. 11b), yet the separation time was much longer at low pH due to the low EOF. Therefore, a compromise between

enantiomeric resolution and analysis time was reached, and all the studies were performed at pH 6.5.

The effect of the ionic strength of the running electrolyte on the enantiomeric resolution is illustrated in Fig. 12. Increasing the ionic strength of the running electrolyte seems to improve the enantiomeric resolution of all analytes. Increasing the ionic strength of the separation electrolyte decreases the EOF as well as the effective electrophoretic mobility of the analytes with an overall decrease in the apparent mobility of the analytes, i.e., increasing the analysis time (results not shown). Also, increasing the ionic strength of the running electrolyte is known to cause a decrease in the CMC of the surfactant and an increase in the aggregation number [39,40]. This will increase the micellized surfactant concentration ( $[S]-CMC$ ) and in turn will increase the number of chiral centers in the micellar form, thus augmenting the solubilization of the various analytes by the micellar phase and increasing the chiral association between the solutes and the chiral micelles, respectively. In addition, increasing the ionic strength has a salting out effect which should afford stronger nonpolar interaction between the solutes and the chiral micelles. Thus, increasing the ionic strength of the running electrolyte results in strengthening both solute solubilization into the micelle and its chiral association with the chiral micelle. These two effects, which arise from increasing the ionic strength of the running electrolyte, seem to increase the enantiomeric resolution of all analytes. On the other hand, increasing the ionic strength resulted in longer analysis time from ca. 13 min at 50 mM sodium phosphate to ca. 30 min at 200 mM sodium phosphate. It should be noted that there is a limit for increasing the ionic strength due to the increase in conductivity, and consequently Joule heating at elevated ionic strength. Under the conditions of Fig. 12, 200 mM phosphate was the limit to which the ionic strength could be increased without introducing undesirable Joule heating effects.

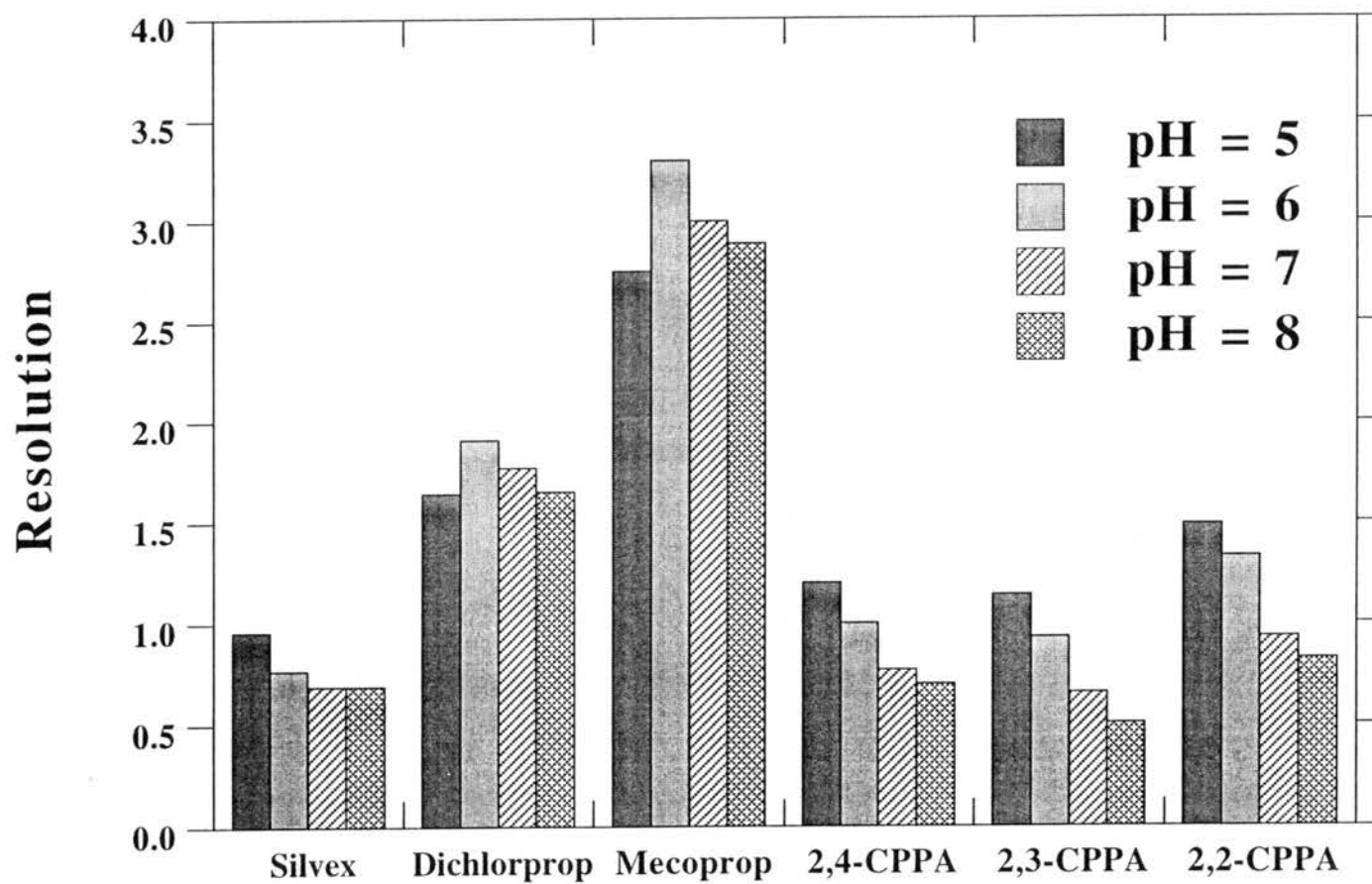


**Figure 10.** Bar graphs of the enantiomeric resolution of phenoxy acid herbicides at different pH values of the running electrolyte. Conditions: running electrolyte, 100 mM sodium phosphate-sodium acetate, various pH values, containing 60 mM OM. Other experimental conditions as in Fig. 8.

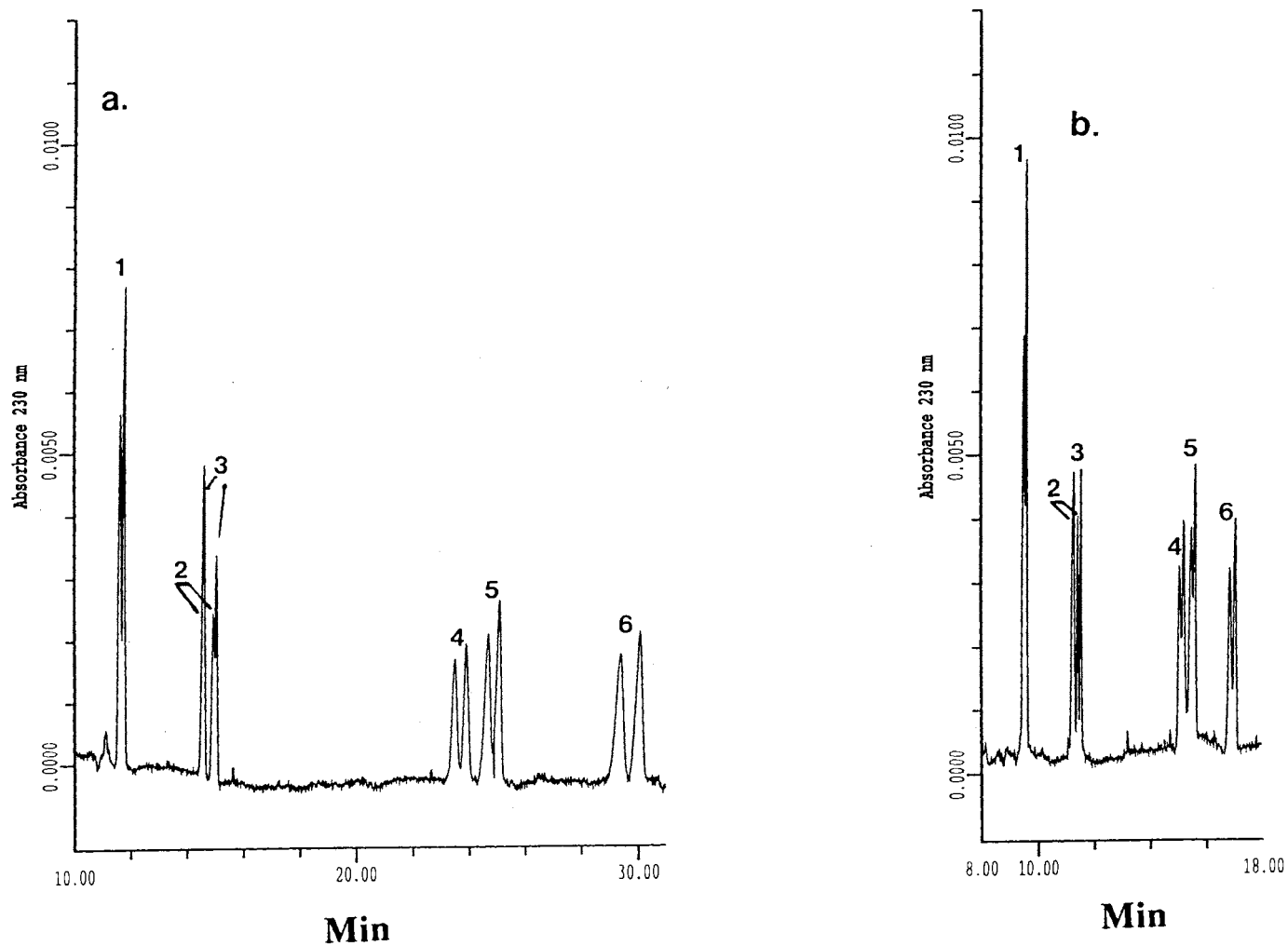


**Figure 11.** Electropherograms of phenoxy acid herbicides at different pH values of the running electrolyte. Conditions: running electrolyte, 100 mM sodium phosphate-sodium acetate, pH 5.0 in (a) and pH 7.0 in (b), containing 60 mM OM. Other experimental conditions as in Fig. 8. Peaks, 1 = silvex, 2 = dichlorprop, 3 = mecoprop, 4 = 2,4-CPPA, 5 = 2,3-CPPA, 6 = 2,2-CPPA.

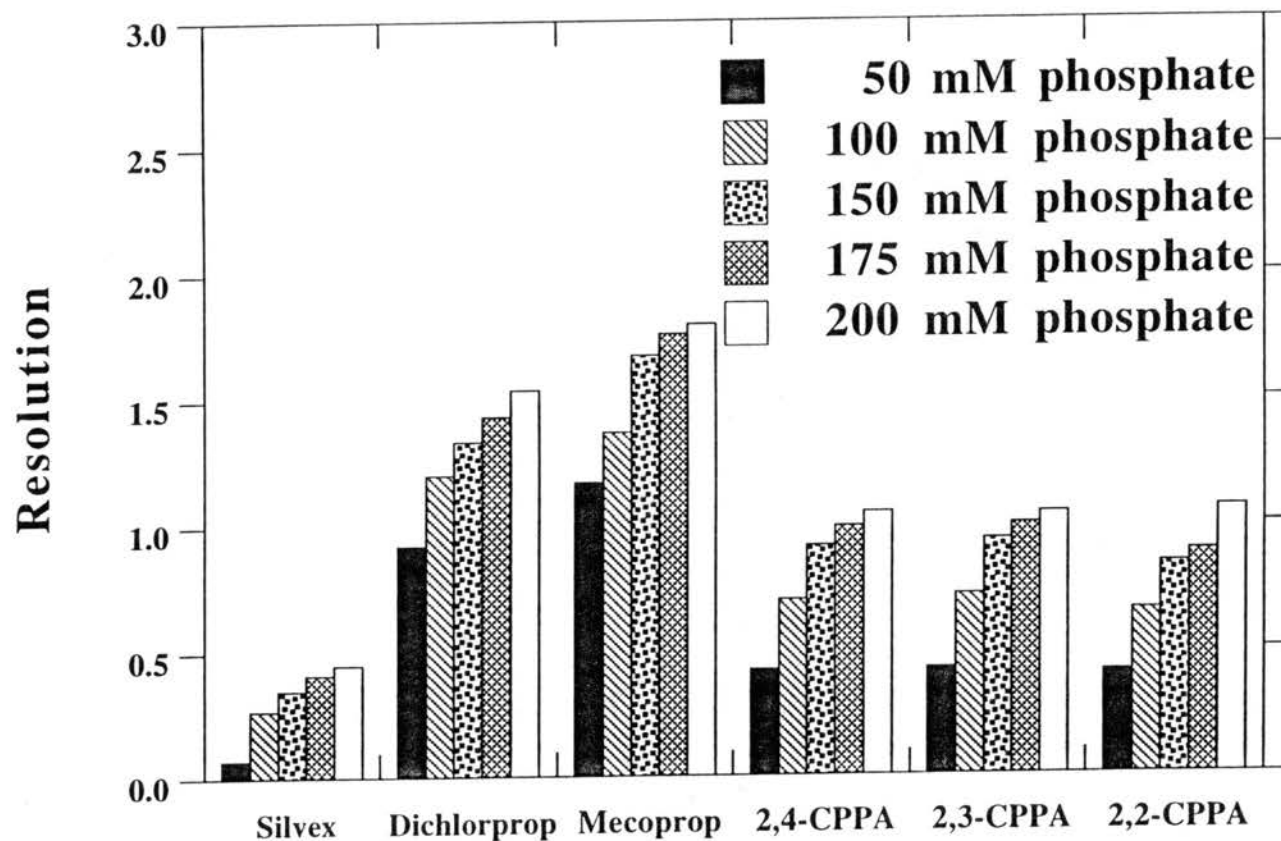


**Figure 12.** Bar graphs of the enantiomeric resolution of phenoxy acid herbicides at different ionic strength of the running electrolyte. Conditions: running electrolyte, various sodium phosphate concentrations, pH 6.5, containing 80 mM OG. Other experimental conditions as in Fig. 4.

### Effect of Methanol

To further gain insight into the underlying of the chiral separation brought about by the electrophoretic systems under investigation and using OM as a typical alkylglucoside surfactant, the effect of the percent methanol in the running electrolyte on the enantiomeric resolution of the phenoxy acid herbicides was examined. As expected, the enantiomeric resolution of the various analytes was affected differently by the addition of methanol to the separation electrolyte, see Fig. 13. The effect of methanol correlates satisfactorily with the hydrophobicity of the analytes. For all practical purposes, the CMC and the aggregation number of the micelle can be considered unaffected by the addition of methanol since in the percent range studied (i.e., from 0% to 10% v/v), there is a slight inhibitory effect of methanol on the micellization process [41]. The enantiomeric resolution of silvex, which is the most hydrophobic compound, improved upon the addition of methanol to the separation electrolyte. This suggests that for this hydrophobic compound, the addition of methanol may have adjusted the degree of penetration of the solute (probably by a competition effect) in the palaside layer to favor better polar interaction with the chiral head group of the surfactant molecule, thus improving the enantioselectivity toward silvex, see Fig. 13. On the other hand, the least hydrophobic analytes, 2,4-, 2,3- and 2,2-CPPAs, suffered an opposite effect. This would suggest that the addition of methanol has weakened the interaction of the solute with the palaside layer thus lowering the probability of the solute to encounter the chiral center of the surfactant and associate with. For dichlorprop and mecoprop (solutes of intermediate hydrophobicity), the enantiomeric resolution was slightly affected for dichlorprop and exhibited a maximum for mecoprop. This behavior can be equally explained by the effect of methanol on modulating the degree of penetration of the solute in the palaside layer and its subsequent interaction with the chiral polar head group. Moreover, the addition of methanol decreased the EOF due to increasing the viscosity of the running electrolyte, and consequently, the analysis time almost doubled upon the addition of 10% (v/v) of methanol to the separation electrolyte.



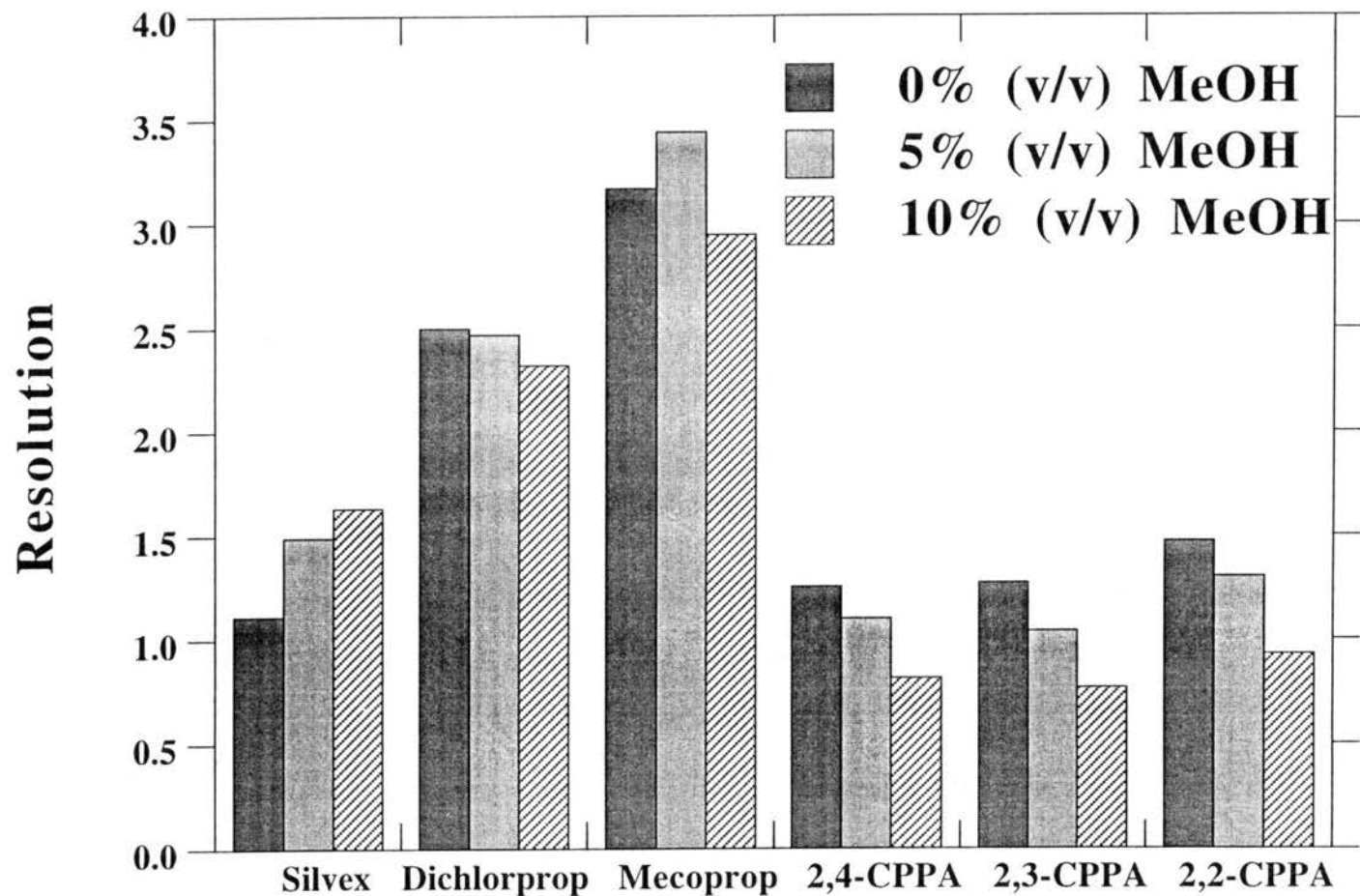


**Figure 13.** Bar graphs of the enantiomeric resolution of phenoxy acid herbicides at different percentages of methanol added to the running electrolyte. Conditions: running electrolyte, 175 mM sodium phosphate, pH 6.5, containing 60 mM OM and various percentage of methanol. Other experimental conditions as in Fig. 8.

### Effect of Temperature

As shown in Fig. 14, decreasing the separation temperature increased the enantiomeric resolution of all analytes. Temperature has various influences on the electrophoretic system under investigation. The effect of temperature on the CMC of surfactants in aqueous medium is complex, the value appearing first to decrease with temperature to some minimum and then to increase with further increase in temperature [38]. The minimum in the CMC-temperature dependence is around 50°C for nonionic surfactants as the ones used in this study [38]. Increasing temperature causes decreased hydration of the hydrophilic group, which favors micellization. This in principle should increase the number of interacting micelles in the temperature range 10 to 30°C and in turn the enantiomeric resolution. However, increasing temperature favors the partitioning of the solute in the aqueous phase, and this may explain the continuous decrease in the enantiomeric resolution as the temperature is increased from 10 to 30°C. Also, increasing temperature decreases the viscosity of the separation buffer. This effect combined with the decrease in the partitioning of the solute in the micelle may have resulted in increasing the effective electrophoretic mobility of all analytes as the separation temperature increased (Fig. 15). This is supported by the sharper increase in the effective electrophoretic mobility of the least hydrophobic analytes (see Fig. 15), which were shown to need high micellar phases to attain enantiomeric resolution (see Figs 5 ,6 and 8).

### Chiral Separation under Optimized Conditions

Optimization of all of the aforementioned parameters (i.e., surfactant concentration, ionic strength and temperature) allowed the enantiomeric resolution of all analytes in a single run using NG (Fig. 16a) OG (Fig. 16b) or OM (Fig. 17). Baseline enantiomeric resolution of all analytes except silvex was attained by performing the separation at 10°C and using 250 mM sodium phosphate buffer, pH 6.5, containing 50 mM NG or 70 mM OG. Again, and as expected, higher enantiomeric resolution for all analytes except silvex

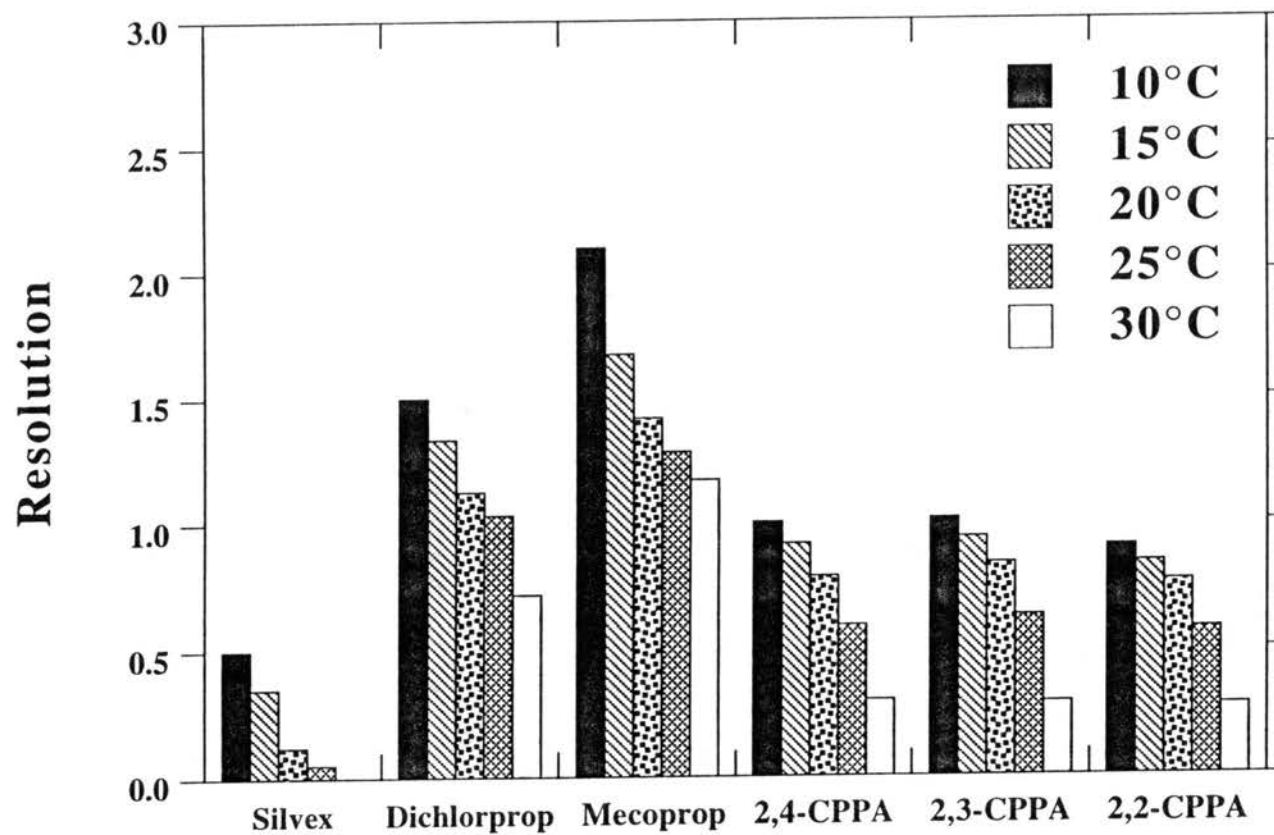


**Figure 14.** Bar graphs of the enantiomeric resolution of phenoxy acid herbicides at different temperatures. Conditions; running electrolyte, 150 mM sodium phosphate, pH 6.5, containing 80 mM OG. Other experimental conditions as in Fig. 4.

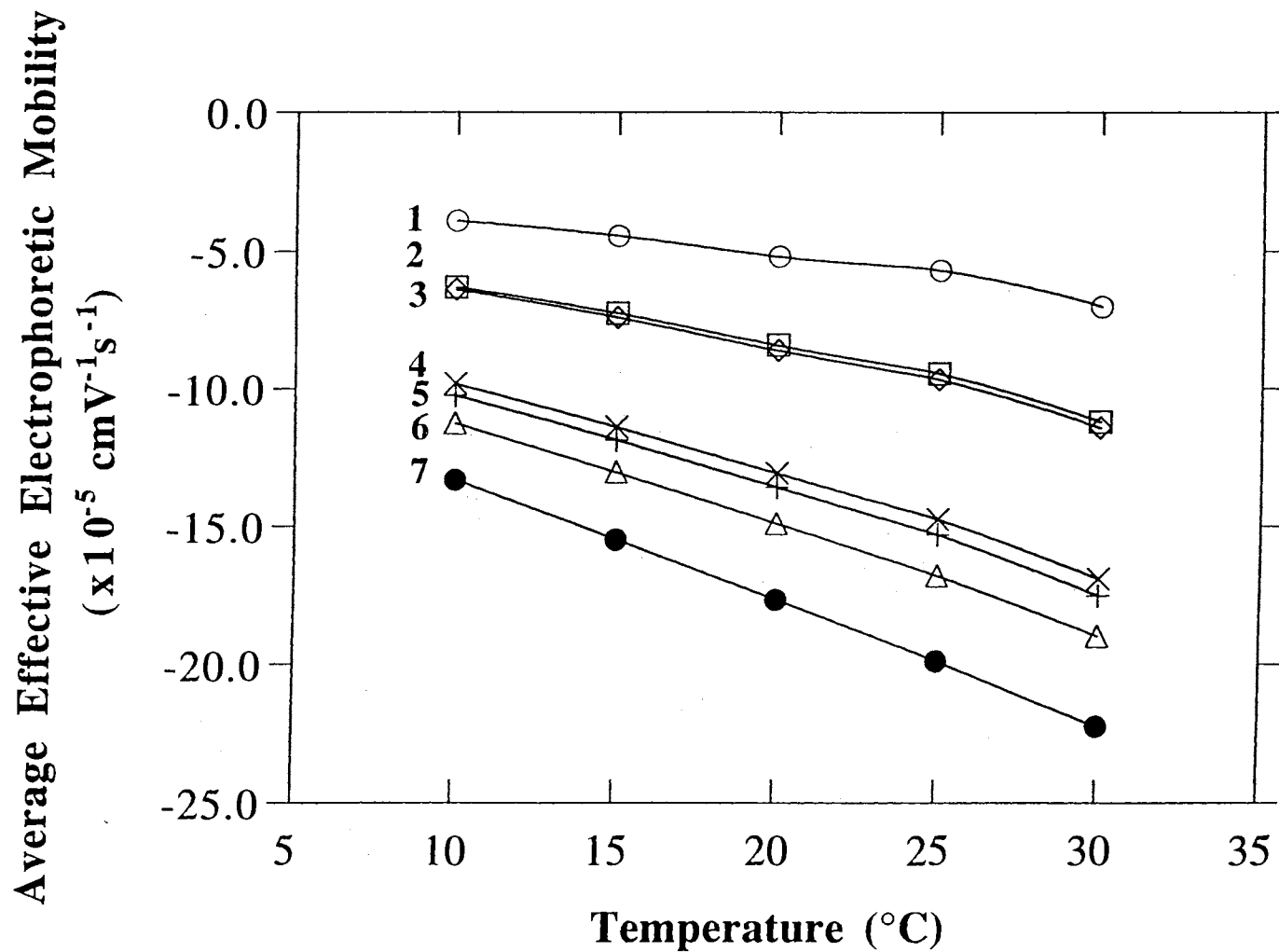


**Figure 15.** Plots of the average effective electrophoretic mobility of phenoxy acid herbicide enantiomers versus separation temperature. Conditions: running electrolyte, 150 mM sodium phosphate, pH 6.5, containing 80 mM OG. Other experimental conditions as in Fig. 4. Curves, 1 = silvex, 2 = dichlorprop, 3 = mecoprop, 4 = 2,4-CPPA, 5 = 2,3-CPPA, 6 = 2,2-CPPA, 7 = 2-PPA.

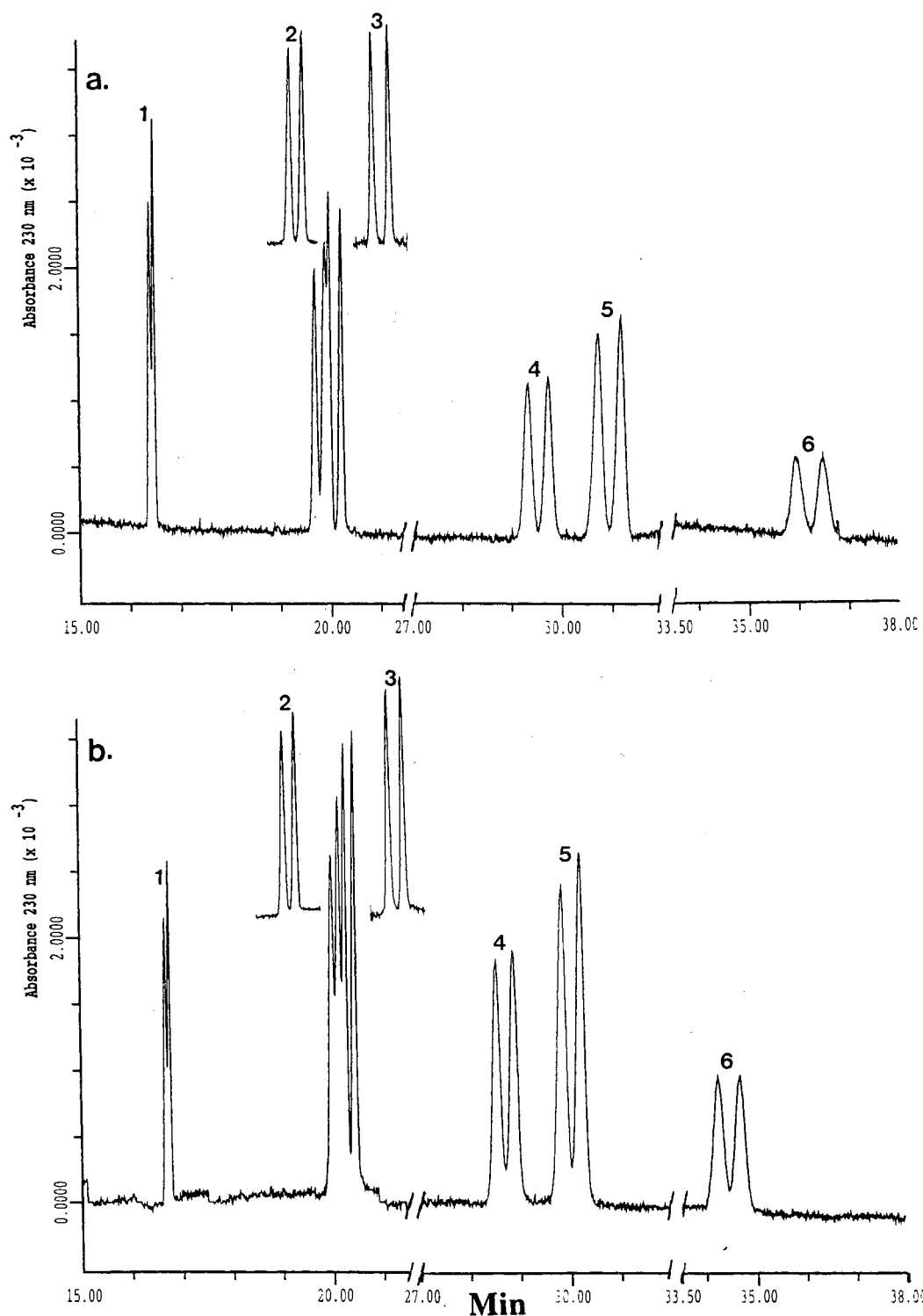


**Figure 16.** Electropherograms of phenoxy acid herbicides depicting optimum enantiomeric resolution using NG (a) or OG (b). Conditions: running electrolyte, 250 mM sodium phosphate, pH 6.5, containing 50 mM NG in (a) and 70 mM OG in (b); temperature, 10°C. Other experimental conditions as in Fig. 4.

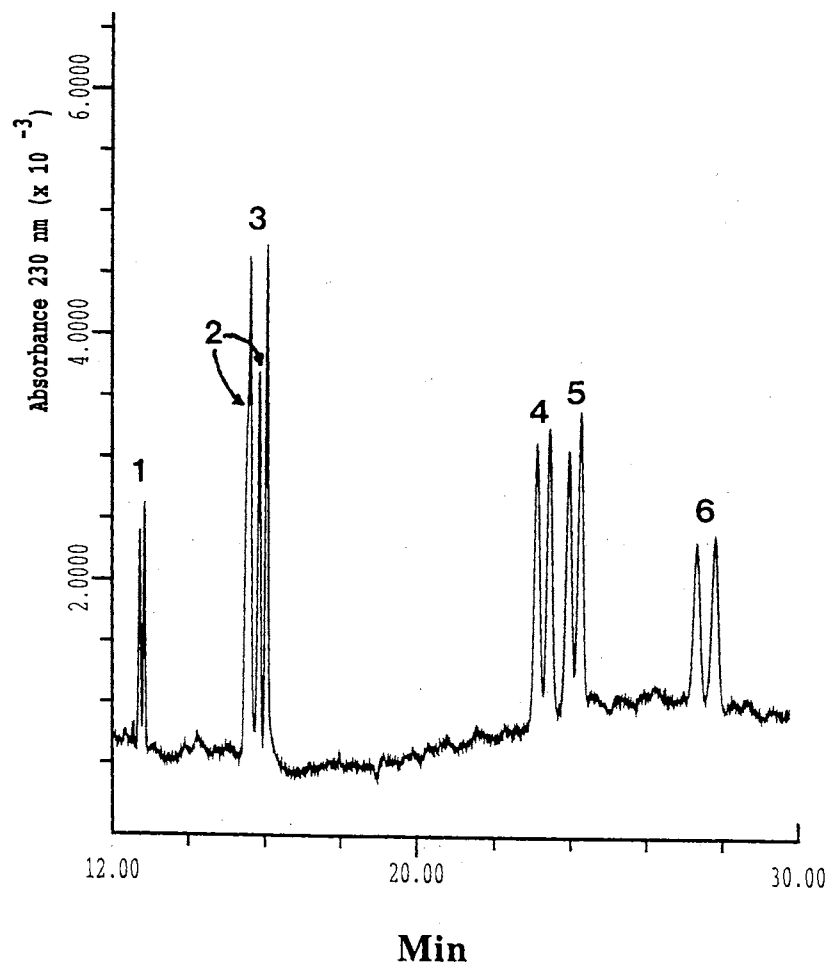


**Figure 17.** Optimum enantiomeric resolutions of phenoxy acid herbicides using OM. Conditions: running electrolyte, 200 mM sodium phosphate, pH 6.5, 60 mM OM; temperature, 10°C. Other experimental conditions as in Fig. 8. Peaks, 1 = silvex, 2 = dichlorprop, 3 = mecoprop, 4 = 2,4-CPPA, 5 = 2,3-CPPA, 6 = 2,2-CPPA.

were attained with NG. Also, NG required less surfactant concentration than OG for maximum resolution. In the case of OM, baseline enantiomeric resolution of analytes including silvex was attained using 200 mM sodium phosphate buffer, pH 6.5, containing 60 mM OM, and performing the separation at 10°C.

#### Enantiomeric Separation of Other Solutes

Although phenoxy acid herbicides served as model solutes to evaluate the properties and utility of alkylglucosides as chiral selectors, the surfactants are also effective in promoting enantiomeric resolution of other solutes investigated in this study including dansyl amino acids, BNPO<sub>4</sub> and pharmaceuticals such as warfarin and bupivacaine.

Dansyl Amino Acids. Chiral separations of dansyl amino acids using OM are illustrated in Fig. 18a-d. Similar to phenoxy acid herbicides, the surfactant concentration required to attain optimum enantiomeric resolution of the five dansyl amino acids under investigation was a function of their hydrophobicity. Enantiomeric resolution of tryptophan and phenylalanine was only attainable at low OM concentrations (i.e., 25-30 mM for tryptophan and 25-40 mM for phenylalanine, Fig. 19 and Fig. 18b), while moderate OM concentrations were needed to attain optimum enantiomeric resolution for leucine, methionine and valine (i.e., 30 mM for leucine and methionine and 40 mM for valine), see Fig. 18 c and d. Like phenoxy acid herbicides, the enantiomeric resolution of all dansyl amino acids was absent at surfactant concentration below CMC (see Fig. 18 a).

The enantiomeric resolution of dansyl amino acids was also attained using OG or NG (Fig. 20). The dependence of the enantiomeric resolution on the concentration of OG or NG followed the same trend observed with OM. However, tryptophan was not enantiomerically resolved at any concentration of OG or NG (Fig. 20). Phenylalanine enantiomeric resolution decreased as the concentration of NG or OG decreased. On the other side of the spectrum, optimum enantiomeric resolution of leucine, valine and methionine was attained at 30 mM OM. Note that no enantiomeric resolution for any

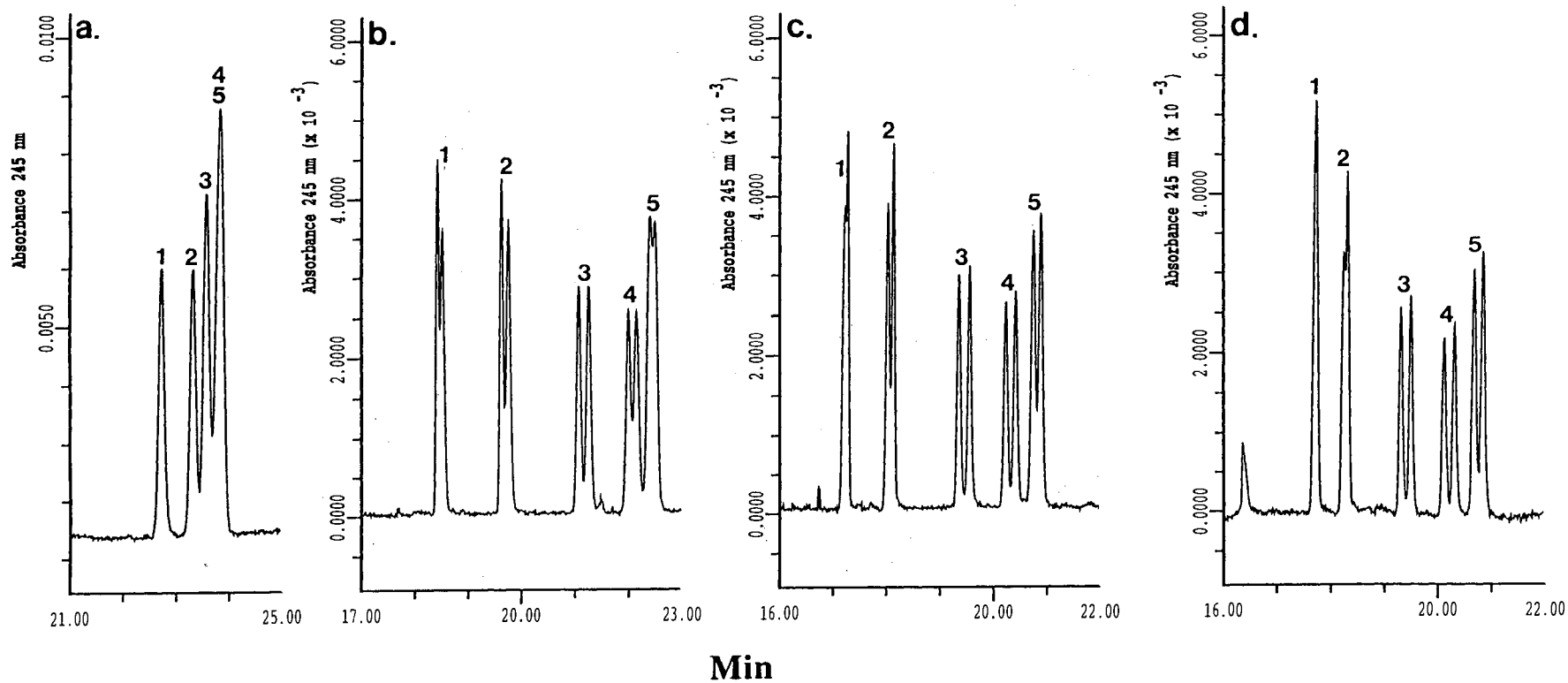


**Figure 18.** Electropherograms of dansyl amino acids. Conditions: running electrolyte, 200 mM sodium phosphate, pH 6.5, containing 10 mM OM in (a), 25 mM OM in (b), 30 mM in (c) and 40 mM OM in (d); voltage, 15 kV. Other experimental conditions as in Fig. 8. Peaks, 1 = tryptophan, 2 = phenylalanine, 3 = leucine, 4 = methionine, 5 = valine.



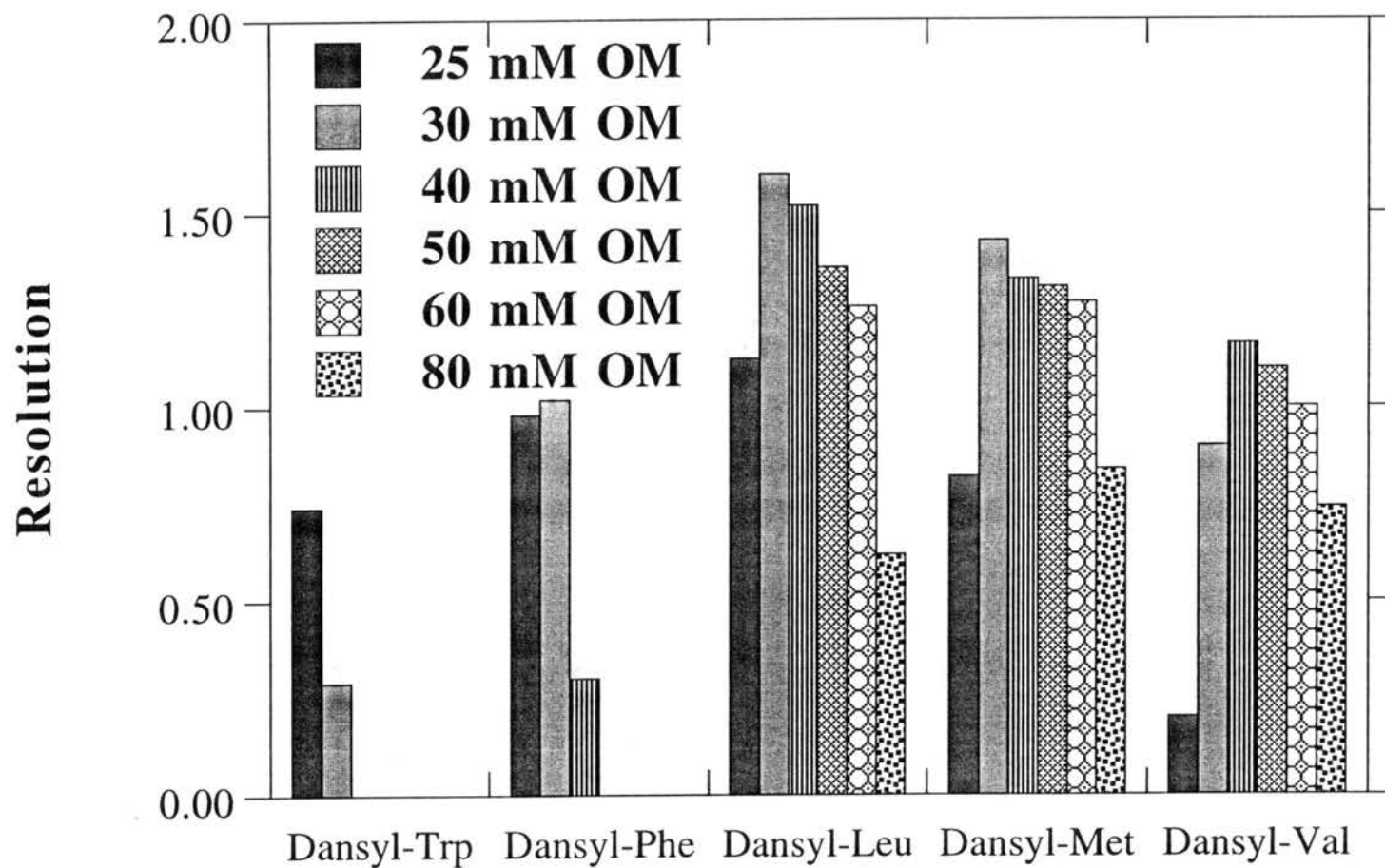


**Figure 19.** Bar graphs of the enantiomeric resolution of dansyl amino acids at different OM concentration. Experimental conditions as in Fig. 18.

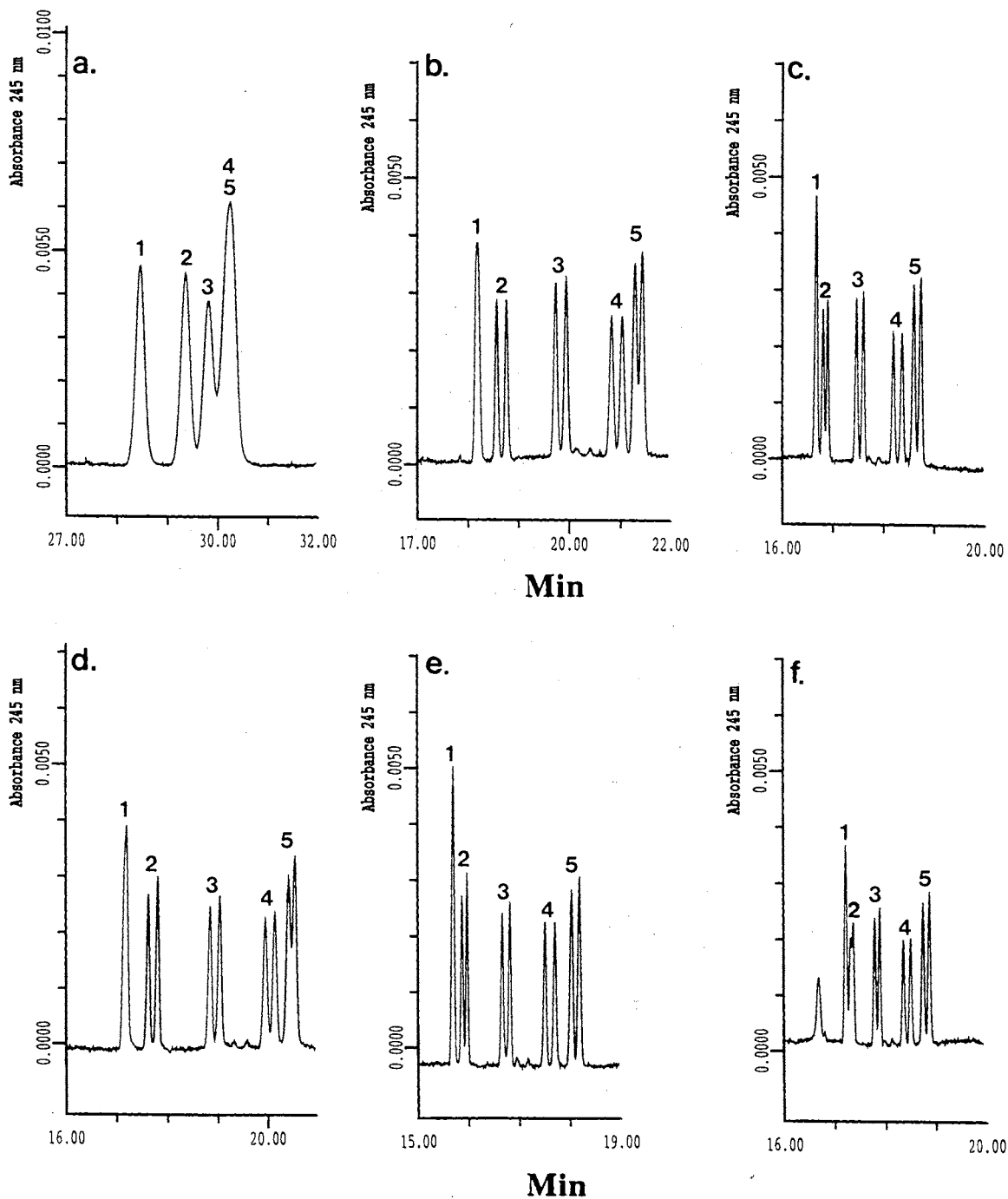


**Figure 20.** Electropherograms of dansyl amino acids. Conditions: running electrolyte, 200 mM sodium phosphate, pH 6.5, containing 10 mM OG (a), 30 mM OG (b), 60 mM OG (c), 10 mM NG (d), 30 mM NG (e) and 60 mM NG (f). Other experimental conditions as in Fig. 4. Peaks, 1 = tryptophan, 2 = phenylalanine, 3 = leucine, 4 = methionine, 5 = valine.

dansyl amino acids was achieved at OG concentration lower than its CMC (Fig. 20a). On the other hand, the enantiomeric resolution achieved at 10 mM NG (Fig. 20d) was expected since the CMC of NG is about 6.5 mM (see Table I). Unlike phenoxy acid herbicides, the values of the enantiomeric resolution achieved using NG or OG were higher than those achieved using OM. However, similar to phenoxy acid herbicides, the migration of the anionic dansyl amino acids were in the order of decreasing hydrophobicity, since the higher is the hydrophobicity of the solute, the higher its solubilization in the micelle which is traveling with the cathodal EOF velocity, and consequently the slower its migration toward the anode.

1,1'-Binaphthyl-2,2'-diylhydrogen phosphate. Optimum enantiomeric resolution of BNPO<sub>4</sub>, which is a very hydrophobic species, was only achievable at low surfactant concentrations (Fig. 21a and 21b). Furthermore, the relatively high hydrophobicity of BNPO<sub>4</sub> permitted its enantiomeric resolution even at surfactant concentrations lower than CMC value of OM (Fig. 21a). The interactions between BNPO<sub>4</sub> and OM monomers were sufficient to achieve the enantiomeric resolution. However, this was not true for OG and the enantiomeric resolution was only achieved at concentrations above CMC (Fig. 21c and 21d). The high hydrophobicity of BNPO<sub>4</sub> was also the reason for which low NG concentrations were required to achieve baseline enantiomeric resolution (Fig. 21e and 21f).

Warfarin. Warfarin, an anticoagulant, was enantiomerically resolved only using OM surfactant. However, the addition of borate to the separation electrolyte was needed to form in situ charged micelles, and consequently enhance the enantiomeric resolution of the warfarin which is weakly acidic (pK<sub>a</sub> of the phenolic group = 5.1 [42]). Since the analysis was performed at low pH (pH 6.5), high borate concentration was needed to charge the

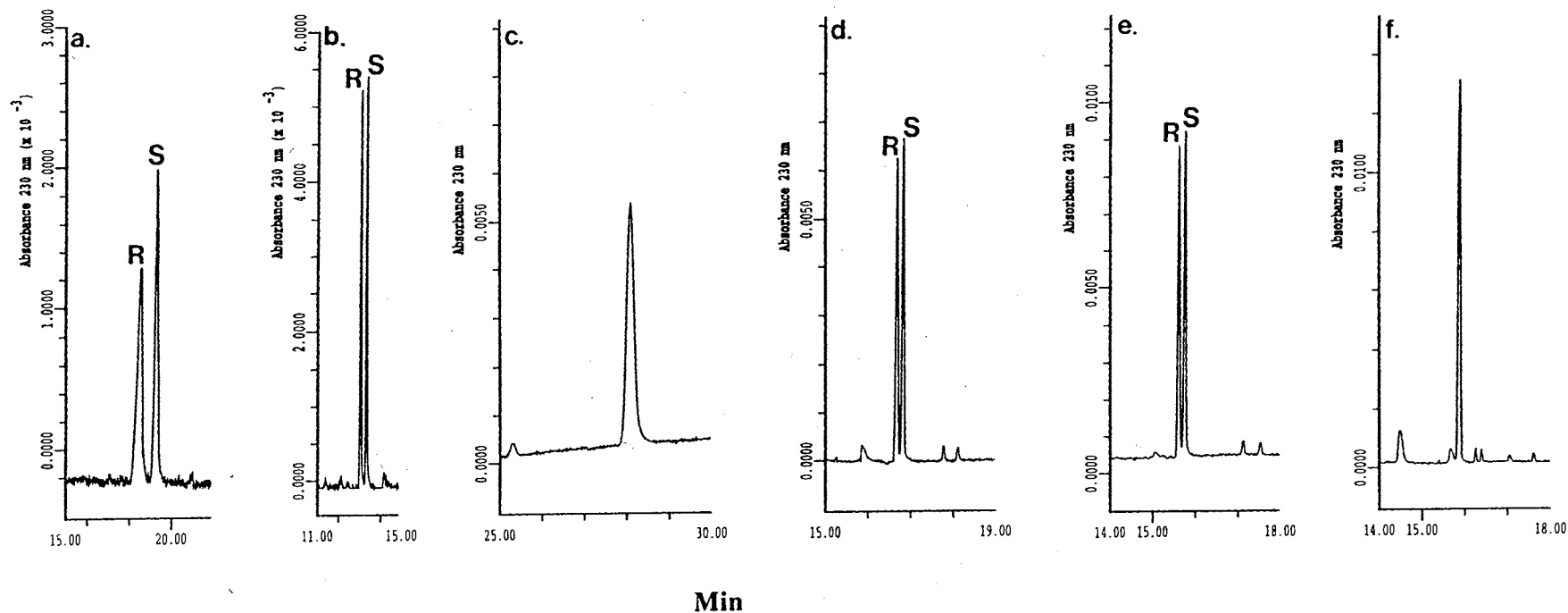


**Figure 21.** Electropherograms of 1,1'-binaphthyl-2,2'-diylhydrogen phosphate. Conditions: running electrolyte, 150 mM sodium phosphate, 400 mM sodium borate, pH 6.5, containing 15 mM OM in (a), and 30 mM OM in (b); and 200 mM sodium phosphate, pH 6.5, containing 10 mM OG in (c), 30 mM OG in (d), 10 mM NG in (e) and 30 mM NG in (f); voltage, 20 kV. Other experimental conditions as in Fig. 4.

micelle. This was explained in a recent report by our laboratory [43] (see Chapter IX). Optimum enantiomeric resolution of warfarin was achieved using a buffer consisting of 250 mM sodium phosphate and 400 mM sodium borate, pH 6.5 containing 60 mM OM (Fig. 22).

Bupivacaine. The enantiomeric resolution of bupivacaine a local anesthetic solute was only attainable at a very high surfactant concentration, i.e., 150 mM. This is due to the fact that bupivacaine is cationic and is migrating faster than the non-ionic surfactant OM which is migrating with the electroosmotic flow. As shown in Fig. 23, optimum enantiomeric resolution was attained using a buffer consisting of 200 mM sodium phosphate and 400 mM sodium borate, pH 6.5, containing 150 mM OM. No enantiomeric resolution was achieved using NG or OG at any concentration (results not shown).

### Conclusions

Three chiral alkylglucoside surfactants, namely n-octyl- (OG) and n-nonyl- $\beta$ -D-glucopyranoside (NG), and octyl- $\beta$ -D-maltopyranoside (OM) were evaluated in the enantiomeric separation of phenoxy acid herbicides and other species. The enantiomeric resolution could be manipulated readily by adjusting the surfactant concentration, ionic strength, pH and separation temperature. The optimum surfactant concentration needed for maximum enantiomeric resolution varied among the different analytes, and was an inverse function of the hydrophobicity of the phenoxy acid herbicides with the most hydrophobic solutes requiring less surfactant concentration for attaining a baseline enantiomeric resolution. Due to the ionic nature of the phenoxy acid herbicides, increasing the pH of the running electrolytes increased the degree of ionization of the acidic herbicides, thus decreasing their association with the chiral micelles and in turn their enantiomeric resolution. Increasing the ionic strength seems to enhance both the solubilization of the solute in the micelle and the chiral interaction of the solute with the micelle with a net increase in enantiomeric resolution. Methanol added at low percent (<10 % v/v) seems to

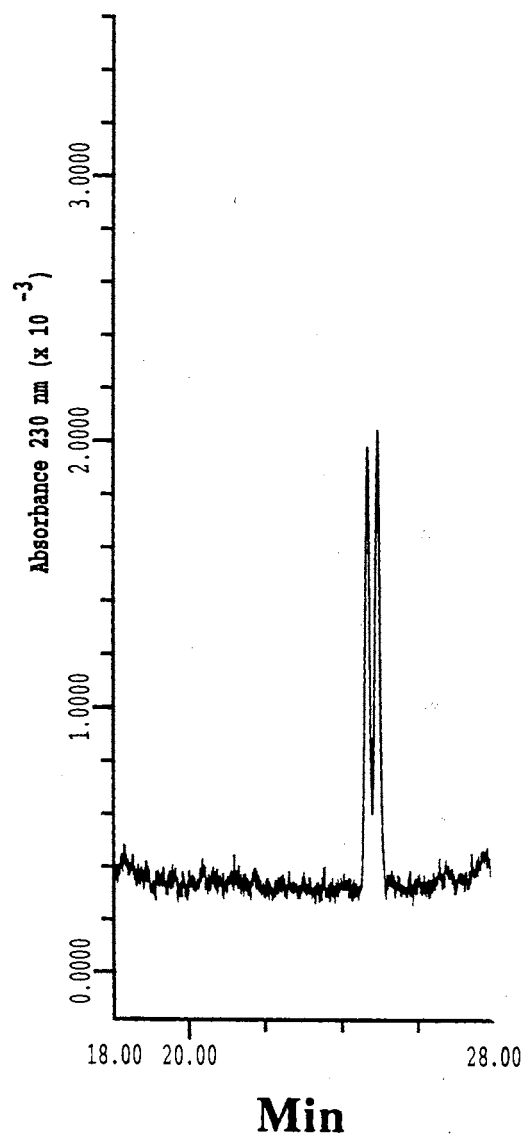


**Figure 22.** Electropherograms of warfarin. Conditions: running electrolyte, 250 mM sodium phosphate, 400 mM sodium borate, pH 6.5, containing 60 mM OM; voltage, 20 kV. Other conditions as in Fig. 4.

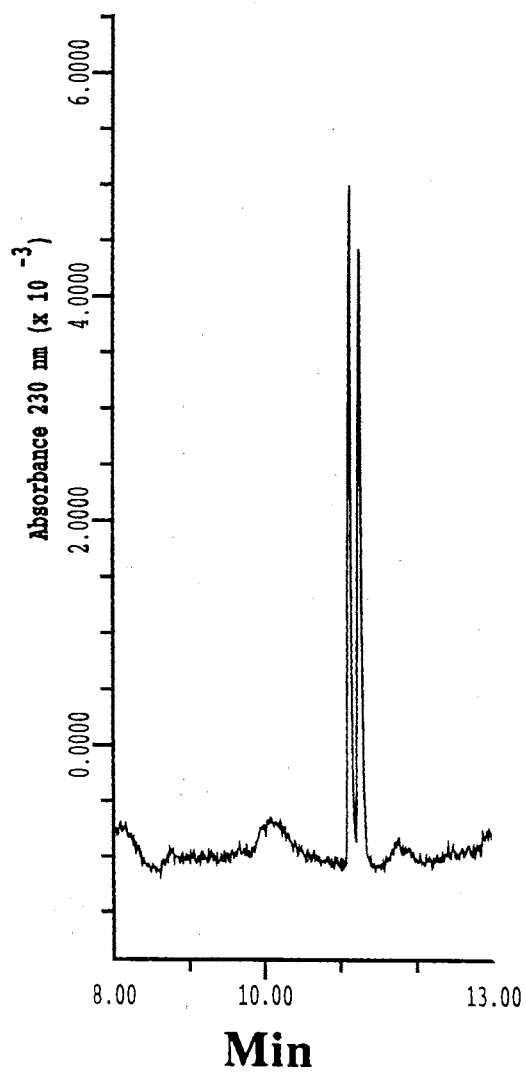


**Figure 23.** Electropherograms of bupivacaine. Conditions: running electrolyte, 200 mM sodium phosphate, 400 mM sodium borate, pH 6.5; voltage, 20 kV. Other experimental conditions as in Fig. 4.

modulate the enantiomeric selectivity by enhancing it for the hydrophobic phenoxy acid herbicides, and decreasing it for the less hydrophobic herbicides. Performing the separation at a subambient temperature favored an enhanced solute-micelle association, and improved enantiomeric resolution.

The three alkylglucoside chiral surfactants were also useful in the enantiomeric separation of some dansyl amino acids, 1,1'-binaphthyl-2,2'-diylhydrogen phosphate, warfarin and bupivacaine. While OM proved useful for the separation of 5 different dansyl amino acids namely tryptophan, phenylalanine, leucine, methionine and valine, OG and NG exhibited chiral recognition for four of the dansyl amino acids but not for tryptophan. However, the enantiomeric resolution achieved using NG and OG were higher than that obtained with OM. Also, the three surfactants exhibited different enantioselectivity toward the 1,1'-binaphthyl-2,2'-diylhydrogen phosphate. The unique enantioselectivity of each surfactant was further exhibited by the fact that only the OM micellar system was able to provide an adequate enantiomeric resolution for warfarin and bupivacaine. In other words, the three surfactants are needed for solving different enantiomeric separation problems.



## References

1. Nishi, N., Kokusenya, Y., Miyamoto, T. and Sato, T., *J. Chromatogr. A* , 659 (1994) 449.
2. Otsuka, K. and Terabe, S., *J. Liq. Chromatogr.* , 16 (1993) 945.
3. Nielen, M.W.F., *J. Chromatogr.* , 637 (1993) 81.
4. Altria, K.D., Walsh, A.R. and Smith, N.W., *J. Chromatogr.* , 645 (1993) 193.
5. Altri, K.D., Goodall, D.M. and Rogan, M.M., *Chromatographia* , 34 (1992) 19.
6. Belder, D. and Schomburg, G., *J. High Resolut. Chromatogr.* , 15 (1992) 686.
7. Soini, H., Reikkola, M.-L. and Novotny, M.V., *J. Chromatogr.* , 608 (1992) 265.
8. Wren, S.A.C. and Rowe, R.C., *J. Chromatogr.* , 603 (1992) 235.
9. Wren, S.A.C., *J. Chromatogr.* , 636 (1993) 57.
10. Fanali, S., *J. Chromatogr.* , 474 (1989) 441.
11. Cruzado, I.D. and Vigh, G., *J. Chromatogr.* , 608 (1992) 421.
12. Guttman, A., Paulus, A., Cohen, A.S., Grinberg, N. and Karger, B.L., *J. Chromatogr.* , 448 (1988) 41.
13. Armstrong, D.W., Tang, Y., Ward, T. and Nichols, M., *Anal. Chem.* , 65 (1993) 1114.
14. Mayer, S. and Schurig, V., *J. High Resolut. Chromatogr.* , 15 (1992) 129.
15. Khun, R., Erni, F., Bereuter, T. and Hausler, J., *Anal. Chem.* , 64 (1992) 2815.
16. Otsuka, K. and Terabe, S., *J. Chromatogr.* , 515 (1990) 221.
17. Dobashi, A., Ono, T., Hara, S. and Yamaguchi, J., *Anal. Chem.* , 61 (1989) 1984.
18. Okafo, G.N. and Camilleri, P., *J. Microcol. Sep.* , 5 (1993) 149.
19. Aiken, J.H. and Huie, C.W., *Chromatographia* , 35 (1993) 448.
20. Busch, S., Kraak, J.C. and Poppe, H., *J. Chromatogr.* , 635 (1993) 119.
21. Barker, G.E., Russo, P. and Hartwick, R.A., *Anal. Chem.* , 64 (1992) 3024.
22. Stalcup, A.M. and Agyei, N.M., *Anal. Chem.* , 66 (1994) 3054.
23. Fanali, S., Ossicini, L., Foret, F. and Bocek, P., *J. Microcol. Sep.* , 1 (1989) 190.

24. Gozel, P., Gassman, E., Michelsen, H. and Zare, R.N., *Anal. Chem.* , 59 (1987) 1984.
25. Tran, A.D., Blanc, T. and Leopold, E.J., *J. Chromatogr.* , 516 (1990) 241.
26. Schutzner, W., Fanali, S., Rizzi, A. and Kenndler, E., *J. Chromatogr.* , 639 (1993) 375.
27. Nishi, H. and Terabe, S., *J. Chromatogr. A* , 694 (1995) 245.
28. Mechref, Y. and El Rassi, Z., *J. Chromatogr. A* , 724 (1996) 285.
29. Mechref, Y. and El Rassi, Z., *Anal. Chem.* , 68 (1996) 1771.
30. Otsuka, K., Kashihara, M., Kawaguchi, Y., Koike, R., Hisamitsu, T. and Terabe, S., *J. Chromatogr. A* , 652 (1993) 253.
31. Otsuka, K. and Terabe, S., *J. Chromatogr.* , 559 (1991) 209.
32. Terabe, S., Miyashita, Y., Ishihama, Y. and Shibata, O., *J. Chromatogr.* , 636 (1993) 47.
33. Ishihama, Y. and Terabe, S., *J. Liq. Chromatogr.* , 16 (1993) 933.
34. Tekel', J. and Kovacicova, J., *J. Chromatogr.* , 643 (1993) 291.
35. Smith, J.T. and El Rassi, Z., *J. Chromatogr. A* , 685 (1994) 131.
36. Smith, J.T. and El Rassi, Z., *J. Microcol. Sep.* , 6 (1994) 127.
37. Neugebauer, J., *A Guid to the Properties and Uses of Detergents in Biology and Biochemistry*, Calbiochem-Novabiochem Corp., San Diego, CA, 1994.
38. Rosen, M.J., *Surfactants and Interfacial Phenomena*, 2nd ed., John Wiley & Sons, New York, 1988.
39. Brito, R.M.M. and Vaz, W.L.C., *Anal. Biochem.* , 152 (1986) 250.
40. Chattopadhyay, A. and London, E., *Anal. Biochem.* , 139 (1984) 408.
41. Bunton, C.A., Gan, L.H., Hamed, F.H. and Moffatt, J.R., *J. Phys. Chem.* , 87 (1983) 336.
42. Hiskey, C.F., Bulloch, E. and Whitman, C., *J. Pharm. Sci.* , 51 (1962) 43.
43. Mechref, Y., Smith, J.T. and El Rassi, Z., *J. Liq. Chromatogr.* , 18 (1995) 3769.

## CHAPTER XIII

# EVALUATION OF OCTYLMALTOPYRANOSIDE CHIRAL SURFACTANT IN THE ENANTIOMERIC SEPARATION OF FLUORESCENTLY LABELED PHENOXY ACID HERBICIDES AND THEIR LIF DETECTION

### Introduction

Many herbicides and pesticides are being applied in the environment as racemic mixtures despite the fact that most often only one enantiomer is biologically active. The consequence of this practice is increasing the concentration of organic pollutants in the environment. The increasing awareness of the ecological hazards associated with the use of racemic herbicides will soon initiate strict government regulations regarding their use. Thus, as there will be a need for efficient chiral separation methods to monitor the enantiomeric content of herbicides formulations and production, there will also be an urgent need for highly sensitive analytical chiral separation methods for the analysis of environmental matrices at the low ppb levels.

In the previous chapter, we have introduced and evaluated chiral alkylglucoside surfactants in the enantiomeric separations of underivatized phenoxy acid herbicides. While these chiral systems will be suitable to determine the enantiomeric content of herbicides in plant production and herbicide formulations where detectability is not an issue, this chapter is concerned with developing a chiral micellar system for the separation of fluorescently labeled phenoxy acid herbicides for their determination by chiral capillary electrophoresis/laser induced fluorescence (CCE/LIF) detection at low levels. The precolumn derivatization is based on the tagging of the phenoxy acid herbicides via their

carboxylic acid groups with 7-aminonaphthalene-1,3-disulfonic acid (ANDSA) in the presence of carbodiimide, thus yielding a stable amide bond between the amino group of the ANDSA tag and the carboxylic acid group of the herbicide. This precolumn derivatization, which was demonstrated recently for phenoxy acid herbicides with CE systems involving cyclodextrins (CDs) and mixed CDs [1] (see Chapter XI), was also applied previously for acidic carbohydrate species by our laboratory [2-4] (Chapters III-V).

Besides providing centers for the sensitive detection of the phenoxy acid herbicides, the precolumn derivatization with ANDSA has increased the hydrophobicity of the herbicides and also imparted these solutes with two strong sulfonic acid groups which are completely ionized over a wide range of pH. As will be shown in this study, these structural alterations introduced by the labeling with ANDSA have in most cases enhanced the chiral recognition of the ANDSA derivatized phenoxy acid herbicides by the OM chiral micellar system under investigation when compared to the native underivatized herbicides.

## Materials and Methods

### Capillary Electrophoresis Instrument

Two Beckman P/ACE instruments (Beckman Instrument, Fullerton, CA, USA) were used in this study, one equipped with a diode array detector and was described in Chapter VI. The other instrument was equipped with an LIF detector and was described in Chapter IX. The detection of underivatized phenoxy acid herbicides was performed at 230 nm. For LIF detection, a fluorescence emission band-pass filter of  $380 \pm 2$  nm was purchased from Corion (Holliston, MA, U.S.A.). The laser beam was rejected with a cut-on filter at 360 nm from Corion. The resulting signal was fed to the computer for archiving and real time display of the electropherograms. The fused-silica capillaries were obtained from Polymicro Technology (Phoenix, AZ, U.S.A.) and had the dimensions of 50 cm to detection window and 57 cm total length with 50  $\mu$ m I.D. and 365  $\mu$ m O.D.. Unless otherwise stated, the temperature of the capillary was maintained at 15 °C by the instrument

thermostating system. Samples were pressure injected at 0.034 bar (i.e., 3.5 kPa) for various lengths of time.

### Reagents and Materials

n-Octyl- $\beta$ -D-maltopyranoside (OM) surfactant was purchased from Calbiochem (La Jolla, CA, USA). The structure and the CMC value of this surfactant are listed in Table I of Chapter XII. Phenoxy acid herbicides including silvex, 2-(2,4-dichlorophenoxy)propionic acid (dichlorprop), 2-(4-chloro-2-methylphenoxy)propionic acid (mecoprop), 2-(4-chlorophenoxy)propionic acid (2,4-CPPA), 2-(3-chlorophenoxy)propionic acid (2,3-CPPA), 2-(2-chlorophenoxy)propionic acid (2,2-CPPA), and 2-phenoxypropionic acid (2-PPA) were purchased from Aldrich (Milwaukee, WI, USA) and from Chem Service (West Chester, PA, USA). The structures of these herbicides are illustrated in Fig. 1 of Chapter XI. All other chemicals used in this study were obtained from the same sources listed in Chapter III.

### Precolumn Derivatization

The seven chiral phenoxy acid herbicides used in this study were tagged with ANDSA according to the procedure previously described in Chapter XI. For the determination of the limit of detection of the ANDSA derivatized phenoxy acid herbicides, the final concentration of the analytes in the reaction mixture was  $5.0 \times 10^{-10}$  M. The entire reaction mixture containing the derivatized phenoxy acid herbicides, excess derivatizing agent, and other components of the reaction mixture was analyzed by CE. A typical example of ANDSA-phenoxy acid herbicides is shown in Chapter XI.

### Fluorescence Measurements

The fluorescence spectra of ANDSA and its phenoxy acid herbicide derivatives were recorded on Spex Industries Model F112 spectrofluorometer (Edison, NJ, USA).

Samples of ANDSA and ANDSA-phenoxy acid derivatives were prepared in 50 mM phosphate buffer, pH 6.5. Fluorescence spectra of ANDSA-phenoxy acid herbicides were obtained from dilute reaction mixtures of ANDSA and EDAC and 30-fold molar excess of herbicides. Under these conditions, a complete conversion of ANDSA to its herbicides derivatives is assumed to be achieved. This was supported by CE analysis of the reaction mixture, where the electropherograms showed no detectable peak for unreacted ANDSA and the formation of the derivatives. The fluorescence spectra for ANDSA and ANDSA-phenoxy acid herbicide are displayed in Fig. 1. ANDSA showed two excitation maxima one at 315 nm while the other was at 350 nm, while the emission maximum of ANDSA was at 450 nm. The derivatization has caused shifts in both the excitation and emission maxima, and the two excitation maxima were shifted to 329 nm and 341 nm, while the emission maximum was shifted to 376 nm. Thus, selecting suitable filters would allow the reduction in ANDSA signal.

#### Field-Amplified Sample-Stacking

On-column concentration was performed according to the field-amplified sample-stacking procedure reported by Chien and Burgi [5,6]. Briefly, approximately 70% of the capillary total length was pressure filled with the derivatized sample prepared in water and then a voltage of 10 kV was applied in the negative polarity mode (i.e., the cathode at the inlet end and the anode at the outlet end of the capillary). Upon the application of this voltage the current initially was 0.6  $\mu\text{A}$  due to the difference in conductivity between the running electrolyte and the large aqueous plug of the sample. As the aqueous sample plug was pumped out of the column by the cathodal EOF, the current kept increasing until it reached its normal value in the absence of the sample plug (i.e., 46  $\mu\text{A}$ ). At this time, the polarity of the system was switched back to the normal configuration (i.e., anode at capillary inlet and cathode at capillary outlet) and the electrophoretic separation was performed.

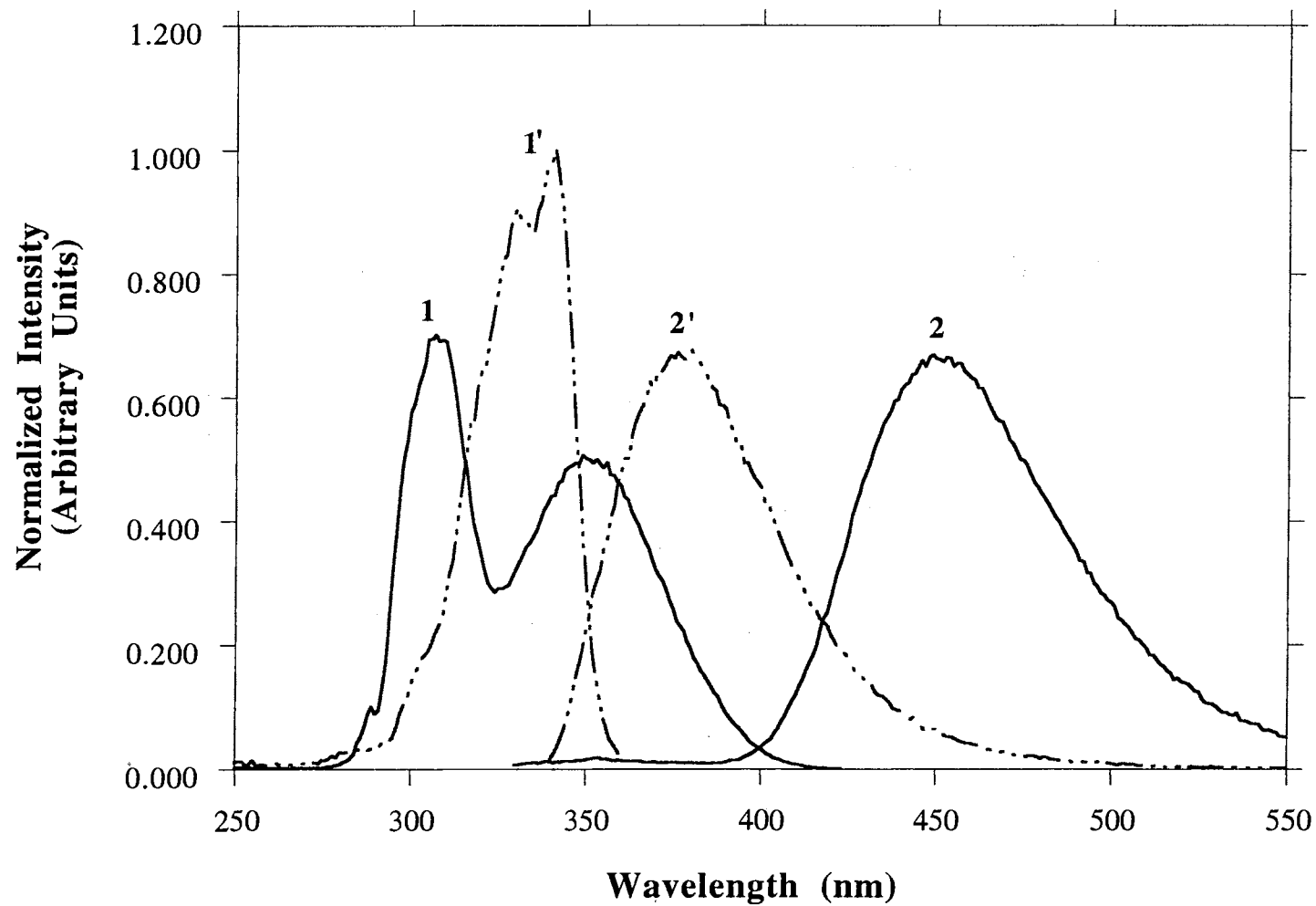


**Figure 1.** Fluorescence spectra of ANDSA and ANDSA-2,2-CPPA. (1) excitation spectrum of ANDSA, (2) emission spectrum of ANDSA, (1') excitation spectrum of ANDSA-2,2-CPPA, and (2') emission spectrum of ANDSA-2,2-CPPA.

## Results and Discussion

### Effect of Tagging with ANDSA on Enantiomeric Resolution

According to the studies in chapter XII involving the evaluation of alkylglucoside surfactants in chiral capillary electrophoresis of underivatized phenoxy acid herbicides, it has been observed that there exists a correlation between the extent of solute solubilization into the alkylglucoside micelle and the enantiomeric resolution. Similar to the underivatized phenoxy acid herbicides, the locus for the solubilization of the ANDSA-phenoxy acid herbicides in the OM micelle is more likely to be in the palaside layer which consists of the hydrophilic head groups of the surfactant molecules and the first few carbon atoms of the alkyl tails. Also, as with the underivatized phenoxy acid herbicides, the ANDSA derivatives will orient their polar sulfonic acid groups toward the polar chiral centers of the OM surfactant while the none polar portion of the ANDSA derivatives will be oriented toward the interior of the micelle in the palaside layer. The major difference between the derivatized and underivatized solutes is that the hydrophobic part of the ANDSA tag would make the solute undergo deeper penetration in the palaside layer than the underivatized herbicides, thus affecting their electrokinetic behavior as well as their chiral recognition by the chiral micelle. One noticeable change is the case of 2-PPA. In fact, underivatized 2-PPA, which is the least hydrophobic phenoxy acid herbicide, was not enantiomerically separated at any OM surfactant concentration. Upon derivatization with ANDSA, the 2-PPA separated enantiomerically as shown in Fig. 2. The tagging with ANDSA allowed the molecule to associate with the palaside layer to a larger extent than in the case of underivatized 2-PPA, a condition that may have favored more encounter between the chiral center of the solute and the chiral head group of the surfactant molecule in the OM micelle, and in turn a better chiral recognition.

Since OM is a nonionic surfactant, its micelle migrates with the cathodal electroosmotic flow (EOF). Therefore, an anionic analyte (whose electrophoretic migration



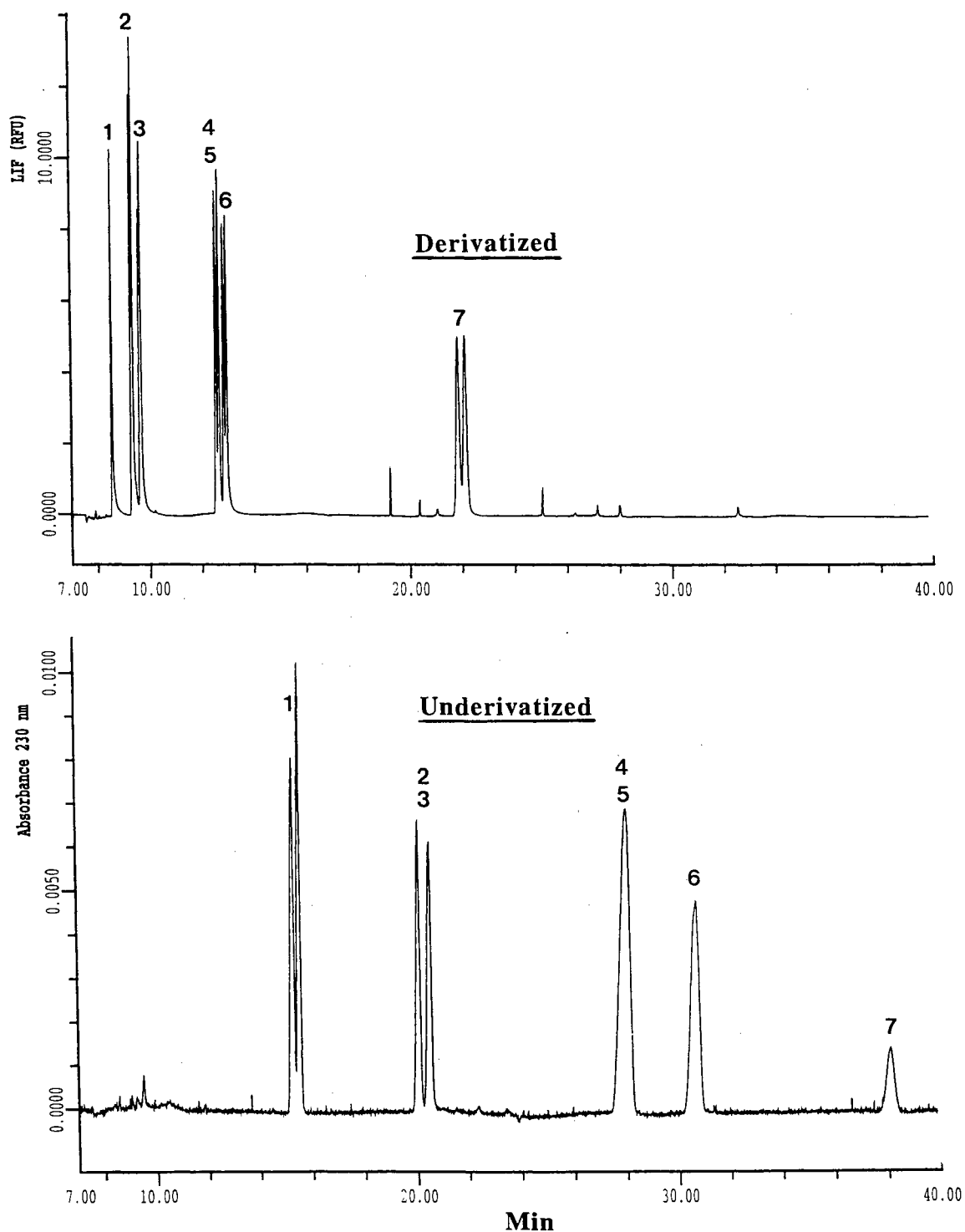


**Figure 2.** Electropherograms of derivatized (a) and underivatized (b) phenoxy acid herbicides. Conditions: running electrolyte, 200 mM sodium phosphate, pH 6.5, containing 30 mM OM; voltage, 25 kV; capillary, bare fused-silica capillary 50 cm (to detection point)/ 57 cm (total length) x 50  $\mu$ m I.D.; temperature, 15°C. Peaks in (a), 1 = ANDSA-silvex, 2 = ANDSA-dichlorprop, 3 = ANDSA-mecoprop, 4 = ANDSA-2,4-CPPA, 5 = ANDSA-2,3-CPPA, 6 = ANDSA-2,2-CPPA, 7 = ANDSA-2-PPA; peaks in (b), 1= silvex, 2= dichlorprop, 3= mecoprop, 4= 2,4-CPPA, 5= 2,3-CPPA, 6 = 2,2-CPPA, 7= 2-PPA.

is in the opposite direction to the cathodal EOF) that associates strongly with the nonionic OM micelle will exhibit a relatively low effective electrophoretic mobility and consequently its migration time will be shorter. Indeed, and as shown in Fig. 2, increasing the hydrophobicity of the analytes through labeling with ANDSA, augmented the analyte-micelle interaction and consequently decreased the migration time as compared to underivatized phenoxy acid herbicides. Although the labeling of the analytes with ANDSA replaced the carboxylic acid group of each phenoxy acid herbicide by two strong sulfonic acid groups, thus increasing the negative charges of each analyte from one to two, apparently the increase in hydrophobicity was more pronounced to the extent that the analysis time was almost one half shorter and decreased from ca. 39 min to ca. 22 min, compare Fig. 2a to 2b. As discussed above, another important feature of the derivatization with ANDSA is the fact that 2-PPA which could not be resolved enantiomerically as an underivatized solute at any surfactant concentration is now readily resolved as an ANDSA-2-PPA derivative, see Fig. 2. Also, 2,4- 2,3- and 2,2-CPPA which required relatively higher OM concentration to undergo enantiomeric separation (see Fig. 8 Chapter XII) are now resolved at lower OM concentration. On the other hand, and as illustrated in Fig. 2, the enantiomeric resolution of dichlorprop and mecoprop decreased as a result of the labeling with ANDSA, and a lower OM concentration is now needed for their enantiomeric resolution (see below for more discussion). However, unlike underivatized silvex, ANDSA-silvex is not resolved enantiomerically even at very low surfactant concentration.

Returning to Fig. 2, the capillary temperature was maintained at 15 °C in all the studies since as the temperature was increased the enantiomeric resolution decreased. The enantiomeric resolution-temperature dependency resembled and paralleled what we described in the previous chapter with underivatized phenoxy acid herbicides using OM and other alkylglucoside surfactants (results not shown).

### Limit of Detection

As shown earlier, the derivatization of phenoxy acid herbicides with ANDSA is very quantitative producing as high as 99.7% yield [1] (Chapter XII). In addition, the derivatization leads to stable derivatives with no side products. Other salient features of the derivatization is improving the sensitivity and selectivity of detection of the phenoxy acid herbicides. Indeed, the derivatization of phenoxy acid herbicides with ANDSA has allowed a detection limit of  $5 \times 10^{-10}$  M which correspond to a 0.1 ppb, a concentration level at which environmental herbicide samples are expected to occur. Moreover, the derivatization procedure was successful even at the limit of detection, i.e.,  $5 \times 10^{-10}$  M, see Fig. 3a. This detection limit is two times lower than what we observed in our recent work with CD and mixed CDs for the enantiomeric separation of ANDSA-phenoxy acid herbicides [1], see Chapter XI. The improvement in the limit of detection with the chiral micellar system under investigation over the previously reported CDs system can be attributed to the presence of a micellar phase, which is known to enhance fluorescence intensity[7].

### Field-Amplified Sample-Stacking of Ultra Diluted Samples

The field-amplified sample-stacking was performed on ultra diluted samples as described in Experimental. Under these conditions (see Fig. 3b), the concentration detection limit was as low as  $10^{-11}$  M (2.21 ppt), which corresponds to a 50 fold lower concentration detection limit than that attained without sample stacking, see above. Also, the samples were successfully derivatized at this low concentration (see Fig. 3c), yet an overnight mixing was required to reach the same efficiency of derivatization as determined from comparing the peak heights of samples derivatized at this low concentration (Fig. 3c) to those prepared by dilution of a  $5 \times 10^{-10}$  M derivatized sample (Fig. 3b).

While the separation efficiency was largely unaffected by the stacking procedure (471,000 plates/m in direct injection as opposed to 464,000 plates/m with stacking), the

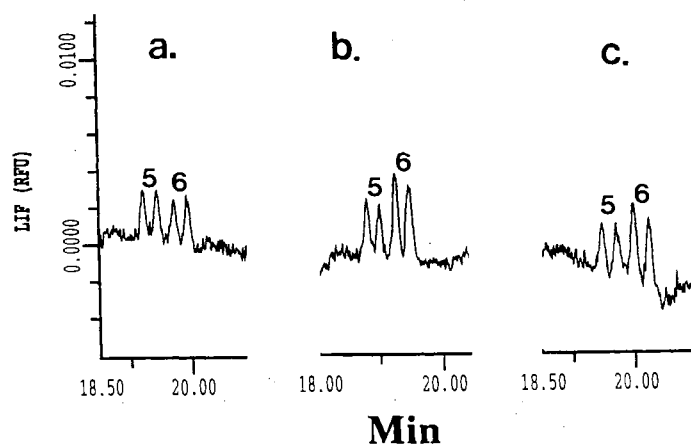


**Figure 3.** Electropherograms of ANDSA-phenoxy acid herbicides obtained without (a) and with (b and c) field-amplified sample-stacking. Conditions: running electrolyte, 200 mM sodium phosphate, pH 6.5, containing 30 mM OM; voltage, 20 kV; capillary, bare fused-silica capillary 50 cm (to detection point)/ 57 cm (total length) x 50  $\mu$ m I.D.; temperature, 15°C, sample injection, 10 sec of pressure injection at 0.034 bar in (a); the procedure for the field-amplified sample stacking used in (b and c) is described in the experimental section. Peaks, 5 = ANDSA-2,3-CPPA, 6 = ANDSA-2,2-CPPA.

enantiomeric resolution slightly decreased from 1.44 to 1.31 and from 1.25 to 1.17 for 2,3-CPPA, and 2,2-CPPA, respectively. In addition, under stacking conditions, the average percent relative standard deviations (%RSD, n=5) of migration time, peak area and peak height were determined to be 1.03, 1.9, and 2.2, respectively. Therefore, the field-amplified sample-stacking procedure hardly reduced the reproducibility of the separation.

#### Effect of Surfactant Concentration

Since increasing the OM concentration, [S], in the running electrolyte results in increasing the micellized surfactant concentration, [S]-CMC, the solubilization of the anionic ANDSA derivatized phenoxy acid herbicides in the OM micellar phase will be increased. This would result in decreasing the effective electrophoretic mobility of the analytes with increasing OM concentration as shown in Fig. 4. The decrease in the average effective electrophoretic mobility was more pronounced for the more hydrophobic analytes, see Fig. 4. Because the tagging with ANDSA has increased the hydrophobicity of all analytes by the same increment, the migration order of the ANDSA-phenoxy acid herbicides paralleled that of their underivatized counterparts. The order of decreasing hydrophobicity of the analytes is silvex >> dichlorprop > mecoprop >> 2,4-CPPA ≥ 2,3-CPPA > 2,2-CPPA >> 2-PPA, which is the reversal of their migration order. This order correlates with the number of non-polar groups substituted on the phenyl ring of the analytes as well as the nature (i.e., methyl or chlorine group) and position of the substituted group (i.e., ortho, meta and para).

Furthermore, the hydrophobicity of the analytes influenced the concentration of the OM surfactant required for optimum enantiomeric resolution of the ANDSA-phenoxy acid herbicides, see Fig. 5. The derivatization with ANDSA has imparted silvex with a relatively strong hydrophobic character which enforced its non-polar interaction with the alkyl tail of the surfactant so that on the average the ANDSA-silvex molecule spend more time deeper in the palaside layer of the micelle. This will distance the chiral center of silvex from

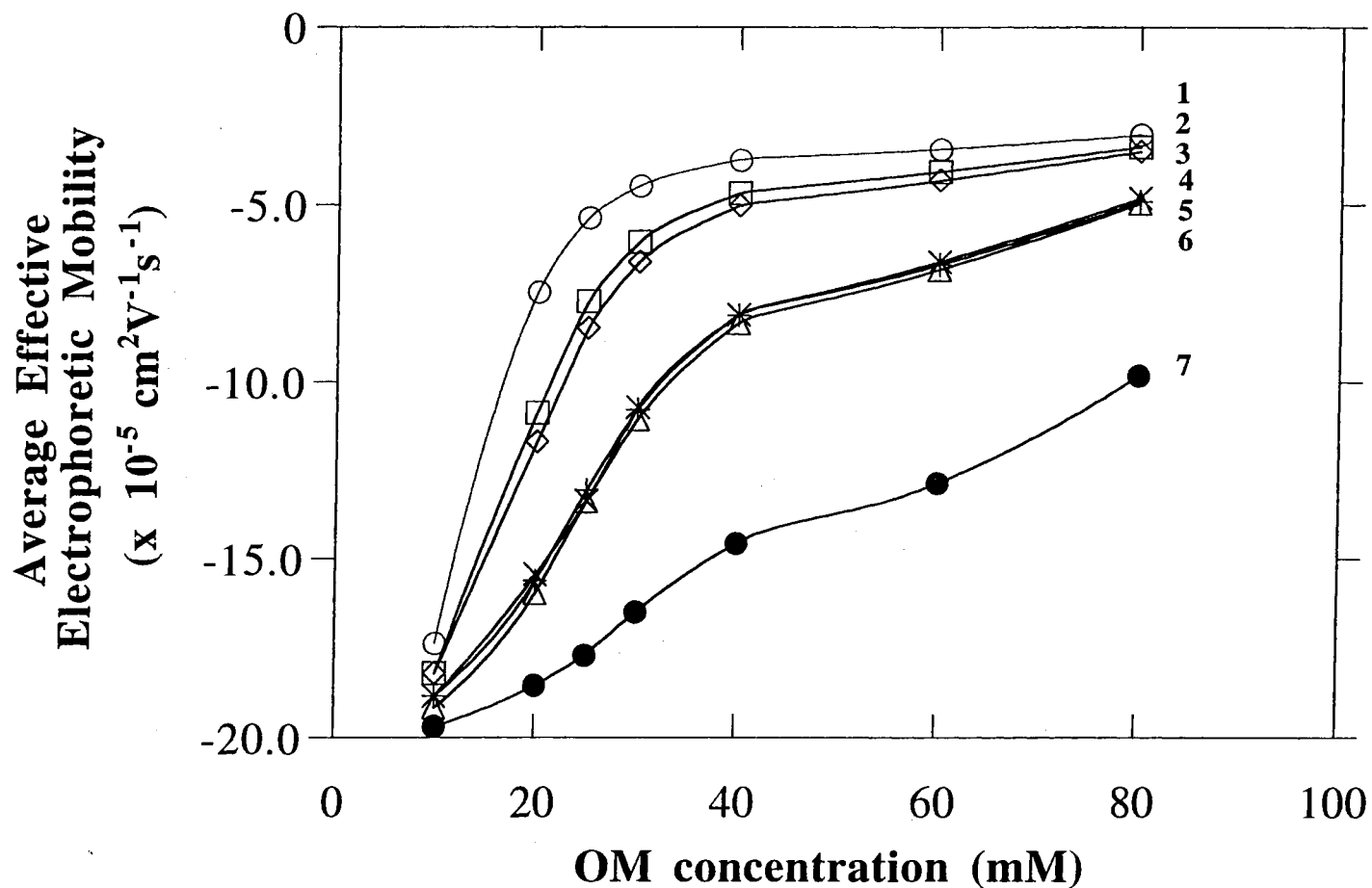


**Figure 4.** Plots of the average effective electrophoretic mobilities of ANDSA-phenoxy acid herbicides versus OM concentrations. Conditions: running electrolyte, 200 mM sodium phosphate, pH 6.5, containing various concentrations of OM; voltage, 20 kV; capillary, bare fused-silica capillary 50 cm (to detection point)/ 57 cm (total length) x 50  $\mu$ m I.D.; temperature, 15°C. Lines, 1 = ANDSA-silvex, 2 = ANDSA-dichlorprop, 3 = ANDSA-mecoprop, 4 = ANDSA-2,4-CPPA, 5 = ANDSA-2,3-CPPA, 6 = ANDSA-2,2-CPPA, 7 = ANDSA-2-PPA.

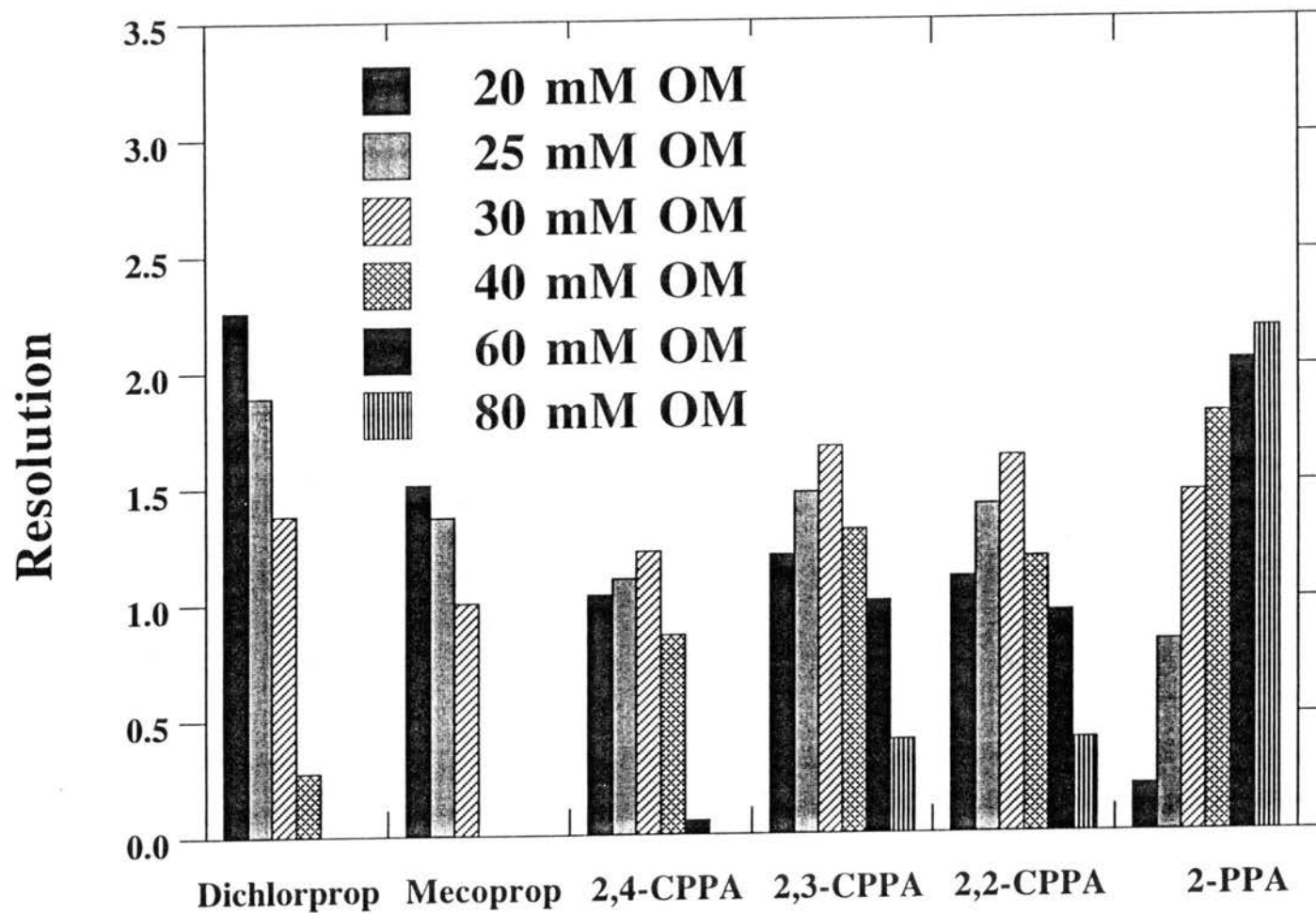


**Figure 5.** Bar graphs of the enantiomeric resolution of ANDSA-phenoxy acid herbicides at various OM concentrations. Conditions: running electrolyte, 200 mM sodium phosphate, pH 6.5, containing 20 mM OM in (a), 30 mM OM in (b) and 80 mM OM in (c). Experimental conditions as in Fig. 4.

interacting with the polar chiral centers of the OM surfactant, a condition that explains the absence of enantiomeric resolution of ANDSA-silvex at any surfactant concentration. On the other hand, the enantiomeric resolution of ANDSA-dichlorprop and ANDSA-mecoprop decreased as the surfactant concentration increased. Due to increasing the micellar phase ratio, increasing the surfactant concentration would increase the nonpolar interaction of the two relatively hydrophobic solutes (i.e., ANDSA-dichlorprop and ANDSA-mecoprop) with the non-polar portion of the palaside layer at the expense of decreasing the interaction with the polar chiral head group of the micelle, thus yielding a decrease in the enantiomeric resolution. The enantiomeric resolution of the solutes of intermediate hydrophobicity such as the ANDSA derivatives of 2,4-CPPA, 2,3-CPPA and 2,2-CPPA reached a maximum resolution at 30 mM OM. This means that 30 mM OM would provide optimum concentration of micellized chiral centers for maximum resolution. Finally, the enantiomeric resolution of 2-PPA, which is the least hydrophobic species, kept increasing as the micellar phase increased (see Fig. 5). However, as the surfactant concentration increased to 80 mM, the resolution of the other analytes was negatively affected (Fig. 6a-c). As shown in Fig. 6a, the enantiomeric resolution of some of the ANDSA derivatized phenoxy acid herbicides was achieved even at surfactant concentration slightly lower than CMC (i.e., 20 mM OM), while this behavior was not observed with the underivatized herbicides. This may be due to the increase in hydrophobicity as a result of derivatization.

#### Effect of pH and Ionic Strength

Unlike the underivatized herbicides whose ionization varies with the pH of the running electrolyte, the ANDSA-phenoxy acid herbicides are completely ionized over a wide range of pH due to the presence of two strong sulfonic acid groups in the ANDSA tag. Due to their strong acidic character, the enantiomeric resolution of the ANDSA-phenoxy acid herbicides was largely unaffected by the pH. Conversely, and as shown earlier [8], the enantiomeric resolution of underivatized phenoxy acid herbicides increased



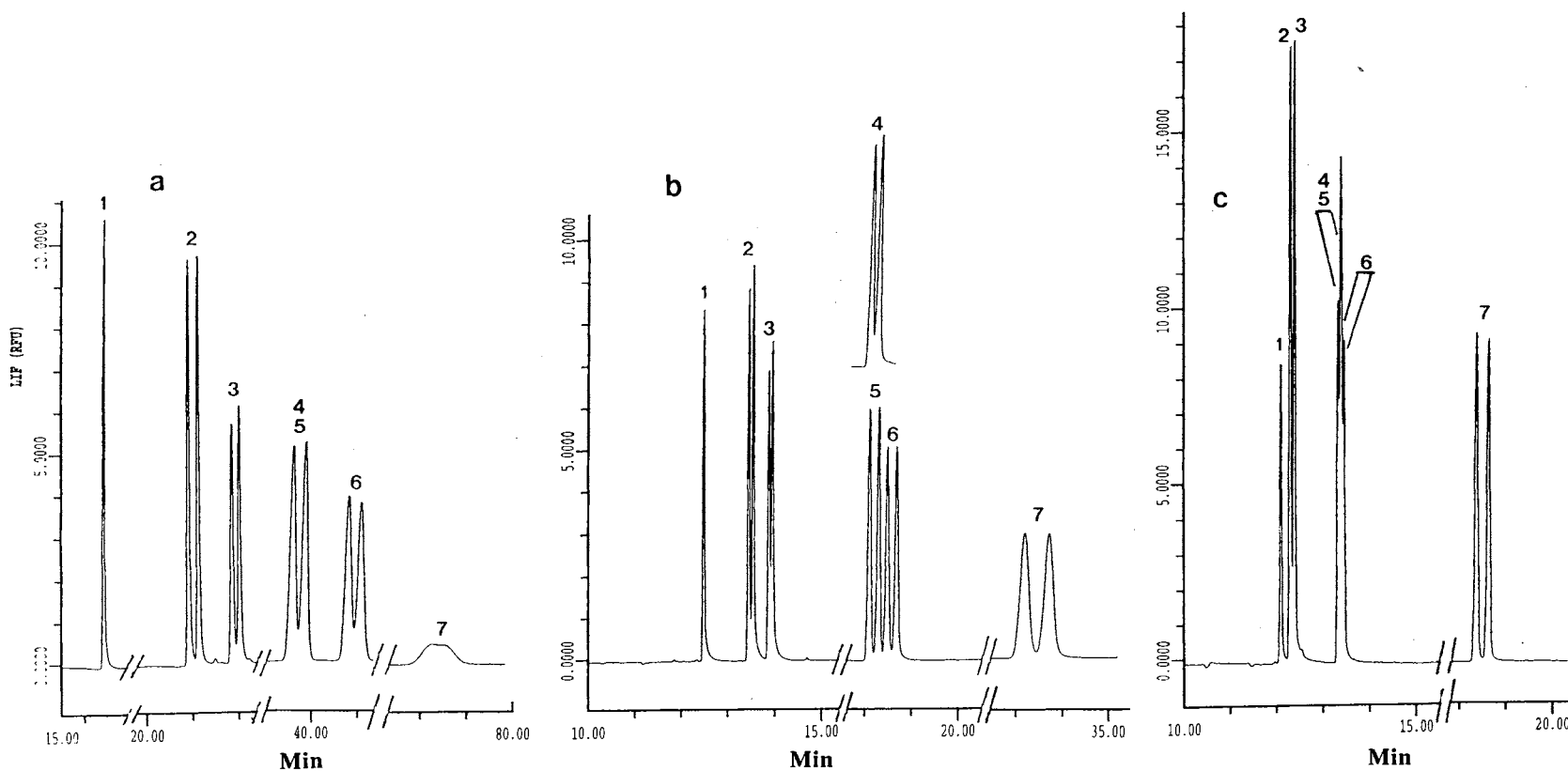


**Figure 6.** Electropherograms of ANDSA-phenoxy acid herbicides at various OM concentrations. Conditions: running electrolyte, 200 mM sodium phosphate, pH 6.5, containing 20 mM OM in (a), 30 mM OM in (b) and 80 mM OM in (c). Other experimental conditions as in Fig. 4. Peaks, 1 = ANDSA-silvex, 2 = ANDSA-dichlorprop, 3 = ANDSA-mecoprop, 4 = ANDSA-2,4-CPPA, 5 = ANDSA-2,3-CPPA, 6 = ANDSA-2,2-CPPA, 7 = ANDSA-2-PPA.

with decreasing pH due to a better solubilization of the solutes in the chiral micellar phase. With the ANDSA-derivatized phenoxy acid herbicides, the only influence the pH has was to accelerate the EOF and in turn reduce the analysis time as the pH was increased. Thus, and as a compromise pH 6.5 was selected for studying the effects of other operating parameters.

The enantiomeric resolution of the various analytes under investigation was affected differently by the increase in the ionic strength of the separation electrolyte. Generally, increasing the ionic strength of the separation electrolyte decreases the EOF and the effective electrophoretic mobility of the analytes. The net result is a decrease in the apparent mobility of the analytes and consequently longer analysis time. Also, increasing the ionic strength is known to decrease the CMC and increase the aggregation number of the OM micelle [8,9]. This would increase the micellized surfactant concentration as well as the concentration of chiral centers in the micellar form. In addition, increasing the ionic strength has a salting out effect which will increase nonpolar interaction with the chiral OM micelle. As can be seen in Fig. 7, the enantiomeric resolution of dichlorprop and mecoprop decreased as the ionic strength of the separation electrolyte increased indicating that the concentration of the chiral centers in the micellar phase has exceeded the optimum value for maximum resolution and/or increasing the ionic strength has resulted in strengthening non polar interaction with the core of the micelle at the expense of the polar interaction with the sugar chiral head groups at the surface of the OM micelle. On the other hand, the enantiomeric resolution for all other analytes has improved as the ionic strength of the separation electrolyte increased. While for 2-PPA (the least hydrophobic solute) this effect was more pronounced, the enantiomeric resolution of 2,4-, 2,3- and 2,2-CPPA increased first when going from 50 to 150 mM phosphate, and then leveled off at higher phosphate concentration (see Fig. 7). This is equivalent to saying that by increasing the ionic strength, the concentration of the chiral centers in the micellar phase has not attained yet the optimum value for maximum resolution for the intermediate and weakly hydrophobic

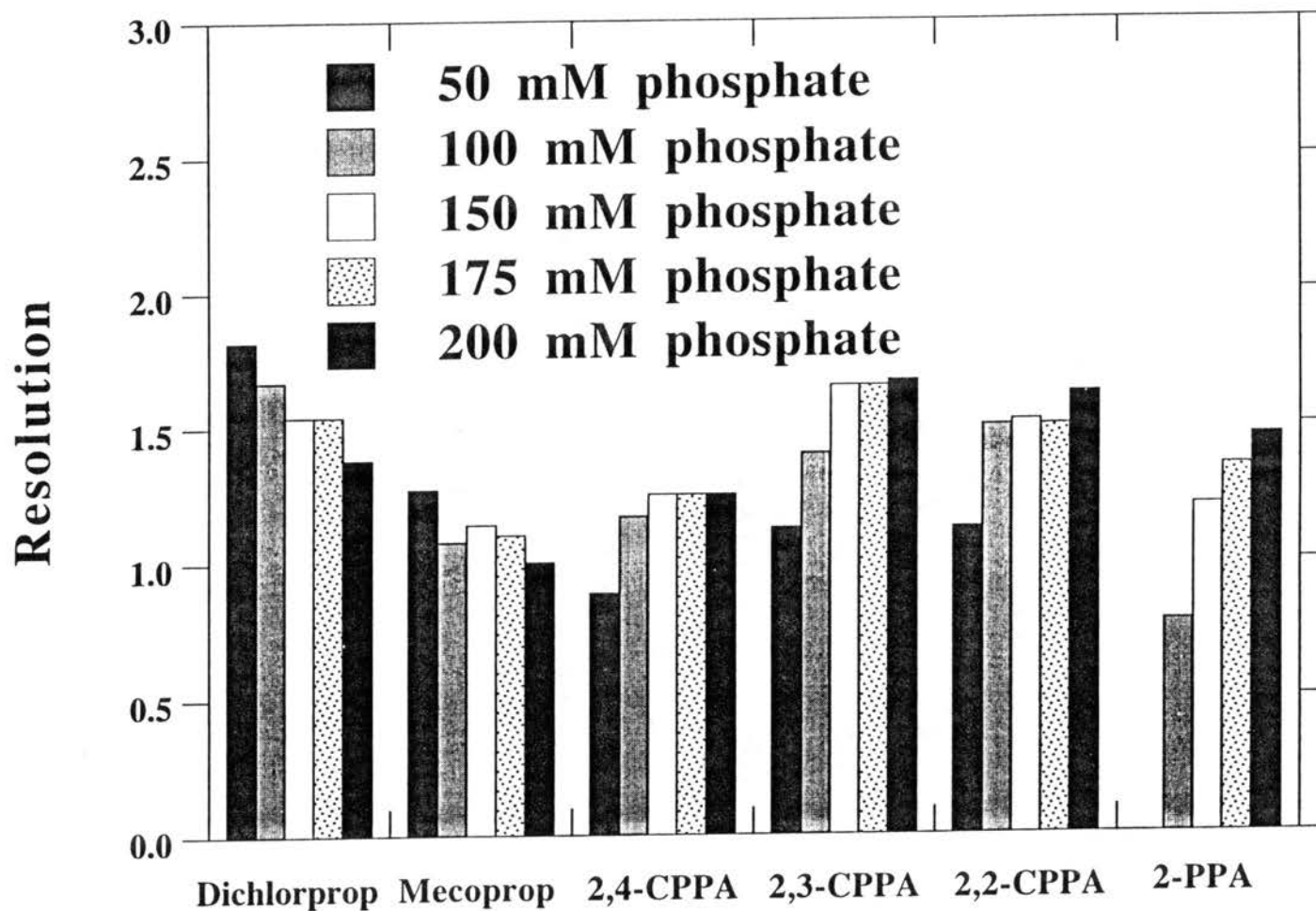


**Figure 7.** Bar graphs of the enantiomeric resolution of ANDSA-phenoxy acid herbicides at various ionic strengths of the separation electrolyte. Conditions: running electrolyte, 50 mM sodium phosphate in (a), 150 mM sodium phosphate in (b) and 200 mM sodium phosphate in (c), pH 6.5, all containing 30 mM OM. Experimental conditions as in Fig. 4.

solutes and/or upon increasing the ionic strength the depth of solute penetration into the palaside layer kept moving in the direction that favored better association of the chiral center of the solute with that of the surfactant.

### Effect of Methanol

The enantiomeric resolution of the various analytes was affected differently by the addition of methanol to the separation electrolytes, see Fig. 8. However, the effect correlated with the hydrophobicity of the analytes. For all practical purposes, the CMC and the aggregation number of the micelle can be considered unaffected by the addition of methanol since in the percent range studied (i.e., from 0% to 10% v/v), there is a slight inhibitory effect of methanol on the micellization process [10]. As can be seen in Fig. 8, while the enantiomeric resolution of dichlorprop and mecoprop improved slightly upon the addition of 5% (v/v) methanol to the separation electrolyte, the enantiomeric resolution of all other analytes decreased as the percentage of methanol was increased. The enantiomeric resolution of the least hydrophobic analytes, 2-PPA, was the most reduced by the addition of methanol to the separation electrolyte. Moreover, the addition of methanol decreased EOF, and the analysis time was almost doubled upon including 5% (v/v) of methanol into the separation electrolyte.

In the case of ANDSA-dichlorprop and ANDSA-mecoprop, the addition of 5% methanol may have adjusted the depth of solute penetration in the palaside layer (most probably by a competition effect) thus favoring a better interaction between the chiral center of the solute and that of the surfactant in the OM micelle. For the intermediate and weakly hydrophobic solutes, the decrease in enantiomeric resolution suggests an opposite effect. In other words, the addition of methanol may have resulted in weakening the interaction of the solute with the palaside layer to the point that it has diminished the probability of the solute to encounter the chiral head group of the surfactant.

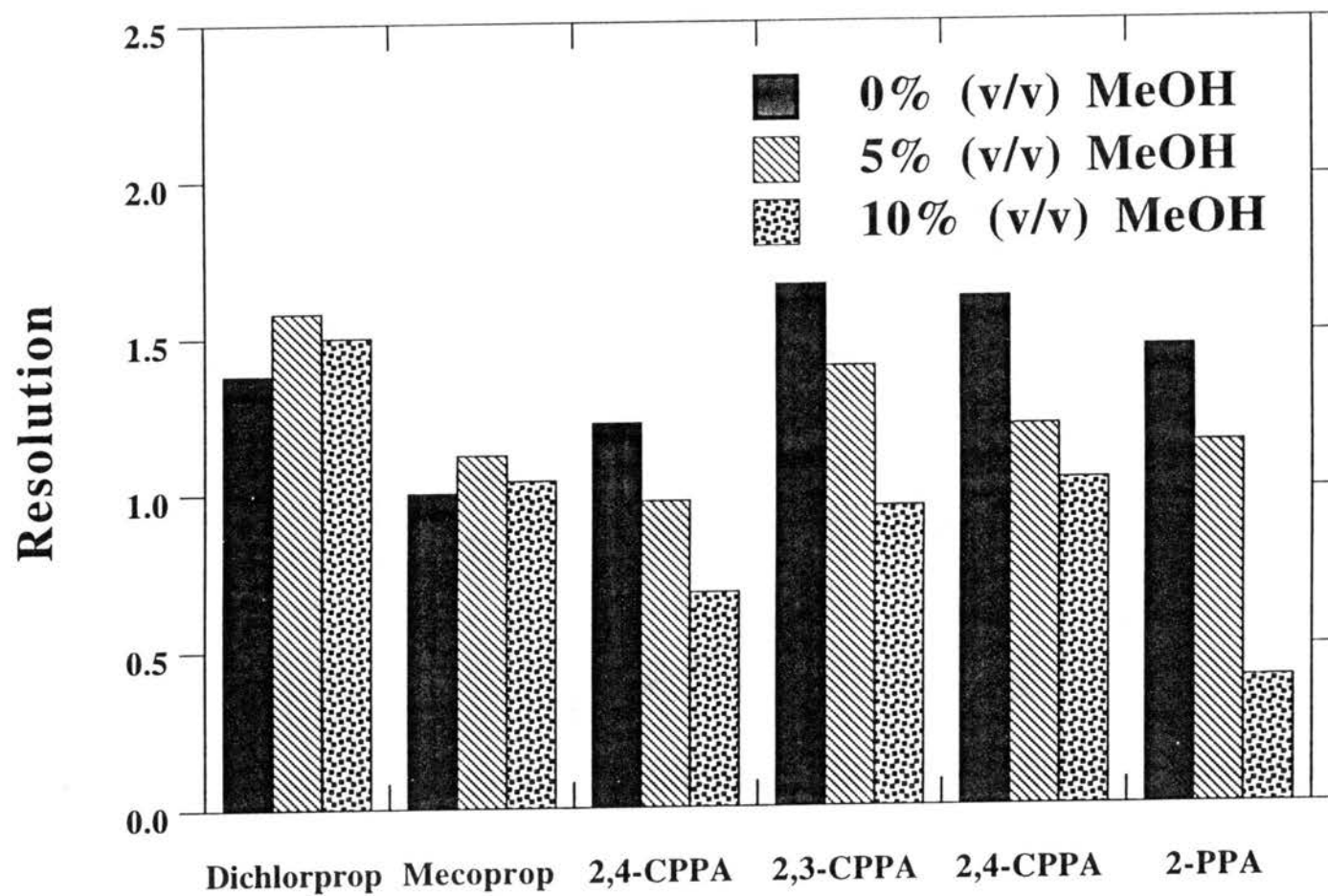


**Figure 8.** Bar graphs of the enantiomeric resolution of ANDSA-phenoxy acid herbicides at various percentage of methanol in the separation electrolyte. Conditions, running electrolyte, 200 mM sodium phosphate, pH 6.5, containing 30 mM OM and various percentage of methanol. Other experimental conditions as in Fig. 4.

## Conclusions

A novel chiral nonionic surfactant, namely octyl- $\beta$ -D-maltopyranoside (OM), was evaluated in chiral capillary electrophoresis of fluorescently labeled phenoxy acid herbicides. The labeling of the analytes with ANDSA permitted a concentration detection limit of  $5 \times 10^{-10}$  M using laser induced fluorescence detection. This limit of detection allowed the determination of ultra diluted solutions of the ANDSA derivatized phenoxy acid herbicides whose concentration was as low as  $10^{-11}$  M (i.e., 2.2 ppt) by applying the concept of field amplified sample-stacking (FASS). The sample injection by FASS did not adversely affect separation efficiencies, resolution and reproducibility of the electrophoretic system. The tagging of the phenoxy acid herbicides with ANDSA increased the hydrophobicity of the analytes, thus favoring an enhanced solubilization of the derivatized herbicides in the OM micellar phase. The net results of this effect were a much shorter analysis time and an improved enantiomeric resolution of the derivatives when compared to underivatized phenoxy acid herbicides. The optimum surfactant concentration required for maximum resolution decreased with increasing the hydrophobicity of the analyte with the least hydrophobic analyte requiring higher surfactant concentration. Because of the two permanently charged sulfonic acid groups of the ANDSA tag, the pH of the running electrolyte had little effect on the enantiomeric resolution of the derivatized herbicides. Due to its salting out effect and increasing the micellized surfactant concentration, increasing the ionic strength of the running electrolyte increased the enantiomeric resolution of the least hydrophobic analytes. Conversely, increasing the percent methanol in the running electrolyte decreased the enantiomeric resolution of the least hydrophobic analytes due to decreasing the strength of solute-micelle association. For hydrophobic analytes, there was an optimum percent methanol for maximum enantiomeric resolution.

## References

1. Mechref, Y. and El Rassi, Z., *Anal. Chem.* , 68 (1996) 1771.
2. Mechref, Y., Ostrander, G.K. and El Rassi, Z., *Electrophoresis* , 16 (1995) 1499.
3. Mechref, Y., Ostrander, G.K. and El Rassi, Z., *J. Chromatogr. A* , 695 (1995) 83.
4. Mechref, Y. and El Rassi, Z., *Electrophoresis* , 15 (1994) 627.
5. Chien, R.-L. and Burgi, D.S., *Anal. Chem.* , 64 (1992) 1046.
6. Chien, R.-L. and Burgi, D.S., *Anal. Chem.* , 64 (1992) 489.
7. Smith, J.T. and El Rassi, Z., *J. Cap. Elec.* , 2 (1994) 136.
8. Brito, R.M.M. and Vaz, W.L.C., *Anal. Biochem.* , 152 (1986) 250.
9. Chattopadhyay, A. and London, E., *Anal. Biochem.* , 139 (1984) 408.
10. Bunton, C.A., Gan, L.H., Hamed, F.H. and Moffatt, J.R., *J. Phys. Chem.* , 87 (1983) 336.

VITA 7

YEHIA SALEM MECHREF

Candidate for the Degree of

Doctor of Philosophy

Thesis: INTRODUCTION OF MEDIA AND REAGENTS FOR THE  
DETERMINATION OF ENVIRONMENTAL AND BIOLOGICAL  
SUBSTANCES BY HIGH PERFORMANCE CAPILLARY  
ELECTROPHORESIS

Major Field: Chemistry

Biographical:

Personal Data: Born in El Mina, Lebanon, September 18, 1966, the son of  
Salem and Fayzah Mechref.

Education: Graduated from El Faysal High School, Jeddah, Saudi Arabia in  
1984; received Bachelor of Science Degree in chemistry from the  
American University of Beirut, Beirut, Lebanon, in July, 1991; completed  
requirements for the Doctor of Philosophy Degree at Oklahoma State  
University in July, 1996.

Professional Experience: August 1992 to present, graduate research and  
teaching assistant, Oklahoma State University.

Professional Organization: Phi Lambda Upsilon,